COLA 2015

International Conference on Laser Ablation 2015

31 August – 4 September 2015

Cairns, Australia

PROGRAM HANDBOOK

www.cola2015.org

International Conference on Laser Ablation 2015

31 August – 4 September 2015

Cairns, Australia

Contents

National Library of Australia Cataloguing-in-Publication entry

Creator:	Conference on Laser Ablation (13th : 2015 : Cairns, Qld.)
Title:	Conference on laser ablation 2015 : program handbook / Prof Andrei Rode.
ISBN:	978 0 64694 286 5 (paperback)
Subjects:	1. Laser ablation—Congresses. 2. Lasers—Industrial applications—Congresses.
Other creators/ contributors:	Rode, Andrei.
Dewey number:	621.366

Welcome

Dear colleagues

Welcome to COLA 2015! This conference is shaping up to be a wonderful exposé of the latest developments in laser ablation and in a broader area of laser-induced modification of material properties. Lasers have become an indispensable tool for processing of materials in nanoscience and nanotechnology, which is one of the fastest growing areas in research globally. The recent appearance of coherent X-Ray free electron lasers, developments in mega-Joule lasers for laser fusion, remarkable achievements in atto-science and toward generation of single-cycle laser pulses show how the area has expanded from a rather limited area of laser ablation presented in the first COLA conferences 20 years ago. The developments are a wonderful example of how the fundamental discoveries of light interaction with matter led to the technological marvels of the past 50 years, from internet to laser surgery. There are real chances that the multidisciplinary research fields of laser material modification will solve major world problems in energy, information, transport and health.

The purpose of this conference is to present a forum for the discussions and exchange of ideas in various areas of laser transformation of materials. This is the first COLA conference in the Southern Hemisphere and we hope that it will enhance interaction and strengthen links between Australian, New Zealand and many international research groups working in this multidisciplinary field. We hope that students and early career scientists will use the COLA 2015 conference as a chance to network widely with researchers from around the world, with the exposure to the broad diversity of this research field and its potential and opportunities. We also hope it will give our more senior colleagues a chance to catch up with old friends and meet many new ones. Finally, we hope that the conference will be enjoyable, enlightening and fun, with a high-quality program and social events to add to what will be a memorable COLA.

We would like to thank the many Committee members and our professional conference organisers Conference Logistics, who have worked hard to prepare the conference and social events for your enjoyment. We would like to extend our warm welcome to you all, and we hope you enjoy the conference technical and social programs.

Andrei Rode, Chair of COLA 2015

On behalf of the Chairs and co-Chairs:
Koji Sugioka, Hong Bo Sun, Marta Castillejo, Leonid Zhigilei, Saulius Juodkazis, Debora Kane

Committees

Conference Chairs

- Andrei Rode, Australian National University, Canberra, Australia
- Koji Sugioka, RIKEN, Japan
- Hong Bo Sun, Ultrafast Opto-Electronic Technologies, JILIN University, China
- Marta Castillejo, Spanish National Research Council, Spain
- Leonid Zhigilei, University of Virginia, USA

Local Organising Committee

Co-Chairs

- Saulius Juodkazis, Swinburne University of Technology, Melbourne, Australia
- Deb Kane, Macquarie University, Sydney, Australia

Members

- Alexander Fuerbach, Macquarie University, Sydney
- Vincent Daria, JC School of Medical Research, Canberra
- Eugene Gamaly, Laser Physics Centre, Australian National University, Canberra
- Jeff Davis, Centre for Coherent X-ray Science, Melbourne
- Robert Sang, Centre for Attosecond Science, Griffith University, Brisbane
- Trevor Smith, Centre for Coherent X-ray Science, University of Melbourne
- Rongping Wang, Laser Physics Centre, Australian National University, Canberra
- Cather Simpson, The Photon Factory, University of Auckland, New Zealand
- Yvonne Durandet, Industrial Research Institute Swinburne, Melbourne
- Esa Jaatinen, Queensland University of Technology, Brisbane
- David Sampson, University of Western Australia, Perth
- Hoe Tan, Australian National University, Canberra
- Liz Micallef, Australian Centre for Nanoscience and Nanotechnology, Canberra
- Jane Carter, Conference Logistics, Australia

Steering Committee

- S. Amoruso (Univ. Naples, Italy)
- C. B. Arnold (Princeton Univ., USA)
- A.P. Caricato (Univ Salento, Italy)
- M. Farsari (FORTH, Crete, Greece)
- E. G. Gamaly (Australian Nat. Univ., Australia)
- W. Husinsky (Vienna Univ. Technol., Austria)
- J. Lunney (Trinity Coll. Dublin, Ireland)
- T. Makimura (Univ Tsukuba, Japan)

- M. Meunier (Ecole Polytech., Canada)
- Y. Nakata (Osaka Univ., Japan)
- T. Okada (Kyushu Univ., Japan)
- S. Orlando (CNR, ISM Tito Scalo, Italy)
- N. Pryds (Tech. Univ., Denmark)
- T. Sakka (Kyoto Univ, Japan)
- J. Schou (Tech. Univ., Denmark)
- K. Sugioka (RIKEN, Japan)
- O. Uteza (Aix-Marseille Univ., France)
- X. Xu (Purdue Univ., USA)
- T. Yabe (Tokyo Inst. Technol., Japan)
- L. Zhigilei (Univ. Virginia, USA)

Advisory Committee

- C. N. Afonso (CSIC, Inst. Opt. Spain)
- D. Baeuerle (Johannes Kepler Univ. Linz, Austria)
- N. Bityurin (Inst. Appl. Physics, Russia)
- J. T. Dickinson (Washington State Univ., USA)
- M. Dinescu (Natl. Inst. Lasers Plasma & Radiat. Phys., Romania)
- J. J. Dubowski (Univ. Sherbrooke, Canada)
- E. Fogarassy (Univ Strasbourg, France)
- C. Fotakis (FORTH, Greece)
- D. Geohegan (Oak Ridge Natl. Lab., USA)
- R. F. Haglund, Jr (Vanderbilt Univ., USA)
- E. Haro-Poniatowski (Univ Autonoma Metropolitana Iztapalapa, México)
- P. R. Herman (Univ. Toronto, Canada)
- W. P. Hess (Pacific NW Natl. Lab., USA)
- M.H. Hong (Natl. Univ. Singapore)
- H. U. Krebs (Univ. Gottingen, Germany)
- T. Lippert (Paul Scherrer Inst., Switzerland)
- B. Luk'yanchuk (DSI, Singapore)
- W. Marine (Aix-Marseille Univ., France)
- K. Murakami (Univ. Tsukuba, Japan)
- H. Niino (ALPROT, Japan)
- R. E. Russo (Univ. Calif. Berkeley., USA)
- R. Stoian (Univ St Etienne, France)
- M. Stuke (Max Planck Inst. Biophys. Chem., Germany)
- M. Takai (Osaka Univ., Japan)
- A. Vertes (George Washington Univ., USA)
- A. Vogel (Med Univ Lubeck, Germany)
- I. Zergioti (Natl. Tech. Univ. Athens, Greece)

General information

Conference venue

Pullman Cairns International Hotel
17 Abbott Street
Cairns QLD

Phone (+61)7 4031 1300

Conference registration desk

The registration desk is located in the Grand Ballroom foyer and will be open for the duration of the conference to serve as your main point of contact for all conference related enquiries. The registration desk can be contacted throughout the conference on mobile +61 448 357 251.

The registration desk will be open during the following times:

Sunday 30 August	1500–1900
Monday 31 August	0800–2030
Tuesday 1 September	0800–2030
Wednesday 2 September	0800–1300
Thursday 3 September	0830–2030
Friday 4 September	0830–1300

Catering

Morning and afternoon teas and lunches will be held each day in the exhibition. Lunches will be served as an informal stand-up buffet. Dietary requirements noted on your registration have been passed on to the catering staff. Vegetarian options are available within the main catering options. A dedicated table is available for those delegates that advised of other specific dietary requirements. Please ask the catering staff to assist if required.

At the Conference Dinner, dietary meals will be provided as requested on your registration. Please advise the banquet staff of your request.

Exhibition hours

The exhibition will be open as follows:

Sunday 30 August	1730–1900
Monday 31 August	0800–2030
Tuesday 1 September	0800–2030
Wednesday 2 September	0800–1300
Thursday 3 September	0830–2030
Friday 4 September	0830–1100

Internet access

Wi fi will be available free of charge to all conference delegates. Please access the **Pullman Cairns Public server** via your device's settings. You will then need to open your browser and you will be prompted for a unique code. Please enter **COLA2015** to continue.

Lost or found property

Please report any lost or found property to the registration desk.

Medical emergency

In case of an emergency, please contact any staff member of the Pullman Cairns International Hotel or the registration desk staff.

Messages

A message board is situated near the conference registration desk and should be checked regularly. Telephone +61 448 357 251.

Mobile phones and pagers

As a courtesy to other delegates and speakers, please ensure all mobile telephones and pagers are turned off or in 'silent' mode during all sessions and social functions.

Name badges

Your name badge is your entry to all sessions, lunches, morning and afternoon teas and the Welcome Cocktail Reception and should be worn at all times.

Participant list

A participant list was emailed to delegates prior to the conference. Anyone who indicated on their registration form that they did not want their name and organisation to appear on the participant list was not included.

Posters

Posters will be located in the Tully Room. The following scheduled sessions have been allocated:

Poster session 1	Monday 31 August	1830–2030
Poster session 2	Tuesday 1 September	1830–2030
Poster session 3	Thursday 3 September	1830–2030

Poster presenters have been asked to stand beside their poster during these times.

Posters will be available for viewing during each of these days during the breaks. The posters on display will change each day. Please refer to the poster program on page 40 for a detailed listing for each of the three days.

Smoking

Please note that smoking is prohibited in all hotels, clubs, restaurants and workplaces in Queensland, as well as in commercial outdoor eating and drinking areas and in outdoor public places. If you wish to smoke you will need to go outside the Cairns Pullman International Hotel conference venue.

Speakers' preparation area

The speakers' preparation area is located in the Grand Ballroom foyer. Upon arrival at the Conference, all speakers who have not previously emailed their presentation, should take it as soon as possible to the speakers' preparation area. Presentations will then be pre-loaded for the appropriate session room. Speakers may run through their presentations in the speakers' preparation area at their leisure.

All speakers are requested to report to their allocated room 20 minutes prior to the start of the session to meet with the session chair and to check that their presentation has been correctly loaded.

Special requirements

If you have not previously advised the Secretariat of any special dietary or disability requirements, please see the staff at the registration desk as soon as possible.

Taxis

13 10 08

Travel to Cairns Airport

A taxi will cost approximately $25.

Sun Palm Transport operates a shuttle service to the Cairns Airport every hour from 0400 to 2000. Bookings can be made on line at http://www.sunpalmtransport.com.au/ or by phoning +61 7 4099 1191.

Useful contact numbers

Airlines

Qantas	13 13 13
Virgin	13 67 89
Jetstar	13 15 38

Local conference secretariat

Conference Logistics
PO Box 6150 Kingston ACT 2604
T +61 2 6281 6624 F +61 2 6285 1336
E conference@conlog.com.au
W www.conferencelogistics.com.au

Social functions

Welcome reception

Sunday 30 August 2015
1800–1900
Grand Ballroom Foyer, Pullman Cairns International Hotel

Join us in the foyer of the Grand Ballroom for Welcome drinks on the evening before the conference.

Cost: Included in all full registrations only. Day delegates and full delegates wishing to purchase additional tickets may purchase these at a cost of $60 per ticket.

Conference dinner

Wednesday 2 September 2015
1900–2200
Daintree Pool Deck, Pullman Cairns International Hotel

Join us on the Daintree pool deck of the Pullman Cairns International Hotel for a three course meal and beverages.

Cost: Included in all full registrations only. Day delegates and full delegates wishing to purchase additional tickets may purchase these at a cost of $120 per ticket.

Poster sessions

Monday 31 August, Tuesday 1 September and Thursday 3 September
1830–2030
Tully Rooms, Pullman Cairns International Hotel

Poster sessions will be held in the Tully Room of the hotel on the above days. Delegates are encouraged to attend the poster sessions as the posters are an integral part of the conference program. Please note that posters will change each session.

Cost: Tickets to each session are included in all full registrations only. Day delegates and full delegates wishing to purchase additional tickets may purchase these at a cost of $40 per ticket per session.

Please refer to the poster program on page 40 for a detailed listing for each of the three days.

Invited speakers

A/Prof Ariando

Department of Physics & NUSNNI-Nanocore, National University of Singapore

After his post-doctoral fellowship at the NanoNed and University of Twente in the Netherlands, A/Professor Ariando moved to the National University of Singapore (NUS) as an assistant professor at the Department of Physics and NUSNNI-Nanocore Institute in 2008, where he initiated and is leading a research group on advanced functional materials with a research focus on physics and devices of multifunctional oxides and control of oxide interfaces at the atomic level. Currently, he manages a research group including four postdoctoral fellows and 10 PhD students. He has published over 70 refereed research articles, including Nature, Science and PRL, on superconducting, magnetic and new emerging properties at thin films, heterostructures, and interfaces of complex oxides, and filed 5 patents. He has been the pioneer of the oxide interface field in Singapore and contributed various important work in the progress and understanding of the two dimensional electron gas at oxide interfaces and in other field of complex oxides. The work has been highlighted in Nature Physics and selected as Editorial's choice in Science magazine. In recognition of his work, he was awarded the Omicron Medal for Nanotechnology and the Young Scientist Award of Faculty of Science NUS.

A/Prof Yves Bellouard

Ecole Polytechnique Fédérale de Lausanne (EPFL), Switzerland

Dr Yves Bellouard is Associate Professor in Microengineering at Ecole Polytechnique Fédérale de Lausanne (EPFL) in Switzerland, where he heads the Galatea lab and the Richemont Chair in micromanufacturing. He received a BS in Theoretical Physics and a MS in Applied Physics from Université Pierre et Marie Curie in Paris, France in 1994-1995 and a PhD in Microengineering from Ecole Polytechnique Fédérale de Lausanne (EPFL) in Lausanne, Switzerland in 2000. Before joining EPFL in 2015, he hold a faculty position at Eindhoven University of Technologies (TU/e) in the Netherlands, for nearly ten years and prior to that, Research Scientist at Rensselaer Polytechnic Institute (RPI) in Troy, New York for about four years where he started working on femtosecond laser processing of glass materials. His current research interests are on new paradigms for system integration at the microscale and in particular laser-based methods to tailor material properties for achieving higher level of integration in microsystems, like for instance integrating optics, mechanics and fluidics in a single monolith. These approaches open new opportunities for direct-write methods of microsystems (3D printing).

Prof Nadezhda Bulgakova

HiLASE, Institute of Physics ASCR, Chech Republic

Professor Nadezhda M. Bulgakova received her PhD degree in Physics and Mathematics from the Institute of Thermophysics (ITP) SB RAS in 1985 for studies of impacts of space flights and transport aircrafts on chemical content and radiation absorption in ionosphere and stratosphere. In 90th she focused on theoretical studies of laser-matter interaction and from 1997 she leads the Group of Laser Ablation Theory in the ITP. Prof Bulgakova has published more than 150 journal papers, conference proceedings and book chapters in English and Russian. In 2010 she received a Marie Curie International Incoming Fellowship and in 2011 she joined the Optoelectronics Research Centre at the University of Southampton for two years. In 2012 Prof Bulgakova was awarded the Diploma Di Merito and Golden Medal of the European Scientific-Industrial Chamber in recognition of contribution to the theory of laser-matter interaction. Since 2014, she works at the HiLASE Centre of the Institute of Physics AS CR, Czech Republic. Her research interests include processes in solid targets absorbing laser radiation; dynamics of plasma plumes during pulsed laser ablation of solids; cluster formation in free gaseous jets and laser-ablation plumes; plasma-chemical reactions.

Prof Henry Chapman

Centre for Free Electron Laser, DESY, Germany

Professor Henry Chapman is a director of the Center for Free-Electron Laser Science at the Deutsches Elektronen-Synchrotron and the University of Hamburg in Germany. He carried out his PhD in X-ray optics at The University of Melbourne, Australia, work for which he was awarded the Bragg Gold Medal from the Australian Institute of Physics. Henry develops methods in coherent X-ray imaging, which began at Stony Brook University in New York. Later, at Lawrence Livermore National Laboratory in California, he led a team to demonstrate the concept of ‘diffraction before destruction’ where an intense X-ray free-electron laser pulse gives rise to a pristine diffraction pattern of an object before its destruction by that pulse. This solves a serious limitation in X-ray structure determination by increasing the tolerable dose for high-resolution imaging and crystallography by many thousands of times. He led a large international collaboration to extend this work to the atomic scale with the method of serial femtosecond X-ray crystallography, which promises to overcome current bottlenecks in protein structure determination. His current research is focused on developing this method and extending it to the smallest possible crystals: that is, single molecules. In 2015 he was a recipient of the Leibniz Prize from the DFG (German Research Foundation).

Prof Ya Cheng

Shanghai Institute of Optics and Fine Mechanics, Chinese Academy of Science, China

Professor Ya Cheng is a professor of the Shanghai Institute of Optics and Fine Mechanics (SIOM), Chinese Academy of Sciences, and the deputy director of the State Key Laboratory of High Field Laser Physics, SIOM. He received his BS from Fudan University, China, in 1993 and PhD from SIOM in 1998. Since 1995, he has been working in the fields related to ultrafast photonics. His current research interests include femtosecond laser micromachining and ultrafast nonlinear optics. He has published more than 100 papers in peer-reviewed journals and given more than 100 invited talks at international conferences. He is an editor of Laser Micro/Nanoengineering and Chinese Physics Letters and a Fellow of the Institute of Physics, UK.

Prof Jean-Philippe Colombier

Universite Jean Monnet, Saint-Etienne, France

Professor Jean-Philippe Colombier graduated in 2002 from Université de Lyon, France. He was with the Commissariat à l'Energie Atomique and received his PhD degree in 2005 from Université Jean Monnet (France). He is currently assistant professor at Université Jean Monnet, and performs his research activities at Laboratoire Hubert Curien, St-Etienne, France. His interests include theoretical approaches related to ultrafast laser interaction with materials and laser processing.

Prof Alessandro De Giacomo

University of Bari, Italy

Dr Alessandro De Giacomo is a staff research professor of the Chemistry Department of the University of Bari in Italy and an associate researcher of the Institute of Inorganic Methodologies and Plasmas of the National Council of the Researches (IMIP-CNR). He has been carrying out fundamental studies on laser induced plasmas in different applications, spacing from material science to analytical chemistry, which include Plasma Assisted Pulsed Laser Deposition, Laser Spectroscopy, Nanoparticles and carbon nanostructures synthesis by pulsed laser ablation in liquid, and Laser Induced Breakdown Spectroscopy for over sixteen years. At the present he is the head of the laser-matter interaction and laser plasmas joint laboratories of University of Bari and IMIP-CNR, whose activities focus on the production of metal nanoparticles for application in biological sciences and for the development of diagnostic tools for space exploration, cultural heritage and geological applications. In addition to this research activity and the academic work, Dr Alessandro De Giacomo is an active member of scientific committees of international conferences and a member of editorial boards of international journals, as well as a reviewer for several funding agencies in Europe.

Prof Min Gu

Swinburne University of Technology, Australia

Professor Min Gu is a Laureate Fellow of the Australian Research Council as well as is Pro Vice-Chancellor (Research Capacity), Director of the Centre for Micro-Photonics and University Distinguished Professor at Swinburne University of Technology. He is a sole author of two standard reference books and over 800 publications in nano/biophotonics. He is an elected Fellow of the Australian Academy of Science as well as the Australian Academy of Technological Sciences and Engineering. He is also an elected fellow of the Australian Institute of Physics, the Optical Society of America, the International Society for Optical Engineering, the Institute of Physics (UK), and the International Institute of Electric and Electronic Engineers. He was President of the International Society of Optics within Life Sciences, Vice President of the Bureau of the International Commission for Optics, and a Director of the Board of the Optical Society of America. He was awarded the Einstein Professorship of the Chinese Academy of Science, the W. H. (Beattie) Steel Medal of the Australian Optical Society, and the Ian Wark Medal and Lecture of the Australian Academy of Science. He was a Finalist of The 2013 Australian Innovation Challenge Competition.

A/Prof Stephen Madden

Australian National University, Australia

A/Professor Steve Madden currently leads research on Chalcogenide, Tellurite, and polysiloxane integrated optical devices at the Laser Physics Centre, Australian National University. His research career in fibre & integrated optics spans the period from 1984 to the present in start-ups, Multi-nationals, and academia covering a diverse range of areas including Liquid Crystals, seven different materials systems for planar devices, all fibre devices, Hybrid integration, Bragg gratings and devices, planar tunable lasers, optical transmission systems and all optical networking, and non-linear effects in SOAs and planar waveguide devices. The spectrum of work has covered fundamental science through to putting new high technology products into volume production and out onto the market. Most recently a strong focus has been on Mid-infrared photonics and rare earth doped planar waveguides, where notable firsts have been achieved in lasing and gain in tellurite and chalcogenide hosts promising a range of new laser opportunities and applications.

Prof Ion Mihailescu

National Institute for Lasers, Plasma, and Radiation Physics, Romania

Main field: Laser interactions; lasers and plasma physics; nanostructured thin films technology, nanopowders generation and characterisation, surface physics and engineering, laser spectroscopy.

Other fields: Biophysics and biomedicine; nano- bio- technologies, gas- and bio- sensors, plasma and laser theory.

Current research interests: Pulsed laser deposition, modification and characterisation of nanostructured thin coatings; matrix assisted pulsed laser evaporation (MAPLE); laser surface studies and processing; biomaterials thin layers; tissue engineering; biomimetic metallic implants; optoelectronics and sensors.

Prof Masa Murakami

Institute of Laser Engineering, Osaka University, Japan

Professor Masakatsu Murakami (Dr Eng., electrical engineering, Osaka University, Japan, 1988) is Professor of Institute of Laser Engineering (ILE), Osaka University. After he defended Doctor thesis, he worked for three years at Max-Planck-Institute for quantum-optics (MPQ) in Germany on laser-matter interaction and heavy ion fusion physics.

After MPQ, he engaged himself in laser isotope separation for two years at Institute for Laser Technology (ILT) in Japan. Since 1993 he has worked at ILE, Osaka University. He now leads a theoretical group at ILE. The scope of current scientific interests concerns interactions with intense laser and matter, high temperature plasma, laser ion acceleration, hydrodynamic phenomena in astrophysics.

Recently he has proposed 'Nanotube Accelerator' (Physics Today 66, (2013) p.17), to generate MeV-order proton beams. The proton beams thus generated will have a number of future applications are expected, including cancer therapy, compact neutron sources, and ion-driven fast ignition for medicine, industry, and fusion energy, respectively.

Prof Stefan Nolte

Friedrich-Schiller-Universität Jena, Germany

Professor Stefan Nolte is a Professor for Laser Physics at the Friedrich-Schiller-University in Jena, Germany, where he is heading the Ultrafast Optics group at the Institute of Applied Physics. He is also head of Laser Materials Processing at the Fraunhofer IOF, Jena. He studied physics at the University of Hannover, Germany, from where he received his diploma in 1995 and his PhD in 1999 on micromachining with ultrashort laser pulses.

His research topic is the application of ultrashort laser pulses with the main focus on ultrashort pulse micromachining and materials modification for industrial and medical applications, where he has been actively engaged since the field's inception in the mid-1990s. This work has spurred the industrial use of ultrashort pulse lasers in materials processing. Apart from ablation and surface structuring another research focus is the three-dimensional structuring within the volume of transparent materials. This opens the opportunity for realising various photonic devices.

The results of this work are published in more than 250 scientific articles in premier peer-reviewed journals, 10 book contributions as well as in more than 300 invited and contributed conference presentations.

Prof Roberto Osellame

Politecnico di Milano, Italy

Professor Roberto Osellame received the Laurea Degree (cum laude) in electronic engineering from the Politecnico di Milano (Italy) in 1996 and the PhD degree in Physics from the Politecnico di Torino (Italy) in 2000. Since 2001 he is a Staff Researcher of the Institute for Photonics and Nanotechnologies (IFN) of the Italian National Research Council (CNR), where he became Senior Researcher in 2007. From 2001 he is also a Contract Professor at the Politecnico di Milano, teaching Physics in the Faculty of Engineering. His research interests include femtosecond laser micromachining of transparent material for the fabrication of quantum photonic and optofluidic devices. He is author of more than 120 publications on major international journals and holds 4 patents in the field of optics and photonics technologies. He has been awarded the 'Ricerca.tissimi' prize of Regione Lombardia as one of the 20 best researchers in the 'life sciences' field. He has been awarded the CNR prize in 2009 for 'results of particular excellence and strategic national and international relevance'. He is a program committee member in CLEO-Europe and Photonics West international conferences. He has been involved in several European projects and has been the Coordinator of FP7-STREP project 'microFLUID'.

Prof David Villeneuve

Attosecond Science Laboratory, National Research Council, Canada

Professor David Villeneuve obtained a PhD in physics from the University of Waterloo in 1980. After a postdoc at the University of Rochester, he joined the National Research Council in Ottawa. He is currently head of the Attosecond Science Group at NRC, and the NRC head of the Joint Attosecond Science Laboratory (JASLab), a joint undertaking between NRC and the University of Ottawa. He has over 170 publications in refereed journals, is an adjunct professor of physics at the University of Ottawa, and is a Fellow of the Royal Society of Canada, of the American Physical Society and of the Optical Society of America. His interests include the generation of attosecond-duration pulses, soft x-ray coherent imaging, high harmonic spectroscopy, and the study of atoms and molecules in intense laser fields.

Prof Martin Wolf

Fritz-Haber Institut der Max Planck, Germany

Professor Martin Wolf received his PhD there in 1991with Gerhard Ertl for studies on surface photochemistry from Freie Universität Berlin. After a postdoc period in Austin, Texas, with Mike White, he set up a laboratory for femtosecond surface spectroscopy at the Fritz-Haber-Institute of the Max-Planck Society and was also a visiting scientist at IBM Yorktown Heights with Tony Heinz. In 2000 he was appointed full professor for experimental physics at the Freie Universität Berlin. Since 2008 he has been director of the Physical Chemistry department at the Fritz-Haber-Institute in Berlin.

His research focuses on the dynamics of elementary excitations at surfaces, interfaces and in solids, ultrafast photoinduced dynamics and transient electronic structure in correlated materials, interfacial electron transfer, photochemistry and vibrational spectroscopy at interfaces.

Dr Vassilia Zorba

Lawrence Berkeley Lab, USA

Dr Vassilia Zorba is a Staff Scientist and Principal Investigator at the Lawrence Berkley National Laboratory in Berkeley CA, where she also serves as the Deputy Director for the Laser Technologies Group. She received her PhD in 2008 from the University of Crete and the Ultraviolet Laser Facility at IESL-FORTH on femtosecond laser surface structuring technologies and biomimetic material functionalisation.

Dr Zorba's current research focuses on ultrafast laser-material interactions and their use in novel optical far- and near-field laser-ablation based spectroscopic techniques. Her research interests include non-linear optics, laser-induced plasma chemistry, and laser ablation-based chemical analysis in electrochemical energy storage, with emphasis on next-generation Li-ion batteries. Dr Zorba's credits include more than 50 publications in peer-reviewed journals, numerous invited talks and the 2011 R&D 100 Technology Award.

Australian National University

Research School of Physics and Engineering

Sponsor and exhibitor information

Platinum co-sponsors

Australian National University
Research School of Physics and Engineering
and Laser Physics Centre

Australian National University

Australian National University—Research School of Physics and Engineering

The Research School of Physics and Engineering represents Australia's largest university based research and teaching activity in the physics discipline. Hundreds of academics, technical staff and students form the School's greatest asset, its people. This critical mass of researchers is of fundamental importance in fostering the kind of interdisciplinary interactions that create modern research excellence.

The underlying impetus of our research is a belief in the fundamental importance of physics to all of science and technology and the key role physics must play in addressing the challenges facing the modern world. For example in medicine, further development of new procedures, such as positron therapy for cancer treatment, will not be possible without advancing the basic physics that underlies them. The communications revolution that is changing the world is driven by physics, and if progress is to continue, research must harness advances in electronic materials, lasers and optoelectronic devices.

There is no better place to study and research physics than The Research School of Physics and Engineering at The Australian National University.

Prof Tim Senden
Director
Research School of Physical Sciences and Engineering
The Australian National University
Building 60, Mills Road
ANU Campus
Canberra ACT 0200

+61 2 6125 5111 [ph]
director@physics.anu.edu.au
http://physics.anu.edu.au/

Gold sponsor

Agilent Technologies

Agilent Technologies

Agilent is a leader in life sciences, diagnostics and applied chemical markets. Agilent provides laboratories worldwide with instruments, services, consumables, applications and expertise, enabling customers to gain the insights they seek.

The market leading Agilent 7900 ICP-MS offers high sensitivity, fast detection and wide dynamic range makes it perfectly suited to laser ablation analysis of a wide range of samples. With sequence control via ICP-MS Mass Hunter software workstation, LA-ICP-MS is highly flexible and can be used to ablate a single spot for inclusion analysis, 'raster' (moving track) for bulk analysis, or for precise depth profiling studies. Contact us for more details.

Direct solid sampling is beneficial in the analysis of archaeological and forensic samples, and for elemental distribution or zonation studies in geochemistry, bio-imaging and environmental monitoring.

Stewart Carter
Agilent Technologies Australia Pty Ltd
679 Springvale Road
Mulgrave VIC 3170

1800 802 402 [ph]
+61 3 9560 2901 [fx]
Agilent_assist@agilent.com
www.agilent.com/chem

Student and Early Career Researcher Sponsor

Australian Nanotechnology Network

The Nanotechnology field is one of the fastest growing areas of research and technology. The Australian Nanotechnology Network (ANN), is dedicated to substantially enhancing Australia's research outcomes in this important field by promoting effective collaborations, exposing researchers to alternative and complementary approaches from other fields, encouraging forums for postgraduate students and early career researchers, increasing nanotechnology infrastructure, enhancing awareness of existing infrastructure, and promoting industry and international links.

The ANN will achieve these goals through its dedication to bringing together all the various groups working in the field of Nanotechnology and related areas within Australia.

The International Conference on Nanoscience and Nanotechnology is the major forum designed to achieve these goals.

Ms Liz Micallef
Australian Nanotechnology Network
Research School of Physical Sciences and Engineering (Building 60)
The Australian National University
Canberra ACT 0200

+61 2 6125 5952 [ph]
+61 2 6125 3915 [fx]
ann@ausnano.net

Student Presentation Prize Sponsor

Centre for Ultrahigh bandwidth Devices for Optical Systems (CUDOS)

CUDOS is a research consortium between seven Australian Universities and national as well as international collaborators in optical science and photonics technology. Funded by the Australian Research Council under the Centres of Excellence program, CUDOS aims to lead research which creates a world-best on-chip photonic platform for information transfer and processing technologies.

Ms Shelley Martin
CUDOS, School of Physics (A28)
The University of Sydney NSW 2006

+61 2 9351 3979 [ph]
+61 2 9351 7726 [fx]
cudos@physics.usyd.edu.au
www.cudos.com.au

Exhibitors

Coherent Scientific

Coherent Scientific specialises in the supply and support of scientific lasers, spectroscopy systems, microscopes and related equipment. We are the local distributor for highly reputable companies such as Bruker, Coherent Inc, Nikon, Princeton Instruments, and TMC. Coherent Scientific has supported its customers for over 25 years with its highly experienced sales and service personnel located throughout Australia and New Zealand.

Coherent Scientific
116 Sir Donald Bradman Drive
Hilton SA 5033

+61 8 8150 5200 [ph]
sales@coherent.com.au
www.coherent.com.au

Lastek Pty Ltd

Lastek Pty Ltd is a specialist distributor of advanced lasers and laser systems. We have been in this business for over 27 years. We are able to install, service, train, repair systems to a high level as well as design and build custom systems. On our display at COLA we will be presenting several major manufacturers of industrial femtosecond lasers, including Light Conversions of Lithuania.

Alex Stanco
Lastek Pty Ltd
10 Reid Street
Thebarton SA 5031

+61 8 84438668 [ph]
+61 8 84438427 [fx]
alex.stanco@lastek.com.au
www.lastek.com.au

Stratpharma

Stratpharma specialises in products for treating open wounds and preventing abnormal scarring; Including Stratamed®, a silicone-based gel dressing approved for non-epithelialised wounds. Stratamed® is invisible when dry, and can be applied immediately after procedures providing faster re-epithelialisation, and leading to a reduction in inflammation and down time for patients. Stratpharma also produces: Strataderm® treating old/new scars; Stratamark® for prevention/treatment of stretch marks and StrataXRT® for treating radiation dermatitis and burns.

Mignon Furnell
Stratpharma
174 Willoughby Road
Crows Nest NSW 2065

1800 567 007 [ph]
+61 2 9437 0777 [fx]
mfurnell@stratpharma.com
www.stratpharma.com

Floor plan

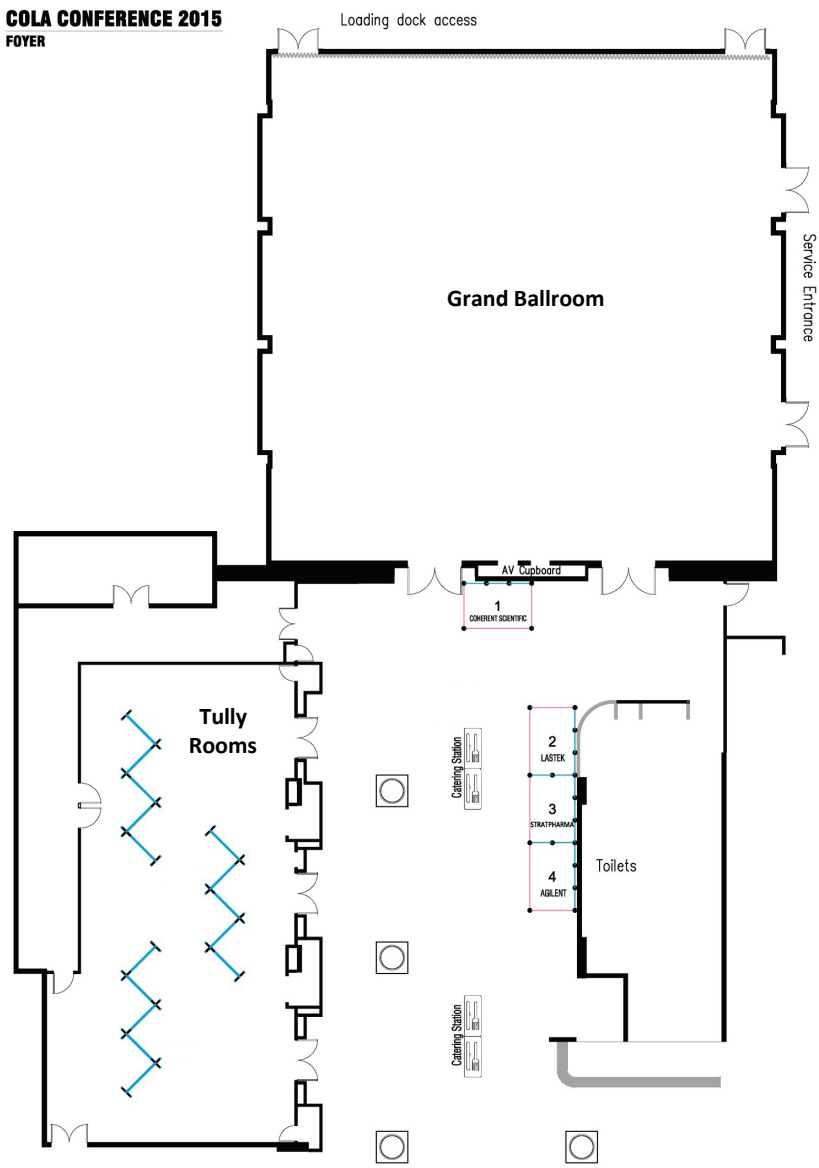
COLA CONFERENCE 2015
FOYER
Loading dock access
Grand Ballroom
Service Entrance
AV Cupboard
1
COHERENT SCIENTIFIC
Tully
Rooms
Catering Station
2
LASTEK
3
STRATPHARMA
4
AGILENT
Toilets
Catering Station

PROGRAM DIVIDER GOES HERE

Program

Sunday, 30 August

1800–1900	WELCOME RECEPTION	Grand Ballroom Foyer Pullman Cairns International Hotel

Monday, 31 August

from 0800		Delegate registration	Grand Ballroom Foyer
0830–1030		**Session 1—Promising New Laser Technologies** Chair: **Prof David Geohegan**, Oak Ridge National Laboratory, USA	Grand Ballroom
0830		Welcome and Opening	
0845	I-01	INVITED **A/Prof Yves Bellouard**, Ecole Polytechnique Fédérale de Lausanne, Switzerland ***Femtosecond laser-induced material modifications to control stress states in silica: a step toward metastable polymorphic phase generation***	
0915	O-01	**Dr Razvan Stoian**, Laboratoire Hubert Curien, CNRS, Université Jean Monnet, France *Spatio-temporal dynamics of non-diffractive ultrafast laser excitation and nanostructuring in bulk silica glass*	
0930	O-02	**Remi Lachaine**, École Polytechnique de Montréal, Canada *Physical mechanisms of bubble formation induced by ultrafast laser irradiation of resonant plasmonic core-shells*	
0945	O-03	**Dr Stefano Orlando**, Institute for Structure of Matter, National Research Council, Italy *Femtosecond Laser texturing of CVD Diamond surface for Solar Conversion Application*	
1000	O-04	**Dr Emmanuel Haro-Poniatowski**, Universidad Autónoma Metropolitana Iztapalapa, Mexico *Synthesis of bismuth-based nanosheets by ultrasound assisted liquid laser ablation*	
1015	O-05	**Dr Tatiana Itina**, Hubert Curien Laboratory, UMR CNRS 5516/Lyon University, France *Ultra-short laser interactions with nanoparticles: from melting and shape change to fragmentation*	
1030–1100		COFFEE BREAK	Grand Ballroom Foyer

1100–1245	**Session 2—Lasers in Nanoscience** Grand Ballroom Chair: **Prof Marta Castillejo**, Instituto de Química Física Rocasolano, CSIC, Spain		
1100	I-02	INVITED **Prof Min Gu**, Swinburne University of Technology, Australia ***Femtosecond laser fabrication for nanophotonics***	
1130	O-06	**Dr Christos Boutopoulos**, École Polytechnique de Montréal, Canada *Mechanism investigations of gold nanoparticle enhanced ultrafast laser near field optical breakdown and nanocavitation*	
1145	O-07	**Tetsuya Shimogaki**, Kyushu University, Japan *Effects of UV-Laser Processing on ZnO Nanocrystals: Controlling the Crystal Growth, Electrical and Optical Properties*	
1200	O-08	**Prof Nikita Bityurin**, Institute of Applied Physics, RAS, Russia *Plasmonic, excitonic and exciton-plasmonic photoinduced nanocomposites*	
1215	O-09	**Prof Xianfan Xu**, Purdue University, USA *Sub-Diffraction-Limit Laser Lithography assisted by Laser-Induced Periodic Surface Structures (LIPSS)*	
1230	O-10	**Dr Yasuhiko Shimotsuma**, Kyoto University, Japan *Self-organization of nanostructures embedded in various materials*	
1245–1400	LUNCH BREAK		Grand Ballroom Foyer
1400–1545	**Session 3—Promising New Laser Technologies** Grand Ballroom Chair: **Prof Michel Meunier**, Polytechnique Montreal, Canada		
1400	I-03	INVITED **Prof Alessandro De Giacomo**, University of Bari, Italy ***Fundamental aspects of Nanoparticles production by laser ablation in liquids***	
1430	O-11	**Dr Marco Ernst**, Australian National University, Australia *Laser welding for handling of thin crystalline Si wafers*	
1445	O-12	**Dr Alexandra Palla-Papavlu**, National Institute for Lasers, Plasma, and Radiation Physics, Romania *Highly sensitive and selective sensor arrays via laser-induced forward transfer*	
1500	O-13	**Dr Richard Russo**, Lawrence Berkeley National Laboratory, USA *Laser Ablation Molecular Isotopic Spectroscopy (LAMIS)*	
1515	O-14	**Dr M Mahjouri-Samani**, Oak Ridge National Laboratory, USA *Controlled Growth of Two-Dimensional Layered Semiconductors from Laser-Synthesized Nanoparticles*	
1530	O-15	**Dr Ricardas Buividas**, Swinburne University of Technology, Australia *Characterisation of femtosecond laser structured cubic-BN*	
1545–1615	COFFEE BREAK		Grand Ballroom Foyer

1615–1800	**Session 4—Promising New Laser Technologies** Grand Ballroom Chair: **Prof Stefan Nolte**, Fraunhofer IOF, Germany	
1615	I-04	INVITED **Prof Martin Wolf**, Fritz Haber Institute of the Max Planck Society, Germany ***Fundamental aspects of laser-matter interaction: Ultrafast dynamics of insulator-to-metal transitions probed by time-resolved photoemission***
1645	O-16	**Dr Elena P Silaeva**, Tokyo University of Science, Japan *Laser-matter interaction in ultra-high DC fields: First-principles calculations*
1700	O-17	**Dr Jian Xu**, RIKEN Center for Advanced Photonics, Japan *Femtosecond laser fabricated electrofluidic devices enabling 3D flexible manipulation and observation of microorganism motions*
1715	O-18	**Prof Michael Withford**, MQ Photonics Research Centre, Australia *3D Integrated Photonics: A new enabling technology for astronomy, telecommunications, sensing and quantum science*
1730	O-19	**Prof Zhisong Xiao**, Beihang University, China *Tuning Dispersion by Controlling Phase Variation in a Ring Resonator Coupled with Mach-Zehnder Interferometer*
1745	O-20	**Dr Maria Isabel Sanchez**, Aix Marseille Université, CNRS, France *Laser induced Forward Transfer for improving fine line metallization in photovoltaic applications*
1830–2030	**Poster Session 1** (see page 40 for details)	Tully Rooms

Tuesday, 1 September

0830–1015	**Session 5—Emerging trends in photoexcitations** Chair: **Prof Martin Wolf**, Fritz-Haber-Institut, Germany		Grand Ballroom
0830	I-05	INVITED **Prof David Villeneuve**, National Research Council, Canada ***High Harmonics and Attosecond Pulses—Seeing Inside Molecules***	
0900	O-21	**Dr Jiri Bulir**, Institute of Physics, ASCR, Czech Republic *Photoluminescence excitation of rare earth doped fluoride films by surface plasmon resonance in the Kretschman configuration*	
0915	O-22	**Nick Cvetojevic**, University of Sydney, Australia *Towards Planet Hunting on a Chip: First Successful On-Telescope Deployment of Integrated 2D-3D Hybrid Photonics using Extreme Adaptive Optics*	
0930	O-23	**Dr Guillaume Duchateau**, Centre Lasers Intenses et Applications (CELIA), France *Laser structuration of dielectric materials by a train of femtosecond pulses through cumulative effects*	
0945	O-24	**Alessandro Maffini**, Politecnico Di Milano, Italy *Laser Cleaning of Pulsed Laser Deposited diagnostic mirrors for nuclear fusion applications*	
1000	O-25	**A/Prof M Cather Simpson**, The University of Auckland, The MacDiarmid Institute for Advanced Materials and Nanotechnology and The Dodd Walls Centre for Quantum and Photonic Technologies, New Zealand *Quantitative Comparison of the Efficiency of Laser Ablation for Bessel, Vortex and Gaussian Beam Shapes*	
1015–1045	COFFEE BREAK		Grand Ballroom Foyer
1045–1230	**Session 6—Lasers in Nanoscience** Chair: **Prof Michael Stuke**, Max-Planck-Institute Goettingen, Germany		Grand Ballroom
1045	I-06	INVITED **Prof Roberto Osellame**, Institute for Photonics and Nanotechnology-CNR, Italy ***Femtosecond laser micromachining for 3D optofluidic devices***	
1115	O-26	**Glen Douglass**, Macquarie University, Australia *Feasibility Study of Femtosecond Laser Written Arrayed Waveguide Gratings*	
1130	O-27	**Dr Michael Lee**, Paul Scherrer Institute, Switzerland *Laser direct-write of complex materials: towards multi-layered micro/nano-structured optoelectronic devices*	
1145	O-28	**Prof Michel Meunier**, Polytechnique Montreal, Canada *Plasmonic nanoparticles enhanced ultrafast laser locally inducing stimulation of hippocampal neurons*	
1200	O-29	**Dr Mitsuhiro Honda**, Institute of Innovative Science and Technology at Tokai University, Japan *ZnO nanostructures prepared through millisecond pulsed laser ablation in liquid*	
1215	O-30	**Prof Anquan Jiang**, Fudan University, China *Temperature dependence of semiconducting BiFeO3 thin films deposited by pulsed laser deposition for resistive memory application*	

1230–1400	LUNCH BREAK		Grand Ballroom Foyer
1400–1545	**Session 7—Pulsed Laser Deposition** Chair: **Prof Nadezhda Bulgakova**, HiLASE Centre, Institute of Physics ASCR, Czech Republic		Grand Ballroom
1400	I-07	INVITED **A/Prof Ariando**, National University of Singapore ***Functional oxide interfaces by pulsed laser deposition***	
1430	O-31	**Shuhei Yada**, Keio University, Japan *Nanostructure formation on PLLA and PLGA by femtosecond laser irradiation*	
1445	O-32	**Prof Martin Ntwaeaborwa**, University of The Free State, South Africa *Cathodoluminescent and photoluminescent properties of pulsed laser deposited thin phosphor films*	
1500	O-33	**Dr Jan Lancok**, Institute of Physics, Academy of Sciences of the Czech Republic, Czech Republic *Fluoride-metals nanostructured films fabricated by Pulsed Laser Deposition with auxiliary Electron beam evaporation*	
1515	O-34	**Prof Ikurou Umezu**, Konan University, Japan *Dynamics of laser ablated colliding plumes in background gas*	
1530	O-35	**Ville Kekkonen**, Picodeon Ltd Oy, Finland *Picosecond pulsed laser deposition of metal and metal-oxide layers with controllable porosity for sensor applications*	
1545–1615	COFFEE BREAK		Grand Ballroom Foyer
1615–1800	**Session 8—Emerging trends in photo-excitations** Chair: **Prof Yves Bellouard**, Ecole Polytechnique Fédérale De Lausanne, Switzerland		Grand Ballroom
1615	I-08	INVITED **Prof Masakatsu Murakami**, Institute of Laser Engineering, Osaka University, Japan ***Proton Beam Generation with Nanotube Accelerator Driven by Ultra-Intense Ultra-Short Laser***	
1645	O-36	**Dr Burkhard Fechner**, Coherent LaserSystems GmbH & Co. KG, Germany *Enabling Laser Applications in Microelectronics Manufacturing*	
1700	O-37	**Dr Philippe Delaporte**, Aix-Marseille University, CNRS, LP3, France *Influence of ink properties on the dynamics of high velocity laser printing*	
1715	O-38	**Amany Gouda**, Department of Physics, Nagoya University, Japan *Formation Mechanism of Periodic Nano-Grating Structure by Weibel Instability*	
1730	O-39	**Andrea Pezzoli**, Politecnico Di Milano, Italy *Pulsed Laser Deposition of tailored Tungsten and Tungsten Oxide films*	
1745	O-40	**Prof Alexander Andreev**, Max Born Institute, Germany *Effective generation of fast particles and X-ray from nano-structured targets irradiated by ultra-short intense laser pulses*	
1830–2030	**Poster Session 2** (see page 44 for details)		Tully Rooms

Wednesday, 2 September

0830–1015	**Session 9—Laser Interactions with Organic and Biological Materials** Chair: **Prof Xianfan Xu**, Purdue Universtiy, USA	Grand Ballroom
0830	I-09	INVITED **Prof Ion Mihailescu**, National Institute for Lasers, Plasma and Radiation Physics, Romania ***Soft pulsed laser technologies for transfer of organic materials***
0900	O-41	**Dr Carmen Ristoscu**, National Institute for Lasers, Plasma and Radiation Physics, Romania *Combinatorial Matrix—Assisted Pulsed Laser Evaporation for fabrication of maps of biomaterials*
0915	O-42	**Dr David McPhail**, Imperial College, United Kingdom *Studies in Laser Cleaning from London Museums Including Some Recent Work Laser Cleaning of PMMA*
0930	O-43	**Dr Anatoliy Vorobyev**, University of Rochester, USA *Biomimetic multifunctional metallic surfaces produced by femtosecond laser*
0945	O-44	**Dr Anna Paola Caricato**, University of Salen, Italy *MAPLE deposition of polymer multilayer structures: overcoming the limitation of solvent-based techniques*
1000	O-45	**Dr Esther Rebollar**, Instituto De Química Física Rocasolano, CSIC, Spain *In situ monitoring of Laser Induced Periodic Surface Structures formation on polymer films by Grazing Incidence Small Angle X-ray*
1015–1045	COFFEE BREAK	Grand Ballroom Foyer
1045–1215	**Session 10—Laser Interactions with Organic and Biological Materials** Chair: **Prof Thomas Lippert**, Paul Scherrer Institut, Switzerland	Grand Ballroom
1045	I-10	INVITED **Prof Henry Chapman**, Center for Free-Electron Laser Science, DESY Synchrotron, Germany ***Diffraction before destruction: Imaging bio-molecules with high-intensity X-ray Free-Electron Laser (XFEL) pulses***
1115	O-46	**Dr Csaba Vass**, University of Szeged, Department of Optics and Quantum Electronics, Hungary *Time-resolved study on periodic microstructure fabrication in polymers*
1130	O-47	**Dr Vincent Daria**, The Australian National University, Australia *Ultrafast laser surgery of dendrites*
1145	O-48	**Prof Michael Ziskind**, Laboratoire De Physique Des Lasers, Atomes Et Mole'cules Laboratoire De Physique, France *Substrate mediated laser ablation and droplet capture for biomolecules analysis by mass spectrometry*
1200	O-49	**Hunjae Jang**, Seoul National University, Korea *Skin ablation for efficient drug delivery via the laser-induced microjet injector*
1215–1300	LUNCH BREAK	Grand Ballroom Foyer
1300–1830	Excursions	
1900–2200	CONFERENCE DINNER	Daintree Pool Deck, Pullman Cairns International Hotel

Thursday, 3 September

0830–1015	**Session 11—Fundamentals of Laser-Material Interactions** Grand Ballroom Chair: **Prof Leonid Zhigilei**, University of Virginia, USA	
0830	I-11	INVITED **Prof Nadezhda Bulgakova**, HiLASE Centre, Institute of Physics AS, Czech Republic ***Numerical modelling of laser interaction with transparent materials: From description to prediction***
0900	O-50	**Prof Juergen Reif**, Brandenburg Tech. University BTU Cottbus-Senftenberg, Germany *Laser Induced Periodic Surface Structures of Thin, Complex Multi-Component Films*
0915	O-51	**Dinithi Namarath**, Queensland University of Technology, Australia *Modelling field propagation with spatially varying light intensity in photorefractive media*
0930	O-52	**Dr Norbert Linz**, University of Luebeck, Institute of Biomedical Optics, Germany *Wavelength dependence of nanosecond IR laser-induced breakdown in water: evidence for multiphoton initiation via an intermediate*
0945	O-53	**Dr Konstantin Khishchenko**, Joint Institute for High Temperatures RAS, Russia *Multiphase equations of state for metals under intense laser influences*
1000	O-54	**Dr Alexey Volkov**, University of Alabama, USA *Non-equilibrium effects in laser-induced plasma plumes*
1015–1045	COFFEE BREAK	Grand Ballroom Foyer
1045–1230	**Session 12—Fundamentals of Laser-Material Interactions** Grand Ballroom Chair: **Dr Richard Russo**, Lawrence Berkeley National Laboratory, USA	
1045	I-12	INVITED **Prof Stefan Nolte**, Friedrich-Schiller-Universität Jena, Germany ***Ultrashort pulse laser processing of transparent materials—potential and applications***
1115	O-55	**Lasse Haahr-Lillevang**, Aarhus University, Denmark *Short-pulse laser excitation of quartz: Experiments and modelling of transient optical properties and ablation*
1130	O-56	**Ayumu Matsumoto**, Kyoto University, Japan *Absorption spectroscopy of atoms in the bubble produced by laser ablation in aqueous solutions*
1145	O-57	**Prof Wolfgang Husinsky**, Technische Universität Wien, Austria *Sub-10fsec to 30 fsec laser ablation: Experimental studies of key features during the first steps of laser ablation around the threshold*
1200	O-58	**Prof Masaki Hashida**, Kyoto University, Japan *Orientation of periodic grating structures controlled by double pulse irradiations*
1215	O-59	**Prof Mishik Kazaryan**, Lebedev Physical Institute of Russian Academy of Sciences, Russia *Laser processing with specially designed laser beam*

1230–1400	LUNCH BREAK		Grand Ballroom Foyer
1400–1545	**Session 13—Pulsed Laser Deposition** Chair: **Dr Razvan Stoian**, Laboratoire Hubert Curien, France		Grand Ballroom
1400	I-13	INVITED **Prof Ya Cheng**, Shanghai Institute of Optics and Fine Mechanics, China ***Nanoscale ablation and 3D structuring in porous glass: mechanism and applications***	
1430	O-60	**Prof Thomas Lippert**, Paul Scherrer Institute, Switzerland *Thin film compositional variations in three distinct pressure regimes during pulsed laser deposition*	
1445	O-61	**Kirill Migdal**, All-Russia Research Institute of Automatics, Russia *Laser-induced spalling of thin metal film from silica substrate followed by inflation of microbump*	
1500	O-62	**Tatsuki Owashi**, Tokai University, Japan *Tin oxide nanostructures prepared by laser ablation in water*	
1515	O-63	**Reece Oosterbeek**, The University of Auckland, New Zealand *Ultrashort pulsed laser ablation threshold dependence on incident wavelength in monocrystalline silicon*	
1530	O-64	**Dr Evgeny Zamburg**, Southern Federal University, Russia *Influence of Plume Parameters on Properties of Nanocrystalline ZnO Films Obtained by Pulsed Laser Deposition*	
1545–1615	COFFEE BREAK		Grand Ballroom Foyer
1615–1800	**Session 14—Pulsed Laser Deposition** Chair: **Prof Deb Kane**, Macquarie University, Australia		Grand Ballroom
1615	I-14	INVITED **Prof Jean-Philippe Colombier**, Laboratoire Hubert Curien, France ***Dynamics of nanostructure formation on metal surfaces induced by ultrashort laser irradiation***	
1645	O-65	**Prof Ovidiu Crisan**, National Institute for Materials Physics, Romania *Interfacial mechanisms and potential applications of novel laser ablated L10-based nanocomposite magnets*	
1700	O-66	**Prof Daniel Bubb**, Rutgers University, USA *The influence of cavitation bubble dynamics and laser fluence on mean particle diameter in laser ablation of metal targets in liquids*	
1715	O-67	**Toshinobu Tanaka**, Graduate School of Information Science and Electrical Engineering, Kyushu University, Japan *Synthesis of Mg-doped ZnO microspheres by laser ablation in air and their crystal and photoluminescence properties*	
1730	O-68	**Dr Johannes Roth**, University Stuttgart, Germany *Molecular Dynamics Simulations of Laser Ablation of Al-Ni alloys and Al-Ni layer systems*	
1745	O-69	**Prof MK Jayaraj**, Cochin University of Science and Technology, India *Enhanced dielectric properties of Bismuth Zinc Niobate-Silver composite thin||films prepared by pulsed laser deposition*	
1830–2030	**Poster Session 3** (see page 49 for details)		Tully Rooms

Friday, 4 September

0830–1015	**Session 15—Laser-Based Analytical Methods** Grand Ballroom Chair: **Dr Koji Sugioka**, Riken, Japan	
0830	I-15	INVITED **Dr Vassilia Zorba**, Lawrence Berkeley National Laboratory, USA ***High-resolution ultrafast laser ablation-based chemical imaging of energy materials***
0900	O-70	**Prof Javier Laserna**, University of Malaga, Spain *LIBS spectroscopy meets the ocean. Chemical analysis of archeological materials in Mediterranean waters*
0915	O-71	**Prof Cristian Focsa**, University of Lille, France *Two-Step Laser Mass Spectrometry (L2MS) analysis of soot particles surface composition: new developments on the VUV single photon*
0930	O-72	**Dr Sebastian Trusso**, Istituto Per I Processi Chimico-Fisici, CNR, Italy *Decoration of silicon nanowires with laser ablated silver nanoparticles for surface-enhanced Raman spectroscopy*
0945	O-73	**Nathan Goodfriend**, University of Edinburgh, United Kingdom *Comparison of fs and ns lasers for Blister-Based Laser-Induced Forward-Transfer*
1000	O-74	**Dr Haizhong Guo**, Institute of Physics, Chinese Academy of Sciences, China *Oxygen vacancies, a crucial role playing on structural, magnetic, and electrical properties of epitaxial manganite thin films*
1015–1045	COFFEE BREAK Grand Ballroom Foyer	
1045–1215	**Session 16—Ultrafast Phenomena and Phase transformations** Chair: **Dr Olivier Uteza**, LP3 – CNRS – AMU, France Grand Ballroom	
1045	I-16	INVITED **A/Prof Stephen Madden**, Australian National University, Australia ***Ultrafast lasers on a chip: Progress towards making the femtosecond world mainstream***
1115	O-75	**Dr Erik Wagenaars**, York Plasma Institute, University of York, United Kingdom *Plasma-Enhanced Pulsed Laser Deposition of metal-oxide films: studying the plasma physics for enhanced process control*
1130	O-76	**Dr Peter Gregorcic**, University of Ljubljana, Slovenia *Resonance effect of the secondary vapor-bubble's oscillations induced by a synchronized delivery of Er:YAG-laser pulses*
1145	O-77	**Dr Rie Tanabe**, Nagaoka University of Technology, Japan *Dynamics of laser-induced cavitation bubble in liquid studied by high-speed stroboscopic videography: Effects of liquid viscosity*
1200	O-78	**Prof Koichi Sasaki**, Hokkaido University, Japan *Dynamics of cavitation bubbles induced by laser ablation in liquid nitrogen at various temperatures*
1215–1300	COLA 2015 Awards and Closing	

Poster program

Monday, 31 August

1830–2030	**Poster Session 1**	Tully Rooms
	Fundamentals of Laser-Material Interactions	
P-001	**Mr Xuewen Wang**, Swinburne University of Technology, Australia *Colour centres in KBr induced by femtosecond laser pulses*	
P-002	**Dr Csaba Vass**, University of Szeged, Department of Optics & Quantum Electronics, Hungary *Study on effects induced by ultrashort laser pulses focused inside transparent materials*	
P-003	**Dr Csaba Vass**, University of Szeged, Department of Optics & Quantum Electronics, Hungary *Two dimensional numerical modeling of TWIN-LIBWE method for interpretation of submicrometer grating fabrication in fused silica*	
P-004	**Dr Olivier Uteza**, Aix Marseille Univ., CNRS, LP3, France *Time-resolved measurement of femtosecond laser energy deposition in fused silica*	
P-005	**Remi Lachaine**, Polytechnique Montréal, Canada *Comparative study of nanoparticle-assisted resonant and non-resonant ultrafast laser nanocavitation*	
P-006	**Prof Haizheng Tao**, Wuhan University of Technology, China *Origin of photoinduced change in optical properties of chalcogenide glass*	
P-007	**Toufik Tamsaout**, Center for Development of Advanced Technologies (CDTA), Algeria *Three-dimensional modelling of laser cutting process with compressible and incompressible assisting gas*	
P-008	**Dr Juan Song**, Jiang Su University, China *The three-level ripples induced by femtosecond laser on a 6H-SiC single crystal and the formation mechanism*	
P-009	**A/Prof Maria Doubenskaia**, Lyon University, Ecole Nationale d'Ingenieurs de Saint-Etienne (ENISE), LTDS Laboratory, France *Integrated analysis of millisecond pulsed laser irradiation of metals by comprehensive optical diagnostics and numerical simulation*	
P-010	**Prof Arvinder Singh**, National Institute of Technology Jalandhar, India *Second Harmonic Generation of q-Gaussian Laser Beam by Localization of Upper Hybrid Wave in Collisionless Plasma*	
P-011	**Prof Nek Shaikh**, Institute of Physics, University of Sindh, Pakistan *Effect of Transverse Magnetic Field on Dynamics of Sn Plasma Produced by CO2 Laser*	

P-012	**Dr Alexander Samokhin**, Prokhorov General Physics Institute, Russian Academy of Sciences, Russia *On different regimes of condensed matter laser ablation: molecular dynamic simulations*
P-013	**Dr Alexander Samokhin**, Prokhorov General Physics Institute, Russian Academy of Sciences, Russia *Laser ablation of absorbing liquids under transparent cover: acoustical and optical monitoring*
P-014	**Dr Mohamad Javad Sobhani**, Iran University of Science and Technology, Iran *Fabrication of 3d microfluidic chanels in PMMA with Nd:YAG laser*
P-015	**Dr Mohamad Javad Sobhani**, Iran University of Science and Technology, Iran *Ns laser fabrication of 2D micro-channels in PMMA followed by wet chemical etching*
P-016	**Dr Smijesh Nadarajan Achary, Prof Reji Philip**, Raman Research Institute, India *Influence of laser pulse width on the ablation of Zinc in nitrogen ambient*
P-017	**Ayumu Matsumoto**, Kyoto University, Japan *Effects of pulse duration on overall temporal behavior of the bubble produced by nanosecond laser ablation in water*
P-018	**Dr Marta Castillejo**, Institute Physical Chemistry 'Rocasolano'—CSIC, Spain *Double Pulse Femtosecond Laser Ablation and Deposition of Co/Zn/S nanostructures*
P-020	**Toufik Tamsaout**, Center for Development of Advanced Technologies (CDTA), Algeria *Optimisation of laser cutting process in relation to the maximum cutting speeds using numerical modelling*
P-022	**Dr Kuo-Cheng Huang**, Instrument Technology Research Center, National Applied Research Laboratories, Taiwan *Section Analysis of Fabric materials Cut Using Ultraviolet Laser Ablation*
P-023	**Prof Dr Alexander Horn**, Laserinstitut Hochschule Mittweida, Germany *Simulation of the spherical aberration by focusing laser radiation in transparent materials: Comparison of different simulation approaches*
P-024	**Dr Arvinder Singh**, National Institute of Technology Jalandhar, India *Excitation of Upper Hybrid Wave by Cross-Focusing of Two Cosh-Gaussian Laser Beams in Preformed Parabolic Plasma Channel*
P-025	**Dr Olivier Uteza**, LP3 – CNRS – AMU, France *Space-time study of microplasmas inside silicon induced by infrared ultrashort laser pulses*
P-026	**Dr Miklós Füle**, Department of Experimental Physics, University of Szeged, Hungary *Structure and surface morphology evolution of amorphous carbon surfaces during transformation by 0.2-20 ps laser pulses*
P-027	**Prof Cristian Focsa**, University of Lille, France *Electrical and optical investigations of plasma plumes generated by femtosecond laser ablation of various metals*

P-028	**Dr Guillaume Duchateau**, Centre Lasers Intenses et Applications (CELIA) / CEA, France *Energy deposition in dielectric materials by few cycles laser pulses*
P-029	**Jason Becker**, CMUXE, School of Nuclear Engineering, Purdue University, USA *Effect of Metal Thermal Properties on LIBS Plasma Emission*
P-030	**Patrick Skrodzki**, CMUXE, School of Nuclear Engineering, Purdue University, USA *Effects of Transverse Magnetic Fields on nanosecond and femtosecond Laser Produced Plasma*
P-031	**Jason Becker**, CMUXE, School of Nuclear Engineering, Purdue University, USA *Improving the conversion efficiency of EUV emission using CO2 reheating of Nd:YAG pre-pulse produced Sn plasma*
P-032	**Dr Wen-Tse Hsiao**, Instrument Technology Research Center, National Applied Research Laboratories, Taiwan *Optical constant of molybdenum film in CuInGaSe solar cell and the estimated ablating temperatures with a moving laser*
P-033	**Prof Marta Castillejo**, Instituto de Química Física Rocasolano, CSIC, Spain *Femtosecond laser ablation plasmas of metals as nonlinear optical media for low order harmonic generation*
P-035	**Chris Baldwin**, Macquarie University, Australia *Nanostructuring of diamond via two photon UV etching at sub-ablation fluences*
	Lasers in Nanoscience—Photonic Fabrication at Nanometer Scale
P-037	**Dr Rosalina Zakaria**, University of Malaya, Malaysia *Laser Annealing of Thin Films using NdYAG laser*
P-039	**Cheng-Yu Shih**, University of Virginia, USA *Molecular dynamics simulation study of femtosecond laser ablation of silver thin films and bulk targets in water environment*
P-040	**Prof Leonid Zhigilei**, University of Virginia, USA *Large-scale atomistic modeling of structural modification of metal surfaces in femtosecond laser processing*
P-041	**Dr Maria Lucia Pace**, CNR – ISM UOS Tito Scalo, Italy *Fs laser pulses for ablation and deposition of noble metal nanoparticles with tunable optical properties*
P-044	**Dr Lebogang Kotsedi**, University of South Africa/iThemba LABS-National Research Foundation, South Africa *Molybdenum thin films interaction with femtosecond laser to form Molybdenum dioxide nanorods*
P-045	**Jeonghong Ha**, Pohang University of Science & Technology, Korea *Plasmonic nanowelding of silver nanowires using a femtosecond laser*
P-046	**Prof Dongsik Kim**, Pohang University of Science & Technology, Korea *Structural transformation of single-walled carbon nanotubes by femtosecond laser irradiation*

P-047	**Prof Wolfgang Husinsky**, Technische Universität Wien, Austria *Influence of the pulse duration on the ablation threshold and the incubation coefficient of copper and silicon upon irradiation by femtosecond laser pulses*
P-048	**Dr Wen-Tse Hsiao**, Instrument Technology Research Center, National Applied Research Laboratories, Taiwan *Surface modification nanoporous titanium oxide films for dye-sensitized solar cell application using Nd:YVO4 and CO2 lasers*
P-049	**A/Prof Ranran Fang**, College of Science, Chongqing University of Posts & Telecommunications, China *Time-resolved microscopy of femtosecond laser-induced surface nanostructures on metal*
P-050	**Dr Won Seok Chang**, Korea Institute of Machinery and Materials, Korea *Design and Fabrication of a Tip-On-Aperture Probe for Resolution Enhancement of Optical Patterning*
P-051	**Dr Won Seok Chang**, Korea Institute of Machinery and Materials, Korea *Fabrication of solution-based electronics using laser selective scanning*
P-052	**Prof Nikita Bityurin**, Institute of Applied Physics, RAS, Russia *Diffusion-assisted laser writing for 3D nanostruturing by means of multiphoton polymerization*
P-053	**Carlos Acosta Zepeda**, Universidad Autónoma Metropolitana, Mexico *Slit diffraction patterning of silicon surfaces by ns-laser irradiation: theory and experiment*
P-054	**A/Prof Yoshiki Nakata**, Institute of Laser Engineering, Osaka University, Japan *Sub-Micron Period Metal Lattices Fabricated by Interfering Ultraviolet Femtosecond Laser Processing*
	Promising New Laser and Optical Technologies
P-055	**Prof Tomasz Tanski**, Institute of Engineering Materials & Biomaterials, Poland *Influence of laser alloying of $AlMg_5Si_2Mn$ on structure and mechanical properties obtained layers*
P-056	**Prof Andrei Rode**, Australian National University, Australia *Mapping laser-induced thermal forces acting on particles in air in a diverging hollow-core vortex beam*
P-057	**Prof Krzysztof Labisz**, Institute of Engineering Materials & Biomaterials, Poland *Ceramic particles feeding in carbon prepared aluminium surface using diode laser*
P-058	**Prof Leonid Zhigilei**, University of Virginia, USA *Strong enhancement of surface diffusion under the action of laser induced nonlinear surface acoustic waves*
P-059	**Chi-Chung Yang**, Instrument Technology Research Center, Taiwan *Hybrid laser cutting technology of Ti-6Al-4V thin sheet using diode-pumped-solid-state ultraviolet laser*

P-060	**Dr Egor Loktionov**, Bauman Moscow State Technical University, Russia *Improvements in combined laser interferometry technique for laser ablation research*
P-061	**Dr Yuji Sato**, Joining & Welding Research Institute, Osaka University, Japan *Investigation of micro structure and surface morphology of Ti64 plate fabricated by vacuum selective laser melting*
P-062	**Dr Maria Lucia Pace**, CNR – ISM UOS Tito Scalo, Italy *Laser ablation parameters as fundamental key factors for controlling the 3D Additive Manufacturing process: considerations*
P-063	**Dr Citlali Sanchez-Ake**, National Autonomous University of Mexico, Mexico *Real-time study of gold nanoparticles formation by pulsed laser annealing*
P-064	**Dr Alexandra Palla-Papavlu**, National Institute for Lasers, Plasma & Radiation Physics, Romania *Fabrication of a lab-on-a-chip device by laser micromachining*
P-065	**Prof David Geohegan**, Oak Ridge National Laboratory, USA *Synthesis of Ultrasmall Nanoparticles by Laser Vaporization as 'Building Blocks' for Nanostructures and Thin Films*
P-067	**Dr Olaf Krueger**, Ferdinand-Braun-Institut, Leibniz-Institut für Höchstfrequenztechnik (FBH), Germany *Precision UV laser scribing for cleaving mirror facets of GaN-based laser diodes*
P-068	**Dr Sayarifah Nur Aqida Syed Ahmad**, University Malaysia, Pahang, Malaysia *Surface modification of AISI H13 tool Steel by laser cladding with NiTi powder*

Tuesday, 1 September

1830–2030	**Poster Session 2**	Tully Rooms
	Promising New Laser and Optical Technologies	
P-069	**Changho Seo**, Department of Mechanical Engineering, POSTECH, Republic of Korea *Removal of 5 nanometer gold particles from solid surfaces by laser-induced spray jet*	
P-070	**Dr Seung-Man Kim**, Korea Institute of Machinery & Materials, Republic of Korea *Laser based edge zone release process for ZoneBOND temporary bonding and debonding*	
P-071	**Dr Jaegu Kim**, Korea Institute Of Machinery And Materials, South Korea *Selective lift-off of GaN LED from sapphire substrate using 266 nm diode-pumped solid-state laser irradiation*	
P-072	**Prof Helena Jelinkova**, Czech Technical University In Prague, Czech Republic *Dysprosium thiogallate laser—source of mid-infrared radiation*	
P-073	**Falko Jahn**, University Of Applied Sciences Mittweida, Germany *Microstructuring of tetrahedral amorphous carbon films (ta-C) using a 248 nm KrF excimer laser*	

P-074	**Dr Peter Gregorcic**, Faculty of Mechanical Engineering, University of Ljubljana, Slovenia *Optimization of laser-pulse energy during selective laser trabeculoplasty by detection of cavitation bubbles formation*
P-075	**Dr Toufik Tamsaout**, Centre De Développement des Technologies Avancées, Algeria *Characterization of titanium oxide layers produced by nanosecond laser irradiation*
P-076	**Dr Mohamad Javad Sobhani**, Iran University of Science and Technology, Tehran, Iran *Characterization and controlling the size and density of polyethersulfone membrane pores with excimer lasers*
P-077	**Prof Dan C. Dumitras**, National Institute for Laser, Plasma & Radiation Physics, Romania *Laser photoacoustic technology for measurement of gas ablation products at sub-ppb level*
P-078	**Robert Donaldson**, Queensland University of Technology, Australia *Creating and utilizing spatially varying light intensity profiles to enhance nonlinear responses*
P-079	**Dr Burkhard Fechner**, Coherent LaserSystems GmbH & Co. KG, Germany *Excimer Laser Assisted Growth of Group IV Alloys*
P-081	**Prof Nikita Bityurin**, Institute of Applied Physics, RAS, Russia *Femtosecond surface nanostructuring by means of colloidal particle lens array*
Pulsed Laser Ablation and Deposition	
P-082	**Kumiko Yokota**, Kobe University, Japan *Laser-detonation facility for acceleration of gaseous materials: Etching and deposition of solid materials*
P-085	**Tei Watanabe**, National Institute of Technology, Anan College, Japan *TiO2 PLD nanocrystalline films supporting Au nanoparticles for application to visible-light-operating plasmonic photocatalysts*
P-086	**Dr Rongping Wang**, Australian National University, Australia *Epitaxial growth of Sc2O3 films on Gd2O3-buffered silicon substrates by Pulsed Laser Deposition*
P-087	**Dr Marco Ernst**, Australian National University, Australia *Nanosecond laser ablation of aluminium-oxide dielectric films for the formation of p-type doped silicon for photovoltaic applications*
P-088	**Takeshi Ueyama**, Graduate School of Information Science & Electrical Engineering, Kyushu University, Japan *Synthesis of ZnO Micro-Spheres by Laser Ablation and Their Application to Refractive Sensor*
P-089	**Eri Ueno**, Hitachi Zosen Corporation, Japan *Numerical analysis of flow field during laser ablation process for formation of Si clusters*

P-090	**Dr Shih-Feng Tseng**, Instrument Technology Research Center, National Applied Research Laboratories, Taiwan *Graphene resistance chip fabricated by ultraviolet laser beams for a high-sensitivity electrochemical impedance spectroscopy*
P-091	**Dr Suwon Kim**, Kyungpook National University *A Study on Laser Joining of Metal and Plastic*
P-093	**Prof Kouichi Takase**, Nihon University, Japan *Vanadium Oxide thin film preparation by PLD for Resistive switching memory In/VOx/Al*
P-094	**A/Prof Masahito Tagawa**, Kobe University, Japan *Property of the hyperthermal CO2 beam formed by a laser-detonation facility for space environmental effect studies in upper Martian*
P-095	**Prof Hendrik Swart**, University of the Free State, South Africa *Luminescence properties of Pulsed Laser Deposited Y2O3:Bi3+ thin films*
P-096	**Yi Sun**, Osaka Institute of Technology, Japan *Flexible Transparent ZnO Thin-Film Transistors by Pulsed Laser Deposition*
P-097	**Dr Sergey Starikov**, Joint Institute for High Temperatures of Russian Academy of Sciences, Russia *Atomistic simulation of surface modification by laser pulse: comparison of models with various scales*
P-098	**Dr Maria Dinescu**, National Institute for Lasers, Plasma and Radiation Physics, Romania *Growth of SrxBa1-xNb2O6 and Ca-doped SrxBa1-xNb2O6 thin films on MgO and Nb:SrTiO3 substrates by PLD and RF-PLD technique*
P-099	**Ville Kekkonen**, Picodeon Ltd Oy, Finland *Picosecond pulsed laser deposition process of porous ceramic coating for Li-ion battery separator film*
P-100	**Dr Jørgen Schou**, DTU Fotonik, Technical University of Denmark, Denmark *Pulsed Laser Deposition of absorber and buffer layer for thin-film earth-abundant solar cells*
P-101	**Dr Maria Dinescu**, INFLPR—National Institute for Laser, Plasma and Radiation Physics, Romania *Small band-gap thin film of doped and pure BiFeO3 obtained by pulsed laser deposition for photovoltaic and photocatalytic applications*
P-102	**Dr Maria Dinescu**, INFLPR—National Institute for Laser, Plasma and Radiation Physics, Romania *Dielectric properties enhancement in epitaxial BCZT thin films with nanoscale strain domains.*
P-103	**Prof Koichi Sasaki**, Hokkaido University, Japan *Spectrum of laser light scattered by nanoparticles in ablation-induced cavitation bubble*
P-104	**Dr Citlali Sanchez-Ake**, National Autonomous University of Mexico, Mexico *NaCl thin films obtained by pulsed laser deposition*
P-105	**Dr Citlali Sanchez-Ake**, National Autonomous University of Mexico, Mexico *A pulsed photo acoustic study of the laser ablation synthesis of Ag nanoparticles in ethanol*

P-106	**Shota Sakaki**, Hokkaido University, Japan *Synthesis of submicrometer-sized spherical particles by laser irradiation in liquid with different laser pulse width*
P-110	**Rongping Wang**, Australian National University, Australia *Growth and Characterization of Y2O3 thin films on Gd2O3 buffered Si substrates using Pulsed Laser Deposition*
P-112	**Owen Bodley**, The University of Auckland / The MacDiarmid Institute for Advanced Materials and Nanotechnology and The Dodd Walls Centre for Quantum and Photonic Technologies, New Zealand *An Apparatus to Control the Spatial Beam Characteristics for Femtosecond Laser Ablation of a Wide Variety of Materials*
P-113	**Rakesh Arul**, The University of Auckland / The Dodd Walls Centre for Quantum and Photonic Technologies and The MacDiarmid Institute for Advanced Materials and Nanotechnology, New Zealand *Laser reduction of graphene oxide to reduced graphene oxide: an experimental and simulated comparison between methods*
P-115	**Thomas Ward**, The University of Auckland / The MacDiarmid Institute for Advanced Materials and Nanotechnology and The Dodd Walls Centre for Quantum and Photonic Technologies, New Zealand *Optimisation of femtosecond laser ablation parameters for efficient cutting of sintered alumina wafers*
P-116	**Zhiwei Han**, The University of Auckland / The MacDiarmid Institute for Advanced Materials and Nanotechnology and The Dodd Walls Centre for Quantum and Photonic Technologies, New Zealand *Femtosecond laser cutting speed optimization for single crystal quartz wafers*
P-117	**Satoshi Ohmuro**, Graduate School of Science and Technology, Nihon University, Nihon *Effect of applied electric field in Pulsed Laser Deposition*
P-118	**A/Prof Tomomas Ohkubo**, Tokyo University of Technology, Japan *Numerical Simulation of Laser Processing of Carbon Fiber Reinforced Plastics Including Combustion Effect*
P-119	**Dr Michal Novotny**, Institute of Physics, Academy of Sciences of the Czech Republic, Czech Republic *The properties of rare-earth doped zinc oxide/phthalocyanine structures for optoelectronics*
P-120	**Dr Takahiro Nakamura**, Institute of Multidisciplinary Research for Advanced Materials, Tohoku University, Japan *Formation of Diamond-Like Carbon Thin Films by Femtosecond Laser Ablation of a Frozen Cyclohexane Target*
P-121	**J.J. Naddeo & Matt Ratti**, Rutgers University, USA *Light Induced Toxicity of Silver Nanoparticles Produced by Laser Ablation in Liquid*
P-123	**Prof Dermot Brabazon**, Dublin City University, Ireland *Confined atmospheric pulsed laser deposition of nanostructured ultrathin films*

P-124	**Dr Andreea Matei**, National Institute for Lasers Plasma & Radiation Physics, Romania *PLD of layered double hydroxides for hydrophobic coatings*
P-125	**Dr Andreea Matei**, National Institute for Lasers Plasma & Radiation Physics, Romania *Thin films of ferrocene derivatives for non-linear optical applications: laser processed thin films and printed pixels*
P-126	**Yong-Won Ma**, Pusan National University, Republic of Korea *Fabrication of Polyimide Spheres by Pulsed Laser at 355 nm*
P-127	**Dr Antonella Lorusso**, Department of Mathematics and Physics 'E. De Giorgi', Italy *Structural and morphological properties of metallic thin films grown by pulsed laser deposition for photocathode application*
P-128	**Prof Jingquan Lin**, Changchun University of Science & Technology, China *Systematic investigation of plasma shock evolution from Al target induced by nanosecond Nd:YAG laser ablation*
P-129	**Dr Zhibin Lin**, Electro Scientific Industries, USA *Experimental and Numerical Studies of Nanosecond Laser Processing for Industrial Micromachining Applications*
P-131	**Dr Ok Sik Kim**, Laser Application Center, South Korea *Laser ablation of CFRP by using picosecond laser and femtosecond laser*
P-132	**Prof Mishik Kazaryan**, Lebedev Physical Institute of Russian Academy of Sciences, Russia *Printing and surface patterning in liquids by laser and ultrasound ablation*
P-133	**Prof Deb Kane**, Macquarie University, Australia *Laser removal of a coating from glass slides of consolidant materials relevant to museum conservation practice*
P-134	**Mr Ryota Kajimoto**, Osaka Institute of Technology, Japan *Preparation of visible-light-responsive titanium oxide by laser ablation in liquid*
P-135	**Prof Miroslav Jelinek**, Institute of Physics ASCR, Czech Republic *Bonds and bio- properties of hybrid laser Cr- doped DLC for implants*
P-136	**Prof Miroslav Jelinek**, Institute of Physics ASCR, Czech Republic *Thermoelectric YbCoSb Laser Prepared Layers*
P-137	**Prof Miroslav Jelinek**, Institute of Physics ASCR, Czech Republic *Scanning thermal microscopy: Characterization of PLD films*
P-138	**Ryuchi Ishihara**, Nihon-University, Japan *Synthesis of Rod-Shaped Iron Nanocrystals Using Blue Laser-Assisted Pulsed-Laser Ablation in Liquid*
P-139	**Dr Kuo-Cheng Huang**, Instrument Technology Research Center, National Applied Research Laboratories, Taiwan *Planar Square-spiral Inductor Generated from the ITO Film Removal by Using UV Laser Ablation*

Thursday, 3 September 2015

1830–2030	**Poster Session 3**	Tully Rooms
	Pulsed Laser Ablation and Deposition	
P-140	**A/Prof Yasutaka Hanada**, Hirosaki University, Japan *Microfabrication of UV transparent fluoric polymer CYTOP using a conventional pulsed green laser*	
P-141	**Young-Joon Han**, Australian National University, Australia *Low temperature micro-photoluminescence spectroscopy on laser doped silicon with different surface condition*	
P-142	**Dr Taeho Ha**, Korea Institute of Machinery & Materials, Republic of Korea *Prototype of Mini-size Er:YAG Laser Skin Perforator*	
P-143	**Dr Peter Gregorcic**, Faculty of Mechanical Engineering, University of Ljubljana, Slovenia *Photodisruption of the elastic membrane with the laser-induced cavitation bubble dynamics: an optodynamic study*	
P-144	**Nathan Goodfriend**, University of Edinburgh, United Kingdom *Blister-based nanosecond laser-induced forward transfer of large molecules and nanoparticles for gas-phase analysis*	
P-145	**Gabriela Gomes**, Centro Brasileiro de Pesquisas Físicas, Brazil *Crystalline hydroxyapatite thin coatings produced by Nd:YAG 532nm Pulsed Laser Deposition at room temperature*	
P-146	**Dr Florent Bourquard**, Laboratoire Hubert Curien, France *Textured graphene synthesis by pulsed laser ablation for surface-enhanced Raman scattering*	
P-147	**Rongping Wang**, Australian National University, Australia *Laser ablation of ZnS nanoparticles in liquids*	
P-148	**Emily Foka**, University of The Free State, South Africa *Effect of substrate temperature on structure and luminescence properties of YVO4:Eu thin films grown by PLD*	
P-149	**Prof Cristian Focsa**, University of Lille, France *Rare earth doped cobalt ferrite thin films grown by PLD: influence of the deposition conditions*	
P-150	**Dr Maria Dinescu**, National Institute for Lasers, Plasma & Radiation Physics, Romania *Tailoring the physical properties of plasma mirrors antireflection coatings*	
P-151	**Dr Luis Escobar-Alarcon**, Instituto Nacional De Investigaciones Nucleares, Mexico *Preparation of vanadium oxide thin films modified with Ag using an hybrid deposition configuration*	
P-152	**Prof Francis Dejene**, University of The Free State, South Africa *Characterization of structural and luminescence properties of blue-green SrAlxOy:Eu2+, Dy3+ thin films deposited by PLD system*	
P-153	**Prof Francis Dejene**, University of The Free State, South Africa *Structural and luminescence properties of yellow Y3Al5012:Ce3+, thin film phosphors prepared by Pulsed Laser Deposition*	

P-157	**Prof Marta Castillejo**, Instituto de Química Física Rocasolano, CSIC, Spain *Pulsed Laser Deposition and Characterization of Single Crystal Cobalt Ferrite Films with Biphase Composition*
P-158	**Dr Anna Paola Caricato**, Department of Mathematics and Physics 'E. De Giorgi', University of Salen, Italy *Decoration of silica nanowires forests with Au nanoparticles by PLD*
P-160	**Dr Florent Bourquard**, Laboratoire Hubert Curien, France *Nitrogen plasma assisted Femtosecond Pulsed Laser Deposition of a-C:N films for environmental analytical microsystems and in situ plume analysis*
P-162	**Stefano Orlando**, CNR-ISM, Italy *ZnSb-based thermoelectric thin films by PLD and combined PLD-sputtering system*
P-163	**Abdub Ali**, University of The Free State, South Africa *The effect of different species of gases on material properties of Eu3+ doped Y2O2S thin films phosphor deposited by Pulsed Laser*
P-164	**Abdub Ali**, University of The Free State, South Africa *Effect of annealing temperature on structural and luminescence properties of Eu3+ -doped Y2O3 red phosphor thin films by PLD method.*
P-168	**Dr Olivier Uteza**, University Aix-Marseille, France *Control and optimization of an energetic sub-picosecond laser-driven hard x-ray K-alpha source with a high pulse repetition rate*
P-169	**Prof Andrei Rode**, Australian National University, Australia *New High-Pressure Silicon Phases Formed in Fs-Laser Induced Confined Microexplosion*
Laser Interactions with Organic and Biological Materials	
P-171	**Prof Jack J. Yoh**, Seoul National University, Korea *Thermal effects on the rapid bubble growth in the laser-induced microjet injector for transdermal drug delivery*
P-172	**Dr Akimichi Shibata**, Keio University, Japan *Biodegradability of poly(lactic-co-glycolic acid) after irradiation of femtosecond laser pulses*
P-173	**Dr Jørgen Schou**, DTU Fotonik, Technical University of Denmark, Denmark *Thin film production from a compressible organic target by laser irradiation: from material destruction at high target pressure to material*
P-174	**Dr Yuji Sato**, Joining & Welding Research Institute, Osaka University, Japan *Femtosecond laser induced periodic nano-structure on PET surface for controlling of cell elongation*
P-176	**Dr Esther Rebollar**, Instituto De Química Física Rocasolano, CSIC, Spain *Simultaneous laser induced periodic nanostructuring and diffraction-assisted micropatterning of thin polymer films*
P-177	**Simon Ashforth**, The University of Auckland / The MacDiarmid Institute for Advanced Materials & Nanotechnology and The Dodd Walls Centre for Quantum & Photonic Technologies, New Zealand *Ultrashort laser ablation of load bearing and skull cortical bone tissue: A comparative study*
P-179	**Dr Egor Loktionov**, Bauman Moscow State Technical University, Russia *Laser ablation of UV curing polymer and compositions*

P-180	**Takuya Kawa**, Graduate School of Engineering, Osaka University, Japan *Periodic Nanostructures Produced on Ti Substrate with Femtosecond Laser for Controlling of Cell Spreading in Multi Direction*
P-181	**Dr Miklos Füle**, High Intensity Laser Laboratory, Department of Exp. Physics, University of Szeged, Hungary *The influence of pulse duration, wavelength and fluence on laser induced structure formation from the viewpoint of dental applications*
P-182	**Dr Premysl Fitl**, University of Chemical Technology Prague, Czech Republic *Patterning of organic semiconductors for photovoltaic applications by LIFT technology*
P-183	**Dr Valentina Dinca**, National Institute for Lasers, Plasma & Radiation Physics, Romania *Human mesenchymal stem cells interaction with nano and microtextured surfaces*
P-184	**Dr Valentina Dinca**, National Institute for Lasers, Plasma & Radiation Physics, Romania *Sericin-tethered graphene artificial composite matrix obtained by MAPLE for MC3T3-E1 pre-osteoblasts studies*
P-185	**Prof Nikita Bityurin**, Institute of Applied Physics, RAS, Russia *Indirect laser surgery*
P-186	**Dr Koji Sugioka**, RIKEN Center for Advanced Photonics, Japan *Hybrid subtractive and additive 3D microprocessing using femtosecond laser for functional biochip fabrication*
Laser-Based Analytical Methods	
P-187	**A/Prof Michael Ziskind**, Laboratoire De Physique Des Lasers, Atomes Et Mole'cules Laboratoire De Physique, France *Development of a real time mass spectrometry instrument for non-invasive ex-vivo and in-vivo analysis based on IR laser ablation*
P-188	**Dr Syarifah Aqida**, Universiti Malaysia Pahang, Malaysia *Interfacial Indentation Test of Laser Surface Modified AISI H13 tool steel thermal barrier coatings*
P-189	**Dr Sung Hyun Pyun**, Korea Institute of Machinery & Materials, South Korea *Laser induced breakdown spectroscopy for in situ elemental analysis of deep sea minerals*
P-190	**Dr Cristina Popa (Achim)**, National Institute for Laser, Plasma and Radiation Physic/University Politehnica, Romania *Laser spectroscopy for noninvasive gas monitoring in patients with dysfunctions*
P-191	**Aparna Neettiyath**, Indian Institute of Technology Madras, India *Analysis of copper sulfide contaminant in solid transformer insulation using vacuum ultraviolet laser induced breakdown spectroscopy*
P-193	**Dr Peter Gregorcic**, Faculty of Mechanical Engineering, University of Ljubljana, Slovenia *Laser-induced breakdown spectroscopy and shadowgraphic analysis of selective thin-layers removal by laser ablation*

P-194	**Patrick Skrodzki**, CMUXE, School of Nuclear Engineering, Purdue University, USA *Role of Material Properties on Signal Enhancement in Nd:YAG-CO2 DPLIBS*
P-195	**Dr Burkhard Fechner**, Coherent LaserSystems GmbH & Co. KG, Germany *Laser Ablation Sampling at Ultrashort Wavelength*
P-196	**Dr Alessandro De Giacomo**, University of Bari, Italy *Nanoparticles Enhanced Laser Induced Breakdown Spectroscopy: applying nanoparticle to LIBS*
P-197	**Prof Dan Dumitras**, National Institute for Laser, Plasma & Radiation Physics, Laser Department, Romania *Spectroscopic analysis of the breath from subjects with type 2 diabetes*
P-198	**Dr Soo-Jin Choi**, Seoul National University, Korea *Advanced experimental design for simultaneous acquisition of laser induced plasma and Raman signals*
P-199	**Prof Nilesh Vasa**, Indian Institute of Technology Madras, India *Suitability of laser-induced breakdown spectroscopy in screening potential additives to mitigate fouling deposits*
P-200	**Dr Valentin Serban Teodorescu**, National Institute For Materials Physics, Romania *Fast atomic diffusion in solid state amorphous thin films irradiated with low fluence laser pulse in UV*
Ultrafast Phenomena and Phase Transformations	
P-203	**Kirill Migdal**, All-Russia Research Institute of Automatics, Russia *Thermodynamics and Kinetics of d-Metals in Two-Temperature States*
P-204	**Dr Masayuki Kakehata**, National Institute of Advanced Industrial Science & Technology (AIST), Japan *Cross-sectional image of femtosecond laser-induced periodic surface structures on yttria-stabilized zirconia*
P-205	**Kirill Migdal**, Landau Institute For Theoretical Physics, Russia *Dynamics of gold and silver films initiated by femtosecond laser pulse*
P-206	**Prof Alexander Horn**, Laserinstitut Hochschule Mittweida, Germany *Case study on the ultrafast laser ablation of thin aluminium films: dependence on laser parameters and film thickness*
P-207	**Dr Antonio Santagata**, CNR – ISM UOS Tito Scalo, Italy *Investigations about oligothiophene donor-acceptors systems*
P-208	**Dr Benoit Chimier**, Université de Bordeaux, France *Hydrodynamic simulation of aluminum target surface irradiated by a femtosecond laser pulse*
P-209	**Atia Tul Noor**, Griffith University, Australia *Dissociative double ionization of acetylene in strong laser field*

COLA-2015

Program

Monday
31 August 2015

Oral presentations

I-01

Femtosecond laser-induced material modifications to control stress states in silica: a step toward metastable polymorphic phase generation

Yves Bellouard
Galatea Lab, STI/IMT, Ecole Polytechnique Fédérale de Lausanne (EPFL)
Rue de la Maladière 71b, Case postale 526, CH - 2002 Neuchâtel Switzerland
yves.bellouard@epfl.ch

1. Summary

Femtosecond laser exposure of silica in the non-ablative regime induces localized volume changes resulting in a stress-field surrounding laser affected zones. Here, we review these effects and illustrate potential applications of laser-induced controlled stress-state in silica, and in particular, we explore its use for the control and localized generation of metastable polymorphic phases of silica.

2. Tunable stress-state during non-ablative exposure of silica

Non-ablative femtosecond laser pulses applied on fused silica induce mainly two types of modifications: homogeneous modifications and self-organized nanogratings [1,2]. Noteworthy, a localized net volume expansion is associated with the occurrence of self-organized nanogratings [3] which orientation affects stress distribution [4]. For shorter pulses (< 200 fs) and low-energy – corresponding to the regime of homogeneous modifications, densification is observed [5]. The laser pulse duration can therefore be used to introduce either tensile and compressive stress, which intensity and direction can be fine-tuned by controlling the pulse energy and the laser polarization.

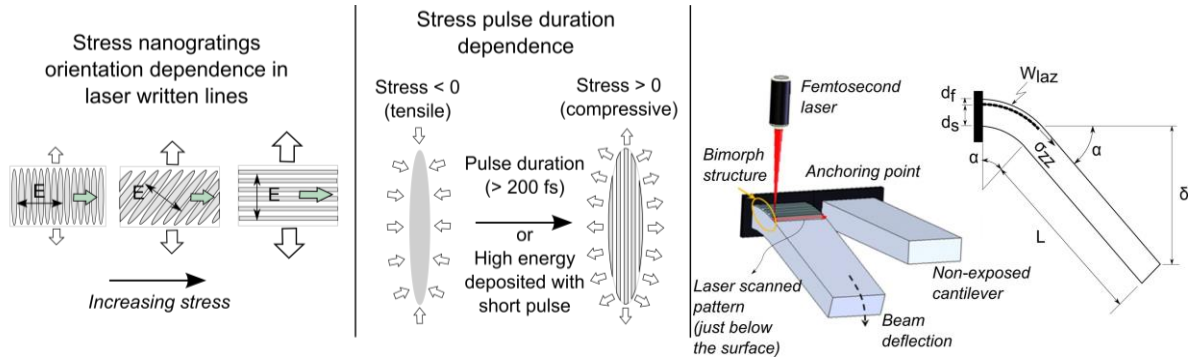

Fig. 1 Left: Illustration of the effect of nanogratings orientation in laser-written line on stress intensity [4]. The maximum intensity is found for nanogratings perpendicular to the writing direction. Middle: stress-state inversion by switching between the continuous modification regime to the regime where nanogratings forms [3,5]. Right: mechanical method based on micro-machined cantilever for measuring quantitatively volume expansion resulting from laser exposure in the non-ablative regime [3].

3. Effect on micromachining, applications of laser-induced stress

The ability to control stress state as illustrated above have practical consequences on the laser exposure process but also interesting applications. As a direct consequence, the stress generated during laser exposure can lead to path-dependent machining if the stress introduced in the material is sufficiently high to induce elastically irreversible transformations, can be used to create controlled stress state (see for instance [6]) and offers a path for high-pressure phase generation in silica. The later has a high innovation technological potential in the field of highly integrated microsystems and more generally for better understanding the formation of high pressure phases in silica which is of particular interest for Earth sciences.

4. References

[1] K. M. Davis, K. Miura, N. Sugimoto, and K. Hirao, "Writing waveguides in glass with a femtosecond laser," Opt. Lett. 21, 1729–1731 (1996).
[2] Y. Shimotsuma, P. G. Kazansky, J. Qiu, and K. Hirao, "Self-Organized Nanogratings in Glass Irradiated by Ultrashort Light Pulses," Phys. Rev. Lett. 91, 247405 (2003).
[3] A. Champion and Y. Bellouard, "Direct volume variation measurements in fused silica specimens exposed to femtosecond laser," Opt. Mater. Express 2, 789–798 (2012).
[4] A. Champion, M. Beresna, P. Kazansky, and Y. Bellouard, "Stress distribution around femtosecond laser affected zones: effect of nanogratings orientation," Opt. Express 21, 24942–24951 (2013).
[5] Y. Bellouard, T. Colomb, C. Depeursinge, M. Dugan, A. A. Said, and P. Bado, "Nanoindentation and birefringence measurements on fused silica specimen exposed to low-energy femtosecond pulses," Opt. Express 14, 8360–8366 (2006).
[6] B. McMillen and Y. Bellouard, "On the anisotropy of stress-distribution induced in glasses and crystals by non-ablative femtosecond laser exposure," Optics Express 23, 86–100 (2015).

O-01

Spatio-temporal dynamics of non-diffractive ultrafast laser excitation and nanostructuring in bulk silica glass

P. K. Velpula, M. K. Bhuyan, J. P. Colombier, and R. Stoian
Laboratoire Hubert Curien, UMR 5516 CNRS, Université de Lyon, Université Jean Monnet, 42000 Saint Etienne
razvan.stoian@univ-st-etienne.fr

Ultrafast laser volume interaction with transparent materials can achieve localized structural transformations and embedded changes of the dielectric function. Matter compaction or rarefaction can be determined by material properties, its thermal history or the level of the energy deposition, having strong influence on the fabrication quality and accuracy in 3D laser-material processing.

Employing non-diffractive nonlinear ultrafast Bessel optical beams with quasi-stationary characteristics allows remarkable potential for energy localization beyond the diffraction limit. The ability to maintain near-constant intensity profiles over an appreciable distance along the propagation direction, sustaining nonlinear absorption, recommends non-diffractive concepts for high aspect ratio submicron structuring applications. Furthermore, in the presence of nonlinear propagation, the material response can be critically determined by the pulse temporal envelope, impacting on photo-inscription regimes, i.e. formation of various types of refractive index structures. If smooth positive index structures can be produced for ultrashort exposure, one-dimensional void structures are obtained for tailored dispersion-engineered pulses, highlighting the important contribution of delayed ionization and light diffusion on excited carriers. Nonlinear simulations confirm the different energy balance driven by the pulse envelope. Thus photoionization mechanisms can be synchronized and self-limiting effects in carrier plasmas can be overcome leading to an unprecedented localization of laser energy on scales well below the incident wavelength, and the laser pulse duration becomes key in deciding the type and morphology of the structures. To understand the formation mechanisms, we specifically follow the characteristic dynamics of electronic excitation and relaxation in confinement conditions and point out particular times of energy deposition, serving as guidelines for time control. Fast electronically-induced structural changes or slower thermodynamic transformations can thus be discriminated. Space- and time-resolved absorption and phase contrast microscopy reveals two main carrier relaxation paths, triggering specific structural and morphological changes of the silica matrix. Fast exciton self-trapping in self-induced matrix deformations results in soft positive index contrast linear traces driven by a swift accumulation of non-bridging oxygen hole centers, a defect marker of this regime. High excitation densities determine a thermomechanical path for the induced modification, visible in the onset of phase-like transition towards low-viscosity states and the release of pressure waves. Nanosized embedded channels are thus created via rarefaction and liquid cavitation, accompanied by the decomposition of the silica matrix, release of oxygen and generation of oxygen deficiency centers. Temporal pulse dispersion engineering allows thus driving unique carrier dynamics and offers precise control over energy deposition down to the 100 nm nanoscale. Extreme high-aspect-ratio uniform void structures can thus be fabricated in conditions of sub-micron transverse light confinement

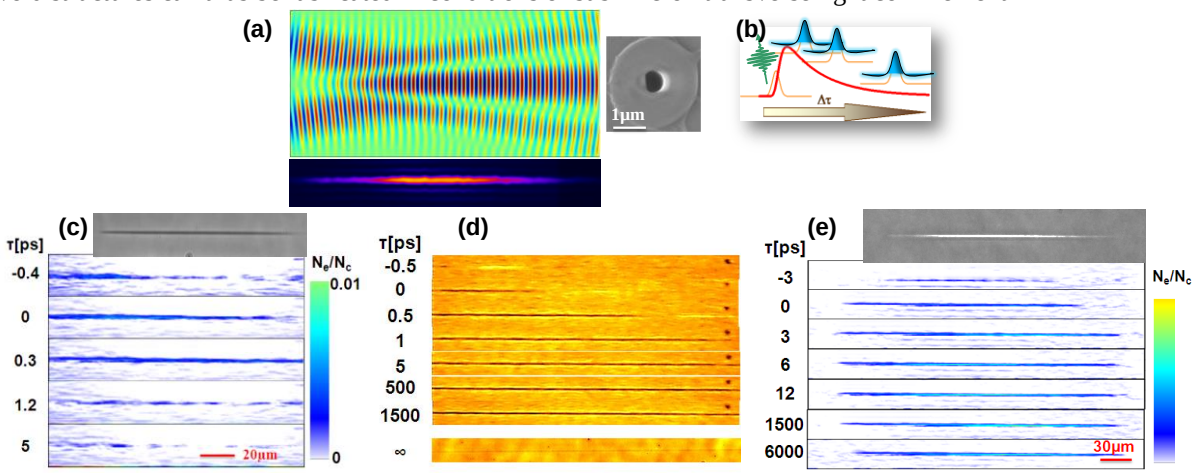

Fig. 1. (a) Example of ultrafast Bessel beam nanostructuring. (b) Concept of time-resolved investigations. (c,d) Fast absorption electronic and phase shifting excitonic effects in positive refractive index change structures observed time time-resolve transmission and phase contrast microscopy. (e) Slow electronic decay for conditions of excitation above the cavitation threshold.

[1] K. Mishchik, C. d'Amico, P. K. Velpula, C. Mauclair, Y Ouerdane, A. Boukenter, and R. Stoian "Ultrafast laser-induced electronic and structural modifications in bulk fused silica" J. Appl. Phys. **114**, 133502 (2013).

[2] M. Bhuyan, P. K. Velpula, J. P. Colombier, T. Olivier, N. Faure, and R. Stoian "Single shot high aspect ratio bulk nanostructuring of fused silica using chirp controlled ultrafast laser Bessel beams" Appl. Phys. Lett. **104**, 021107 (2013).

O-02

Physical mechanisms of bubble formation induced by ultrafast laser irradiation of resonant plasmonic core-shells

R. Lachaine[1], P.Y. Lajoie[1], C. Boutopoulos[1,2], E. Boulais[3], M. Meunier[1]

[1]*Department of Engineering Physic, Laser Processing and Plasmonics Laboratory, École Polytechnique de Montréal, 2500 Chemin de Polytechnique, Montréal, Québec, H3T 1J4*

[2]*SUPA, School of Physics and Astronomy, University of St. Andrews, North Haugh, St. Andrews, KY16 9SS, UK*

[3]*Massachusetts Institute of Technology, Department of Biological Engineering, 77 Massachusetts Avenue, Cambridge, MA, USA 02139*

E-mail: remi.lachaine@polymtl.ca

The generation of bubbles around plasmonic nanoparticles has drawn lots of attention in the past decade. The use of nanoparticles to locally produce bubbles finds many applications in the biomedical field such as nanosurgery and cell transfection [1].

In previous work, we have shown that micron-size bubbles can be generated by irradiating off-resonance gold nanoparticles (NPs) with near infrared ultrafast laser pulses [2]. We demonstrated that cavitation is controlled by the production of nanoplasma in the vinicity of the NPs rather than by the heating of the particle. Producing these bubbles require peak laser fluences above 150mJ/cm^2, which is high enough to hinder some biomedical applications. Using resonant silica/gold core-shell nanoparticles (CSs) enable reducing the cavitation threshold, owing to the wide tunability of their plasmon resonance.

In this work, we use CSs to produce micron-size bubbles with peak fluences around 15mJ/cm^2, about 10 times lower than with NPs, while avoiding the complete CSs explosion. A complete study of the CSs damages have been performed using TEM and in-situ spectroscopy. We found the existence of three damaging regimes in which the CSs are subsequently cracked, melted and completely degraded (Figure 1).

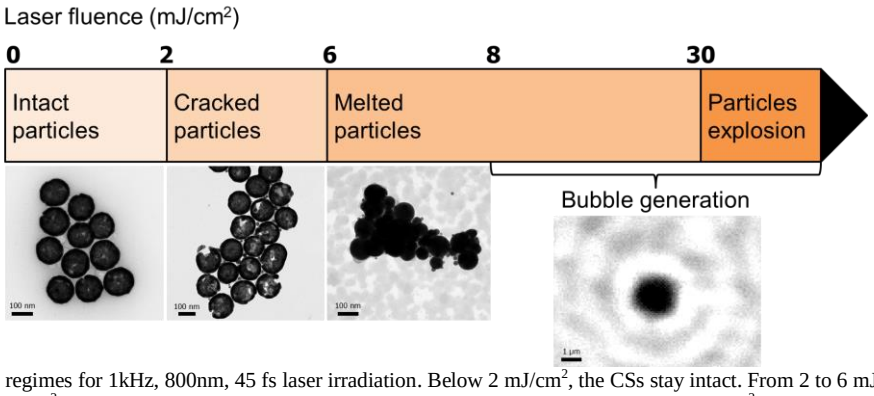

Fig. 1. CSs damaging regimes for 1kHz, 800nm, 45 fs laser irradiation. Below 2 mJ/cm^2, the CSs stay intact. From 2 to 6 mJ/cm^2, they crack open. From 6 to 30 mJ/cm^2, CSs melt into spherical NPs. Bubbles are generated for fluences above 8 mJ/cm^2. Finally, the CSs explode for fluence higher than 30 mJ/cm^2.

We then characterized the bubble generation using scattering pump-probe technique and shadowgraphy imaging, focusing on the physical mechanisms leading to the bubble formation. Bubbles can arise from two main energy sources: heat transfer from the hot particles and plasma relaxation in the water surrounding those particles. For picosecond pulses, only the heat transfer contributes to bubble formation. However, for ultrafast pulses (45fs), we show that a combination of those two mechanisms leads to cavitation, facilitating bubble production. Indeed, generating similar bubbles requires twice the amount of energy per pulse when its duration is increased from 45fs to 150ps. This is consistent with modeling results based on nonlinear plasma contribution that become significant for femtosecond pulses.

This unique combination of laser heating and plasma production opens up new possibilities to further reduce the bubble generation threshold without completely destroying the plasmonic nanoparticles in the process.

[1] E. Boulais, R. Lachaine, A. Hatef, and M. Meunier, "Plasmonics for pulsed-laser cell nanosurgery: Fundamentals and applications," Journal of Photochemistry and Photobiology C: Photochemistry Reviews**17**, 26-49 (2013).

[2] E. Boulais, R. Lachaine, and M. Meunier, "Plasma mediated off-resonance plasmonic enhanced ultrafast laser-induced nanocavitation," Nano Letters**12**, 4763-4769 (2012).

O-03

Femtosecond Laser texturing of CVD Diamond surface for Solar Conversion Application

P. Calvani[1,*], A. Bellucci[1,3], M. Girolami[1], S. Orlando[2], and D. M. Trucchi[1]

[1]*Institute for Structure of Matter, National Research Council, Via Salaria km 29.300, 00015 Monterotondo Scalo, Rome, Italy*

[2]*Institute for Structure of Matter, National Research Council, U.O.S. Tito Scalo, Zona Industriale 85050 Tito Scalo (PZ), Italy*

[3]*Physics Department, University of Rome Sapienza, Piazzale Aldo Moro 2, 00185 Roma, Italy*

**Corresponding Author e-mail address: paolo.calvani@ism.cnr.it*

Nanoscale periodic texturing on diamond surface has been performed by femtosecond laser and optimized on CVD polycrystalline diamond to obtain a significant increase of optical absorbance and, specifically, of responsivity to visible and infrared radiation (Fig. 1, left). The horizontal polarized laser beam has been focused perpendicularly to the diamond plate surface with a fluence of 20 mJ/cm^2 so that plates have been treated with an intensity higher than the diamond damage threshold. Fs-laser ultrashort pulses induced a controlled periodicity of ripples of 170 nm and length of several μm (Fig. 1, right), able to dramatically increase the diamond absorption[1], which is intrinsically visible-blind due the wide bandgap of 5.47 eV.

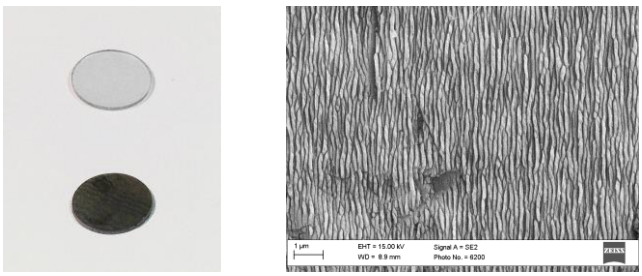

Fig. 1. Left: Comparison of Optical Grade CVD diamond before (top) and after (bottom) the Fs-laser treatment. Rigth: SEM image of Optical Grade CVD diamond surface treated by Fs-laser where the formation of nanoscale periodic structures is evident.

The surface treatment has been performed in a high vacuum chamber (<10^{-7} mbar) by moving the X axis of the X-Y translational stage with different speed resulting in a variation of the effective treatment dose on the sample. A study of the influence of dose on absorbance and responsivity has been performed, highlighting an optimum condition. A defect engineering strategy is at the basis of the surface texturing, supported by the evidence of an enhanced responsivity (about 100 times and 10 times at 350 nm and 500 nm, respectively, higher than the untreated one, shown in Fig. 2). The operating mechanisms of the first optimized surface-textured diamond is discussed and explained by disentangling the optical enhancement from an electronic increased density of states within the diamond bandgap. The enhanced diamond sensitivity to solar radiation, demonstrated for the first time, can open the path for development of high performance wide spectrum detectors as well as solar energy converters based on PETE (photon-enhanced thermionic emission) energy converters[2].

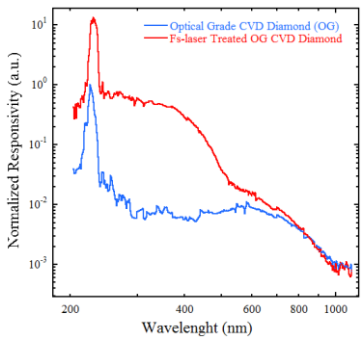

Fig. 2. Responsivity of Optical Grade CVD diamond before and after the treatment: the enhancement due to the Fs-laser treatment is evident, especially in visible range.

References

[1] P. Calvani, A. Bellucci, M. Girolami, S. Orlando, V. Valentini, A. Lettino, and D. M. Trucchi, "Optical properties of femtosecond laser-treated diamond," *Appl. Phys. A Mater. Sci. Process.*, vol. 117, no. 1, pp. 25–29, 2014.

[2] J. W. Schwede, I. Bargatin, D. C. Riley, B. E. Hardin, S. J. Rosenthal, Y. Sun, F. Schmitt, P. Pianetta, R. T. Howe, Z.-X. Shen, and N. a Melosh, "Photon-enhanced thermionic emission for solar concentrator systems.," *Nat. Mater.*, vol. 9, no. 9, pp. 762–7, Sep. 2010.

O-04

Synthesis of bismuth-based nanosheets by ultrasound assisted liquid laser ablation

E. Velarde-Granados[1,2], L. Escobar-Alarcón[1,*], D.A. Solís-Casados[2], O Olea-Mejía[2], M. Espinoza-Pesqueira[3], E. Haro-Poniatowski[4]

[1] *Departamento de Física, Instituto Nacional de Investigaciones Nucleares, Apdo. Postal 18-1027, México DF 11801, México.*
[2] *Centro Conjunto de Investigación en Química Sustentable UAEM-UNAM, Toluca, Estado de México, 50200, México.*
[3] *Departamento de Tecnología de Materiales, Instituto Nacional de Investigaciones Nucleares, Apdo. Postal 18-1027, México DF 11801, México.*
[4] *Departamento de Física, Universidad Autónoma Metropolitana Iztapalapa, Apdo. Postal 55-534, México, D.F., México.*
** Corresponding author: luis.escobar@inin.gob.mx.*

Abstract.
The preparation of nanostructures, such as nanoparticles, nanowires and nanotubes, have become the focus of intense studies over the last few years due to their potential applications. Among the physical techniques, the laser ablation of solids in liquid media has emerged as an important route for the synthesis of nanostructures. The preparation of bismuth nanosheets ablating a high purity Bi target immersed in water subjected to an ultrasound wave is reported. The effect of the laser fluence used for ablation on the size and shape of the nanostructures synthesized was investigated. The nanosheets were characterized by Transmission Electron Microscopy (TEM), Energy Dispersive X-ray Spectroscopy (EDS), UV-Vis and Raman spectroscopies. The obtained results reveal the formation of nanosheets with square-like shape and sizes from approximately 140 to 543 nm as is showed in the figure 1. The bismuth nanosheets, are highly crystalline and depending on the conditions of preparation, either Bi or Bi_2O_3 are obtained. UV-Vis measurements show the typical band absorption characteristic of bismuth with nanometric size. Raman spectra confirm the formation of Bi or Bi_2O_3 nanostructures. The presence or of the ultrasound wave together with appropriate energy densities seems to favor the formation of nanosheets. Further studies of this particular effect are underway.

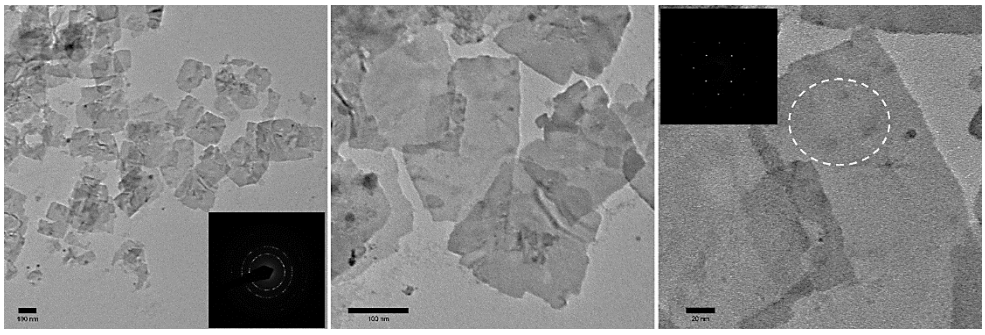

Fig. 1. Bismuth-based nanosheets prepared in distilled water, under ultrasonic conditions, using the third harmonic of a Nd: YAG laser, 355 nm, 5 ns of pulse duration, working at a repetition rate of 10 hertz.

O-05

Ultra-short laser interactions with nanoparticles: from melting and shape change to fragmentation

Tatiana E. Itina and Laure Delfour

Hubert Curien Laboratory, UMR CNRS 5516/Lyon University, Bât F, 18 rue du Prof. Benoît Lauras, Bat. B, 42000, Saint-Etienne, France

Femtosecond lasers are powerful tool used not only for nanoparticle synthesis but also that can help to trigger nanoparticle size and to better control over their size distributions [1-2]. The resulted nanoparticles are particularly attractive for bio-sensing, medical application, as well as for catalysis. In the present paper, we consider ultrashort laser interactions with nanoparticles both in vacuum and in liquids. The objective is to elucidate the major mechanisms of particle fragmentation in order to better control over nanoparticle shape and sizes. First, laser energy absorption is considered. The roles of laser wavelength, particle size and concentration are underlined. Then, ultra-short laser-induced dynamics of nanoparticles is considered by using molecular dynamics simulations. The obtained results help us to elucidate the roles of thermal, mechanical and electrostatic effects in the particle decomposition. It is found that as a result of a quite moderate ultra-short laser irradiation, voids can be formed in the initially spherical metallic particles turning them into hallow ones. With the increase in laser fluence, particle decomposition is observed resulting from both thermal and mechanical effects (Fig 1.).

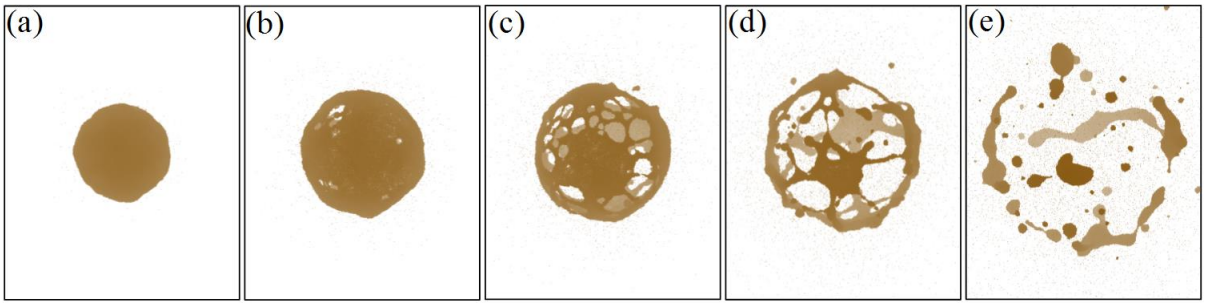

Fig1. Fragmentation dynamics calculated for a gold particle of 15 nm. Here, laser parameters are the following: laser wavelength λ = 400 nm, laser pulse duration is 150 fs, laser fluence F = 100 mJ/cm² calculated (a) –at time delay of 46 ps, (b) – at 86.5 ps, (c) – at 119.5, (d) – at 165 ps, and (e) - at 281 ps after the beginning of the laser pulse.

Furthermore, a series of calculations are performed to elucidate the major particle decomposition mechanisms as a function of particle size and laser parameters. On one hand, we calculate laser fluences required to reach the Coulomb explosion and for particle boiling (F_{ce} and F_{th}, respectively in Fig. 2). On the other hand, the absorbed laser fluence depends on the absorption cross-section. The corresponding absorbed fluence is referred as F_{abs} in the Figure. The intersections of the absorption curve with F_{ce} (r) and with F_{th} (r) are then determined.

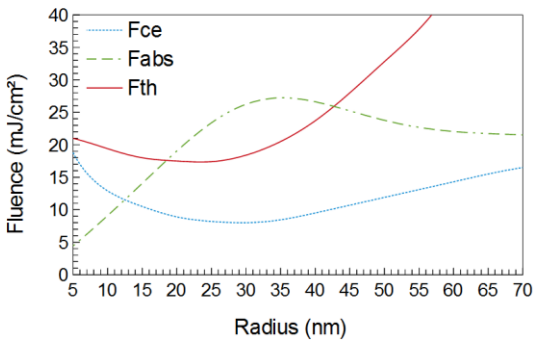

Fig; 2. Laser fluences as a function of the particle radius : absorbed fluence (green), lowest laser fluence needed for the particle to boil (red) or to undergo Coulomb explosion (blue).

The performed analysis allows us to predict optimum laser parameters for nanoparticle size manipulation, but also to recommend nanoparticle properties for the enhanced absorption, which is particularly interesting for the development of novel energy sources and for photo-thermal applications.

[1] Werner, D.; Furube, A.; Okamoto, T.; Hashimoto, S. *J. Phys. Chem. C*, **115**, 8503–8512 (2011)
[2] Pyatenko, A.; Yamaguchi, M.; Suzuki, M. *J. Phys. Chem. C*, **113,** 9078–9085 (2009).

I-02

Femtosecond laser fabrication for nanophotonics

Min Gu

Centre for Micro-Photonics and CUDOS
Faculty of Science, Engineering, Technology
Swinburne University of Technology
Hawthorn, Victoria 3122, Australia

When a femtosecond laser beam is focused by a high numerical aperture objective, it can be confined to a diffraction-limited region. The highly spatially and temporally concentrated focal volume can result in nonlinear effects such as two-photon absorption in a variety of media, enabling the fabrication of three-dimensional structures at a micro-scale. Therefore, femtosecond laser fabrication is a powerful tool toward the development of ultimate 3D photonic devices. We will show our new achievement on optically-digitalised holography for floating display. Because of the increasing demand for realising nano-geometries, the diffraction-limited resolution associated with femtosecond laser fabrication should be overcome to access to the nano-scale. We will show how this diffraction limit can be broken in the development of superresolution photoinduction-inhibited nanolithography (SPIN) and the application of SPIN in optical big data storage.

O-06

Mechanism investigations of gold nanoparticle enhanced ultrafast laser near field optical breakdown and nanocavitation

C. Boutopoulos[1,2], A. Dagallier[1], R. Lachaine[1], D. Rioux[1], A. Hatef[3], E. Boulais[4], Michel Meunier[1]

[1]*Laser Processing and Plasmonics Laboratory, Engineering Physics Department, Polytechnique Montréal, Montréal, Québec H3C 3A7, Canada*
[2]*SUPA, School of Physics and Astronomy, University of St. Andrews, North Haugh, St. Andrews, KY16 9SS, UK*
[3]*Nipissing Computational Physics Laboratory, Nipissing University, North Bay, Ontario, P1B 8L7, Canada*
[4]*Massachusetts Institute of Technology, Department of Biological Engineering, 77 Massachusetts Avenue, Cambridge, MA, USA 02139*
e-mail address: christos.boutopoulos@polymtl.ca

Plasmonic nanoparticle (NP)-enhanced laser nanocavitation (or plasmonic bubble (PB)) is crucial for a variety of biomedical research fields such as cancer treatment, imaging, disease detection, drug and gene delivery. Our group recently demonstrated that PB generation with near-infrared off-resonance femtosecond (fs) laser irradiation minimizes the laser energy absorption by the AuNPs, thus ensuring the preservation of their optical and structural properties [1]. In this work, we further investigate the role of the near-field and laser pulse width in the nanocavitation mechanism around threshold laser fluences. In order to ensure a systematic alteration of the near-field we used a variety of AuNPs with sizes ranging from 80 nm to 210 nm. Pulse widths in the range from 70 fs to 5 ps pulse at 800 nm wavelength were examined. We employed single-particle ultrafast imaging for PB detection (Fig. 1a and 1b), while the AuNP disintegration at high fluences was examined by *in-situ* dark field imaging. Experimental results were correlated with plasma calculations around the vicinity of the AuNP and modelling of the AuNP thermodynamic response.

We observed a clear dependence of both the nanocavitation laser fluence threshold ($F_{PB,th}$) and the AuNP disintegration laser fluence threshold ($F_{D,th}$) on the nanoparticles size. Depending on the AuNP size and the laser pulse width, the $F_{D,th}$ / $F_{PB,th}$ ratio varies between ~ 3.5 to ~ 7, indicating a broad processing window. Within this processing window, the AuNPs present noticeable ability to generate multiple PB without any decrease in cavitation efficiency. AuNPs excitation in the fs regime optimizes the effect in terms of both threshold sharpness and processing window. We calculated the effective power density threshold at the AuNP poles (I_{ef_th}), which considers the AuNP size dependent near-field enhancement (Fig. 1c). We show that I_{ef_th} is almost independent of the particle size for a given pulse duration. Furthermore, I_{ef_th} values are in good agreement with the reported power density range for conventional optical breakdown, caused by laser focusing in aqueous media [2]. These findings, in agreement with our analytical plasma modelling, indicate that the optical breakdown is the dominant nanocavitation mechanism for the PB generation at the threshold regime, within the 70 fs - 5 ps pulse width range. AuNP disintegration was observed for high laser fluences. The disintegration mechanism will be discussed using both experimental and simulation results.

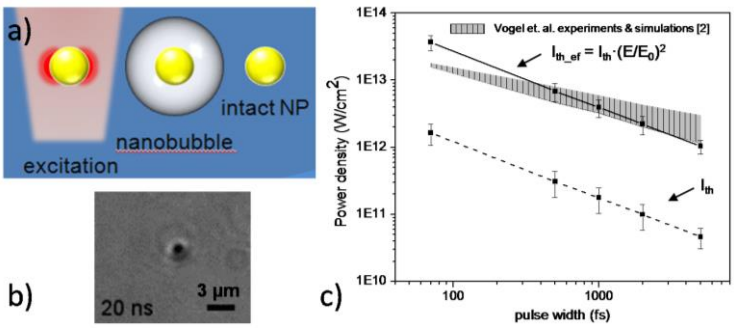

Fig.1: (a) Schematic representation of PB generation (b) Pump probe PB image at 20 ns (c) Dependence of the nanocavitation power density threshold (I_{th}) and effective power density threshold ($I_{ef\_th} = I_{th} \cdot (E/E_0)^2$) on the laser pulse width. The hatched area indicates the reported power density range for conventional optical breakdown, caused by laser focusing in aqueous media [2]. The relatively good overlap indicates that the near field amplification optical breakdown is the dominant nanocavitation mechanism.

In conclusion, systematic alteration of the AuNP near-field and laser pulse width enabled insights into the AuNP enhanced off-resonance laser nanocavitation mechanism. Indeed, optical breakdown around the AuNP poles was proved as the dominant mechanism in the 70 fs - 5 ps regime. Optimum selection of the AuNP size (150 nm -170 nm) and laser pulse width (70 fs) minimizes the PB generation threshold and prevents AuNP disintegration for an extended laser processing window. The latter can be the basis for further development of PB-based nanosurgery as a unique therapeutic tool for safe *in vivo* treatments.

[1] E. Boulais, R. Lachaine, and M. Meunier, "Plasma mediated off-resonance plasmonic enhanced ultrafast laser-induced nanocavitation," Nano Letters **12**, 4763-4769 (2012).

[2] A. Vogel, J. Noack, G. Hüttman, and G. Paltauf , "Mechanisms of femtosecond laser nanosurgery of cells and tissues," Applied Physics B, 81(8), 1015–1047 (2005); A. Vogel et. al., "Roles of Tunneling, Multiphoton Ionization, and Cascade Ionization for Femtosecond Optical Breakdown in Aqueous Media" public research project report (2009).

O-07

Effects of UV-Laser Processing on ZnO Nanocrystals: Controlling the Crystal Growth, Electrical and Optical Properties

T. Shimogaki[1], M. Takahashi[1], M. Yamasaki[1], T. Fukuda[1], M. Higashihata[1], H. Ikenoue[1]
D. Nakamura[1], Y. Nakata[2], T. Okada[1]
[1]Department of Information Science and Electrical Engineering, Kyushu University, 530-1 West 2, 744 Oaza Motooka, Fukuoka, Japan
[2]Institute of Laser Engineering, Osaka University, 2-6 Yamadaoka, Suita, Osaka, Japan
E-mail: shimogaki@laserlab.ees.kyushu-u.ac.jp

Zinc Oxide (ZnO) nanocrystals, which are characterized by their unique configurations, fine structures and large surface-to-volume ratio, are expected to be the building blocks of novel photo electronic devices. In particular, one-dimensional-grown ZnO nanocrystals can be ultraviolet light emitting diodes (UV-LED) with high efficiency due to their large surface area and excellent crystallinity. It is difficult, however, to control the electrical property of ZnO nanocrystals for practical applications because of their quite-small sizes. Therefore, many researchers are trying to establish the fabrication method of morphology and position-controlled ZnO nanocrystals using catalyst or zinc acetate layers as seed layers. [1-3] In this study, we report the controllability of electrical and optical property of ZnO nanocrystals and the high-throughput fabrication of ZnO nanocrystals using some kinds of UV-laser processes. These processes do not require any seed layer or catalyst, so that they have a great potential to improve the conventional procedures of the study filed of ZnO nanocrystals.

ZnO nanocrystals were fabricated by various UV-laser processing. The core technique of crystal-growth is nanoparticle-assisted pulsed laser deposition (NAPLD). Densely-packed ZnO nanorods, which are shown in Fig. 1(a), were fabricated by NAPLD on a *c*-cut sapphire substrate. We have achieved to fabricate *p-n* homo junction on ZnO nanorods using phosphorous-ion implantation followed by UV-laser annealing. [4]

Additionally, periodically-aligned ZnO nanowires, which have more suitable structures for UV-LEDs, UV-LDs and field emitters, were obtained by the development of NAPLD. A ZnO buffer layer with the thickness of about 150 nm was deposited by conventional pulsed laser deposition on an *a*-cut sapphire substrate. Subsequently, it was laser-patterned with four-beam interference UV-laser. The surface of ZnO buffer layer was ablated periodically, as shown in inset of Fig. 1(b). A circular area with diameter of about 150 μm was patterned by only one pulse of interference UV-laser, as shown in Fig. 1(b). Then, ZnO nanowires were fabricated on the laser-patterned ZnO buffer layer by NAPLD. Figure 1(c) shows obtained periodically-aligned ZnO nanowires after ultrasonic cleaning process, which was performed to remove excess ZnO nanowires. It was found that each ZnO nanowire has good crystallinity and photoluminescence property. Additionally, rectified *I-V* characteristics was obtained after phosphorous-ion implantation followed by UV-laser annealing.

Thus, we have demonstrated the effectiveness of some kinds of UV-laser processes on the study of ZnO nanocrystals. These techniques can accelerate the study field of applying ZnO nanocrystals to photo electronic devices or other devices.

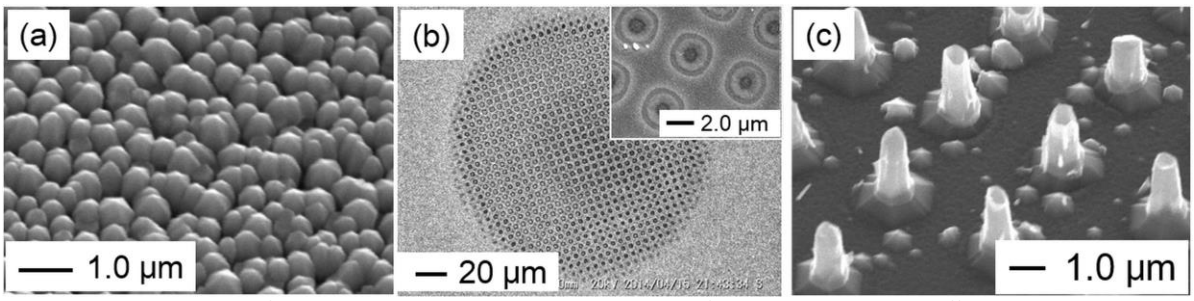

Fig. 1(a) An SEM image of densely-packed ZnO nanorods, (b) SEM images of the laser-patterned ZnO buffer layer, the inset is high magnification view, (c) An SEM image of periodically-aligned ZnO nanowires grown on the laser-patterned ZnO buffer layer.

[1] X. Wang, C. J. Summers and Z. L. Wang, *Nano* Lett., **4**, 423 (2004).
[2] Y. H. Kim, N. S. Baek, K. H. Kim and S. D. Jung, *J. Sol-Gel. Sci. Technol*., **64**, 304 (2012).
[3] Y. Tak and K. Yong, *J. Phys. Chem. B*, **109**, 19263 (2005).
[4] T. Shimogaki, K. Okazaki, D. Nakamura, M. Higashihata, T. Asano and T. Okada, *Opt. Express*, **20**, 15247 (2012).

O-08

Plasmonic, excitonic and exciton-plasmonic photoinduced nanocomposites

N. Bityurin[1], A. A. Smirnov[1], A. Afanasiev[1], N. Ermolaev[1], N. Agareva[1], V. Bredikhin[1], A. Pikulin[1], N. Sapogova[1], L. A. Smirnova[2], E. Salomatina[2], I. Glazova[2]

[1]Institute of Ap[plied Physics, RAS, Nizhniy Novgorod, Russia
[2]Nizhniy Novgorod State University, Nizhniy Novgorod, Russia
E-mail: bit@appl.sci-nnov.rul

UV irradiation of materials consisting of a polymer matrix that possesses precursors of different kinds followed by annealing can result in creation of nanoparticles within the irradiated domains. Such photoinduced nanocomposites are promising for photonics applications due to the strong alteration of their optical properties compared to initial nonirradiated materials [1].

We report our results on the synthesis and investigation of plasmonic, excitonic and exciton-plasmonic photo-induced nanocomposites. Plasmonic nanocomposites contain metal nanoparticles of noble metals (gold, silver, etc.) with pronounced plasmon resonance [2]. Excitonic nanocomposites possess semiconductor nanoclusters (quantum dots) [3].

Exciton-plasmon media consisting of both quantum-sized semiconductor nanoparticles and plasmonic metal nanoparticles placed in a dielectric matrix are of an increasing scientific interest. Materials of this kind have unique optical properties, such as the giant optical nonlinearity and the complex luminescent behavior, especially in the case when the exciton and plasmon frequencies of the particles are close to each other. These materials can be used to implement "active" 3D plasmonics, which deals with plasmonic structures in the media with inverted population of the electron states. It is important that in case of photo-induced nanocomposites before the irradiation such the media do not contain any nanoparticles, being totally homogeneous. The nanoparticles are induced by the laser and thus are localized only within the irradiated domains.

With plasmonic photoinduced nanocomposites, we investigate PMMA+ Au precursors. Here, we theoretically and experimentally consider opportunities to control the size distribution of nanoparticles using special regimes of laser material alteration. In particular, we examine the effect of laser swelling on kinetics of nanoparticles formation.

With excitonic photoinduced nanocomposites, we investigate PMMA+CdS precursors of different kinds. We follow the pulse-to pulse kinetics of laser induced green luminescence pumped by UV CW laser for different concentration of precursor and different modes of sample preparation. We employ nanosecond pulses of the UV harmonics of a Nd:YAG laser at different fluences and repetition rates. This allows us to determine the mechanisms of precursor reduction and nanoparticle formation. We also obtain and investigate samples containing precursors of both Au and CdS. It is important that CdS nanoparticle luminescence spectrum is close to the plasmon resonance band of the gold nanoparticles.

One of the most intriguing problems with exciton-plasmon photoinduced nanocomposites is obtaining the correlated spatial distribution of plasmonic and excitonic nanoparticles. With this respect, we analyze the opportunities provided by the plasmonic nanoparticles inserted into the bulk of a transparent medium to modify the material by laser light irradiation [4]. We separately consider two different mechanisms of material alteration by femtosecond laser pulses. First, we analyze a photochemical reaction initiated by the two-photon absorption of light near the plasmonic nanoparticle within the matrix. We show that the spatial distribution of the products of such a reaction changes the symmetry of the material, resulting in the appearance of anisotropy in the initially isotropic material or even in the loss of the center of symmetry. Second, we analyze the efficiency of a thermally-activated chemical reaction at the surface of a plasmonic particle and the distribution of the product of such a reaction just near the metal nanoparticle irradiated by an ultrashort laser pulse.

[1] Nikita M. Bityurin, "Laser Nanostructuring of Polymers", in, "Fundamentals of Laser – Assisted Micro- and Nanotechnologies", Edited by V. P. Veiko, V. I. Konov , Springer International Publishing, Switzerland, 2014, pp. 293-314.
[2] N. Bityurin, A. Alexandrov, A. Afanasiev, N. Agareva, A. Pikulin, N. Sapogova, L. Soustov, E. Salomatina, E. Gorshkova, N. Tsverova, L. Smirnova, "Photoinduced nanocomposites—creation, modification, linear and nonlinear optical properties", Applied Physics A, 112, 135 (2013).
[3] F. Antolini, E. Burresi, L. Stroea, V. Morandi, L. Ortolani, G. Accorsi, and M. Blosi, "Time and Temperature Dependence of CdS Nanoparticles Grown in a Polystyrene Matrix", Journal of Nanomaterials, 2012, ID 815696 (2012).
[4] A. A. Smirnov, A. Pikulin, N. Sapogova, N. Bityurin, "Femtosecond laser irradiation of plasmonic nanoparticles in polymer matrix: implications for photothermal and photochemical material alteration", Micromachines 5, 1202 (2014).

O-09

Sub-Diffraction-Limit Laser Lithography assisted by Laser-Induced Periodic Surface Structures (LIPSS)

Woongsik Nam[1,2], Xiaolong He[1,2,3], and Xianfan Xu[1,2,*]

[1]*School of Mechanical Engineering, Purdue University, West Lafayette, IN 47906, USA*
[2]*Birck Nanotechnology Center, Purdue University, West Lafayette, IN 47906, USA*
[3]*School of Mechatronics Engineering, Harbin Institute of Technology, Harbin 150001, PR China*
[*]*xxu@purdue.edu*

For the past decades, advances in optical techniques and processing have achieved a rapid reduction in the feature size of nanostructures. In particular, optical lithography has been the primary tool to create the fine-scale patterns required for nano-fabrication. However, as the feature size shrinks beyond the diffraction limit of light, conventional optical lithography can no longer improve the required high resolution. Although several alternative lithographic techniques, such as extreme ultraviolet lithography, nano-imprint lithography, and two-photon laser direct writing lithography have demonstrated their capability to achieve high resolution, these approaches require either high-cost, complex systems, or offer limited flexibility. On the other hand, direct writing of laser-induced periodic surface structures (LIPSS) has been an active area of ongoing examination as a flexible and low-cost method to create features well below the processing laser wavelength. LIPSS can form on nearly all kinds of materials, including metals, semiconductors, and insulators [1,2], but the poor quality and the random nature of LIPSS have remained an obstacle to widespread applications. In this work, we demonstrate a laser-direct-writing technique to exploit the small feature size of LIPSS for lithography. The formation of LIPSS is deliberately controlled and sub-20 nm feature sizes are demonstrated on photoresist (Fig. 1 and Fig. 2). Our approach has the capability to create *a single line* by controlling the laser power such that only the centre fringe in the LIPSS pattern exceeds the required processing power threshold. This is unlike other LIPSS techniques where multiple, periodic line structures are formed. The created features are characterized using scanning electron microscopy (SEM) and atomic force microscopy (AFM). We expect that our approach could be a promising alternative for high-resolution lithography with its simplicity and flexibility.

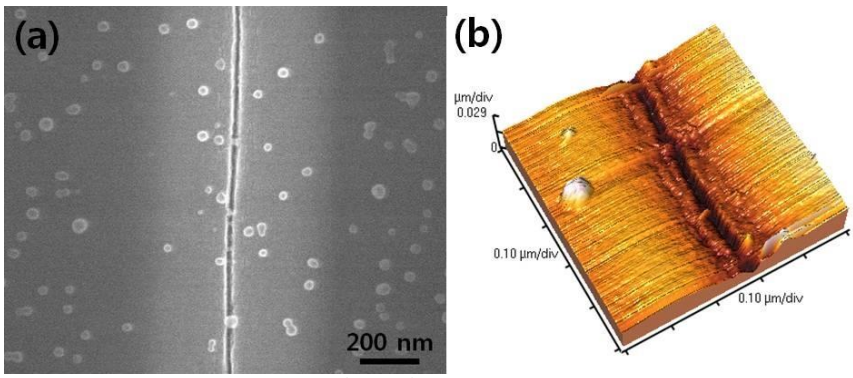

Fig. 1. (a) SEM and (b) AFM images of a line feature created using the laser-direct-write lithography

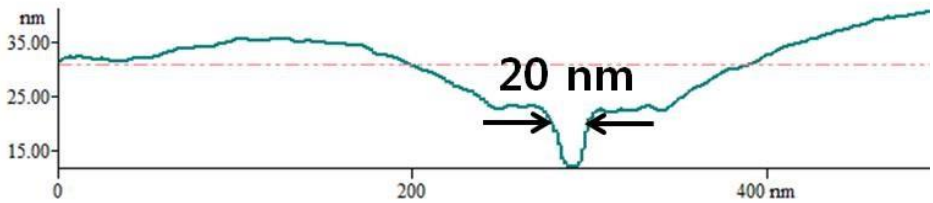

Fig. 2. Height profile of a line feature created using the laser-direct-write lithgraphy

References

[1] B. Öktem, I. Pavlov, S. Ilday, H. Kalaycıoğlu, A. Rybak, S. Yavaş, M. Erdoğan, and F. Ö. Ilday, "Nonlinear laser lithography for indefinitely large-area nanostructuring with femtosecond pulses," Nature Photonics **7**, 897 (2013).

[2] J. E. Sipe, J. F. Young, J. S. Preston, and H. M. van Driel, "Laser-induced periodic surface structure I: theory," Phys. Rev. B **27**, 1141 (1983).

O-10

Self-organization of nanostructures embedded in various materials

Y. Shimotsuma[1], T. Kurita[1], S. Kubota[1], A. Murata[1], T. Sei[1], M. Sakakura[2], K. Miura[1]
[1]*Department of Material Chemistry, Kyoto University, Kyoto 615-8510, Japan*
[2]*Society-Academia Collaboration for Innovation, Kyoto University, Kyoto 615-8510, Japan*
E-mail address: yshimo@func.mc.kyoto-u.ac.jp

Space-selective nanostructuring inside various materials has been accomplished by focused irradiation of femtosecond laser pulses. In the case of isotropic material such as glass [1,2], the localized form-birefringence can be successfully induced. We have proposed the mechanisms of the self-organization based on the interference between the electric field component of the incident light and the generated electron plasma wave [3]. Whereas, another group has also proposed the formation mechanism of nanoplanes due to nanoplasmonic effects [4]. More recently, we have also revealed that periodic nanostructures were formed inside single crystal of silicon (c-Si) and gallium phosphide (GaP) by using the infrared femtosecond laser double-pulse configuration [5]. Self-organized nanostructures inside semiconductor could be induced empirically only if it is indirect band gap semiconductor. The strained silicon regions with a width of about 100 nm are self-aligned parallel to the polarization direction of the first arriving pulses, despite of the polarization direction of the secondly arriving pulses. AFM inspections reveal that such strained silicon nanostructures exhibit high electric conductivity and low thermal conductivity [5]. The formation mechanisms would be interpreted in terms of the electrostrictive force through the interaction between electron-hole plasma and phonon. We have observed backscattering electron images (BEIs) on the polished sample surfaces to the depth of focal spot location inside SiO_2 glass, GeO_2 glass, c-Si, GaP, gallium nitride (GaN) and gallium arsenide (GaAs) crystal (Fig. 1). Although BEI for c-Si and GaP are analogous to the nanogratings constituted by oxygen deficiencies inside of glass, the principal difference in the periodic nanostructure between c-Si and SiO_2 glass is the alignment direction of the periodic nanostructure. These stripe-like darker regions in the BEI correspond to lower-density material. Although there is a big difference in refractive index between c-Si and SiO_2 glass, the period of the nanostructures for c-Si ($\Lambda \sim 200$nm) is similar to that for SiO_2 glass. Furthermore, the dark regions with a width of $t \sim 100$ nm were aligned parallel to the polarization direction of the first arriving pulses (E^{1st}), despite of the polarization direction of the secondly arriving pulses (E^{2nd}). In addition, the similar periodic nanostructure of c-Si was observed in GaP. On the other hand, we have also carried out the observation of the modified region inside GaAs after the femtosecond double-pulse irradiation. No apparent periodic nanostructures were observed in the case of the direct-transition type semiconductors, such as GaAs and GaN. In the case of GaN, the nanovoids are distributed in the triangular shape corresponding to the hexagonal wurtzite type crystal structure without depending on the laser polarization. Another group has also observed that the formation of periodic strained layers associated with nanovoids inside a SiC single crystal [6]. Since a SiC is an indirect band gap semiconductor, their results are consistent with our interpretation that the nanostructures can be formed inside a material only if it is an indirect bandgap semiconductor. Apart from the basic understanding, such periodic nanostructures will open the door to the innovative applications including the 5-dimensional optical storage, polarization imaging sensor and the self-contained thermoelectric devices.

Material	SiO_2 glass	GeO_2 glass	Si	Si	GaP	GaN	GaAs
Polarization direction	E ↕	E ↕	E^{1st} ↕ E^{2nd} ↕	E^{1st} ↕ E^{2nd} ↔	E^{1st} ↕ E^{2nd} ↕	E ↕	E^{1st} ↕ E^{2nd} ↕
BEIs	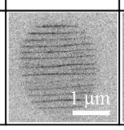	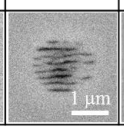	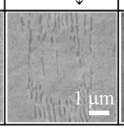	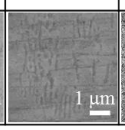	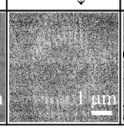	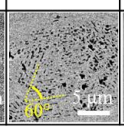	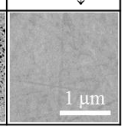

Figure 1: Backscattering electron images (BEIs) on the polished sample surfaces to the depth of focal spot inside various materials. E^{1st} and E^{2nd} indicate the polarization direction of the first and the second arriving pulse in double-pulse train respectively.

[1] Y. Shimotsuma, M. Sakakura, P. G. Kazansky, M. Beresna, J. Qiu, K. Miura, and K. Hirao, "Ultrafast manipulation of self-assembled form birefringence in glass," Adv. Mater. **22**, 4039 (2010).
[2] T. Asai, Y. Shimotsuma, T. Kurita, A. Murata, S. Kubota, M. Sakakura, K. Miura, F. Brisset, B. Poumellec, and M. Lancry, "Systematic control of structural changes in GeO_2 glass induced by femtosecond laser direct writing," J. Am. Ceram. Soc. *In press* (2015).
[3] Y. Shimotsuma, P. G. Kazansky, J. Qiu, and K. Hirao, "Self-organized nanogratings in glass irradiated by ultrashort light pulses," Phys. Rev. Lett. **91**, 247405 (2003).
[4] V. R. Bhardwaj, E. Simova, P. P. Rajeev, C. Hnatovsky, R. S. Taylor, D. M. Rayner, and P. B. Corkum, "Optically produced arrays of planar nanostructures inside fused silica," Phys. Rev. Lett. **96**, 057404 (2006).
[5] M. Mori, Y. Shimotsuma, T. Sei, M. Sakakura, K. Miura, H. Udono, "Tailoring thermoelectric properties of nanostructured crystal silicon fabricated by infrared femtosecond laser direct writing," Phys. Status Solidi A *In press* (2015).
[6] T. Okada, T. Tomita, S. Matsuo, S. Hashimoto, Y. Ishida, S. Kiyama, and T. Takahashi, "Formation of periodic strained layers associated with nanovoids inside a silicon carbide single crystal induced by femtosecond laser irradiation," J. Appl. Phys. **106**, 054307 (2009).

I-03

Fundamental aspects of Nanoparticles production by laser ablation in liquids

M. Dell'Aglio[2], O. De Pascale[2], R. Gaudiuso[2], G. Valenza[1], A. De Giacomo[1,2]

[1]*Department of Chemistry, University of Bari, Via Orabona 4, 70125 Bari-Italy*
[2]CNR-IMIP, Via Amendola 122/D, 70126 Bari-Italy

In the last decade Pulsed Laser Ablation in Liquids (PLAL) has been widely investigated from the fundamental point of view, and various theories have been proposed. Although many important achievements have been obtained by the scientific community, many aspects still need to be clarified and many contradictions arise when comparing the interpretation of similar experiments carried out by different authors. In this paper we have reconsidered previous works focused on specific processes and stages of the PLAL, in order to outline a modern and comprehensive point of view of the overall physical aspects of PLAL. Experiments of single and double pulse Laser Ablation in Liquids (LAL) were carried out for studying the production of nanoparticles (NPs) in water, which revealed the fundamental role of plasma evolution and relaxation, as well as cavitation bubble dynamics produced by the laser plasma itself, in the formation of nanostructure and in their corresponding properties. Different techniques were used for studying the phenomena occurring during LAL at different conditions (single pulse [1], double pulse and external pressure [2]). These include Optical Emission Spectroscopy and fast camera shadowgraph for studying the laser induced plasma characteristics and other shadowgraph-like experiments for the cavitation dynamics and material ejection, and combination of spectroscopic and microscopic techniques for investigate the correlation between the ablation process and the produced nano particles [3,4].

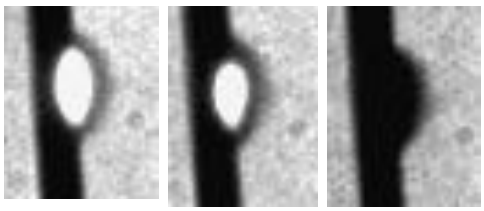

Fig. 1. Plasma evolution and cavitation bubble formation during LAL.

[1] A. De Giacomo, M. Dell'Aglio, A. Santagata, R. Gaudiuso, O. De Pascale, P. Wagener, G. C. Messina, G. Compagnini and S. Barcikowski "Cavitation dynamics of laser ablation of bulk and wire-shaped metals in water during nanoparticles production" Phys. Chem. Chem. Phys. **15**, 3083(2013)

[2] A. De Giacomo, A. De Bonis, M. Dell'Aglio, O. De Pascale, R. Gaudiuso, S. Orlando, A. Santagata, G.S. Senesi, F. Taccogna, R. Teghil "Laser ablation of graphite in water in a range of pressure from 1 to 146 atm using single and double pulse techniques for the production of carbon nanostructures" J. of Phys. Chem. C **12**,115 (2012)

[3] M. Dell'Aglio, R. Gaudiuso, R. ElRashedy, O. De Pascale, G. Palazzo, A. De Giacomo, Collinear double pulse laser ablation in water for the production of silver nanoparticles, Phys.Chem. Chem. Phys., **15**, 20868, (2013)

[4] M. dell'Aglio, R. Gaudioso, O. De Pascale, A. De Giacomo "Mechanisms and processes of pulsed laser ablation in liquids during nanoparticle production" Appl. Sur. Sci. doi: 10.1016/j.apsusc.2015.01.082.

O-11

Laser welding for handling of thin crystalline Si wafers

M. Ernst[1,2], V. Steckenreiter[2], S. Kajari-Schröder[2], and R. Brendel[2,3]
[1]*Centre for Sustainable Energy Systems, Australian National University, Canberra, Acton ACT 2601, Australia*
[2]*Institute for Solar Energy Research Hamelin (ISFH), 31860 Emmerthal, Germany*
[3]*Department Solar Energy, Institute of Solid-State Physics, Leibniz Universität Hannover, 30167 Hannover, Germany*
E-mail: marco.ernst@anu.edu.au

1. Introduction

Thin crystalline Si films (< 100 µm) are used in many applications, such as sensors [1, 2], photovoltaic absorbers [3], and optical and particle filters [4]. Such thin crystalline Si films are difficult to handle [5] and break easily under standard semiconductor processing. We present a laser welding process for the mechanical connection of a thin Si film with a separate stabilizing support that is also made of crystalline Si. We aim at easing low volume handling of very thin compact and porous Si layers in the laboratory. We join the thin Si film and a thick Si support wafer by laser welding without contaminating the Si wafers with any foreign materials. We measure the tear-off stresses as a function of the laser energy and investigate the chemical and mechanical stability in typical semiconductor processes such as plasma deposition, oxidation, and wet chemical cleaning.

2. Laser welding procedure and results

The laser welding procedure is performed with a pulsed laser with a wavelength of 1064 nm, a pulse duration of 1.3 µs, and average pulse energy of 1.4 mJ. We investigate the laser welding procedure for two cases. With this process we join an approximately 30 µm-thick macroporous Si layer to a Si frame with a typical thickness of 200 µm to 300 µm (case 1) and two approximately 80 µm-thick crystalline Si films (case 2).

Figure 1a shows a cross-sectional SEM micrograph of the laser joint for case 1. The sample was prepared by breaking. The heating by the laser pulse melts and ejects Si from the porous Si layer and from the substrate. Some of the molten Si solidifies at the interface of the substrate and the thin macroporous Si layer and establishes thereby a mechanical connection.

Figures 1b shows a top view SEM micrograph of the laser welding spot after separating the joined wafers of case 2 by applying sufficient mechanical force. The micrograph shows about 20 µm-wide solidified Si melt around the laser spot. A small area fraction of this molten Si shows a flat surface. We attribute this flat region to the area that was broken when separating the two Si layers.

We test the processing stability of our laser joints with processes that are typically used for fabricating Si solar cells. Furthermore, we determine the tensile strength of the laser joints. Figure 1c shows the effective tear-off stress σ as a function of the laser pulse energy E_p with five laser pulses per position. The effective tear-off stress σ increases from (16.9 ± 8.0) kPa to (49.9 ± 14.3) kPa with increasing laser pulse energy.

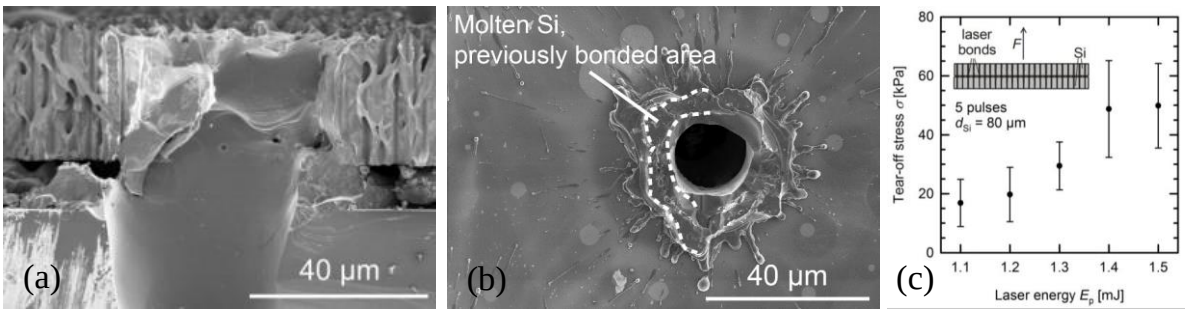

Fig. 1. (a) Cross-sectional SEM micrograph of a laser-welded spot for case 1. (b) Top view SEM micrograph of a laser welding spot after mechanical separation of the films (case 2). (c) Tear-off stress σ as function of laser energy E_p.

3. References

[1] N. Massad-Ivanir, L. M. Bonanno-Young, Y. Mirsky, A. Nahor, A. Sa'ar, and E. Segal, "Rapid detection of bacteria by 'direct-cell-capture' onto porous Si lamellar gratings," in Porous Semiconductors - Science and Technology (PSST), 2012, pp. 100–101.
[2] D. Vega, J. Reina, and A. Rodriguez, "Macroporous silicon photonic crystals for gas sensing," in Spanish Conference on Electron Devices (CDE) (2013), pp. 143–146.
[3] R. Brendel and M. Ernst, "Macroporous Si as an absorber for thin-film solar cells," Phys. Status Solidi RRL **4**, 40 (2010).
[4] V. Lehmann, R. Stengl, H. Reisinger, R. Detemple, and W. Theiss, "Optical shortpass filters based on macroporous silicon," Appl. Phys. Lett. **78**, 589 (2001).
[5] J. Hermanowski, "Thin wafer handling — Study of temporary wafer bonding materials and processes," in IEEE International Conference on 3D System Integration (3DIC), 2009, pp. 1–5.

O-12

Highly sensitive and selective sensor arrays via laser-induced forward transfer

M. Filipescu[1,2], A. Palla Papavlu[1,2], M. Dinescu[2], A. Wokaun[1], T. Lippert[1]
1 General Energy Research Department, Paul Scherrer Institut, 5232 PSI Villigen, Switzerland
2 National Institute for Lasers, Plasma, and Radiation Physics, 077125 Magurele, Romania
Corresponding Author e-mail address: mihaela.filipescu@inflpr.ro

Environmental monitoring of air pollution is of great interest for industry, e.g. automotive (detection of polluting gases from cars), health, and chemical plants as well as for many research groups to develop better systems. Since sensors are the main components in products and systems used to detect different analytes in air, there are always new and innovative sensor technologies emerging. Several key requirements for sensors include sensitivity, response speed, reversibility, energy consumption, and fabrication costs. Therefore, cheap devices on light and flexible substrates i.e. plastic or paper are required.

Here, we focus on the application of carbon nanotubes (CNT) as sensor material which can be used in room temperature operable devices. The most important drawback for the application of CNTs is the necessity to find techniques to deposit them with high enough conductivity on the active area of a chemiresistor. Therefore, we evaluated laser-induced forward transfer (LIFT) as a new approach to fabricate CNT sensor arrays, for the detection of low analyte concentrations.

In LIFT, a laser beam is focused through a transparent support plate onto the backside of a photodegradable triazene polymer (TP) thin film coated with the material to be transferred (CNT). The TP acts as a dynamic release layer and also protects the material to be transferred from direct laser irradiation. Each single laser pulse promotes the transfer of the thin film material onto a receiver substrate (flexible paper, polyethylene terephthalate (PET), polyimide) that is usually placed parallel and facing the thin film at a short distance. The donor-receiver system is placed on a *xyz* stage, thus allowing the fabrication of well-defined 2D and 3D patterns.

As the functionality of the LIFT-ed sensors depends on the LIFT parameter, an optimization of the process parameters was performed first, followed by a physicochemical characterization of the active material, while the performance of the laser-printed devices was evaluated by exposure to different analyte vapors. Different sensitivities (in the ppb range) and selectivity to the selected chemical agents have been measured, thus proving the feasibility of our LIFT approach for applications in sensors and biosensors.

This work was supported by the Commission for Technology and Innovation (KTI-Nr. 16713.1 PFNM-NM) and Scientific Exchange Programme between Switzerland and the New Member States of the European Union (project no. 13.251).

O-13

Laser Ablation Molecular Isotopic Spectroscopy (LAMIS)

RICHARD E. RUSSO[1,2*], XIANGLEI L. MAO[1], AND ALEX A. BOL'SHAKOV[2]

[1]***Lawrence Berkeley National Laboratory, Berkeley, USA,*** *rerusso@lbl.gov*
[2]***Applied Spectra, Inc, Fremont,CA USA,***

Laser ablation is an excellent technology for rapidly measuring the chemistry (elemental and isotope content) of a sample. The laser pulse duration and energy drives the process of ablation, which converts a portion of a sample into a luminous optical plasmas that condenses to a fine aerosol. Chemical analysis is instantaneous by measuring the emission spectra in the optical plasma, or by transporting the aerosol to a secondary source for excitation and analysis. No sample preparation or consumables are needed. The physics of the laser matter interaction influences chemical analysis capabilities, including range of elements detected, sensitivity of converting laser photons to ablated mass, and accuracy and precision of analysis. Traditionally, laser ablation sampling has been coupled with ICP-MS (Inductively Coupled Plasma Mass Spectrometry) for sensitive isotopic analysis. Alternatively, optical emission from the luminous plasma initiated by the ablation process at the sample surface can be monitored and provide elemental analysis and in some cases isotopic analysis. This well-known optical approach is called LIBS (Laser-Induced Breakdown Spectroscopy). Overall, LIBS is not ideally suited for isotopic analysis due to poorly resolved spectral shifts in atomic and ionic spectra from isotopes, especially in atmospheric pressure laser plasmas. However, our new technology LAMIS (Laser Ablation Molecular Isotopic Spectroscopy) shows the ability to perform isotope measurements in these laser plasmas at atmospheric pressure. By expanding the capabilities of classical LIBS to emphasize the measurement of molecular emission spectra in addition to elemental, LAMIS provides the ability to measure all elements and their isotopes, especially light elements like Li, Be, C, N, O which are impossible with XRF. Molecular isotopic shifts are orders of magnitude greater than atomic and ionic transitions. By measuring molecular emission spectra as the plasma cools, isotopic spectral splitting is enhanced up to several orders of magnitude. We developed LAMIS to date by demonstrating its ability to measure B, C, H, D, Sr and other isotopes. We demonstrated low percent levels for sensitivity and have experimental plans to meet ppm levels. For some isotopes, we have achieved < 0.1% precision. The talk will describe the isotope work that has been reported in LIBS plasmas and show how LAMIS expands those capabilities.

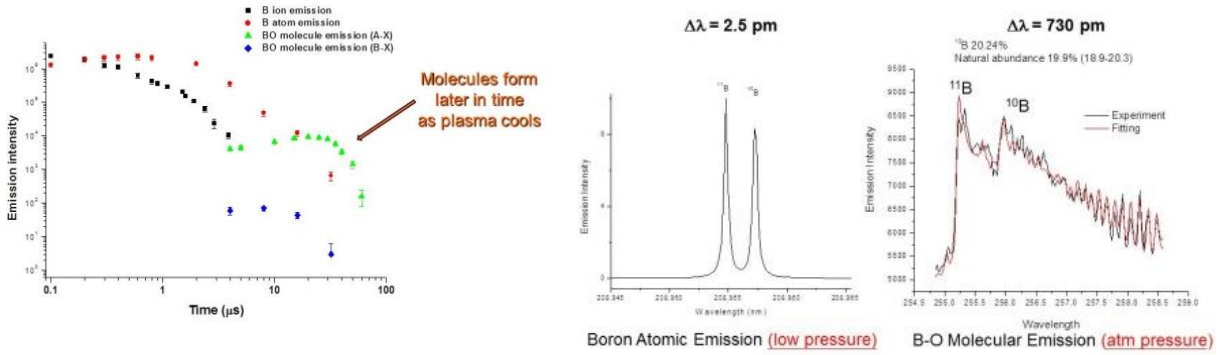

Time dependent emission of species in the laser plasma. Atomic versus molecular isotope emission spectra.

References:

1. R.E. Russo, J.J . Gonzlaez, X.L. Mao, V. Zorba and J. Yoo, *Laser Ablation in Analytical Chemistry, Feature Article,* Analytical Chemistry, 85, 6162 (2013).
2. Arnab Sarkar, Xianglei Mao, George C.-Y. Chan, Richard E. Russo, *Laser Ablation Molecular Isotopic Spectrometry of Water for* $_1D^2/_1H^1$ *ratio analysis,* Spectrochimica Acta B, 88 p46-53 (2013).
3. R.E. Russo, X.L. Mao, J.J. Gonzalez and J. Yoo, *Femtosecond versus Nanosecond Laser Pulse Duration for Laser Ablation Chemical Analysis,* Spectroscopy 28(1) 1 (2013).
4. Mao, X.L., Bol'shakov, A.A., Perry, D.L., Sorkhabi, O., and Russo R.E., *Laser Ablation Molecular Isotopic Mass Spectrometry (LAMIS): Strontium and It's Isotopes, Spectrochimica Acta B66, 767-775 (2011).*
5. Russo, R.E., A.A. Bol'shakov, X.L. Mao, C.P. McKay, D.L. Perry, and O. Sorkhabi, *Laser Ablation Molecular Isotope Mass Spectrometry (LAMIS), Spectrochimica Acta, Part B, Vol. 66, Issue 2, pp. 99-104, (2011).*
6. Russo, R.E., T.W. Suen, A.A. Bol'shakov, J. Yoo, O. Sorkhabi, X.L. Mao, J.J. Gonzalez, D. Oropeza, and V. Zorba. *Laser Plasma Spectrochemistry, J. Analytical At. Spectrometry, Vol 26, 1596 (2011).*

O-14

Controlled Growth of Two-Dimensional Layered Semiconductors from Laser-Synthesized Nanoparticles

M. Mahjouri-Samani[1], M. Tian[3], K. Wang[1], C. M. Rouleau[1], A. A. Puretzky[1], G. Eres[2], I. N. Ivanov[1], K. Xiao[1], M. A. McGuire[2], G. Duscher[3], D. B. Geohegan[1]

[1]Center for Nanophase Materials Sciences, Oak Ridge National Laboratory, Oak Ridge, TN, USA
[2]Materials Science and Technology Division, Oak Ridge National Laboratory, Oak Ridge, TN,USA
[3]Dept. of Materials Science and Engineering, University of Tennessee, Knoxville, TN, USA
E-mail: mahjourisamm@ornl.gov

Two-dimensional layered semiconducting materials, notably the metal chalcogenides and dichalcogenides (GaS, GaSe, GaTe, InSe, *etc.* and MoS_2, WS_2, $MoSe_2$, $NbSe_2$, *etc*.) have recently attracted significant renewed attention due to the novel physical, chemical, electrical and optical properties that can emerge when they are isolated in nanosheets of single- or few-layer thickness [1,2]. Developing new methods for the facile synthesis of layered materials is crucial for emerging applications in functional devices.

Here we demonstrate the use of pulsed laser vaporization (PLV) to form stoichiometric nanoparticles that serve as building blocks for the synthesis of 2D GaSe and $MoSe_2$ layered semiconductors [3,4]. Our PLV approach offers a new synthesis solution to address the challenges of conventional vapor phase growth methods (e.g., CVD), by taking advantage of the spatial confinement of the ablation plume in relatively high background gas pressures to preserve the stoichiometric transfer of material from a bulk target to predefined locations on the substrate while providing sufficient kinetic energy for surface diffusion. After ablation of crystalline targets, the propagation of the laser ablation plume was characterized by *in situ* ICCD-imaging and ion probe analysis. As shown in Fig. 1, we demonstrate the formation of 2D crystals in either nanosheet networks (200 nm domain sizes) or large single crystalline domains (100 µm lateral sizes) with controlled stoichiometry, number of layers, crystallite size, and growth location. Small-domain nanosheet networks are formed by direct deposition of stoichiometric nanoparticles onto heated substrates in an argon background pressure of ~1 Torr.

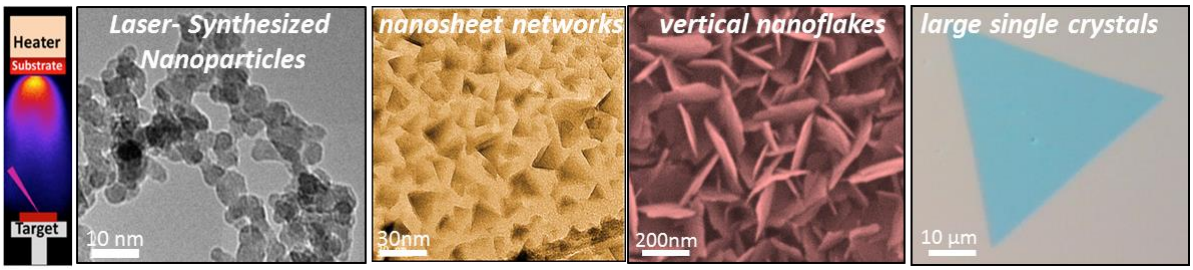

Fig. 1. Growth of 2D nanosheet with different sizes and orientations from laser-synthesised nanoparticles.

To grow large 2D crystals from nanoparticles grown by laser vaporization, room temperature-deposited nanoparticles were sandwiched between two substrates to form a confined vapor transport growth system. Heating from the source substrate side in an inert background gas develops a natural temperature gradient that evaporates the confined nanoparticles from the source substrate to the cooler receiver substrate where crystalline 2D nanosheets are observed to grow in pre-patterned locations. This novel PLV-based synthesis and processing method offers a unique approach for the controlled growth of large-area, metal chalcogenides with a controlled number of layers and sizes in patterned growth locations for optoelectronics and energy related applications.

[1] M. Chhowalla, et al. "The chemistry of two-dimensional layered transition metal dichalcogenide nanosheets" *Nature Chem.* **5**, 263-275 (2013).
[2] S. Z. Butler, et al. "Progress, challenges, and opportunities in two-dimensional materials beyond graphene" *ACS Nano* **7**, 2898-2926 (2013).
[3] M. Mahjouri- Samani, R. Gresback, M. Tian, K. Wang, A. A. Puretzky, C. M. Rouleau, G. Eres, I. N. Ivanov, K. Xiao, M. A. McGuire, G. Duscher, and D. B. Geohegan "Pulsed Laser Deposition of Photoresponsive Two- Dimensional GaSe Nanosheet Networks" *Advanced Functional Materials* **24**(40), 4365 (2014).
[4] M. Mahjouri-Samani, M. Tian, K. Wang, A. Boulesbaa, C.M. Rouleau, A.A. Puretzky, G. Eres, M.A. McGuire, B.R. Srijanto, K. Xiao, G. Duscher, and D.B. Geohegan, "Digital Transfer Growth of Patterned 2D Metal Chalcogenides by Confined Nanoparticle Evaporation,"*ACS Nano* **8**, 11567 (2014).

Research was supported by the U.S. Department of Energy, Office of Science, Basic Energy Sciences (BES), Materials Sciences and Engineering Division and performed in part as a user project at the Center for Nanophase Materials Sciences, which is a DOE Office of Science User Facility.

O-15

Characterisation of femtosecond laser structured cubic-BN

R. Buividas[1,2], I. Aharonovich[3], G. Seniutinas[1,2], L. Rapp[4], X. Wang[1,2], A. V. Rode[4]
T. Taniguchi[5], S. Juodkazis[1,2]

[1]*Centre for Micro-Photonics, Swinburne University of Technology, Hawthorn, VIC 3122, Australia*
[2]*Melbourne Centre for Nanofabrication, 151 Wellington Road, Clayton, VIC 3168, Australia*
[3]*University of Technology Sydney, Thomas St, Ultimo, NSW 2007 Australia*
[4]*Laser Physics Center, Research School of Physics & Engineering, Australian National University, ACT 0200, Australia*
[5]*National Institute for Materials Science, 1-1 Namiki Tsukuba Ibaraki 305-0044 Japan*
E-mail: rbuividas@swin.edu.au

Cubic-BN has mechanical properties similar to diamond however it is not oxidizing at high temperatures in air ambient. Its low-pressure hexagonal phase has a 2D graphene structure with appealing optical, mechanical, and electrical properties; bandgap of c-BN is 6.4 eV and bulk modulus 400 GPa.

Laser pulses of 230 fs duration at 1030 nm and 515 nm wavelengths were focused at a 20 µm depth below the surface of a facet plane inside c-BN crystals. Millimeter-sized grains of c-BN were formed at high pressure conditions using belt-type high pressure apparatus [1]. Tight focusing with numerical aperture NA = 1.42 was implemented to form arrays of damage sites recorded at different pulse energies E_p at a single pulse conditions. Strong contrast changes were observed at threshold values of E_p = 4.5 nJ (515 nm) and 80 (1030 nm) estimated at the focus. Separation between irradiation spots was 10 µm to eliminate a cross talk for void-formation and optical characterisation. For comparison, dense sub-surface array of void-structures were fabricated with 800 nm /150 fs pulses focused with NA = 0.95 at a 10 µm depth.

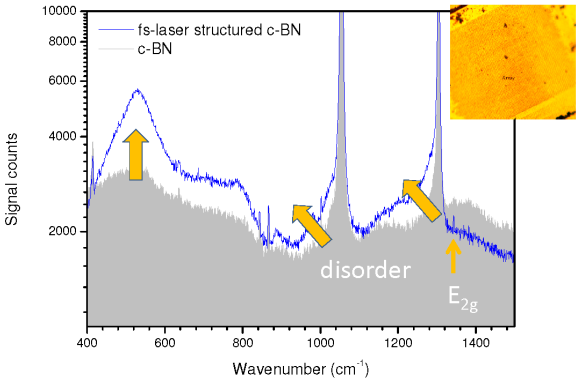

Fig 1. Raman spectra of sub-surface array of void-structures recorded with 800 nm/150 fs pulses. Excitation wavelength of Raman scattering was 785 nm.

Raman scattering and photoluminescence (PL) was measured from the laser modified void-structures in c-BN. Characteristic TO and LO phonon modes were observed with small broadening at the high-energy side of the modes (**Fig. 1**). Back-scattered Raman signal excited by 785 nm irradiation was collected with NA = 0.4 lens averaging response from area with several void-structures. Wide peak at 520 cm^{-1} was the largest modification observed from sub-surface void-structures (800 nm/150 fs). Presence of a lower density h-BN was not confirmed in the void-structures which would be recognisable by its 1350 cm^{-1} E_{2g} mode [2]. Under 405 nm excitation, PL from the void regions (**Fig. 2(a)**) has recognizable features which can be identified as atomic neutral nitrogen N emission at 455, 556, 577 nm [3]. This implies that photolysis of c-BN occurred under high intensity driven by nano-/micro-explosion at the focus. N atoms should be trapped inside the laser shocked region of the void-structure. Molecular N_2 PL which occurs in 300-400 nm window was out of the range of observation in this first test. The PL excited at 405 nm/30 ps illumination showed close to a single exponential decay with time constant of 4 ns (**Fig.2(b)**); under the 532 nm/100 ps excitation the decay was similar 4 ns (not shown here). The PL decay times from the laser structured regions and pristine c-BN were similar; only intensity was different. Formation of voids in materials with the highest bulk modulus exceeding pressures at the Earth's center can bring fundamental understanding how high- pressure/temperature materials are formed. Conditions at the focal region and energy deposition are discussed.

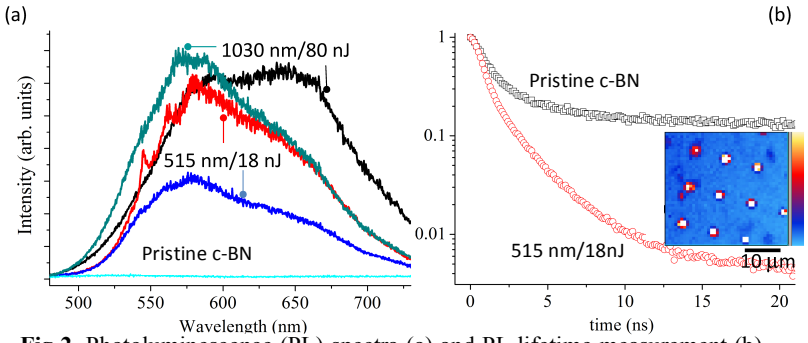

Fig 2. Photoluminescence (PL) spectra (a) and PL lifetime measurement (b) under 405 nm 30 ps excitation from void-structures and pristine c-BN. The inset in (b) shows typical confocal PL map.

References

[1] T. Taniguchi, K. Watanabe, S. Koizumi, I. Sakaguchi, T. Sekiguchi, S. Yamaoka, Ultraviolet Light Emission from Self-Organized p–n Domains in Cubic Boron Nitride Bulk Single Crystals Grown Under High Pressure, Appl. Phys. Lett. 81 (22) 4145 (2002).

[2] S. Reich, A. C. Ferrari, R. Arenal, A. Loiseau, I. Bello, and J. Robertson, Resonant Raman scattering in cubic and hexagonal boron nitride, Phys. Rev. B 71, 205201 (2005).

[3] M. A. Uman, Lightning (Dover Publications, Inc., New York 1984).

I-04

Fundamental aspects of laser-matter interaction: Ultrafast dynamics of insulator-to-metal transitions probed by time-resolved photoemission

Martin Wolf
Fritz Haber Institute of the Max Planck Society,14195 Berlin, Germany
E-mail wolf@fhi-berlin.mpg.de

Photoexcitation of insulating or semiconducting materials above the band gap leads to non-equilibrium processes on ultrafast timescales. Depending on excitation density their dynamics are governed by exciton formation and electron-phonon scattering or more complex processes like material ablation or laser induced phase transitions. Examples are charge-density wave (CDW) materials where at low temperatures a periodic lattice distortion leads to an opening of an electronic gap at the Fermi surface. Here we study femtosecond laser excitation of wide band gap semiconductors as well as more complex materials with strong electron-phonon coupling and many-body correlation effects leading to the formation of insulating, broken symmetry ground states. We use time- and angle-resolved photoemission spectroscopy (trARPES) to study surface excition formation (ZnO) as well as ultrafast insulator-to-metal (IM) transitions in several materials (VO_2, $TbTe_3$, $TiSe_2$).

On ZnO surfaces we observe the formation surface-bound excitons within only 200 fs after photoexcitation, which are stable in the presence of a charge accumulation layer caused by hydrogen adsorption. Strong excitation close to the Mott limit enhances the screening of the Coulomb interaction and reduces the exciton formation probability [1]. On the other hand, for the correlated electron material VO_2, strong photoexcitation leads to an quasi-instantaneous band gap collapse upon photo-excitation, followed by hot carrier relaxation within 200 fs. In conjunction with many body theory, these results show that the photoinduced phase transition is caused by doping of the valence band with photoholes, leading to an significantly enhanced screening of the Coulomb interaction and drastic band gap renormalization [2]. Furthermore, we have studied the ultrafast dynamics of the electronic structure during photo-induced phase transition in the in charge-density wave compounds $TbTe_3$, $DyTe_3$ and $TiSe_2$. Using trARPES we can directly map the transient changes of the Fermi surface and the opening and closing of the CDW gap (see Fig.1) [3]. For $TiSe_2$ we find an unusual binding energy dependence of relaxation rate back to the CDW phase and scaling like the imaginary part of a model self-energy [4]. This is identified as a signature of strong electron-hole scattering driving the electronic instability in phase transition in $TiSe_2$.

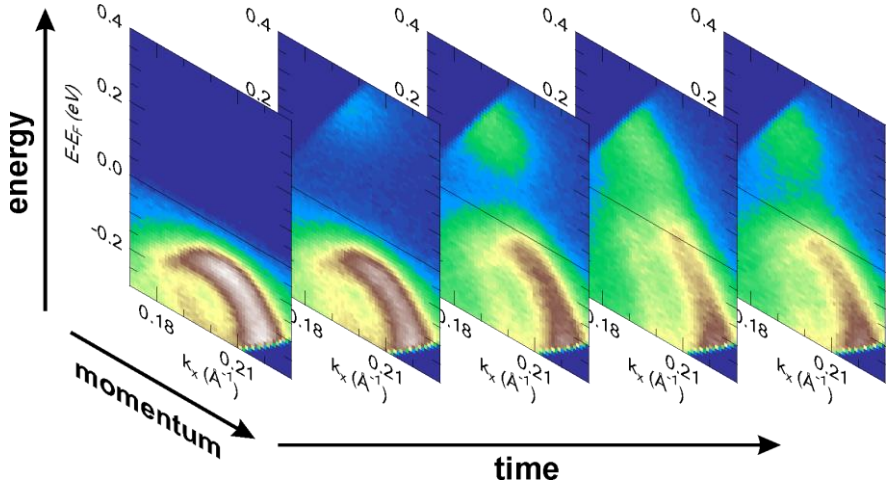

Fig. 1. Time- and momentum-resolved photoemission spectroscopy of the ultrafast band gap collapse in $DyTe_3$ after fs laser excitation.

[1] J.-C. Deinert, *et al*, Phys. Rev. Lett. **113**, 057602 (2014)
[2] D. Wegkamp, *et al*., Phys. Rev. Lett. **113**, 216401 (2014)
[3] L. Rettig, J.-H. Chu, I. R. Fisher, U. Bovensiepena, and M. Wolf, Faraday Discussions **171**, 299 (2014)
[4] C. Monney, *et al*, Phys. Rev. B **85**, 235150 (2012); C. Monney, *et al* (under review).

O-16

Laser-matter interaction in ultra-high DC fields: first-principles calculations

E.P. Silaeva[1], K. Uchida[1], K. Watanabe[1], M.L. Karahka[2], H.J. Kreuzer[2], A. Vella[3]

[1]*Department of Physics, Tokyo University of Science, 1-3 Kagurazaka, Shinjuku-ku, Tokyo 162-8601, Japan*

[2]*Departement of Physics & Atmospheric Science, Dalhousie University, 6310 Coburg Rd., Halifax, NS B3H 4R2, Canada*

[3]*Groupe de Physique des Materiaux, Université de Rouen, Avenue de l'Université - BP12 76801 Saint Etienne du Rouvray, France*

E-mail: elena.silaeva@gmail.com

When a semiconductor or insulator is subjected to high electrostatic DC field, its electrical and optical properties can be strongly altered [1,2]. This phenomenon has dramatic consequences in the domains of Atom Probe and Field Ion Microscopies, Field Emission Microscopies and many field-effect nano-devices, where a semiconductor or insulator nanostructure is biased to a high voltage and DC field can reach huge values up to 1 V/Å (Fig. 1a). Moreover, ultrafast lasers are often employed in these techniques to attain better performance. Thus, the study of laser-matter interaction in high DC field becomes crucial for the advancement in these domains.

In this work, using first-principles calculations we study the behavior of Si and MgO atomic clusters in high DC field and illuminated with a laser pulse (Fig. 2b). First, we performed Density-Functional Theory (DFT) calculations and showed that the HOMO-LUMO gaps of Si and MgO clusters drastically decrease in DC field on the order of 1V/Å (Fig. 1c). Note that HOMO-LUMO gap for molecules and atomic clusters corresponds to band-gap for bulk materials. Then, Time-Dependent DFT study allowed us to introduce the laser illumination and calculate the absorption spectra of Si cluster, demonstrating clear features of the DC-field-induced change in the electronic structures. Finally, the combined TD-DFT and Molecular Dynamics calculations [3] showed that at sufficiently high DC fields, femtosecond laser pulse can trigger the detachment of a Si atom from the cluster.

The theoretical results can be verified using Atom Probe setup (Fig. 1a) [4]. By measuring a flux of atoms emitted from a biased Si and MgO nano-tip as a function of fs-laser pulse intensity and wavelength, we follow experimentally the changes of absorption related to the presence of high DC field.

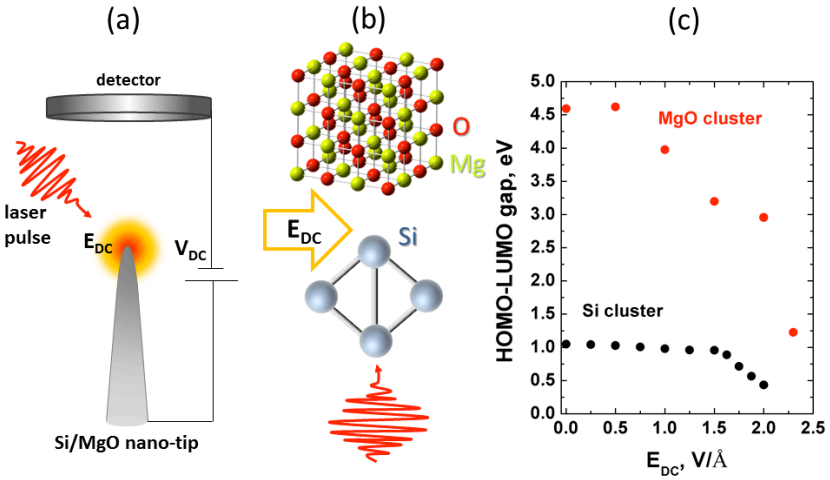

Fig. 1. (a) Typical setup of Atom Probe and Field Ion Microscopy with a semiconductor or insulator nano-tip biased to high DC voltage V_{DC}; (b) MgO and Si atomic clusters used in first-principles calculations, DC field E_{DC} direction is shown by the arrow (c) HOMO-LUMO gaps of clusters as a function of applied DC field.

We gratefully acknowledge the financial support from Tokyo University of Science.

[1] M. Durach, A. Rusina, M. F. Kling, and M. I. Stockman, "Metallization of Nanofilms in Strong Adiabatic Electric Fields," Phys. Rev. Lett. **105**, 086803 (2010).

[2] E. P. Silaeva, L. Arnoldi, M. L. Karahka, B. Deconihout, A. Menand, H. J. Kreuzer, and A. Vella, "Do Dielectric Nanostructures Turn Metallic in High-Electric dc Fields?," Nano Lett. **14**, 6066 (2014).

[3] J. Haruyama, C. Hu, and K. Watanabe, "First-principles molecular-dynamics simulation of biphenyl under strong laser pulses by time-dependent density-functional theory," Phys. Rev. A **85**, 062511 (2012).

[4] A. Vella, "On the interaction of an ultra-fast laser with a nanometric tip by laser-assisted Atom Probe Tomography: A review," Ultramicroscopy **132**, 5 (2013).

O-17

Femtosecond laser fabricated electrofluidic devices enabling 3D flexible manipulation and observation of microorganism motions

J. Xu[1], H. Kawano[2], A. Miyawaki[2], K. Midorikawa[1], K. Sugioka[1,*]
[1]*RIKEN Center for Advanced Photonics, 2-1 Hirosawa, Wako, Saitama 351-0198, Japan*
[2]*RIKEN Brain Science Institute, 2-1 Hirosawa, Wako, Saitama 351-0198, Japan*
E-mail: ksugioka@riken.jp, jxu@riken.jp

Dynamic observation and analysis of the motion of microorganisms is of importance to understand the functions of specific regions in biosamples such as a flagellum for biologists. For this purpose, e. g., studying the rapid motion of the flagellum, a slide glass with a cover glass or a pertri dish is generally used under an optical microscopy equipped with a high-speed camera and a high numerical-aperture objective lens. However, due to the limitation of visually imaging volumes and long observation time, it is very difficult to efficiently capture the flagellum's moving images and thereby analyze the movement dynamics. We previously reported the use of glass microchip with three-dimensional (3D) microfluidic structures fabricated by femtosecond (fs) laser for scaling down the observation site as well as preventing the evaporation of water in the medium, which successfully performed the dynamic observation of 3D motion of *Euglena gracilis* (one kind of single-celled, motile microorganisms) with extraordinarily reduced observation time [1]. Considering random swimming behavior of *Euglena* cells in the previous work, 3D flexible control of the swimming direction of cells in a nondestructive manner will enable us to perform more functional observation for preciously quantitative analysis of flagellar movement. In this paper, we propose the use of monolithically integrated electrofluidic devices in glass based on hybrid fs laser microfabrication for flexible electro-orientation and high-performance observation of 3D motion of *Euglena* cells. In this process, 3D glass microfluidic structures with the smooth inner surface are first prepared by fs laser direct-write modification followed by annealing, successive chemical etching and additional annealing processes. Then, using the same laser, the water-assisted laser ablation on the internal walls of fabricated glass microfluidic structures is performed in a space-selective manner. Finally, the electroless metal plating performs the selective deposition of conductive metal structures on the ablated regions to realize electrofluidics [2]. Compared with conventional fabrication methods, electrodes with designable geometries can be flexibly prepared at any positions in microchannels by this technique. To test the electro-orientation performance, *Euglena* cells were introduced into electrofluidic devices as shown in Fig. 1. As seen from Figs. 1a, 1c and 1e, the cells were randomly swimming in the channels when no electric field was applied. Once the proper electric field was applied between the electrodes, the movement of cells dramatically changed to be bidirectionally oriented along the direction of electric field (Figs. 1b, 1d and 1g). Particularly, swimming of cells can be oriented along z-direction using outlined square electrodes formed at the top and bottom of the channel (see Fig. 1d), which makes it much easier to observe the flagellar motion from the front side. In contrast, four electrodes confronting each other at a right angle formed on the bottom of the channel successfully demonstrate controllable electro-orientation of cell movement in the x-y plane by changing the direction of electric field generated in the microscale space (Figs. 1f and 1h). The fabricated electrofluidic devices allow us to perform tracking observation of specific cells manipulated with the electric field with high efficiency as well as to quantitatively analyze the effects of electrical forces on manipulation.

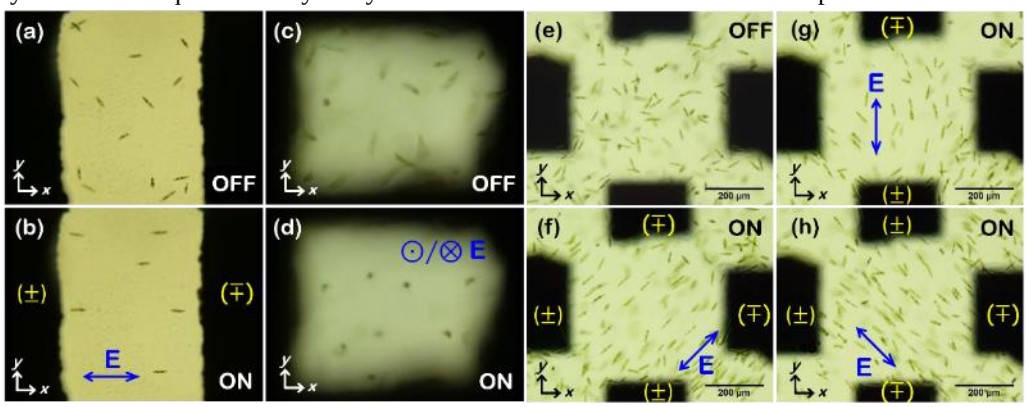

Fig. 1. 3D manipulation of movement of *Euglena* cells in fs laser fabricated electrofluidic devices. (a-b) a pair of electrodes formed at the bottom of a channel; (c-d) outlined square electrodes formed at the top and bottom of a channel. (e-h) four electrodes confronting each other form at the bottom of a channel. Black areas are the electrodes. "ON" and "OFF" refer to electric power. "±" and "∓" indicate the transient polarity of the applied AC electric field (10 Vp-p, (b) 0.9 MHz and (d, f, g, h) 2 MHz), i.e., "±" and "∓"mean the opposite polarities. The arrows indicate the direction of electric field. Electrode spacing in (a-b) and side length of the observation widow in (c-d) are ~500 μm.

References

[1] Y. Hanada, K. Sugioka, H. Kawano, I. S. Ishikawa, A. Miyawaki, and K. Midorikawa, *Biomed. Microdevices*, **10**, 403 (2008).
[2] J. Xu, D. Wu, Y. Hanada, C. Chen, S. Z, Wu, Y. Cheng, K. Sugioka, and K. Midorikawa, *Lab Chip*, **13**, 4608 (2013).

O-18

3D Integrated Photonics: A new enabling technology for astronomy, telecommunications, sensing and quantum science

S. Gross, I. Spaleniak, Z. Chaboyer, A. Arriola, M. Ams, P. Dekker, A. Fuerbach, L. Helt, M. J. Steel and M. Withford

MQ Photonics Research Centre & Centre for Ultrahigh-bandwidth Devices for Optical Systems (CUDOS), Department of Physics and Astronomy, Macquarie University, NSW 2109, Australia

michael.withford@mq.edu.au

There is an ever-growing need for compact and low cost integrated optical devices for use in applications such as communications and sensing. Standard technologies used for the fabrication of such guided wave devices include ion exchange and etching of silicon-on-insulator and silica-on-silicon wafers. These are inherently 2D in nature. A relatively new fabrication method that also shows good promise in this field is that of ultrafast laser direct-writing. It was shown in 1996 that focussed ultrafast laser pulses can induce a permanent refractive index change inside dielectric media; a process initiated via various nonlinear mechanisms. Because the absorption is nonlinear, material modification remains localised at the focal point where the laser intensity is highest. Thus, by translating the material through the focus of an ultrafast laser beam, a pathway of refractive index change can be produced. By varying the writing geometry, the material and ultrafast laser properties, 2D and 3D optical waveguide devices with different characteristics can be fabricated in the bulk of many transparent materials. In addition, ultrafast laser direct writing can be applied to a range of different glasses (and crystals) without the requirement for photosensitivity, and different glass geometries including bulk, fibre and micro-structured fibre.

The capacity for 3D architectures enables device designs that are not achievable using standard planar fabrication methods based on lithography. Embedded waveguide circuitry inside a single piece of bulk glass introduces additional advantages such as high tolerance to vibration and temperature variations. These attributes have been exploited to create integrated photonic lanterns that map multimode light to single mode channels [1], multimode-multimode filters [2], high bandwidth mode selectors [3] and pupil remappers planned for future exoplanet searches [4]. The wavelength range of passive devices of this type span from the visible to the mid – IR, with low propagation losses of < 0.3 dB/cm measured from 1.0 to 4.0 µm. Recent outcomes of 3D integrated photonics applied to the fields of astronomy, telecommunications and quantum science will be presented.

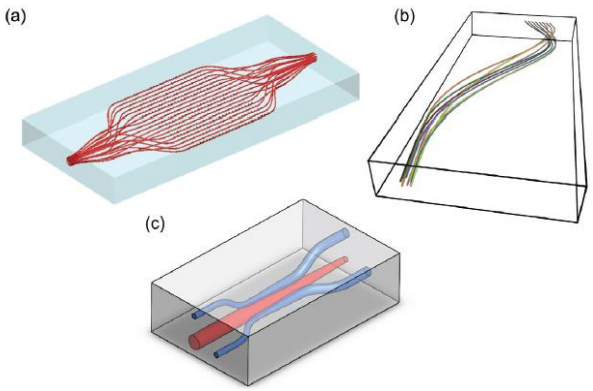

Fig. 1. (a) 3D sketch of two photonic lanterns back-to-back connected by 19 identical waveguide Bragg-gratings for OH-emission suppression during astronomical observations. (b) 3D pupil-remapping chip consisting *of* 8 precisely path length-matched waveguides designed for aperture masking interferometry for the detection of exo-planets. (c) Tapered coupler for multiplexing and de-multiplexing of spatial modes in future space-division multiplexed optical communication systems.

[1] I.Spaleniak, N. Jovanovic, S. Gross, M. J. Ireland, J. S. Lawrence and M. J. Withford, "Integrated photonic building blocks for next-generation astronomical instrumentation II: the multimode to single mode transition", Opt. Exp., **21** 27197 (2013).

[2] I. Spaleniak, S. Gross, N. Jovanovic, R. J. Williams, J. S. Lawrence, M. J. Ireland and M. J. Withford, "Multiband processing of multimode light: combining 3D photonic lanterns with waveguide Bragg gratings", Laser & Photon. Rev., **8** L1 (2014).

[3] S. Gross, N. Riesen, J. D. Love and M. J. Withford, "Three-dimensional ultra-broadband integrated tapered mode multiplexers", Laser & Photon. Rev., **8**. L81 (2014).

[4] N. Jovanovic, P. G. Tuthill, B. Norris, S. Gross, P. Stewart, N. Charles, S. Lacour, M. Ams, J. Lawrence, A. Lehmann, C. Niel, G. D. Marshall, G. Robertson, M. Ireland, A. Fuerbach and M. J. Withford, "First starlight demonstration of an integrated pupil-remapping interferometer: A new technology for high contrast exoplanetary imaging", J. Monthly Notices of the Royal Astronom. Soc., **427** 806 (2012).

O-19

Tuning Dispersion by Controlling Phase Variation in a Ring Resonator Coupled with Mach-Zehnder Interferometer

Hao Zhang, Jiayang Chen, Junjie Jin, Jian Lin, Long Zhao, Zhuanfang Bi, Anping Huang, Zhisong Xiao†

Key Laboratory of Micro-nano Measurement-Manipulation and Physics (Ministry of Education), School of Physics and Nuclear Energy Engineering, Beihang University, Beijing 100191, China
Corresponding Author e-mail address: zsxiao@buaa.edu.cn

Abstract

The group velocity of light pulses v_g can be controlled in dedicated media through material dispersion, in which the group velocity may be lower than the light velocity in vacuum c (slow light) or larger than c (fast light) or negative (backwards light). Otherwise, tuning dispersion to control the group velocity can also be attained through structural dispersion such as optical ring resonators which are very dispersive around its resonant frequency. In a ring resonator there are two methods to control v_g : one is tuning coupled coefficient between ring resonator and straight optical waveguide, the other is introducing active gain to change propagation loss in the resonator. However, the coupled coefficient is determinated by processing technology and cannot be changed after fabricating. And introducing active gain such as doping rare-earth ions Er^{3+} into optical waveguide material is a complicated process. What's more, tuning range of the group velocity of light is limited by the luminescence capability of rare-earth ions in the optical waveguide material. In this paper, we propose a ring resonator coupled with Mach-Zehnder Interferometer (MZI) structure in which the dispersion is tunable through two phase shift variation points in the MZI's arm and into the ring resonator respectively. In this way, the group velocity of light into the ring resonator can be controlled easily into the "slow light", "fast lgiht" and "backwards light" region and in this structure we can obtain positive and negative group velocity in larger range than a single ring resonator coupled with a straight optical waveguide structure. Moreover, the capability of tuning dispersion of the cascade of MZI-coupled resonator structure is analysed and compared with cascade of ring resonator structure.

References

[1] H. Uranus and H. Hoekstra, "Modeling of Loss-Induced Superluminal and Negative Group Velocity in Two-Port Ring-Resonator Circuits," J. Lightwave Technol. **25**, 2376-2384 (2007).
[2] J. E. Heebner, R. W. Boyd, and Q. H. Park, "Slow light, induced dispersion, enhanced nonlinearity, and optical solitons in a resonator-array waveguide," Physical Review E **65**, 036619 (2002).
[3] R. W. Boyd, and D. J. Gauthier, "Controlling the Velocity of Light Pulses," Science, **326** (5956), 1074-1077 (2009).
[4] W. Green, R. Lee, G. DeRose, A. Scherer, and A. Yariv, "Hybrid InGaAsP-InP Mach-Zehnder Racetrack Resonator for Thermooptic Switching and Coupling Control," Opt. Express **13**, 1651-1659 (2005).
[5] T. Ye, Y. Zhou, C. Yan, Y. Li, and Y. Su, "Chirp-free optical modulation using a silicon push-pull coupling microring," Opt. Lett. **34**, 785-787 (2009).

O-20

Laser Induced Forward Transfer for improving fine line metallization in photovoltaic applications.

M.I. Sanchez-Aniorte, A.P. Alloncle, T. Sarnet, P. Delaporte
Aix Marseille Université, CNRS, LP3 UMR 7341, 13288, Marseille, France
E-mail: sanchez@lp3.univ-mrs.fr

Introduction

Grand challenges to create new front metallization techniques in photovoltaics focus considerable attention on LIFT approach. This alternative method aims to overcome the limitations of the well-established and mature screen-printing technique. Such limitations are for instance: restrictions in the grid pattern design, high temperature steps, and poor aspect ratio of the line contact [1]. Although different new front contact metallization concepts have been studied like ink-jet printing, light induced plating or photolithography, etc., most of them require relatively complicated or expensive processing steps and are not attractive for industrial production [2, 3]. As a result it is desirable to find innovative metallization techniques to improve the cell efficiency without significantly increasing the cost. As mentioned before, a very promising metallization concept, which can be implemented in production lines, is based on a single-step LIFT from thick film Ag inks [4]. But many challenges remain before obtain high-quality, robust and high performance LIFT contacts formation and it is required a fully theoretical and experimental assessment.

With this intention the direction which is followed by Lasers, Plasmas and Photonic Processes Institute (LP3) was to develop and optimize LIFT technique to create front side metallization for photovoltaic applications. This paper presents the results of a study of LIFT technique to create high quality and good relation aspect contacts prepared from thick Ag-based inks. The process provides precision deposits of silver inks films onto a working substrate. The beam of a picosecond pulsed laser (Continuum Leopard SS-10-SV Nd:YAG, 10hz, 50ps, at 355 nm third harmonic) is imaged on the donor. The receiver substrates are located on micrometer translation systems (x, y, z). The laser pulses interact with the liquid film and propel the ink away from the substrate. The ejected material exhibits different regime of ejection depending of the viscosity of the liquid [5, 6]. We focus on this paper on the ejection of high viscosity paste. For successful LIFT front contact formation a full understanding of the fluid dynamics of the accelerating ink films is critical.

Finally, complete morphological study was carried out with Scanning Electron Microscopy (SEM), Energy Dispersive X-ray (EDX) spectrometry and Confocal microscopy. The fluid dynamics of the ejected material has been studied by time-resolved imaging technique. The results and fundamental investigations of the processes underlying the technique illustrate the role played by different laser parameters in the evolution of microstructure and electrical properties of the deposited material.

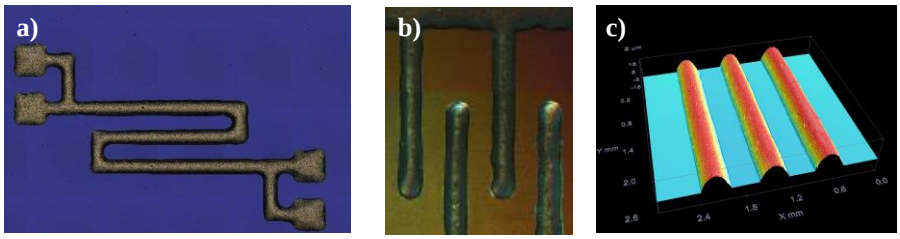

Fig.1. LIFT printed lines of Ag NP paste (NPS from Harima Inc.) annealed at 220°C during one hour. The line width is 180 µm. a) printing on Si, b) printing on polyimide c) the analysis of the lines by confocal microscopy demonstrates a very good homogeneity and spatial resolution obtained with the LIFT process.

References

[1] G. Poulain, C. Boulord, D. Blanc, A. Kaminski, M. Gauthier, C. Dubois, B. Semmache, M. Lemiti, "Direct laser printing for high efficiency silicon solar cells fabrication" Applied Surface Science, Vol. 257, Issue 12, pp. 5241-5244 (2011).

[2] M.A. Green, "Third generation photovoltaics: solar cells for 2020 and beyond". Physica E. Vol.14, pp.65-70 (2002).

[3] A. Lennon, Y.Yao, S. Wenhamm "Evolution of metal plating for silicon solar cell metallization. " Progress in Photovoltaics: Research and Applications (2012).

[4] E. Breckenfeld, H. Kim, R.C.Y. Auyeung, N. Charipar, P. Serra, A. Piqué, "Laser-induced forward transfer of silver nanopaste for microwave interconnects", Applied Surface Science, Vol. 331, pp. 254-261 (2015).

[5] E. Biver, L. Rapp, A.P. Alloncle, P. Serra, P. Delaporte, "High-Speed Multi-Jets Printing using Laser Forward Transfer : Time-Resolved Study of the Ejection Dynamics", Optics Express, Vol. 22, pp. 17122–17134 (2014).

[6] L. Rapp, J. Ailuno, A. Alloncle, and P. Delaporte, "Pulsed-laser printing of silver nanoparticles ink: control of morphological properties" Opt. Express, Vol. 19, pp. 21563-21574 (2011).

Monday
31 August 2015

Poster presentations

P-001

Colour centres in KBr induced by femtosecond laser pulses

Xuewen Wang[1], Ričardas Buividas[1], Saulius Juodkazis[1,2]

[1]Centre for Micro-Photonics, Faculty of Science, Engineering and Technology,

Swinburne University of Technology, Hawthorn, VIC 3122, Australia

[2]Melbourne Centre for Nanofabrication, 151 Wellington Road, Clayton, VIC 3168, Australia

E-mail: xuewenwang@swin.edu.au

Colour centres in alkali halides have many practical applications in high density memory devices, tunable lasers, single molecule trapping, and super-continuum sources [1-4]. For these applications a simpler femtosecond laser direct write method can be used. It is the most efficient and controllable 3D coloration as compared to electron, ion bombardment and X or γ ray irradiation. One layer of exposed laser regions was coloured in pure KBr crystal at a 100 μm depth with direct laser writing (DLW). KBr become dark blue in locations irradiated by 1030 nm wavelength, 220 fs duration pulses focused by a numerical aperture NA = 0.7 objective lens. The 5 mm long lines with 2 μm separation were fabricated with 5 - 20 nJ (at focus) energy pulses at pulse density of 10 pulses per 1 μm and 1 mm/s scan speed. The absorption spectrum as shown in Fig. 1a with five distinct bands designated as V, F, R1, R2 and M bands, which were in good accordance with the theoretical prediction for the alkali halides [5]. Each band has a particular charge pattern illustrated in Fig. 1b. From the absorption spectrum, the density of colour centres was calculated using Smakula formula (Fig. 1b). The density of the F centre was estimated as high as 5.3 x 10^{18}cm^{-3}, which colored KBr in dark blue. Under the red(white) light illumination centered at F-band the coloration faints. When structural damage was created with 20 nJ pulses (irradiance 3.6 TW/cm^2) the coloration becomes permanent at the focal region where structural changes of crystal matrix are created. Polarization effects of the writing beam on the transmission of a linearly polarized light at the colour center absorption band were investigated.

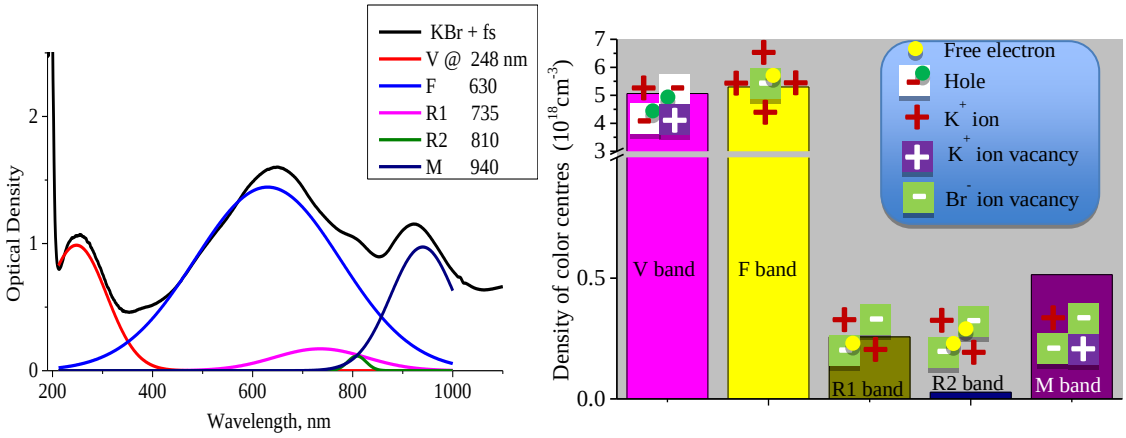

Fig.1 (a). The absorption spectrum of KBr after DLW with fs-laser pulses. (b) The density of different colour centres and their configuration (e.g., F centre was formed by a Br^- ion vacancy with a trapped electron.)

References

[1] V. V. Ter-Mikirtychev et al., "Stable room-temperature tunable color center lasers and passive Q-switchers," Prog. Quant. Electron. **20**, 219 (1996).

[2] E. J. Caine, et al. "Optical data storage in LiF using electron beam encoding," J. Vac. Sci. Technol. B. **16**, 3232 (1998).

[3] L. Nony, et al. "Observation of Individual Molecules Trapped on a Nanostructured Insulator," Nano Lett. **4**, 2185 (2004).

[4] J. Nimsch, et al. "LiF, an underestimated supercontinuum source in femtosecond transient," Opt. express **21**(14), 17060 (2013).

[5] H. Ivey, "Spectral Location of the Absorption Due to Color Centers in Alkali Halide Crystals," Phys. Rev. **72**, 341 (1947).

P-002

Study on effects induced by ultrashort laser pulses focused inside transparent materials

Béla Hopp[1], Tomi Smausz[2,1], Tamás Gera[1], Judit Kopniczky[1], Csaba Vass[1], Martin Ehrhardt[3], Pierre Lorenz[3], Klaus Zimmer[3]

[1]*Department of Optics and Quantum Electronics, University of Szeged, H-6720 Szeged, Dóm tér 9, Hungary*
[2]*MTA-SZTE Research Group on Photoacoustic Spectroscopy, University of Szeged, 6720 Szeged, Dóm tér 9, Hungary*
[3]*Leibniz-Institut für Oberflächenmodifizierung e. V., Permoserstr. 15, 04318 Leipzig, Germany*
Corresponding Author e-mail address: bhopp@physx.u-szeged.hu

1. Introduction

Tight focusing of femtosecond laser pulses gives the possibility of reaching ultrahigh intensities and creating extreme conditions during laser pulse - material interactions.

Formation of particular structures consisting of nanovoids has potential applications in plasmonics and nanophotonics. Such voids can be produced in transparent dielectric materials by single- or multipulse irradiation with focused high intensity femtosecond lasers [1]. It was demonstrated that the focusing of the laser power in a volume of diameter in the order of the laser wavelength can result in multiple ionization of the atoms forming a quickly expanding plasma and shock wave with pressures in the order of terapascals [2]. Since this pressure value exceeds with orders of magnitude the strength (Young modulus) of the irradiated material, at the compressing and rarefaction period of the shock wave reversible (melting/solidifying) and irreversible phase changes (e.g. transition from crystalline into amorphous state) can occur. Besides the amorphous material the presence of nano-crystallites with increased density was also demonstrated by transmission electron microscopic and X-ray diffraction studies [3, 4].

Our aim was to study effects induced by focusing of femtosecond laser pulses inside different optical materials and to form modified regions around the produced nanovoids having optical and mechanical properties different from that of starting material.

2. Experiments and results

Pulses of a Ti-sapphire laser (CPA-2001, Clarc MRX: λ=775 nm, FWHM=150 fs) operated at 1 kHz repetition rate were focused into the transparent targets with an 50X microscope objective (NA=0.8). During the processing the target was placed onto an XYZ translator and was continuously scanned over a range of 0.5×0.5×0.2 mm^3 resulting in a 3D array of 50×50×10 focal sites, each of them receiving one single laser shot. The pulse energy reaching the sample surface was varied in 7-170 µJ range. The irradiated materials were fused silica, YVO_4, $CaCO_3$, KTiOPO4 (KTP) and $LiNbO_3$. The polarisation plane was set as to avoid the multiple focusing in anisotropic samples.

The threshold pulse energy for void formation was estimated for the applied materials. The largest lateral size of the produced voids was ~4µm. At the elevated pulse energies the cracking of the crystals was observed which makes difficult the study of effects related to high energy shock waves generated inside the materials.

The prepared voids and their neighbouring layers could be analysed after proper cutting, polishing and etching of the samples. The characteristic properties of the modified volumes were examined with different methods: optical microscopy, micro-Raman spectroscopy, electron microscopy and optical energy dispersive X-ray spectroscopy. On the basis of the obtained results further, more detailed studies will be made using promising experimental parameters.

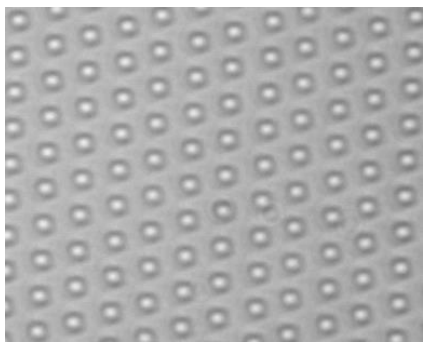

Fig. 1. Optical microscopic image of an array of voids produced in $LiNbO_3$ at 170 µJ pulse energy.

3. References

[1] S. Juodkazis, H. Misawa, T. Hashimoto, E. G. Gamaly, and B. Luther-Davies, Appl. Phys. Lett. **88** 201909 (2006)
[2] E. E. Gamaly, S. Juodkazis, K. Nishimura, H. Misawa, B. Luther-Davies, L. Hallo, P. Nicolai, and V. Tikhonchuk, Phys. Rev. B **73** 214101 (2006)
[3] S. Juodkazis, H. Misawa, E.G. Gamaly, B. Luther-Davies, A.V. Rode, L. Hallo, P. Nicolai, and V.T. Tikhonchuk, AIP Conf. Proc. Vol **955** 1041 (2007)
[4] V. Mizeikis, S. Kimura, N.V. Surovtsev, V. Jarutis, A. Saito, H. Misawa, and S. Juodkazis, Appl. Surf. Sci. **255** 9745–9749 (2009)

P-003

Two dimensional numerical modeling of TWIN-LIBWE method for interpretation of submicrometer grating fabrication in fused silica

C. Vass[1,2], A. Kemeci[1], B. Hopp[1]
[1]*Department of Optics and Quantum Electronics, University of Szeged, H-6720 Szeged, Dóm tér 9, Hungary*
[2]*ELI-HU Non-Profit Ltd.., Dugonics tér 13, H-6720 Szeged, Hungary*
Corresponding Author e-mail address: vasscsaba@physx.u-szeged.hu

The periodically structured transparent materials have a wide range of application possibilities: these can be applied as transmission gratings, in sensing and special spectroscopy techniques (OWLS), etc. The two-beam interferometric laser-induced backside wet etching (TWIN-LIBWE) method is a well suited, competitive procedure for structuring of these materials (especially for grating fabrication in fused silica surface) due to the achievable high resolution (reachable minimum grating period is ≈100 nm) and good controllability [1].

The reachable minimum grating period is limited in TWIN-LIBWE by optically: the applied laser wavelength, the incident angle and the relevant refractive indexes determined the achievable minimum grating period. Beside this obvious optical limitation, the thermal effects also limit the achievable resolution. If the heat diffusion length [2] is comparable with the grating constant, the material can be removed not only from the intensity maximums of the interference pattern, but from the minimums, too. This could be the reason that the modulation depth of structure drastically decreased if the period reach the magnitude of the heat diffusion length [1]. However, the heat diffusion length does not describe completely the lateral heat diffusivity. Therefore our motivation was to simulate numerically the grating fabrication during TWIN-LIBWE procedure to verify our above described assumptions. We aimed to study the effects of lateral heat diffusion in this periodical irradiation pattern on the resulted grating structure. To achieve this objective, we extended our previously published one dimensional LIWBE model [3-4] to two dimensional, including the lateral heat diffusion.

The material removal during LIBWE procedure can be attributed to basically thermal (high temperature target surface), chemical (modification of hydrocarbon absorber and the carbon contamination of target surface) and mechanical (high pressure jet and bubble) effects. The latter one was not taken into account in this model. During our calculation the two-dimensional heat flow equation was solved by the finite differences method. The phase changes and the temperature-dependent thermal parameters of the relevant materials are included. The absorption of thin, carbon contaminated fused silica film and the removal of boiled layer from the transparent target surface are also taken into consideration. The incoming laser intensity has sinusoidal profile: one grating period was taking into account with the consideration of proper boundary conditions. In our model the heat can propagate both perpendicularly to the liquid-target boundary and parallel to the surface (perpendicularly the grooves). The average laser fluence and the grating periods were swept in the following ranges: fluence: 200-600 mJ/cm^2; period: 100-1000 nm. The etched profiles were perfectly calculated with our model.

The results were similar as we expected: in the smaller period cases (p=100 and 200 nm) the lateral heat diffusion become dominant and the modulation depth decreases, while for higher periods (p>5-600 nm) the decreasing of modulation depth is not significant.

[1] Cs. Vass, K. Osvay, T. Véső, B. Hopp, " Submicrometer grating fabrication in fused silica by interferometric laser induced backside wet etching technique ", Appl. Phys. A **93**, 69-73 (2008)
[2] D. Bäuerle, Laser Processing and Chemistry, 3rd edn. (Springer, Berlin, 2000)
[3] Cs. Vass, B. Hopp, T. Smausz, F. Ignácz, "Experiments and numerical calculations for the interpretation of the backside wet etching of fused silica", Thin Solid Films **453-454** 121-126 (2004)
[4] Cs. Vass, J. Budai, Z. Schay, B. Hopp, "Interpretation and Modeling of Laser-Induced Backside Wet Etching Procedure", JLMN-Journal of Laser Micro/Nanoengineering **5**(1) 43-47 (2010)

P-004

Time-resolved measurement of femtosecond laser energy deposition in fused silica

O. Utéza, M. Lebugle, M. Sentis, and N. Sanner

Aix Marseille Univ., CNRS, LP3 UMR 7341, 163 avenue de Luminy C.917, 13288 Marseille, France

Corresponding Author e-mail address: uteza@lp3.univ-mrs.fr

Pump-and-probe experiments are routinely implemented in science to investigate the physical mechanisms governing matter transformation submitted to an external excitation [1]. In this context, due to their brevity, femtosecond pulses are an ideal tool to study the dynamics of the physics taking place during laser-matter interaction [2].

In this work, we develop laser-matter interaction experiments with a 500 fs pump pulse and a 60 fs probe pulse, with their characterization relying on an adapted frequency-resolved optical gating technique [3]. Major advantage of the developed set-up is that the time calibration is directly realized in-situ (*using the sample itself*), and in the exact configuration of the pump-probe experiment, thus allowing us to determine with high precision the dynamics of laser energy deposition in dielectrics.

In particular, by monitoring the change of transient optical properties read by the short probe, we are able to retrace the time-resolved evolution of pump absorption by the free-electron plasma developing at the surface of a fused silica target irradiated by a single femtosecond pulse as a function of laser fluence (see Figure 1 as an example for F = 3.9 $F_{th,LIAT}$, with $F_{th,LIAT}$ the laser-induced ablation threshold fluence) [4]. The precise calibration of time zero allows us to measure precisely the effective duration of i) absorption of the fs laser pulse and ii) of plasma relaxation as well as iii) the characteristics of the plasma mirror formed at the surface of the transparent material. These results and related knowledge help to fully understand laser energy deposition and ionization in dielectrics and to optimize laser-based micromachining processes [5,6].

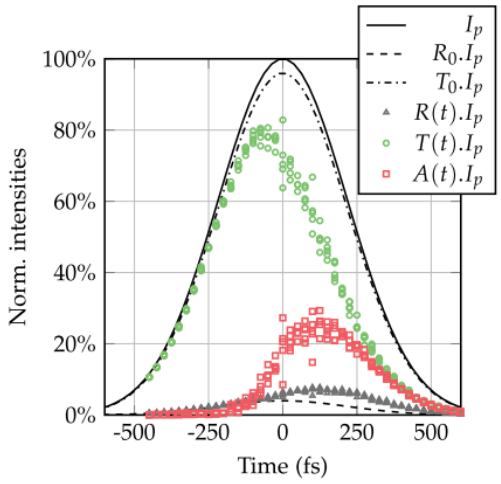

Fig. 1. Transmitted (green circles), reflected (grey triangles) and absorbed (red squares) intensity fractions of the pump pulse resulting from the interaction with the plasma at $3.9F_{th,LIAT}$. The black dashed and dash-dotted lines indicate the reflectivity and transmissivity of SiO_2 at rest, respectively. $F_{th,LIAT}$ = 5.8 J/cm², with F expressed in terms of peak fluence ($F = \frac{2E}{\pi w_0^2}$). In these experiments, $w_0 \cong 14.1$ µm.

Acknowledgements.

Financial support of CNRS through the PICS n°45052 is gratefully acknowledged. We also thank Prof. E. Gamaly and Prof. A. Rode for valuable discussions.

References

[1] J-C. Diels, W. Rudolph in, *Ultrashort laser pulse phenomena*, (Acad. Press, San Diego, 1996).
[2] A. Horn in, *Ultra-fast Material Metrology*, (Wiley-VCH, Weinheim, 2009).
[3] R. Trebino, *Frequency-Resolved Optical Gating: The Measurement of Ultrashort Pulses* (Kluwer Academic Pub., Dordrecht, 2002).
[4] M. Lebugle, N. Sanner, N. Varkentina, M. Sentis, O. Utéza, "Dynamics of femtosecond laser absorption of fused silica in the ablation regime", J. Appl. Phys. **116**, 063105 (2014).
[5] G.M. Petrov, J. Davis, "Interaction of intense ultra-short laser pulses with dielectrics", J. Phys B: At. Mol. Opt. Phys. **41**, 025601 (2008).
[6] M. Lebugle, N. Sanner, O. Utéza, and M. Sentis, "Guidelines for efficient direct ablation of dielectrics with single femtosecond pulses", Appl. Phys. A **114**, 129-142 (2014).

P-005

Comparative study of nanoparticle-assisted resonant and non-resonant ultrafast laser nanocavitation

R. Lachaine[1], C. Boutopoulos[1,2], A. Dagallier[1], P.Y. Lajoie[1], D. Rioux[1],E. Boulais[3], Michel Meunier[1]

[1]Laser Processing and Plasmonics Laboratory, Engineering Physics Department, Polytechnique Montréal, Montréal, Québec H3C 3A7, Canada

[2]SUPA, School of Physics and Astronomy, University of St. Andrews, North Haugh, St. Andrews, KY16 9SS, UK

[3]Massachusetts Institute of Technology, Department of Biological Engineering, 77 Massachusetts Avenue, Cambridge, MA, USA 02139

E-mail: remi.lachaine@polymtl.ca

Plasmonic nanoparticle (NP)-enhanced laser nanocavitation (or plasmonic bubble (PB)) is crucial for a variety of biomedical research fields such as cancer treatment, imaging, disease detection, drug and gene delivery [1]. In this paper, we present a comparative study of nanobubble generation using non-resonant gold nanoparticles (AuNPs) and resonant silica/gold core-shell nanoparticles (CSs) under infrared ultrafast laser irradiation. We investigated the different PB generation mechanisms and the cavitation/disintegration thresholds using a variety of techniques, such as pump-probe single NP imaging, scattering pump-probe PB detection, *in-situ* dark-field imaging, *in-situ* spectroscopy and TEM.

For non-resonant AuNPs, we investigated the role of the near-field and laser pulse width in the nanocavitation mechanism around nanocavitation threshold laser fluences. In order to ensure a systematic alteration of the near-field we used a variety of AuNPs with sizes ranging from 80 nm to 210 nm. We observed a clear dependence of both the nanocavitation laser fluence threshold ($F_{PB,th}$) and the AuNP disintegration laser fluence threshold ($F_{D,th}$) on the AuNP size. Depending on this size and the laser pulse width, the $F_{D,th}$ / $F_{PB,th}$ ratio varies between ~ 3.5 to ~ 7, indicating a broad processing window. Within this processing window, the AuNPs present noticeable ability to generate multiple micron-size PBs with fluences ranging from 80 to 200 mJ/cm^2 without any decrease in cavitation efficiency. Further experimental investigations and plasma modeling both show that optical breakdown is the dominant mechanism for the PB generation in the fs regime. Ultrafast AuNPs excitation thus enabled the PB generation without any particle damaging.

For resonant CSs, we observed micron-size PB generation with fluences ranging from 8 to 20mJ/cm^2, 10 times lower than with AuNPs, while avoiding the complete particle destruction. The PB formation can arise from two main energy sources: heat transfer from the hot particles and plasma relaxation in the water surrounding those particles. For ultrafast pulses, we show that a unique combination of those two mechanisms leads to cavitation, facilitating PB production. A complete TEM CSs damaging characterization revealed three damaging regimes in which the CSs are subsequently cracked, melted and completely destroyed. We show the existence of a processing window for which the CSs are melted (not destroyed) and can generate PB.

Comparing the two particle types, non-resonant AuNPs result in an optical breakdown driven cavitation mechanism that leaves the particles intact. Generating PB requires relatively high fluences, in the order of few hundreds of mJ/cm^2. Those high fluences could limit *in-vivo* treatments. On the other hand, resonant CSs result in a unique combination between heat transfer and breakdown cavitation mechanisms followed by CSs melting. This melting limits the possibility of multiple treatments using the same particles. However, generating PB with resonant CSs requires much lower fluences than with non-resonant AuNPs. This low fluence (few tenths of mJ/cm^2) could allow for treatment in deeper tissue.

In conclusion, we demonstrate that ultrafast laser PB generation strongly depends on the NP selection. Future *in-vivo* applications would have to meet both low threshold treatment and NP integrity requirements. In this context, our findings can be the basis for further development of PB-based nanosurgery as an efficient therapeutic tool.

[1] E. Boulais, R. Lachaine, A. Hatef, and M. Meunier, "Plasmonics for pulsed-laser cell nanosurgery: Fundamentals and applications," Journal of Photochemistry and Photobiology C: Photochemistry Reviews**17**, 26-49 (2013).

P-006

Origin of photoinduced change in optical properties of chalcogenide glass

Haizheng Tao[1]*, Pengpeng Wang[1], Zhiyong Yang[2], Rongping Wang[3]

[1] *State key laboratory of silicate materials for architectures (Wuhan University of Technology), Wuhan, 430070, P.R. China*

[2] *School of Physics and Electronic Engineering, Jiangsu Normal University, Xuzhou, Jiangsu 221116, P.R.China*

[3] *The Australian National University, Laser Physics Centre, Canberra, ACT 2600*

* *Correspondent author, E-mail: thz@whut.edu.cn*

Chalcogenide glasses have been intensively investigated during the last several decades due to their potential applications in many fields such as information storage and integrated optics. Recently significant achievements have been made regarding the understanding of microscopic mechanism of some photo-induced effects. However, the nature of many intriguing phenomena in these glasses is not well understood. In this report, the phenomena of photoinduced transmitting change and photoinduced second harmonic generation in chalcogenide glass were focused. Based on the detailed structural characterization before and after irradiation, together with corresponding theoretical analysis, the origin of the above-mentioned photoinduced phenomena in chalcogenide glass is proposed.

References

[1] Tao HZ*, Yang ZY, Lucas P, Origin of photo-induced transmitting oscillations in chalcogenide glasses, Optics Express, 2009, 17(20): 18165-18170.

[2] Tao HZ, Zhao XJ, Liu QM, Optical non-linearity in nano- and micro-crystallized glasses, Journal of Non-Crystalline Solids, 2013, 377: 146-150

[3] Han XC, Tao HZ*,Gong LJ,Wang XY,Zhao XJ,Yue YZ, Origin of the frequency shift of Raman scattering in chalcogenide glasses, Journal of Non-Crystalline Solids 391 (2014) 117–119.

[4] Lin CG, Tao HZ*, Zheng XL, Pan RK, Zang HC, Zhao XJ*, Second Harmonic Generation in IR-transparent β-GeS2 Crystallized Glasses, Optics Letters, 2009, 34(4):437-439.

[5] Tao HZ*, Lin CG, Gu SX, Jing CB, Zhao XJ, Optical Second Order Nonlinearity of the Infrared Transmitting 82GeS2·18CdGa2S4 Nanocrystallized Chalcogenide Glass, Applied Physics Letters, 2007, 91(1)011904-1～3.

P-007

Three–dimensional modeling of laser cutting process with compressible and incompressible assisting gas

T. Tamsaout, E.H. Amara
Laser Material Processing Team
Center for Development of Advanced Technologies (CDTA),
PO. Box 17, Baba-Hassen, 16303 Algiers, Algeria
E-mail : ttamsaout@cdta.dz, amara@cdta.dz

Abstract

The understanding of the fundamental physical phenomena occurring during laser cutting of metals is still only slightly understood. Indeed, the models used in literature are often highly simplified and focuses on some effects such as considering the cutting gas as a force balance applied to the gas–material interface, neglecting other important physical mechanisms. In the presented work, a three–dimensional model has been constructed to study laser cutting process in the case of compressible and incompressible applied inert gas. It is based on the Navier–Stokes equations with the energy conservation one and the implementation of the volume-of-fluid (VOF) method to track the formation of the kerf. The laser energy which is absorbed at the cutting front is introduced as source term into the energy equation. By using a phase change model, we simulate the dynamics and geometry of a growing laser-cutting generated kerf until it becomes fully developed. All these physics are coupled and solved simultaneously by Fluent CFD®.

The figure below shows sequences of kerf formation evolution under the effect of assisting gas jet.

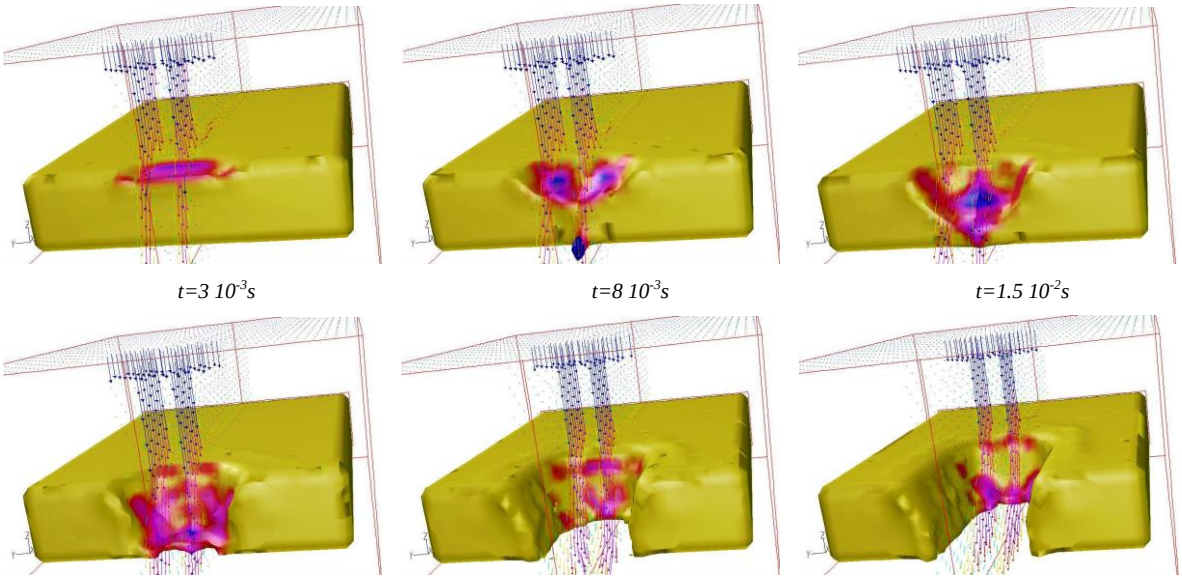

Fig. 1. Kerf formation during laser cutting process at different time step *t.*

References

[1] S. Markus Gross, "On gas dynamic effects in the modelling of laser cutting process," Appl. Math. Mod. **30**, 307–318 (2006).
[2] K. Kheloufi and E.H. Amara, "Numerical investigation of the effect of some parameters on temperature field end kerf width in laser cutting process," Physics Procedia. **39**, 872–880 (2012).
[3] S. Sun and M. Brandt, *Non-traditional Machining Processes - Research Advances*, chapter 2, *Laser Beam Machining*, J.P. Davim ed. (Springer–Verlag, London, 2013).
[4] E.H. Amara, K. Kheloufi, and T. Tamsaout, "Process velocity effect on melt film dynamics during laser cutting of metals," Proc. ICALEO2014, **107**, Laser Institute of America, USA.

P-008

The three-level ripples induced by femtosecond laser on a 6H-SiC single crystal and the formation mechansim

Juan Song[1], Wenjun Tao[1], Min Gong[2], Junyi Ye[2], Ye Dai[2], Guohong Ma[2]
[1]School of Material Science and Engineering, Jiangsu University, Zhenjiang 212013, China
[2]Physics Department, Shanghai University, Shanghai 200444, China
E-mail: ddvsh@163.com

1. Introduction

For controlling of the physical properties of 6H-SiC as functional devices, microstructuring of 6H-SiC by femtosecond lasers has been intensively studied[1]. In this paper, by a line-scanning laser irradiation at different velocities, the textured 6H-SiC surface progressively involved from first 200nm-period ripples, then 580nm-period ripples, and finally to 315nm ripples. The finite-diference-time-domain method(FDTD) was adopted to analyse the formation mechanism of the three-level ripples.

2. Experiments and results

In our experiment, a laser beam of 800 nm,120-fs and 1kHz was focused by a 5× microscopic objective on the surface of a (0001) 6H-SiC wafer. For laser fluence of 2.2 J/cm^2, as the moving velocity of the laser focus decreased from 1000 μm/s to 100 μm/s, the morphologies of the ablation lines are shown in Fig.1, which demonstrate the progressive growth of 200nm, 580nm, 315nm-period ripples.

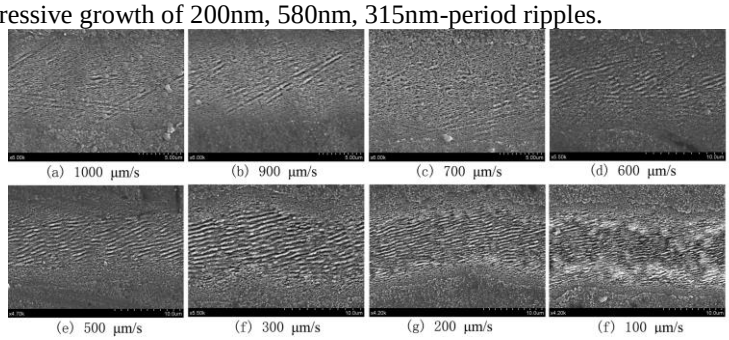

Fig.1 Scanning electron microscopic images of the ablation lines inscribed at velocities from 1000 μm/s to 100μm/s.

3. Discussion and conclusion

We agree with the proposal of M. Obara that the interference of incident wave with the wave scattered by surface scratches is the most possible reason for inducing 200nm-period and 580nm-period ripples[2]. Main discussions were focused on the orientation characteritics of ripples that M. Obara did not consider. Both isolated scratches (Fig.2(a-d))and crossed scratches with different orientation angles (Fig.2e) were constructed.. The detailed FDTD simulation in Fig.2 indicate that for scratches oriented 90° with respect to laser polarization generate a pair of strongest ripple-like optical field enhancement compared to scratches with other orientation angles ,which generate most competitive ripples perpendicular to laser polarization. In Fig.3(a), a group of NSW ripple is constructed to analyse their interaction with the incident wave. The simulated results of Fig.3(b) show that periodic optical field enhancement appears among the 580nm-period ripple gap, which is responsible for the formation of 315nm-period MSW ripples.

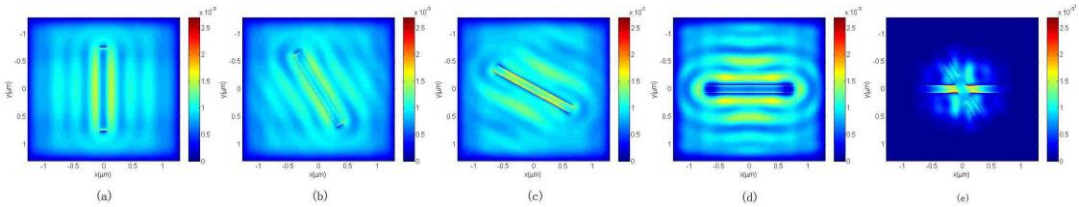

Fig.2 Simulated optical field energy distributions for the isolated scratches oriented at (a) 0° (b) 30° (c)60° (d)90° with respect to y-direction laser polarization and the crossed scratches (e)

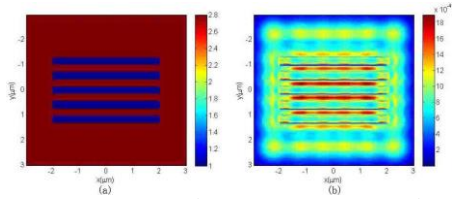

Fig.3 Schematic model of 580nm-period ripples (a) and the optical field energy distribution after their interaction with incident wave (b).

References

[1] Q.Z. Zhao, F. Ciobanu, S. Malzer, and L. J. Wang, "Enhancement of optical absorption and photocurrent of 6H-SiC by laser surface nanostructuring," Appl. Phys. Lett. 91, 121107 (2007).

[12] G. Obara, H. Shimizu, T. Enami, E. Mazur, M. Terakawa, and M. Obara, "Growth of high spatial frequency periodic ripple structures on SiC crystal surfaces irradiated with successive femtosecond laser pulses," Opt. Express **21**, 26324-26334 (2013).

P-009

Integrated analysis of millisecond pulsed laser irradiation on metals by comprehensive optical diagnostics and numerical simulation

M.Doubenskaia, I. Smurov
Lyon University, Ecole Nationale d'Ingénieurs de Saint-Etienne (ENISE), LTDS Laboratory,
58 rue Jean Parot, 42023 Saint -Etienne Cedex 2, France
e-mail : igor.smurov@enise.fr

Physical phenomena in pulsed Nd:YAG laser irradiation with millisecond pulse duration could be considered as the most simple case of laser – material interaction: thermodynamic equilibrium, heat transfer as the main energy transfer mechanist, limited convection in a shallow molten pool with flat surface, no intensive evaporation and plasma formation [1,2]. However it appears that when applying comprehensive optical diagnostics supported by numerical simulation, the real situation is not so simple and evident: to explain evolution of surface temperature evaporation should be taken into account in mathematical model, restoration of real temperature measured by pyrometer is not possible without definition of emissivity variation with temperature, interaction of metallic vapour with laser beam exists even at low energy density flux such as the order of 10^5 W/cm^2.

Comprehensive analysis of heat-and mass transfer under the pulses of Nd:YAG laser irradiation on INOX 304L substrates was carried out by simultaneous application of complimentary optical diagnostic tools. The following optical devices were used: (a) original multi-wavelength pyrometer in the near infrared range (1,370- 1,531 µm); (b) IR-camera FLIR Phoenix RDASTM equipped by InSb sensor with 3 to 5 µm band pass arranged on 320x256 pixels array; (c) Phantom V7.1 camera with SR-CMOS monochrome sensor, up-to 105 frames per second for 64x88 pixels array. Laser irradiation parameters: variation of energy per pulse in the range 15-30 J at a constant pulse duration of 10 ms with and without protective gas (Ar). True temperature was restored based on the method of multi-wavelegths pyrometry; this way, melting/solidification was analysed. Emissivity hysteresis with temperature was found. Variation of intensity of the surface evaporation visualised by camera Phantom V7.1 was linked with the surface temperature evolution.

Variation of the melt life-time, duration of solidification and the instant when melting starts with parameters of pulsed action obtained from pyrometer measurements are compared with the results of numerical simulation.

The influence of initial surface roughness on near-surface mass transfer was analysed: It was shown that rapid heating and evaporation of the micro-picks at the surface, in particular in case of high initial roughness, strongly contribute to material removal from the irradiated surface. Evaporation and micro-particles ejection in case of high surface roughness was seen even before the beginning of melting.

References

[1] W. Steen, J. Mazumder, *Laser Material Processing*, 4th Edition, (Springer, 2010).
[2] G. Gladush, I. Smurov, *Laser Processing of Materials: Theory, Experiment*, (Springer-Verlag, Berlin, 2011).

P-010

Second Harmonic Generation of q-Gaussian Laser Beam by Localization of Upper Hybrid Wave in Collisionless Plasma

Arvinder Singh and Naveen Gupta
National Institute of Technology Jalandhar
arvinder6@lycos.com

This paper presents a scheme of second harmonic generation (SHG) of an intense q-Gaussian laser beam in a hot collisionless plasma magnetized perpendicular to the direction of propagation of laser beam. On account of $\nabla \times B$ force, an upperhybrid wave (UHW) at pump frequency is generated. Following moment theory approach in W.K.B approximation the solution of the pump laser beam has been obtained. Filamentary structures of the laser beam are observed due to ponderomotive nonlinearity. There filaments are the regions of very high intensity and hence the UHW gets localized in these regions thereby producing steep density gradients in the transverse direction that in turn act as a source of S.H.G of pump beam. Numerical simulations have been carried out to have appreciation of laser filamentation and to delineate its effect on localization of UHW as well as on conversion efficiency of second harmonics. It has been observed that that intensity profile of the laser beam and strength of static magnetic field have significant effect on localization of UHW as well as on conversion efficiency of second harmonics.

P-011

Effect of Transverse Magnetic Field on Dynamics of Sn Plasma Produced by CO_2 Laser

Nek M Shaikh[1, 2], N Amin[1, 3], Y Tao[1], and M S Tillack[1]
[1]*Center for Energy Research, University of California, San Diego, 9500 Gilman Drive, La Jolla, CA, USA 92093-0417*
[2]*Institute of Physics, University of Sindh, Jamshoro, Pakistan 76080*
[3]*Department of Physics, University of Agriculture, Faisalabad, Pakistan*
E-mail: neksheikh@yahoo.com

Abstract:

In the present work we report the effect of magnetic field on the emission intensity of the neutral and singly ionized transition line, spatial and temporal variation in the plasma properties of the tin plasma in vacuum produced by the CO_2 laser. The plasma electron temperature is inferred by the Boltzmann plot method from singly ionized Sn emission lines, and plasma electron density is inferred using Stark broadened profiles. In the temporal variations, the temperature with and without magnetic field of 0.64T is estimated as (1.48-0.63) eV and (1.04- 0.58) eV at the delay of (200 – 1100) ns. Another experiment the electron temperature is measured in the range of (0.53 - 1.28) eV, and electron density is measured in the range of (9.19×10^{15} - 7.45×10^{16}) cm^{-3}, as the laser intensity is varied from (1×10^{10} to 2.5×10^{10}) W/cm^2. The plasma shielding effect has been observed within the laser intensities of ($2\times10^{10} – 2.5\times10^{10}$) W/cm^2.

In order to get more information regarding the time taken by a particular state of the constituent to evolve after the onset of plasma, TOF emission studies were made for tin with and without magnetic field. This technique gives details on the velocity and K.E of the emitted particles. TOF profiles were taken at different distances from the target surface with and without magnetic field, in order to study the effect magnetic field. Time resolved studies were made for Sn II (556.19 nm) and Sn I (317.5 nm) species at a distance of 0mm, 1mm, 2mm and 3mm from the target surface in the presence and absence of the magnetic field. The expansion velocities of the Sn II were found to be greater than the excited neutrals. The expansion velocities of Sn II at 556.19 nm for 1mm distance from the surface with and without magnetic field were found to be 0.19×10^6 cm/sec and 0.23×10^6 cm/sec respectively. Similarly, expansion velocities of Sn II at 556.19 nm for 3mm distance from the surface with and without magnetic field were found to be 0.27×10^6 cm/sec and 0.32×10^6 cm/sec respectively. The observed deceleration of neutrals and ions compared to the field free case is consistent with magnetohydrodynamics model in which K.E of expansion is converted into joule heating.

We explain the results by considering the role of various atomic processes viz. electron impact excitation and recombination

References:

1. Harilal S S, O'Shay B, and Tillack M S, Mathew M V **.** *J. Appl. Phys* **98,** 013306 (2005)
2. Nek. M. Shaikh, Y. Tao, R. A. Burdt, S. Yuspeh, N. Amin, and M. S. Tillack, "Spectroscopic analysis of temperature and density of Sn plasma produced by a CO_2 laser," *Journal of Applied Physics* **108,** 083109 (2010).
3. Ajai Kumar, R.K. Singh, V. Prahlad, And H.C. Joshi,"Effect of magnetic field on the expansion dynamics of laser-blow-off generated plasma plume: Role of atomic processes", Laser and Particle Beams **28,** 121–127 (2010),

P-012

On different regimes of condensed matter laser ablation: molecular dynamic simulations

A.A. Samokhin[1], V.I.Mazhukin[2], A.V.Shapranov[2], M.M. Demin[2]

[1]*Prokhorov General Physics Institute,Russian Academy of Sciences, Vavilov Str., 38, 119991 Moscow, Russia*

[2]*M.V. Keldysh Institute of Applied Mathematics, Russian Academy of Sciences, Myusskaia sq. 4, 125047 Moscow, Russia*

E-mail address: asam40@mail.ru

Absorption of intense laser pulses gives rise to various non equilibrium processes in condensed matter which result in ablation of irradiated materials. Some of the processes are not sufficiently investigated and need more adequate descriptions than that formulated in previous decades and used [1] until today without necessary modifications.

Here the laser ablation processes are analyzed in the framework of molecular dynamic simulations combined with continual description of electron subsystem in metals. At nanosecond pulse duration in metal (Al) film targets with 48 and 430 nm thickness which is initially in liquid states with temperature 6400 K four different ablation regimes are observed depending on laser pulses intensities: surface evaporation, explosive (volume) boiling, spinodal decomposition and supercritical fluid expansion [2-4]. At shorter (picosecond) pulses spallation effect (see, *e.g.* [5,6]) due to negative pressure values generated in the thin film (48 nm) is also observed. Thin dielectric films demonstrate similar behavior except for repetitive explosive boiling process observed in 430 nm metal film.

Appearance of explosive boiling in metals irradiated with intense laser pulses is not evident beforehand because of high values of thermal conductivity and small radiation penetration length. Nevertheless, the explosive boiling process at absorbed radiation intensity I = 44 MW/cm^2 is clearly visible in Fig 1a which shows several flying away target fragments formed after explosions at earlier moments 1.16 ns, 1,5 ns and 1.79 ns. The fragments with initially well defined boundaries then become thinner and disintegrate due to surface evaporation process. Remnants of the first fragment which was formed due to the first explosion at 0.71 ns are not visible here. Fig 1b shows spinodal decomposition regime where density fluctuations have no such distinct boundaries as in the explosive boiling case. Initial thickness of the explosive boiling fragment is of the order radiation penetration length (about 10 nm). This result means, in particular, that in theoretical description of the explosive boiling process in irradiated metals [1] it is necessary to take properly into account finite value radiation penetration length.

Pressure pulses generated during explosive boiling in the considered model have durations 100-200 ps with amplitudes 200-300 bar above preceding recoil pressure level and they can be used as experimental markers for near critical region approaching.

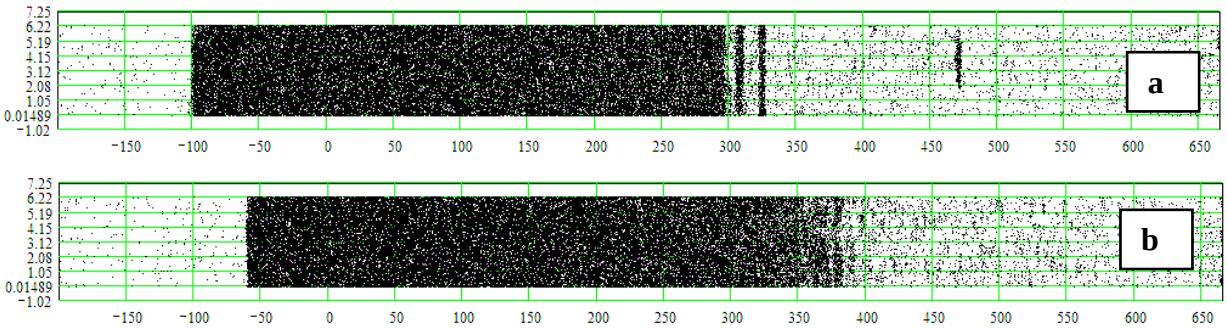

Fig 1. Snapshots of irradiated (from the right) metal film at t = 1.82 ns after the radiation pulse with constant intensity I = 44 MW/cm^2 is switched on (a), and at t =0.73 ns with I = 88 MW/cm^2 (b)

References

[1] M. Q. Jiang, Y. P. Wei, G. Wilde, L. H. Dai. "Explosive boiling of a metallic glass superheated by nanosecond pulse laser ablation". Appl. Phys. Let. **106**, 021904 (1-6), (2015).

[2] V.I.Mazhukin, A.A. Samokhin, M.M. Demin,A.V.Shapranov. "Explosive boiling of metals upon irradiation by a nanosecond laser pulse" Quantum Electronics. **44**, No. 4, 283–285, (2014).

[3] V.I.Mazhukin, A.A. Samokhin, M.M.Demin, A.V.Shapranov. "Modeling of nanosecond laser vaporization and explosive boiling of metals". Mathem. Montisnigri. **29**, 68 - 90, (2014).

[4] V.I.Mazhukin, A.A. Samokhin, A.V.Shapranov, M.M.Demin. "Modeling of thin film explosive boiling - surface evaporation and electron thermal conductivity effect". Mater. Res. Express, **2**, No. 1, 016402 (1-9), (2015).

[5] C. Wu, L.V. Zhigilei. "Microscopic mechanisms of laser spallation and ablation of metal targets from large-scale molecular dynamics simulations", Appl. Phys. *A*, **114,** 11-32, (2014).

[6] A. Ionin, S. I. Kudryashov, L. V. Seleznev, "Thermal Melting and Ablation of Silicon by Femtosecond Laser Radiation". J. Exp. Theor. Phys., **116**, No. 3, 347–362, (2013).

P-013

Laser ablation of absorbing liquids under transparent cover: acoustical and optical monitoring

A.A. Samokhin, N.N. Il'ichev, P.A. Pivovarov, A.V. Sidorin
Prokhorov General Physics Institute,Russian Academy of Sciences, Vavilov Str., 38, 119991 Moscow, Russia
E-mail address: asam40@mail.ru

Phase transitions are among many others non equilibrium processes which take place during laser ablation of condensed matter. Despite a lot of papers on the theme experimental investigations of the phase transition and related phenomena in laser ablation remain somewhat incomplete, in particular, due to a lack of simultaneously measured different parameters in the experiments. In interesting papers [1,2], *e.g.*, the lack of straightforward experimental information on pressure behavior in irradiated targets impedes unambiguous quantitative interpretation of the results obtained.

In Ref [3] it was shown how the recoil pressure and irradiated surface displacement can be measured simultaneously during action of nanosecond laser pulses with periodically modulated intensity.

In the present work this method combined with optical diagnostic is used to investigate laser ablation of absorbing liquids (water, ethanol) under transparent cover. Erbium laser pulses (wavelength 2.94 μ, 200 ns duration) are delivered to the liquid surface covered with different plates (silica, sapphire and lithium fluoride) transparent to the laser radiation. In water the radiation absorption length is about 1 μ. Optical monitoring set up consists of probe laser beam (cw-laser, wavelength 0.53 μ, 150 mW) directed to the boundary surface plate-liquid at 10 deg. Reflected signals were detected by photodiode with nanosecond time resolution.

Observed optical signals have threshold behavior and last for about several hundred microseconds at laser fluency 0.1 – 0.6 J/cm^2. Occurrence of optical signals during action of laser pulse is consistent with the results [4] where the bipolar photoacoustic signals were observed in the case of covered liquid surface. Such photoacoustic signals are typical for the free surface case and suggest vapor cavity formation under the transparent cover. Optical signals end which is rather abrupt correlates with arising acoustical perturbations. Our results also suggest cavity formation beneath the transparent plate boundary when the surface of plate is covered by submicron layer of liquid. Fig.1 shows optical signals oscillations after the laser pulse ending.

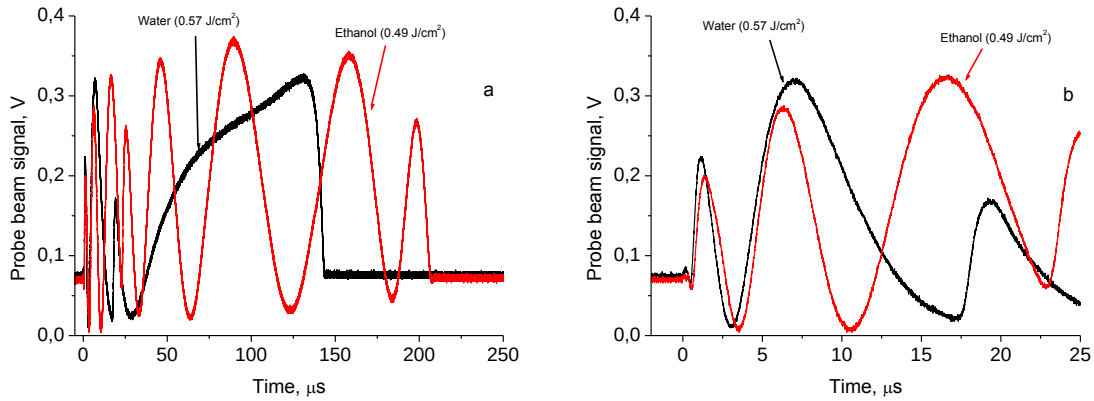

Fig. 1. Reflected probe beam signals from ethanol and water, covered by sapphire plate; a) full length the signals, b) initial part of the signals.

References

[1] F. Lang, P. Leiderer, "Liquid–vapour phase transitions at interfaces: sub-nanosecond investigations by monitoring the ejection of thin liquid films", New J. of Phys., **8**, 14 (2006).
[2] C. Porneala, D.A. Willis, "Time-resolved dynamics of nanosecond laser-induced phase explosion", J. Phys. D: Appl. Phys. **42**, 155503 (2009).
[3] A.A. Samokhin, N.N. Il'ichev, "On photoacoustic monitoring of laser evaporation front movement", Q. Electronics, **40**, 659- 660 (2010).
[4] A.A.Samokhin, N.N.Il'ichev, P.A.Pivovarov, A.V.Sidorin, "Analysis of photoacoustic monitoring of laser ablation in the case of laser pulseswith periodically modulated intensity", Math. Montis., **30**, 46-55 (2014).

P-014

Fabrication of 3D microchanels in PMMA by Nd:YAG laser

H. Pazokian[1], M.Javad. Sobhani[2], M. Mollabashi[2], H. Amiri[1], S.Safaei[2]
[1]*Laser and Optic research school, Tehran, Iran*
[2]*Department of Physic,Iran University of Science and Technology, Tehran, Iran*
Email: h_pazokian2005@yahoo.com, h_pazokian@iust.ac.ir

Nowadays, microfluidic chips are very attractive for different application especially medical ones. Among various methods used for fabrication of microfluidic devices, fs laser direct writing has been addressed by several researchers [1-3]. Using fs pulses leads to clean ablation with at least thermal damage to the surrounding area. On the other hands, in ns laser ablation, the surface roughness of the orders of microns formed on the ablated area. However typical microfluidic structures are on the orders of ten to hundred microns. Then this amount of roughness is acceptable. In this paper, we study ns direct writing of microchanels in PMMA. The second harmonic of a Q-switch Nd:YAG laser ($\tau \sim 8\ ns$) is used as irradiation source. The effect of laser parameters on the quality and dimensions of channels is investigated.

[1]K. Sugioka, Y. Hanada, K. Midorikawa, "Three-dimensional femtosecond laser micromachining of photosensitive glass for biomicrochips". Laser & Photon Rev **4**:386–400(2010)
[2] K. Sugioka, Y. Cheng, "Integrated microchips for biological analysis fabricated by femtosecond laser direct writing". MRS Bull **36**:1020–1027(2011)
[3] Y. Liao, Y. Ju, L. Zhang et al, "Three-dimensional microfluidic channel with arbitrary length and configuration fabricated inside glass by femtosecond laser direct writing" Opt Lett 35:3225–3227(2010)

P-015

Ns laser fabrication of 2D micro-channels in PMMA followed by wet chemical etching

H. Pazokian[1], S.Safaei[2], M. Mollabashi[2], H. Amiri[1], M.Javad. Sobhani[2]
[1]*Laser and Optic research school, Tehran, Iran*
[2]*Department of Physic,Iran University of Science and Technology, Tehran, Iran*
Email: h_pazokian2005@yahoo.com, h_pazokian@iust.ac.ir

Ns laser ablation is used for the fabrication of 2D microfluidic channels in PMMA. Influence of operating parameters such as the pulse energy, the translation speed, the focal length of the lens, the number of pulses and the repetition rate on the quality and depth of channels is investigated. A chemical wet etching by HNO3 solution is used after irradiation to improve the surface quality of the fabricated channels. The optimum time for a define concentration of the solution is found.

P-016

Influence of laser pulse width on the ablation of Zinc in nitrogen ambient

N.Smijesh and Reji Philip*

Raman Research Institute, C.V. Raman Avenue, Sadashivanagar, Bangalore 560 080, India.

Corresponding Author E-mail: reji@rri.res.in

We report time of flight (TOF) spectral measurements of laser produced plasmas(LPP) generated by irradiating a solid Zinc target withlasers of nanosecond (7 ns, 1064 nm) and femtosecond (100 fs, 796 nm) pulse durations respectively, carried out in a broad ambient pressure range of 0.05 to 100 Torr of Nitrogen. At the relatively high input fluence of ~ 16 J/cm^2 used, fast and slow atomic species are found to appear at different times in the TOF spectra, the dynamics of which are primarily determined by the pulse durations of the irradiating laser[1-3]. In fs LPP, the average speed of fast species is unaffected by an increase in ambient pressure, while in ns LPP average speed is found to reduce with pressure. Slow species shows a sharp peak in TOF spectra with a narrow velocity distribution for fs LPP, indicating a large number density (N_e) and low electron temperature (T_e), which is confirmed through optical emission spectroscopic studies. Whereas for ns LPP, the TOF of slow species is found to have more broadened profile due to strong plume-laser interaction. The dynamics of slow species is heavily influenced by the presence of shock waves, which leads to the occurrence of a much slower species at larger pressures. The optimum ambient pressure for maximum emission intensity and emission life time isdetermined to be 10 Torr.

References.

[1] S. Amoruso, R. Bruzzese, C. Pagano, and X. Wang, Appl. Phys.A **89,**1017 (2007).
[2] S. Amoruso, G. Ausanio, R. Bruzzese, M. Vitiello, and X. Wang, Phys. Rev. B **71**, 033406 (2005).
[3] B. Verhoff, S. S. Harilal, J. R Freeman, P. K. Diwakar, and A. Hussanein, J. Appl. Phy. **112**, 093303 (2012).

P-017

Effects of pulse duration on overall temporal behavior of the bubble produced by nanosecond laser ablation in water

A. Matsumoto[1], A. Tamura[1], A. Kawasaki[1], T. Honda[1], P. Gregorčič[2], N. Nishi[1], K. Amano[1], T. Sakka[1]

[1]Department of Energy and Hydrocarbon Chemistry, Kyoto University, Kyoto, Kyoto 615-8510, Japan

[2]Faculty of Mechanical Engineering, University of Ljubljana, Aškerčeva 6, 1000 Ljubljana, Slovenia

E-mail: matsumoto.ayumu.78w@st.kyoto-u.ac.jp

1. Introduction

Liquid-phase laser ablation is expected to be applied to various applications, such as underwater in-situ elemental analysis and synthesis of nanoparticles in liquid. However, the mechanism is not fully clarified due to complex interactions among pulsed laser, solid, liquid, plasma and bubble induced in the process. To improve the performance of the elemental analysis and the synthesis of nanoparticles, we have to understand the behavior of the ablated species and the bubble, and their relationship should be also controlled. Plasma emission images and shadowgraph images have been observed to investigate the ablated species and the bubble. However, in the case of the shadowgraphy multiple events are required to capture the bubble dynamics during its whole lifetime. Therefore, it is difficult to evaluate the temporal behavior precisely since in our case the shot-to-shot fluctuations are significant. Gregorčič et al. have used a laser-beam-transmittance probe (LBTP) to measure the whole bubble dynamics from a single pulse [1]. In the case of LBTP the continuous-wave (CW) illumination probe is needed to illuminate the interaction area. The portion of the CW laser is scattered and deflected by the bubble. Thus, the transmitted light power, which is collected by a lens to a photodetector, decreases by increasing the bubble's diameter. In such a way, the whole bubble dynamics is detected from a single laser shot, which is especially important in the case of non-repeatable conditions due to the significant shot-to-shot fluctuations. In the present study, the behavior of the ablated species and the bubble induced by laser ablation in water are investigated by employing LBTP. We study the effects of laser-pulse duration, which could control the relationship between the ablated species and the bubble [2].

2. Experimental

A Q-switch Nd:YAG laser with the wavelength of 1064 nm, the pulse duration of 20 ns (short pulse) or 100 ns (long pulse), and the pulse energy of 6 mJ (fixed) was focused onto a Cu target in water. As a CW probe we used a He-Ne laser (632.8 nm) expanded by 10 times by using a beam expander. The probe passed through the bubble on the ablation spot in the direction parallel to the target surface. The transmitted probe light was collected by a lens into a photodiode. The photodiode signal was measured by an oscilloscope. In the case that we observed the signal immediately after the laser irradiation, the band-pass interference filter (632 ± 1.5 nm) was placed in front of the photodiode to avoid the detection of the plasma emission as well as the scattered light of the pulsed laser. The temporal profile of the pulsed laser was observed by another photodiode which detects the reflected light from a beam splitter that was placed on the laser pathway.

3. Results and discussion

When a bubble starts to expand the LBTP signal decreases since less light is transmitted through the interaction area. In our experiments, the several negative peaks were obtained in the LBTP signal due to multiple oscillations of the bubble. Here, the amplitude and the duration of a single peak in LBTP signal decreases with the repetition. From peak widths, which were from ~10 μs to ~100 μs, the time of a single bubble oscillation can be obtained. The peaks attributed to the third and subsequent bubbles in the case of the short pulse had higher amplitude and were wider than that in the case of the long pulse, although the peaks attributed to the first bubble were almost the same for the both cases. This is probably because the ablated species remains in the bubble in the case of the long pulse compared to the case of the short pulse, which may enhance the viscosity of the bubble. Unexpectedly, a scattering signal with the width of ~1 μs was observed immediately after the laser irradiation. This is probably related to the ejection and dispersion of the ablated species into the water phase. The beginning of the signal was steep and the profile fluctuated shot-by-shot in the case of the short pulse compared to the case of the long pulse. This might indicate that relatively large amount of the ablated species are ejected into the water phase in the case of the short pulse in contrast to the case of the long pulse. This could affect the contents of the bubble and consequently the repetition behavior of the bubble might be changed as discussed above.

[1] P. Gregorčič, M. Jamšek, M. Lukač, M. Jezeršek, "Synchronized delivery of Er:YAG-laser-pulse energy during oscillations of vapor bubbles, J. LA&HA **2014**, 14 (2014).

[2] T. Sakka, A. Tamura, A. Matsumoto, K. Fukami, N. Nishi, and B. Thornton, "Effects of pulse width on nascent laser-induced bubbles for underwater laser-induced breakdown spectroscopy," Spectrochim. Acta, Part B **97**, 94 (2014).

P-018

Double Pulse Femtosecond Laser Ablation and Deposition of Co/Zn/S nanostructures

I. Lopez-Quintas[1], E. Rebollar[1], D. Avila-Brande[2], J. G. Izquierdo[3], L. Bañares[3], M. Castillejo[1], R. de Nalda[1], M. Martín[1]

[1] *Instituto de Química Física Rocasolano, Consejo Superior de Investigaciones Científicas CSIC, Serrano 119, 28006 Madrid, Spain*
[2] *Departamento de Química Inorgánica I. Facultad de Ciencias Químicas, Universidad Complutense Madrid, 28040 Madrid, Spain*
[3] *CLUR and Departamento de Química Física I. Facultad de Ciencias Químicas, Universidad Complutense Madrid, 28040 Madrid, Spain*
E-mail: mmm@iqfr.csic.es

1. Abstract

Ultrafast laser ablation techniques are powerful tools for the synthesis and processing of materials; fs pulses, shaped in different temporal and spatial configurations, can be used to influence the outcome of material ablation either acting on the laser/target interaction dynamics [1] or by the control of the phase state of the ablation plasma [2]. Nanostructures consisting of II-VI semiconductors doped with transition metal atoms can potentially bear magnetic and optical functionalities [3]. In previous work [4] we have investigated the ablation of Co/ZnS targets irradiated by two 100 fs pulses, at 800 nm with individual pulse energies below the threshold for ion detection by TOF-MS; with pulses separated by time delays in the range of 0 to 300 ps, the yields of Co, Zn and S ions were found to be strongly dependent on the relative energy and delay between the two pulses.

In this work the products deposited by double pulse (DP) ablation were collected on appropriate substrates and the dependence on delay and pulse energy of the composition, morphology and structure of the deposits was investigated. Previously the DP ablation plasma was studied by Optical Emission Spectroscopy to characterize the composition and dynamics of the ejected neutrals. DP ablation and deposition was carried out under vacuum and the growth of the deposit layer on Si substrates was monitored "in situ" by measuring the varying reflectivity of a He-Ne beam.

The threshold fluence of a single fs pulse (SP), giving rise to a measurable layer of deposited material, was investigated by atomic force microscopy (AFM). Analysis of the deposit layer obtained after 10^6 laser shots showed that SP ablation at a fluence of ~ 0.15 Jcm^{-2} yielded a ~10 nm thick layer on the Si substrate whereas a layer nearly one order of magnitude thicker was obtained with 10^6 DP sequences of two identical pulses of the same fluence, delayed by 1 ps. Moreover, the layer height measured at delays of 300 ps between pulses was five times larger than the expected from two uncoupled single fs pulses. The AFM images are shown in Figure 1.

Finally, we unambiguously show that the delay between the pulses, in the picoseconds range, plays a determining role on the total yield of the ablation process. This fact, and the more subtle effects on the composition of the PLD-synthesized deposits, will be discussed in terms of the efficiency of the laser energy coupling and the relaxation processes in the material.

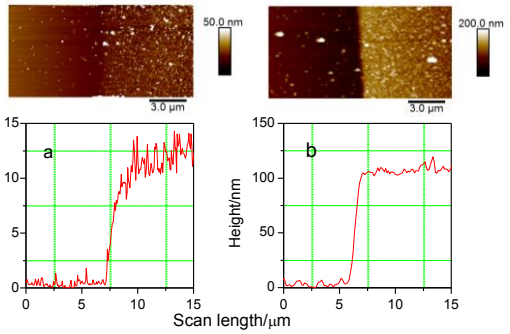

Fig. 1. AFM images of Co/Zn/S deposits produced by: a) Single fs PLD, F=0.15 Jcm^{-2}, 10^6 laser shots, b) Double fs PLD, with identical pulses delayed by 1ps, at the same fluence and number of DP sequences than in a).

2. References

[1] L. Englert, B. Rethfeld, L. Haag, M. Wollenhaupt, C. Sarpe-Tudoran, T. Baumert, "Control of ionization processes in high band gap materials via tailored femtosecond pulses" Opt. Expr. **15**, 17855 (2007).
[2] F. Bourquard, T. Tite, A-S. Loir, C. Donnet, F.Garrelie, "Control of the graphite femtosecond ablation plume kinetics by temporal laser pulse shaping: effects on pulsed laser deposition of diamond-like carbon" J. Phys.Chem. C **118**, 4377-4385 (2014).
[3] S.J. Pearton, W.H. Heo, M. Ivill, D.P. Norton, T. Steiner, "Dilute magnetic semiconducting oxides", Semicond. Sci. Technol. **19**, R59-R74 (2004).
[4] I. Lopez-Quintas et al. "Double pulse fs-laser investigation of the ablation dynamics of Co/ZnS". In preparation.

P-020

Optimisation of laser cutting process in relation to the maximum cutting speeds using numerical modelling

K. Kheloufi, E. H. Amara, T. Tamsaout
Centre for Development of Advanced Technologies, Algiers, Algeria
E-mail: kkheloufi@cdta.dz

Abstract

Laser cutting of steel is nowadays a well established industrial process. Manufacturers using laser cutting in their production are particularly interested in attainment of high cutting speeds for maximization of productivity and cutting reproducibility by Optimization of the processing parameters.

In the present study, the maximum cutting speed is investigated as a function of laser power and gas jet velocity. For this purpose, a three-dimensional transient finite volume model has been constructed, based on the Navier–Stokes equations and energy conservation equation for the description of momentum and heat transport phenomena, and the Volume of Fluid (VOF) method for free surface tracking. The Fresnel absorption model is used to handle the absorption of the incident wave by the surface of the liquid metal and the enthalpy-porosity technique is employed to account for the latent heat during melting and solidification of the material. The main objective of using a transient phase change model in the current case is to simulate the dynamics and geometry of a growing laser-cutting generated kerf until it becomes fully developed.

It was observed that when the cutting speed is increased high enough for a given laser power level, a maximum cutting speed is reached beyond which the laser power is insufficient to produce complete cutting. The maximum cutting speed is defined as the speed for which the calculated cutting profile is just deep enough to cut through a workpiece of a given thickness.

The results show that maximum cutting speed increases by rising the laser power and assist gas velocity. The results indicate an intense influence of the laser power on the maximum cutting speed.

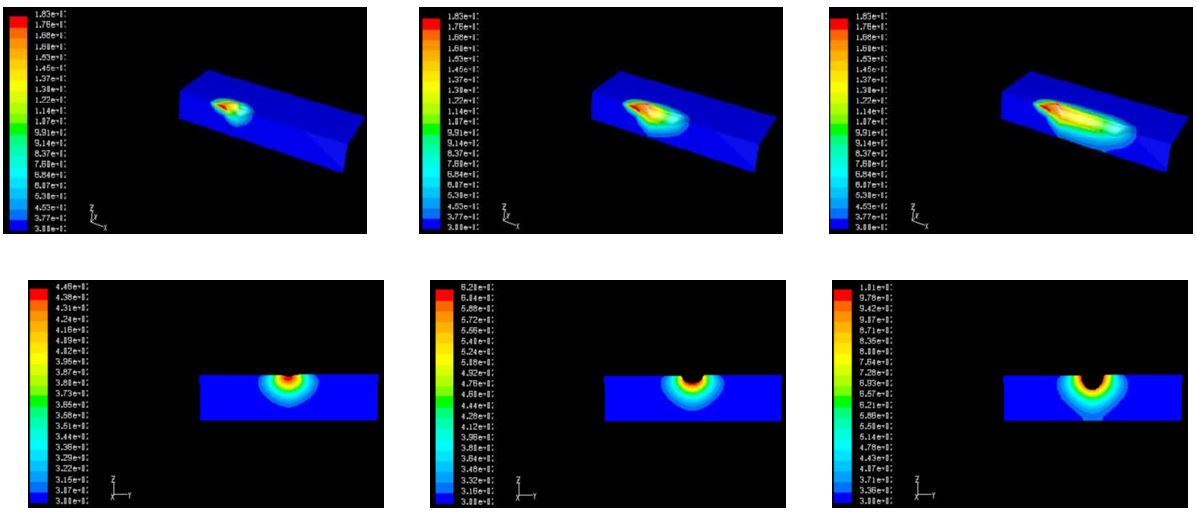

Fig. 1. Temperature distribution and groove formation during laser processing of 1 mm thickness sheet steel.

References

[1] K. Kheloufi, E. H. amara, "Numerical Investigation of the Effect of Some Parameters on Temperature Field and Kerf Width in Laser Cutting Process," Physics Procedia, Vol. **39**, 2012, Pages 872–880.

P-022

Section Analysis of Fabric materials Cut Using Ultraviolet Laser Ablation

Hsin-Yi Tsai, Chih-Chung Yang,Wen-Tse Hsiao, Kuo-Cheng Huang*

Instrument Technology Research Center, National Applied Research Laboratories
20, R&D Rd. VI, Hsinchu Science Park, Hsinchu 300, Taiwan
*E-mail: huangkc@narlabs.org.tw**

Laser ablation is widely applied in cutting, engraving, and marking and it is regarded as a novel technique in the fashion clothing industry. In the past, the fabrics such as cotton, silk, lace, polyester and leather, were cut by using traditional tools (i.e. knife or shear). However, these tools would be easily wearing after a period of time and sometimes the edge of some fabrics would be fraying. To solve the above problems, the laser cutting technology with the characteristics of fast, high precision, repeatability and high flexibility of shapes can be applied. Therein, the thermal properties and quality of cut surface on cloth-reinforced polyester was discussed in previous study [1-2], and the laser technology applied in fabrication of three-dimensional patterns for textiles was represented in recent years [3-4]. However, the properties and the edge effects of the fabrics before and after the laser ablation were not investigated.

This article aims to analyze the variation of the component and the contour of fabrics cut using ultraviolet laser system with a wavelength of 355 nm. The processing parameters include the laser powers, pulsed frequencies, scanning speeds can be adjusted, and the shrink ratio and the oxidation degree are discussed. Then, the suitable parameters in cutting process for fabrics are determined. The experiments and the results showed; 1) the cross section and the morphology of the composite materials cutting by the laser ablation and knife were evaluated by three-dimensional confocal laser scanning system and discussed; 2) the powers and pulsed frequency were fixed at 14 W and 100 kHz, and the scanning speed ranged from 5 to 30 mm/s to develop the repeat cycles and shape distortion of silk materials. The results showed scanning speed of 5 mm/s and repeat 6 cycles would cause the minimum distortion of silk; 3) the pulsed frequency was adjusted from 60 to 200 kHz to analyze the oxidation and carbonize degree at the edge of non-woven. In addition, the suitable parameters of laser systems for different types of fabric were investigated as the reference information and the laser cutting system can provide the high speed, without fraying and smooth edge of patterns for clothing industry.

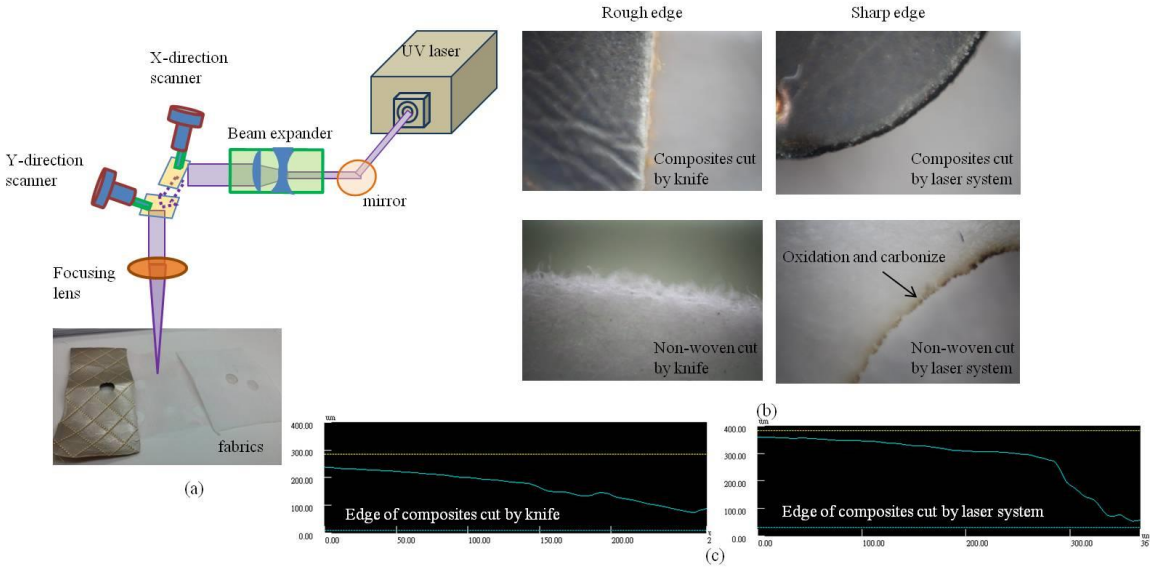

Figure 1: (a) Schematic of the fabric cutting using laser ablation, (b) the microscopic and (c) the profile images of edge of fabrics cut using knife and laser ablation.

[1] V. Tagliaferri, A. Di llio, Crivelli Visconti, "Laser cutting of fibre-reinforced polyesters", Composites 16(4), 317-325, (1985).
[2] M. D. Mello, "Laser Cutting of Non-Metallic Composites",Proc. SPIE Laser Processing: Fundamentals, Applications and Systems Engineering, 28 (1986).
[3] F. Vidal, R. Gonzálex, M. Fontán, P. Rico, D. Piñeiro, "Development of a Flexible Robotic Cell for Laser Cutting of 3D Foam and Preformed Fabric", Robotics in Smart Manufacturing, 371, 91-100 (2013).
[4] A. Garcia-Diaz, I. Fernández-lglesias, E. Piñeiro, I. Coto, F. Vidal, and D. Piñeiro, "Vision-Based Automation of Laser Cutting of Patterned Fabrics", Robotics in Smart Manufacturing, 371, 170-178 (2013).

P-023

Simulation of the spherical aberration by focusing laser radiation in transparent materials: Comparison of different simulation approaches

M. Olbrich[1], T. Viertel[2], J. Kubistova[1], R. Ebert[1], A. Fischer[1], J. Bliedtner[2] and A. Horn[1]

[1]*Laserinstitut Hochschule Mittweida, University of Applied Sciences Mittweida, Technikumplatz 17, 09648 Mittweida, Germany*

[2]*Fachbereich SciTec, Ernst-Abbe-Hochschule Jena, Carl-Zeiss-Promenade 2, 07745 Jena, Germany*

Email: molbrich@hs-mittweida.de

The possibility of creating micro cavities, cracks or refractive index modifications due to the interaction of laser radiation with transparent materials by focusing the laser radiation into the material offers many promising applications. Holographic data storage, laser-written waveguides or optical gratings are some examples [1,3]. For further improvements in the quality of the named applications, a deep understanding of the involved processes during the laser radiation material interaction is necessary. In this work, the change of the laser intensity distribution by spherical aberration caused by the transition of the radiation from air to matter is discussed. The simulations are compared with experimental data with respect to the calculated intensity distributions and the lateral size of the laser-generated cavities.

Experiments were performed producing micro cavities by ultrashort-pulsed laser radiation (wavelength $\lambda = 1030$ nm, pulse duration (sech²) $\tau_H = 180$ fs, gaussian beam diameter before objective $d_\sigma = 5$ mm, pulse energy $E_p = 60 – 230$ nJ) PMMA (refractive index $n = 1.48$, surface at $z = 0$) at the optical distances $d_{opt} = n \cdot z_0$ by using an infinity-corrected microscope objective with $NA = 0.65$, focal length $f = 4$ mm. z_0 represent the set geometrical positions with 50 µm, 80 µm, 110 µm, 140 µm and 170 µm. The threshold intensity was estimated to $I_{thr} = 27$ TW/cm². Longer cavities are formed when the radiation is focused deeper into the transparent material (Fig. 1).

Simulations were performed to interpret the results including the calculation of the beam propagation in air and PMMA using a propagation operator, like Kirchhoff's diffraction formula or the Spectrum of Planes Waves (SPW), which is based on Fast Fourier Transformation (FFT) [1]. Another approach for beam propagation is solving the Maxwell equation e. g. by Finite Differences Time Domain (FDTD) [2]. Kirchhoff's diffraction formula and FDTD can be used unrestricted but have a long computation time in which FDTD has the highest computational effort. While SPW is very fast, it has only a restricted applicability. To avoid these restrictions, some solutions are given and discussed, which includes a semi-analytical proceeding of Kirchhoff's diffraction formula, automatic refinement of the sampled area for the SPW, and the coupling of the two approaches with FDTD. All simulations were performed using Graphic Processor Units (GPU) to reduce the calculation time.

The calculation with Kirchhoff's diffraction formula of the intensity distribution describes the same effects that were observed in the experiments (Fig. 1 and 2). Due to an increasing spherical aberration with increasing depth of the material, the beam size gets larger and the threshold intensity for the modification of the material is not reached anymore. This calculation could also be achieved by an analytical solution [3]. However, the further work will include simulations of the temperature distribution due the heating of matter and thermal stress induced by ultrashort pulsed laser radiation leading to non-ideal simulation conditions. In that case, an analytical solution is no longer valid.

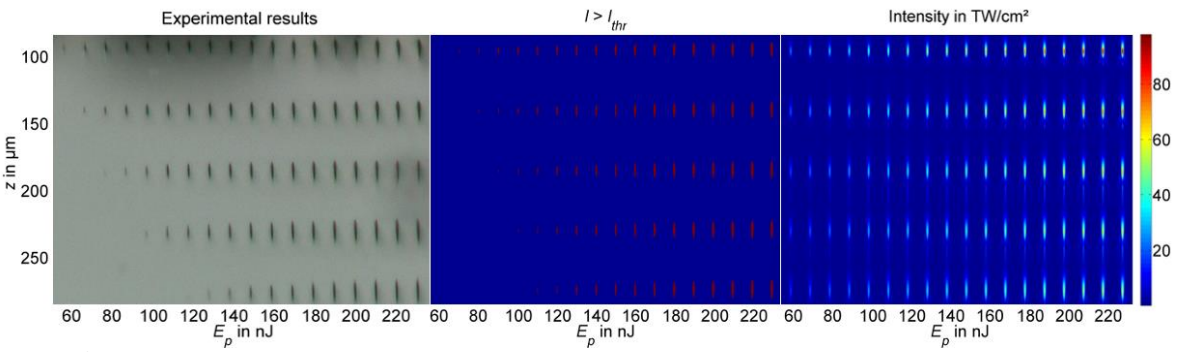

Fig. 1. Left: Laser-induced cavities by ultrashort laser radiation in PMMA for different pulse energies at distinct z-positions (surface z = 0, light microscopy). Right: calculated intensity distribution corresponding to the experimental parameters. Middle: Area with higher intensity than I_{thr}

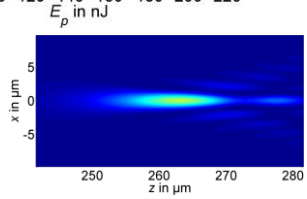

Fig. 2. Calculated Intensity distribution at the beam waist for $d_{opt} = n \cdot 170$ µm and $E_p = 230$ nJ

[1] F. Träger, *Handbook of Lasers and Optics*, 1st. ed., (Springer, New York, 2007)

[2] A. Z. Elsherbeni, and V. Demir, *The finite-difference time-domain method for electromagnetics with MATLAB® simulations*, 1st. ed., (SciTech Pub, Raleigh, NC, 2009)

[3] A. Marcinkevičius, V. Mizeikis, S. Juodkazis, S. Matsuo, and H. Misawa, "Effect of refractive index-mismatch on laser microfabrication in silica glass", Appl. Phys. A: **76**, 257-260 (2003)

P-024

Excitation of Upper Hybrid Wave by Cross-Focusing of Two Cosh-Gaussian Laser Beams in Preformed Parabolic Plasma Channel

Naveen Gupta and Arvinder Singh
National Institute of Technology Jalandhar
naveenenterprises0@gmail.com

This paper presents a scheme for excitation of upper hybrid wave (UHW) by beating two Cosh-Gaussian (ChG) laser beams in a preformed parabolic plasma channel magnetized in a direction perpendicular to propagation of laser beams. The mechanism for laser induced nonlinearity is assumed to be a ponderomotive force. The ponderomotive force depends not only on the intensity of first laser beam but also on that of second laser beam. Therefore, the dynamics of one laser beam is governed by that of other and hence cross-focusing of the two laser beams takes place. Starting from Maxwell's the coupled differential equations governing the evolution of spot size of laser beams with distance of propagation have been derived with the help of moment theory approach in W.K.B approximation. Numerical simulations have been carried out to investigate the effect of laser as well as channel parameters on cross-focusing of the laser beams and further to delineate its effect on power of generated UHW. It has been observed that decentered parameters of the laser beams and strength of static magnetic field have significant effect on excitation of UHW.

P-025

Space-time study of microplasmas inside silicon induced by infrared ultrashort laser pulses

A. Mouskeftaras[1]*, M. Chanal[1], R. Clady[1], A.V. Rode[2], M. Chambonneau[1], M. Sentis[1], O. Utéza[1], D. Grojo[1+]

1- Aix-Marseille University, CNRS, LP3 UMR 7341, F-13288, Marseille, France
2- Laser Physics Centre, Australian National University, Canberra ACT 0200, Australia
*Email adresses: *mouskeftaras@lp3.univ-mrs.fr, currently at alexandros.mouskeftaras@epfl.ch ; +grojo@lp3.univ-mrs.fr*

Long-wavelength femtosecond lasers are highly desirable for three-dimensional (3D) microfabrication applications in semiconductors that are opaque at the fundamental wavelength of Ti:sapphire lasers. However, experiments show that the intrinsic properties of narrow gap materials prevent the occurrence of confined breakdown in the bulk with tightly focused interaction arrangements.

We perform a pump-probe microscopy experiment at 1300-nm wavelength and ≈50 fs pulse duration [1] to investigate the specificity of microplasmas formed by two-photon ionization [2] when the beam is focused below the surface of silicon crystals (NA=0.3). Figure 1 shows an image of a plasma acquired for a delay of 10 picoseconds after the interaction of a pulse of ≅ 10 nJ energy.

This allows us to study the space-time characteristics of the plasmas for laser intensities up to 10^{12} W/cm^2. The measurements reveal a self-limitation of the excitation at a maximum free-carrier density of ≅ 10^{19} cm^3, which is more than one order of magnitude below the threshold for permanent modification. In parallel, we perform a pump self-absorption measurement to translate the observations in terms of energy balance inside the material and discuss the potential factors that prevent bulk micromachining. We observe that the plasma develops in a pre-focal region for pump pulse energies exceeding 40 nJ leading to a clamping of the intensity at the focus. This is a major reason for the saturation of the maximum free-carrier density that can be achieved. At higher pulse energies, the shape of the microplasma is changed progressively. The observation likely relies on nonlinear propagation effects due to the low threshold for self-focusing in silicon. The overall results underline the limits in local control of silicon excitation, which are inherent to the use of single near-infrared ultrashort Gaussian pulses.

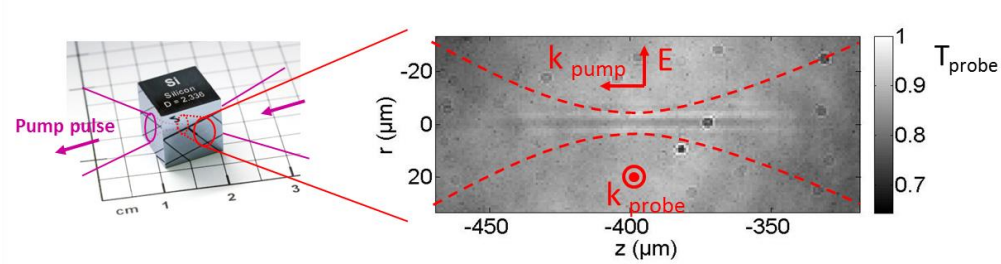

Fig. 1: Intensity of the transmitted probe (a.u.) in presence of a pump pulse (10 nJ, 10 ps delay) as acquired with the experimental arrangement. The microplasma is visible (black stripe associated with inverse Bremstrahlung absorption) at the focus of the pump beam.

In addition, the experiment allows us also to study directly free-carrier dynamics in bulk silicon. We observe that the plasma cylinders expand in 2D and we measure a microplasma lifetime of ≅ 1.5 ns. By combining the observations with simulations, we extract directly the free-carrier diffusion coefficient and recombination time in bulk silicon as a function of free-carrier density up to ≅ 10^{19} cm^3. This provides an original set of experimental data which must be beneficial for modelling the responses of silicon in various contexts.

[1] Mouskeftaras, A. *et al.* Self-limited underdense microplasmas in bulk silicon induced by ultrashort laser pulses. *Appl. Phys. Lett.* **105,** 191103 (2014).
[2] Grojo, D. *et al.* Long-wavelength multiphoton ionization inside band-gap solids. *Phys. Rev. B* **88,** 195135 (2013).

P-026

Structure and surface morphology evolution of amorphous carbon surfaces during transformation by 0.2-20 ps laser pulses

J. Csontos[1], J. Budai[1], Z. Tóth[2], M. Füle[3]

[1]*Departement of Optics and Quantumelectronics, University of Szeged, Hungary, H-6720, Szeged, Dóm tér 9.*

[3]*Department of Oral Byology and Experimental Dental Research, University of Szeged, Hungary, H-6720, Szeged, Tisza Lajos Krt 64.*

[3]*Department of Experimental Physics, University of Szeged, Hungary, H-6720, Szeged, Dóm tér 9.*

Corresponding Author e-mail address:miklos.fule@gmail.com

1. Introduction

Different kinds of amorphous materials are used in industry and science for various purposes: they serve as protecting materials, solar cell base materials, biocompatible coatings for implants, etc. The surface texture of these materials modified by laser pulses below or above the ablation threshold plays an important role in different applications: the surface area can be increased, cell adhesion can be modified etc. The laser induced processes are strongly influenced by the ambient and laser pulse parameters: wavelength, fluence, and pulse number[1]. In our earlier experiments the surface texture formation processes were studied on different type of crystalline materials[2] as function of the pulse number and laser fluence. Based on these results a possible scheme for the formation processes was sketched, but further examination is needed to reveal the processes being most significant from point of view of surface texturing.

A further parameter of which variation can help to determine the main processes of surface texturing is the duration of the laser pulse. Its variation in the 100 fs to several tens of ps range allows investigating the effect of processes of different characteristic times (electron thermalization, electron phonon interaction, rearranging the bonding system, phonon relaxation, fixation of bonding structure). Increasing the pulse duration causes decreasing cooling rate in the laser heated material which can lead to increase the size of the ordered domains in the amorphous material, effecting the bonding structure besides surface morphology. In this paper our results concerning the pulse duration and pulse number dependence of the surface texture formation and bonding structure modification of different carbon surfaces just below the ablation threshold are presented.

2. Experimental realization

A titanium sapphire and a unique excimer-dye laser system were used on different kind of carbon surfaces. The energy, pulse duration time and repetition rate of titanium sapphire pulses were 175 μJ, 0.03-30 ps and 100 Hz, respectively. In case of the excimer dye laser system these parameters were 5 mJ/200 μJ, 0.2-30 ps and 1 Hz, respectively. The number of pulses was varied from 1 to 100. The textured and transformed surfaces were investigated by field emission scanning electron microscopy (FESEM) and Raman spectroscopy.

3. Results

In our previous work[3] diamond-like amorphous layers were deposited by pulsed laser deposition. As can be seen on the FESEM images in Fig. 1. TiS laser treatment results in appearance of surface texture in 20-50 nm scale.

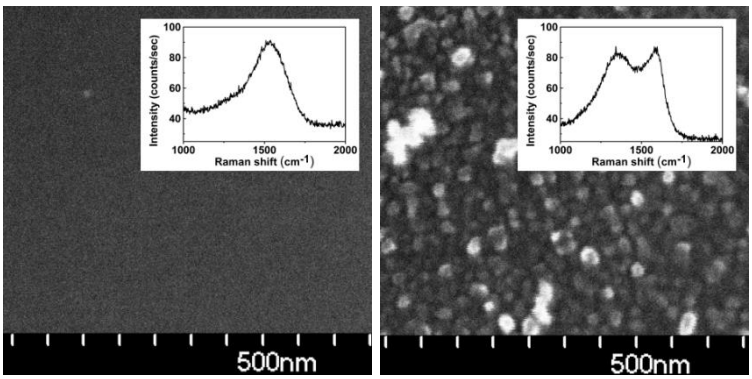

Fig 1. SEM image and Raman spectrum of the intact (left) and the TiS laser modified amorphous carbon layer (right).

Raman spectra of laser treated area shows characteristic changes in the bonding structure (as an example see insets in Fig.1.). After laser treatment the diamond-like layer transforms to a more graphitic-like amorphous carbon layer. The dependence of surface structure scale length and the change in sp^3/sp^2 ratio on laser pulse duration and other processing parameters will be presented.

References

1 J. Csontos, Z. Pápa, A. Gárdián, M. Füle, J. Budai and Z. Toth "Spectroscopic ellipsometric and Raman spectroscopic investigations of pulsed laser treated glassy carbon surfaces," Appl. Surf. Sci. Article in Press (2015)

2 M. Füle, A Gárdián, J. Budai and Z. Tóth, "Comparative Study of the Surface Nanostructure Formation on Different Surfaces Generated by Low Number of fs Laser Pulses" J. Laser Micro/Nanoeng. **10**, 74 (2015)

3 J. Budai, Z. Tóth, A. Juhász, G. Szakács, E. Szilágyi, M. Veres and M. Koós "Reactive pulsed laser deposition of hydrogenated carbon thin films: The effect of hydrogen pressure" J. Appl. Phys. **100** 043501. (2006)

P-027

Electrical and optical investigations of plasma plumes generated by femtosecond laser ablation of various metals

S.A. Irimiciuc[1,2] ,S. Gurlui[2], P. Nica[3], M. Agop[3], M. Osiac[4], C. Focsa[1]

[1] *Laboratoire de Physique des Lasers, Atomes et Molécules, Université Lille 1, 59655 Villeneuve d'Ascq, France*
[2] *Faculty of Physics, Alexandru Ioan Cuza University, 700506 Iasi, Romania*
[3] *Department of Physics, Gh. Asachi Technical University, 700050 Iasi, Romania*
[4] *Faculty of Physics, University of Craiova, 200585 Craiova, Romania*
E-mail: cristian.focsa@univ-lille1.fr

Plasma plumes generated by femtosecond laser ablation on several metals (W, In, Te, Mn, Ni, Cu, Al) were studied by optical and electrical means. The aim of these experiments has been to investigate the link between the plasma parameters (electron temperature, particle density, plasma potential, expansion velocity) and the physical properties of the targets (electrical and thermal conductivities, melting, boiling points etc.). The experiments were performed at various background pressures ($10^{-2} \div 10^{-5}$ Torr), target biases and probe-target axial distances. The probe current was analyzed in terms of a shifted Maxwell-Boltzmann distribution function. Similar temporal behaviors were found for both positive and negative polarities. Consequently, we hypothesize that unified distribution functions should exist for both types of charged particles. This was further confirmed by common oscillation frequencies evidenced in both polarities. Plasma temperatures ("hot" and "cold" particles) and average charge states were deduced from the model. Moreover, by applying various probe biasing voltages and collecting the plasma current, the I-V characteristics were reconstructed at different evolution times, in order to study the temporal evolution of plasma proprieties. Two different behaviors of laser generated plasma plumes were evidenced, with an important effect of the applied target bias at short evolution times.

The optical investigations were focused on studying the dynamics of the expanding plume as well as of the excited plasma particles. Background pressure was proved to be the major factor on the expanding velocity of the global plume. The target bias only influenced the expansion of plume produced on materials with low atomic mass. ICCD imaging revealed the presence of two or three plasma structures, depending on the background pressure, result which is in good agreement with the Langmuir probe investigations.

P-028

Energy deposition in dielectric materials by few cycles laser pulses

G. Duchateau[1], B. Chimier[1], L. Barilleau[1], A. Bourgeade[2]
[1]*Université de Bordeaux-CNRS-CEA, CELIA, UMR 5107, 351 Cours de la Libération, 33405 Talence, France*
[2]*CEA/CESTA, 15 Avenue des Sablères, 33114 Le Barp, France*
Corresponding Author e-mail address: duchateau@celia.u-bordeaux1.fr

Optical materials such as silica, Sb_2O_3 (BK7), KH_2PO_4 (KDP), or sapphire, are commonly used in laser systems for pulse shaping or to be structured to obtain new optical functionalities as wave guides, nano-gratings, etc. These materials are dielectrics with large bandgaps which electronic properties may significantly evolve when interacting with intense femtosecond (fs) laser pulses. At the same time, laser-pulse characteristics such as the frequency spectrum may be strongly affected in the course of propagation. The modifications of electronic properties initiate with the photo-ionization stage. It is followed by the laser-assisted electron dynamics in the conduction band leading to the energy deposition in the lattice and possible ablation. The latter can be accurately described by modelling coupled electron dynamics and laser propagation.

In the case of short pulses of tens of fs, spectral broadening becomes significant and the assumption of a fixed monochromatic wave should be abandoned, i.e. *time-dependent* descriptions are required. The best way to describe the propagation of short laser pulses in dielectric materials under these conditions is to solve numerically the three-dimensional Maxwell equations [1]. A good candidate for modeling the primary ionization stage is the so-called BVkP approach, which is based on Bloch-Volkov states describing the quantum dynamics of an electron in both the lattice and laser electric fields [2]. It has been shown to correctly account for the possible temporal evolution of the frequency spectrum through the time-dependent electric field, thus being able to describe consistently the simultaneous presence of various multiphoton orders due to spectral broadening or temporal evolution due to a frequency chirp for instance. An illustration is provided by Fig. 1 with the following parameters: 100fs, 413nm, 50TW/cm^2, and bandgap of 9eV. The electron density evolution consists of peaks corresponding to the absorption of different numbers of photons. This time-dependent ionization model has been coupled to a code solving the Maxwell's equations to account for a temporal evolution of the pulse frequency spectrum [1]. An illustration of this effect is provided by Fig. 2 which shows the evolution of the maximum of the free-electron density as a function of the propagation distance in a frequency converter KDP crystal with parameters: 80fs, 633nm, 7.5TW/cm^2, and bandgap of 7.8eV. When the frequency conversion is not allowed, the black curve shows an exponential decrease in the electron density associated with the depletion of the laser pulse. When frequency conversion takes place (red curve), this behavior is dramatically changed due the additional ionization path created by the second-harmonic generation. When the latter becomes significant, roughly after a few tens of µm of propagation, the two-photon ionization rate is such that it compensates the laser depletion leading to the observed increase in the density.

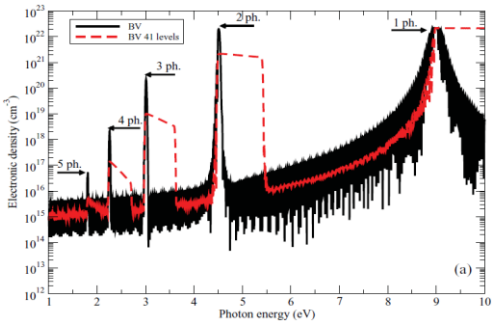

Fig. 1. Laser-induced free electron density (see text)

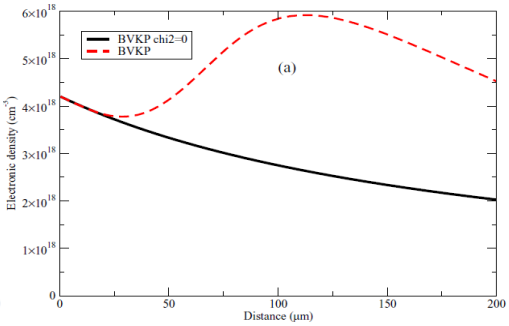

Fig. 2. Evolution of the density in case of frequency conversion (see text)

In the case of ultra-short pulses of a few fs which may have less than 2 optical cycles, the BVkP ionization model remains fully valid whereas the well-known Keldysh formula should no longer be used since it has been established for stationary conditions. Regarding the electron dynamics in the conduction band, electron heating based on collisional processes may not be significant since temporal interval between two collisions lies in the fs range, i.e. the pulse duration. Within this regime, electron heating may take place through direct multiphoton transitions between states of the conduction band [3]. A quantum description of this process as well as its introduction in the Maxwell's equations will be presented. Preliminary results show a strongly nonlinear heating and subsequent energy deposition with respect to the laser intensity.

[1] G. Duchateau and A. Bourgeade, "Influence of the time-dependent pulse spectrum on ionization and laser propagation in nonlinear optical materials," Phys. Rev. A **89**, 053837 (2014).
[2] A. Bourgeade and G. Duchateau, "Time-dependent ionization models designed for intense and short laser pulse propagation in dielectric materials," Phys. Rev. E **85**, 056403 (2012).
[3] H. Bachau et al, "Electron heating in the conduction band of insulators irradiated by ultrashort laser pulses," Phys. Rev. B **74**, 235215 (2006).

P-029

Effect of Metal Thermal Properties on LIBS Plasma Emission

J. R. Becker, P. J. Skrodzki, P. K. Diwakar, and A. Hassanein

Center for Materials Under eXtreme Environment (CMUXE), School of Nuclear Engineering,

Purdue University, West Lafayette, IN 47906, USA

Email address: becker32@purdue.edu

Abstract

Laser-induced breakdown spectroscopy (LIBS) serves as an efficient, non-invasive method for material analysis through ablation of target materials with single or multiple lasers followed by investigation of the spectral characteristics of materials plasmas. Laser-material interaction plays a critical role in the evolution of LIBS plasma which ultimately affects the LIBS spectral response. This study demonstrates the role of sample thermal properties on LIBS signal intensity, continuum emission, species persistence, plasma temperature, and plasma electron density. This information is crucial in optimizing the parameters for improvement of LIBS signal for various applications. The plasma was generated using a 1064 nm, 9 ns full width half maximum (FWHM) laser pulse from Nd:YAG laser. Nine different metals have been selected for this study, ranging from low-z to high-z materials. These metals were selected based on their varying atomic mass, melting point, boiling point, ionization potential, thermal parameters, and optical properties. Signal intensity, S/N, S/B, species persistence, and continuum emission were determined for all samples at various laser pulse energies and correlated to thermal properties of the metal samples. Principal component analysis and dendogram analysis were performed to identify dominating material properties influencing LIBS plasma emission. Shadowgraphy of LIBS plasma induced shockwaves showed varying shockwave velocity, which was correlated to laser-material interactions. Detailed mechanisms of laser-material interactions and influence of material properties on LIBS plasma are discussed.

P-030

Effects of Transverse Magnetic Fields on Nanosecond and Femtosecond Laser Produced Plasma

N. Shah, P.K. Diwakar, A. Hassanein

Center for Materials Under Extreme Environment, School of Nuclear Engineering,

Purdue University, West Lafayette, Indiana 47907, USA

Email address: shah109@purdue.edu@purdue.edu

Laser produced plasmas (LPP) are used for many applications including LIBS, EUV production, pulsed laser deposition (PLD), and nanoparticle generation, where both nanosecond and femtosecond pulses have been used. A magnetic field is able to manipulate LPP properties for plasma confinement, debris mitigation, plasma focusing, emission enhancement, etc. In this study, the influence of transverse magnetic field on both nanosecond and femtosecond laser produced plasma is presented. To generate a nanonsecond plasma, a Continuum Surelite Nd:YAG pulse laser (λ:1064 nm and FWHM:6 ns) is used, while for femtosecond LPP, a Ti:Saphire (λ:800 nm and FWHM:40 fs) pulse laser is used to ablate 3 different samples: aluminum, brass, and tungsten. A permanent magnetic trap was designed with nearly uniform magnetic field of 0.8T. Samples were ablated using varying fluences (spot size and energy) in vacuum. Three different plasma diagnostics were used to study the dynamics of the transient plasma. Faraday cup analysis was used to determine the velocity (kinetic energy) and ion flux. It was observed that fluence and atomic mass of the target material play critical roles in determining the reduction in velocity in the presence of magnetic field. Secondly, fast photography was performed using an intensified charged coupled device (ICCD) to study the plume dynamics. In the presence of transverse magnetic field, the plume expansion was confined; the plume front traveled a shorter distance as compared to free expanding plasma. Femtosecond LPP appear to be significantly influenced by laser fluence in determining the LPP plume shape as well as expansion in the presence of magnetic field. Finally, optical emission spectroscopy was used to determine the temperature, electron density, and ionization rate of the plasma plume. In the presence of transverse magnetic field, enhancement in the emission of some ionic lines was observed along with a slight reduction in electron density and increase in plasma temperature.

P-031

Improving the conversion efficiency of EUV emission using CO_2 reheating of Nd:YAG pre-pulse produced Sn plasma

J. P. Oliver, A. Mohanta, M. P. Polek, P. K. Diwakar, T. S. Sizyuk, A. Hassanein

Center for Materials Under Extreme Environment, School of Nuclear Engineering
Purdue University, West Lafayette, Indiana 47907, USA
E-mail: oliver36@purdue.edu

Current photolithography methods utilize a 193 nm light source in the microfabrication of electronic circuits. While this technique has served its purpose for the past three decades, an inherent restriction on the minimum detail prescribed to an etching process is imposed by the large photon wavelength limits its continued practice. In meeting this challenge, next-generation lithography technologies are being developed to reduce the limits of wafer etching. Extreme ultraviolet lithography (EUVL) is a leading lithography technique in next-generation lithography due to the small 13.5 nm photon emission from tin and the availability of 2%-BW Mo/Si multilayer mirrors with 70% reflectivity. In order to meet the throughput demand, a high conversion efficiency of EUV light is required. Additional techniques have shown that the conversion efficiency of 13.5 nm light can be improved by exercising pre-pulse LPP of Sn followed by CO_2 laser reheat.

This study is to optimize the conversion efficiency (CE) of 13.5 nm Sn-based light by varying several parameters – spot size and wavelength of pre-pulse Nd:YAG laser, and time delay between pulses. Using HEIGHTS package, the effect of spot size on EUV emission and conversion efficiency was studied. The modeling results were then compared with the experimental findings to further benchmark and optimize the experiments. Spot sizes of the Nd:YAG laser were varied to identify the optimal focus for enhanced conversion efficiency. The experiment was conducted with both single-pulse Nd:YAG and double-pulse Nd:YAG with CO_2 laser reheat. Inter-pulse delay study was conducted to identify the behavior of CE across a range of time delays, making note of the optimal time delay producing the highest CE. This procedure was then repeated operating the Nd:YAG laser at its 266 nm fourth-harmonic. The experiment was conducted using a TEA CO_2 laser (τ_p = 35 ns, λ = 10.6 μm) and Nd:YAG laser (τ_p = 6 ns, λ = 1064 nm) capable of operating at fourth harmonic. An absolutely calibrated EUV Power Tool coupled with a 1 GHz digital oscilloscope was implemented to determine the CE, and the EUV emission spectra were acquired from an EUV transmission grating spectrograph (TGS).

P-032

Optical constant of molybdenum film in CuInGaSe solar cell and the estimated ablating temperatures with a moving laser

C.C. Yang, W. T. Hsiao, S. F. Tseng, D. Chiang
Instrument Technology Research Center, National Applied Research Laboratories, Hsinchu 30076, Taiwan R.O.C.
e-mail: dony@itrc.narl.org.tw

1. Introduction

The laser is a versatile tool for surface patterning and direct microstructure machining on a variety of materials. It helps in the solar cell industries to operate the edge isolation for the square silicon wafer cells and to scribe a large area thin film panel into isolated, individual cells for the thin film solar cells. The direct observations on the edge isolation and cell scribing are difficult because the time period of interaction between laser and material is short, usually less than μs, and the laser spot is small, usually in the range of the μm. That is the reason why the experimental phenomena from the material ablations influenced by the laser operational parameters are well-documented, however, the mechanism discussions or interaction descriptions are few. The simulation can provide an efficient method to shine a light on the material and light interaction mechanism. A nano-second laser pulse is applied on the molybdenum metal film deposited on a glass substrate and the temperature profile in this substrate is examined with the time. The calculated maximum temperature are reasonably to explain the lower laser fluence required for condition, in which the laser penetrates the substrate before hits the metal film, than that for condition, in which the laser hits first the metal film [1]. We also extend the numerical method to evaluate the temperature when the laser is moving relatively to the working piece.

2. Numerical methods

We use the Matrix method first to solve the optical constants of the examined materials from their reflectance and transmittance measurements with the wavelengths. The laser parameters and the materials used in this simulation are given in table 1. The laser wavelength used is 355 nm and a pulsed train with different frequency is applied to determine the response of Mo film to the laser when the laser is stationary. An alternating direction-implicit technique is used to solve the two-dimensional heat condition partial differential equation with time.

3. Preliminary Calculated Results

The material properties used in the simulation are list in Table 1. Two schematic structures are plotted in Fig. 1. The laser penetrates into the glass substrate, hits the Mo film and goes through the air, shown in case I. The laser goes through air layer, hits the Mo film and enters into the substrate, shown in case II. The reflectance and transmittance of a Mo film of 97 nm thick on glass substrate varied with wavelengths and their corresponding optical constants are shown in Fig. 2. The temperature distributions along the laser central axis for case I at the 10 W for 25 ns are shown in Fig. 3 and the temperature distributions for case II are shown in Fig 4. The calculated temperatures in case I are much higher than that for case II.

Table 1: Material characteristics used in simulation

	thickness	n	k	Cp	κ	Tm
Glass	25 μm	1.56	0.	2.10	0.0105	-
Mo	0.5 μm	0.42	1.09	2.57	1.38	2896
Air	100 μm	1.0	0.	0.0013	0.00024	-

n= refraction index, k= extinction coefficient, Cp= heat capacity in terms of J/cm3-k, κ= thermal conductivity in terms of J/cm-k-s, Tm= melting temperature in terms of kelvin

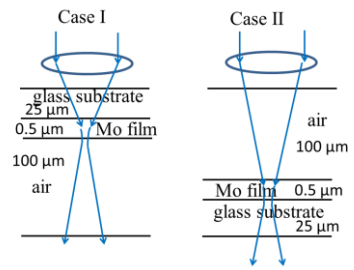

Fig. 1 two schematic diagrams

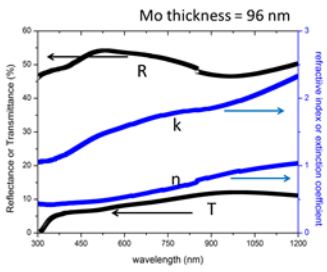

Fig. 2 optical constants of Mo film

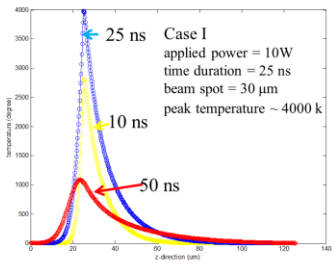

Fig. 3 temperature distribution for case I, the peak temperature is 4000 k

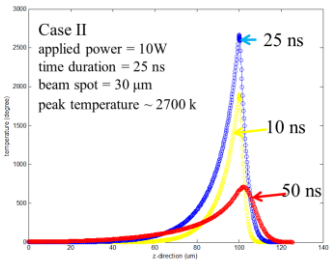

Fig. 4 temperature distribution for case II, the peak temperature is 2700 k

[1] G. Heise, M. Englmaier, C. Hellwig, T. Kuznicki, S. Sarrah, and H. P. Huber, "Laser Ablation of Thin Molybdenum Films on Transparent Substrates at Low Fluences", Appl. Phys. A., **102**, 173-178 (2011)

P-033

Femtosecond laser ablation plasmas of metals as nonlinear optical media for low order harmonic generation

M. Oujja[1], J. G. Izquierdo[2], L. Bañares[2], R. de Nalda[1], M. Castillejo[1]

[(1)]Instituto de Química Física Rocasolano, CSIC, Serrano 119, 28006 Madrid, Spain

[(2)]Departamento de Química Física, Facultad de Ciencias Químicas (Unidad Asociada I+D+i al CSIC), Universidad Complutense de Madrid, 28040 Madrid, Spain

E-mail: marta.castillejo@iqfr.csic.es

Laser ablation plasmas are current subject of study as media to generate short wavelength coherent radiation by nonlinear optical frequency up-conversion [1]. In particular, for metal targets under femtosecond irradiation, the presence of nanoparticles in the laser plume brings specific advantages associated with resonant enhancement of the conversion efficiency, extension of the cut-off frequency of the newly generated radiation and others [2].

In this work we examine the nonlinear response of complex metal plasmas, generated by femtosecond laser ablation, by using them as media for third and fifth-order harmonic generation (HG) of a 1064 nm 8-ns Nd:YAG driving laser. The experimental set up, based on a system described previously [3,4] includes the use of 80-fs ablating pulses, centred at 800 nm, generated in a Ti:sapphire system. Full electronic control of the relative timing between the femtosecond (ablation) and nanosecond (HG driving) pulses, together with the control of the geometry of the interaction, allowed to search optimum delays, distances from the target and ablation focusing conditions. Complementary diagnostic of the ablation plumes, carried out by optical emission spectroscopy (OES), allowed collecting both time-resolved 2D projections of the broadband emission and 1D spatially-resolved spectra.

The work covered the metals Ag, Cu, Al and Mn, for which both common trends and markedly differing features were found. Among the behaviours shared by all materials it is interesting to note that the ablation beam focusing conditions on the metal surface played the most determining role on the overall nonlinear response, and also on the optimum delay for HG. This is shown in Fig. 1 for the case of Cu. On the contrary, it was found that both the global nonlinear response, and the relative efficiency for third and fifth HG were strongly dependent on the choice of the metallic target.

As also exemplified in Fig. 1, the harmonic signal presents a characteristic dependence with the delay between the fs ablation event and the ns driving pulse, which accounts for the contribution to the nonlinear signal of various plume species in different temporal ranges. Correlation with OES measurements in the corresponding plumes has allowed distinguishing the contribution of atomic ions and neutrals and nanoparticles to the low order nonlinear response of the studied plumes.

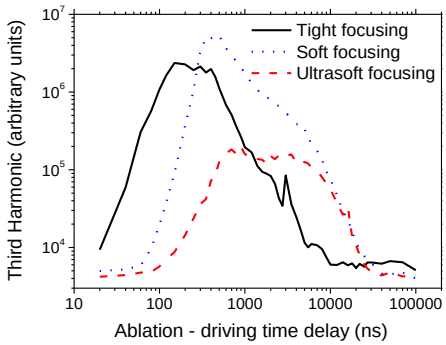

Fig. 1. Third harmonic generation in a fs-laser ablation Cu plasma, as a function of the delay between the fs ablation event and the ns driving pulse, and for three different focussing geometries of the ablation laser.

References

[1] R. A. Ganeev, *Plasma Harmonics*, (CRC Press, Boca Raton, 2014).

[2] R.A. Ganeev, T. Witting, C. Hutchison, V.V Strelkov, F. Frank, M. Castillejo, I. Lopez-Quintas, Z. Abdelrahman, J.W.G. Tisch, and J.P. Marangos, "Comparative studies of resonance enhancement of harmonic radiation in indium plasma using multi-cycle and few-cycle pulses," Phys. Rev. A. **88**, 033838 (2013).

[3] R. de Nalda, M. Lopez-Arias, M. Sanz, M. Oujja, and M. Castillejo, "Harmonic generation in ablation plasmas of wide bandgap semiconductors," Phys. Chem. Chem. Phys. **13,** 10755 (2011).

[4] M. Lopez-Arias, M. Oujja, M. Sanz, R.A. Ganeev, G.S. Bolataev, N.Kh. Satlikov, R.I. Tugushev, T. Usmanov, and M. Castillejo, "Low-order harmonic generation in metal ablation plasmas in nanosecond and picosecond laser regimes," J. Appl. Phys. **111**, 043111. (2012).

P-035

Nanostructuring of diamond via two photon UV etching at sub-ablation fluences

C. G. Baldwin, J. E. Downes, R. P. Mildren
Department of Physics and Astronomy, Macquarie University, Sydney, NSW, 2109, Australia
Email: chris.baldwin@mq.edu.au

Two photon UV etching of diamond is a relatively newly discovered process, wherein exposure of a diamond surface in air to UV light with fluence below the ablation threshold results in slow, controllable removal of material with average rates typically much less than one atomic layer per pulse. Numerous experiments have been performed to investigate the properties if this process, the results of which will be presented. These include measurements of etch rate under a variety of conditions, imaging of nanostructures arising from etching, analysis of surface chemical states via x-ray spectroscopy, post-process modification of complex nanostructures by UV etching, and observation of the behaviour of etching as a function of oxygen partial pressure.

It has been found that the rate of material removal has a quadratic dependence on the laser intensity, and the profile of etched pits are proportional to the square of the etching beam's intensity profile; both of which are indicative of a two photon process[1]. It also appears to be thresholdless – average etch rates have been observed from as low as 10^{-9} nm/pulse to as high as 10^{-2} nm/pulse with consistent behaviour. The presence of atmospheric oxygen is necessary for etching to occur [2], indicating that the process is photo-chemical in nature and sustained by surface oxidation. X-ray spectroscopy has found the etched diamond surface to be free of graphite (which is normally associated with the laser ablation of diamond), and instead shows a clean, oxygen terminated surface. The lack of redeposited detritus indicates that material leaves as highly volatile species; likely CO or CO_2.

Etching also causes roughening of the surface, as the diamond tends to form microfacets along (111) planes. Interestingly, the morphologies of these structures are strongly dependent on the angle between the polarisation of the etching laser and the underlying crystal lattice. Figure 1 shows an example of a (001) oriented surface and the differences in nanostructure which arise from rotation of the beam polarisation. This seems to indicate an interaction with highly directional components of the surface – likely surface bonds.

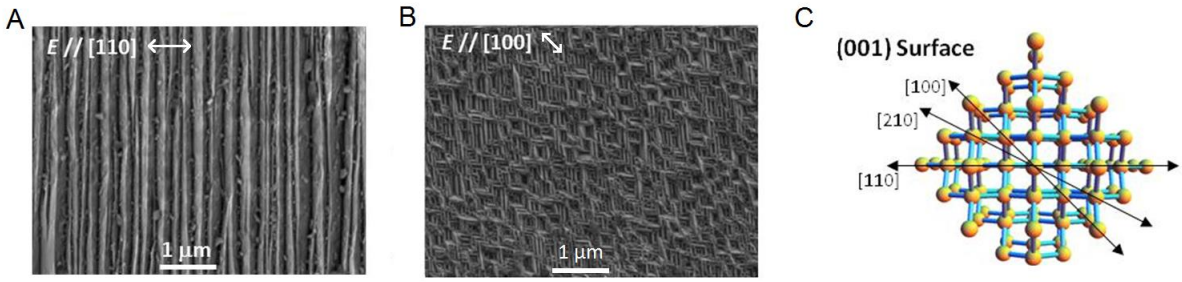

Fig. 1. SEM images of (111) faceting on deeply etched (100) surfaces (A, B), with writing beam polarisation indicated. C shows how the etching beam polarisations relate to the crystal lattice.

These characteristics of material removal, which to the authors' knowledge are distinctive to diamond, have led to a broad description of a 'cold' etch mechanism where two photon absorption occurs at the diamond surface, which results in the ejection of carbon and oxygen atoms followed by readsorption of oxygen from the atmosphere to regenerate the oxygen termination layer. However, many aspects of the mechanism are poorly understood. Important characteristics that determine minimum feature size, as well as the smoothness and chemical characteristics of etched surfaces are yet to be elucidated. Crucially, little is known about the two photon excitation and how it results in the desorption of material. It is the goal of our ongoing work to learn more about the etching mechanism, both to identify physical processes not observed elsewhere, as well as to assess the viability of UV etching for technological applications.

References

[1] R. P. Mildren, J. E. Downes, J. D. Brown, B. F. Johnston, E. Granados, D. J. Spence, A. Lehmann, L. Weston, and A. Bramble, "Characteristics of 2-photon ultraviolet laser etching of diamond," Opt. Mater. Express **1**, 576-585 (2011)

[2] V. V. Kononenko, M. S. Komlenok, S. M. Pimenov, V. I. Konov, "Photoinduced laser etching of a diamond surface", Quantum Electron, **37** (11), 1043–1046, (2007).

P-037

Laser Annealing of Thin Films using NdYAG laser

G.C. Lee[a], Y.S. Ong[b], W. Kam[b], K.S. Hamdan[b], R. Zakaria[b], and C.S. Lim[a]

[a] *Department of Mechanical, Materials and Manufacturing Engineering, University of Nottingham Malaysia Campus*

[b] *Photonics Research Centre, Faculty of Science, University of Malaya*

rozalina@um.edu.my

ABSTRACT

In this report, experiment was performed to study the effect of pulsed laser annealing of two different types of thin films using Nd:YAG laser at fundamental wavelength (1064nm). The two thin films been subjected to pulsed laser annealing are: amorphous-silicon (a-Si) thin film and gold (Au) thin film. For a-Si thin film, the samples are annealed with single laser pulse at different laser fluence to obtain polycrystalline (poly-Si) thin films. From the result obtained, it was proven that the crystallinity of poly-Si thin films increases as the laser fluence increases up to 3J/cm^2 with no ablation effect observed. However, the result shown that a-Si thin filmed annealed with the fluence of 2.1J/cm^2 and 3J/cm^2 contains large number of defects within crystalline structure formed. Also, the higher the fluence is used to anneal a-Si thin film; higher internal compression stress will reside within the microstructure of poly-Si thin film produced. Also, it was discovered that laser annealing of Au thin film with fundamental wavelength laser enables formation of gold nanoparticles (AuNPs) through. It was also proven that the maximum absorbance and respective wavelength of maximum absorbance of AuNPs are tunable through manipulation of the laser annealing parameter, at which annealing Au thin film using higher fluence or greater number of laser pulses will greatly enhancement in absorbance of AuNPs.

P-039

Molecular dynamics simulation study of femtosecond laser ablation of silver thin films and bulk targets in water environment

Cheng-Yu Shih, Chengping Wu, Maxim V. Shugaev, and Leonid V. Zhigilei

Department of Materials Science and Engineering, University of Virginia, 395 McCormik Road, Charlottesville, Virginia 22904-4745, USA
E-mail: cs5fg@virginia.edu

Laser ablation of metal target in liquid environment is actively used for generation of clean colloidal nanoparticles with unique shapes and functionalities. The fundamental mechanisms responsible for the nanoparticle formation and the key processes that control the nanoparticle size distributions are not yet fully understood. In this presentation, we report the results of the first atomistic simulations of laser ablation of metal targets in liquid environment. A model combining a coarse-grained representation of liquid (parameterized for water), a fully atomistic description of laser interactions with metal targets, and advanced acoustic impedance matching boundary conditions is developed for the simulations. The model is implemented in a computationally-efficient parallel code, which is used to perform a series of large-scale simulations of laser ablation of thin silver films deposited on a silica substrate and a bulk silver target.

In contrast to the laser ablation in vacuum, where the superheated Ag undergoes an explosive decomposition into liquid droplets and vapor, the phase decomposition in the liquid environment is partially suppressed and the hot metal vapor/clusters ejected from the irradiated target are localized in a low-density mixing region where the liquid is brought to the supercritical state. Due to the soft confinement provided by the water environment, a thin Ag molten layer forms between the region of high density Ag vapor and the supercritical water as shown in right frame of the Figure. The thin Ag molten layer acts as a source of Ag vapor for continuous growth of nanoparticles in the supercritical water. The main nanoparticle formation mechanism is the condensation of clusters from the Ag vapor, followed by coalescence and coarsening within the supercritical water region. The results of the simulations support the notion of the important role of the cavitation bubble in the process of nanoparticle formation, often suggested in interpretation of experimental observation. The simulations also predict that larger nanoparticles can be generated at high fluence, when active water motion incurs the instability of the floating molten metal layer. The distinct contributions of the vapor condensation and disintegration of a thin metal layer lead to the formation of a bimodal nanoparticle size distribution commonly observed in experiments performed at high laser fluences.

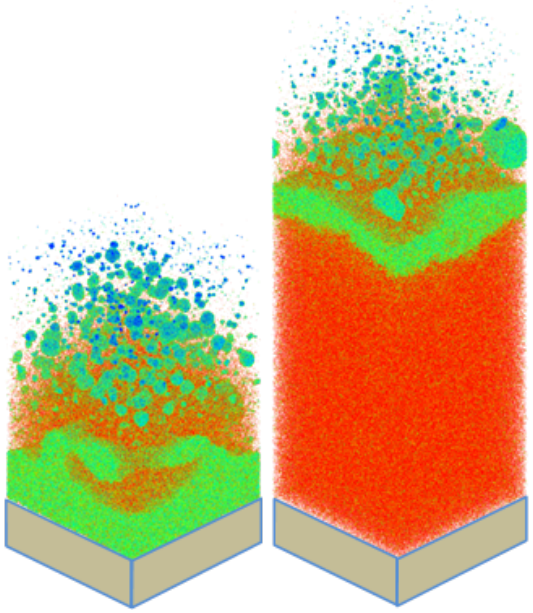

Figure. Snapshots of atomic configurations obtained in molecular dynamics simulations of laser ablation of a 20 nm Ag film in water environment. The snapshots are shown for 3 ns after irradiation by a 40 fs laser pulse at an absorbed fluence of 400 J/m^2 (left) and 700 J/m^2 (right). The films are initially located on a silica substrate shown by the solid boxes at the bottom. The water is blanked in the snapshots to provide a clear view of the metal nanoparticles generated in the water-Ag mixing region. The Ag atoms are colored by their potential energies, from red color for vapor-phase Ag atoms to green color for hot liquid layers/droplets and to blue color for small clusters quenched due to the interaction with supercritical water.

P-040

Large-scale atomistic modeling of structural modification of metal surfaces in femtosecond laser processing

Chengping Wu, Maxim V. Shugaev, Eaman T. Karim, and Leonid V. Zhigilei

Department of Materials Science and Engineering, University of Virginia, 395 McCormik Road, Charlottesville, Virginia 22904-4745, USA

E-mail: lz2n@virginia.edu

Large-scale atomistic simulations are performed to investigate the relations between the basic mechanisms of laser interaction with metals, laser-induced non-equilibrium structural and phase transformations, and the resulting microstructure of laser-treated regions. Two series of simulations are reported in this presentation.

The first series of simulations is motivated by the experimental observation of surface "swelling" of metal targets irradiated at laser fluences below the spallation/ablation threshold [1,2]. The simulations performed for single-crystal Ag targets irradiated by femtosecond laser pulses predict the concurrent occurrence of the fast laser melting and the dynamic relaxation of laser-induced stresses that leads to the generation of sub-surface voids in the transiently melted surface region of the target. Rapid cooling and resolidification of the melted region can trap the voids by the advancing solidification front and result in the formation of a subsurface porous region with an effective increase in the volume of the material (*i.e.*, "swelling") within the laser spot. The ultrafast cooling of the surface region also creates conditions for massive crystal nucleation and generation of a nanocrystalline surface layer. The layer contains a high density of stacking faults, twins, and pentagonal structural elements, suggesting high hardness and possible enhancement of catalytic activity of the surface [2].

The second series of simulations is motivated by the results of recent electron backscatter diffraction measurements [3] that suggest a substantial influence of crystallographic orientation of single-crystal metal targets on the generation and accumulation of crystal defects [4,5]. We investigate the physical origin of this influence in a series of large-scale simulations of femtosecond laser processing of Ni and Cr targets with different crystallographic orientations.

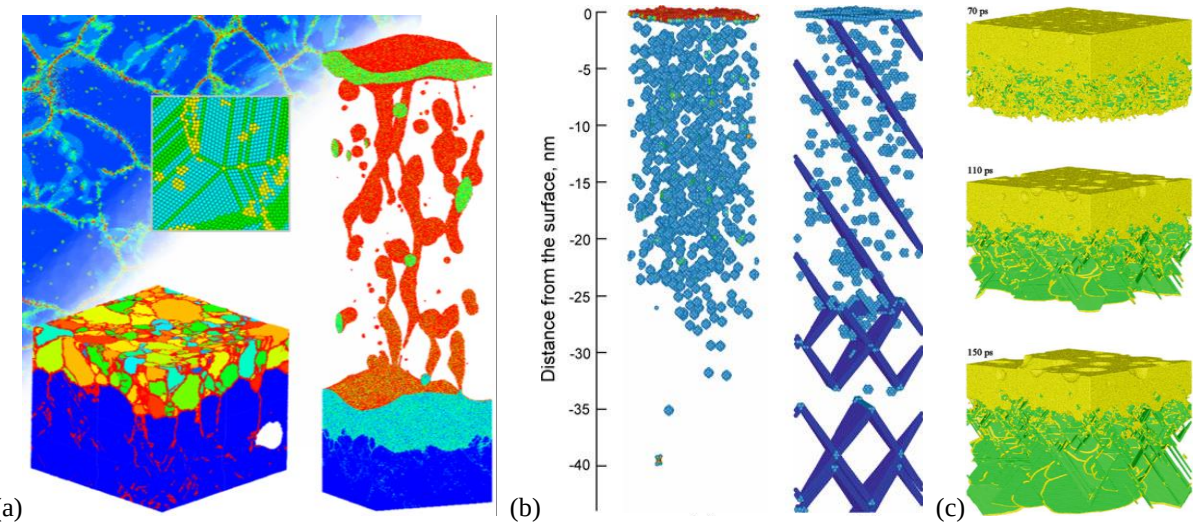

Figure. Snapshots from large-scale atomistic simulations of laser-induced structural modification of metal targets. The simulations are for Ag and Cr targets and are described in Refs. [2] for (a), [4] for (b), and [5] for (c).

References

[1] J.-M. Savolainen, M. S. Christensen, and P. Balling, Material swelling as the first step in the ablation of metals by ultrashort laser pulses, *Phys. Rev. B* **84**, 193410, 2011.

[2] C. Wu, M. S. Christensen, J.-M. Savolainen, P. Balling, and L. V. Zhigilei, Generation of sub-surface voids and a nanocrystalline surface layer in femtosecond laser irradiation of a single crystal Ag target, *Phys. Rev. B* **91**, 035413, 2015.

[3] X. Sedao, C. Maurice, F. Garrelie, J.-P. Colombier, S. Reynaud, R. Quey, F. Pigeon, Influence of crystal orientation on the formation of femtosecond laser-induced periodic surface structures and lattice defects accumulation, *Appl. Phys. Lett.* **104**, 171605, 2014.

[4] E. T. Karim, C. Wu, and L. V. Zhigilei, Molecular dynamics simulations of laser-materials interactions: General and material-specific mechanisms of material removal and generation of crystal defects, in *Fundamentals of Laser-Assisted Micro- and Nanotechnologies*, Springer Series in Materials Science, Vol. **195**, Edited by V. P. Veiko and V. I. Konov (Springer International Publishing Switzerland, 2014), pp. 27-49.

[5] C. Wu, E. T. Karim, A. N. Volkov, and L. V. Zhigilei, Atomic movies of laser-induced structural and phase transformations from molecular dynamics simulations, in *Lasers in Materials Science*, Springer Series in Materials Science, Vol. **191**, Edited by M. Castillejo, P. M. Ossi, and L. V. Zhigilei (Springer International Publishing Switzerland, 2014), pp. 67-100.

P-041

Fs laser pulses for ablation and deposition of noble metal nanoparticles with tunable optical properties

M.L. Pace[1], A. Guarnaccio[1], F. Ranù[1], D. Trucchi[2], A. De Bonis[3], R. Teghil[3], S. Orlando[1], D. Mollica[1], G.P. Parisi[1], A. Santagata[1*]

(1) CNR – ISM UOS Tito Scalo, Zona Industriale, 85050 Tito Scalo (PZ) – ITALY
(2) CNR – ISM UOS Montelibretti, Via Salaria km 29.300, 00015 - Monterotondo Scalo (RM) – ITALY
(3) Dipartimento di Scienze, Università degli Studi della Basilicata,Viale dell'Ateneo Lucano 10, 85100 Potenza -ITALY
**Corresponding Author e-mail address: antonio.santagata@cnr.it*

The capability of generating nanoparticles by direct ablation of metals through the use of fs laser pulses has been widely confirmed, during the last years, both theoretically and experimentally. The process is characterized by a large fraction of nanoparticles which, as reported by Tsakiris *et al*. [1] can be in the range of 90% of the ablated material.

In the work here presented the tunability of Au, Ag and Cu core nanoparticles generated by a 800 nm, 120 fs Ti:Sa laser in different vacuum conditions is reported. Uv-vis, XRD, XPS, TEM and SEM techniques have been used in order to characterize the obtained deposits. The outcome display promising perspectives in controlling the tunability of the plasmonic features by varying the experimental conditions employed. With this regard the role played by nanoparticles' distribution, coalescence and growth seems to be fundamental in determining the optical properties observed. The presence of nanoparticle shell structures, especially for Cu where Cu_2O can be considered the most probable species to be formed, do not determine the final properties of the deposit where, instead, the collective noble metal core nanoparticle characteristics play a major role. The comparison among results obtained by the three noble metals highlight how simple experimental parameters changes can tune the plasmonic properties of the nanoparticles generated by fs laser ablation and provide straightforward benefits for potential optical applications.

[1] N. Tsakiris, K.K. Anoop, G. Ausanio, M. Gill-Comeau, R. Bruzzese, R. S. Amoruso, L.J. Lewis, "Ultrashort laser ablation of bulk copper targets: Dynamics and size distribution of the generated nanoparticles", J. Appl. Phys. 115, art. n. 243301 (2014).

P-044

Molybdenum thin films interaction with femtosecond laser to form Molybdenum dioxide nanorods.

L. Kotsedi[1-2]

[1] *UNESCO-UNISA Africa Chair in Nanosciences-Nanotechnology, College of Graduate Studies, University of South Africa, Muckleneuk ridge, PO Box 392, Pretoria-South Africa.*
[2] *Nanosciences African Network (NANOAFNET), iThemba LABS-National Research Foundation, 1 Old Faure road, Somerset West 7129, PO Box 722, Somerset West, Western Cape Province, South Africa.*
Corresponding Author e-mail (Kotsedi@tlabs.ac.za)

Abstract

In this study thin films of molybdenum were deposited on glass substrate using the electron beam evaporator. These films were then exposed to the femtosecond fibre laser with the fundamental wavelength of 1064nm and the repetition rate of 78.5 MHz and pulse duration 298 fs. The laser-irradiated samples were then studied using the Raman spectroscopy, atomic force microscopy and high-resolution scanning electron microscope. From the Raman shift data the effect of the laser exposure was the formation of the molybdenum dioxide layer, the scanning electron microscope micrographs showed the nanorods like structure that has formed of on the irradiated sample, the density of the nanorods was increasing as the laser fluence increased. Atomic force microscope scan was taken on the irradiated area and 3D images were generated to further consolidate the results of the scanning electron microscope. Resistance measurement as a function of temperature was conducted on the sample to study the effect of the conductivity of the thin film after the laser exposure.

References:

[1] M. Maaza , B. D. Ngom, S. Khamlich, J. B. Kana Kana, P. Sibuyi, D. Hamidi, S. Ekambaram, J. Nanopart. Res. (2012) 14:714, DOI 10.1007/s11051-011-0714-3

[2] V.P. Veiko, G.A. Kotov, M.N. Libenson, M.N. Nildtin, Sov. Phys. Dokl . 18 (1973) 83

P-045

Plasmonic nanowelding of silver nanowires using a femtosecond laser

Jeonghong Ha[1], Dongsik Kim[1]

[1]*Department of Mechanical Engineering, Pohang University of Science and Technology, Pohang 790-784, Republic of Korea*

E-mail: dskim87@postech.ac.kr

Silver nanowire (AgNW) networks have attracted substantial attention as a promising alternative to indium tin oxide (ITO) films owing to their excellent electrical, optical, and mechanical properties. Welding of AgNW junctions has also emerged as a topic of fundamental and practical importance related with fabrication of future electronics. Successful post-treatment methods such as thermal annealing, Joule heating, pressuring, and plasmonic welding have been reported [1-3]. In this work, we demonstrate that ultrafast laser irradiation can weld junction of AgNWs effectively, significantly reducing the thermal side effects (Fig. 1). A Ti:sapphire femtosecond laser (wavelength = 800 nm; full width at half maximum FWHM = 50 fs) and a KrF excimer laser (wavelength = 248 nm, FWHM = 25 ns) were employed to form nanowelded junctions between neighboring AgNWs under various conditions. The morphological and structural changes were analysed by scanning electron microscopy (SEM) and transmission electron microscopy (TEM). The four-point probe technique was employed to obtain the sheet resistance of the AgNW networks. Transmittance spectra were measured for AgNW films on polyethlylene terephthalate (PET) substrates using a UV-Vis-near IR spectrometer. The laser treatment could reduce the sheet resistance of a AgNWs film to 25 Ω/□ with a transmittance of 93% (Fig. 2). The thermal side effects were negligible in the case of femtosecond laser irradiation while the excimer laser irradiation caused significant melting and breakup of the network.

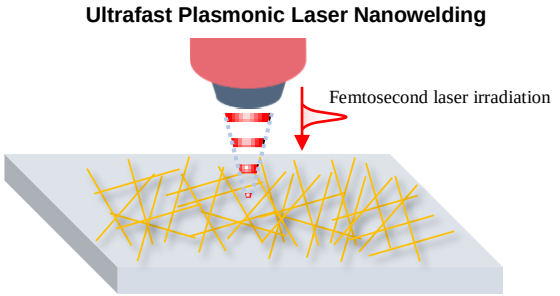

Fig. 1 Schematic of plasmonic laser nanowelding of AgNWs by femtosecond laser.

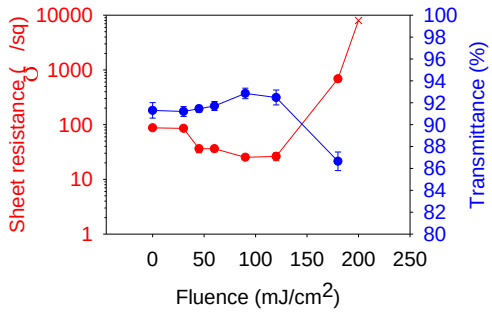

Fig. 2 Sheet resistance and transmittance of AgNW films after fs laser irradiation varying laser fluuce.

[1] J. Y. Lee, S. T. Connor, Y. Cui, and P. Peumans, "Solution-processed metal nanowire mesh transparent electrodes," *Nano Lett.* **8**, 689 (2008).

[2] Y. Lu, J. Y Huang, C. Wang, S. Sun, and J. Lou ,"Cold welding of ultrathin gold nanowires," Nat. Nanotech. **5**, 218-224 (2010).

[3] E. C. Garnett, W. Cai, J. J. Cha, ,F. Mahmood, S. T. Connor, M. G. Christoforo, Y. Cui, M. D. McGehee, and M. L. Brongersma, "Self-limited plasmonic welding of silver nanowire junctions," Nat. Mater. **11**, 241-249 (2012).

P-046

Structural transformation of single-walled carbon nanotubes by femtosecond laser irradiation

Jeonghong Ha[1], Hyun Young Jung[2], Yung Joon Jung[2], Jaegu Kim[3], and Dongsik Kim[1]
[1]*Department of Mechanical Engineering, Pohang University of Science and Technology, Pohang 790-784, Republic of Korea*
[2]*Department of Mechanical and Industrial Engineering, Northeastern University, Boston, Massachusetts 02115, United States*
[3]*Korea Institute of Machinery and Materials, Daejeon 305-343, Republic of Korea*
E-mail: dskim87@postech.ac.kr

There is a growing need for technologies to transform the structure of carbon nanotubes (CNTs) and to generate molecular junctions between adjacent tubes because the performance of a CNT network significantly deteriorates due to weak van der Waals interactions between tubes [1]. Previous studies demonstrated significant advances in transforming the CNT structures with formation of covalently bonded junctions between adjacent CNTs by electron beam irradiation [2] and Joule heating [3]. In this work, femtosecond laser irradiation is employed as a tool to induce structural transformations in CNTs (Fig. 1) since an ultrashort laser pulse can selectively deposit energy over a period shorter than the electron phonon relaxation time. We demonstrate that femtosecond laser irradiation can transform single-walled nanotubes (SWNTs) into multi-walled nanotubes (MWNTs) and form molecular junctions between adjacent SWNTs by femtosecond laser irradiation (Fig. 2). A Ti:sapphire femtosecond laser (wavelength = 800nm, full width half maximum = 50 fs, pulse energy E < 3 mJ, repetition rate = 1 kHz) was employed in the experiment. By inducing the structural transformation, which depended strongly on the number of incident laser pulses, the electrical conductivity of CNT networks could be enhanced substantially.

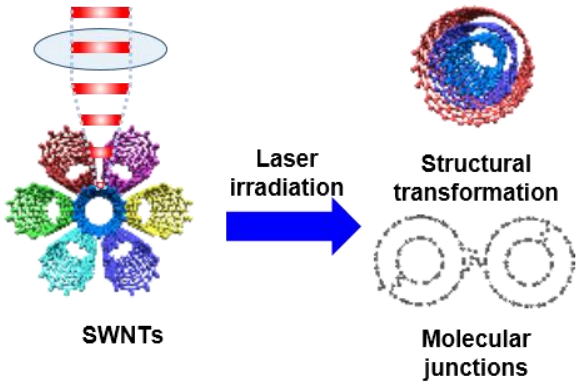

Fig. 1 Schematic of the structural transformation of SWNTs by femtosecond laser irradiation.

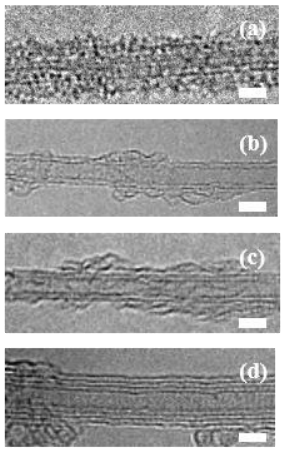

Fig. 2 TEM images of CNTs (a) before and (b)-(d) after laser irradiation with increasing pulse number.

[1] R. Saito, R. Matsuo, G. Dresselhaus, and M. Dresselhaus, "Anomalous Potential Barrier of Double-Wall Carbon Nanotube," Chem. Phys. Lett. **348**, 187 (2001).
[2] M. Terrones, F. Banhart, N. Grobert, J.-C. Charlier, H. Terrones, and P. M. Ajayan, "Molecular junctions by joining single-walled carbon nanotubes," Phys. Rev. Lett. **89**, 0755051–0755054 (2002).
[3] C. Jin, K. Suenaga, S. Iijima, "Plumbing carbon nanotubes," Nat. Nanotech. **3**, 17-21 (2008).

P-047

Influence of the pulse duration on the ablation threshold and the incubation coefficient of copper and silicon upon irradiation by femtosecond laser pulses.

Chandra S.R.Nathala[1,2], Ali Ajami, Andreas Assion[2], Wolfgang Husinsky[1]*

1) Institute for Applied Physics, Vienna Technical University, Vienna, Austria

2) Femtolasers Produktions GmbH, Vienna, Austria

** husinsky@iap.tuwien.ac.at*

Laser micromachining of surfaces for applications in Nano-technology require precise information of ablation threshold values. Several authors have reported the ablation threshold values for different materials, however only few authors have investigated the dependence of pulse duration on ablation threshold values [1-5]. In this paper we present the ablation studies of copper and silicon using ultra-short pulses of 30-550fs duration in vacuum environment. The threshold fluence is determined using diameter-regression method and time-of-flight (TOF) technique where the ion emission and neutral emission are recorded. We also determined the threshold values for electron emission in air environment. The dependence of pulse duration on threshold fluence for multi pulse ablation, ablation rates and incubation coefficients are reported for these materials. A comparison of the threshold values determined by various techniques is presented.

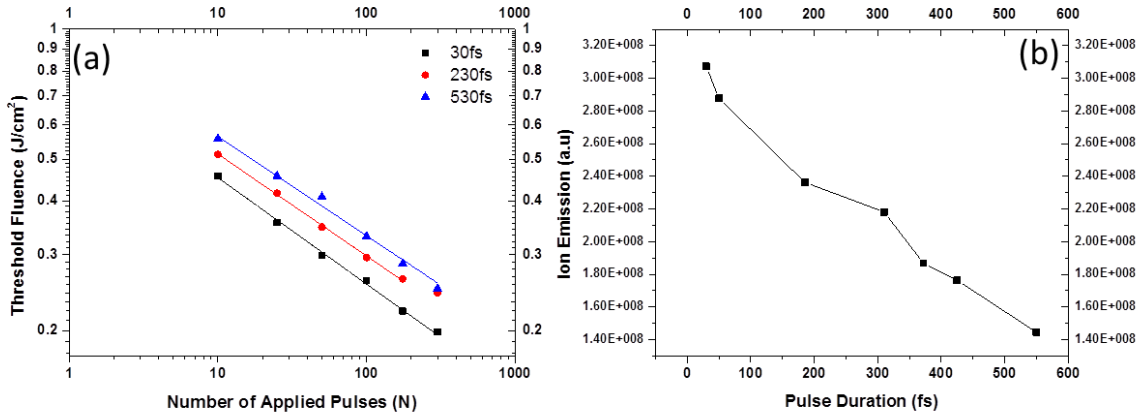

Fig. 1a. Dependence of multi-shot threshold fluence values of copper on pulse duration and Fig. 1b. Dependence of Silicon ion emission on pulse duration.

This work was supported by the Österreichische Forschungsförderungsgesellschaft (FFG) Project# 834325.

References:

1. M. Lenzner, J. Krüger, S. Sartania, Z. Cheng, C. Spielmann, G. Mourou, W. Kautek, and F. Krausz, "Femtosecond Optical Breakdown in Dielectrics," Physical Review Letters **80**, 4076-4079 (1998).

2. M. Hashida, A. F. Semerok, O. Gobert, G. Petite, Y. Izawa, and J. F. Wagner, "Ablation threshold dependence on pulse duration for copper," Applied Surface Science **197–198**, 862-867 (2002).

3. J. Byskov-Nielsen, J.-M. Savolainen, M. Christensen, and P. Balling, "Ultra-short pulse laser ablation of copper, silver and tungsten: experimental data and two-temperature model simulations," Appl. Phys. A **103**, 447-453 (2011).

4. B. N. Chichkov, C. Momma, S. Nolte, F. von Alvensleben, and A. Tünnermann, "Femtosecond, picosecond and nanosecond laser ablation of solids," Appl. Phys. A **63**, 109-115 (1996).

5. B. C. Stuart, M. D. Feit, S. Herman, A. M. Rubenchik, B. W. Shore, and M. D. Perry, "Nanosecond-to-femtosecond laser-induced breakdown in dielectrics," Physical Review B **53**, 1749-1761 (1996).

P-048

Surface modification nanoporous titanium oxide films for dye-sensitized solar cell application using Nd:YVO_4 and CO_2 lasers

W.T. Hsiao[1*], C.C. Yang[1], K.Y. Yang[3], N.N. Chu[1], S.F. Tseng[1], C.K. Chung[1], D. Chiang[1], K.C. Huang[1], K.M. Lin[2], M.F. Chen[3]

[1] *Instrument Technology Research Center, National Applied Research Laboratories, Hsinchu 30076, Taiwan*
[2] *Department of Mechanical Engineering, Southern Taiwan University of Science and Technology, Tainan 71005, Taiwan*
[3] *Department of Mechatronics Engineering, National Changhua University of Education, Changhua 50007, Taiwan*
Corresponding Author e-mail address: wentse@narlabs.org.tw

1. Introduction

The utilization of fossil energy with its resulting discharge of exhaust gas has become the primary cause of the greenhouse effect, leading to dangerous environmental consequences. With the energy crisis and increased environmental awareness in late years, many nations are actively seeking to employ renewable energy resources such as solar photovoltaic, wind energy, potential energy, and biomass energy. Of these, one of the best options may be photovoltaic solar power generation engineering, such as silicon based and thin films solar cells. Nano-scale titanium oxide (TiO_2) films are used as a working electrode for dye-sensitized solar cells (DSSCs) due to its high efficiency performance. However, the surface morphology of the working electrode can significantly influence cell efficiency. Therefore, the several studies were reporting the surface modification on the TiO_2 electrode for DSSCs [1-3]. This study investigated the laser surface modification characteristics of TiO_2 films using Nd:YVO_4 (1064nm, pulsed mode) and CO_2 (10600 nm, continuous wave (CW) mode) laser source combined with moving stage and galvanometric scanning unit with varying parameters, including laser fluence, scanning times, pulse repetition frequency, speed of moving stage and scanning unit.

2. Experimental detail

The commercial TiO_2 thin films with thickness of 100 nm were prepared using radio-frequency magnetron sputtering on soda-lime glass substrates, the material properties used in the experiments are listed in Table 1. To enhance the performance characteristics of the TiO_2 films, the Nd:YVO_4 and CO_2 lasers was adopted to surface modification in ambient air. Adjustment of the surface modification parameters is detailed as follows: To obtain favorable surface modification results (i.e., to prevent micro cracks and damage to the substrate), the laser beam was defocused on the surface of substrates with a distance of 20 mm. The laser fluence varied among 20, 40, and 60 mJ/cm^2, and the dual-axis moving stage and scanning speeds varied among 9, 90, and 900 mm/s, respectively. To yield favorable surface modified quality, a vertical spacing path with equal spacing of 1 mm was used for each treatment path as shown in Figure 1.

Table 1: Material characteristics used in experiments

Substrate	Film thickness (nm)	Transmission (400-800nm)
Soda-lime glass (1.1 mm)	100	> 80%

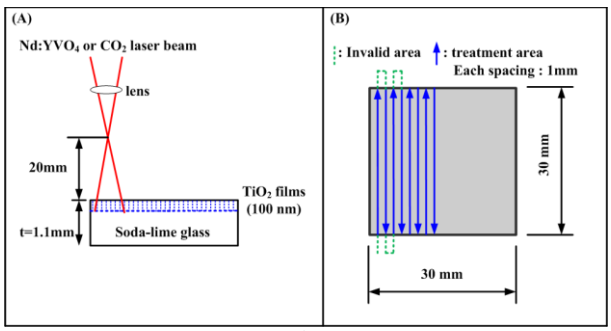

Fig. 1. Schematic diagram of the experimental set-up.

3. Performance characteristics evaluation

The film characteristics were systematically analyzed using a field emission scanning electron microscope, an atomic force microscope (AFM), X-ray diffraction (XRD) equipment, and ultraviolet–visible–near-infrared (UV-vis-NIR) spectrophotometer. The experimental results indicate that varying the laser fluence, scanning times, pulse repetition frequency, and speed was strongly affected the optical and structural characteristics of the TiO_2 films.

[1] M. Y. Pu and J. Z. Chen, "Improved performance of dye-sensitized solar cells with laser-textured nanoporous TiO_2 photoanodes," Mater. Lett. **66** 162-164 (2012).

[2] H. Kim, G. P. Kushto, C. B. Arnold, Z. H. Kafafi and A. Pique, "Laser processing of nanocrystalline TiO_2 films for dye-sensitized solar cells," Appl. Phys. Lett. **85**, 464-466 (2004).

[3] H. Kim, R. C. Y. Auyeung, M. Ollinger, G. P. Kushto, Z. H. Kafafi, A. Piqué, "Laser-sintered mesoporous TiO_2 electrodes for dye-sensitized solar cells," Appl. Phys. A: Mater. Sci. Proc. **83**,73-76 (2006).

P-049

Time-resolved microscopy of femtosecond laser-induced surface nanostructures on metal

Ranran Fang[1, 2], A.Y. Vorobyev[2], and Chunlei Guo[2]

[1] College of Science, Chongqing University of Posts and Telecommunications, Chongqing, 400065, China
[2]The Institute of Optics, University of Rochester, Rochester, New York, 14627, USA
E-mail: ranranfang2@gmail.com

Surface nano/microstructures play an important role in modifying physical, chemical, and biomedical properties of materials. In recent years, direct nano/microstructuring of a solid surface using femtosecond (fs) laser pulses [1] has become a subject of active researches due to many useful applications in such areas as optoelectronics, plasmonics, microfluidics, biomedicine, nanomaterials, and others. Although there have been a few studies on physical processes underlying the formation of laser-induced surface nanostructures [2-4], clear understanding of these processes is lacking. To further advance the understanding of physical processes governing the formation of the femtosecond laser-induced surface nanostructures, we perform a study on time evolution of the morphology of a metal surface from its melting up to its resolidification. The surface morphology evolution is studied using a femtosecond pump-probe microscopy technique. Our study is focused on laser-induced irregular nanostructures, which are commonly generated at low laser fluence. Using time-resolved imaging of the irradiated surface, we find three characteristic times of: (1) Onset of a change in morphology of the melted surface (transient surface structures in a liquid phase), (2) Onset of resolidification of the surface nanostructures, and (3) Complete resolidification of the surface nanostructures for ablation in laser fluence range between 0.1 and 1 J/cm^2. Our study shows that these characteristic times are a function of incident laser fluence. Increasing laser fluence causes the transient structures onset time to decrease, while the resolidification onset time and complete resolidification time to increase. Explanation of the observed evolution of surface nanostructures is given in terms of available theoretical mechanisms of femtosecond laser ablation.

References

[1] A.Y. Vorobyev and C. Guo, "Direct femtosecond laser surface nano/microstructuring and its applications," Laser Photonics Rev. 7(3) 385-407 (2013).
[2] E. Stratakis, V. Zorba, M. Barberoglou, C. Fotakis, and G. Shafeev, "Laser writing of nanostructures on bulk Al via its ablation in liquids," Nanotechnology **20**, 105303 (2009).
[3] T. Y. Hwang, A. Y. Vorobyev, and C. Guo, "Ultrafast dynamics of femtosecond laser-induced nanostructure formation on metals," Appl.
Phys. Lett. 95, 123111 (2009).
[4] B. J. Demaske, V.V. Zhakhovsky, N. A. Inogamov, and I. I. Oleynik, "Ablation and spallation of gold films irradiated by ultrashort laser pulses," Phys. Rev. B 82, 064113 (2010).

P-050

Design and Fabrication of a Tip-On-Aperture Probe for Resolution Enhancement of Near-Field Patterning

J.-B. Kim[1], and W. S. Chang[2*]

[1]3D Group, Future Device R&D Lab., Advanced Research Institute, LG Electronics Inc., 16 Woonyeon-dong, Seocho-gu, Seoul 137-724, Republic of Korea

[2] Nano Mechanical Systems Research Division, Korea Institute of Machinery & Materials, 104 Sinseongno, Yuseong-gu, Daejeon, 305-343, Republic of Korea

E-mail: paul@kimm.re.kr

The tip of a tip-on-aperture (TOA) probe is illuminated through an aperture at the near-field of the probe and electromagnetic interaction between the structure sharp tip at the end of the probe and the surface is used for measurements and materials processing. A novel TOA probe is described, which has a polygonal cross-sectioned tip that can make the strong and local enhancement of electromagnetic field[1,2]. A right triangular pillar was selected as optimal shape of the tip among the several polygonal pillars. The electromagnetic energy distributions at the near-field of the probe and of a typical TOA probe (with circular tip) were calculated numerically, and the results were analyzed. The results show that a TOA probe with a triangle tip confines electromagnetic energy within the smaller area than a typical tip-on-aperture probe, and has 6.7 times the maximum intensity. Moreover, the electric field distributions at the near-field of a TOA probe were calculated numerically to analyze the effects of polarization direction on the characteristics of measurement and processing. A TOA probe is asymmetric for the axis, since it has a probe at metal coated layer on the aperture. The geometrical relationship between this asymmetric shape and polarization direction is the reason for the change of the electromagnetic energy distributions. Numerical analysis shows that a TOA probe can make the best use of the tip for high resolutions when the tip is located on the parallel axis with the polarization direction. After analyzing the trend in the magnitude of the electric field, it was proposed that a localized, enhanced field at the tip apex was caused by the local electric field at the aperture and surface plasmons excited and propagating on the outer surface of the probe.

An NSOM probe is a tinned, metal coated optical fiber with an aperture. To fabricate a TOA NSOM probe, a tip is generated at the end of the probe. FIB processing is applied to the process to make an aperture and a tip, so the aperture and the tip are generated at the same time. With this process, possibilities to fabricate TOA probes with various tips and were shown. And resolution enhancement for optical measurement and patterning was verified using the TOA probe fabricated in this study.

References

[1] M. Stähelin, M. A. Bopp, G.. Tarrach, A. J. Meixner, and I. Zschokke-Gränacher, “Temperature profile of filber tips used in scanning near-field optical microscopy” Appl. Phys. Lett. **68,** 2603 (1996).

[2] H. G. Frey, F. Keilmann, A. Kriele, and R. Guckenberge, “Enhancing the resolution of scanning near-field optical microscopy by a metal tip grown on an aperture probe” Appl. Phys. Lett. **81,** 5030 (2002).

P-051

Fabrication of solution-based electronics using laser selective scanning

Sukyoung Ji[1,3], Wontea Park[2], Yong-Young Noh[2], Won Seok Chang[1,3]

[1]Department of Nanomechatronics, University of Science and Technology, 156, Gajeongbuk-ro, Yuseong-gu, Daejeon 305-343, Korea

[2]Department of Energy and Materials Engineering, Dongguk University, Pildong 3-ga, Jung-gu, Seoul, Korea, 100-715

[3]Department of Nanomechanics, Korea Institute of Machinery and Materials, 156, Gajeongbuk-ro, Tuseong-gu, Deajeon 305-343,Korea

E-mail: paul@kimm.re.kr

The fabrication of conductive micro- and nanoscale patterning for electronics application is one of the most important processes. Conventional methods such as vacuum metal deposition and photolithography require expensive vacuum environment, high processing temperature, and toxic chemicals and so on. In this study we present a fine patterning method of conductive lines on polyimide (PI) and glass substrate using silver (Ag) nanoparticles on based on laser scanning for an alternative process method[1,2]. Controlled laser irradiation can realize selective scanning of conductive ink without damaging the substrate. Thus, this technique easily creates fine patterns on heat-sensitive substrates such as flexible plastics. The selective laser sintering of Ag nanoparticles was managed by optimizing the conditions for the various laser scan velocity (1.0-20 mm/s) and power (10-150 mW) in order to achieve a small gap-size, high electrical conductivity, and fine roughness. The fabricated electrodes had a minimum channel length of 5 μm and conductivity of 4.2×10^5 S/cm (bulk Ag has a conductivity of 6.3×10^5 S/ cm) on the PI substrate. This method successfully applied to fabricate an organic filed effect transistor (OFET) with a poly(3hexylthiophene) (P3HT) channel material. Characteristics of P3HT OFET showed 0.1 $cm^2/V \cdot S$ of hole mobility, -21.6 V of threshold voltage, and -21.1 V/dec of sub-threshold swing, respectively.

References

[1] S. H. Ko, H. Pan, C. P. Grigoropoulos, J. M. J. Frechet, C. K. Luscombe, and Dimos Poulikakos, "Lithography-free high-resolution organic transistor arrays on polymer substrate by low energy selective laser ablation of inkjet-printed nanoparticle film", Appl. Phys. A **92**, 579 (2008).

[2] S. H. Ko, H. Pan, C. P. Crigoropoulos, C. K. Luscombe, J. M. J. Frechet, and D. Poulikakos, "Air stable high resolution organic transistors by selective laser sintering of ink-jet printed metal nanoparticles", Appl. Phys. Lett. **90**, 141103 (2007).

P-052

Diffusion-assisted laser writing for 3D nanostruturing by means of multiphoton polymerization

A. Pikulin and N. Bityurin
Institute of Applied Physics, RAS, Nizhniy Novgorod, Russia
E-mail: bit@appl.sci-nnov.ru

The photopolymerization process locally initiated by multiphoton absorption of the laser light provides the most versatile modern nanofabrication and nanoprototyping technologies [1-2]. Arbitrarily-shaped three-dimensional solid structures can be made with submicron detail by means of the direct writing with a focused ultrashort-pulse laser beam. Modern polymerizable resins allow for creation of highly transparent and mechanically stable structures for applications in photonics, optoelectronics, plasmonics, micro-electromechanical and microfluidic systems. Biocompatibility of some polymers is important for biomedical applications.

To improve the spatial resolution of the nanostructuring, the technique of diffusion-assisted laser writing (DALW) has been recently introduced [3]. This technique relies on the diffusion of the radical quencher (or the inhibitor), deliberately admixed into the polymerizable resin. Under the certain irradiation conditions, the consumption of the quencher in the focal spot of the beam is being compensated by means of the diffusion from the surrounding non-irradiated volume. As a result, the non-equilibrium quasi-stationary distribution of the quencher concentration with a pronounced zero-minimum within the focal spot is formed. Unless the local quencher concentration is close to zero, the polymerization process is prohibited. Thus, actual polymerization volume becomes constrained by the quencher distribution. Both the minimal size of a single polymer feature (line or voxel) and the minimal distance between the polymer features can be improved.

In this work, we theoretically study the limiting capabilities of DALW. We analyze the effect of the kinetic constants, the diffusion coefficients, the writing speed and the beam average power on the polymer feature size.

[1] Z. Sekkat and S. Kawata, "Laser nanofabrication in photoresists and azopolymers," Laser Photon. Rev. 8, 1 (2014).
[2] M. Malinauskas, M. Farsari, A. Piskarskas, and S. Juodkazis, "Ultrafast laser nanostructuring of photopolymers: A decade of advances," Phys. Rep. 533, 1 (2013).
[3] I. Sakellari, E. Kabouraki, D. Gray, V. Purlys, C. Fotakis, A. Pikulin, N. Bityurin, M. Vamvakaki, and M. Farsari, "Diffusion-Assisted High-Resolution Direct Femtosecond Laser Writing," ACS Nano 6, 2302 (2012).

P-053

Slit diffraction patterning of silicon surfaces by ns-laser irradiation: theory and experiment.

C. Acosta-Zepeda[1], P. Saavedra[2], G. Mecalco[1], N. Batina[3], I. Morales-Reyes[3], J. Bonse[4], E. Haro-Poniatowski[1]

[1]*Departamento de Física,* [2]*Departamento de Matemáticas,* [3]*Departamento de Química, Universidad Autónoma Metropolitana Iztapalapa, Av. San Rafael Atlixco No. 186, Col. Vicentina, C.P. 09340 México D. F., México.*

[4]*BAM Bundesanstalt für Materialforschung und -prüfung, Unter den Eichen 87, D-12205 Berlin, Germany.*

caz@xanum.uam.mx

Pulse laser irradiation of surfaces can have very different effects depending on several processing parameters such as pulse duration, wavelength, and energy density among others [1]. In this work we take benefit from laser irradiation and the optical diffraction effect to realize complex surface structures, reaching micrometer precision on the lateral scale, and nanometer accuracy in the vertical direction. Using the *diffraction assisted method* (DAM) technique, the morphology of Si wafer surfaces is modified with a single laser pulse, passing through a diffraction mask, chosen as slit of 75 µm width here. Subsequently, the surface topographyis characterized by atomic force microscopy (AFM). Fig. 1(a) shows the experimental set-up for the laser irradiation experiments of a single-crystalline silicon wafer.

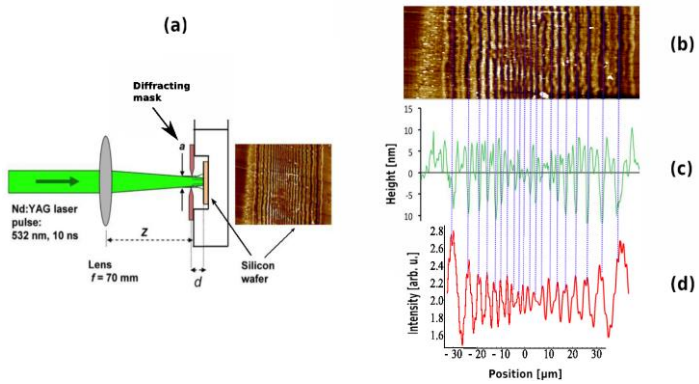

Fig. 1. Experimental set-up for diffraction-assisted micropatterning of the silicon wafer. Typical distances: *Z* (from lens to mask 60 mm), *a* (slit width 75 µm), *d* (sample to mask distance 100-200 µm), and *f* (focal length of the lens 70 mm) (a). AFM topography image (b) of a DAM-micropatterned region on a silicon wafer surface. A cross-sectional height profiles is shown in (c) and the corresponding calculated diffracted intensity profile in (d).

The diffraction pattern is generated by a single pulse (532 nm, 10 ns, beam diameter 3 mm), generated from frequency-doubled Nd-YAG laser, at a distance d typically a few hundreds of micrometers behind the diffracting slit, which is illuminated at a distance of Z~60 mm through a f=70 mm focal length lens. The structured light illumination field resulting from the diffraction, locally modifies the material (Fig. 1(b)) via melting and displacing fluid flows (Marangoni effect), giving rise to parallel groove-shaped features, with depths up to 10 nm (Fig. 1(c)). That grooves are produced in the regions where the intensity of diffraction pattern is maximum, as seen in the intensity profile calculated with Fresnel diffraction theory (Fig. 1(d)). In order to have a quantitative comparison with experiments we calculate the materials response as approximated analytical solution of a fluid-flow at the surface. In a first step, this includes the calculation of the temperature distribution and the location of the liquid-solid interface, both as a function of time. The equations to be solved are the heat conduction equation in liquid and solid with appropriate spatio-temporal boundary conditions.

$$\frac{\partial T(z,t)}{\partial t} - \frac{\partial}{\partial z}\left(D\,\frac{\partial T(z,t)}{\partial z}\right) = P(z,t) \qquad (1)$$

In a second step, we use the numerical solution of Eq. (1), to predict a two-dimensional fluid flow, solving numerically the continuity equation and Navier-Stokes Eqs. (2), as described in reference [2].

$$\boldsymbol{\nabla}\cdot\boldsymbol{u} = 0, \quad \nabla^2\boldsymbol{u} = 0 \qquad (2)$$

The results of the calculated melt displacements will be compared with experimental topography patterns.

References

[1] E. Haro-Poniatowski, C. Acosta-Zepeda, G. Mecalco, J. L. Hernández-Pozos, N. Batina, I. Morales-Reyes, J. Bonse, "Diffraction-assisted micropatterning of silicon surfaces by ns-laser irradiation," J. Appl. Phys. **115**, 224309 (2014).

[2] T. Schwarz-Selinger, D. G. Cahill, S. -C. Chen, S.-J. Moon, C. P. Grigoropoulos**,** "Micron-scale modifications of Si surface morphology by pulsed-laser texturing," Phys. *Rev. B.* **64**, 155323 (2001).

P-054

Sub-Micron Period Metal Lattices Fabricated by Interfering Ultraviolet Femtosecond Laser Processing

Yoshiki Nakata[1], Yoshiki Matsuba[1], Noriaki Miyanaga[1]
[1]Institute of Laser Engineering, Osaka University, 2-6 Yamadaoka, Suita, Osaka, 565-0871 Japan
nakata-y@ile.osaka-u.ac.jp

1. Introduction

Micron or sub-micron metal lattices have been identified as a fundamental component in nano-photonics and include metamaterials which show a negative refractive index and harmonic conversion [1]. Most of them have been fabricated by electron beam (EB) lithography or a focused ion beam (FIB). These methods are ineffective in terms of time and cost, so alternate methods have been researched. Among them, interfering ultra-short pulse laser processing has been investigated: the photonic structure of polymers [2], grating inside dielectrics [3] and material surfaces [4] have been fabricated. We have been investigating this technique since 2000 and have fabricated 2D [5] or 3D [6] nanostructures in lattices. The period of the lattices is the key parameter that defines the characteristics of devices, and the shortest period is restricted by laser wavelength.

In this experiment, we used the second-harmonic (SH) wave of a femtosecond laser at 785 nm. The period was shortened to 760 nm, and characteristic nanostructures in the lattice were fabricated.

2. Experimental set-up

A femtosecond laser system operated at 785 nm with a typical pulse width of 240 fs was used. An SH wave was generated by a barium borate (BBO) nonlinear crystal. It was split into four first-order diffracted beams by a transmission beam splitter, and they were interfered via two convex lenses forming a demagnification system. Here, gold thin film deposited on a silica glass by magnetron sputtering was used as a target.

3. Gold nanostructures in sub-micron lattice

Figure 1 (a) and (c) shows the SEM images of the textured surface on 100 nm thick gold thin film with processing energy of 6.3 μJ and 16.6 μJ. Figure 1 (b) and (d) shows corresponding bird's eye views. The period was 760 nm, 40% shorter than the shortest period of 1.3 μm processed by basic wavelength [7]. At lower energy, a nanobump measuring 310 nm in width was fabricated. On the other hand, a mixed structure of nanowhisker and nanodrop was fabricated at higher energy. The diameter of a droplet was 84 nm, which is also 40% smaller than that processed with a 1.3 μm period case. They are formed via thermal processes such as melting and freezing, which are known as SLS (Solid-Liquid-Solid) processes. The absorption coefficient at ultraviolet is far higher than that at near infrared. This technique can shorten the period, minify the unit structure and improve the energy coefficient.

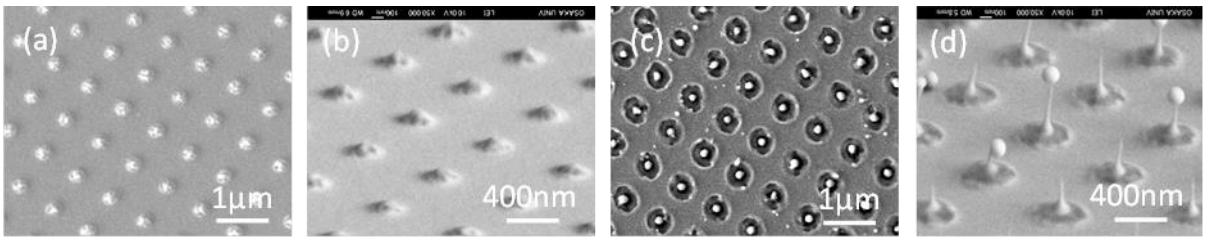

Fig. 1. (a) and (c) are top views of the textured surfaces of 100 nm thick gold films processed at 6.3 and 16.6 μJ respectively. (b) and (d) are corresponding bird's eye views.

References

[1] A. N. Grigorenko, A. K. Geim, H. F. Gleeson, Y. Zhang, A. A. Firsov, I. Y. Khrushchev and J. Petrovic, "Nanofabricated Media with Negative Permeability at Visible Frequencies", Nature **438**, 335 (2005).
[2] T. Kondo, V. Mizeikis, S. Matsuo, K. Ueno, and H. Misawa, "Three-dimensional Micro- and Nano- Structures of Materials by Tightly Focused Laser Radiation", Bull. Chem. Soc. Jpn. **81**, 411 (2008).
[3] K. Kawamura, M. Hirano, T. Kurobori, D.. Takamizu, T. Kamiya and H. Hosono, "Femtosecond-laser-encoded Distributed-feedback Color Center Laser in Lithium Fluoride Single Crystals", Appl. Phys. A **84**, 311 (2004).
[4] P. Simon, J. Ihlemann, "Machining of Submicron Structures on Metals and Semiconductors by Ultrashort UV-laser Pulses", Appl. Phys. A **63**, 505 (1996).
[5] Y. Nakata, T. Okada and M. Maeda, "Fabrication of Dot Matrix, Comb and Nanowire Structures Using Laser Ablation by Interfered Femtosecond Laser Beams", Appl. Phys. Lett. **81**, 4239 (2002).
[6] Y. Nakata, T. Okada and M. Maeda, "Nano-sized Hollow Bump Array Generated by Single Femtosecond Laser Pulse", Jpn. J. Appl. Phys. **42**, L1452 (2003).
[7] Y. Nakata, T. Hiromoto, N. Miyanaga, "Mesoscopic Nanomaterials Generated by Interfering Femtosecond Laser Processing", Appl. Phys. A **101**, 471 (2010).

P-055

Influence of laser alloying of AlMg5Si2Mn on structure and mechanical properties obtained layers

W. Pakieła, T. Tański, Z. Brytan, K. Labisz

Division of Materials Processing Technology, Management and Computer Techniques in Materials Science, Institute of Engineering Materials and Biomaterials, Silesian University of Technology, Konarskiego Str 18A, 44-100 Gliwice, Poland

Tomasz.Tanski@polsl.pl, Wojciech.Pakiela@polsl.pl, Zbigniew.brytan@polsl.pl,Krzysztof.Labisz@polsl.pl

Abstract

The goal of this paper was the investigation of laser treatment influence on the microstructure, mechanical and tribological properties of the surface layer obtained during the laser treatment using fiber laser (FL). The performed laser treatment involves remelting and feeding of Inconel 625 powder into the aluminium surface. As a base material was used aluminium alloy AlMg5Si2Mn. The Inconel powder was introduced in the remelting zone by means of milled on surfaces two or three grooves with a depth of 0.5 to 1 mm. The size of applied to alloying Inconel powder was in the range 150 - 220 µm. In order to remelting the aluminium alloy surface has been used the fiber laser, with an applied power of the laser beam 3 kW. The linear laser scan rate of the beam was set 0.5 m/min. Based on the performed investigations it was possible to obtain the layer consisting of the heat affected zone, transition zone and remelted zone (Fig. 1), without cracks and defects as well as has with a much higher hardness value compared to the non remelted material. For investigation of the obtained structure there was used light as well scanning and transmission electron microscopy. This investigation with appliance of a FL laser for Al alloys makes it possible to obtain or develop, interesting technology very attractive for different industry branches [1, 2].

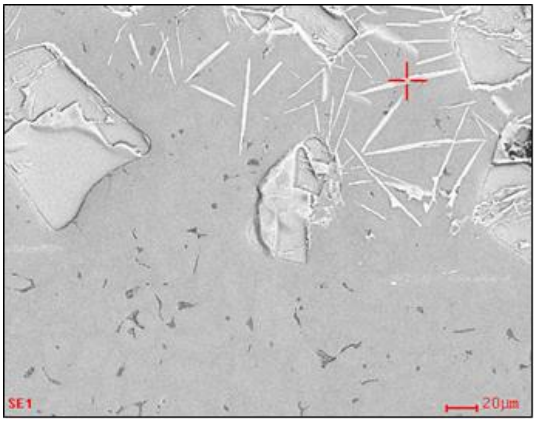

Fig. 1 transition zone between the remelting zone and heat affected zone

References

[1] [13] T. Tanski, Determining of laser surface treatment parameters used for light metal alloying with ceramic powders, Materialwissenschaft und Werkstofftechnik 45/5 (2014)333-343 DOI: 10.1002/mawe.201400232

[2] E. Kennedy, G. Byrne, D. N. Collins, Review of the use of high power diode lasers in surface hardening, Journal of Materials Processing Tech 155-156 (2004) 1855-1860.

P-056

Mapping laser-induced thermal forces acting on particles in air in a diverging hollow-core vortex beam

Niko Eckerskorn,[1] Richard Bowman,[2,3] Richard A. Kirian,[4] Jochen Küpper,[4] Henry N. Chapman,[4] Miles J. Padgett,[2] Andrei V. Rode[1]

[1]*Laser Physics Centre, RSPE, The Australian National University, Canberra ACT 0200 Australia*
[2]*Department of Physics and Astronomy, University of Glasgow, Glasgow G12 8QQ, UK.*
[3]*Queens' College, Cambridge Nanophotonics Centre, Cavendish Laboratory, University of Cambridge, CB3 0HE, UK*
[4]*Center for Free-Electron Laser Science, DESY, Notkestrasse 85, 22607 Hamburg, Germany*

avr111@physics.anu.edu.au

Optical trapping of light absorbing particles in gas environment has shown to be governed by optically induced thermal or photophoretic forces [1-3]. The applied photophoretic force propels a particle when an incident light beam nonuniformly heats the surface of the particle [3-5]. Optical guiding of absorbing particles by photophoretic force over large distances in open air was recently realised by an optical pipeline [4,5]. It was performed using a vortex beam, a donut-like intensity structure with a high-intensity ring of light that surrounds a dark core. Optical vortices create a ring-shaped transverse intensity distribution, while the particles are trapped at the intensity minima. Photophoretic force depends on the particle size relative to the mean-free path of gas molecules, absorption of laser light, and thermal conductivity. In the presented levitation experiments the thermal force is two to three orders of magnitude larger than the radiation–pressure force, rendering opaque particles impervious to conventional optical traps.

Here we present the results on quantitative evaluation of the photophoretic force and trapping stiffness by levitating graphite particles and carbon-coated glass shells of calibrated sizes in a vertically directed diverging hollow-core vortex beam. The axial equilibrium position of a suspended particle with known mass in the diverging beam with known intensity distribution immediately provides the axial force acting on the particle. Changing the beam power changes the intensity on the particle surface, which in turn force the particle to find a new equilibrium position. In the transverse plane. The trap's stiffness was measured using well-established position tracking with a fast CCD [6]. By repeating such experiments with different particle sizes and at different pressure we calibrate the force acting on the particle in the beam. The measurements were conducted at various air pressures from 0.1-1.5 bar and compared with the light pressure forces evaluated for the known intensity illuminating the particle.

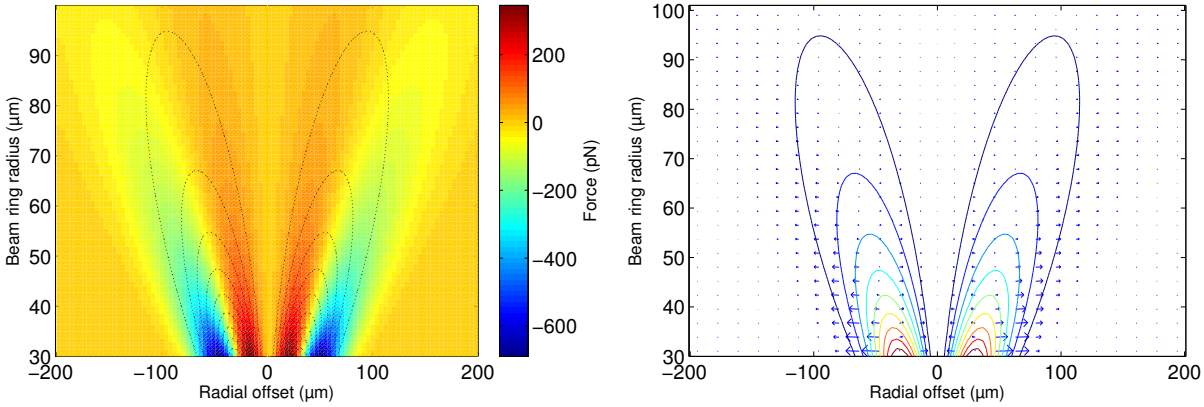

Figure 1. Measured force acting on a spherical carbon coated glass shell or graphite sphere (r=1µm), situated in linearly polarized first order vortex beam (LG01) carrying 1 W, under atmospheric pressure. The left panel shows the magnitude of the vectorial force (red – towards the axis, blue – away from axis) as displayed in the right panel. The contour overlays indicate the intensity distribution.

The forces recovered from our experiments range around ~10^{-10} N per Watt of total power in the beam, at atmospheric pressures, see Fig. 1, with force increasing near linearly with decrease of pressure. The maximum intensity encountered by the particle is ~30 kW/cm^2, given a maximum particle radius to vortex 'ring' radius of 1/30. Intensities of this order of magnitude are suitable for handling biological samples without damage. The results provide grounds to link the position and size of a spherical particle in an arbitrary intensity distribution to the value of photophoretic and light pressure forces under various gas pressures.

[1] E. J. Davis, G. Schweiger, *The Airborne Microparticle* (Springer, Berlin, 2002).
[2] D. McGloin, *et.al.*, *Optical manipulation of airborne particles*, Faraday Discussions **137**, 335-350 (2008).
[3] V. G. Shvedov, et al., *Optical guiding of absorbing nanoclusters in air*, Opt. Ex. **17**, 5743- 5757 (2009).
[4] V. G. Shvedov, et al, *Giant optical manipulation*, Phys. Rev. Lett. **105**, 118103 (2010).
[5] N. Eckerskorn, et al., *Hollow Bessel-like beam as an optical guide for a stream of particles*, Opt. Ex. **21**, 30492-30499 (2013).
[6] R. W. Bowman M. J. Padgett, *"Optical trapping and binding,* J. Opt. **76**, 026401 (2013).

P-057

Ceramic particles feeding in carbon prepared aluminium surface using diode laser

K. Labisz[1],T. Tański[1], Z. Brytan[1], W. Pakieła[1]
Division of Materials Processing Technology, Management and Computer Techniques in Materials Science,
Institute of Engineering Materials and Biomaterials, Silesian University of Technology,
Konarskiego Str 18A, 44-100 Gliwice, Poland
Corresponding Author e-mail address: krzysztof.labisz@polsl.pl

Abstract
Introduction of ceramic powders into surface layer of ceramic particles into engineering metal alloys is a very well know and widely used technique. The new approach to it is to obtain fine distributed nano-size particles involved in the al matrix using the traditional laser technology.
In this paper are presented the results of microstructure investigation of the surface layer of cast aluminium-silicon-copper alloys after heat treatment alloyed and/ or remelted with ceramic carbide phase especially WC ceramic powder using High Power Diode Laser (HPDL). The surface layer was especially for the reason of reducing the reflectivity of the surface layer, what is the main problem in the up-to date MMC (Metal Matrix composites) production. For characterisation of the obtained microstructure there were used electron microscopy methods with EDS microanalysis and SAD (Selected Area Diffraction) methods. By mind of scanning electron microscopy, using secondary electron detection, was it possible to determine the deformation process and distribution of ceramic WC powder phase occurred in the alloy after laser treatment in relation to different silicon addition (Figs. 1 and 2).

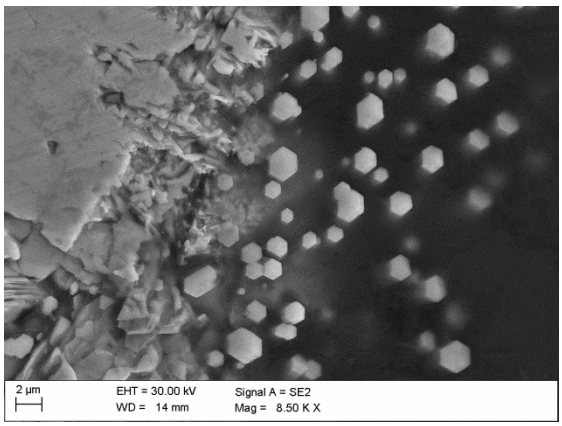

Fig. 1 WC alloying AlSi7Cu4

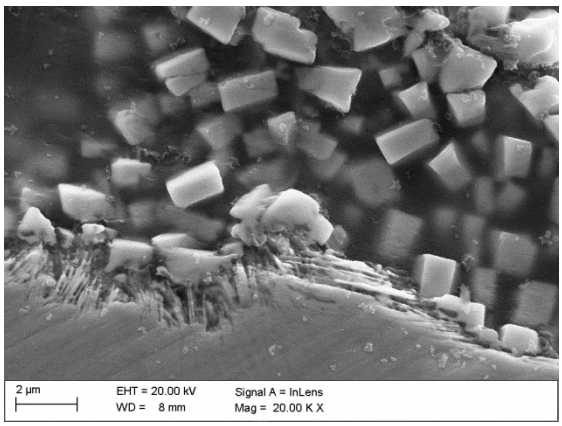

Fig. 1 WC alloying AlSi9Cu4

The structure of the surface laser changes in a way, revealing three zones - the remelting zone, the heat influence zone, the intermediate zone placed over the Al substrate. The structural changes of the fed ceramic powder, its distribution and morphology as well as the microstructure of the matrix material influence the functional properties especially wear resistance, hardness and corrosion resistance of the achieved layer. Concerning the laser treatment conditions for laser surface hardening also the basic treatment parameters were studied like: laser power, laser scan speed and ceramic powder feed rate. This investigation with appliance of HPDL laser for Al alloys makes it possible to obtain fine distributed nanosized particles in the surface what makes it interesting and very attractive for automobile and machine industry [1, 2].

References

[1] A. Lisiecki, "Welding of thermomechanically rolled fine-grain steel by different types of lasers", Arch. Metall. Mater. **59(4)**, 1625-1631 (2014).
[2] K. Labisz, "Microstructure and mechanical properties of HPDL laser treated cast aluminium alloys", Materials Science and Engineering Technology **45**, 314-324 (2014).

P-058

Strong enhancement of surface diffusion under the action of laser induced nonlinear surface acoustic waves

Maxim V. Shugaev,[1] Anthony J. Manzo,[2] Chengping Wu,[1] Vladimir Yu. Zaitsev,[1,3]

Henry Helvajian,[2] and Leonid V. Zhigilei[1]

[1]*Department of Materials Science & Engineering, University of Virginia, 395 McCormik Road, Charlottesville, Virginia 22904-4745, USA*
[2] *Physical Sciences Laboratories, The Aerospace Corporation, P.O. Box 92957, Los Angeles, CA 90009-2957, USA*
[3] *Division of Hydrophysics and Hydroacoustics, Institute of Applied Physics, Uljanova St. 46, Nizhny Novgorod, 603950, Russia*
E-mail: lz2n@virginia.edu

Short pulse laser irradiation of a strongly absorbing target can produce strong transient stresses in the region of the laser energy deposition and result in the generation of acoustic pulses (bulk and surface waves) capable of producing structural changes in the target material at substantial distances from the absorption region. Laser generation of surface acoustic waves (SAWs), in particular, is actively used in many practical applications, ranging from nondestructive evaluation of mechanical properties and surface defects to "atomization" of liquid samples for mass spectrometry analysis. The ability of SAWs to affect atomic/molecular-level surface processes, however, remains largely unexplored and is generally considered implausible due to the large mismatch between the relatively low frequencies of the acoustic waves, typically sub-MHz, and the THz-range vibrational frequencies characteristic of atoms and molecules adsorbed on a surface.

In this presentation we report the results of a joint computational – experimental study aimed at exploring the ability of strong laser-generated acoustic waves to produce non-thermal atomic rearrangements in the regions of the irradiated targets that are not directly affected by the laser heating. The experimental study of the diffusion of small Au clusters on a silicon surface tracked with fluorescence microscopy provides the direct evidence of surface mobility enhancement of molecular species using a wide bandwidth (100 MHz) acoustic source generated by pulsed laser irradiation [1]. The diffusion enhancement is recorded at a distance of about 1 cm from the source. The experimental observations are explained based on the results of large-scale molecular dynamics simulations of non-linear SAW propagation and interaction with surface molecular adsorbates [2]. The results of the simulations demonstrate that while the initial sinusoidal SAW has only a moderate effect on the surface diffusion [3], the wave profile sharpening and shock front formation lead to a very strong, more than 4500-fold, enhancement of the diffusion coefficient [2]. A detailed analysis of the simulation results reveals that the strong diffusion enhancement can be attributed to the dynamic coupling of high frequency harmonics of the non-linear SAW with cluster vibrational modes. While a less dramatic 19-fold increase in the effective diffusion coefficient is observed in experiments for SAWs generated by nanosecond pulse laser irradiation at 100 Hz repetition rate, the linear scaling of the enhancement with the number of the SAW pulses passing through the diffusion region per unit time suggests that a much stronger enhancement can be achieved at higher laser repetition rates. The results of this study may have practical implications in chemical catalysis, low temperature thin film growth, and mass spectrometry of heat sensitive molecules. At a general level, the results indicate that the acoustic activation at ultrasonic frequencies can serve as an effective substitution for heat in a broad range of applications.

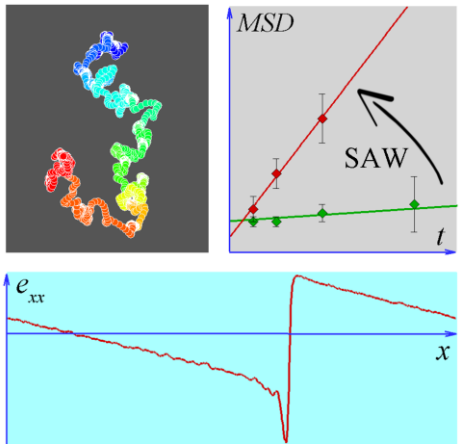

Figure. Schematic representation of the results of the experimental and computational investigation of the acoustic enhancement of surface mobility. A typical simulated trajectory of an atomic cluster is shown in the upper left frame. The cluster is set into motion by the non-linear sharpening of the SAW (bottom frame). The results of the simulations are used to explain the experimental observations of the increase in the mean square displacement of the clusters in the presence of SAWs (upper right frame).

1. A. J. Manzo and H. Helvajian, Proc. SPIE **8969**, 896908, 2014.
2. M. V. Shugaev, A. J. Manzo, C. Wu, V. Yu. Zaitsev, H. Helvajian, and L. V. Zhigilei, submitted, 2015.
3. C. Wu, V. Yu. Zaitsev, and L. V. Zhigilei, *J. Phys. Chem. C* **117**, 9252-9258, 2013.

P-059

Hybrid laser cutting technology of Ti-6Al-4V thin sheet using diode-pumped-solid-state ultraviolet laser

C.C. Yang*, W.T. Hsiao, H.Y. Tsai, K.C. Huang
Instrument Technology Research Center, National Applied Research Laboratories, Hsinchu 30076, Taiwan
Corresponding Author e-mail address: jjyang@narlabs.org.tw

1. Introduction

Titanium alloy is gradually used in the aerospace and medical industries due to the noticeable mechanical and chemical properties such as light, high strength, good corrosion resistance, nice thermal conductivity and easy manufacturing for complicated components. Especially, Ti-6Al-4V (Grade 5) is a widely used for medical materials due to its excellent biocompatibility and mechanical properties for the human body. However, the titanium alloy material is not easy for machining; therefore, nontraditional micromachining methods [1-2] were presented, such as ultrasonic machining (USM), electric discharge machining (EDM), electron beam machining (EBM), laser beam machining (LBM), are useful and powerful for microstructure fabrication, especially in micro hole of a high aspect ratio. Hybrid laser cutting technology of the titanium alloys thin sheet using UV laser system was proposed in this study.

2. Experimental

Commercial Ti-6Al-4V (Grade 5) alloy thin sheet with thickness of 100 μm are used in these experiments. To investigate the influence on the characteristics (i.e., cutting profile, oxidation, and residual properties) of thin titanium alloy sheet laser cutting by various different operating parameters including laser fluence, machining times, pulse repetition frequency and speed was proposed. The micro hole cutting procedure of the three steps was as follows and shown in Fig. 1 (a-c).

Step1：The contour portion of the micro holes was removed using a fluence laser beam in order to speed up the ablation rate of material and decrease machining time, in Fig. 1 (a).

Step2：Adjusted focus position of focal lens. High fluence laser beams were used to trim residuals and to ensure roundness in the bottom circle of micro holes, in Fig. 1 (b).

Step3：High fluence laser beams were used to trim residuals and to ensure roundness in the top circle of micro holes, in Fig 1 (c).

We significantly compare the relationship between the micromachining parameters of micro hole with UV laser drilling system on titanium alloys to determine the cutting profile, oxidation, and residual properties of the micro holes. These parameters would help us perform the fabrication of a 5x5 matrix, micro holes with a diameter of 600 μm.

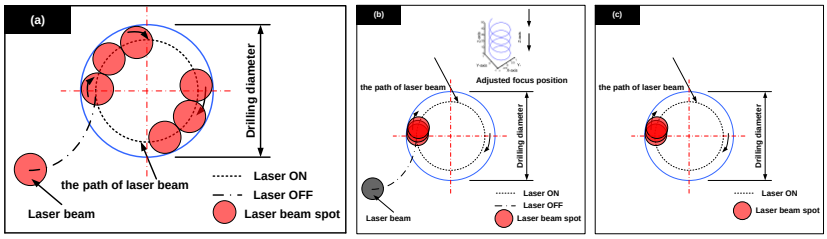

Fig. 1. Schematic diagram of the micro holes cut steps.

3. Preliminary matrix hole cutting results

Fig.2 shows the optical microscope image of Ti-6Al-4V (Grade 5) alloy thin sheet with diameter of 600μm. As the figures could be observed that the contour profile has sharp edge and excellent roundness. In addition, by using the present hybrid cutting method has the little heat affected zone of the cutting region.

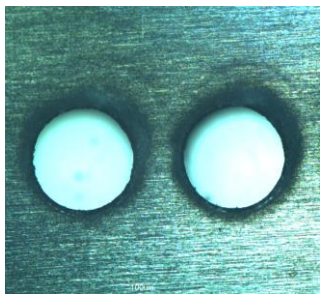

Fig. 2. Optical microscope image of the cutting holes.

[1] N. F. Ren, L. L. Jiang, D. Liu, L.V. Liu, Q. Wang, "Comparison of the simulation and experimental of hole characteristics during nanosecond-pulsed laser drilling of thin titanium sheets," Int. J. Adv. Manuf. Tech. **76** 735-743 (2015).

[2] H. Kim, G. P. Kushto, C. B. Arnold, Z. H. Kafafi and A. Pique, " Artificial intelligence based modeling and optimization of heat affected zone in Nd:YAG laser cutting of duralumin sheet," J.Intell. Fuzzy Syst. **27**, 1545-1555 (2014).

P-060

Improvements in combined laser interferometry technique for laser ablation research

E. Loktionov[1], A. Pavlov[1], Yu. Protasov[1], V. Telekh[1]
[1]Bauman Moscow State Technical University, 2nd Baumanskaya str. 5-1, 105005 Moscow, Russia
E-mail address: stcpe@bmstu.ru

1. Introduction

Imaging and quadrature phase shift interferometry of laser irradiated surface and laser-induced gas-plasma flows has been used to investigate laser ablation processes in a number of works. Processing of experimental data obtained using of these techniques reveals some data insufficiency or results ambiguity, e.g. caused by surface shielding or unknown ablated mass flow rate. Previously [1], we used Michelson scheme for surface & Mach-Zehnder – for plume interferometry. Although some valuable results were obtained [2], there were several restrictions and complications in techniques implementation due to temporal coherence of probing ultra-short laser pulses, reflective properties of irradiated surface and probing wavelength to ablation crater ratio. Also beam-splitting interferometers are not always suitable for multi-wavelength probing and are sensitive to optical paths fluctuations. To solve these problems we investigated performance of the modified Nomarski scheme for multi-wavelength plume and speckle surface interferometry.

2. Experimental performance

Nomarski scheme, where probe beam is split after object in birefringent Wollaston prism (Fig. 1), has been used for laser-induced plasma flows interferometry in [3] for $n_e \sim 10^{19}$ cm^{-3} plumes, but in original phase contrast layout resolved electron density lower threshold could be reduced by ca. 3 orders of magnitude (at sub-mm optical path scale). Another feature of this scheme is an ability of easy interference periods inclination and spacing regulation (by prism position and rotation), the latter is extremely useful for quadrature and irradiated surface speckle interferometry. Absence of reflective optical elements makes Nomarski scheme very convenient for multi-wavelength interferometry, that has been implemented by us for 400 and 800 nm probes using single color-CCD. Each of wavelengths images sole treatment results (e.g. for Al-film ablation at ambient conditions) in ca. 5 times electron density mismatch (0.45 and 2.4 10^{18} cm^{-3}), combined treatment gives intermediate (1.1 10^{18} cm^{-3}) value of this parameter and also density of atoms (2.3 10^{19} cm^{-3}), the latter data are invaluable for the cases when ablated mass flow rate can't be evaluated or plume consists of target vapors and background gas. Speckle surface interferometry scheme is based not on reflected wave-front shift, but on projected interference periods distortion, this method is suitable for multi-μm crater depths poorly analyzed using interference microscopy.

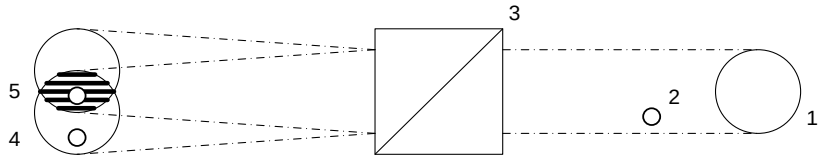

Fig. 1. Nomarski interferometer principle (1 – probe beam, 2 – object, 3 – Wollaston prism, 4 – absorption and 5 – interference image)

3. Conclusions

Use of Nomarski interferometer provides abilities to simplify optical scheme justification (including setting interference period), multi-wavelength and ultra-short pulses probing, to reduce optical paths fluctuation issues, and to broaden application range.

The results have been obtained at "Beam-M" (RFMEFI59014X0001) facility at BMSTU.

1. E.Y. Loktionov, A.V. Ovchinnikov, Y.Y. Protasov, and D.S. Sitnikov, "Experimental diagnostic module for ultrafast combined interferometry of the processes of interaction of ultrashort laser pulses with condensed media in vacuum," Instrum. Experiment. Techn. **53**, 416 (2010).
2. E.Y. Loktionov, Y.Y. Protasov, V.D. Telekh, and R.R. Khaziev, "Complex Processing of Interferograms of Light-Erosion Gas-Plasma Streams in Vacuum," Instrum. Experiment. Techn. **56**, 46 (2013).
3. P. Hough, C. McLoughlin, T.J. Kelly, S.S. Harilal, J.P. Mosnier, and J.T. Costello, "Time resolved Nomarski interferometery of laser produced plasma plumes," Appl. Surf. Sci. **255**, 5167 (2009).

P-061

Investigation of microstructure and surface morphology of Ti64 plate fabricated by vacuum selective laser melting

Yuji Sato[1], Masahiro Tsukamoto[1], Yorihiro Yamashita [2], Daichi Tanigawa [3], Nobuyuki Abe[1]
[1]*Joining and welding research institute, Osaka university (11-1 Mihogaoka, Ibaraki-shi , Osaka, 567-47,Japan)*
[2] *Industrial Research Institute of Ishikawa, (2-1 Kuratsuki, Kanazawa, Ishikawa 920-8203, Japan)*
[3] *Graduate school of engineering, Osaka University (1-1 Yamadaoka, Suita-shi, Osaka, 565-0871 Japan)*
sato@jwri.osaka-u.ac.jp

1. Introduction

Selective laser melting (SLM) process, as one of additive manufacturing (AM) technologies, is useful way as direct and complicated shape formation [1]. We demonstrated that Ti6Al4V plates were fabricated 3D structure by SLM process in vacuum. Titanium alloys are clinically employed for artificial bones and hard tissue implants in humans because of their light, nonmagnetic, weather resistant, and biocompatibility properties, but they are difficult to form into complicated structures, such as bionic structures, because they are difficult to cut as machine materials. In our previous study, Ti 64 plates fabricated by vacuum SLM process were investigated correlation between the surface morphology and laser power density. From the results, the surface roughness was depended on the laser power density. At the laser power density of 5.7×10^5 W/cm^2, the surface roughness improved from 60 μm to 0.62 μm.

In this study, in order to investigate the laser melting and solidification dynamics, a process of Ti 64 alloy plate (10mm x 10mm x1 mm), which fabricated by vacuum SLM, was captured by high speed video camera. It was also determined that crystal orientation was evaluated with X-ray diffraction.

2. Experimental procedure and results

The SLM system employs a single-mode fiber laser with a wavelength of 1064 nm and a maximum output power of 300 W in a continuous wave. A three-axis galvanic mirror setup was used to focus on the powder surface by using a z-axis lens. The Gaussian laser beam has a diameter of 60 μm at the $1/e^2$ intensity point. The chamber's pressure was set to 1.0×10^{-2} Pa to prevent the Ti64 powder from oxidizing. The base plate of the powder bed was vertically dropped in determined steps, and Ti64 powder supplied from the powder feeder was then smoothed by a roller on top of the powder bed. The single-mode fiber laser irradiated and melted the powder bed to make a molten pool in order to form 2D metallic structures. A linear raster scan pattern was employed with a scan vector length of 10 mm. These processes are then repeated to build up a 3D fabricated sample.

Melting and solidification dynamics of vacuum SLM process were observed at an oblique view to 45 degrees of the laser with high speed video camera (Fig.1). And the Ti64 plated fabricated by vacuum SLM was evaluated with XRD and SEM to investigate the crystal orientation. From the results, it was recorded from the powder peaks of α (1011), α (0002), α (1010), and α (1012) that the crystal orientation is composed mainly of martensitic alpha. Diffraction peaks corresponding to β (110) were detected in vacuum SLM processed samples.

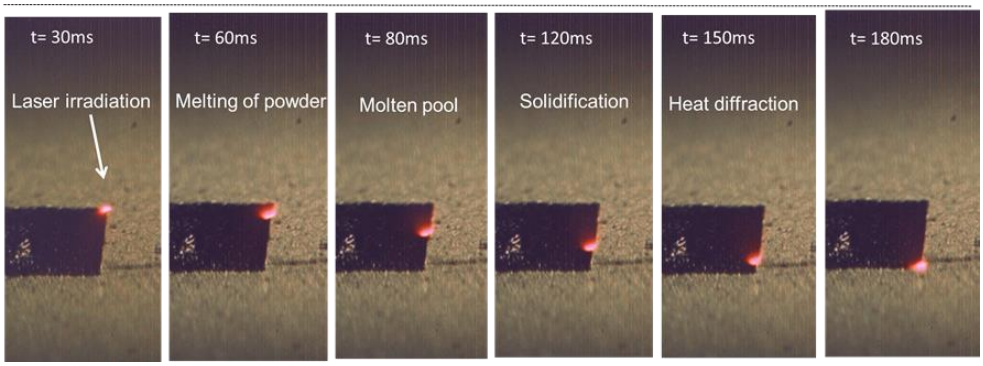

Fig.1 observation of melting and solidification dynamics of Ti64 powder with the high speed video camera.

1. Edson Costa Santos, Masanari Shiomi, Kozo Osakada, Taha Laoui, "Rapid manufacturing of metal components by laser forming" International J. of Machine Tools and Manufacture **46** pp.1459-1468 (2006)

P-062

Laser ablation parameters as fundamental key factors for controlling the 3D Additive Manufacturing process: considerations

M.L. Pace[1], A. Guarnaccio[1], F. Ranù[1], D. Trucchi[2], D. Mollica[1], S. Orlando[1], G.P. Parisi[1], A. Santagata[1*]

(1) CNR – ISM UOS Tito Scalo, Zona Industriale, 85050 Tito Scalo (PZ) – ITALY

(2) CNR – ISM UOS Montelibretti, Via Salaria km 29.300, 00015 - Monterotondo Scalo (RM) – ITALY

**Corresponding Author e-mail address: antonio.santagata@cnr.it*

The ability of processing through laser beams different kind of powders for direct production of components with complex geometries by 3D printing has been gaining an impressive and growing attention for specific industrial applications. The process which can be distinguished as Selective Laser Sintering or Selective Laser Melting is even considered, more generally, as Additive Manufacturing where layer by layer material is built by interaction between a laser beam and a powder bed. All effects occurring during the interaction between the laser beam and the powder properties are usually neglected and phenomenological approaches are rather followed. From the work here presented some considerations related to the defect observed during the employment of the Additive Manufacturing process such as: balling, pores production, thermal stresses, micro-structural inhomogeneities, presence of unprocessed powder, capillary instability and so on will be discussed. With this aim, laser parameters (power, spot size, duration, wavelength) both, in plane laser scanning and vertical powder bed translation features (speed, pattern and spacing) power properties (size, density, distribution, composition and layer thickness) already reported in literature will be introduced.

In such a way a deep insight view about the effects played by these parameter will be reported in order to provide some indications on the manifold mechanisms involved. Although non equilibria processes can be considered, thermal effects will be taken into account in first approximation. The rapid heating of the powder due to the laser beam energy transfer process followed by a rapid cooling rate can provide a local latent heat during the solidification process and induce unexpected phases of the final manufactured component. On these bases and taking into account other hypothesis connected to the underneath heat diffusion of the growing up piece of manufacture, heat accumulation effects and sharp decrease of the melted material viscosity, the presence of different kind of defects can be foreseen. In this manner the generated 3D component features and the production parameters used in this survey will be considered for drawing a relationship between fundamental mechanisms occurring during the laser ablation process and the Additive Manufacturing technique.

P-063

Real-time study of gold nanoparticles formation by pulsed laser annealing

C. Sánchez-Aké[1], J. Martínez[1], F. Álvarez[1], T. García-Fernández[2], R. Castañeda-Guzmán[1], M. Villagrán-Muniz[1]

[1] Laboratorio de Fotofísica, Centro de Ciencias Aplicadas y Desarrollo Tecnológico, Universidad Nacional Autónoma de México, Apartado Postal 70-186, México D.F., C.P. 04510, México

[2] Universidad Autónoma de la Ciudad de México (UACM), Prolongación San Isidro 151, San Lorenzo Tezonco, México D.F., C.P. 09790, México

E-mail: citlali.sanchez@ccadet.unam.mx

The synthesis of metallic nanoparticles (NPs) either covered or embedded in transparent dielectric materials has recently received great attention for its possible applications as plasmonic structures. There are several methods to synthesize metal NPs such as chemical synthesis, photoreduction, thermal and laser annealing among others. The formation of NPs on the surface of different substrates by laser annealing results from the irradiation with nanosecond laser pulses of metal thin films grown previously on these substrates. The main advantages of this method include high precision of nanoparticles placement, room temperature processing in atmospheric conditions and freedom of chemical wastes and lithography requirements [1]. Moreover, it has been shown than for a laser fluences above a threshold, the NPs can be implanted into glass substrates [2,3].

This work focuses on the fabrication of gold NPs on both glass and fused silica substrates via laser annealing of Au films using a Nd:YAG laser (355 nm of wavelength and 7 ns of pulse duration). This study is aimed at the better understanding of the mechanisms involved during the annealing. For this, real-time optical absorption, laser beam deflection and pulsed photoacoustic measurements were used to monitor the formation of the NPs as a function of the laser fluence and the number of pulses. The influence of the film thickness, the laser repetition rate and the background pressure on the characteristics of the NPs was also studied. The obtained NPs were characterized by SEM, AFM and UV-Vis optical absorption. The current assessment shows that the annealing induces physical processes with duration of hundreds of microseconds.

[1] M.J. Beliatis, N.A. Martin, E.J. Leming, S.R.P. Silva, S.J. Henley, "Laser ablation direct writing of metal nanoparticles for hydrogen and humidity sensors", Langmuir **27**(3), 1241 (2011).

[2] S.J. Henley, M.J. Beliatis, V. Stolojan, S.R.P. Silva, "Laser implantation of plasmonic nanostructures into glass", Nanoscale **5**, 1054 (2013).

[3] M. Dubiel, M. Heinz, M. Stiebing, J. Meinertz, J. Ihlemann, Th. Rainer, "Generation and characterization of plasmonic nanostructures in glass surfaces by means of excimer and solid state laser irradiation", in Proceedings of SPIE, Ed. Allan D. Boardman, Vol. 9163, 91631M (2014).

P-064

Fabrication of a lab-on-a-chip device by laser micromachining

A. Palla Papavlu, M. Filipescu, F. Stokker, V. Dinca, M. Dinescu
Lasers Department, National Institute for Lasers, Plasma, and Radiation Physics, Magurele 077125, Romania
Corresponding Author e-mail address: alexandra.papavlu@inflpr.ro

Pathogenic microorganisms such as *E-coli* are the third leading cause of hospital associated infections. *E-coli* microorganisms have the capability to adapt to different environments and modify their pathogenic properties, thus appearing the possibility of acquisition and transfer of these genes from and to other pathogens. Therefore, the design and fabrication of new diagnostic systems which can be used in the field of environmental monitoring and control, but also for medicine, and public health are of paramount importance.
This study deals with the design and fabrication of a microfluidic lab-on-chip system to perform the amplification of DNA (through real-time PCR) from *E-coli*. Micro-channels and micro-cavities have been fabricated by laser direct-write in different polymers i.e. PDMS, PMMA for their application in 3D microfluidic systems. Both a Nd:YAG (10 Hz at 1064 nm) and an ArF (193 nm) laser have been used for irradiation. Channel and micro-cavity morphology, dimensional accuracy, and surface conditions have been investigated by optical microscopy, atomic force microscopy, and scanning electron microscopy. The difference in width between bottom and top surface has been also studied. In addition, metallic and dielectric thin films are necessary for the integration of the heating elements to carry out DNA amplification. Both for the insulation and conducting purposes materials with high temperature coefficient of resistance i.e. amorphous hydrogenated silicon carbide (a-SiC:H) and Ni have been deposited by pulsed laser deposition.
Our results indicate that the laser micromachining techniques applied here represent an important technical support for the realization of low-cost lab-on-a-chip systems with wide-ranging applications in chemical and biological analysis and clinical diagnostics.

This work was supported by a grant from MEN-UEFISCDI, project PN-PCCA 34/2014.

P-065

Synthesis of Ultrasmall Nanoparticles by Laser Vaporization as "Building Blocks" for Nanostructures and Thin Films

David B. Geohegan[1], M. Mahjouri-Samani[1], M. Tian[3], K. Wang[1], C. M. Rouleau[1], A. A. Puretzky[1], G. Eres[2], K. Xiao[1], M. A. McGuire[2], G. Duscher[3]

[1]*Center for Nanophase Materials Sciences, Oak Ridge National Laboratory, Oak Ridge, TN, USA*
[2]*Materials Science and Technology Division, Oak Ridge National Laboratory, Oak Ridge, TN,USA*
[3]*Dept. of Materials Science and Engineering, University of Tennessee, Knoxville, TN, USA*
E-mail: geohegandb@ornl.gov

Pulsed laser vaporization (PLV) and pulsed laser deposition (PLD) are versatile nonequilibrium techniques used to discover a wide range of nanostructures synthesized by condensation, vapor-liquid-solid, or condensed phase growth in the gas phase (e.g., discovery of C_{60}, single-wall carbon nanotubes and nanohorns, nanowires, etc.), and all types of thin films (from oxide superconductors and multiferroics to 2D materials such as graphene and metal chalcogenides) [1]. However, it has been unclear how gas-phase nanoparticles produced during PLV incorporate into thin films and nanostructures during PLD.

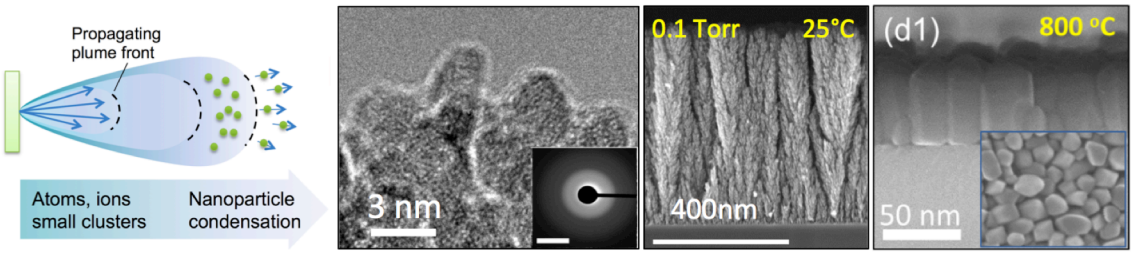

Fig. 1. Pulsed laser vaporization of solid TiO_2 targets for the formation of pure fluxes of "amorphous" ultrasmall nanoparticles (TiO_2 < 5 nm, shown) was used to synthesize mesoporous nanoparticle architectures at room temperature (25°C, in 0.1 Torr oxygen, d = 5 cm, 1 Hz), or crystalline nanostructures of various metastable phases at elevated temperature (800°C, otherwise same conditions, yielding anatase TiO_2 crystalline nanorods).

Here we describe the general phenomena of the formation and assembly of 'amorphous' ultrasmall nanoparticles (UNPs) in pulsed laser ablation plumes confined by background gases, and their role as transformable "building blocks" for the synthesis of mesoscale nanoparticle architectures, nanorods, and thin films with interesting metastable phases. We concentrate on TiO_2. Using *in situ* time-resolved diagnostics (ICCD imaging, ion probe, LIF) and *ex situ* advanced electron microscopy (SEM, TEM, atomic-resolution Z-contrast scanning TEM, nano-beam electron diffraction (NBED), EELS) we characterize both the plume conditions and "amorphous" UNPs produced and collected on room-temperature substrates, and their individual transformations to crystalline phases upon post annealing. As shown in Fig. 1, when deposited at room temperature nearly pure UNP architectures are formed which, when annealed, transform into polycrystalline nanorods can be used as electrodes for dye-sensitized solar cells or photocatalytic water splitting [2]. However, when deposited at elevated temperature, we reproducibly obtain crystalline nanostructures with metastable phases, such as TiO_2(B) nanosheets, or anatase nanorods (shown). Theory and simulation, along with NBED and EELS data indicate that the evolution of a particular crystalline phase and preferred growth orientation is linked to the elimination of defects and ordering of TiO_6 octahedral units made possible by the metastable nature of the "amorphous" nanoparticle "building blocks".

Thus, metastable UNPs synthesized by PLV are found to carry the target stoichiometry and transformability to a substrate for the catalyst-free formation of nanostructures and films with metastable phases, depending on their size and arrival rate – explaining a longstanding mystery in PLD. Similar plume conditions and stoichiometric amorphous UNP "building blocks" were recently used to synthesize 2D metal chalcogenide nanosheets and large single crystals, indicating the generality of the technique [3,4].

Research was supported by the U.S. Department of Energy, Office of Science, Basic Energy Sciences (BES), Materials Sciences and Engineering Division and performed in part as a user project at the Center for Nanophase Materials Sciences, which is a DOE Office of Science User Facility.

[1] D.B. Geohegan, et al., "Laser Interactions for the Synthesis and *in situ* Diagnostics of Nanomaterials," Ch. 7 in *Lasers in Materials Science,* **191**, 143-173 (Springer, Switzerland, 2014).
[2] F. Sauvage, F. Di Fonzo, et al., "Hierarchical TiO_2 Photoanode for Dye-Sensitized Solar Cells," *Nano Lett.* **10** (7), 2562-2567 (2010).
[3] M. Mahjouri-Samani, et al., "Pulsed Laser Deposition of Photoresponsive Two-Dimensional GaSe Nanosheet Networks" *Advanced Functional Materials* **24**(40), 4365 (2014).
[4] M. Mahjouri-Samani, et al., "Digital Transfer Growth of Patterned 2D Metal Chalcogenides by Confined Nanoparticle Evaporation," *ACS Nano* **8**, 11567 (2014).

P-067

Precision UV laser scribing for cleaving mirror facets of GaN-based laser diodes

J.-H. Kang, M. Spevak, S. Einfeldt, O. Krüger
Ferdinand-Braun-Institut, Leibniz-Institut für Höchstfrequenztechnik (FBH), Gustav-Kirchhoff-Str. 4, 12489 Berlin, Germany
E-mail: olaf.krueger@fbh-berlin.de

Group-III nitride compound semiconductors (AlInGaN) are of immense interest for laser diodes (LDs) because they can theoretically cover an emission range from the infrared (InN) to the UV (AlN). The present work focuses on LDs emitting at short wavelengths, i.e., in the blue to ultraviolet (UV) region, which consist of InGaN multi-quantum well (MQW) structures and AlGaN cladding layers grown on GaN wafers. Besides growing good-quality lattice-matched ternary alloys, the patterning of narrow ridge waveguides, the formation of Ohmic contacts with low resistivity to the p-type layers as well as the precise cleaving of facets forming the cavity mirrors of Fabry-Pérot LDs are essential for efficient laser operation. Smooth mirror facets are crucial for high output power, deposition of high-quality coatings with defined reflectivity, and device reliability for edge emitting LDs. The threshold current density of the LDs will be corrupted by rough or nonparallel facets. The group-III nitride layers crystallize in wurtzite structure having a hexagonal lattice, which makes it particularly challenging to cleave rectangular laser bars. Furthermore, the AlGaN cladding layers are lattice mismatched to the GaN substrate and the resulting strain typically causes the wafers to be concavely bowed. Hence, diamond scribing and cleaving, which is well-established for GaAs and InP LDs, suffers from low yield due to imprecise breaking of the GaN-based wafers. In this paper we will show that laser scribing provides a versatile method to fabricate GaN LD dies with high-quality facets. Complemental to our previous work about laser scribing of sapphire to cleave GaN-on-sapphire LDs [1], here we focus on facet formation of GaN-based LDs on GaN substrate. We used a nanosecond-pulsed laser (pulse length < 30 ns) with a wavelength of 355 nm to scribe the material followed by cleaving.

The epitaxial layer structures of the LDs targeting laser wavelengths of 420 nm are around 5 microns thick and were grown on 2 inch GaN substrates of two vendors by metal-organic vapor phase epitaxy. A simple fabrication process for broad-area laser diodes was performed on quarters of 2 inch wafers using contact lithography, metal deposition by electron beam evaporation, and contact formation by rapid thermal annealing. After completion of wafer processing, laser scribing was performed in ambient air on the front of the wafer (epi-side). Using alignment marks on the wafer, pattern recognition, and an air-bearing XY stage coupled to a galvanometer scanner the laser spot was precisely positioned with respect to existing structures on the wafer. The laser beam was focused to a diameter of about 15 µm using a telecentric F-teta objective with a focal length of 56 mm. The bandgap energy of the GaN substrate is 3.4 eV and corresponds to an absorption edge at 365 nm, i.e., at the irradiation wavelength of 355 nm GaN absorbs, decomposes and ablates. Debris caused by laser processing was removed by diluted hydrochloric acid. The 200 µm thick wafers were then affixed to a supporting tape and cleaved by hitting a blade against the back (substrate-side) using a commercial breaker tool.

Laser processing parameters, such as pulse energy, pulse repetition frequency (PRF), scan velocity, and number of repetitive scribing were optimized to avoid damage to the active LD region. Scribe depth and pattern were adjusted to the cleaving process to assure reliable die separation. For pulse energies between 1 µJ and 45 µJ at PRF = 20 kHz and single scan at 100 mm/min trench depths between 15 µm and 180 µm were obtained. For the mirror facets a precise alignment to the crystal's natural cleaving plane (GaN's m-plane) is essential. Also, the laser scribe lines must be precisely aligned to properly guide the cleaving. To avoid collateral damage of the epitaxial layer stack, e.g., by thermal effects, a skip-and-scribe pattern was applied leaving non-scribed sections where the active laser regions (p-contacts) are located. A distance of 70 µm between the ends of the laser processed lines and the edges of the p-contacts was chosen such that the broken line keeps the cleaving in the designated track. The trenches scribed perpendicular to the mirror facets must be sufficiently deep to force the hexagonal lattice to break along them. These lines were continuous and run in a distance of more than 200 µm parallel to the active lasing section (p-contacts).

The dies were carefully inspected by scanning electron microscopy and process parameters were optimized to minimize particle contamination and formation of terraces at the mirror facets. Also, experiments with two different water-soluble protective coatings were carried out to prevent adhesion of debris on the wafer surface during laser processing but have not shown a significant advantage. Crystal cracks due to thermal stress caused by local heating of the material during laser processing could be avoided by choosing gentle process conditions. No defects in the MQW could be detected by scanning cathodoluminescence measurements. Also, luminescence and laser spectra of the laser processed LDs did not show evidence for device degradation. Threshold current densities are comparable with LDs fabricated by diamond scribing. All data collected so far prove the concept of laser-assisted fabrication of mirror facets for GaN-based LDs.

[1] J. R. van Look, S. Einfeldt, O. Kruger, V. Hoffmann, A. Knauer, M. Weyers, P. Vogt, and M. Kneissl, "Laser Scribing for Facet Fabrication of InGaN MQW Diode Lasers on Sapphire Substrates," IEEE Photon. Technol. Lett. **22** (6), 416 (2010).

P-068

Surface modification of AISI H13 tool Steel by laser cladding with NiTi powder

B. Norhafzan[1], S.N. Aqida[1,2], E. Chikarakara[3], D. Brabazon[3]

[1]*University Malaysia Pahang,26600 Pekan, Pahang, Malaysia*

[2]*Automotive Engineering Centre, Universiti Malaysia Pahang, 26600 Pekan, Pahang, Malaysia*

[3]*Advanced Processing Technology Research Centre, Dublin City University, Dublin, Ireland*

Email: norhafzan23@gmail.com

Abstract

This paper presents laser cladding of NiTi powder on AISI H13 tool steel surface. The cladding process was conducted using Rofin DC-015 diffusion-cooled CO_2 laser system with wavelength of 10.6 µm. The NiTi powder was pre-placed on H13 tool steel surface. The laser beam was focused to a spot size of 90 µm on the sample surface. The laser parameters were set to give 1515 and 1138 W peak power, 18 and 24 % duty cycle and a 2300 to 3500 Hz laser pulse repetition frequency (PRF). Hardness, properties of the modified layer were characterized by Matsuzawa MMT-X7 Vickers Hardness Tester with Vickers indenter. Metallographic study, chemical composition and phase analysis were conducted using scanning electron microscope (SEM), energy dispersive x-ray spectrometer (EDXS) and x-ray diffraction (XRD) analysis. Results showed that hardness of modified layer increased two times of the substrate material. The analysis detected α-ferrite and NiTi phase presence in the modified layer. The metallographic study show high metallurgical bonding between substrate and modified layer. These findings are significant to enhance surface properties for the lifetime of components and repair them when worn.

Index terms - Laser cladding, microhardness, XRD analysis, EDXS, NiTi

Tuesday
1 September 2015

Oral presentations

I-05

High Harmonics and Attosecond Pulses -- Seeing Inside Molecules

David Villeneuve
Joint Attosecond Science Laboratory, National Research Council and University of Ottawa
100 Sussex Drive, Ottawa ON Canada
David.Villeneuve@nrc.ca

High Harmonic Spectroscopy (HHS) employs femtosecond high harmonic generation as a method to study the electronic structure of molecules. In many ways it is a time-reversed version of photoelectron spectroscopy, with the advantage that the energy, phase and polarization of the emitted photons can be measured for a broad range of energies simultaneously. By applying impulsive laser alignment methods, these measurements can be made in the molecular frame. The original HHS experiment showed that we could look inside a molecule at its electronic structure, and form the image of a single molecular orbital [1].

High harmonic spectroscopy employs two timescales – femtosecond and attosecond. The attosecond time scale results from the sub-optical-cycle nature of the process, and can reveal electron dynamics [2]. The femtosecond time scale enables pump-probe techniques to be employed. We have shown [3] that we can follow the photo-dissociation of bromine, in which we observe short-term dynamics by quantum interference between atomic centers, and long-term dynamics by interference of electron trajectories between separate atoms. We observed the transition between a molecule and distinguishable atoms.

Applying homodyne high harmonic spectroscopy to NO_2, we can see population transferring between two diabatic states as the excited state wave packet traverses near the conical intersection [4].

Finally, we can observe multi-electron effects, such as 4d-5p interactions associated with the giant resonance in xenon atoms [5].

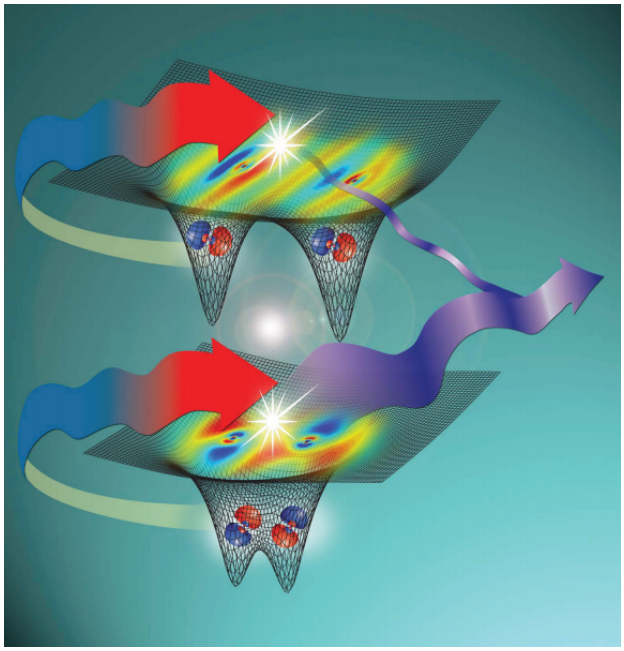

[1] J. Itatani, J. Levesque, D. Zeidler, H. Niikura, H. Pépin, J. C. Kieffer, P. B. Corkum and D. M. Villeneuve, Tomographic imaging of molecular orbitals, Nature (London) 432, 867-871 (2004).

[2] Olga Smirnova, Yann Mairesse, Serguei Patchkovskii, Nirit Dudovich, David Villeneuve, Paul Corkum, Misha Yu. Ivanov, High harmonic interferometry of multi-electron dynamics in molecules, Nature (London) 460, 972-977 (2009).

[3] H. J. Worner, J. B. Bertrand, D. V. Kartashov, P. B. Corkum and D. M. Villeneuve, Following a chemical reaction using high-harmonic spectroscopy, Nature (London) 466, 604 (2010).

[4] H. J. Wörner, J. B. Bertrand, B. Fabre, J. Higuet, H. Ruf, A. Dubrouil, S. Patchkovskii, M. Spanner, Y. Mairesse, V. Blanchet, E. Mével, E. Constant, P. B. Corkum, D. M. Villeneuve, Conical Intersection Dynamics in NO2 Probed by Homodyne High-Harmonic Spectroscopy, Science 334, 208 (2011).

[5] A. D. Shiner, B. E. Schmidt, C. Trallero-Herrero, H. J. Wörner, S. Patchkovskii, P. B. Corkum, J-C. Kieffer, F. Légaré, D. M. Villeneuve, Probing collective multi-electron dynamics in xenon with high-harmonic spectroscopy, Nature Physics 7, 464 (2011).

O-21

Photoluminescence excitation of rare earth doped fluoride films by surface plasmon resonance in the Kretschman configuration

Jiří Bulíř, Tomáš Zikmund, Michal Novotný, Ján Lančok, Libor Juha
Institute of Physics, Academy of Sciences of the Czech Republic, Na Slovance 2, 182 21 Prague 8, Czech Republic
Corresponding author e-mail: bulir@fzu.cz

We report on excitation of the photoluminescence of rare earth doped fluoride by means of the surface plasmon resonance of Al layer. The advantage of this method is high efficiency of the excitation, which is applicable to ultra-thin films. The p-polarized UV diode laser light is coupled to surface plasmon resonance using a fused silica prism in a Kretschman configuration. The angular dependence of reflected intensity is measured using a theta-2theta goniometer. The surface plasmon at resonance condition induces the luminescence in the adjacent doped fluoride layer. The luminescence is collected using a fiber optics and detected by a spectrophotometer. For the experiment, we used pure LiF films and doped by Eu, Pr and Yb. The fluoride layer was deposited on Al-coated fused silica substrate by electron beam evaporation. For the experiment, we prepared several samples with thickness up-to 20 nm. We studied effect of color center enhancement in doped fluoride structure upon pulsed laser irradiation. We used KrF excimer laser (wavelength 248 nm) and capillary discharge XUV laser (wavelength 46.9 nm) for the fluoride layer treatment. The results shows that the induced color center photoluminescence can be enhanced by rare earth doping. Optical constants and thickness of the prepared fluoride film were studied by spectroscopic ellipsometry in the wavelength range from 245 nm to 1000 nm. The results were analytically compared with the theoretical simulation of angular dependence of p-polarized reflectivity and electric field intensity induced in the fluoride films.

O-22

Towards Planet Hunting on a Chip: First Successful On-Telescope Deployment of Integrated 2D-3D Hybrid Photonics using Extreme Adaptive Optics

Nick Cvetojevic[1,2,3], Nemanja Jovanovic[4], Simon Gross[5], Izabella Spelaniak[6], Christian Schwab[7], Barnaby Norris[3], Michael J. Withford[1,5], Peter Tuthill[3], Olivier Guyon[4,8], and Jon S. Lawrence[2]

[1]*Centre for Ultrahigh bandwidth Devices for Optical Systems (CUDOS), School of Physics, University of Sydney, Sydney, Australia*
[2]*The Australian Astronomical Observatory (AAO), Level 1, 105 Delhi Rd, North Ryde, NSW, Australia*
[3]*Sydney Institute for Astronomy (SIfA), School of Physics, University of Sydney, NSW 2006, Australia*
[4]*National Astronomical Observatory of Japan, Subaru Telescope, 650 North A'Ohoku Place, Hilo, HI, 96720, U.S.A.*
[5]*MQ Photonics Research Centre, Dept. of Physics and Astronomy, Macquarie University, NSW, Australia*
[6]*School of Photonics & Quantum Sciences, Heriot-Watt University, Edinburgh, UK*
[7]*NASA Sagan Fellow, Department of Astronomy & Astrophysics, Pennsylvania State University, PA-16802, U.S.A.*
[8]*Steward Observatory & College of Optical Sciences, University of Arizona, Tucson, AZ, 85721, U.S.A.*
E-mail: nickc@physics.usyd.edu.au

The next generation of telescopes currently under construction are vastly larger than any previously built. While their monumental size will allow astronomers to peer deeper into space, a fundamental scaling law means that instrumentation used by astronomers on these telescopes dramatically increases in both size and cost [1]. This imposes an immediate obstacle for the next generation of instrumentation, and in particular spectroscopic instruments, which are used extensively in the hunt for habitable Earth-like planets in distant solar systems. Furthermore, detecting Earth-like planets places extreme requirements on spectrograph performance in terms of exceptionally high resolution and stability. Constructing conventional spectrographs in this parameter space has led to spiralling costs and complexity, and proved to be the primary limiting factor for the field. Integrated on-chip photonics can potentially provide an unparalleled improvement in spectrograph sensitivity and stability. However, until now, such devices have not been deployed and tested on telescopes with sufficiently high coupling to demonstrate the advantage over competing bulk-optic state-of-the-art instruments.

In this body of work we designed, fabricated, prototyped, and deployed a new kind of hybrid photonic circuit that combines a lithographically fabricated planar Arrayed Waveguide Grating (AWG) micro-spectrograph and a 3D integrated photonic lantern (multimode-to-single mode tapered transition) [2-3], fabricated in bulk glass using the femtosecond laser direct write technique. The AWG and lantern (and an injection multimode fibre) form a single integrated monolithic device (Fig.1) capable of taking the atmospherically distorted light from the telescope's focal plane, converting it to a series of diffraction-limited (single mode) inputs, and dispersing them simultaneously to form multiple output spectra.

We employed the SCExAO extreme adaptive optics facility at the Subaru Telescope on Mauna Kea, Hawaii, to achieve unprecedented levels of on-sky coupling (~60% and higher) directly into a commercially available fibre (with laboratory benchmarking demonstrating coupling as high at 87% is possible). The measured throughput from the telescope focus to the detector was 42%, outperforming high-resolution bulk optic spectrographs, especially on large telescopes.

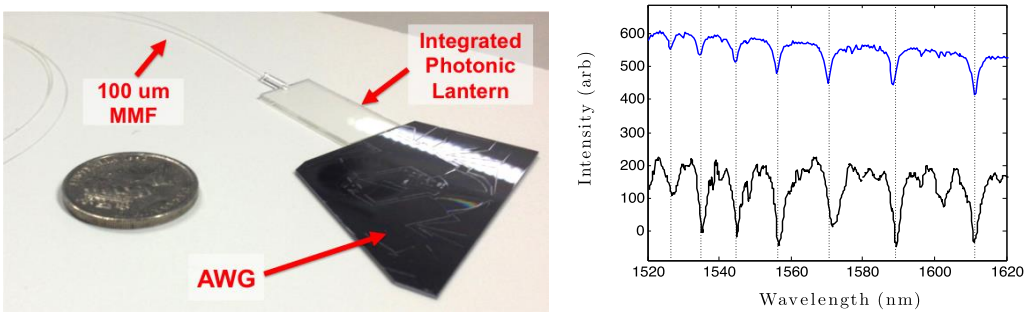

Fig. 1. After the telescope light is injected into a multimode-mode fibre it is transported to an integrated photonic lantern and the spectrograph chip (left), which disperses the starlight at NIR wavelengths. The acquired spectrum (right) of the star HD135153 is shown in black, alongside a sample spectrum in blue. The Hydrogen Brackett series of absorption lines from the star's atmosphere are marked.

[1] J. J. Bland-Hawthorn, and A. Horton, "Instruments without optics: an integrated photonic spectrograph," Proc. SPIE 6269, **21** (2006).
[2] V. Coud´e du Foresto, M. Faucherre, N. Hubin, and P. Gitton, "Using single-mode fibers to monitor fast Strehl ratio fluctuations. Application to a 3.6 m telescope corrected by adaptive optics," A&AS **145**, pp. 305–310, (2000).
[3] Christian Schwab, Sergio G. Leon-Saval, Christopher H. Betters, Joss Bland-Hawthorn and Suvrath Mahadevan, "Single Mode, Extreme Precision Doppler Spectrographs" Proc. IAU 403 (2012).

O-23

Laser structuration of dielectric materials by a train of femtosecond pulses through cumulative effects

E. Smetanina[1], O. Caulier[1], B. Chimier[1], S. Skupin[1], A. Bourgeade[2], K. Mishchik[1], J. Lopez[1], C. Javaux Léger[3], C. Hoenninger[4], R. Kling[3], Y. Petit[5], T. Cardinal[5], L. Canioni[1], V. Tikhonchuk[1], G. Duchateau[1]

[1]*Université de Bordeaux-CNRS-CEA, CELIA, UMR 5107, 351 Cours de la Libération, 33405 Talence, France*

[2]*CEA/CESTA, 15 Avenue des Sablères, 33114 Le Barp, France*

[3]*ALPhANOV, Rue François Mitterand, 33400 Talence, France*

[4]*AMPLITUDE SYSTEMES, 11, avenue de Canteranne, Cité de la Photonique, 33600 Pessac, France*

[5]*Université de Bordeaux-CNRS, ICMCB, UPR 9048, 87 avenue du Dr. A. Schweitzer, 33608 Pessac cedex, France*

Corresponding Author e-mail address: duchateau@celia.u-bordeaux1.fr

1. Introduction and general phenomenology of the physical processes

Optical materials can be structured by laser pulses to get new material functionalities in various scientific area going from photonics to medicine. For instance, wave guides, nano-gratings, emergence of nonlinear optical properties for data storage [1], cutting and welding of materials are applications of great interest. Structuration driven by a train of laser pulses is strongly emerging due to its advantages: table top laser facility, very well controlled structuration with energy deposition accuracy in the nJ range by adjusting the number of pulses, etc. The material structuration due to pulse-to-pulse cumulative effects should be deeply understood to design specific structures. This may be achieved by modelling the main physical processes and their possible coupling. Briefly, each laser pulse first induces photo-ionization and heats the conduction electrons which can then transfer their energy to the lattice. That leads to a local increase in the material temperature together with heat diffusion and thermally-activated ions migration on longer timescales. Since the laser pulse is partially absorbed, the electron dynamics and the pulse propagation are closely coupled. Due to the low heat diffusion coefficient of dielectric materials, the laser energy may be accumulated in the absorption region, leading to high temperatures even if the single pulse energy is too low to induce itself any significant material modification. A general modelling including all the above-mentioned processes will be presented, including the two following applications of interest.

2. Nanostructures formation in silver-doped phosphate glasses

Here a phosphate glass doped with initially uniformly distributed Ag^+ ions is irradiated. The laser-induced ionization first leads to the formation of Ag^0 atoms through the reaction $Ag^+ + e^- \rightarrow Ag^0$. The latter specie may then associate with Ag^+ to form Ag_2^+, which exhibits luminescence properties allowing to observe the spatial size of modified zone. Fig. 1(a) shows the emergence of a micrometric ring structure after an irradiation by 10^7 laser pulses [1] with parameters: 1030 nm, 470 fs, 1.2 µm of waist, 100 nJ, 10MHz. Due to the migration of charged species, a static electric field originates leading to the formation of nonlinear optical properties. A model including laser heating, heat diffusion, and thermally-activated diffusion and kinetic reactions of the various silver species, allows us to account for the observed structure (Fig. 1(b)). Details of the modelling, mechanisms for cumulative effects, and influence of laser parameters on the ring characteristics will be presented.

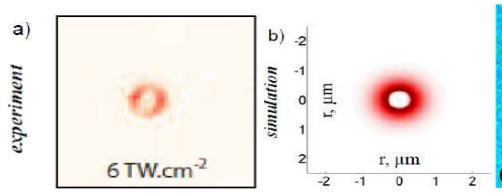

Fig. 1. (a) Experimental and (b) predicted ring structure (Section 2).

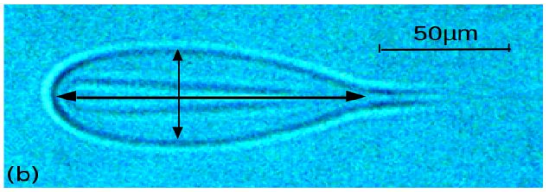

Fig. 2. Laser affected zone in sodalime (Section 3)

3. Refractive index modifications in sodalime glasses

Modification of Sodalime glasses irradiated by a train of 500 laser pulses with various repetition rates (RR) is addressed. Each pulse with 300fs duration, 1030nm wavelength and µJ energy, is focused by a 10x objective in the glass. The affected zone exhibits a particular comet-like shape with characteristic longitudinal and transverse lengths (Fig. 2). Experimental investigations show that this structure only appears for RR larger than roughly 100kHz. Then, both lengths increase with respect to the RR up to 500kHz. In order to shed light on the underlying cumulative effects taking place, the energy deposition is obtained by simulating the laser pulse propagation through a Forward Maxwell code [2]. The thermal effects are modelled by solving a heat diffusion equation with the deposited laser energy as initial condition. The softening temperature is considered as the threshold for a permanent index modification of the matter. The obtained evolutions of both characteristic lengths with respect to the RR are in a good agreement with the experimental data, demonstrating that the material modifications originate from heat accumulation and subsequent phase transition.

[1] G. Papon *et al*, "Fluorescence and second harmonic generation correlative microscopy to probe space charge separation and silver cluster stabilization during direct laser writing in a tailored silver-containing glass," Optical Materials Express **3**(11), 1855-1861 (2013).

[2] L. Bergé *et al*, "Ultrashort filaments of light in weakly ionized optically transparent media," Rep. Prog. Phys. **70**, 1633 (2007).

O-24

Laser Cleaning of Pulsed Laser Deposited diagnostic mirrors for nuclear fusion applications

A. Maffini[1], A. Uccello[2], D. Dellasega[1,2], M. Passoni[1,2]
[1]Dipartimento di Energia, Politecnico di Milano, Via Ponzio 34/3, 20133 Milano, Italy
[2]Istituto di Fisica del Plasma "P. Caldirola", CNR, via R. Cozzi 53, 20125 Milano, Italy
e-mail address: alessandro.maffini@polimi.it

Laser cleaning technique has attracted more and more attention from scientist and engineers as a powerful tool for many high-tech applications, in which a solvent-free cleaning process, easy to automate and gentler than abrasive techniques, is required [1].

In the field of nuclear fusion research, laser cleaning is a potential candidate for the cleaning of the delicate First Mirrors (FMs), essential components of the diagnostic systems in future fusion reactors like ITER [2]. Due to the complex interactions with ITER harsh environment, the FMs' surface may be covered by the materials eroded from the reactor main chamber, leading to a dramatic decrease of FMs reflectivity which can have an ultimate impact on the reactor safety and economics [3]. An effective laser cleaning process has to remove the contaminants without damaging the mirror surface nor altering its optical properties.

In this work, the laser cleaning of ITER FMs is investigated in details, following an integrated approach in which a single Nd:YAG nanosecond laser source is exploited to i) produce rhodium (Rh) coatings suitable as FMs, ii) deposit ITER-relevant contaminants onto mirrors' surface and iii) study the laser cleaning process of the ITER-like diagnostic mirrors.

Nanostructured, high-reflective Rh films with realistic properties as FM coatings (i.e. reflectivity, mechanical properties, behavior under reactor-relevant conditions) are produced by means of Pulsed Laser Deposition (PLD) [4-6] and are used as test system for cleaning.

The great versatility of the PLD technique is also exploited to deposit ITER-relevant contaminants with controlled features on mirrors' surface. By properly controlling the deposition it is possible to tune finely the properties of the contaminants. Previously, we successfully cleaned tokamak-like carbon layers deposited on Rh mirror surface [7,8]. Here we discuss the cleaning of tungsten- and aluminium- (as beryllium proxy) based contaminants, with different composition, degree of oxidation, morphology (from compact dense layer to open, very porous structure) and thickness (from 100 nm up to 1 μm).

Laser damaging tests are performed on bare Rh coatings, in order to find a range of laser parameters (fluence, wavelength, number of pulses) safe for the cleaning experiments.

The mirrors are cleaned using the fundamental Nd:YAG wavelength (NIR, λ=1064 nm) or its fourth harmonic (UV, λ=266 nm). The laser fluence per pulse varies from ~100mJ/cm^2 to ~400mJ/cm^2. A suitable remote handling procedure is developed to clean samples of some cm^2 in a few minutes in vacuum condition. Coatings morphology and composition are assessed by SEM, EDS and Raman spectroscopy before and after the contamination and after cleaning. The specular reflectivity (R_{spec}) of the mirrors is characterized using UV-Vis-NIR spectrophotometry before and after cleaning.

We observe that the cleaning effectiveness depends on the contaminant composition, morphology and optical properties. Nevertheless, by properly choosing the laser parameters, a satisfactory recovery of R_{spec} (from 70% to 90% of the original value for $\lambda > 400$ nm) is achieved for most of the samples here considered, thus proving the robustness and the adaptability of the technique also in the context of nuclear fusion industry and research.

An investigation of the structural and morphological changes experienced by the contaminant during the laser irradiation, and their impact on the efficacy of the cleaning process, is also presented. Finally, the effect of repeated cycles of cleaning-contamination-cleaning on the mirrors' performances is discussed.

[1] D. M. Kane, *Laser Cleaning II*, (World Scientific Publishing, Singapore, 2006)
[2] http://www.iter.org
[3] A. Litnovsky et al., "Progress in research and development of mirrors for ITER diagnostics", Nucl. Fusion, **49**, 075014 (2009)
[4] M. Passoni, et al.," Nanostructured rhodium films produced by pulsed laser deposition for nuclear fusion applications", J. Nucl. Mater. **404**, 1 (2010)
[5] A. Uccello, et al., "Nanostructured rhodium films for advanced mirrors produced by Pulsed Laser Deposition", J. Nucl. Mater. **432**, 261 (2013)
[6] A. Uccello, et al., "Deuterium plasma exposure of Rh films: Role of morphology and crystal structure", J. Nucl. Mater. **446**, 106 (2014)
[7] A. Uccello, et al., "Laser cleaning of pulsed laser deposited rhodium films for fusion diagnostic mirrors", Fus. Eng. Des. **88**, 1347 (2013)
[8] A. Maffini, et al., "Laser cleaning of diagnostic mirrors from tokamak-like carbon contaminants", J. Nucl. Mater. doi: 10.1016/j.jnucmat.2014.10.016 (2014)

O-25

Quantitative Comparison of the Efficiency of Laser Ablation for Bessel, Vortex and Gaussian Beam Shapes

M. Cather Simpson[1,2,3,4*], Reece N. Oosterbeek[1,3], Simon Ashforth[1,3,4], Owen Bodley[1,3]

[1] *The Photon Factory, The University of Auckland, Auckland, New Zealand*

[2] *School of Chemical Sciences, The University of Auckland, Auckland, New Zealand*

[3] *The MacDiarmid Institute for Advanced Materials and Nanotechnology and The Dodd Walls Centre for Quantum and Photonic Technologies, New Zealand*

[4] *Department of Physics, The University of Auckland, Auckland, New Zealand*

** Corresponding author email: c.simpson@auckland.ac.nz*

Ultrafast laser micromachining using pulses of < 10 ps duration is a rapidly growing field with applications in areas as diverse as microelectronics, surgery, and dentistry [1]. The mechanism of ultrafast laser ablation gives it significant advantages over longer pulsed and CW laser machining. The initial excitation is multiphoton in nature, and the ultrashort duration effectively decouples the electron and phonon degrees of freedom. Because of these key features, ultrafast laser micromachining is often described as "cold cutting," able to work for virtually any material, and able to beat the Rayleigh criterion [2]. Unfortunately, despite these tremendous advantages, femtosecond laser micromachining is currently to slow for widespread use in industry.

Here, we apply a new custom-built laser micromachining apparatus to the dependence of the laser ablation efficiency upon the spatial beam shape. The ablation threshold is a routinely used to evaluate ablation for different conditions. A number of established techniques are used to measure this parameter, including the least visible damage, diameter regression, and volume regression [3]. These have significant limitations, however. The first is strongly subjective. The latter often require many time consuming measurements, and have been developed with the assumption of a Gaussian beam shape. The diagonal scan method, first proposed by Samad *et al.* [4], reduces the number of measurements, but also assumes a Gaussian beam. The current ablation threshold methods are thus inappropriate for a rational comparison of laser ablation as a function of beam shape.

We extend the diagonal scan method to allow the ablation threshold to be measured for non-Gaussian beam shapes of vortex and Bessel beams. For vortex beams we obtain an expression for the damage radius ρ as a function of propagation length z, followed by integration to determine the maximum damage radius:

$$F_{th} = \frac{-|l|(|l|+1)^{|l|}E_0}{|l|!\,\pi e^{|l|+1}\rho_{max}^2} W_{-1}\left(\frac{|l|+1}{-|l|e^{1+\frac{1}{|l|}}}\right)$$

F_{th} is the ablation threshold in J/cm^2, E_0 is the pulse energy in J, ρ_{max} is the maximum damage radius in cm, l is the vortex charge, and W_{-1} is the non-principal branch of the Lambert Omega function [5]. We also evaluate the pulse superposition N to explore incubation effects.

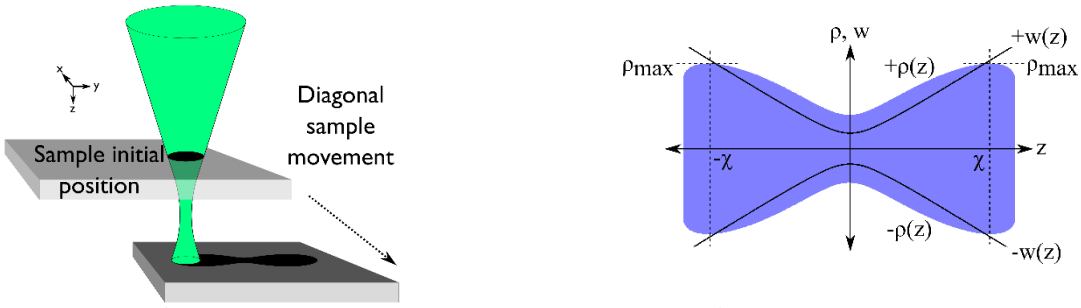

Fig. 1. (Left) The diagonal scan method. (Right) Calculated damage radius for a vortex beam diagonal scan.

In contrast to vortex beams, the fluence distribution of a Bessel beam could not be analytically solved to obtain the damage radius. To extend this technique to Bessel beams, we have therefore developed a numerical solution method to determine the ablation threshold for n^{th} order Bessel beams, based on measurement of the maximum feature radius from a diagonal scan ablation feature. Experimental and theoretical comparison of the efficiency of femtosecond laser ablation with a variety of wavelengths, beam shapes and number of pulses is shown as a function of incident laser pulse energy.

References

[1] J. Kruger, W. Kautek, "Ultrashort Pulse Laser Interaction with Dielectrics and Polymers", Adv. Polym. Sci. **168**, 247 (2004)

[2] M. D. Perry et al. "Ultrashort pulse laser machining of dielectric materials", J. Appl. Phys., **85**, 6803 (1999)

[3] N. Sanner, et al. "Measurement of femtosecond laser-induced damage and ablation thresholds in dielectrics" Appl. Phys. A Mater. Sci Process., **94**, 889 (2009)

[4] R. E. Samad, N. D. Vieira Jr., "Geometrical method for determining the surface damage threshold for femtosecond laser pulses", Laser Phys. **16**, 336 (2006)

[5] R.M. Corless et al. "On the LambertW Function", Adv. Comput. Math., **5**, 329 (1996)

I-06

Femtosecond laser micromachining for 3D optofluidic devices

Roberto Osellame
Institute for Photonics and Nanotechnologies – National Research Council (IFN-CNR), Piazza Leonardo da Vinci 32, 20133 Milan (Italy)
e-mail address: roberto.osellame@polimi.it

Femtosecond laser micromachining is rapidly becoming a major player in processing transparent materials. Being contactless, maskless, cost-effective and capable of 3D structuring it proved to be a unique technology raising interest both in scientific as well as in industrial applications. In addition, femtosecond laser micromachining includes many different processes, from gentle modification of materials for waveguide writing, to subtractive approaches like ablation or laser assisted etching to produce microchannels, to additive approaches like two-photon polymerization to produce 3D micro/nano structures. The combination of these processes enables the fabrication of highly innovative devices that integrate microfluidic with optics, giving rise to the so-called optofluidics [1]. A first example of hybrid microfabrication consists in the combination of waveguide writing with femtosecond laser irradiation followed by chemical etching (FLICE) for microchannel creation. This very powerful platform produced several innovative and effective devices in the field of optofluidics [2]. One of the most interesting applications is the on-chip manipulation and analysis of cells. These complex operations, that usually require massive equipment and specialized personnel, can be performed in devices with an extremely small footprint, in the order of a few millimeters, in an almost completely automatized way. In an optofluidic device fabricated by femtosecond lasers, unprecedented 3D layouts are possible, which take advantage of optical forces, delivered by waveguides, to trap and deform cells, sort them and count them [3,4] (see Fig. 1(a)).

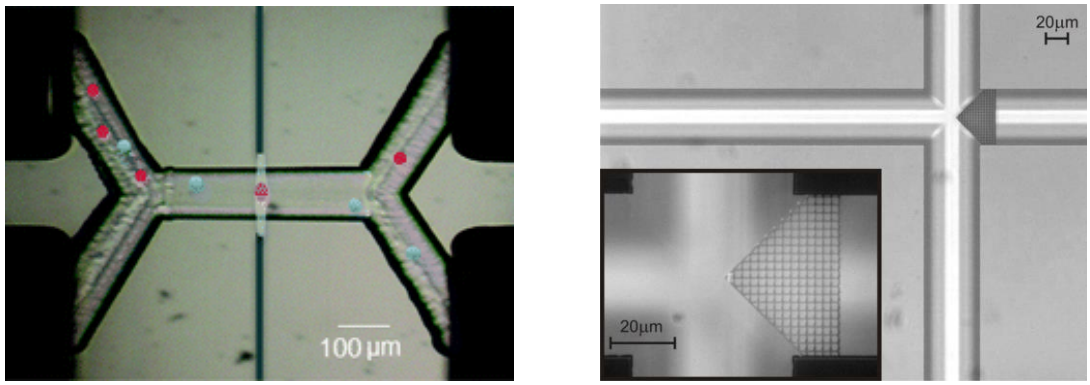

(a) (b)

Fig, 1. (a) An optofluidic cell sorter conditioned on the real-time measurement of the cell mechanical deformability [3]. (b) Microscope image of a porous filter fabricated by two-photon polymerization inside a commercial microfluidic device [4].

A second example of hybrid fabrication consists in combining the microchannel formation with two-photon polymerization. This allows producing 3D micro/nano structures inside a microchannel. One example is the fabrication by two-photon polymerization of a porous filter inside an already sealed microchannel [5] (Fig. 1(b)). This filter can be custom-tailored with pore sizes as small as a few hundred nanometers and can be used to filter plasma from whole blood.

Potentials of hybrid femtosecond laser micromachining are still largely unexplored, but the possibility to combine photonic and microfluidic networks together with three-dimensional micro/nanostructures will definitely make this technology one of the most versatile and powerful microfabrication techniques available.

[1] D. Psaltis, S.R. Quake and C. Yang, "Developing optofluidic technology through the fusion of microfluidics and optics," *Nature* **442**, 381 (2006).
[2] R. Osellame, H.J.W. M. Hoekstra, G. Cerullo and M. Pollnau, "Femtosecond laser microstructuring: an enabling tool for optofluidic lab-on-chips," *Laser Photonics Rev*. **5**, 442 (2011).
[3] T. Yang, P. Paiè, G. Nava, F. Bragheri, R. Martinez Vazquez, P. Minzioni, M. Veglione, M. Di Tano, C. Mondello, R. Osellame and I. Cristiani, "An integrated optofluidic device for single-cell sorting driven by mechanical properties" *Lab Chip* **15**, 1262 (2015).
[4] P. Paiè, F. Bragheri, R. Martinez Vazquez and R. Osellame, "Straightforward 3D hydrodynamic focusing in femtosecond laser fabricated microfluidic channels," *Lab Chip* **14**, 1826 (2014).
[5] L. Amato, Y. Gu, N. Bellini, S. M. Eaton, G. Cerullo and R. Osellame, "Integrated three-dimensional filter separates nanoscale from microscale elements in a microfluidic chip," *Lab Chip* **12**, 1135 (2012).

O-26

Feasibility Study of Femtosecond Laser Written Arrayed Waveguide Gratings

G. Douglass[1], F. Dreisow[2], S. Gross[1] S. Nolte[2] and M. J. Withford[1]
[1]*Centre for Ultrahigh bandwidth Devices for Optical Systems (CUDOS)*
MQ Photonics Research Centre, Department of Physics & Astronomy, Macquarie University, NSW 2109, Australia
[2]*Institute of Applied Physics, Fredrich-Schiller-University Max-Wien-Platz 1,07743 Jena, Germany*
E-mail: glen.douglass@students.mq.edu.au

Abstract: The prospect of fabricating arrayed waveguide gratings (AWGs) using the femtosecond laser direct write technique is investigated. Here we successfully demonstrate the fabrication of planar slab waveguides that act as free propagation zones (FPZ), low loss adiabatic tapers and manufacturing strategies to inscribe AWGs 'on-the-fly'.

AWGs (Fig: 1a) have recently been utilised as integrated compact, low loss, 'on-chip' spectroscopic sensors for applications including bio-medicine [1] and astronomy [2]. Since these devices are currently lithographically fabricated, the development of new prototypes require small scale fabrication runs that are expensive and time consuming. Here the laser direct-write technique is proposed as a fast and cost effective alternative for rapidly prototyping new devices. To laser fabricate an AWG both single mode waveguides and large planar slab waveguides are required. To date there has only been three reports on the fabrication of slab waveguides [3-5]. These previous examples however have not fabricated slab waveguides large enough for AWGs.

Here we demonstrate the fabrication of large slab waveguides in boro-aluminosilicate glass (Eagle2000) using a 5.1 MHz repetition rate 50 fs pulse Ti: sapphire oscillator. Slab waveguides were fabricated using the multi-scan technique with a 0.4µm pitch and translation speed of 2000mm/min. These slabs have a refractive index contrast of $1.5\text{x}10^{-3}$ and a transverse standard index deviation of 1.97% relative to the slab index change. Propagation of light within the slabs (Fig: 1b) shows linear diffraction as expected. Low loss linear adiabatic tapers were also developed and shown to reduce the losses at the FPZ-waveguide array interface by 90% (Fig: 1c). Fabrication of a complete AWG using a continuous contouring technique to avoid lossy defects has been demonstrated. Techniques to control the phase in the waveguide array will be presented.

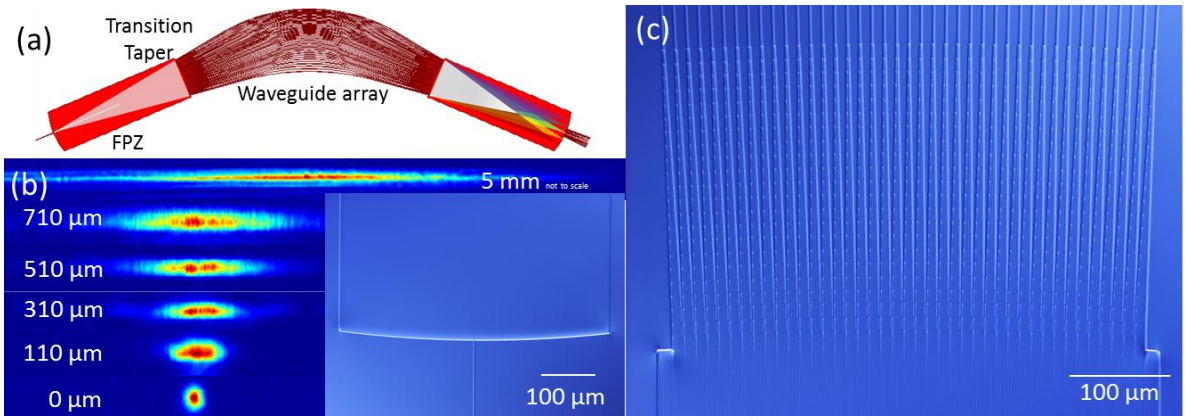

Fig. 1. (a) Schematic of an array waveguide grating. (b) Near-field profiles of light diffraction at different propagation lengths in a laser written slab waveguide seen to the right. (c) DIC image from a complete AWG prototype displaying the low loss adiabatic tapers.

References

[1] Y. Komai, H. Nagano, K. Kodate, K. Okamoto, and T. Kamiya, "Application of Arrayed-Waveguide Grating to Compact Spectroscopic Sensors," Jpn. J. Appl. Phys. **43**, 5795-5799 (2004)

[2] N. Cvetojevic, N. Jovanovic, C. Betters, J. S. Lawrence, S. C. Ellis, G. Robertson, and J. Bland-Hawthorn, "First starlight spectrum captured using an integrated photonic micro-spectrograph," Astron. Astrophys., **544**,L1 (2012)

[3] W. Watanabe, Y. Note, and K. Itoh, "Fabrication of multimode interference waveguides in glass by use of a femtosecond laser." *Opt. Lett.*, **30**, 2888-90 (2005)

[4] S. Ghosh, N. D. Psaila, R. R. Thomson, B. P. Pal, R. K. Varshney, and A. K. Kar. "Ultrafast laser inscribed waveguide lattice in glass for direct observation of transverse localization of light," *Appl. Phys. Lett.*, **100**, (2012)

[5] A. Szameit, F. Dreisow, M. Heinrich, R. Keil, S. Nolte, A. Tunnermann, and S. Longhi, "Geometric Potential and Transport in Photonic Topological Crystals", Phys. Rev. Lett. **104**, 1-4 (2010).

O-27

Laser direct-write of complex materials: towards multi-layered micro/nano-structured optoelectronic devices

Michael M. Lee, and Thomas Lippert
Paul Scherrer Institute, General Energy Research Department, CH-5232 Villigen PSI, Switzerland
michael.lee@psi.ch

Laser-direct writing (LDW) is a remarkably simple method to fabricate highly ordered and functional micro/nano structured systems from a wide range of materials. The versatility of LDW enables complex materials to be deposited as a liquid, paste or solid with lateral directionality and high selectivity resulting in efficient material usage. Pastes and solids may be deposited with well-defined geometries (tuneable by rudimentary optics) and into functional 3D structures assembled through layer-by-layer direct-writing [1]. The ability to pattern structures with great repetition rate, high reproducibility and well-defined spatial coordinates has led to the realisation of metamaterials by LDW [2]. In this work we utilize LDW as a means to provide metallization for high performance Si solar cells. Here, we detail the challenges of conformal coating of micron-scale electrodes of silver nanopastes over rough, randomly textured, pyramidal structures (see Fig. 1); we quantify the suppression of defects in the active layers through fluorescence spectroscopy; and we study the morphological and electronic properties of the deposited silver electrodes. Finally, we provide a progress report on the laser-direct writing of an exciting new breed of materials for optoelectronics: organic-inorganic hybrid perovskites [3].

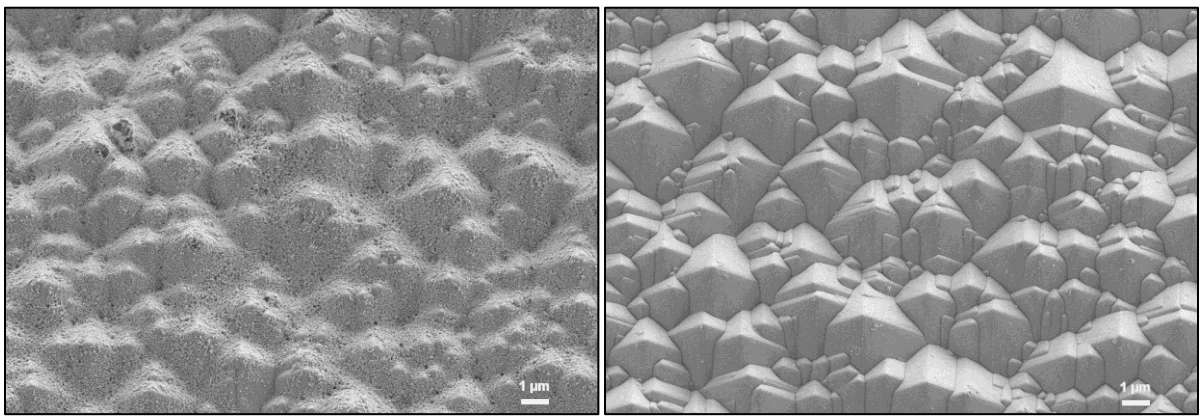

Fig. 1. Scanning electron micrographs of textured thin film Si solar cells with (left) and without (right) laser printed Ag electrodes

[1] J. Wang, R. C. Y. Auyeung, H. Kim, N. A. Charipar, and A. Piqué, "Three-Dimensional Printing of Interconnects by Laser Direct-Write of Silver Nanopastes", Adv. Mater., **40**, 4462 (2010).
[2] H. Kim, J. S. Melinger, A. Khachatrian, N. A. Charipar, R. C. Y. Auyeung, and A. Piqué, "Fabrication of terahertz metamaterials by laser printing", Optics Lett., **35**, 4039 (2010).
[3] M. M. Lee, J. Teuscher, T. Miyasaka, T. N. Murakami, and H. J. Snaith, "Efficient Hybrid Solar Cells Based on Meso-Superstructured Organometal Halide Perovskites", Science, **338**, 643 (2012).

O-28

Plasmonic nanoparticles enhanced ultrafast laser locally inducing stimulation of hippocampal neurons

M. Meunier[1], F. Lavoie-Cardinal[2], E. Bergeron[1], C. Boutopoulos[1], C. Salesse[2], A. Dagallier[1], R. Lachaine[1], and P. De Koninck[2]

[1]Department of Engineering Physics, Laser Processing and Plasmonics Laboratory, Polytechnique Montréal, 2500 Chemin de Polytechnique, Montréal, Québec, H3T 1J4
[2]Institut universitaire en santé mentale de Québec, 2601 de la Canardière, Québec, Québec, G1J 2G3
E-mail: michel.meunier@polymtl.ca

The physiology of neurons and neuronal circuits is often studied by applying various external stimuli including mechanical, electrical, chemical and more recently optical. Light-induced stimulation with optogenetic tools is a well-established and powerful approach to study circuit function[1]. However, it remains difficult with all these techniques to stimulate locally the cell membrane at the nm to µm scale, which would be useful to study the cellular behaviors governing neuronal and dendritic functions. We have developed a new and alternative technique to locally apply a stimulus on neurons using a near-infrared (NIR) ultrafast laser and plasmonic gold NPs (AuNPs). Upon off-resonance irradiation, numerical simulations show that a series of highly localized phenomena at the nanoscale occurred around the AuNPs, including charge creation, heat transfer, pressure wave and eventually nanocavitation[2,3]. Pump-probe experiments indicate that few hundreds nm to µm size bubbles could be formed around the AuNPs in close proximity with the cell membrane (Figure 1a and b)[4]. Functionalized AuNPs can target specific antigens on the targeted cells (Figure 1c) and induce various highly localized stimuli that may include a combination of mechanical (pressure wave and bubbles), thermal and possibly electrical effects, depending on laser parameters and AuNPs properties. Figure 1d shows a simulation result of a pressure wave interacting locally with a cell membrane located 20 nm from the AuNP surface.

We tested this hypothesis *in vitro* on rat hippocampal neurons. We have developed a technique to effectively functionalized 100 nm AuNPs with antibodies targeting specific cell membrane receptors[5]. These stable functionalized AuNPs were incubated with neurons. Then, regions of interest on somato-dendritic domains with one or more AuNPs were irradiated with a 800 nm femtosecond pulsed laser. We monitored the neuronal response with confocal imaging of Ca^{2+} fluctuations using GCaMP6 and with patch clamp electrophysiology. Our results indicate that we are able to induce localized or widespread Ca^{2+} elevation inside the neurons, depending on i) laser intensity, ii) surface area of illumination, or iii) number of functionalized AuNPs on targeted cells. Discussion on the physical mechanisms will be presented based on simulation results and pump-probe experiments.

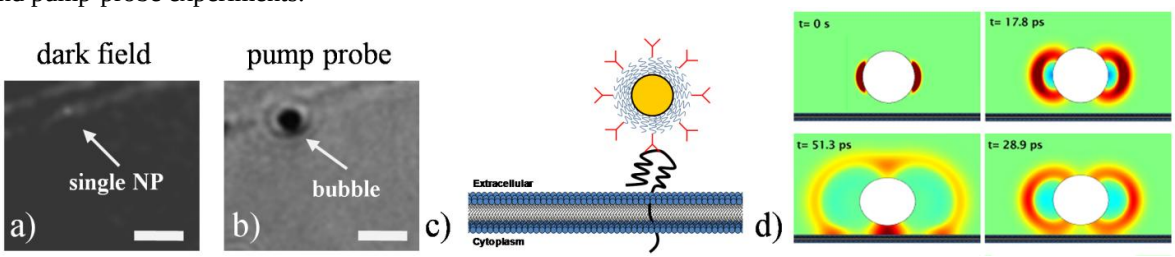

Figure 1: (a) Dark field image of a single 100 nm AuNP bound on a cell. (b) Upon irradiation with a laser pulse, a bubble is generated in close proximity to the cell membrane and detected with pump-probe imaging (scale bar is 3 µm) (c) Cell targeting with stable AuNPs functionalized with antibodies. (d) Numerical simulation results showing a pressure wave after an irradiation of a 100 nm AuNP by a 45 fs NIR pulse. The cell membrane (at the bottom of each image) is located at 20 nm from the AuNP surface.

References

[1] Fenno, Lief, Ofer Yizhar, and Karl Deisseroth. "The development and application of optogenetics." Annual review of neuroscience 34 (2011): 389-412.
[2] E. Boulais, R. Lachaine, A. Hatef, and M. Meunier, "Plasmonics for pulsed-laser cell nanosurgery: Fundamentals and applications", Journal of Photochemistry and Photobiology C: Photochemistry Reviews 17, 26-49 (2013).
[3] E. Boulais, R. Lachaine, and M. Meunier, "Plasma mediated off-resonance plasmonic enhanced ultrafast laser-induced nanocavitation", Nano Letters 12, 4763-4769 (2012).
[4] C. Boutopoulos, E. Bergeron and M. Meunier "Plasmonic bubble mediated single near infrared femtosecond laser pulse cell perforation", submitted to Biomedical Optics Express (2015).
[5] E. Bergeron, C. Boutopoulos, R. Martel, A. Torres, C. Rodriguez, J. Niskanen, J-J Lebrun, F. M. Winnik, P. Sapieha, and M. Meunier, "Cell-specific optoporation with near-infrared ultrafast laser and functionalized gold nanoparticles", submitted to ACS Nano (2015).

O-29

ZnO nanostructures prepared through millisecond pulsed laser ablation in liquid

Mitsuhiro Honda[1], Tatsuki Owashi[2], Shusuke Bitoh[2], Satoru Iwamori[2], Sergei A Kulinich[1]

1 Institute of Innovative Science and Technology, Tokai University, Hiratsuka, Kanagawa, Japan

2 Department of mechanical engineering, Tokai University, Hiratsuka, Kanagawa, Japan

E-mail address: hm842891@tsc.u-tokai.ac.jp

Zinc oxide (ZnO) nanostructures are attractive candidates for a variety of applications, such as gas sensors, photocatalysts, UV LEDs, and nanoscale electronic and optoelectronic devices [1]. The precise control of size, shape, chemical composition and crystallinity of ZnO nanostructures is still a challenge for their use. We prepared ZnO nanostructures with various sizes and shapes through millisecond pulsed laser ablation in liquid. By changing pulse width, laser power and liquid, the product size and shape could be controlled. For the characterization of ZnO nanostructures, transmission electron microscope (TEM) measurement, X-ray photoelectron spectroscopy (XPS), X-ray diffraction (XRD) analysis, and Raman spectroscopy were conducted. Figure 1 shows TEM images of ZnO nanostructures prepared using water as a liquid medium. The pulse widths were 0.5 ms and 2 ms, while the laser powers were 1 kW and 5 kW. Nanorod-shaped structures are well seen. With increasing pulse width from 0.5 ms to 2 ms, the aspect ratio of ZnO nanorods was observed to be higher. The increment of the laser power leads to the reduction in size. Figure 2 shows a representative XRD pattern and XPS spectra of a prepared sample. Based on the XRD pattern, the analyzed sample has a hexagonal structure. The XPS spectra indicate that the sample is composed of Zn and O. When using ethanol as a liquid in LAL, the shape of structures was close to sphere. With increasing the pulse width from 0.5 ms to 2 ms, the diameter of nanoparticles became larger. XPS and XRD spectra showed that the composition of prepared structures were zinc and oxygen atoms. We conclude that ZnO nanostructures with the shapes of nanorods and nanospheres, with various sizes, were prepared by millisecond pulsed laser. The ZnO nanostructures prepared by laser ablation in liquid are promising for the applications where extremely pure nanomaterials are needed, for example, bio-imaging and surgery.

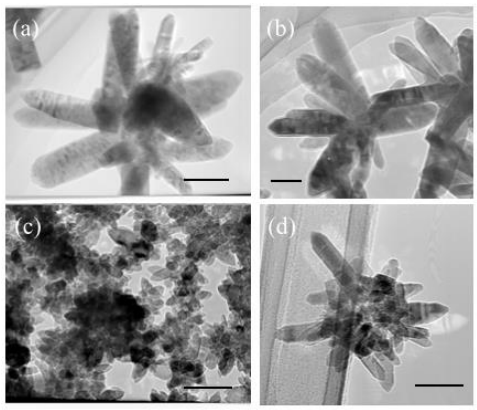

Figure 1 TEM images of ZnO nanostructures prepared with laser parameters of (a) 0.5 ms, 1 kW, (b) 2 ms, 1 kW, (c) 0.5 ms, 5 kW and (d) 2 ms, 5 kW. Water was used as a liquid medium. Scale bars indicate 100 nm.

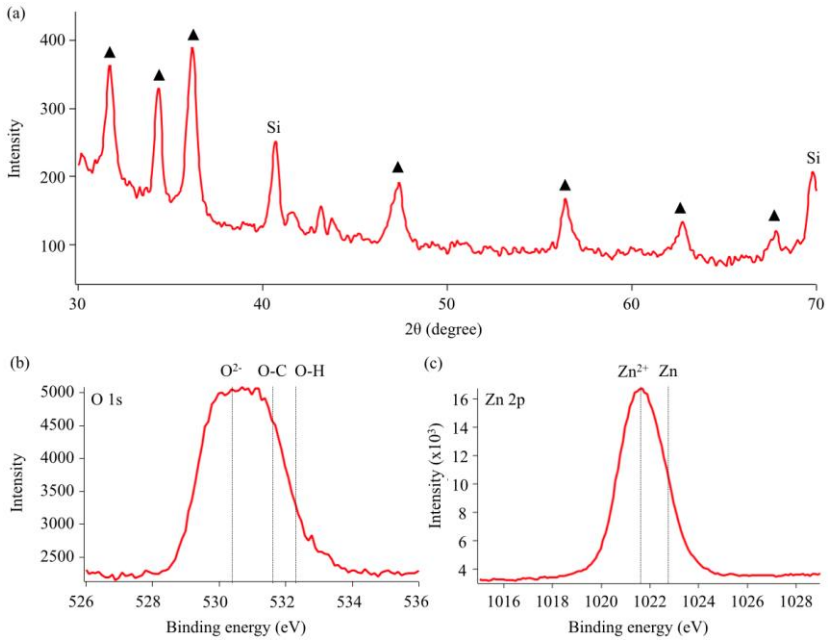

Figure 2 (a) XRD pattern and (b), (c) XPS spectra of ZnO prepared with the pulse width of 2 ms, the power of 1 kW. In (a), triangles indicate peaks of hexagonal ZnO, and the peaks marked with Si correspond to silicon substrate.

References

[1] A. K-Radzimska and T. Jesionowski," Zinc Oxide—From Synthesis to Application: A Review," Materials, **7**, 2833 (2014)

O-30

Temperature dependence of semiconducting $BiFeO_3$ thin films deposited by pulsed laser deposition for resistive memory application

A. Q. Jiang and J.W. Meng
State Key Laboratory of ASIC & System, the School of Microelectronics, Fudan University, Shanghai 200433, China
E-mail: aqjiang@fudan.edu.cn

Conducting ferroelectric materials have exhibited emergent electronic properties, including significant electroresistance effects in switchable ferroelectric diodes [1] and multiferroic/ferroelectric tunnel junctions [2] and intriguing charge conduction in ferroelectric domain walls [3], which have attracted considerable attention in high-speed switching and high-density memories as well as in ultrafast electro-optical devices. Ferroelectric-resistive memories based on ferroelectric diodes have demonstrated the ability of high resistive ON/OFF ratios, high speeds and low write powers with the high reproducibility by controlling polarization orientation. Here we fabricated semiconducting (00*l*) $BiFeO_3$ (BFO) thin films with the thicknesses of 30-40 nm on $SrRuO_3/SrTiO_3$ substrates using a pulsed laser deposition technique. The growth mode of BFO thin film can been controlled by the underlay $SrRuO_3$ bottom electrodes. It was found that the $SrRuO_3$ thin film was 3D island formation at laser energy density of 2.5 J/cm^{-2} but a 2D layer-by-layer growth mode when the energy density was reduced down to 1.5 J/cm^{-2}, as shown in Fig. 1. Above-layer growth modes of BFO thin films match with $SrRuO_3$ exactly, though the growing conditions are the same. The 2D thin film at 300 K shows switchable ON/OFF diode currents upon polarization flipping near a negative coercive voltage, which is nevertheless absent from the 3D thin film. From a positive-up-negative-down pulse characterization technique, we measured domain switching current transients in both semiconducting thin films after deduction of time-dependent leakage currents, where doman switching time can be adjusted in the range of ns-ms through the resistance adjustment of the circuit RC time constant. These current transients can be further transformed into standard polarization-voltage (*P-V*) hysteresis loops. The *P-V* hysteresis loops after 1 μs-retention time show the preferred domain orientation pointing to bottom electrodes in a 3D thin film. This poor polarization retention can be improved considerably in a 2D thin film. From these *P-V* hysteresis loops, we extracted domain switching time dependence of coercive voltage at temperatures of 78 - 300 K, as shown in Fig. 2. It is found that the coercive voltages in semiconducting ferroelectric thin films are much higher than those in insulators. Finally, an equivalent resistance model in description of free-carrier compensation of the domain boundary charge during domain growth is developed to interpret this difference. Thes semiconducting thin films can be further integrated into the elements of ferroelectric resistive memories with the sizes of a few tens of nanometers with readout currents on the order of nA.

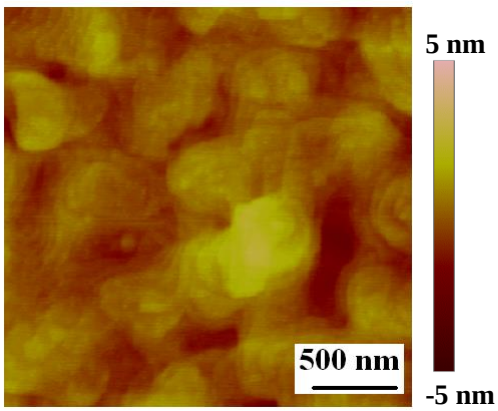

Fig. 1. Micrograph of atomic force microscopy for a 2D $BiFeO_3/SrRuO_3/SrTiO_3$ thin film.

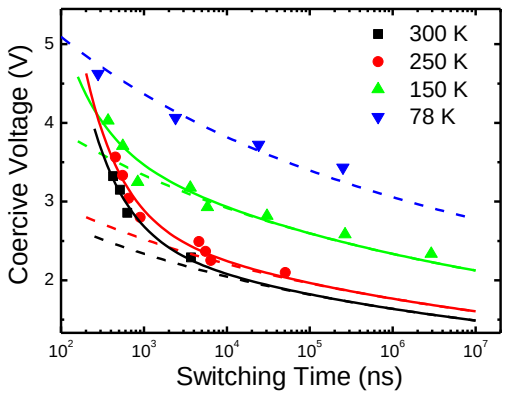

Fig. 2. Domain switching time dependence of coercive voltage for a 2D thin film at different temperatures. The solid lines are the best fitting of the data in a semiconducting thin film in comparison to the dotted lines for a ferroelectric insulator.

References

[1] A. Tsurumaki, H. Yamada, and A. Sawa, "Impact of Bi Deficiencies on Ferroelectric Resistive Switching Characteristics Observed at p-Type Schottky-Like Pt/$Bi_{1-\delta}FeO_3$ Interfaces," Adv. Funct. Mater. **22**, 1040 (2012).
[2] V. Garcia, S. Fusil, K. Bouzehouane, S. Enouz-Vedrenne, N. D. Mathur, A. Barthelemy, and M. Bibes, "Giant Tunnel Electroresistance for Non-destructive Readout of Ferroelectric States," Nature **460**, 81 (2009).
[3] P. Maksymovych, S. Jesse, P. Yu, R. Ramesh, A. P. Baddorf, and S. V. Kalinin, "Polarization Control of Electron Tunneling into Ferroelectric Surfaces," Science **324**, 1421 (2009).

I-07

Functional oxide interfaces by pulsed laser deposition

Ariando

Department of Physics & NUSNNI-Nanocore
National University of Singapore
Email: ariando@nus.edu.sg
Site: http://staff.science.nus.edu.sg/~ariando/

Research effort is being made to explore fundamental properties of new materials and their potential impact for future device applications. Recent advances in pulsed laser deposition technique have enabled the growth of atomic-scale thin film and layer-by-layer design of heterostructures, providing unprecedented structural perfection and control of their physical properties which offer potential solutions to the fundamental limits of scalability of conventional semiconductor technology. New physical properties and behavior that are absent in bulk can be engineered.

Among different material systems, complex oxides offer opportunities to develop multifunctional (nano)-devices, owing to the large variety of physical properties resulting from the complex interplay between the electronic, orbital, spin and structural degrees of freedom. This potential is further enhanced by the possibility to combine various oxides in the forms of atomically controlled heterostructures and interfaces, as demonstrated by the discovery of two-dimensional electron gas (2DEG) at the interface between two complex oxide insulators, in particular at the interface between a polar (e.g. $LaAlO_3$) and nonpolar (e.g. $SrTiO_3$) oxides. In this talk, I will present our research effort on oxide interfaces at the National University of Singapore; from basic understanding to tuning the physical properties of the 2DEG by material engineering at atomic level and by electric-field effects. The growth of various oxide interfaces by pulsed laser deposition and the observation of new emerging electronic and magnetic properties and direct imaging and electric field tuning of ferroelectric domain walls at oxide interfaces will be presented.

O-31

Nanostructure formation on PLLA and PLGA by femtosecond laser irradiation

S. Yada[1], A. Shibata[1], S. Yukawa[1], M. Terakawa[1,2]
[1]*School of Integrated Design Engineering, Keio University, 3-14-1 Hiyoshi, Kohoku-ku, Yokohama 2223-8522, Japan*
[2]*Department of Electronics and Electrical Engineering, Keio University, 3-14-1 Hiyoshi, Kohoku-ku, Yokohama 2223-8522, Japan*
E-mail: terakawa@elec.keio.ac.jp

Biodegradable polymers have been attracting increasing attention in tissue engineering due to its biodegradability and high biocompatibility. *In vitro* studies of cell biology revealed that cells are able to sense their extra-cellular environment and receive signals that regulate cellular functions such as adhesion, morphology, migration and differentiation. Since chemically and geometrically modified material surface are known to affect such cellular functionalities, several methods to process surface of biodegradable polymers have been studied. Among other methods, laser processing has advantages in surface processing of biodegradable polymers because it provides dry processing without using a toxic chemical component and in processing of complex-shaped surfaces even after molding. We have reported successful formation of laser-induced periodic surface structure (LIPSS) on poly-L-lactic acid (PLLA), a typical and widely used biodegradable polymer, by femtosecond laser irradiation. In this work, we investigate LIPSS formation on PLLA and poly(lactic-co-glycolic acid) (PLGA) under various irradiation conditions: number of laser pulses, laser fluence, laser wavelength (266, 400 and 800 nm) and laser pulse duration (100 fs to 2.04 ps) to reveal the optimal irradiation condition for LIPSS formation. Biodegradation of PLLA and PLGA was also studied after laser irradiation. As shown in Fig. 1, LIPSS were formed at different incident wavelengths: 266 nm [Fig. 1(a)], 400 nm [Fig. 1(b)] and 800 nm [Fig. 1(c)]. LIPSS was likely formed with 400 nm wavelength compared to 800 nm as electron excitation via multiphoton absorption is likely to occur. However, with 266 nm wavelength, only shallow LIPSS were formed. This result suggests that certain thermal ablation is necessary to form LIPSS on PLLA. To further discuss thermal properties in LIPSS formation, pulse width and repetition rate dependency of LIPSS formation was also studied. LIPSS were formed with wider window of laser irradiation conditions at repetition rate of 1 kHz compared to 100 Hz. It was also found that pulse width of 100 fs is more likely to form LIPSS compared to 2.04 ps. These results suggest the requirement of adequate amount of heat, sufficient interval for photochemical reaction, and high peak intensity to form LIPSS. The biodegradation test shows that the biodegradability of both PLLA and PLGA remained after laser irradiation. For PLLA, the biodegradation characteristics did not change drastically before and after laser irradiation, however, for PLGA the ablation crater formed after laser irradiation at 400 nm expand drastically compared to that formed by 800 nm. Although the surface roughness increased after biodegradation by elapse of time, LIPSS remained almost unchanged for more than 100 min. [Fig. 2]. We could conclude that hydrolysis less occurred on LIPSS due to its hydrophobicity.

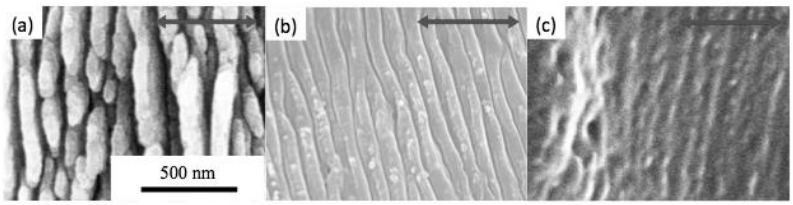

Fig. 1. SEM images LIPSS formed on PLLA under the irradiation condition of (a) 1.0 J/cm^2 for 10000 pulses at 800 nm, (b) 0.40 J/cm^2 for 5000 pulses at 400 nm, (c) 7.5 mJ/cm^2 for 5000 pulses at 266 nm. The bi-directional arrows indicate laser polarization.

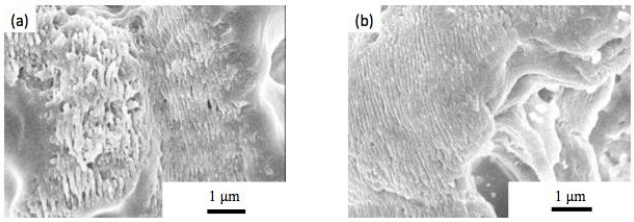

Fig. 2. SEM images of LIPSS formed at 75 mJ/cm^2 with 12000 pulses at 400 nm (a) before and (b) after degradation for 80 minutes.

O-32

Cathodoluminescent and photoluminescent properties of pulsed laser deposited thin phosphor films

O.M. Ntwaeaborwa and H.C. Swart

Department of Physics, University of the Free State, Bloemfontein, South Africa

Corresponding Author e-mail address: ntwaeab@ufs.ac.za

Phosphors have many uses today, such as information display, medical imaging, and theft prevention. The phosphors are often used as powders, even though thin films offer higher resolution and better chemical stability. We have investigated the cathodoluminescent (CL) and photoluminescent (PL) properties of thin films of several phosphors (e.g. $SrAl_2O_4:Eu^{2+},Dy^{3+}$; SiO_2:PbS; $SiO_2:Ce^{3+},Tb^{3+}$ and $CaS:Eu^{2+}$) that were ablation deposited onto Si (100) substrates using either conventional pulsed laser deposition (PLD) or pulsed reactive crossed beam laser ablation (PRCLA). Several deposition parameters were varied, including vacuum versus partial pressure of gas (O_2 or Ar), type of laser pulse, and substrate temperature using either a 307 nm XeCl or 248 nm KrF excimer laser. The CL spectrum and intensity were measured in vacuum from films irradiated with 2 keV electrons for a prolonged period of time, while PL data were collected in air under excitation by either a 325 nm HeCd laser or a monochromatized xenon lamp. Both the CL and PL intensities were strongly dependent on the deposition conditions and post-deposition annealing. Data from scanning electron microscopy (SEM) and atomic force microscopy (AFM) show that the major influence of the deposition conditions on the CL/PL intensity was through changes in the morphology and topography of the films, which affects light scattering and out-coupling. Finally, the CL intensity from the films decreased significantly during prolonged electron beam irradiation. The degraded CL intensity resulted from the formation of non-luminescent oxide layers on the film surfaces. The chemical composition and electronic states of the 'dead' layers were analyzed using x-ray photoelectron spectroscopy (XPS). The influence of the various deposition conditions on the luminescent intensities will be discussed. The mechanism leading to lower CL intensities will be concluded to be electron stimulated surface chemical reactions.

Figure 1 shows the PL spectra of the pulsed laser deposited $SrAl_2O_4:Eu^{2+},Dy^{3+}$ thin films prepared in different background gases with the film prepared in argon showing the highest PL intensity and the least PL intensity was observed from the film prepared in vacuum. The surface topography of the films in figure 2 shows that the films prepared in vacuum was smoother than those prepared in oxygen and argon. This explains why the film prepared in vacuum was less intense than those prepared in oxygen and argon.

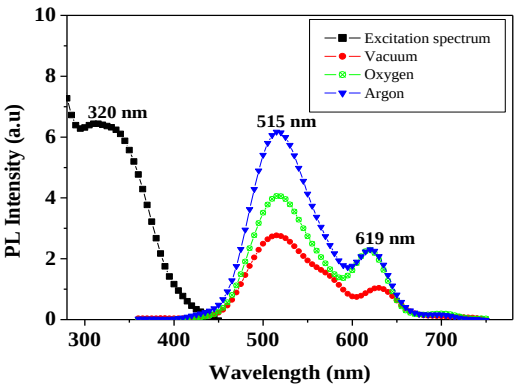

Fig. 1. The PL spectra of the $SrAl_2O_4:Eu^{2+},Dy^{3+}$ films prepared in different atmospheres

.

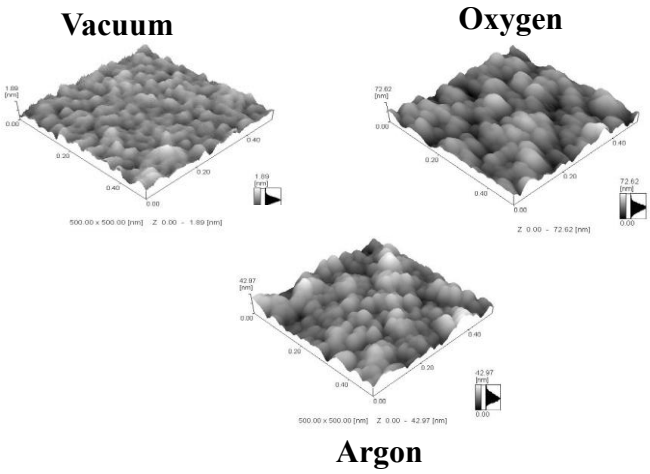

Fig. 2. The AFM images of the films prepared in different atmospheres.

O-33

Fluoride-metals nanostructured films fabricated by Pulsed Laser Deposition with auxiliary Electron beam evaporation

J. Lančok[1], M. Novotný[1], N Abdellaoui[2], J. Bulíř[1], J. Kopeček[1], A. Pereira[2], J. Vlček[1], B. Moine[2]

1) Institute of Physics, Academy of Sciences of the Czech Republic, Na Slovance 2, 182 21 Prague 8, Czech Republic

2) Institut Lumière Matière, UMR5306 Université Lyon 1-CNRS, Université de Lyon 69622 Villeurbanne cedex, France

Corresponding Author e-mail address: lancok@fzu.cz

Fluoride materials occupy an original and strategic position in modern optics. The fluorides exhibit unique optical features (low pohonon energy, high transparency in UV region, low refractive indices for infrared radiation) associated with the presence of rare-earth (RE) ions, which make them excellent candidates for variety of optoelectronics and photonics applications. One of the way how to enhance luminescence properties of Re^{3+} ions is using plasmonic behaviour of metallic nanoparticles (NPs) [1].

Most of the plasmonic research has so far focused on "classical" materials Ag and Au. Beyond this noble metals however, other, less used metals exist, whose specific characteristic could significantly bring new functionalities [2]. For example Al NPs yield an localised surface plasmon (LSP) resonance within the deep ultraviolet optical range [2] and by tuning the size of the NPS the resonance frequency could be shifted up visible spectral range. As was demonstrated in [3] the Al plasmonic behaiviour could endhanced the luminescence properties of the Eu doped oxide film. Despite potential and low cost of Al, the exploitation of its plasmonics is very recent and still facing both scientific and technical challenges. One of the crucial problems is the degradation of plasmonic properties induced by rapid oxidation. This problem could be solved by using fluorides matrices, which will embed the Al NPs.

In our work we demonstrated successfully fabrication of either pure fluoride or RE doped fluoride thin films with metals NPs by means of combination of two PVD deposition techniques: Pulsed Laser Deposition (PLD) by means of pulsed Nd:YAG laser operated at 266 nm and Electron Beam Evaporation (EBE). The fluoride thin films were fabricated be EBE [4] while the PLD technique is very suitable to fabricate metals NPs or to ablate very precisely amount of materials for RE doping [3]. The silver and aluminium NPs embedded by CaF_2 films were fabricated by PLD with auxiliary EBE (fluoride matrix) at UHV deposition chamber. Before the deposition the vacuum chamber was evacuated down to 10^{-7} Pa to minimise the oxygen contamination. The thickness and optical properties of the films was investigated in-situ by spectral reflectometry.

The nanometric size distribution of RE doping was performed by PLD from metallic targets during CaF_2 deposition by EBE. The precise level of doping was easily controlled by the repetition rate of laser. The separation between RE^{3+} ions and metallic NPs were performed by computer controlled targets system together with the appropriate triggering of the pulsed laser with a purpose to study the influence of the fluorescence properties similar to work presented for oxides [3]. The prepared layers were analysed by spectral ellipsometer in the spectral range from 245 to 1000 nm. Characteristic interference oscillations are seen in the curves of spectral dependence of ellipsometric angles psi and delta. The analysis of the measured date revealed an absorption band at about 375 nm and 250 nm, which corresponds to localized plasmon resonance of incorporated silver and aluminium NPs, respectively. The plasmon resonance absorption band was parameterised using Lorentz oscillator model in the dispersion curve [5]. The excitation and luminescence spectra were measured in consequence of the metals NPs and nanometric distribution in the films. The results were compared and discussed with the results of analysis structural properties performed by methods (SEM, HRTEM, AFM, XRD).

Our experiments show great potential of combination of EBE and PLD for fabrication of metallic NPs in fluoride matrices. The plasmonics structure also some other "non usual metals", which exhibits either plasmonics behaviour in UV such as Bi, or could easily oxidised like Cu could be also prepared by the similar way.

[1] P. N. Prasad, *Nanophotonics* _Wiley, New York, 2004

[2] G. Maidecchi, G. Gonella, R.P. Zaccaria et all., "Deep Ultraviolet Plasmon Resonance in Aluminum Nanoparticle Arrays" ACS NANO **7** (2013) 5834

[3] N Abdellaoui, A Pereira, A Berthelot, B Moine, N P Blanchard and A Pillonnet, "Plasmonic enhancement of Eu:Y_2O_3 luminescence by Al percolated" Nanotechnoogy **26** (2015) 095701

[4] A. Guille, A. Pereira, A. Bensalah-Ledoux, B. Moine, M. Novotný, J. Bulíř, P. Fitl, J. Lančok, "Sensitization of Pr^{3+} ions by Eu^{2+} ions in CaF_2 thin films deposited by evaporation" J Appl Phys, 114 (2013) 203509.

[5] J. Bulir, M. Novotny, A. Lynnykova, J. Lancok, "Preparation of nanostructured ultrathin silver layer"J. of Nanophotonics 5 (2011) 051511.

O-34

Dynamics of laser ablated colliding plumes in background gas

I. Umezu[1], Y. Hashiguchi[1], H. Fukuoka[2], N. Skamoto[3], T. Aoki[1], A. Sugimura[1]

[1]*Department of Physics Konan University, 8-9-1 Okamoto, Kobe 658-8501, Japan*

[2]*Department of Mechanical Engineering, Nara National College of Technology, Nara 639-1080, Japan*

[3] *Department of Science and Engineering, Iwaki Meisei University, Iwaki 970-8551 Japan*

E-mail:umezu@center.konan-u.ac.jp

Pulsed laser ablation in background gas is well known as one of the methods to prepare nanoparticles. Dynamics of plume expansion, which depends on background gas pressure, is essential for formation of nanoparticles. Collision of two plumes induces drastic change in plume expansion dynamics and accordingly modification of nanoparticles structure is expected. In the present paper, two pulsed lasers and targets are equipped and plumes from both targets are collided head-on[1-2]. Effects of delay time between two laser pulses, t_d, are discussed. We found that non-luminous Si species in emission-decayed plume is re-excited by collision with counter plume and re-emission is observed. This technique might be applied for preparation of core/shell nanostructures.

Si and Ge targets were placed at opposed position and they were irradiated by delay controlled two pulsed lasers. Helium gas was introduced in a chamber and kept at constant pressure. Plume collision dynamics was controlled by varying timing of laser pulses. The Si target was irradiated at t=0 followed by irradiation of the Ge target at t= t_d. Expansion dynamics of the plumes was measured using the ICCD camera equipped with spectrometer. Spectroscopic method enables us to measure expansion of Si and Ge plume individually.

When background gas pressure is around 150Pa, the stagnation layer is formed and the plume expansion is suppressed by the counter plume at t_d=0. The delay time, t_d , was varied under this background pressure. The expansion dynamics of Si plume is similar to that of simultaneous irradiation, t_d=0, when delay time t_d is less than 1 μs. Emission of the Si plume decays with time and disappears at t= 5 μs. Therefore, when t_d > 5 μs, emission of Si plume cannot be observed just before the Ge target is irradiated. Interestingly, the emission of Si species is observed around the Ge target after the irradiation of the Ge target. These results indicate that non-luminous Si species in the emission-decayed Si plume reach around the Ge target and is re-excited by collision with luminous Ge plume. The intensity and time constant of the Si re-emission gradually decrease up to about t_d=55μs and sudden decrease is observed above this delay time as shown in Fig.1. Since the time constant of the plume increases with the collision of atomic species in the plume, the reduction of time constant corresponds to the decrease in the collision. Figure 1 indicates that the collision of atomic species rapidly decreases above t_d=55 μs. One of the possible origins of the decrease in the collision is the formation of the Si nanoparticles, which results in decrease in the number of the atomic Si species. The previous report has shown that the formation of Si nanopaticles starts from a few hundred μs after the irradiation[3]. If we take into account difference in experimental conditions, agreement with the previous report is not bad. This result implies a possibility to control the structure of nanopaticles by setting delay time. When delay time is larger than 55 μs, collision between the Si nanopaticles and the Ge atomic species and formation of Si nanopaticles covered by Ge thin layer, that is Si/Ge core/shell structure, is expected. The result of energy dispersive X-ray spectrometers equipped with the transmission electron microscope measurement is consistent with the existence of Si/Ge core/shell structure.

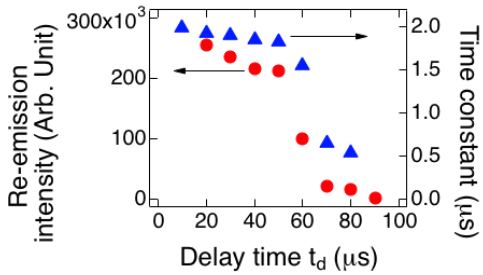

Fig. 1. Intensity and time constant of re-emitted Si species as a function of delay time t_d.

References

[1] I. Umezu, N. Sakamoto, H. Fukuoka, Y. Yokoyama, K. Nobuzawa, and A. Sugimura, "Effects of collision between two plumes on plume expansion dynamics during pulsed laser ablation in background gas," Appl. Phys. A **110**, 629 (2012).

[2] I. Umezu, S. Yamamoto, and A. Sugimura, "Emission induced by collision of two plumes during pulsed laser ablation," Appl. Phys. A **101**, 133 (2010).

[3] J. Muramoto, T. Inmaru, Y. Nakata, T. Okada, and M. Maeda, "Spectroscopic imaging of nanoparticles in laser ablation plume by redecomposition and laser-induced fluorescence detection," Appl. Phys. Lett. **77**, 2334 (2000).

O-35

Picosecond pulsed laser deposition of metal and metal-oxide layers with controllable porosity for sensor applications

V. Kekkonen, S. Chaudhuri, F. Clarke, J. Kaisto, J. Piirto, A. Zolotukhin, J. Liimatainen
Picodeon Ltd Oy, Piisilta 1, FI-91100 Ii, Finland
E-mail: ville.kekkonen@picodeon.com

Picodeon Coldab® industrial Pulsed Laser Deposition (PLD) platform has been utilized for generating layers of various metals (e.g. Cu, Au, Pt, W) and metal-oxides (e.g. Al_2O_3, TiO_2, WO_3). By controlling laser parameters and deposition conditions, the layer structures can be designed to be either porous with controllable level of porosity or fully dense with neither pores nor pinholes.

Nowadays, thin layers of a couple to hundreds of nanometers, either fully dense or with defined level of porosity, find their use in wide range of applications from optics and electronics to biomedicine. A major application area of metal-oxide nano-layers is sensors. In particular nanostructured porous coatings and nanoparticles are used as sensing layers and catalysts in gas sensors. Furthermore, a gas sensor structure in some cases requires dense metal-oxides and metals as a passivation layers and heaters respectively. Both mentioned layers could be produced by PLD as sequential processes, which makes PLD highly attractive.

Picodeon Coldab® PLD platform enables industry-standard level of wafers processing and allows effective manufacturing of various coating layers for wide range of applications. Here, we demonstrate production of coating layers consisting of metal or metal-oxide nanoparticles of controllable size with exceptional uniformity across 4” wafers. Furthermore, we report performance of the sensing layers in functional gas sensors with and without catalyst particles. Technical approaches for efficient control of the coatings porosity and particle size are discussed.

I-08

Proton Beam Generation with Nanotube Accelerator Driven by Ultra-Intense Ultra-Short Laser

M. Murakami[1], K. Yamanoi[1], H. Miura[1], H. Azechi[1], M. Tanaka[2], T. Kaneko[3], T. Kato[3], T.M. Jeong[4], I.J. Kim[4], S. Ter-Avetisyan[4], C.H. Nam[4]

[1]*Institute of Laser Engineering, Osaka University, Osaka 565-0871, Japan*
[2]*Department of Engineering, Chubu University, Aichi 487-8501, Japan*
[3]*Department Electronic Engineering, Tohoku University, Sendai 980-8579, Japan*
[4]*Center for Relativistic Laser Science, Institute for Basic Scienece, Gwangju 123, Korea*
E-mail: murakami-m@ile.osaka-u.ac.jp

Ion acceleration driven by ultraintense ultrashort laser pulses has been intensively studied in the past decade, because a number of future applications can be expected using such MeV-oder protons. For practical use of the accelerated ions, it is crucial to produce high-quality proton beams that are monoenergetic and collimated. Carbon nanotubes (CNTs) are hardy and versatile, with remarkable material and electronic properties. And they could be useful in some extreme conditions as well. We here propose a novel ion acceleration scheme using CNTs [1, 2], where embedded hydrogen-rich fragments - which could be water ice, paraffin, or some other low-Z material but were modeled as hydrogen nanotubes - are irradiated by an intense laser to eject substantial numbers of electrons. Due to the resultant unique electrostatic field, the nanotube and the embedded materials play the roles of the barrel and bullets of a gun, respectively, to produce highly collimated and quasimonoenergetic proton beams. Such beams are of great interest in fields as diverse as medicine, fusion energy, and materials engineering.

Figure 1 shows the schematic view of the nanotube accelerator. The double-nested nanotubes are irradiated by an ultrashort ultraintense laser pulse. The outer carbon nanotube is assumed to be chemically adsorbed with heavy atoms such as gold, while the inner nanotube is made of light materials such as hydrogen and carbon to form the projectiles. After blowing off the electrons, the remaining nanotubes composed of positive ions generate a unique electrostatic Coulomb field so that the inner ions are accelerated along the axis symmetrically toward both ends of the outer nanotube. The size of CNT for the simulation was 30 nm. Particle simulations has demonstrated that quasimonoenergetic protons with an energy of about 1.5 MeV are produced. If the hydrogen atoms are replaced by carbon atoms, the maximum ion energy increases to 10 MeV for the same target structure.

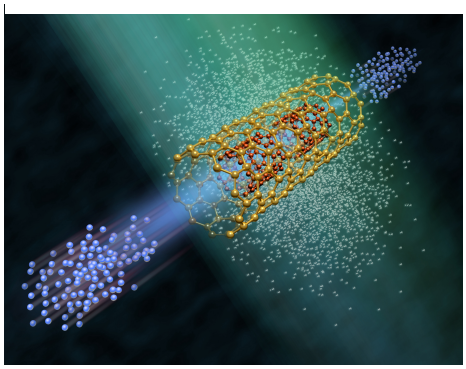

Fig. 1 Schematic view of Nanotube Acceleartor

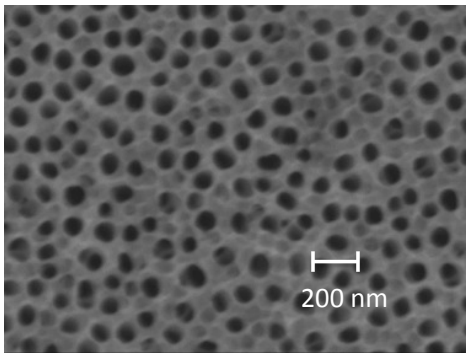

Fig. 2 Top view of the nano-target for experiment

We have conducted experiment to show that such nano-structures can produce MeV-order protons, using Peta-Watt laser. Figure 2 shows the top view of SEM image of the nanotube target used in the experiment, that is made of Titanium-Oxide. The diameter and the axial length of the nanotubes are about 100 nm and 2 microns, respectively. Those nanotube structures are put on the surface of a 100 micron-thick Titanium plate, the opposite surface of which is then irardiated by an intense femt-second laser pulse at an intensity of ~ 10^{20} W/cm^2. The proton signals obtained by the experiment are very interesting; Without the nanostructures, no signal was observed, while with the nanotube structues 10 MeV protons are obtained. This suggests there exists an unrevealed physical mechanism to enhance proton generation under the exsintence of nanostructures on the rear surface.

[1] M. Murakami, M. Tanaka, "Generation of high-quality mega-electron volt proton beams with intense-laser-driven nanotube accelerator." *Appl. Phys. Lett*. **102**, 163101 (2013).
[2] S.G. Benka, "Proton beams from a nanotube accelerator." Physics Today **66** (June issue), 17 (2013).

O-36

Enabling Laser Applications in Microelectronics Manufacturing

R. Delmdahl[1], B. Fechner[1], R. Paetzel[1], J. Brune[1], E. Rea[2]
[1]Coherent LaserSystems GmbH & Co. KG, Hans-Boeckler-Str. 12, D-37079 Goettingen, Germany
[2]Coherent, Inc., 5100 Patrick Henry Drive, Santa Clara, CA 95054, USA
E-mail: ralph.delmdahl@coherent.com

Abstract

This paper will provide a detailed overview of the most recent advances and emerging laser applications used in the processing diverse materials for both the flat panel display and printed circuit board industries.

Higher power UV and shorter pulse length laser sources are enabling component and device manufacturers in the consumer electronics industry to shrink device dimensions and create completely new device geometries. Recently developed laser processes in combination with new materials are helping designers build a whole new generation of thinner, lighter, more battery friendly portable and wearable devices. The unique characteristics of lasers allow users to harness photons to cut, ablate, drill, anneal, pattern or join materials precisely and selectively without mechanical force and with feature sizes not possible with any type of mechanical tool. This paper will give a overview of exciting new applications for lasers, including fine patterning of conductors, laser lift-off carrier separation, microvia drilling in glass and polymers and seed metal patterning for ultra-fine featured IC substrates. We will detail processes that are in full 24/7 production and review the relevant types of ultra-high precision laser sources.

O-37

Influence of ink properties on the dynamics of high velocity laser printing

D. Puerto[1], E. Biver[1,2], A.-P. Alloncle[1], Ph. Delaporte[1]
[1]Aix-Marseille University, CNRS, LP3 laboratory Campus de Luminy, C.917, Marseille, France
[2]Oxford Lasers Ltd., Unit 8, Moorbrook Park, Didcot, OX11 7HP, United Kingdom
E-mail: delaporte@lp3.univ-mrs.fr

The deposition of conductive lines of few tens of micrometers width is of prime interest for the manufacturing of electronic devices, especially on flexible substrates. Laser printing, based on LIFT process (Laser-Induced Forward Transfer), always appears very attractive for such application. This technique allows the deposition of silver nanoparticle inks with a wide range of viscosities [1, 2] and the formation of 2D/3D structures with high resolution [3]. The dynamics of formation and expansion of the liquid jet, which is the basic mechanism of the LIFT process in liquid phase, has been extensively studied by means of time-resolved shadowgraphy [4, 5, 6].

Recently, micrometer conductive lines have been laser printed at velocities up to 4m/s in multi-passes configuration with a picosecond laser operating at 500kHz and a scanning mirror to move the laser at the surface of the donor film [7]. Time-resolved shadowgraphy studies showed that the instabilities induced by the interactions between two adjacent cavitation bubbles and/or two adjacent liquid jets prevent the deposition of a continuous line in a single step at high velocity with standard silver nanoparticle inks (20% silver content) [8, 9]. In this study, we investigate the influence of silver ink donor film properties (thickness, density, viscosity) on the dynamics of the liquid transfer at high velocity and the morphologies of the printed lines. In particular, we observe a new deposition mechanism when inks with higher densities (40% silver content) are used to print conductive lines at high velocity. As shown in figure 1b, all the successive jets are linked together and the specific properties of this ink maintain the stability of this multi-jet structure. In these conditions, we printed 30µm width silver lines at velocities up to 17m/s in a single pass, using a UV picosecond laser operating at 1MHz.

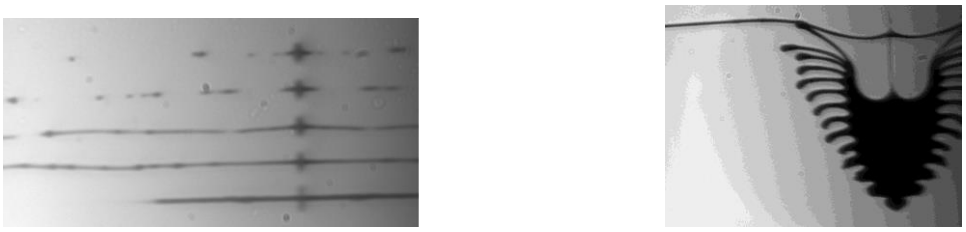

(a) (b)

Fig. 1. Shadowgraphy images of ink transfer at high velocity. (a) 20% silver content ink, ps operating at 500kHz, image taken 9µs after the first shot (5 jets). (b) 40% silver content ink, ps operating at 1MHz, image taken 13.9µs after the first shot (13 jets). Only the left part of the images must be considered, the right part being a mirror effect from the ink donor film.

[1] L. Rapp, J. Ailuno, A.-P. Alloncle, Ph. Delaporte, 'Pulsed-laser printing of silver nanoparticles ink: control of morphological properties', Optics Express **19** (22), 21563–21574, (2011)

[2] S. A. Mathews, R. C. Y. Auyeung, H. Kim, N. A. Charipar, A. Piqué, 'High-speed video study of laser-induced forward transfer of silver nano-suspensions', J. of Appl. Phys. **114**, 064910 (2013)

[3] J. Wang, R. C. Y. Auyeung, H. Kim, N. A. Charipar, A. Piqué, 'Three-Dimensional Printing of Interconnects by Laser Direct-Write of Silver Nanopastes', Adv. Mater. **22**, 4462–4466, (2010)

[4] M. Duocastella, J. M. Fernández-Pradas, J. L. Morenza, and P. Serra, 'Time-resolved imaging of the laser forward transfer of liquids', J. of Appl. Phys. **106**, 084907 (2009)

[5] M. S. Brown, N. T. Kattamis, C. B. Arnold, 'Time-resolved dynamics of laser-induced micro-jets from thin liquid films', Microfluid Nanofluid **11**, 199-207, (2011)

[6] C. Boutopoulos, I. Kalpyris, E. Serpetzoglou, I. Zergioti, 'Laser-induced forward transfer of silver nanoparticle ink: time-resolved imaging of the jetting dynamics and correlation with the printing quality', Microfluid Nanofluid **16**, 493-500, (2014)

[7] L. Rapp, E. Biver, A. P. Alloncle, Ph. Delaporte, 'High-Speed Laser Printing of Silver Nanoparticles Ink', J. of Laser Micro/NanoEnginnering **9** (1), 5-9, (2014)

[8] E. Biver, L. Rapp, A. P. Alloncle, P. Serra, Ph. Delaporte, 'High-Speed Multi-Jets Printing using Laser Forward Transfer: Time-Resolved Study of the Ejection Dynamics', Optics Express **22** (14), 17122–17134, (2014)

[9] A. Patrascioiu, C. Florian, J.M. Fernández-Pradas, J.L. Morenza, G. Hennig, P. Delaporte, P. Serra, 'Interaction between jets during laser-induced forward transfer', Applied Physics Letters **105**, 014101 (2014)

O-38

Formation Mechanism of Periodic Nano-Grating Structure by Weibel Instability

A.M. Gouda,[1] H. Sakagami,[2] T. Ogata,[1] M. Hashida,[3] and S. Sakabe [3]

[1] *Department of Physics, Nagoya University, Nagoya, 464-8602, Japan*

[2] *National Institute for Fusion Science, Toki, Gifu 509-5292, Japan*

[3] *Institute for Chemical Research, Kyoto University, Gokasho, Uji, Kyoto 611-0011, Japan*

Email:amany.gouda@nifs.ac.jp

1. Introduction

Use of an ultra-fast laser irradiation has opened a new window for forming periodic nano-grating structures on the metal surface [1]. The formation mechanism of the periodic nano-grating structure has been investigated by 2D PIC code [2]. Irradiating the laser pulses of 500 fs pulse, wavelength 800 nm, incidence angle 0º, p-polarized and intensity of 10^{18} W/cm^2-µm^2, the formation of periodic nano-grating structures has been confirmed, and the new formation mechanism has been identified by the Weibel instability.

2. Simulation Work

In the simulation, we have assumed low density mimic plasma in front of the target plasma instead of initially preformed plasma in the experimental area. Under the effect of the laser beam on hydrogen plasma which is used to facilitate the calculation instead of metal plasma, counter streams of electrons have been formed. The first stream is called the fast electron stream and it flows in the propagation direction of the laser beam with lower electron density. Conversely, the second stream of higher electron density is called the return stream, and it flows in the reverse direction of the fast stream to maintain the current neutrality. If the magnetic field perturbation exists, both streams have been bent under the effect of Lorentz force. This bending causes net currents, which enhance initial magnetic field. This growth of the magnetic field is well-known as the Weibel instability. The degree and the direction of bending can be easily analyzed. The enhancement to the magnetic field leads to concentration of the return electron density near the plasma boundary.

The magnetic field and the electron current density at t= 200 fs are shown in Fig. 1 (a) and (b), respectively. The structure between the magnetic field and the electron current density in figures proves the growth of the Weibel instability. As return electrons are concentrated by the magnetic field near the boundary, which are shown in Fig. 1 (c), the electron density increase and tips are formed at the boundary. These tips are essential for forming the periodic nano-grating structures.

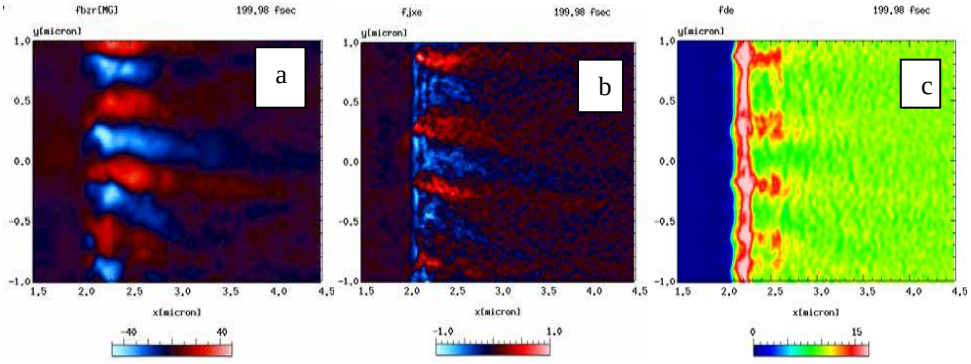

Fig.1. shows the physical values which used to explain periodic nano-grating formation mechanism. (a) the magnetic field, (b) the net electron current density and (c) the electron density profiles.

Reference

[1] M.Hashida, H.Sakagami, S.Sakabe and L.Gemin, Journal of Laser Micro-Nanoengineering.9, 234-237, 2014.

[2] T. Ogata, H. Sakagami, M. Hashida and S. Sakabe, Proc. of 13th International Symposium on Laser Precision Microfabrication, Washington DC, June 12-15, P-We-3 (2012).

O-39

Pulsed Laser Deposition of tailored Tungsten and Tungsten Oxide films

A. Pezzoli[1], D. Dellasega[1,2], V. Russo[1], C. Conti[3], M. Passoni[1,2]

[1]*Dipartimento di Energia, Politecnico di Milano, via Ponzio 34/3, 20133 Milano, Italy*

[2]*Istituto di Fisica del Plasma "P.Caldirola", Consiglio Nazionale delle Ricerche, Via Roberto Cozzi 53, 20125 Milano, Italy*

[3] *Istituto per la Conservazione e la Valorizzazione dei Beni Culturali, Consiglio Nazionale delle Ricerche, via Roberto Cozzi 53, 20125 Milano, Italy*

E-mail: andrea.pezzoli@polimi.it

In this work, Pulsed Laser Deposition (PLD) is exploited to produce W and WO_x films with tailored properties. In particular, the effect of ablation and deposition parameters on film properties and modifications induced by post-deposition annealing treatments are investigated.

Because of Tungsten (W) properties, such as high thermal stability, hardness and low electrical resistivity, W films are extensively studied, mostly as barrier layers in the field of semiconductor integrated circuits, absorption layers in X-ray lithography and layers in multi-layer X-ray mirrors [1]. In the field of nuclear fusion, W coatings are used for plasma-facing components in tokamaks [2]. W oxide films are deeply investigated due to their electronic and optical properties that make this material a good solution in electrochromic devices [3] and gas sensors [4].

Due to the strict connection between films properties and their morphology, structure, crystallographic phase and stoichiometry, it is necessary to have fine parameter control during deposition and post-deposition treatments in order to realize films with the appropriate properties required by the specific application field.

In previous works we demonstrated the PLD capability to deposit W-based coatings with a wide range of structures and morphologies and different types of nanostructured W [5]. W coatings are dense, non-porous and exhibit different crystalline structures, from nanocrystalline to "amorphous-like", with high levels of nanometric defects; materials with "amorphous-like" structure are deeply investigated because they exhibit peculiar and enhanced properties, such as resistance towards highly aggressive environments (e.g. plasma). Furthermore, we deposited W-O [6] and W-N systems, in which gas (O, N) could be either bounded or trapped in films as impurities.

In this work, the role of crucial PLD parameters, such as laser wavelength and fluence and background gasses pressure, was explored in order to understand how they influence films properties. All films were characterized by high resolution SEM, XRD, EDXS, Raman spectroscopy. Moreover, electrical resistivity measurements were used to estimate defects concentrations in films [7]. Firstly, the effect of different wavelengths (λ=532 nm and λ=1064 nm) on films nanostructure was addressed. Successively, the effect of laser fluence, in relation with laser energy and laser focalization, was investigated. Fine control in films properties and also in content of gasses (Ar, He and O) trapped in films were achieved by using different background noble gasses (Ar, He) during films deposition. Furthermore the confinement effects due to different pressures of He and Ar were explored in relation with film properties. Moreover, preliminary results of films deposited with PLD assisted by an Ar plasma were presented. Finally, using a reactive gas (O), W-O systems with peculiar properties, in relation with pressure used during deposition processes, were obtained: it was possible to deposit compact metallic films with a high concentration of trapped O or sub-stoichiometric amorphous W oxide (a-WO_{3-x}) films with structure from compact to porous. All the films were annealed at different conditions of temperature and time. In particular, three representative types of W coating were selected to be annealed. Using characterization techniques above mentioned, modifications due to thermal processes were evaluated in order to understand the films defects, crystallinity and morphology variations. Finally, it was achieved a proper control in films properties, such as the films stoichiometry and structure, by annealing W-O systems.

[1] N. Radić, A. Tonejc, J. Ivkov, P. Dubček, S. Bernstorff and Z. Medunić, "Sputter-deposited amorphous-like tungsten", Surf. Coat. Tech. **180-181**, 66-70 (2004).

[2] C. Ruset, E. Grigore, I. Munteanu, H. Maier, H. Greuner, C. Hopf, V. Phylipps, G. Matthews and JET-EFDA Contributors, "Industrial scale 10µm W coating of CFC tiles for ITER-likeWall Project at JET", Fusion Eng. Des. **84**, 1662-1665 (2009).

[3] M. Regragui, V. Jousseaume, M. Addou, A. Outzourhit, J.C. Bernéde and B. El Idrissi, "Electrical and optical properties of WO_3 thin films", Thin Solid Films **397**, 238-243 (2001).

[4] A. Ponzoni, V. Russo, A. Bailini, C.S. Casari, M. Ferroni, A. Li Bassi, A. Migliori, V. Morandi, L. Ortolani, G. Sberveglieri and C.E. Bottani, " Structural and gas-sensing characterization of tungsten oxide nanorods and nanoparticles ", Sensor Actuat. B-Chem. **153**, 340-346 (2011).

[5] D. Dellasega, G. Merlo, C. Conti, C. E. Bottani, and M. Passoni, "Nanostructured and amorphous-like tungsten films grown by pulsed laser deposition", J. Appl. Phys. **112**, 084328 (2012).

[6] A. Pezzoli, D. Dellasega, V. Russo, A. Gallo, P.A. Zeijlmans van Emmichoven and M. Passoni, "Thermal annealing and exposure to divertor-like deuterium plasma of tailored tungsten oxide coatings", J. Nucl. Mater. (2014), http://dx.doi.org/10.1016/j.jnucmat.2014.11.035

[7] Angela Furrer, Matteo Seita, Ralph Spolenak, "The effects of defects in purple $AuAl_2$ thin films", Acta Mater. **61**, 2874-2883 (2013).

O-40

Effective generation of fast particles and X-ray from nano-structured targets irradiated by ultra-short intense laser pulses

A.A Andreev[1,2,3]

1) Max Born Institute, Berlin, Germany

2) ELI-ALPS, Szeged, Hungary

3) Sankt Petersburg State University, St. Petersburg, Russia

Abstract

Interaction of an ultrashort and ultraintense laser pulse with nano-structured targets is considered. Maximum energy of fast particles, conversion efficiency of laser energy to fast ion one and the divergence of particle beams are compared for various types of targets. The optimal is the target with the maximum absorption and the minimum mass. One variant of efficient target consist of a bunch of parallel or tapered carbon nanofibers. Such targets generate effectively a big current of relativistic electrons, propagating along the fibers and following their curvature. It follows that the optimal fiber thickness should be of several length of the skin layer of the electrical field and has to be in the order of magnitude of tens of nanometers. The distance between the fibers can vary between several Debye radiuses up to values of a few laser wavelengths. Collecting all fibers in only one allows to reduce the transverse size of fast electron cloud. The density of the energy flux of the hot electrons in such bunch, propagating along one nanofiber exceeds several times the intensity of the laser pulse. The absorption of laser energy in optimal nanostructure targets is about 100%. The factor of conversion of laser energy in energy of fast ions for such target can come approximately to tens percents. Efficient conversion of fundamental laser radiation into characteristic sub-femtosecond X-ray radiation and generation of tunable up-converted radiation are predicted. The results of the simulations were compared with the experimental data and have shown a good coexistence.

Tuesday
1 September 2015

Poster presentations

P-069

Removal of 5 nanometer gold particles from solid surfaces by laser-induced spray jet

Changho Seo, Hyeseong Sin and Dongsik Kim*
Department of Mechanical Engineering, POSTECH, Pohang, 790-784, Republic of Korea
** Corresponding Author e-mail address: dskim87@postech.ac.kr*

Removal of nanoscale particles from solid surfaces will be increasingly important in semiconductor industry [1]. Laser-induced spray jet cleaning has recently been proposed as one of the promising techniques for nanoscale particle removal [2]. When an intense laser pulse is focused inside a liquid droplet, laser-induced plasma is generated. Expansion of the plasma breaks up the droplet, forming a pulsed micro spray jet. The speed of jet is high enough to remove the nanoscale particles from solid surfaces [3]. In this work, we examine the cleaning power of the cleaning process using 5 nm gold particles. Additionally, the effect of the liquid cleaning agent on the cleaning performance was analysed for isopropyl alcohol (IPA) and deionized water (DIW). Pulsed micro spray jet composed of micron-sized atomized droplets much smaller than the original droplet was produced with velocity up to ~700 m/s. Particles were then removed by hydrodynamic impact, i.e., direct impingement of atomized droplet and/or the radial flow generated by the droplets [4]. The process parameters, such as laser energy, plasma position and droplet size, were adjusted to maximize the cleaning power. Remaining particles and surface damage were analysed by transmission electron microscopy (TEM), atomic force microscopy (AFM) and scanning electron microscopy (SEM). The results indicate that the spray jet using DIW could remove 5 nm gold particles from the silicon surface with no surface damage (Fig. 1). The spray jet using IPA as a non-water cleaning agent could remove the 10 nm gold particle. The cleaning power of IPA was slightly lower than that of DIW, but it could eliminate the watermark problem without a special rinsing and drying process.

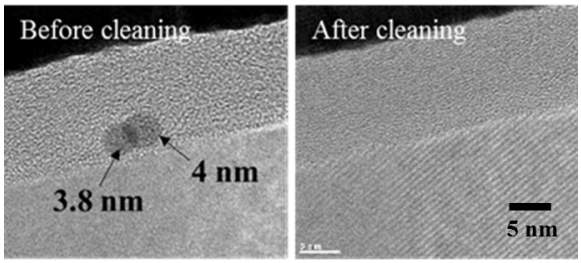

Figure 1 TEM images of the sample surface with 5 nm gold particles (a) before and (b) after cleaning.

[1] International Technology Roadmap for Semiconductors (ITRS), http://www.itrs.net/Links/2012ITRS/Home2012.htm (2012).
[2] D. Ahn, D. Jang, T.-Y. Choi, and D. Kim, "Surface processing technique based on opto-hydrodynamic phenomena occurring in laser-induced breakdown of a microdroplet" Appl. Phys. Lett. **100**, 104104 (2012).
[3] D. Ahn, J. Ha, and D. Kim, "Development of an opto-hydrodynamic process to remove nanoparticles from solid surfaces" Appl. Surf. Sci. **265**, 630 (2013).
[4] Y. Seike, K. Miyachi, T. Shibata, Y. Kobayashi, S. Kurokawa, and T. Doi, "Silicon wafer cleaning using new liquid aerosol with controlled droplet velocity and size by rotary atomizer method" Jpn. J. Appl. Phys. **49**, 066701 (2010).

P-070

Laser based edge zone release process for ZoneBOND temporary bonding and debonding

Seung-Man Kim[1], Jae-Hak Lee[1], Jun-Yeob Song[1], Chang-Woo Lee[1], Tae-Ho Ha[1], Yong-Jin Kim[1], Hyun-Joong Kim[2], Seung-Woo Lee[2]

[1]*Department of Ultra-Precision Machines and Systems, Korea Institute of Machinery and Materials, Yuseong-gu, Daejeon 305-343, Republic of Korea*

[2]*Laboratory of adhesion and Bio-Composites, Program in Environmental Materials Science, Research Institute for Agriculture And Life Science, Seoul National University, Seoul 151-921, Republic of Korea*

E-mail: kimsm@kimm.re.kr

1. Introduction of laser based EZR process

Thin wafer handling is extremely important for 3D multichip packaging because ultra-thin wafers of below 50 μ m thickness are difficult to produce and easy to break. Temporary bonding and debonding(TBDB) is necessary process for thin wafer handling. Device wafers that are attached to rigid carrier wafers using temporary adhesives in temporary bonding process don't break during thinning and patterning process. After that processes, the thin wafers can be detached to carrier wafers by debonding process, and ultra thin device wafers are finally produced without breakage. The TBDB process using ZoneBOND carriers are recently introduced as powerful solution for thin wafer handling [1]. The ZoneBond carriers have two zones; the edge zone possesses a full adhesion in several millimeter widths, while the center zone has a lower adhesion. In order to separate ZoneBONB carriers to the thin device wafers after bonding process, the edge zone only need to release. In this study, the laser based edge zone release(EZR) shown in figure.1 is presented as a faster debonding method without damages for ZoneBOND TBDB process. In addition, the results of feasibility tests to find optimal debonding valuables of laser are shown in this paper.

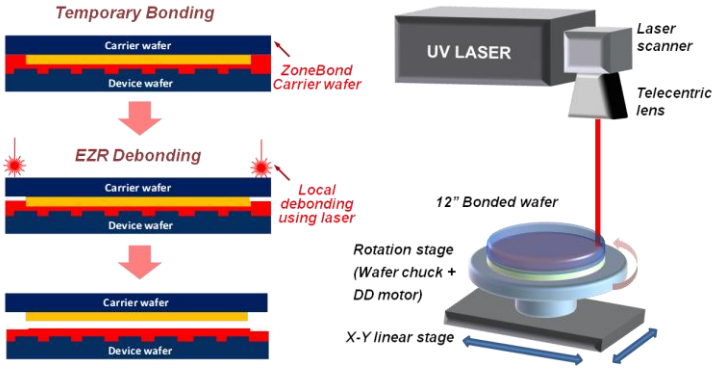

Fig.1 Laser based edge zone release process for ZoneBOND TBDB

2. Characteristics of temporary adhesives and laser sources for laser based EZR process

The adhesive used for this research has thermal curing characteristics [2-3]. The adhesive absorbs 355 nm wavelengths light with 40 % absorbance. For Laser EZR debonding process, 355 nm UV ns pulse laser with about 5 watts power and 50 kHz repetition rate irradiates the adhesive. The heat generated by absorbed light in the adhesive makes that the adhesive turns gels to films which have little adhesive by thermal curing.

3. Experimental results and discussion

Debonding feasibility tests using bonded specimens with chip size were conducted to find optimal debonding conditions that the device wafers can be easily detached from ZoneBOND carrier wafers without damages from laser irradiation. From these tests, the optimal process valuables such as the laser energy density, pulse overlap index and stage rotation speed are determined. The laser based EZR deboning test for a full size ZoneBOND wafer is finally demonstrated using the optimal process valuables in this work.

4. References

[1] T. Matthias, F. Huysmans, J Burggraf, D. Burgstaller, P. Lindner, "Room temperature debonding- An enabling technology for TSV and 3D integration," IEEE-EPTC. **14th**, 236 (2012).

[2] S. -W. Lee, J. –W. Park, C. –H. Park, D. –H. Lim, H. –J. Kim, J. –Y. Song, J. –H. Lee, "UV-curing and thermal stability of dual curable urethane epoxy adhesives for temporary bonding in 3D multi-chip package process," Int. J. Adhes. Adhes. **44**, 138 (2013)

[3] C. –H. Park, S. -W. Lee, J. –W. Park, H. –J. Kim, "Preparation and characterization of dual curable adhesives containing epoxy and acrylate functionalities," React. Funct. Polym. **73** (2013)

P-071

Selective lift-off of GaN LED from sapphire substrate using 266 nm diode-pumped solid-state laser irradiation

Jaegu Kim[1], Jae-Hyun Kim[1], Sung-Hak Cho[1], and Kyung-Hyun Whang[1]

[1]*Nano-Convergence Mechanical Systems Research Division, Korea Institute of Machinery and Materials, Daejeon 305-343, Republic of Korea*

E-mail: gugu99@kimm.re.kr

The demand of selective lift-off of GaN LED from sapphire substrate should be necessary for the repair of the damaged LED which comes out in many complicated process. When the damaged LED occurs, one should eliminate it and replace new single LED in same position. In addition, one can handle a LED with high degree of freedom in manipulation when we have single LED. Mainly, Excimer laser (193 nm ArF, 248 nm KrF and 308 nm XeCl) is used for lift-off GaN LED by projection technique in wafer level transferring. To get single GaN LED with an area of 100 μm x 100 μm, we demonstrate that a 266 nm diode-pumped solid-state laser irradiation with a direct writing technique is applicable to lift off single GaN LED from the sapphire substrate to the thermal release flexible tape. For an optimal condition of lift-off, we investigated the effects of laser processing parameter such as focal position, scanning speed, pulse overlap and laser power. We found out the irradiation power per unit area plays an important role for a good lift-off quality regardless of a fluence energy which is in higher or lower regime.

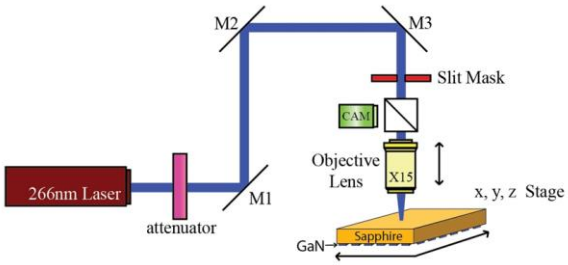

Fig. 1 Experimental setup for selective laser lift-off

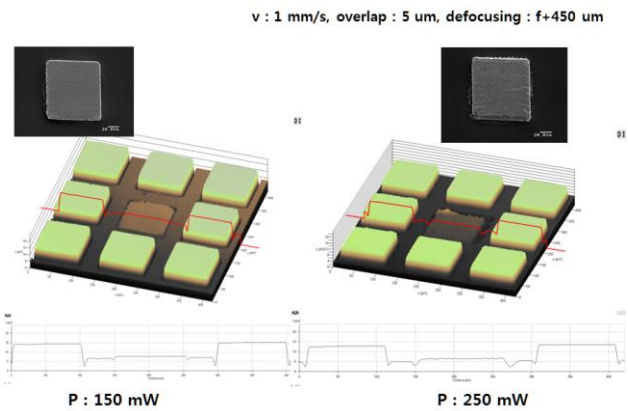

Fig. 2 SEM and confocal images of separated GaN LED (100 μm x 100 μm) and sapphire substrate

P-072

Dysprosium thiogallate laser – source of mid-infrared radiation

H. Jelinková[1], M. E. Doroshenko[2], V.V.Osiko[2], J. Šulc[1], M. Jelínek[1], M. Němec[1]
V.V. Badikov[3], D.V. Badikov[3]
[1]Czech Technical University in Prague, Faculty of Nuclear Sciences and Physical Engineering
Brehova 7, 115 19 Prague 1, Czech Republic
[2]AM Prokhorov General Physics Institute of RAS, Laser Materials and Technology Research Center
Vavilova 38-D, 119991 Moscow, Russian Federation
[3]Kuban State University, May 9th Street 46a, 350040 Krasnodar, Russian Federation
helena.jelinkova@fjfi.cvut.cz

1. Introduction

Due to growing demand of using laser radiation for atmospheric investigation and also for spectroscopic or medical purposes, a compact and reliable laser sources in mid-IR (2-5 µm) spectral region are required. One of effective laser materials allowing to cover this spectral region can be a lead thiogallate crystal doped by dysprosium ions (Dy:$PbGa_2S_4$ – Dy:PGS) [1]. The capability of Dy^{3+} ions in low phonon energy PGS crystal to generate various wavelengths has not been fully investigated yet. Previously most attention was paid to lasing at $^6H_{11/2}$ - $^6H_{13/2}$ transition with pumping by 1.32 µm, 1.66 µm or 1.7 µm radiation [2, 3]. In this work we studied the transitions originating from $^6H_{9/2}$+$^6F_{11/2}$ level and terminating at $^6H_{11/2}$ or $^6H_{13/2}$ levels (Fig.1 - left) resulting in generation of 5.4 µm and 2.4 µm radiation, respectively, and compare it with the 4.3 µm line generation. The properties of oscillations at 2.4 µm were studied also for cryogenic temperatures.

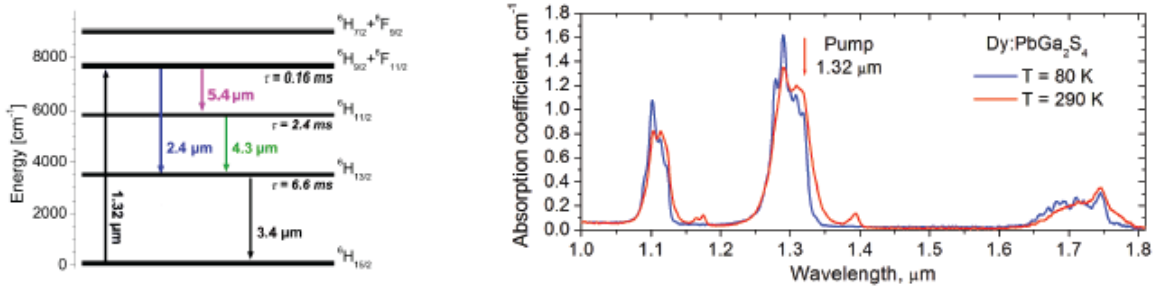

Fig.1. Energy level diagram of Dy^{3+} ion in $PbGa_2S_4$ crystal (left);
Dy:$PbGa_2S_4$ absorption coefficient dependence on wavelength for temperatures of 80 K and 290 K (right).

2. Dy:PGS laser characteristics

Dysprosium doped lead thiogallate crystal with diameter 19.2 mm and length 16.2 mm synthesized using Bridgman technique in quartz ampoules from the melt served as an active medium for developed mid-IR laser. The concentration of the Dy^{3+} in melt was 0.7 at %. The dependence of absorption coefficient on wavelength for room and liquid nitrogen temperature is seen in Fig. 1-right. As pump source Nd:YAG laser operating in free-running mode was used with the 160 mJ output energy, the pulse length of 200 µs and wavelength 1.318 µm. In case of 5.5 µm radiation lasing at RT the maximum reached energy was 107 µJ. As the same condition the maximum pulse energy for 2.4 µm radiation was 2.35 mJ with efficiency of 8.5 %. For 2.4 transition and low temperature (80 K), the threshold was sufficiently (~3 times) lower and the efficiency increased (1.4 times).

4. Conclusions

Different Dy:PGS laser transitions originating from $^6H_{9/2}$+$^6F_{11/2}$ level suitable for 1.32 µm pumping were investigated. Laser generation at 2.4, 4.3, and 5.4 µm with the maximum pulse energy of 2.35 mJ, 850 µJ, and 450 µJ respectively, were obtained at RT. It proves that Dy:PGS material can be used for generation laser radiation in the interesting mid-IR region. From the low temperature spectroscopic measurements it follows that the temperature decrease down to 80 K does not influence strongly the absorption spectrum of Dy^{3+} ions. Laser generation at 4.3 µm was not influenced significantly by the temperature decrease. In the case of 2.4 µm generation the laser threshold decreased at 80 K.

4. References

[1] T. T. Basiev, M. E. Doroshenko, V. V. Osiko, and D. V. Badikov, "Mid IR laser oscillations in new low phonon PbGa2S4:Dy3+ crystal," OSA Trends in Optics and Photonics, Eds. C. Denman and I. Sorokina, OSA Proceedings Series 75, Optical Society of America **98**, TuB10 (2005).
[2] J. Šulc, H. Jelínková, M. E. Doroshenko, T. T. Basiev, V. V. Osiko, V. V. Badikov, and D. V. Badikov, "Dysprosium doped PbGa2S4 laser excited by diode pumped Nd:YAG laser," Optics Letters **35**, 3051–3053 (2010).
[3] H.Jelinkova, M.E.Doroshenko, M.Jelinek, J.Sulc, T.T.Basiev, V.V.Osiko, V.V.Badikov, and D.V.Badikov, "Resonant pumping of dysprosium doped lead thiogallate by 1.7 µm Er:YLF laser radiation," Laser Phys. Lett., 349–353 (2011).

P-073

Microstructuring of tetrahedral amorphous carbon films (ta-C) using a 248 nm KrF excimer laser

F. Jahn[1], A. Engel[1], R. Böttcher[2], S. Weißmantel[1]

[1]University of Applied Sciences Mittweida, Technikumplatz 17, 09648 Mittweida, Germany
[2]3D-Micromac AG, Technologie-Campus 8, 09126 Chemnitz, Germany
Email: falko.jahn@hs-mittweida.de

The special properties of tetrahedral amorphous carbon (ta-C) films with low internal stress, such as extremely high hardness in the range of 60 GPa and low friction coefficient in the range of 0.15, result in increasing interest for using them in industrial applications. For some applications it may, however, be beneficial to modify the surface of those films by microstructuring, for example.

A method for microstructuring of thin films of ta-C on different substrates will be presented. With this method the microstructures are fabricated using a KrF excimer laser LPX Pro 305 F by Coherent, Inc. with a wavelength of 248 nm. The laser micromachining station along with its specification concerning laser parameters, beam guidance, beam shaping and positioning of the samples will be presented.

The microstructures were generated on ta-C films by using mask projection technique. Depending on the mask geometry and the structuring parameters the produced structures have different shapes, sizes and depths. Several selected structuring examples will be presented, two of these are shown in Fig. 1. For measuring the microstructures surface profilometry, scanning electron and optical confocal microscopy were used.

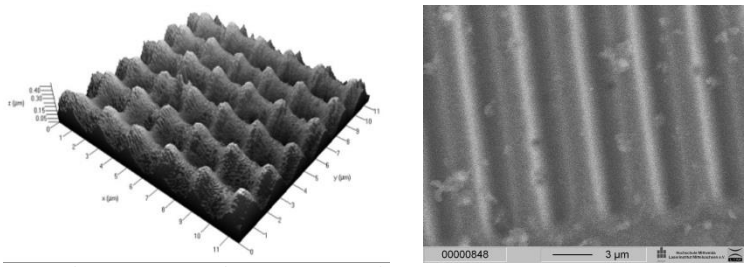

Fig. 1. Examples of microstructures fabricated in ta-C films by excimer laser mask projection technique.

It will be demonstrated that mask projection technique with a wavelength of 248 nm is suitable to produce microstructures with resolutions down to a few micrometers in ta-C films. Optimum structures can result in reduced friction coefficients of less than 0.05. The hardness of the structured films was found, however, to decrease simultaneously down to values in the range of 35 to 40 GPa. Thus it remains still very high so that microstructured ta-C films may have tremendous potential for tribological applications.

Further investigations on the modified ta-C films were directed to the relationship between the microstructure and the mechanical properties, the results of which will also be presented. There were indications that the microstructures are not only the effect of material ablation but also of phase changes. Particularly, it was found that the structured regions were higher than neighboring unstructured regions, which can be accounted for by sp^3 to sp^2 bonding transformation in the amorphous carbon films due to the microstructuring process. Further experimental results on this and on the microstructure of the transformed hard films along with calculations supporting the assumption will be the final main part of the presentation.

P-074

Optimization of laser-pulse energy during selective laser trabeculoplasty by detection of cavitation bubbles formation

P. Gregorčič*[1], J. Pribošek[1], J. Jakiša[1], A. Vrečko[2], B. Vedlin[2], R. Grčar[3], J. Diaci[1], J. Možina[1]

[1]*Faculty of Mechanical Engineering, University of Ljubljana, Aškerčeva 6, 1000 Ljubljana, Slovenia*

[2]*Optotek d.o.o., Tehnološki park 21, SI-1000, Ljubljana, Slovenia*

[3]*Eye Clinic Irman, Savinjska cesta 2, 3310 Žalec, Slovenia*

E-mail: peter.gregorcic@fs.uni-lj.si

The selective laser trabeculoplasty (SLT) is a pulse-laser treatment for the reduction of intraocular pressure in eyes with open angle glaucoma and ocular hypertension [1]. It was introduced by Latina and Park [2], who demonstrated the possibility of selective targeting of the pigmented trabecular meshwork cells by using a Q-switched frequency-doubled Nd:YAG laser with low fluences. This enables treatment without producing collateral damage to the adjacent non-pigmented eye cells and tissues. Moreover, in comparison with an older technique, called argon laser trabeculoplasty [3], the SLT method does not cause coagulation of the trabecular tissue. Instead, the selective absorption in melanin stimulates and facilitates draining of aqueous humour.

The trabecular meshwork cells contain melanin granules, which absorb visible light. This absorption in the pigment turns the absorbed laser-pulse energy in a local rise of the tissue temperature. In such a way, the fluid is vaporized on the surface of melanin granules and therefore micro-meter (transient intracellular) cavitation bubbles are formed around the laser-irradiated cells containing the pigment [4]. By increasing the laser-pulse energy the radius of these bubbles grows to the dimensions, when they become visible by ophthalmoscopy.

The cavitation bubbles induced by selective absorption of the laser pulse represent a kind of microscopic underwater explosions leading to cavitation damage. The cavitation damage is confined to the scale of single cells containing the pigment only when pulse energy is low enough to produce bubbles that are only few micro-meters in size [5]. Consequently, proper setting of the laser energy is essential for ensuring that the target cells are successfully and selectively treated without creating excess damage to the tissue. To ensure this, the operation protocol of SLT is as follows. The spot size is fixed during the entire treatment (typically 400 μm), while laser pulses have wavelength of 532 nm and are shorter than 5 ns. The treatment starts with low energy (typically 0.8 mJ) and it is increased or decreased by an increment of 0.1 mJ until the threshold energy is achieved [6]. The threshold energy is defined as the energy, where the ophthalmologist visually recognizes the formation of cavitation bubbles by ophthalmoscopy. When bubbles are visually detected, the operating surgeon lowers the laser energy just below the threshold for bubbles' formation. In such a way the ophthalmologist subjectively regulates the laser energy during the operation.

Since an automatic method to monitor the bubbles' formation can make the SLT process more reliable and less time consuming [5], we have developed an automatic detection of cavitation bubbles formation on the patient's eye [7]. In this contribution we will present *ex-vivo* and *in-vivo* experiments, the optical system for image acquisition and the solution for image processing that enable us to develop the automatic adjustment of the laser-pulse energy during the treatment. This allows the execution of the procedure closer to the threshold for the cavitation bubble's formation, thereby making the entire procedure more reproducible and effective.

[1] J. M. Shi and S. B. Jia, "Selective laser trabeculoplasty," Int. J. Ophthalmol. **5**, 742 (2012).

[2] M. A. Latina and C. Park, "Selective Targeting of Trabecular Meshwork Cells - in-Vitro Studies of Pulsed and CW Laser Interactions," Exp. Eye Res. **60**, 359 (1995).

[3] A. M. Bovell, K. F. Damji, W. G. Hodge, W. J. Rock, R. R. Buhrmann, and Y. I. Pan, "Long term effects on the lowering of intraocular pressure: selective laser or argon laser trabeculoplasty?" Can. J. Ophthalmol. **46**, 408 (2011).

[4] C. P. Lin and M. W. Kelly, "Cavitation and acoustic emission around laser-heated microparticles," Appl. Phys. Lett. **72**, 2800 (1998).

[5] C. P. Lin, "Selective absorption by melanin granules and selective cell targeting" in, *Lasers in Ophthalmology – Basic, Diagnostic and Surgical Aspects: a Review*, F. Fankhauser and S. Kwasniewska ed. (Kugler Publications, The Hague, 2003).

[6] M. A. Latina and D. H. Gosiengfiao, "Selective laser trabeculoplasty," in, *Lasers in Ophthalmology – Basic, Diagnostic and Surgical Aspects: a Review*, F. Fankhauser and S. Kwasniewska ed. (Kugler Publications, The Hague, 2003).

[7] A. Vrečko, B. Vedlin. J. Jakiša, P. Gregorčič, "Ophthalmic laser device," EU patent application (2014).

P-075

Characterization of titanium oxide layers produced by nanosecond laser irradiation

F. Hamadi[1], T. Tamsaout[1], E.H. Amara[1], A.H. Kellou[2]

[1]*Equipe Traitement des Matériaux par Laser, CDTA, PO. Box 17 Baba-Hassen, 16303 Algiers, Algeria*

[2]*Laboratoire Electronique Quantique, Faculté de Physique, USTHB, PO. Box 32 El-Alia, Bab-Ezzouar, Algiers, Algeria*

fhamadi@cdta.dz

1. Abstract

The laser marking technique is used to induce colors on titanium surface by varying the different processing parameters. The issued beam from a Q-switched diode pumped Nd:YAG green laser (=532 nm. $_{pulse}$=5 ns) scans the treated material surface under normal atmospheric conditions. The aim of our study is to determine the effects of the working parameters (i.e. pulse frequency, beam scanning speed, and pumping energy) and those raising, when these parameters are combined. We can cite the accumulated fluencies and the overlapping rate of the laser impacts, on the resulting mark quality. From the experimental results, we can conclude that the accumulated fluencies and scanning speed are the most important operating parameters during laser marking, since they strongly influence the surface roughness, the surface reflectance and the occurrence of several oxide phases like TiO, TiO_2 (TiO_2, anatase and rutile).

The figures below show SEM images, EDS spectrums and the contents of mass and atomic identified items for the titanium oxides obtained at different scanning speeds.

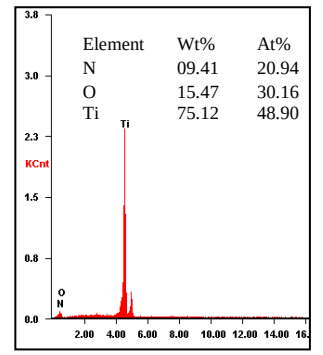

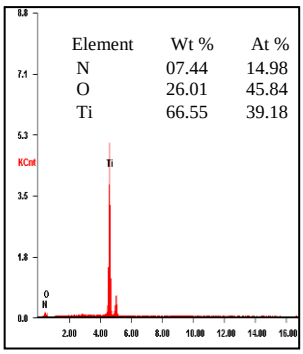

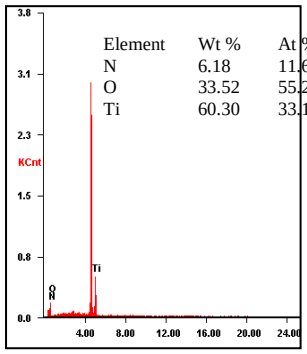

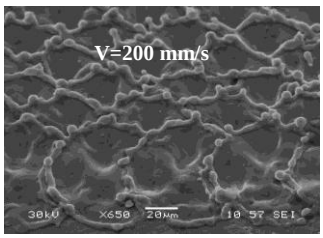

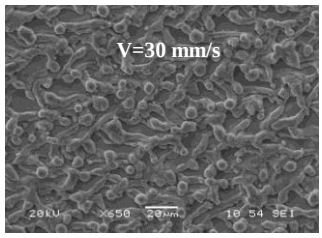

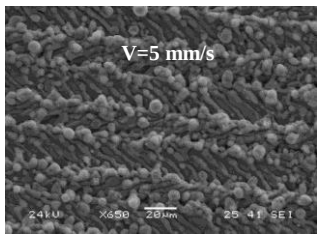

2. References

[1] L. Lavisse, P. Berger, M. Cirisan, J. M. Jouvard, S. Bourgeois and M. C. Marco de Lucas, "Influence of laser–target interaction regime on composition and properties of surface layers grown by laser treatment of Ti plates"J. Phys. D: Appl. Phys. **42**, 245303 (2009).

[2] A. Peréz del Pino, J. M. Fernandez-Pradas, P. Serra, J. L. Morenza, "Coloring of titanium through laser oxidation: comparative study with anodizing", Surf &Coating Technol. **187**, 106-112, (2004).

[3] C. Langlade, A. B. Vannes, J. M. Krafft, J. R. Martin, "Surface modification and tribological behaviour of titanium and titanium alloys after YAG-laser treatments", Surf & Coating Technol. **100-101,** 383-387, (1998).

[4] A. Peréz del Pino, P. Serra, J. L. Morenza, "oxidation of titanium through Nd: YAG laser irradiation", Appl. Surf. Sci. **197–198**, 887-890, (2002).

[5] L. Lavisse, D. Grevey, C. Langlade, B. Vannes, "the early stage of the laser induced oxidation of titanium substrates", Appl. Surf. Sci. **186**, 150-155 (2002).

P-076

Characterization and controlling the size and density of polyethersulfone membrane pores with excimer lasers

Hedieh Pazokian[a*], Adeleh H.P Mehrabadi[b], Mahmoud Mollabashi[b], Jalal Barzin[c], Mohammad Javad Sobhani[b]

[a] *Laser and Optic Research School, Tehran, Iran*

[b]*Department of Physic, Iran University of Science and Technology, Tehran, Iran*

[c]*Biomaterial Department, Iran Polymer and Petrochemical Institute, Tehran, Iran*

Corresponding author Email: h_pazokian@iust.ac.ir

Abstract

Polyethersulfone membrane with different compositions of polyvinyl pyrrolidone blend was irradiated with XeCl and ArF excimer lasers. The morphology of the irradiated surface was examined with scanning electron microscopy. The pore density and mean value of the pore sizes were measured following different irradiation conditions. The results show that the number density and size of pores on the surface of the membrane is changed with laser irradiation. These changes affect more by the inner structure and less the composition of the membrane.

References:

[1]Vourch M, Balannec B, Chaufer B, Dorange G. 2008 Desalination.**219**(1):190-202.

[2]Kunal Pal, Ajit K. Banthia, Majumdar DK. 2007 AAPS Phar mSciTech.**8**(1):E1-E5.

[3]Yang Q, Adrus N, Tomicki F, Ulbricht M. 2011 Journal of Materials Chemistry.**21**(9):2783-811.

P-077

Laser photoacoustic technology for measurement of gas ablation products at sub-ppb level

Dan C. Dumitras
National Institute for Laser, Plasma and Radiation Physics, 409 Atomistilor St., PO Box MG-36, 077125 Bucharest, Romania
and University Politehnica of Bucharest, Faculty of Applied Sciences, 313 Splaiul Independentei St.., 060042 Bucharest, Romania
E-mail: dan.dumitras@inflpr.ro

A very sensitive photoacoustic instrument was designed and implemented to measure precisely trace gas concentrations at sub-ppbV (parts per billion by volume) level. Laser photoacoustic spectroscopy (LPAS) is primarily a calorimetric technique and, as such, differs completely from other previous techniques, as the absorbed energy can be determined directly, instead of via measurement of the intensity of the transmitted or backscattered radiation. A home-built, frequency-stabilized CO_2 laser was used as a laser source which is tunable in the range 9.2-10.8 μm. In this infrared region hundreds of molecular gases/vapors of environmental concern for atmospheric, industrial, medical, military, and scientific spheres exhibit strong absorption bands and their concentration can be accurately measured. The most important features of this gas sensor include high sensitivity and selectivity, large dynamic range, high accuracy and precision, good temporal resolution, ease of use, versatility, reliability, robustness, and multicomponent capability [1]. Also, at small laser power levels the saturation effects are negligible [2].

A typical experimental setup based on resonant LPAS principles is shown in Fig. 1. The continuous wave laser radiation is amplitude-modulated by a mechanical chopper operating at an acoustic resonance frequency of the photoacoustic (PA) cell. It is then focused by a lens and directed through the resonant PA cell. The transmitted laser power is monitored with a powermeter (signal P_L in Fig. 1). Inside the cell the radiation produces pressure modulation recorded by a microphone as an acoustical signal V, which is processed by a lock-in amplifier locked to the chopper frequency. The normalized absorption can then be deduced as being proportional to V/P_L ratio.

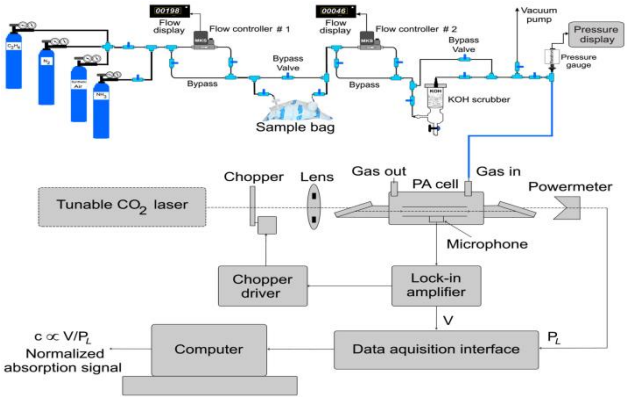

Fig. 1 Typical laser photoacoustic setup for trace gas measurements.

We calibrated our PA cell with the widely used reference gas ethylene, whose absorption coefficients are accurately known at CO_2-laser wavelengths [3]. In particular it exhibits a characteristic absorption peak at the 10P(14) laser transition at 949.49 cm^{-1}. Using this PA cell and an optimized experimental arrangement (for a resonance frequency of 564 Hz and a quality factor of 16.1) we measured a cell responsivity R = 433 V-cm/W. With the total responsivity of the four microphones $S_{M\ tot}$ = 80 mV/Pa (20 mV/Pa each), a cell constant C = 5410 Pa-cm/W can be calculated [4]. The minimum detectable concentration obtained by us in ethylene (0.58 ppbV with a low power laser and 0.21 ppbV with a high power laser) are the best values reported in the literature, improving this parameter by a factor of 6.5 in the first case and by a factor of 18 in the second case. In a molecular gas with a high absorption coefficient (e.g. SF_6), the minimum detectable concentration could be as low as 0.026 ppbV.

With this instrument we measured absorption coefficients for ethylene, ammonia, carbon dioxide, ethanol and methanol, human biomarkers, surgical smoke, cigarette smoke, plant hormones, ablation products etc.

1] D.C. Dumitras, A.M. Bratu and C. Popa., in *CO_2 Laser – Optimisation and Application*, D.C. Dumitras ed. (Intech, Croatia, 2012)
[2] D.C. Dumitras, S. Banita, A.M. Bratu, R. Cernat, D.C.A. Dutu, C. Matei, M. Patachia, M. Petrus and C. Popa, "Ultrasensitive CO_2 laser photoacoustic system", Infrared Phys. Technol. **53**, No. 5, pp. 308-314 (2010)
[3] D.C. Dumitras, D.C. Dutu, C. Matei, A.M. Magureanu, M. Petrus and C. Popa, "Laser photoacoustic spectroscopy: principles, instrumentation, and characterization", J. Optoelectron. Adv. Mat. **9**, No. 12, pp. 3655-3701 (2007)
[4] A.M. Bratu, M. Petrus, M. Patachia and D.C. Dumitras, "Carbon dioxide and water vapors detection from surgical smoke by laser photoacoustic spectroscopy", U.P.B Sci. Bull., Series A **75**, No. 2, pp. 139-146 (2013)

P-078

Creating and utilizing spatially varying light intensity profiles to enhance nonlinear responses

R. Donaldson, E. Jaatinen
Queensland University of Technology, Brisbane, Queensland 4000, Australia
E-mail: robert.donaldson@hdr.qut.edu.au

The modification of the optical and material properties of material systems is reliant on high light intensity, and is usually only possible by utilising laser light[1]. Typical laser systems produce a beam with an intensity characterised by a Gaussian distribution in cross section, such as the rectilinear Hermite-Gaussian or cylindrical Laguerre-Gaussian modes. Thus the bulk of research performed into investigating intensity dependent nonlinear optical effects utilizes or assumes a TEM_{00} fundamental Gaussian mode light intensity distribution. However, this particular distribution may not be optimal for inducing a specific nonlinear effect or may lead to other unwanted outcomes such as sample damage. In this paper, we seek to generate superimposed combinations of higher order Gaussian (HOG), or non-Gaussian (NG) beams and understand their effect on the sample and in inducing nonlinear optical response.

Here we use spatially varying beam profiles produced by HOG or NG beams in the particular application of zscan, a common experimental technique that involves scanning a sample material along the direction of beam propagation through a tightly focussed laser beam [2].Since nonlinear effects are intensity dependent, a stronger nonlinear response will occur at the beam focus than away from this location and by measuring the difference the materials nonlinear properties can be characterized. This widely adopted technique is useful as it is easy to implement and can quite quickly and accurately determine the sample materials nonlinear absorption and refraction.

To induce significant nonlinear optical response in a sample often requires peak intensities that can approach the damage threshold of the material. Therefore, when conducting a zscan experiment there exists the real risk of increasing the incident laser light intensity too high, damaging the sample through ablative or thermal effects. Often then there needs to be a balance between the intensity needs of the nonlinear process against the possibility of damaging the sample. In this paper it is proposed that modified Gaussian beam profiles such as the 'doughnut' or TEM_{01}^{*} mode have the potential to produce significant nonlinear response while lowering the risk of sample damage. Compared to a TEM_{00} fundamental mode Gaussian beam, the doughnut has lower peak intensity while maintaining a higher average intensity. This combination of attributes ensures that sufficient intensity is applied to the sample that the desired nonlinear effect can be evoked, while maintaining intensity below the damage threshold.

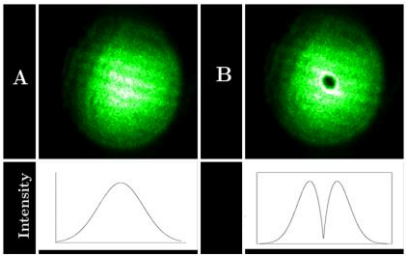

Fig. 1. Gaussian mode (A) and doughnut mode (B) produced by SLM.

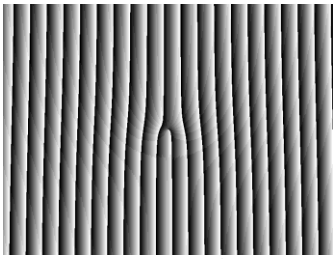

Fig. 2. Forked hologram for producing doughnut modes via SLM.

In this paper we demonstrate techniques and methods to realize the doughnut mode and other user defined beam profiles as shown in figure 1.

Initially, these profiles were developed computationally using a nematic SLM via diffractive holography, as shown in figure 2. However the SLM has a low damage threshold, limiting its use. Given that zscan typically uses intense pulsed radiation intensities one solution that allows use of the SLM is continuous wave version of zscan[3]. However, this would be problematic in samples with weaker nonlinearities. Other solutions discussed here for the physical realisation of HOG or NG beams are phase plates, novel lenses (axicon), etc. Gauss-Bessel beams have some potential utility in enhancing the zscan process[4], and are readily usable with the simple addition of an axicon lens into the zscan array.

By experiments both physical and numerical this paper will investigate and compare the effectiveness or not of these different beam profiles on the nonlinear diffraction and refraction using the zscan approach.

[1] R. W. Boyd, *Nonlinear Optics*, 3rd. ed., (Academic Press, San Diego).
[2] M. Sheik-Bahae, et al., "Sensitive measurement of optical nonlinearities using a single beam," IEEE J. Quantum Electron., **26**(4), 760-769 (1990)
[3] A. Siahmakoun, D. Breitling, and R. A. Najaf-Zadeh, "Continuous-Wave Z-Scan Measurement of Photorefractive SBN:60," Appl. Opt., **39**(29), 5360-5366 (2000)
[4] S. Hughes, and J.M. Burzler, "Theory of z-scan measurements using Gaussian-Bessel beams," Phys. Rev. A, **56**(2), R1103-R1106 (1997)

P-079

Excimer Laser Assisted Growth of Group IV Alloys

S. Chiussi[1], S. Stefanov[1], C. Serra[2], A. Benedetti[2], D. Buca[3], J. Schulze[4], B. Fechner[5], R. Delmdahl[5]

[1]*Departamento Física Aplicada, Universidade de Vigo, E.S.I. Industriales, E-36310 Vigo, Spain*
[2]*CACTI, Universidade de Vigo, E-36310 Vigo, Spain*
[3]*Peter-Grünberg-Institut 9 (PGI 9-IT), Forschungszentrum Jülich, 52425 Jülich, Germany*
[4]*Institut für Halbleitertechnik (IHT), Pfaffenwaldring 47, 70569 Stuttgart, Germany*
[5]*Coherent LaserSystems GmbH & Co. KG, Hans-Boeckler-Str. 12, D-37079 Goettingen, Germany*
E-mail: ralph.delmdahl@coherent.com

Abstract

Fabrication of Photonic Integrated Circuits (PICs) using CMOS compatible direct bandgap Group-IV heterostructures is of increasing concern from scientific, technological, and economic point of view. Growth of group IV alloys, such as the Silicon-Germanium-Tin (SiGeSn) binaries and ternaries through CMOS compatible techniques is therefore of particular interest. Pulsed Laser Induced Epitaxy (PLIE) is a reliable and CMOS compatible laser assisted technique that therefore sparked particular interest. This thin film fabrication route is best to be based on UV-excimer laser systems as broad beam irradiation tools. In view of transferring PLIE from lab to fab, it is of advantage that excimer laser technology has been dramatically improved over the last two decades in terms of beam quality, power stability and component lifetimes. Apart from established hetero-epitaxial growth techniques, like Molecular Beam Epitaxy (MBE) and Chemical Vapour Deposition (CVD), PLIE using powerful, short wavelength excimer lasers can be regarded as a particularly fast and precise processing route for CMOS compatible group IV alloys. This contribution will concentrate on PLIE using 193 nm excimer lasers. The PLIE technique (see fig.1) is based on rapid local melting of a heterostructure with the elements desired in the final alloy and fast solidification of the molten volume, that are induced by 25 ns short ArF-Excimer laser pulses and are completed within very short time scale (<500 ns). Synthesis of epitaxial (Si)GeSn alloys with above 10% Sn in large areas and of SiGeSn/GeSn micropatterns, through scanning and mask projection assisted PLIE, respectively, will be discussed. Emphasis will be placed on the influence of laser processing parameters on compositional and structural properties of the epitaxial alloys.

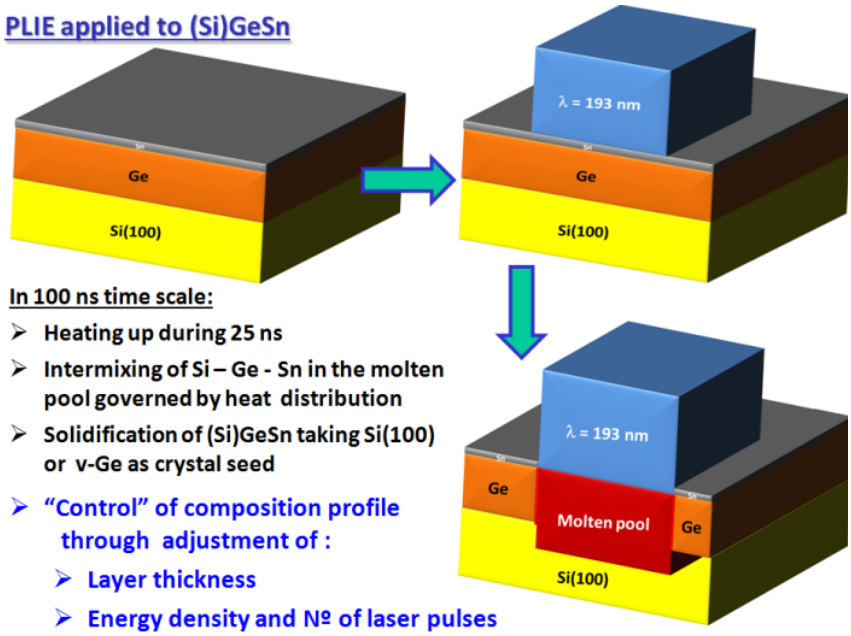

Fig. 1. Schematics of the PLIE technique for producing (Si)GeSn alloys.

References

[1] S. Stefanov, J. C. Conde, A. Benedetti, C. Serra, J. Werner, M. Oehme, J. Schulze, S. Chiussi, "Silicon germanium tin alloys formed by pulsed laser induced epitaxy," Thin Solid Films **520**, 3262 (2012)

[2] R. Delmdahl and R. Paetzel, "Excimer Laser Technology Trends," J. Phys. Appl. Phys. **47**, 1-7 (2013).

P-081

Femtosecond surface nanostructuring by means of colloidal particle lens array

N. Bityurin, A. Afanasiev, A. Pikulin, V. Bredikhin, and N. Mitin
Institute of Applied Physics, RAS, Nizhniy Novgorod, Russia
E-mail: bit@appl.sci-nnov.ru

We consider laser nanostructuring of material surface by means of colloidal particle lens array.
Here, the monolayer of dielectric micro- or nanospheres placed right on the surface acts as an array of near-field lenses that focus the laser radiation into the multitude of distinct spots, allowing formation of many structures in a single stage [1].
Experimentally, the layer of polystyrene spheres with diameters of about the wavelength of the second harmonic of a Ti:Sapphire laser deposited to a dielectric substrate focuses the radiation of the second harmonic (SH) and does not focus the radiation of the fundamental frequency (FF). When using two-color laser pulses (FF+SH) for surface nanostructuring by means of colloid particle lens array, the second harmonic provides seed structure formation while the FF radiation provides energetic effect [2]. We experimentally show that converting several percent of the energy of the FF pulse to the SH offers opportunity to obtain structures on the surface by means of the spheres with the diameter close to the wavelength of the second harmonic. It is not possible to obtain such structures only by means of the FF radiation. At the same time, the formation of the structures by means of the solely SH requires significantly higher energy density than the energy density of the SH within the two-color pulse. Thus, the use of the two-color pulses allows significant increase in the structure recording density comparing to the opportunity provided by the initial FF beam and allows one to enlarge the processed area comparing to the opportunity provided by the highly focused pure SH beam.
The spherical shape of microparticles is not optimal for the beam focusing due to strong aberrations. In the case of silica or polymeric microspheres with refractive index of about 1.5, the field maximum is situated close to the surface of the sphere resulting in a small aspect ratio of the obtained nanostructures. In the case of the higher refractive index, the maximum is placed inside the sphere, thus rendering such particles inapplicable for the surface nanostructuring.
In this work, we study the possibility to employ spheroidal microparticles instead of the spherical ones in order to reduce the aberrations. With self-made FDTD code, we calculate the laser field intensities provided by monolayers of spheroidal particles and analyze the advantages and disadvantages of such focusing systems for surface nanomodification. In particular, we demonstrate the possibility to improve the aspect ratio of the nanostructures and increase the density of the modification spots.

[1] A. Pikulin, A. Afanasiev, N. Agareva, A. P. Alexandrov, V. Bredikhin, and N. Bityurin, "Effects of spherical mode coupling on near-field focusing by clusters of dielectric microspheres.," Opt. Express 20, 9052 (2012).
[2] N. Bityurin, A. Afanasiev, V. Bredikhin, A. Alexandrov, N. Agareva, A. Pikulin, I. Ilyakov, B. Shishkin, and R. Akhmedzhanov, "Colloidal particle lens arrays-assisted nano-patterning by harmonics of a femtosecond laser," Opt. Express 21, 21485–21490 (2013).

P-082

Laser-detonation facility for acceleration of gaseous materials: Etching and deposition of solid materials

K. Yokota, K. Ide, J. Ohira, Y. Yamasaki, K. Morimoto, H. Asada, M. Tagawa
Kobe University, Rokko-dai 1-1, Nada, Hyogo 657-8501, Japan
E-mail: yokota@mech.kobe-u.ac.jp

1. Introduction

Spacecraft orbiting low Earth orbit (LEO), where 200 to 500 km in altitude, has been subjected to severe material degradation by the hyperthermal collisions of O-atoms in upper atmosphere of Earth [1]. Simulation of the hyperthermal collision phenomena in laboratory requires a formation of intense O-atom beam with velocity of 8 km/s that corresponds to orbital velocity of spacecraft. Acceleration of electrically neutral O-atom beam has been achieved by the laser-induced detonation of O_2 gas. However, the collision phenomena in sub-LEO region which is lower than 200 km in altitudes, needs to simulate simultaneous collisions of O-atoms and N_2 in the same collision velocity, i.e., different collision energies due to their different molecular masses. In this presentation, we introduce the laser-detonation facility to form multiple composition beams with different energies for sub-LEO material degradation studies, which has deposition capability as well.

2. Apparatus

The laser detonation O-atom beam source used in this study was developed at Kobe University in order to study high-energy collision of O-atom with solid materials [2]. This source is based on an original design by Physical Sciences Inc. (PSI). The laser-detonation beam source uses a pulsed supersonic valve (PSV) and a carbon dioxide laser (10.6 μm, 5-7 J pulse^{-1}) [3]. The target gas supplied to PSV is preliminary mixed by the gas mixture system installed in the gas supply line with a buffer tank. The PSV introduces target gas into the nozzle and the laser light is focused into the gas in the nozzle. The energy for dissociation and acceleration of target gas is provided by the inverse Bremsstrahlung process. The hyperthermal atomic beam, thus generated, was characterized by a time-of-flight (TOF) distribution measured by a quadrupole mass spectrometer (QMS) with a scintillation detector that is installed in the beam-line. Translational energies of the species in the beam were calculated using TOF distributions with the flight length of 238 cm.

3. Results and Discussion

Compositions of the beam formed by the premixed target gases were analyzed by TOF-QMS spectra. It has been found that the gas composition introduced in the nozzle was close to the mixture ratio set by the gas mixture system between the mixture ratios of 10-90%. Firing the TEA CO_2 laser pulse decomposes N_2 into N as well as O_2 into O. This is not suitable for simulating high-energy collision effect of N_2 in sub-LEO region. In order to avoid the decomposition of molecules in the target gas, N_2 was replaced to Ar. The TOF-QMS spectra of O, O_2 and Ar indicated that the decomposition of O_2 was promoted by the addition of Ar in the laser-induced plasma. It has also been clearly observed that the high-energy collision of chemically inactive Ar accelerates the mass-loss rate of polymeric materials induced by O-atoms, which has not been considered in the space material society. This system was also applied for material deposition to the substrate surfaces. CH_4 gas was selected as a test case. It was demonstrated that diamond-like carbon film with microscopic hardness of 50-60 GPa was successfully deposited on Si(001) substrate.

4. Conclusions

Hyperthermal multiple composition beam can be formed with a laser-detonation beam facility in Kobe University. The beam composition of O_2 and Ar mixture beam could be controlled by the gas mixture system. Since the effect of Ar addition into O-atom beam is clearly observed, effect of high-energy collision needs to be considered for material degradation phenomena in sub-LEO region. The laser-detonation system introduced in this presentation is capable to be applied both for etching and deposition of solids.

Acknowledgments

A part of this study was supported by the Grant-in-Aids for Scientific Research from the JSPS contract No. 25289307 and 26289322; and the Coordination Funds for Promoting Aerospace Utilization from the MEXT, Japan.

References

[1] S. K. R. Miller, B. Banks, "Degradation of spacecraft materials in the space environment", MRS Bulletin .**35**, 1 (2010) 20-34.
[2] K. Yokota, S. Yasuda, A. Mizutani, M. Tagawa "Relative electron impact ionization probabilities of O, O_2 and Ar components in the laser-detonation hyperthermal beams," Jpn. J. Appl. Phys., **52** (2013) 038002.
[3] T. K. Minton, D. J. Garton, in, Chemical dynamics in extreme environments, R.A. Dressler ed. (World Scientific, Singapore, 2001).

P-085

TiO_2 PLD nanocrystalline films supporting Au nanoparticles for application to visible-light-operating plasmonic photocatalysts

T. Watanabe[1], F. Kikuchi[2], T. Tabuchi[1], T. Yoshida[1], I. Umezu[3], and M. Haraguchi[2]

[1] *Course of Chemical Engineering, National Institute of Technology, Anan College, Anan, Tokushima 774-0017, Japan*

[2] *Institute of Technology and Science, The University of Tokushima, 2-1 Josanjima-cho, Tokushima 770-8506, Japan*

[3] *Department of physics, Konan University, Kobe 658-8501, Japan*

E-mail: 6141030@st.anan-nct.ac.jp

1. Introduction

In recent several years, plasmonic excitation phenomena of noble metal nanoparticles have been introduced to visible-light-operating photocatalysts [1]. Focusing on photocatalytic particles, first of all, high purity and highly controlled composition are important. Secondary, nanometer-sized synthesis is significant because of increasing specific surface areas to realize high catalytic activities. Pulsed laser deposition (PLD) in reactive background gases is a candidate process to synthesize high performance nanocrystalline TiO_2 photocatalysts [2]. In this study, we prepare TiO_2 nanocrystalline films supporting Au nanoparticles using PLD in O_2 background gas.

2. Experiments

The TiO_2 nanocrystalline films were formed by the PLD of a TiO_2 target in O_2 background gases. O_2 gas was introduced into the vacuum chamber and maintained at constant pressure 13 Pa. The fourth harmonics of a Nd:YAG laser beam (wavelength: 266 nm, pulse width: 6 ns, energy density: 2.4 J/(cm^2・pulse), pulse energy: 50 mJ/pulse, repetition rate: 10 Hz) was focused onto the TiO_2 target for 15 min. Distance from the target to the unheated deposition Si substrates was 25 mm. Au thin films were deposited on the TiO_2 nanocrystalline filmes by resistance-heating vacuum evaporation with 4 nm apparent thickness. The specimens were annealed at 300ºC for 3.0 h in a furnace. During the annealing process, as-deposited island-like Au balled to nanoparticles. We used a methylene blue (MB) decomposition method. The TiO_2 nanocrystalline films supporting Au-nanoparticle on the Si substrates in MB aqueous solution (0.01 mmol/L), were irradiated by an excitation light (interference-filtered Xe arc lump: 490-500 nm, irradiation density: 3 W/m^2).

3. Results and Discussion

Figure 1 shows a plane-view image by FESEM of the Au nanoparticles on the TiO_2 nanocrystalline film. It was found that the Au nanoparticles of which mean diameter was about 10 nm were dispersed on the TiO_2 nanocrystalline film. The photocatalytic activities were described by absolute values of absorbance decrease of the 664 nm peak (|*ΔAbs.*|). In this experimental condition, little portion of the incident light could excite and decompose shorter wavelength tail of the 664nm absorption peak, directly. Therefore, we introduced "net |*ΔAbs.*|" defined as follow: (|*ΔAbs.*|: Au nanoparticles/TiO_2 films/Si sub.)-(|*ΔAbs.*|: TiO_2 films/Si sub.). These results are shown in Fig. 2. The net |*ΔAbs.*| increased linearly with increasing irradiation time. It means that our TiO_2 PLD nanocrystalline films supporting Au nanoparticles verified visible-light-operating photocatalytic activity which can be attributed to the plasmonic excitation.

Even though this result is primitive, we expect to refine the composite photocatalysts by tuning the size and number density of the Au nanoparticles, and introducing secondary agglomerated structures of primary TiO_2 nanocrystallites, to increase specific surface area of these. In addition, surface localized plasmonic resonance band of Au nanoparticles are in the wavelength range of 500-600 nm. Hence, it is necessary to change MB as indicator to anything not having the absorption band in this wavelength range.

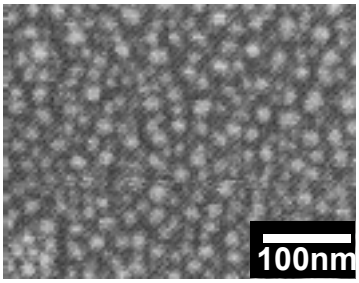

Fig. 1 SEM plane-view image of Au nanoparticles on TiO_2 nanocrystalline film .

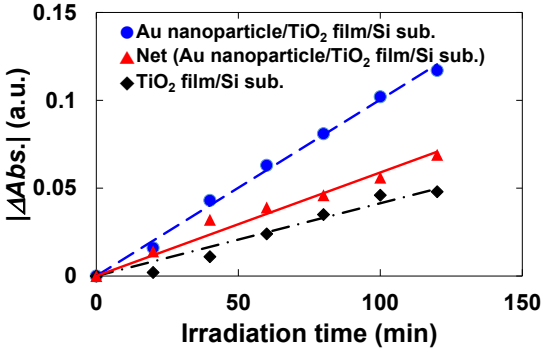

Fig. 2 Photocatalytic activity of TiO_2 PLD nanocrystalline films supporting Au nanoparticles.

[1] P. Wang, B. Huang, Y. Dai and M-H. Whangbo, Phys. Chem. Chem. Phys. **14**, 9813 (2012).

[2] T. Yoshida, N. Yagi, R. Nakagou, A. Sugimura and I. Umezu, Appl. Phys. A **117**, 223 (2014).

P-086

Epitaxial growth of Sc_2O_3 films on Gd_2O_3-buffered silicon substrates by Pulsed Laser Deposition

Joseph Paulraj, Rongping Wang, Matthew Sellars and Barry Luther-Davies

Laser Physics Centre, Research School of Physics and Engineering, Australian National University, Acton, Canberra, ACT 0200, Australia
Corresponding Author e-mail address: rongping.wang@anu.edu.au

We aim at developing waveguide devices that can transform the performance of the gradient echo quantum memory based on bulk crystals. Essentially this requires thin crystalline films of rare-earth doped oxides with low levels of impurities and defects. We therefore investigated the optimal conditions to prepare high quality Sc2O3 films on Gd2O3-buffered silicon wafers using pulsed laser deposition technique since (1) integration of the oxide on silicon will be compatible with standard semiconductor processing; (2) the oxides have minimum lattice mismatching with silicon; (3) there is a refractive index contrast between oxide and silicon in order to create the waveguide-based devices. Under the optimal conditions, X-ray θ-2θ scan of the film showed that, sharp oxide (222) peaks overlaid with silicon (222) and rocking curve of Sc_2O_3 (222) peak has a full width at half maximum(FWHM) of 0.10°. In-plain epitaxial relationship was confirmed by X-ray pole figure where Sc_2O_3 (111) is parallel to Silicon(111). High resolution Transmission electron microscopy images in Figure 1 indicated clear interfaces and perfect lattice images with sharp electron diffraction dots. All these confirm that the oxide films we deposited on silicon are single crystalline with high quality.

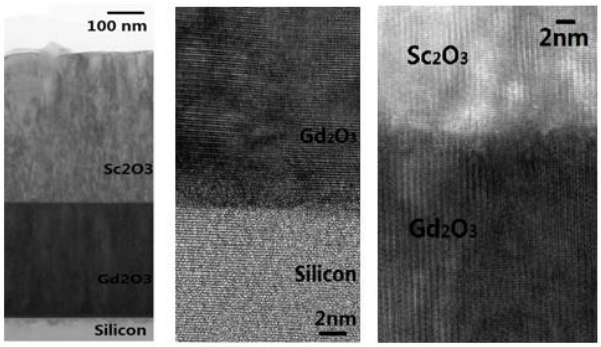

Figure 1. (left) morphology of the interface; (middle) high resolution image of the interface between silicon and Gd_2O_3; (right) high resolution image of the interface between Ga_2O_3 and Sc_2O_3.

P-087

Nanosecond laser ablation of aluminium-oxide dielectric films for the formation of p-type doped silicon in silicon photovoltaic applications

Daniel Walter[1], Evan Franklin[1], Andreas Fell[1], Marco Ernst[1]
[1]*Centre for Sustainable Energy Systems, Australian National University, Canberra, ACT, 2601, Australia*
E-mail: daniel.walter@anu.edu.au

1. Introduction

Laser ablation of dielectric films is a promising fabrication technique for silicon photovoltaics. High efficiency silicon solar cells require localised, micro-scale contacts, where the dielectric film is selectively removed and the subsurface region of the silicon substrate chemically doped. In the laboratory, this has traditionally required photolithography processing, a low-throughput technique that is of limited applicability in industrially environments. In contrast, nanosecond to continuous wave laser ablation of dielectric thin films has been shown to achieve both dielectric patterning and silicon doping simultaneously. In photovoltaic applications, the anti-reflection surface coatings are optically transparent, and incident laser irradiation from the UV to the near-infrared is predominantly absorbed in the silicon substrate. With optimised laser energies, the corresponding rise in substrate temperature vaporises the dielectric, while simultaneously melting the silicon substrate. The laser-vaporised elements of the dielectric diffuse into the melt and, if the dielectric is of a suitable elemental composition, form a doped region that favours electrical contact with low resistance and low electronic recombination. As a result, complex multi-step photolithography processing can be replaced by a single, indirect laser ablation process.

2. Results

In this work, we present a fundamental analysis of laser ablation and concurrent silicon doping via the irradiation of aluminium oxide-coated silicon substrates with a single pulse of a homogenised, 248 nm, nanosecond pulse-length excimer laser system. Aluminium oxide (Al_2O_3) is a high-performance, so-called 'passivating' dielectric film that is also rich in aluminium, a p-type dopant element in silicon. Thus, Al_2O_3 laser-ablation/doping is an attractive processing step for high efficiency cell techniques. We consider the Al_2O_3 film in two configurations: as a single layer, from 5 to 20 nm thick, and as an intermediate layer in a 20 nm Al_2O_3, 80 nm titanium dioxide (TiO_2) stack. We characterise the rate of ablation, the depth and elemental composition of the doped region, and the changes in surface electronic recombination, all as a function of energy density.

In the stack configuration, the TiO_2 layer strongly absorbs the 248 nm laser radiation, resulting in direct laser ablation as confirmed by profilometry measurements (Fig. 1, left). Nonetheless, aluminium doping is still observed, both as a result of thermal energy transfer to the substrate, and via the transmission of a portion of the laser energy following ablation of the TiO_2 layer within the pulse duration. As a single layer, Al_2O_3 is highly transparent at 248 nm, resulting in indirect ablation at a threshold energy density. The melt-phase diffusion, however, does not discriminate between dopant species, resulting in substantial doping with both aluminium and oxygen, as demonstrated by SIMS measurements (Fig. 1, right). Characterisation of the electronic recombination properties of Al- and O-doped silicon provides evidence for the formation of highly recombination active Al-O complexes. Implications for solar cell performance will be briefly discussed.

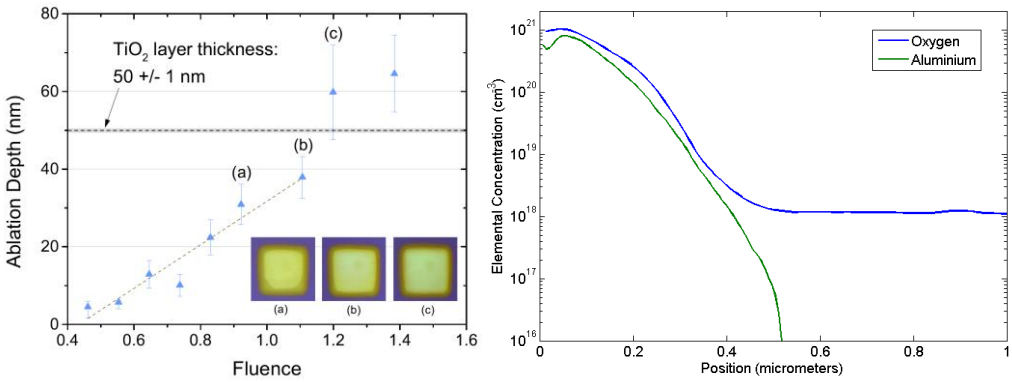

Fig. 1. (left) The ablation rate of Al_2O_3/TiO_2 dielectric stack using measured with profilometry illustrating the direct and uniform ablation of the TiO_2 capping layer, and (right) the concentration profile of both aluminium and oxygen in the silicon substrate following indirect ablation of a 20 nm Al_2O_3 layer with a single excimer laser pulse at 1.5 J cm^{-2}. The dopant depths are equivalent to those achieved with traditional solid-state furnace diffusion in silicon.

P-088

Synthesis of ZnO Micro-Spheres by Laser Ablation and Their Application to Refractive Sensor

T. Ueyama[1], Y. Satou[1], M. Higashihata[1], D. Nakamura[1], H. Ikenoue[1], and T. Okada[1]

[1]Graduate school of information science and electrical engineering, Kyushu University, 744 Motooka, Nishi-ku, Fukuoka 819-0395, Japan

ueyama@laserlab.ees.kyushu-u.ac.jp

1. Introduction

The microsized resonators have attracted attention as a sensing device [1,2]. The resonance mode called whispering gallery mode (WGM) arise from light confinement within a resonator via total internal reflection and has high Q factor. The WGM spectrum shifts in response to the refractive index change surrounding of the resonator [1,2]. These WGM resonators are generally made from silica or polystyrene, so that they require to guide light into the resonators using a coupling fiber [1]. In addition, the resonators have a limitation on the refractive index of the surrounding materials, which must be less than that of the resonator, or light can not be confined in the resonator. On the other hand, we have succeeded in fabricating ZnO microspheres by a simple laser ablation method in air [3]. In addition, ultraviolet WGM lasing from the photoexcited ZnO microsphere have achieved, which does not need to guide light and enable to deal with high refractive indices up to that of ZnO. In this study, we investigated surface refractive index dependence on the oscillation peak of a photoexcited ZnO microsphere.

2. Fabrication of ZnO microspheres

ZnO microspheres were fabricated by ablating a ZnO sintered target on which Nd:YAG laser (λ = 1064 nm) was focused in the air. The fabricated ZnO microspheres were coated with a SiO_2 film by spin coating to fix on a substrate and prevent dissolving of ZnO in water. Figure 1 (a) show the SEM image of the ZnO microsphere coated with a SiO_2. We have confirmed that the synthesized ZnO microspheres have wurtzite-structured ZnO crystal from the X-ray diffraction and micro-Raman measurement [3].

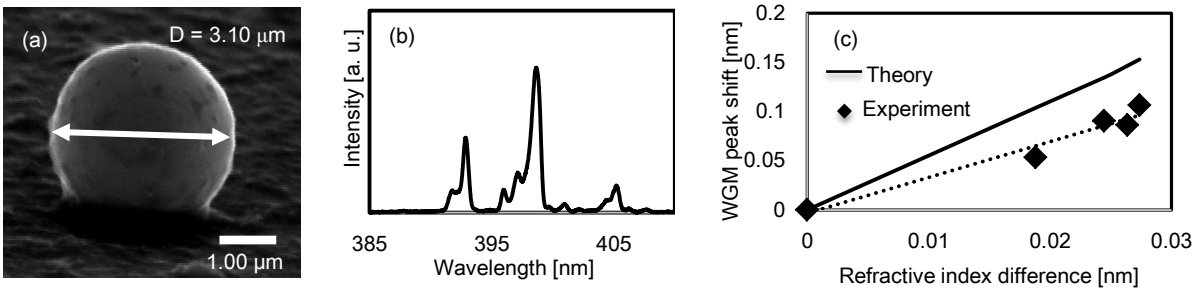

Fig. 1 (a) SEM image of the ZnO microsphere coated with SiO_2. (b) The lasing spectrum from the ZnO microsphere photoexcited by Nd:YAG laser (λ = 355 nm). (c) The WGM peak shifts in respons to refractive index change

3. Experiment results

Figure 1 (b) shows the WGM spectrum from the ZnO microsphere in water under photoexcitation by Nd:YAG laser (λ = 355 nm). Modal structure from the ZnO microsphere were observed in UV region, which corresponds to the near band edge emission in ZnO. The mode spacing of the lasing spectra corresponds to the WGM-theoretical mode spacing. With increasing the refractive index of the surrounding liquid (water ethanol mixtures), a red-shift in the peak wavelength of the WGM spectrum was observed. Figure 1 (c) shows that the experimental peak shift as a function of the refractive index difference, and theoretical line [4] is also shown. The sensitivity of the ZnO microsphere is 3.64 nm/RIU (refractive index unit) which is slightly small compared with that of theoretical calculation (5.56 nm/RIU). It may due to the SiO_2 thin film coating the ZnO microsphere. The degradation of the peak shift can be reduced with a thinner coating film.

4. References

[1] N.M. Hanumegowda, C.J. Stica, B.C. Patel, I. White, and X. Fan, "Refractometric sensors based on microsphere resonators," Appl. Phys. Lett. **87**, 201107 (2005).

[2] S. Pang, R.E. Beckham, and K.E. Meissner, "Quantum dot-embedded microspheres for remote refractive index sensing" Appl. Phys. Lett. **92**, 221108 (2008).

[3] K. Okazaki, T. Shimogaki, K. Fusazaki, M. Higashihata, D. Nakamura, and N. Koshizaki, "Ultraviolet whispering-gallery-mode lasing in ZnO micro/nano sphere crystal," Appl. Phys. Lett. **101**, 211105 (2012).

[4] S. Schiller and R. L. Byer, "Asimptotic expansino of morphological resonance frequencies in Mie scattering," Opt. Lett. **16**, 1138 (1991)

P-089

Numerical analysis of flow field during laser ablation process for formation of Si clusters

E.Ueno[1], N.Fukuda[2], H.Fukuoka[3], M.Yaga[4], I.Umezu[5], M.Han[6], T.Takiya[1]

[1] *Hitachi Zosen Corporation, 2-11, Funamachi 2-chome, Taisho-ku, Osaka, 551-0022, Japan*

[2]*Office of society-Academia Collaboration for Innovation, Kyoto University, Yoshida-Honmachi, Sakyo-ku, Kyoto, 606-8501, Japan*

[3]*Nara National collage of Technology, 22 Yata, Yamatokoriyama, Nara 639-1080, Japan*

[4]*Faculty of Engineering, University of the Ryukyus, 1 Senbaru Nishiura-cho, Nakagami-gun, Okinawa, 903-0213, Japan*

[5]*Department of Physics, Konan University, 8-9-1, Okamoto, Higashinada-ku, Hyogo, 658-8501, Japan*

[6] *Department of Materials Science and Engineering, Nanjing University, 22 Hankou Road, Nanjing 210093, China*

E-mail: eri_u@hitachizosen.co.jp

1. Introduction

Among many techniques to prepare clusters, pulsed laser ablation (PLA) under background gas is a good technique to acquire clusters with the desired size under strong a non-equilibrium state [1]. However spectroscopic observation of plume dynamics have little information on effects of shock waves on cluster formation. However, diffraction and reflection of shock waves are important for cluster formation and growth. In the present work, we perform numerical investigations about the flow field between the silicon target and substrate.

2. Numerical procedure

To solve the entire flow field in the closed space, it is necessary to know the state of vapor atoms of the target material in the vicinity of the outlet of the Knudsen layer under laser irradiation.

We assume that the original energy of the pulsed laser, E_{las}, can be divided into four terms as

$$E_{las}=E_{ref}+E_{evap}+E_{trans}+E_{ion} \quad (1)$$

Here, E_{ref} is the energy loss by surface reflection, E_{evap} is the energy expended for evaporation of the target material, E_{trans} is the energy given to translational movement of the vapor atoms, and E_{ion} represents the energy spent for ionization of the vapour atoms. The energy E_{evap} can be estimated under the assumption that the number of vaporization atoms is proportional to the logarithm of the effective laser fluence [2]. The distribution ratio of remaining energies is determined to balance the translational kinetic energy with the ionizing energy of the vapor atoms. Temperature and pressure at the outer boundary of Knudsen layer is obtained from the solution of the Boltzmann equation and is determined by Clausius-Clapeyron equation, respectively.

We use the one- and two-dimensional Eulerian equations for the governing equations. The equations were solved by a finite volume method using total variation diminishing (TVD) scheme. The third-order Runge-Kutta scheme was adopted for time integration in order to estimate the traveling shock wave interacting with the expanding plume and with the deposition substrate.

3. Results and Discussions

The results of two-dimensional analysis under the thermodynamic conditions are shown in Fig.1. In each figure, the top and bottom sides represent substrate and target, and the left and right side is the centerline of plume and the free surface, respectively. The left and right figures in (A) ~ (D) show gas pressure and cluster density, respectively. Elapsed times after laser irradiation are indicated at the left top of each figure. The accelerated cluster growth near the plume front is apparent due to the influence of the reflected shock wave in (D) of Fig.1.

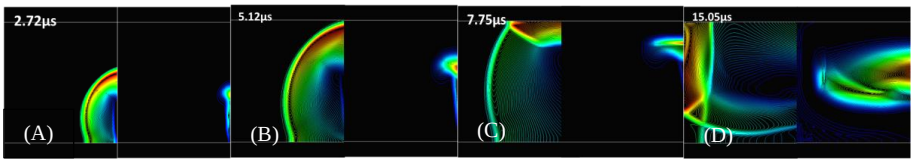

Fig. 1. Density distribution of shock wave and generated clusters (20mm×20mm)

4. Conclusions

We performed numerical investigations about the flow field in the closed space. The accelerated cluster growth near the plume front is apparent due to the influence of the reflected shock wave. Based on the results, we could confirm that growth of clusters is promoted by the influence of the reflected shock wave.

5. References

[1] Patrone, L.,Nelson, D., Safarov, V.I., Giorgio, S., Sentis, M. and Marine, W. “Synthesis and properties of Si and Ge nanoclusters” produced by pulsed laser ablation, Appl. Phys. A69 [Suppl.], S217-S221(1999)

[2] M.Stafe et al. in, *Pulsed Laser Ablation of Solids*, (Springer Verlag, Berlin, 2014).

P-090

Graphene resistance chip fabricated by ultraviolet laser beams for a high-sensitivity electrochemical impedance spectroscopy

S.F. Tseng[1], W.T. Haiso[1], C.K. Chung[1], P.Y. Cheng[2], Y.S. Lin[3], C.H. Chen[1], S.C. Chien[2]

[1]*Instrument Technology Research Center, National Applied Research Laboratories, Hsinchu 30076, Taiwan*

[2]*Department of Mechanical Engineering, National Chiao Tung University, Hsinchu 30010, Taiwan*

[3]*Department of Chemical Engineering, National United University, Miaoli 36003, Taiwan*

Corresponding author e-mail address: tsengsf@itrc.narl.org.tw

1. Introduction

An emulsion is a mixture of two immiscible liquids consisting of oil-in-water or water-in-oil [1]. The emulsion products include foodstuffs, cosmetics, paints, agrochemicals, pharmaceuticals and oils [2]. To estimate the stability of emulsion products is an important factory that not only can affect the appearance and safety of manufactures but also directly affect the safety and pleasure of consumer's purchase. Some of different inspection skills of emulsion stability were discussed, including machine vision, electrical conductivity, photodensitometry, droplet counting, light scattering, centrifugation and droplet lifetime [3-6]. Consequently, this study aims to develop graphene resistance chips of a high-sensitivity electrochemical impedance spectroscopy (EIS) used for helping the users to measure rapidly the stability of emulsion products. This instrument can record with parallel continuous real-time data during the dynamic behavior of phase change emulsion (PCE).

2. Experiments

The graphene-based multilayer films are coated on the glass substrate by the Mayer rod method. Figure 1 shows the schematic diagram of the ultraviolet laser (wavelength 355 nm) processing system combined with a XY-axis laser scanning system. This machined system can adjust laser parameters including the laser fluence, the pulsed repetition frequency, and the scanning speed of galvanometers to pattern the finger electrode structures on graphene films as the resistance chips. Figure 2 shows the schematic diagram of finger electrode structures of graphene resistance chips. The ablated gap of each finger electrode is 500 μm. The ablated line width and depth, edge quality, and three-dimensional (3D) topography of the patterned graphene films are observed and analyzed using a confocal laser scanning microscope. In addition, the reagent with only 0.3 mL volume can immediately use to inspect different types and concentrations of emulsions and to investigate the effects of the stability of emulsion products.

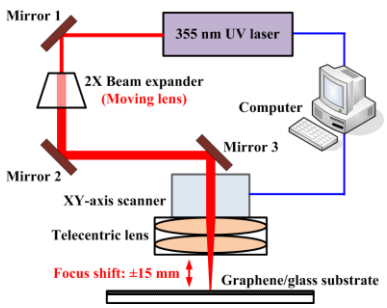

Fig. 1. The schematic diagram of the UV laser processing system.

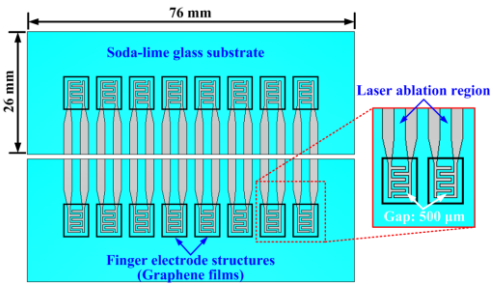

Fig. 2. The schematic diagram of graphene resistance chips.

3. Summary

This study presents the fabrication of graphene-based resistance chip by UV laser beams for a high-sensitivity electrochemical impedance spectroscopy. The finger electrode structures have a clear and uniform ablated depth and edge quality after the fast, maskless, and flexible laser processing by selecting optimal parameters. In the future, the developed instrument can deal with a great quantity of the requirements of emulsion products and can save the inspection time and the manpower cost.

4. References

[1] T. Sakai, "Surfactant-free Emulsions," Curr. Opin. Colloid Interface Sci. **13**, 228-235 (2008).

[2] B. P. Binks, *Modern Aspects of Emulsion Science*, ed., (Royal Society of Chemistry, Cambridge, 1998).

[3] Y. S. Lin, W. L. Chou, C. H. Yang, K. S. Huang, E. C. Wang, C. Y. Chen, Y. H. Lin, and H. M. Huang, "A Real-time Impedance-sensing Chip for the Detection of Emulsion Phase Separation," Phys. Rev. Lett. **34**, 1743-1748 (2013).

[4] J. Rao and D. J. McClements, "Food-grade microemulsions and nanoemulsions: Role of oil phase composition on formation and stability," Food Hydrocoll. **29**, 326-334 (2012).

[5] L. Doki, V. Krstonosic, and I. Nikoli, "Physicochemical characteristics and stability of oil-in-water emulsions stabilized by OSA starch," Food Hydrocoll. **29**, 195-192 (2012).

P-091

A Study on Laser Joining of Metal and Plastic

S.Kim[1], O.Kim[1], J.Oh[1], Y.Kim[1], H.Kim[2]
[1]*Laser Application Center, Kyungpook Nation University, 80 Daehak-ro, Buk-gu, Daegu, South Korea*
[2]*School of Electronics Engineering, Kyungpook Nation University, 80 Daehak-ro, Buk-gu, Daegu, South Korea*
E-mail: suspect3@knu.ac.kr

Recently, several researchers have studied about excellent properties of material. Furthermore, Researchers have been issued joining of heterogeneity materials that having different unique properties. Among joining of heterogeneity materials, joining technique of thermoplastics used generally using by low power of diode laser system. And, research to joining of plastic and metal have been studied these days.[1,2]

In existing method of bonding plastic, laser-beam is transmitted to the upper layer and lower layer absorbed laser-beam. And then, the absorbed laser-beam changes the heat energy and it characteristics strong bonding properties. However, when joining of metal and plastic, the joining force is weaker than the joining of plastic and plastic.[3-5]

So, we studied the joining characteristics and enhance adhesion of metal and plastic. First of all, we confirmed that a phenomenon of mutual between plastic and metal transmission joining The material used in the experiment is SUS(SUS316L) and PC(Polycarbonate). PC is thickness 5mm and have transmittance of 91%. SUS is thickness 2mm. Laser source has a wavelength of 1070nm, beam size 10mm, output power 79.57W. And the melting point(about 300℃) of the PC kept by adjustment of processing speed

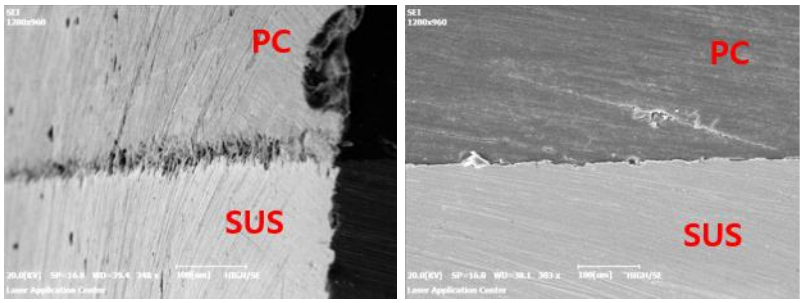

(a) joining image (b) joining section

Fig. 1 PC and SUS304 joining with a Diode Laser

In order to enhance excellent joining force, we experimented a number of ways such as reducing the gap between the each material, fine patterning surface of the SUS by femtosecond laser, surface texturing. So, the melted PC were tested to more sturdy attach to the joining surface of SUS.

[1] S. Katayama, Y. Kawahito, “Laser direct joining of metal and plastic”, Scripta Materialia, 59, 1247-1250(2008)
[2] K.W. Jung, Y. Kawahito, M. Takahashi and S.Katayama, “Laser direct joining of carbon fiber reinforced plastic to zinc-coated steel.”, Materials and Design, 47, 179-188(2013)
[3] M. Seo, K. Ryu and G. Nam, “Study on the laser transmission-welding of thermoplastics”, JKSPE. Vol 22. No. 9.(2005)
[4] A. Roesner, S. Scheik, A. Olowinsky, A. Gillner, U. Reisgen and M. Schleser, “Laser Assisted Joining of Plastic Metal Hybrids”, Physics Procedia, 12, 370-377(2011)
[5] X. Tan, J. Zhang, J. Shan, S. Yang and J. Ren, “Characteristics and formation mechanism of porosities in CFRP during laser joining of CFRP and steel”, Composites: Part B, 70, 35-43(2015)

P-093

Vanadium Oxide thin film preparation by PLD for Resistive switching memory In/VOx/Al

K. Takase[1], Y. Tanimoto[1], S. Kurumi[2], K. Suzuki[2]

[1]*Department of Physiscs, Science and Technology, Nihon University, 1-8 Kanda-Surugadai, Chiyoda-ku, Tokyo, 101-0062 Japan*

[2]*Department of Electrical Engineering, Science and Technology, Nihon University, 1-8 Kanda-Surugadai, Chiyoda-ku, Tokyo, 101-0062 Japan*

takase@shotgun.phys.cst.nihon-u.ac.jp

1. Introduction

Recently, next generation memories such as ferroelectric RAM (FRAM), phase change RAM (PRAM), magnetic RAM (MRAM), resistive change RAM (ReRAM) with non-volatility have been extensively studied due to the fast response speed. In ReRAM consisted of a sandwich structure (metal/insulator/metal), many combinations of metallic and insulating materials have been investigated. A Mott insulator, which is basically in a metallic state in "*one electron picture*", is a treasure house of physical properties, for example superconductivity, giant magnetoresistance, metal – insulator transition, because they are well controlled by electron correlations. With regard to application to ReRAM, a metal – insulator transition, which is not a classical thermodynamic phase transition but a quantum phase transition, has been expected due to their extremely fast response speed of the order of femtosecond [1]. When choosing a Mott insulator from many choices, it is very important for controlling electron correlation to select a material with small U/t, where U is a Coulomb integral and t is a transfer integral. In this study, we have focused on vanadium oxide with small U/t from Zaanen-Sawatzky-Allen phase diagram [2]. There are many phases in vanadium oxides. For a practical application, an insulating state at room temperature is, of course, required in the high temperature phase. So, VO_2, V_2O_5 are our targets. In this study, we have tried phase control of vanadium oxides using pulsed laser deposition (PLD) with oxygen gas and fabricated an In/VO_x/Al ReRAM which can be operated at room temperature.

2. Experimental

VO_x was prepared using PLD with oxygen gas on an Al metal substrate, where an ablation source was a Nd:YAG laser with wavelength = 355 nm and laser fluence = 1.2 J/cm^2, a background pressure was 10^{-3} torr, and an oxygen flow rate was 500 sccm. The substrate temperature was kept to 390 °C. X-ray diffraction (XRD) measurement was carried out to evaluate the phase of the deposited oxide thin film. Indium metal as the top electrode was attached on the VO_x surface. The current – voltage (I - V) characteristics were measured by a conventional two-probe method at room temperature, where the current was limited to 1 mA in a "SET" process, switching from a high resistance state to a low resistance state, to guard a device from a complete dielectric breakdown.

3. Results and Discussions

XRD profiles consist of peaks from V_2O_3 with others and they are different from our target materials. The I - V characteristics measured by a mono-polar operation using a voltage sweep mode indicate clear switching behaviors. The initial state of this capacitor is a high resistance state (insulating state). This means that the composition ratio deviates from V_2O_3 due to the existence of other impurity phases because the high temperature state of pure V_2O_3 at room temperature is a metallic state. At the threshold voltage (SET voltage), the resistance state changes to a low resistance state (metallic state). Once the bias voltage returns to zero and applying again without a current limit, the current increase with bias voltage, following to Ohm's law and drops off suddenly at another threshold voltage (RESET voltage). In this way, our capacitor which could endure 110 times I - V tests indicates non-volatile properties in the I - V characteristics.

We will show the other results for samples prepared under different conditions and discuss the sample preparation and the switching properties of our ReRAM on the day.

7. References

[1] S. Iwai, M. Ono, A. Maeda, H. Matsuzaki, H. Kishida, H. Okamoto, and Y. Tokura, Phys. Rev. Lett. 91, 057401 (2003).

[2] J. Zaanen, G. A. Sawatzky and J. W. Allen, Phys. Rev. Lett. 55, 418 (1985).

P-094

Property of the hyperthermal CO_2 beam formed by a laser-detonation facility for space environmental effect studies in upper Martian atmosphere

M. Tagawa, A. Hatsuda, K. Yokota
Kobe University, Rokko-dai 1-1, Nada, Hyogo 657-8501, Japan
E-mail: tagawa@mech.kobe-u.ac.jp

1. Introduction

Hyperthermal collisions of molecule in upper atmosphere of planets severely affect spacecraft materials. On Earth, O-atom, which is dominant upper atmospheric species in the altitude of 200–800 km, is widely recognized as a major origin of material erosion. For simulating material erosion phenomena in the ground-based facility, acceleration of electrically neutral O-atom is achieved by using pulsed CO_2 laser [1]. On the other hand, hyperthermal collision of CO_2 could lead to material degradation in upper Martian atmosphere. CO_2 is chemically inert compared to O-atom; however, collision energy of CO_2 in the beginning of aerobraking phase is greater than that in the low Earth orbit (LEO). For simulating this event in the Earth-based facility, acceleration of CO_2 over 8 km/s is needed. We have attempted to form hyperthermal CO_2 beam in our laser-detonation facility and analyze the basic beam formation properties.

2. Apparatus

The laser detonation atomic beam source used in this study is reported in the companion paper [1]. However, gas mixture system was not used in this study and 99.8% CO_2 gas was used as target gas. The hyperthermal CO_2 beam was characterized by a time-of-flight (TOF) distribution measured by a quadrupole mass spectrometer (QMS) with a scintillation detector that is installed in the beam-line. Translational energies of the species in the beam were calculated using TOF distributions with the flight length of 238 cm. On the other hand, composition of the beam was analyzed from the area intensity of the TOF-QMS spectra with considering relative ionization cross-sections.

3. Results and Discussion

A similar experiment related to energy accommodation of CO_2 molecule was performed in NASA/JPL in 1995, which was published in 2004 [2]. In this study CO_2 beam at 12 eV (7.4 km/s) was formed, however, the CO_2 fraction was as low as 40%. It was not an ideal pure CO_2 beam, however, the energy accommodation of CO_2 was not affected by the other components in the beam, thus, the accurate experiment on the energy accommodation could be performed with this beam. However, the other components, especially high-energy or chemically active species, could affect the material degradation phenomena. Therefore, precise beam characterization including impurity analysis was carried out in this study. As a result, it was analyzed that the CO_2 fraction in the beam was 44% at the translational energy of 3.5 eV and 30% at 5.4 eV. The other components observed in the beam were C, O, CO and O_2. These species were formed by the decomposition of CO_2 molecule in the laser plasma. The experimental results clearly indicated that the pure CO_2 beam, which is required to material degradation simulations in upper Martian atmosphere, is difficult to form by the current laser-detonation facility. A new idea for prevent decomposition of CO_2 molecule in the laser-induced plasma in nozzle is needed.

4. Conclusions

Hyperthermal CO_2 beam formed by the laser-detonation source was analyzed by the TOF-QMS system. Decomposition of CO_2 molecule in the laser-induced plasma produced C, O, CO and O_2 impurities in the beam as high as 60%. Such high-energy or chemically active species could affect the results on material degradation during exposure. A method to restrict the decomposition of CO_2 molecule in the nozzle should be developed for future space environmental studies in Martian or Venusian atmosphere.

Acknowledgments

A part of this study was supported by the Grant-in-Aids for Scientific Research from JSPS contract Nos. 25289307 and 26289322; and also by the joint research project of the Institute of Laser Engineering, Osaka University. A support through the Coordination Funds for Promoting Aerospace Utilization from the MEXT, Japan is also appreciated.

References

[1] K. Yokota, K. Ide, J. Ohira, Y. Yamasaki, K. Morimoto, H. Asada, M. Tagawa, " Laser-detonation facility for acceleration of gaseous materials: etching and deposition of solid materials," COLA2015, (2015) companion paper.

[2] T. K. Minton, M. Tagawa, G. M. Nathanson, "Energy accommodation in hyperthermal gas-surface collisions: relevance to aerobraking in planetary atmospheres," J. Spacecraft Rockets, **41**, 3 (2004) 389-396.

P-095

Luminescence properties of Pulsed Laser Deposited $Y_2O_3:Bi^{3+}$ thin films

R. M. Jafer[1,2] , A Yousif [1,2], E Coetsee[1], OM Ntwaeaborwa[1], HC Swart[1]

[1] *Department of Physics, University of the Free State, P.O. Box 339, Bloemfontein, ZA 9300, South Africa.*

[2]*Department of Physics, Faculty of Education, University of Khartoum, P.O. Box 321, Postal Code 11115, Omdurman, Sudan.*

Corresponding Author e-mail address: swarthc@ufs.ac.za

1. Introduction

Pulsed laser deposition (PLD) is a reliable method to fabricate oxide thin films, with the major advantage of the material being stoichiometry transferred from a multi-component ablation target to a growing thin film [1]. However, it is well known that such favourable results do not occur under all experimental conditions [2]. Therefore different deposition parameters for each kind of material need to be optimized to get the films with the desired properties. Parameters that may play a role are the ambient atmosphere, substrate temperature, laser pulse energy density and pulse repetition rate. $Y_2O_3:Bi^{3+}$ thin films have been deposited at 300 °C on Si (100) substrates using the PLD technique with an energy density of 38 mJ/cm^2. The influence on the film structure, morphology and optical properties of different background deposition atmospheres (base, O_2, and Ar pressure) were investigated.

2. Results

Cubic and monoclinic phases of Y_2O_3 were observed, with X-ray diffraction (XRD), that have preferential orientations of (222) and (003) respectively. The brightest emission was observed from the film which was deposited in the O_2 ambient pressure, fig. 1 (a), indicating that O_2 was the best ambient atmosphere for growing the $Y_2O_3:Bi^{3+}$ thin films. The photoluminescence (PL) of cubic Y_2O_3: Bi^{3+} phosphor powder shows broad spectra that range from 375 nm to 650 nm with a maximum at 495 nm. This peak consisted of three emission bands in the blue and green regions. All peaks are related to the $^3P_1$–$^1S_0$ transition of the Bi^{3+} ion situated in a monatomic cluster placed on the two sites with S_6 and C_2 symmetry of the Y_2O_3 matrix [3]. But the interesting observation was the emission spectra of the Y_2O_3: Bi^{3+} thin film phosphor. A shift of the green emission from 495 nm to ~ 460 nm as well as the variation of the intensities of the PL spectra was recorded. It is well known, that Bi^{3+} ions are commonly used to probe host characteristics due to their luminescence that is highly sensitive to the coordination of the activator site [4]. Therefore, these observations maybe linked with the change in the structure that was observed with XRD measurements. The existence of two crystal phases of Y_2O_3 (cubic and monoclinic), caused a change in the environment around the Bi^{3+} ion which has an impact on the luminescence emission position of Bi^{3+}. The surface roughness, grain shape and size were influenced by the deposition environment. Fig. 2 shows an example of the Atomic Force Microscopy (AFM) image of one of the O_2 samples.

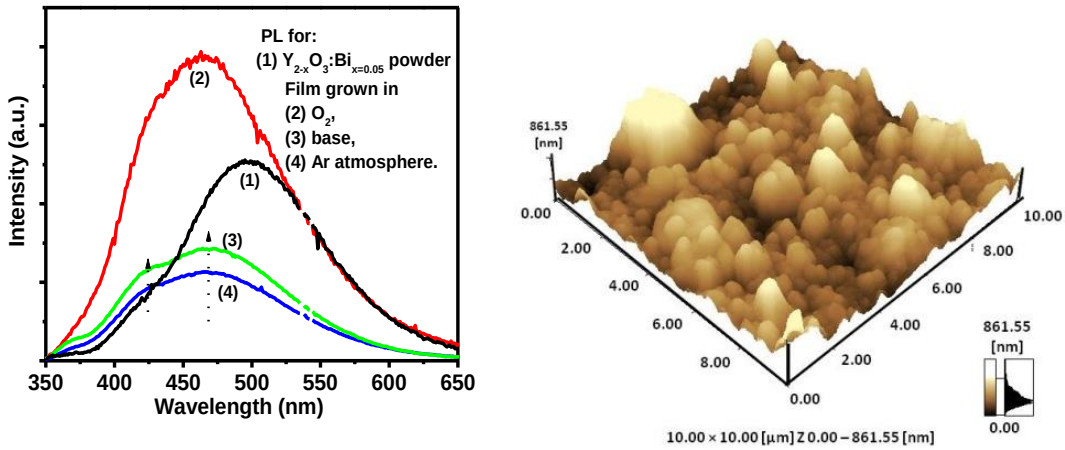

Fig. 1. (a) PL spectra upon a 325 nm He-Cd laser excitation of $Y_{2-x}O_3:Bi_{x=0.005}$ of (1) powder, and (2), (3) and (4) for the thin film deposited in O_2, base and Ar pressure. (b) AFM image of the O_2 sample.

3. References

[1] S. Acquaviva , E. D'Anna , M.L. De Giorgi, M. Fernandez, A. Luches, G. Majni, S. Luby, E. Majkova, "Transfer of stoichiometry during pulsed laser ablation of multicomponent magnetic targets", *Appl. Surf. Sci*. **248,** 286 (2005).

[2] A. Yousif, H.C. Swart, O.M. Ntwaeaborwa, "Improved luminescence properties of pulsed laser deposited $Y_3(Al,Ga)_5$:Tb thin films by post deposition annealing", *J. of Lumin.* **143,** 201 (2013).

[3] R. M. Jafer, E. Coetsee, A. Yousif, , R.E. Kroon, O.M. Ntwaeaborwa, H.C. Swart, "X-ray Photoelectron Spectroscopy and luminescent properties of $Y_2O_3:Bi^{3+}$ phosphor", *Appl. Surf. Sci. doi:10.1016/j.apsusc.2015.01.009*.

[4] A. Yousif, Vinod Kumar, H. A. A. Seed Ahmed, S. Som, L. L. Noto, O. M. Ntwaeaborwa, H. C. Swart, "Effect of Ga^{3+} doping on the photoluminescence properties of $Y_3Al_{5-x}Ga_xO_{12}:Bi^{3+}$ phosphor", *ECS J. of Solid State Sci. and Techn.* **3 (11),** R222 (2014).

P-096

Flexible Transparent ZnO Thin-Film Transistors by Pulsed Laser Deposition

Y. Sun, K. Ashida, T. Maemoto, S. Sasa
Nanomaterials Microdevices Research Center, Osaka Institute of Technology
5-16-1 Omiya, Asahi-ku, Osaka 535-8585, Japan
E-mail: d1d14301@st.oit.ac.jp

Flexible and transparent electronic devices such as an electric circuit and a display have been attracting much attention recent years. In these electronic devices, thin film transistors (TFTs) are very important part for controlling the flow of electric current. Amorphous oxide semiconductors are focused as a material to a development of a transparent and flexible devices. Zinc-oxide (ZnO) based devices have been reported by our groups so far [1] because it is a transparent electrode material of low cost and having extremely low toxicity. We reported fully transparent ZnO-TFTs by using Al-doped ZnO (AZO) low resistivity electrodes on glass substrates and a transconductance (g_m) of 150 μS/mm and ON/OFF ratio of 6.6×10^6 were obtained [2]. In this work, we report the fabrication and characterization of transparent ZnO-TFTs on flexible plastic substrates by pulsed laser deposition (PLD).

Figure 1 shows a schematic diagram of a fabricated ZnO-TFT. SiO_2 thin-films as a buffer layer between ZnO-TFTs and polyethylene naphthalate (PEN) substrates were grown by electron beam physical vapor deposition. 40 nm thick ZnO channel layers and 100 nm thick HfO_2 gate insulators, 100 nm thick AZO electrodes of ZnO-TFTs were grown by PLD. A Nd:YAG laser (4^{th} harmonic, 266 nm) was used for ablation of the oxide material ceramic at room temperature. All fabrication process were under 100 °C. Figure 2 shows the photomicrograph of fabricated ZnO-TFTs and the devices are hard to identify visually by eyes. We characterized the fabricated transparent ZnO-TFTs. Figure 3 shows the typical output characteristics of a 3 μm length gate (L_G) device. The device had a g_m of 252 μS/mm and an ON/OFF ratio of 5.6×10^5. From these results, we succeeded in fabricating the fully transparent ZnO-TFTs on PEN substrates and the characteristics can be comparable with the ZnO-TFTs on glass substrates. The ZnO-TFTs were also characterized in bending states. Figure 4 shows the characteristics of a bending ZnO-TFT. We started the measurement with the flat state, then the radius of a curvature is changed to 5 mm, and finally returned to the flat state again. The g_m and ON/OFF ratio decreased after bending, however the g_m recovered after returning the state.

[1] Y. Kimura et al., Jpn. J. Appl. Phys. 52, 06GE09 (2013).
[2] Y. Sun et al., IEEE Xplore, DOI: 10.1109/IMFEDK.2014.6867064 (2014).

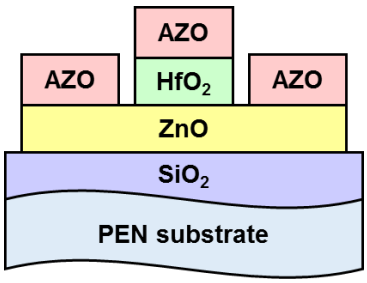

Fig. 1. Schematic diagram of fabricated ZnO-TFT on PEN substrate.

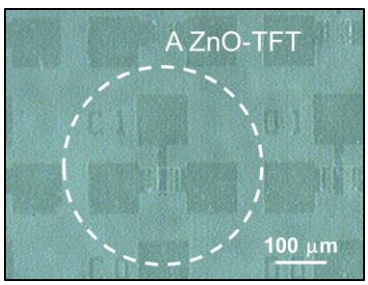

Fig. 2. A photomicrograph of a transparent ZnO-TFT.

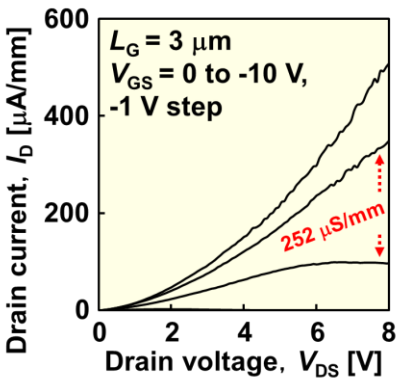

Fig. 3. Output characteristics of the ZnO-TFT.

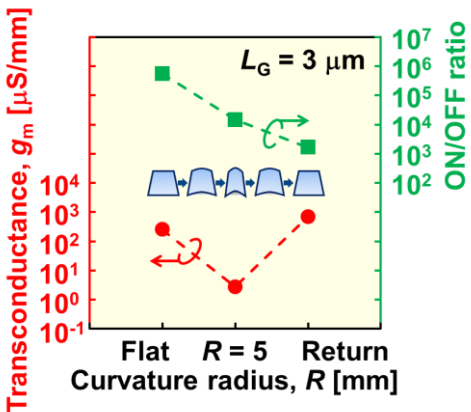

Fig. 4. Effect of bending radius.

P-097

Atomistic simulation of surface modification by laser pulse: comparison of models with various scales

S. Starikov, V. Pisarev
Joint Institute for High Temperatures of RAS, Moscow 125412, Russia
E-mail: starikov@ihed.ras.ru

Over the past years, the experimental works focus on nonlocal character of the surface modification by laser pulse. Now it is clear that all irradiated surface is involved in the modification process. The complete description of the experimental data may be given by the full-scale atomistic simulation of such process with micrometer-length scales in all three dimensions (3D-simulation). In this work the femtosecond laser pulse modification of surface is studied for aluminium (Al) and gold (Au) by use of two-temperature atomistic simulation [1-3]. The results are obtained for various atomistic models with different scales: from pseudo-one-dimensional to full-scale three-dimensional atomistic simulation. The surface modification after laser irradiation can be caused by ablation and melting. At low energy of laser pulse, the nanoscale ripples on surface may be induced by the melting without laser ablation. In this case the nanoscale changes of the surface are due to the splash of molten metal under temperature gradient. The laser ablation occurs at a higher pulse energy when a crater is formed on the surface. There are essential differences between Al ablation and Au ablation. The swelling and voids formation as the first step at the shock-wave-induced ablation are obtained for both metals. However, the simulation of ablation in gold shows existence of additional nonthermal type of ablation which is associated with electron pressure relaxation. This type of ablation takes place at surface layer, at a depth of several nanometers and does not induce swelling.

[1] G. Norman, S. Starikov, V. Stegailov, P. Zhilyaev and I. Saitov "Atomistic modeling of warm dense matter in the two-temperature state" Contrib. Plasma Phys. **53**, 129 (2013).

[2] S. Starikov, A. Faenov, T. Pikuz, I. Skobelev, V. Fortov et al, "Soft picosecond X-ray laser nanomodification of gold and aluminum surfaces" Appl. Phys. B. **116**, 1005 (2014).

[3] V. Pisarev and S. Starikov "Atomistic simulation of ion track formation" J. Phys.: Condens. Matter. **26**, 475401 (2014).

P-098

Growth of $Sr_xBa_{1-x}Nb_2O_6$ and Ca-doped $Sr_xBa_{1-x}Nb_2O_6$ thin films on MgO and Nb:$SrTiO_3$ substrates by PLD and RF-PLD technique

G. Stanciu[1, 2], N. D. Scarisoreanu[1], R. Birjega[1], V. Ion[1], A. Andrei[1], M. Dinescu[1]

1. *National Institute for Lasers, Plasma and Radiation Physics, Magurele, Romania 077125*
2. *University Politehnica of Bucharest, Faculty of Applied Chemistry and Material Science, Bucharest, Romania, 011061*

E-mail: dinescum@nipne.ro

Pulsed laser deposition (PLD) and radio-frequency assisted pulsed laser deposition (RF-PLD) have been used to growth highly textured ferroelectric SBN thin films with different Sr/Ba ratio, undoped and Ca-doped. Pure SBN and Ca-doped ceramic targets were first prepared by solid-state reaction method using pure reagent $SrCO_3$, $BaCO_3$, $CaCO_3$ and Nb_2O_5 powders as starting materials. (001) MgO and Nb:$SrTiO_3$ have been used as substrates for films deposition. Morphological and structural properties characterization of SBN/SCBN layers were performed by Atomic Force Microscopy and X-ray diffraction while the optical properties (refractive index and extinction coefficient) were measured by spectroellipsometry. Studies on the influence of Ca dopant and of Sr/Ba ratio on ferroelectric characteristics were carried out.

Keywords: SBN, Ferroelectric, Thin films, PLD, RF-PLD

Acknowledgements: This work has been funded by the Sectoral Operational Programme Human Resources Development 2007-2013 of the Ministry of European Funds through the Financial Agreement POSDRU/159/1.5/S/132397.

P-099

Picosecond pulsed laser deposition process of porous ceramic coating for Li-ion battery separator film

V. Kekkonen, S. Chaudhuri, F. Clarke, J. Kaisto, J. Liimatainen, J. Piirto, M. Siltanen, A. Zolotukhin
Picodeon Ltd Oy, Piisilta 1, FI-91100 Ii, Finland
E-mail: ville.kekkonen@picodeon.com

Pulsed laser deposition (PLD) is well-known for its versatility and ability to produce thin-film coatings of high-quality and with tailored properties. The process enables deposition of a wide variety of materials, is able to preserve stoichiometry in material transfer, provides good adhesion between the coating and the substrate, and can be done at room temperature. Furthermore, the properties of the coating can be adjusted by controlling the laser parameters affecting the ablation process, by controlling the environment in the deposition chamber affecting the material transfer from target to substrate, and by controlling the substrate conditions affecting the growth of the material layer on the substrate. With these advantageous features of the process, it is possible to produce coatings for many different applications. However, PLD technology has not really expanded from laboratory-scale materials research and has not yet been utilized in large scale industrial production.

Picodeon Coldab® PLD platform with special scanning technology enables production rates and scalability which are required for high volume industrial production. In addition to the general advantages of conventional PLD, Coldab® ultra-short PLD process offers continuous material flow and low thermal budget processing through high pulse repetition rate and ultra-short (<10 ps) laser pulses.

Because of the ever-growing need for energy storage, there is a demand for solutions to improve the performance and safety of batteries. Separator film used in lithium-ion batteries is a high-volume product where the specific features of Coldab® coating process can be applied to produce a coating which improves the properties and performance of the product. The separator film is a porous polymer membrane separating the anode and the cathode in lithium-ion batteries at the same time allowing the Li-ions pass through. In order to improve the safety, stability, and longevity of the batteries, the separator film needs to be coated with a porous ceramic layer which provides additional mechanical support and thermal stability but does not affect the passage of ions through the separator. In Picodeon's process, a microporous AlO_x layer, specifically designed for the separator-film application, is deposited on the polymer membrane with good adhesion. The microstructure of the AlO_x is shown in Fig. 1.

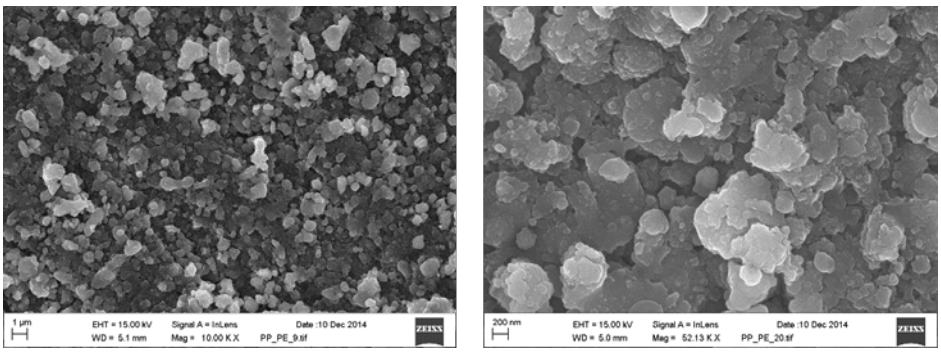

Fig. 1. Surface SEM images of the porous AlOx coating for a separator film of a Li-ion battery show that the layer consists of flakes with diameter of the order of 1 µm. In the image on the left-hand side, the magnification is 10k, and on the right-hand side, the same coating is shown with 50k magnification.

Thanks to the low thermal budget of the process, the coating can be applied without damaging the polymer membrane. Analysis results show that the properties of the coated membrane (ionic resistivity, permeability, and thermal and mechanical performance) are able to give the batteries the expected improvement in performance. In addition, roll-to-roll compatibility and high production rate of Picodeon's Coldab® process enable straightforward scaling of the process to industrial production.

P-100

Pulsed Laser Deposition of absorber and buffer layer for thin-film earth-abundant solar cells

Andrea Cazzaniga[1], Rebecca Bolt Ettlinger[1], Stela Canulescu[1], Nini Pryds[2] and Jørgen Schou[1,*]
[1]*DTU Fotonik, Technical University of Denmark, 4000-DK, Roskilde, Denmark.*
[2]*DTU Energy Conversion, Technical University of Denmark, 4000-DK, Roskilde, Denmark.*

E-mail: josc@fotonik.dtu.dk

Abstract

Cu_2ZnSnS_4 (CZTS) is a promising absorber layer for thin-film solar cells with a direct bandgap at 1.5 eV, a high absorption coefficient $>10^5 cm^{-1}$ and an estimated efficiency of about 27 % [2]. Its structure is very similar to that of $CuIn_xGa_{1-x}Se_2$ (CIGS), which is now a mature material for thin-film solar cells with an efficiency of 21 %. However, In and Ga in the CIGS solar cells are rare elements, and in addition, Ga can be considered as a toxic material. Therefore, earth-abundant and non-toxic alternative materials are needed such as CZTS, for which the current record solar cell efficiency is 8.4 % when combined with a CdS buffer layer [2]. Why the achieved efficiency is so much lower than the expected maximum, is not clear [1]. One likely reason is recombination at the interface between absorber and buffer layer, namely the heterojunction between the CZTS and CdS layer. Here we investigate the use of ZnS as alternative buffer layer to CdS. The ZnS layer (60 nm thick) and the CZTS layer (600 nm thick) are deposited in the same run with sequential Pulsed Laser Deposition (PLD). An advantage of using PLD is the possibility of depositing both CZTS and ZnS at a substrate temperature of 300 °C, which is the optimum temperature for depositing the CZTS layer. (By using using evaporation techniques the sticking coefficient of ZnS at 300 °C is very low). Moreover, ZnS is very stable at high temperatures compared to CdS, so an annealing treatment in a sulfurized atmosphere can be subsequently performed to improve both the crystallinity of the CZTS layer and the electrical contact at the interface. We will compare the electrical properites of the CZTS/ZnS heterojunction made with sequential-PLD with a similar structure where ZnS is deposited with a standard chemical solution process. The films produced with PLD are deposited under high vacuum ($p < 10^{-6}$ mbar) using a KrF excimer laser at 248 nm with 26 ns pulse width. The targets are made of sintered powder with the Cu_2ZnSnS_4-stoichiometry. Subsequently the films will be annealed in sulfurized atmosphere at 550 °C after deposition. The preparation of the films can be handled easily, since the Cu_2ZnSnS_4 layer requires 1 hour deposition at 10 Hz (500 – 600 nm) and the ZnS layer 5 minutes deposition at 10 Hz (50 – 100 nm). The j-V curve of the full solar cells made on Mo-coated SLG will also be presented.

[1] S. Siebentritt, Thin Solid Films 535, 1-4 (2013)
[2] B. Shin, O. Gunawan, Y. Zhu, N.A. Bojarczuk, S.J. Chey, S. Guha, Prog. Photovolt. Res. Appl. 21, 72 (2013).

P-101

Small band-gap thin film of doped and pure BiFeO3 obtained by pulsed laser deposition for photovoltaic and photocatalytic applications.

V. Ion [1], N.D. Scarisoneanu[1], A. Andrei [1], R. Birjega[1], A.I. Bercea [1, 2] M. Dinescu [1]

[1] National Institute for Laser, Plasma and Radiation Physics, 409 Atomistilor, Magurele, Romania;
[2] University of Bucharest, Faculty of Physics, 405 Atomistilor St, RO-077125, Magurele, Romania
E-mail address: nicu.scarisoreanu@inflpr.ro

The perovskite materials with a small band gap value such as bismuth ferrite (BiFeO3- BFO) have become very attractive for photovoltaic and photocatalytic applications. BFO exhibit both ferroelectric and ferromagnetic properties with a high remnant ferroelectric polarization (95 μC/cm2) and Curie temperature (Tc~1103 K). The band gap value of BiFeO3 (Eg~2.71 eV) corresponds to the maximum absorptivity at visible wavelengths and, if doped with Yttrium or Lanthanum, the band gap value can be decreased even more. In this work, BFO and La, Y-doped BFO thin films were deposited using pulsed laser deposition method (PLD) on various substrates. The purpose of this study was to obtain thin films of La, Y- doped BFO with small values of the band gap and to evaluate their photocatalytic applications. A parametric study on the influence of the substrate and substrate temperature during deposition on the properties of the La, Y- doped BFO thin layer was carried out. The band gap values (Eg) of the films were determined by spectroscopic ellipsometry (SE) and the structural features by X-ray diffraction (XRD) and transmission electron microscopy (HR-TEM). The local piezoelectric response, multiferroic and photocatalytic properties of the BFO and La, Y-doped BFO thin films have been studied using PFM, magnetoresitive and dielectric/ferroelectric spectroscopy.

P-102

Dielectric properties enhancement in epitaxial BCZT thin films with nanoscale strain domains.

N.D. Scarisoreanu[1], F. Craciun[2], V. Ion[1], R. Birjega[1] and M. Dinescu[1]

[1] *National Institute for Laser, Plasma and Radiation Physics, 409 Atomistilor, Magurele, Romania*
[2] *CNR-ISC, Istituto Dei Sistemi Complessi, Via del Fosso del Cavaliere 100, Rome, Italy*
E-mail address: nicu.scarisoreanu@inflpr.ro

Lead-free $(Ba_{1-x}Ca_x)(Zr_yTi_{1-y})O_3$ (BCZT) bulk materials exibit similar piezoelectric and ferroelectric properties with lead-based materials such as $Pb(Zr_xTi_{1-x})O_3$ (PZT). These superior properties are due to the existence of a triple point of morphotropic phase boundary (MPB) were the enhancement of electrical or mechanical responses appears. We report on the electrical and structural properties of epitaxial strained thin films of BCTZ with composition around MPB. The BCTZ thin films were deposited using pulsed laser deposition method (PLD) on SrTiO3, LaAlO3 and GdScO3 substrates. The thin films structural features and induced microstrain due to the lattice misfit between the pseudocubic lattice parameter of BCTZ and the used substrates were studied by X-ray diffraction (XRD) and high resolution transmission electron microscopy (HR-TEM). The dielectric properties (relative permittivity of about 2200 and tangent loss ~ 1-1.5% at frequency of 10 KHz) have been obtained by dielectric spectroscopy. The local piezoelectric properties (d33~280 pm/V), polarization dynamics and switching characteristics of the samples were investigated by piezoresponse force microscopy technique (PFM).

P-103

Spectrum of laser light scattered by nanoparticles in ablation-induced cavitation bubble

Koichi Sasaki and Masato Takeuchi
Division of Quantum Science and Engineering, Hokkaido University, Kita 13, Nishi 8, Kita-ku, Sapporo 060-8628, Japan
sasaki@qe.eng.hokudai.ac.jp

1. Introduction

In a previous work, we carried out an experiment of laser light scattering around a cavitation bubble induced by laser ablation in water [1]. As a result, we detected the scattered laser light from the region corresponding to the inside of the cavitation bubble. This experimental result indicates that the inside of the cavitation bubble is the reaction field for the growth of nanoparticles in liquid-phase laser ablation. In addition, it was observed that nanoparticles were stored inside the cavitation bubble until its collapse. Since the cavitation bubble had a high temperature and a high pressure at the collapse [2], the structure of nanoparticles was affected by the dynamics of the cavitation bubble [3,4]. In this work, we measured the spectrum of scattered laser light to examine "the qualitative evolution" of nanoparticles in liquid-phase laser ablation.

2. Experiment

A titanium target was installed in a vessel which was filled with distilled water. The target was irradiated by the focused beam of an Nd:YAG laser (532 nm) from the normal direction. Another Nd:YAG laser (532 nm) was used for the light scattering experiment. The YAG laser beams for scattering were injected into the ablation area from the parallel direction to the target surface at various delay times after the irradiation of the YAG laser pulse for ablation. The distance between the target surface and the YAG laser beam for scattering was roughly 1 mm. The scattered laser light was focused onto the entrance slit of a triple-grating spectrograph. The triple-grating spectrograph was composed of three diffractive gratings with 1800 grooves/mm, a Rayleigh block, an intermediate slit, and a charge-coupled device camera with an image intensifier (an ICCD camera). The Rayleigh block worked as a sharp notch filter at the laser wavelength, so that the intense light at the laser wavelength, which was caused by Rayleigh/Mie scattering and unexpected scattering on optical components, was eliminated efficiently. The spectrum of the scattered laser light around the laser wavelength was measured with the help of the triple-grating spectrograph. The ablation space was also illuminated by an expanded cw laser beam at 532 nm from the opposite direction to the optical path which connected the ablation point and the triple-grating spectrograph. The triple-grating spectrograph with widely opened slits connected the cw laser and the ICCD camera, and we captured the shadowgraph image of the cavitation bubble by using the same optical alignment as that in the laser light scattering experiment. The image of the scattered laser light was also captured using the ICCD camera of the triple-grating spectrograph by removing the Rayleigh block and by opening the slits widely.

3. Results and discussion

When the target was not irradiated by the YAG laser beam for ablation, the spectrum of the scattered laser light coincided well with the spectrum of Raman scattering of liquid water. When the target was irradiated by the YAG laser pulse for ablation, we detected the image of the scattered laser light in the region corresponding to the cavitation bubble. This means that the experimental result reported in the previous paper [1] was reproduced in the present experimental apparatus. We measured the spectrum of the scattered laser light by placing the Rayleigh block and by narrowing the slits of the triple-grating spectrograph. At a short delay time of 100 μs after the irradiation of the ablation laser pulse, we observed the disappearance of the Raman spectrum of liquid water in the region corresponding to the cavitation bubble, and detected no scattered laser light in the shifted wavelength region from the laser wavelength. The disappearance of the Raman spectrum of liquid water is reasonable since liquid water is kicked out by the cavitation bubble. On the other hand, the negligible scattered laser light in the shifted wavelength region indicates that the laser light scattered by nanoparticles in the cavitation bubble had a negligible Raman shift. This suggests that nanoparticles at this delay time are metallic. We detected scattered laser light in the shifted wavelength region from the laser wavelength at a delay time of 200 μs, suggesting the oxidation of nanoparticles. However, we observed no clear peaks in the spectrum of the scattered laser light, which suggested the amorphous structure of oxidized nanoparticles. Although nanoparticles collected after this experiment showed Raman peaks of TiO_2, we could not identify the delay time for the change in the structure from amorphous to crystalline in the present experiment.

[1] W. Soliman, N. Takada, and K. Sasaki, Appl. Phys. Express **3**, 035201 (2010).
[2] W. Soliman, T. Nakano, N. Takada, and K. Sasaki, Jpn. J. Appl. Phys. **49**, 116202 (2010).
[3] N. Takada, A. Fujikawa, N. Koshizaki, and K. Sasaki, Appl. Phys. A, **110**, 835 (2013).
[4] W. Soliman, N. Takada, N. Koshizaki, and K. Sasaki, Appl. Phys. A, **110**, 779 (2013).

P-104

NaCl thin films obtained by pulsed laser deposition

C. Sánchez-Aké[1], E.V. Mejía-Uriarte[1], D.R. Acosta[2]

[1] Centro de Ciencias Aplicadas y Desarrollo Tecnológico, Universidad Nacional Autónoma de México, Apartado Postal 70-186, México D.F., C.P. 04510, México

[2] Instituto de Física, Universidad Nacional Autónoma de México, Apartado Postal 70-186, México D.F., C.P. 04510, México

E-mail: citlali.sanchez@ccadet.unam.mx

Crystalline insulating thin films are promising substrates to support nanostructures when it is necessary to reduce charging effects with the support. For example, this kind of materials can be used in systems where the ultra-thin film acts as a tunnel barrier improving the performance of a device [1]. Moreover, crystalline and insulating films have been also used to control the growth of oriented metal nanocrystals and nanoparticles [2]. Most of the materials used to support and electronically isolate nanostructures for technological applications are crystalline oxide and alkali halides thin films. However, crystalline oxide thin layers are usually oxygen deficient. Alkali halides thin films have been deposited mainly by evaporation in Knudsen effusion cells since this technique allows growing ultra thin films crystalline oriented [3].

There are few previous reports of alkali halides films grown by pulsed laser deposition (PLD) technique even though this method has been used successfully for deposition of other cubic materials. Arieta et al. [4] deposited polycrystalline films by PLD on glass and silicon substrates founding that the crystalline orientation strongly depends on the substrate. However to our knowledge, there are no other studies of the effect of the background pressure on the crystallinity of NaCl films and the formation of the film increasing the number of laser pulses. We report the epitaxial growth of NaCl films on silicon and glass substrates by PLD. The structure of the films was characterized by X-ray diffraction and their morphology was studied by scanning electron microscopy. The effects of Ar background pressure on the crystallinity of the films have been investigated. The evolution of the film growth was also studied. Our results prove that PLD is suitable to grow oriented crystalline NaCl layers of micrometer dimensions.

[1] A. Tekiel, J. Topple, Y. Miyahara, P. Grütter, "Layer-by-layer growth of sodium chloride overlayers on an Fe(001)-p(1x1)O surface", Nanotechnology **23**, 505602 (2012).

[2] X. Sun, M.P. Felicissimo, P. Rudolf, F. Silly, "NaCl multi-layer islands grwon on Au (111)-(22x√3) probed by scanning tunneling microscopy", Nanotechnology **19**, 495307 (2008).

[3] M. Pivetta, F. Patthey, M. Stengel, A. Baldereschi, W. D. Schneider, "Local work funstion Moiré pattern on ultrathin ionic films: NaCl on Ag (100)", Phys. Rev. B **72**, 115404 (2005).

[4] A. Arieta, S. Mera, R. Diamant, M. Fernández-Guasti, R. Sosa, L. Escobar-Alarcón, A.F. Muñoz, E. Haro-Poniatowski, "Synthesis and caharacterization of sodium chloride thin films obtained by pulsed laser deposition", Appl. Phys. A **69**, S491-S493 (1999).

P-105

A pulsed photo acoustic study of the laser ablation synthesis of Ag nanoparticles in ethanol

M. A. Valverde Alva[1], T. García Fernández[2], E. Esparza Alegria[3], C. Sánchez Aké[4], R. Castañeda Guzman[4], M. Villagrán Muniz[4], J. L. Sánchez Llamazares[5], C. F. Sánchez Valdés[5], C. E. Márquez Herrera[6]

[1]Posgrado en Ciencia e Ingeniería de Materiales, Universidad Nacional Autónoma de México (UNAM), México D.F., C.P. 04510, México.
[2]Universidad Autónoma de la Ciudad de México (UACM), Prolongación San Isidro 151, Col. San Lorenzo Tezonco, México D.F., C.P. 09790, México.
[3]Facultad de Ciencias, Universidad Autónoma de México (UNAM), México D.F., C.P. 04510, México.
[4]CCADET, Universidad Nacional Autónoma de México (UNAM), México D.F., C.P. 04510, México.
[5]Instituto Potosino de Investigación Científica y Tecnológica A.C., Camino a la Presa San José 2055, Col. Lomas 4ª sección, San Luis Potosí, S.L.P., C.P. 78216, México
[6]Departamento de Ingeniería Metarlurgica, Facultad de Química, Universidad Autónoma de México (UNAM), México D.F., C.P. 04510, México.
E-mail: citlali.sanchez@ccadet.unam.mx

Laser ablation in liquids has received much attention as a novel nanoparticle-production technique due to its procedural simplicity and its potential applications. However this technique has some important drawbacks due to the dynamical nature of the process, in which the concentration and size of the nanoparticles (NPs) change with the number of pulses during the ablation. In this work a pulsed photoacoustic (PA) technique has been used to study the synthesis by laser ablation of silver nanoparticles (Ag-NPs) in a glass cuvette filled with 10 mL of ethanol. For the PA analysis two piezoelectric sensors were attached to the cuvette and target, respectively. Samples were produced by using a pulsed Nd:YAG laser with 1064 nm of wavelength and 7 ns of pulse duration; the laser pulse energy was varied from 10 to 100 mJ. Higher concentrations of Ag-NPs were obtained for higher laser energies. Transmission electron microscopy micrographs show that the obtained NPs were spherical in shape with an average size of around 10 nm; they show a plasmon absorption peak around 400 nm. The root mean square (RMS) value of the PA signal was found to be proportional to the fluence of the laser ablation pulses. The absorption and scattering of the laser pulse by the increasing number of NPs appearing in the colloidal solution leads to a rapid decrease in the RMS value of the PA signal reducing the fluence of the laser shots impacting on the target. After approximately 100 laser pulses, the different colloidal solution produced exhibited a similar PA response, regardless of the values of input energy of the laser pulses. The repetition rate increment of the laser pulses, in the range from 1 to 10 Hz, leads to the increment of the transmittance and therefore of the production rate of nanoparticles. The fast photography technique, which was used to study the evolution of ablation bubbles, confirmed that PA technique allows determining the precise moment of the first implosion of the bubble. Thus, using PA signal we studied the dependence on the number, energy and frequency of the laser pulses of the moment of the bubble's implosion. Our results show that the PA technique can be used to follow and analyze in-situ and in real time the formation of Ag-NPs by laser ablation in ethanol.

P-106

Synthesis of submicrometer-sized spherical particles by laser irradiation in liquid with different laser pulse width

S. Sakaki[1], N. Koshizaki[1], H. Ikenoue[2], T. Tsuji[3], Y. Ishikawa[4]

[1]*Hokkaido University, Kita 13, Nishi 8, Kita-ku, Sapporo, Hokkaido 060-8628, Japan*
[2]*Kyusyu University, 744 Motooka, Nishi-ku, Fukuoka, 819-0395, Japan*
[3]*Shimane University, 1060 Nishikawatsu-cho, Matsue, Shimane, 690-8504, Japan*
[4]*National Institute of Advanced Industrial Science and Technology, 1-1-1 Higashi, Tsukuba, Ibaraki, 305-8565, Japan*
E-mail: sakaki.shota@frontier.hokudai.ac.jp

Recently, Ishikawa et al reported that submicrometer-sized spherical particles are fabricated by pulsed laser irradiation to colloidal nanoparticles dispersed in liquid [1]. By this method, the synthesis of submicrometer-sized spherical particles of various materials is possible [2]. The particle heating-melting-evaporation model well explains this process [3]. Nanoparticles dispersed in liquid medium absorb pulse energy from laser light, are heated, and finally melted. These melted and fused particles maintain their spherical shape by surface tension and are solidified in the same shape. Therefore, spherical particle fabrication is influenced by several laser parameters, such as wavelength, pulse width, pulse frequency, and laser fluence. Here, we investigate the effect of laser pulse width on fabricated particles.

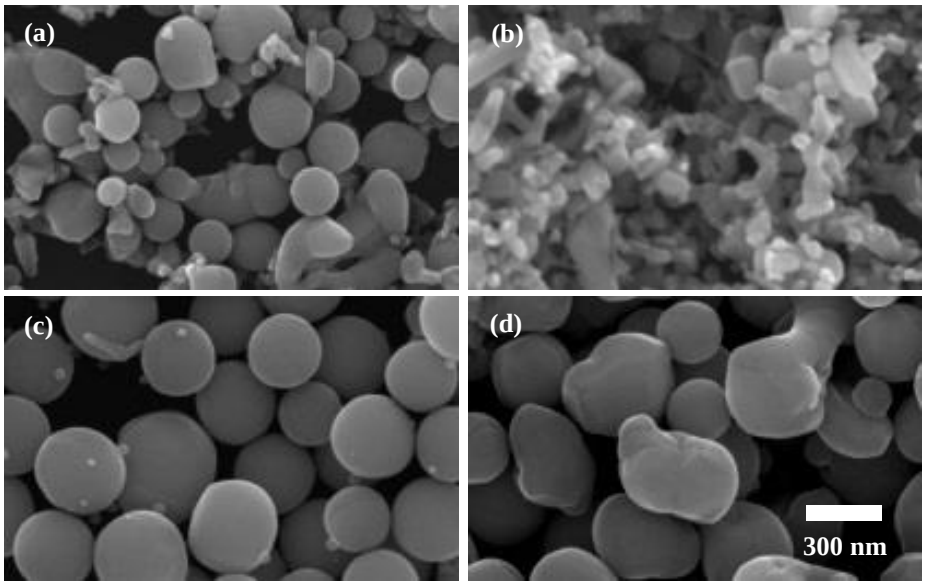

Fig. 1. SEM images of ZnO particles obtained by KrF excimer laser irradiation at the laser fluence of 67 mJ pulse^{-1} cm^{-2} with (a) original laser pulse (pulse width: 50 ns), (b) stretched laser pulse (pulse width: 70 ns) and those obtained at 150 mJ pulse^{-1} cm^{-2} with (c) original laser pulse and (d) stretched laser pulse.

ZnO submicrometer-sized spherical particles were already reported to be obtained using the third harmonic of Nd:YAG laser (wavelength: 355nm, pulse width: 10 ns, pulse frequency: 30 Hz) [4]. In our experiment, we used KrF excimer laser (wavelength: 248 nm, pulse width: 50 ns, pulse frequency: 100 Hz) and irradiated onto ZnO nanoparticles (< 100 nm, Aldrich) dispersed in de-ionized water for 8 min. We also used a pulse stretcher equipped with the KrF excimer laser to have a longer pulse width of 70 ns by delaying a part of pulsed laser light. At the laser fluence of 67 mJ pulse^{-1} cm^{-2}, spherical particles and shapeless raw nanoparticles were simultaneously observed (Fig. 1a). In contrast, no spherical particles were produced by laser irradiation with the stretched pulse (Fig. 1b). At 150 mJ pulse^{-1} cm^{-2}, submicrometer-sized spherical particles were well obtained (Fig. 1c) with 50-ns laser pulse. But, angulated particles appeared after laser irradiation with stretched pulse (Fig. 1d). This result suggests that large pulse width causes the loss of heating energy by heat transfer to liquid medium.

[1] Y. Ishikawa, Y. Shimizu, T. Sasaki, and N. Koshizaki, "Boron carbide spherical particles encapsulated in graphite prepared by pulsed laser irradiation of boron in liquid medium" Appl. Phys. Lett. 91, 161110 (2007)

[2] H. Wang, A. Pyatenko, K. Kawaguchi, X. Li, Z. Swiatkowska-Warkocka, and N. Koshizaki, "Selective pulsed heating for the synthesis of semiconductor and metal submicrometer spheres" Angew. Chem. Int. Ed. 49, 6361–6364 (2010)

[3] A. Pyatenko, H. Wang, N. Koshizaki, and T. Tsuji, "Mechanism of pulse laser interaction with colloidal nanoparticles" Laser Photonics Rev. 7, 596–604 (2013)

[4] H. Wang, N. Koshizaki, L. Li, L. Jia, K. Kawaguchi, X, Li, A. Pyatenko, Z. Swiatkowska-Warkocka, Y. Bando, and D. Golberg, "Size-tailored ZnO submicrometer spheres: bottom-up construction, size-related optical extinction, and selective aniline trapping" Adv. Mater. 23, 1865–1870 (2011)

P-110

Growth and Characterization of Y_2O_3 thin films on Gd_2O_3 buffered Si substrates using Pulsed Laser Deposition

Joseph Paulraj, Rongping Wang, Matthew Sellars and Barry Luther-Davies
Laser Physics Centre, Research School of Physics and Engineering, Australian National University, Mills Road, Acton, Canberra, ACT 0200, Australia
E-mail: joseph.paulraj@anu.edu.au

Abstract
Thin films of rare-earth doped 1% Eu: Y_2O_3 have been grown on Gd_2O_3 buffered Si substrates using pulsed laser deposition. A KrF excimer laser at a wavelength of 248nm with energy 200mJ and repetition rate of 1-5 Hz was used to ablate the Y_2O_3 ceramic target. Y_2O_3 thin films were grown at different substrate temperatures (700°C, 800°C & 900°C) at an oxygen pressure of 4.5pa [3]. The thin films have been characterized using X-ray (Cu $K_{\alpha 1}$ radiation, $\lambda = 0.15405$ nm) diffraction measurements. θ-2θ scans revealed that the films were grown in the Y_2O_3 (2 2 2) direction at $2\theta = 29.10°$, FWHM 0.15°. X-ray pole figure analysis along (2 2 2), $2\theta = 29.159°$ showed three symmetrical diffraction dots at an angular separation of 120° with a minimum FWHM 1.4°, exhibiting higher order of crystallographic orientation of the c-axis normal to the substrate and the films were epitaxial and single-crystalline [1]. The FWHM increases when the substrate temperature in increased further. The films were further investigated using Raman spectroscopy and the corresponding peak shifts were identified as compared to the target and substrate. The PL spectra [4] show the emissions from Eu^{3+} incorporated in Y_2O_3 corresponding to the transitions $^5D_0 - {}^7F_2$ & $^5D_0 - {}^7F_1$.

References
[1] J.J. Araiza, M. Cardenas, C. Falcony, V.H. Mendez-Garcia & G. Contreras-Puente, "Structural, optical and electrical characteristics of yttrium oxide films deposited by laser ablation", **J. Vac.Sci. Technol. A 16 (6)**, Nov 98.

[2] Sean L. Jones, D. Kumar, K.-G. Cho, R. Singh and Paul H. Holloway, "Pulsed laser deposition of Y_2O_3: Eu thin film phosphors", **Displays 19**, 151-167 (1999).

[3] Shaoqiang Zhanga and Rongfu Xiaob, "Yttrium oxide films prepared by pulsed laser deposition", **Journal of Applied Physics, Volume 83, Number 7**, (1998).

[4] S. Ray, P. Pramanik, A. Singha, and Anushree Roy, "Optical properties of nanocrystalline Y_2O_3: Eu3+**", Journal of Applied Physics 97, 094312** (2005)

P-112

An Apparatus to Control the Spatial Beam Characteristics for Femtosecond Laser Ablation of a Wide Variety of Materials

Owen Bodley[1,2], Simon Ashforth[1,2,3], Reece N. Oosterbeek[1,2], M. Cather Simpson[1,2,3,4*]

[1] *The Photon Factory, The University of Auckland, Auckland, New Zealand*

[2] *The MacDiarmid Institute for Advanced Materials and Nanotechnology and The Dodd Walls Centre for Quantum and Photonic Technologies, New Zealand*

[3] *Department of Physics, The University of Auckland, Auckland, New Zealand*

[4] *School of Chemical Sciences, The University of Auckland, Auckland, New Zealand*

** Corresponding author email: c.simpson@auckland.ac.nz*

Ultrafast laser micromachining as a materials processing technique offers promising advantages to a wide range of fields, from the dicing of chips in the semiconductor industry [1] to the surgical treatment of hard tissues like teeth and bone [2,3]. Ultrafast pulses can produce cuts whose widths are just a few hundred nanometres and the locally affected area can be less than a micron [4]. Despite these advantages, ablation rates remain too slow for widespread industrial adoption. As part of a large, systematic study of the parameters hypothesized to influence the efficiency of laser ablation, we have constructed a custom-built laser micromachining stage that allows us to, among other things, alter the spatial and temporal pulse characteristics of our 100 fs, 800 nm laser pulses

The custom matching system has inspection and machining turrets (Fig. 1). Samples are manipulated by a 5-axis stage that includes two N-661 Miniature Linear Stages with NEXACT(R) drives. These provide motion in the horizontal x and y directions. Movement in the vertical (z) direction is controlled by a Thorlabs PT1-Z8 motorized translation stage. Samples can be aligned relative to the incident beam via a Thorlabs GNL20/M dual-axis goniometer. Samples are moved between the inspection and machining turrets via a Thorlabs 300 mm linear translation stage with integrated controller and stepper motor.

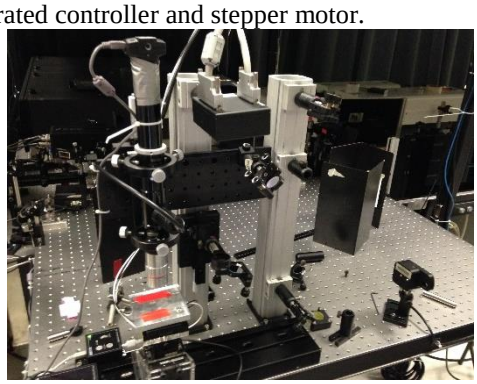

Fig. 1. Custom-built femtosecond laser micromachining system, with spatial beam shaping.

Machined features are inspected using a custom microscope consisting of Edmond Optics 2.0x TV Tube, manual upper zoom with iris, mitutoyo coaxial focusable lower module VIS 7X Zoom and illuminated by a Dolan-Jenner MI-150 fiber optic illuminator. The magnified image is captured by a Thorlabs DCC1645C camera.Incident pulses are arbitrarily captured by a 5046ER Laser Metrics pulse picker with custom synchronization circuit and attenuated by a 2-EWP-T-7882-M ultrafast watt pilot motorized attenuator. The pulses are spatially shaped using a Hamamatsu X10468 LCOS Spatial Light Modulator. Low precision pulse control is via a Thorlabs SH05 optical beam shutter and SC10 controller.

The user operates the system via custom software, programmed in C# and using the WinForms framework. The Thorlabs stages are controlled using the publically available FTDI wrapper class and the communication to the other elements is by the Microsoft SerialPort class. Image capture and display is performed via the open source AForge.net library. Buttons enable direct control of each element; users can program complex motion using simple macro commands. Custom computer generated holograms and pre-computed CGH images can be implemented. To facilitate usability, hardware–computer communication and CGH computations are performed asynchronously, leaving the main UI thread clear for user interaction. Using this system, we compare the ultrafast laser micromachining efficiencies of conventional Gaussian beams with Bessel and vortex beams.

References

1. Jian Cheng, Chang-sheng Liu, Shuo Shang, Dun Liu, Walter Perrie, Geoff Dearden and Ken Watkins “Review of ultrafast laser materials micromachining” **46** Opt. Laser Technol. (2013)
2. P.H. Wu, C WCheng, C.P. Chang, T.M. Wu and J KWang “Fabrication of large-area hydrophobic surfaces with femtosecond-laserstructured molds”, **21** J. Micromech. Microeng. (2011)
3. B. Girard, M.R. Armstrong, B.C. Wilson, C.M.L Clokie and R.J. Dwayne Miller, “Effects of Femtosecond Laser Irradiation on Osseous Tissues” **39** Lasers in Surgery and Medicine (2007)
4. Koji Sugioka and Ya Cheng, “Ultrafast lasers—reliable tools for advanced materials processing”, **3** Light Sci Appl (2014)

P-113

Laser reduction of graphene oxide to reduced graphene oxide: an experimental and simulated comparison between methods

Rakesh Arul[1,2,3], Jacob W. Martin[1,2,3], Reece N. Oosterbeek[1,3], John Robertson[4], M. Cather Simpson[1,2,3,5*]

[1] The Photon Factory, The University of Auckland, Auckland 1142, New Zealand
[2] School of Chemical Sciences, The University of Auckland, Private Bag 92019, Auckland 1142, New Zealand
[3] The Dodd Walls Centre for Quantum and Photonic Technologies and The MacDiarmid Institute for Advanced Materials and Nanotechnology, New Zealand
[4] School of Applied Sciences, Auckland University of Technology, Auckland, New Zealand
[5] Department of Physics, The University of Auckland, Private Bag 92019, Auckland 1142, New Zealand
** Corresponding Author e-mail: c.simpson@auckland.ac.nz*

The rapid development of graphene-based technologies over the past decade has been explosive. A major focus of this field is finding methods for the mass production of high quality graphene for use in fabrication of electronic devices. Laser reduction to produce reduced graphene oxide has been performed with Lightscribe® DVD drives [1] and a range of pulsed lasers [2, 3]. Despite the presence of defects induced by the laser reduction process, reduced graphene oxide shows promise; this approach has been used to create supercapacitors [1], sensors [4] and battery anode materials [5]. The readily scalable nature of the process, the one-step reduction and patterning of devices, and the ability to tune the conductivity by varying laser parameters makes this method very attractive. Therefore, insight into the ultrafast mechanism of ablation is crucial to develop improved methods to produce reduced graphene oxide - despite a number of studies, there is still uncertainty as to the exact mechanism of this process [6].

In this study, we present a direct comparison between three different laser-induced reduction methods for producing reduced graphene oxide – Lightscribe® laser reduction (780nm wavelength, Lightscribe DVD drive, Hewlett-Packard Inc., USA), nanosecond UV laser reduction (248nm wavelength, 5ns pulse duration, Xantos XS, Coherent Inc., USA), and femtosecond laser reduction (800nm wavelength, 110fs pulse duration, Legend Elite, Coherent Inc., USA).

Characterisation of the reduced graphene oxide was carried out using Raman spectroscopy (alpha300 R, WiTEC GmbH, Germany), X-ray Photoelectron Spectroscopy (Axis UltraDLD, Kratos Ltd., UK.) and X-ray Diffraction (Empyrean, PANalytical B.V., Netherlands). Using these techniques, the optimal laser processing conditions for reduction were determined. The quality of these reduced graphene films was also compared to that of the Lightscribe® reduced films.

Reactive force field simulations using ReaxFF have previously been applied to the thermal reduction of graphene oxide [7]. Here we couple the experimental work with simulations to investigate the effects of different amounts and types of oxygen species on graphene on the subsequent thermal annealing and quality of graphene produced. Simulations were performed to model the reduction caused by ultrashort and long laser pulses, corresponding to the lasers that were used to reduce the graphene oxide films. The subsequent structure and dynamics of the graphene/graphene oxide system was studied. Further comparisons to the characterisation data collected from the reduced graphene oxide film were made to validate the model.

The combination of experimental data and molecular dynamics simulations used in this study provide valuable insight into the reduction processes occurring during laser reduction of graphene oxide.

References

1. El-Kady, M.F. and R.B. Kaner, "Scalable fabrication of high-power graphene micro-supercapacitors for flexible and on-chip energy storage." Nature communications, **4** 1475. (2013)
2. Sokolov, D.A., et al., "Excimer laser reduction and patterning of graphite oxide." Carbon, **53** 81-89. (2013)
3. Trusovas, R., et al., "Reduction of graphite oxide to graphene with laser irradiation." Carbon, **52** 574-582. (2013)
4. Robinson, J.T., et al., "Reduced graphene oxide molecular sensors." Nano letters, **8** 3137-3140. (2008)
5. Zhu, X., et al., "Nanostructured reduced graphene oxide/Fe2O3 composite as a high-performance anode material for lithium ion batteries." Acs Nano, **5** 3333-3338. (2011)
6. Zhang, Y.L., et al., "Photoreduction of Graphene Oxides: Methods, Properties, and Applications." Advanced Optical Materials, **2** 10-28. (2014)
7. Bagri, A., et al., "Structural evolution during the reduction of chemically derived graphene oxide." Nat Chem, **2** 581-587. (2010)

P-115

Optimisation of femtosecond laser ablation parameters for efficient cutting of sintered alumina wafers

Thomas Ward[1,2], Reece N. Oosterbeek[1,2], Andrew Rodda[3], Simon Ashforth[1,2,4], Owen Bodley[1,2], M. Cather Simpson[1,2,4,5*]

[1] *The Photon Factory, The University of Auckland, Auckland, New Zealand*
[2] *The MacDiarmid Institute for Advanced Materials and Nanotechonology and The Dodd Walls Centre for Quantum and Photonic Technologies, New Zealand*
[3] *Aeroqual Ltd., Auckland, New Zealand*
[4] *Department of Physics, The University of Auckland, Auckland, New Zealand*
[5] *School of Chemical Sciences, The University of Auckland, Auckland, New Zealand*
** Corresponding author email: c.simpson@auckland.ac.nz*

In this study, we explore the femtosecond laser ablation method for cutting of sintered alumina wafers, which have a variety of commercial uses. Our goal is to increase cutting speed, reduce kerf width and minimize the heat affected zone.

Femtosecond laser ablation was carried out using an amplified Ti:Sapphire laser (Mantis (oscillator) and Legend Elite (amplifier), Coherent Inc., USA), which provides 110 fs pulses at a repition rate of 1 kHz, and a maximum pulse energy of 3.5 mJ. The alumina used was polycrystalline sintered Al_2O_3, AD-96R (CoorsTek, USA.).

To optimise the laser processing technique, a range of different parameters were trialled: focal length, focal position, incident laser power and processing speed. Lenses with focal lengths ranging from 50 to 300 mm were tested. A longer focal length increases the Rayleigh length allowing deeper ablation, but also widens the beam waist, decreasing the peak intensity. The position of the focal point within the sample was also varied, to position a greater portion of the beam intensity within the sample and thereby increase machining depth. Additionally the laser power applied relative to shot density (processing speed) was investigated to determine how the ablation response changed. For all ablation conditions the kerf width, cut quality and heat affected zone were measured.

A clear positive correlation was found between ablation depth and focal length (Fig. 1) across powers of 210 to 900 mW. Positioning the focal point of the laser beam within the sample was found to provide the maximum ablated depth; the optimal depth varied with incident laser power. The effect of processing speed was also investigated (Fig. 1). As expected, we observe a decrease in ablation depth with increasing processing speed, though this effect is very gradual. We can increase processing speed up to 250x from 10 to 2500µm/s, while suffering a depth reduction of only ~33% - this is an extremely useful result for increasing processing efficiencies for industrial applications.

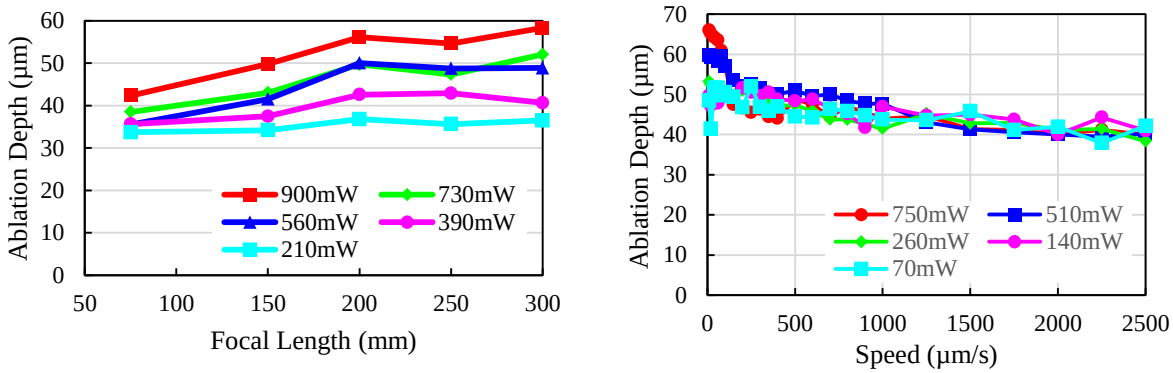

Fig. 1. (Left) Effect of lens focal length on the ablation depth for various laser powers. (Right) Effects of power on ablation depth for different processing speeds.

From the range of tests carried out, we demonstrate the optimal conditions for cutting of alumina using femtosecond laser ablation, including the preferred focal length, focal position, power, and speed settings. These tests represent a thorough investigation of the parameter space with promising applications for improving machining efficiencies.

P-116

Femtosecond laser cutting speed optimization for single crystal quartz wafers

Zhiwei Han[1,2], Reece N. Oosterbeek[1,2], Simon Ashforth[1,2,3], Owen Bodley[1,2], M. Cather Simpson[1,2,3,4*]

[1] The Photon Factory, The University of Auckland, Auckland, New Zealand

[2] The MacDiarmid Institute for Advanced Materials and Nanotechnology and The Dodd Walls Centre for Quantum and Photonic Technologies, New Zealand

[3] Department of Physics, The University of Auckland, Auckland, New Zealand

[4] School of Chemical Sciences, The University of Auckland, Auckland, New Zealand

** Corresponding author email: c.simpson@auckland.ac.nz*

Single crystal quartz is a widely used material in the microelectronics industry, with applications such as quartz crystal resonators being a key component in many integrated circuits. These resonators must have high structural and edge quality to ensure accurate resonance properties. Current mechanical dicing methods used to cut these components utilise diamond saw blades, which are expensive and wear down rapidly [1]. This issue, coupled with the material wastage from the width of the saw blade and damage zone from the mechanical friction, represents a significant cost to the industry. If laser micromachining could be applied here, significant improvements could be made including reductions in cut widths and increased flexibility of cut shapes.

Femtosecond laser micromachining is an excellent candidate for application in this area. The ultrashort pulse duration allows materials transparent to the laser wavelength, such as quartz, to be laser machined, and provides high cut quality with little or no heat affected zone [2]. The major drawback to this method is the slow processing time - currently femtosecond laser cutting takes too long to be used in this setting.

In this work we explore the available laser machining parameter space to determine optimal machining conditions for different types of laser micromachined features. We measure the effectiveness of the available laser power as a function of modifying the focal length, focal point position and laser wavelength. The effect of focal length was studied using uncoated BK7 lenses with focal lengths in the range of 50 to 300mm. We applied pulses from an amplified Ti:Sapphire laser (Coherent Legend Elite) with 110 fs duration at a 1kHz repetition rate. The maximum pulse energy available was approximately 3mJ. The beam was also directed through an optical parametric system (TOPAS, Light Conversions) to alter the wavelength of the output pulse to between 270 and 2600 nm. Quartz wafers were single crystal quartz, 100 mm diameter, 500 µm thick.

References

[1] Krishnan Venkatakrishnan and Bo Tan "Thin silicon wafer dicing with a dual-focused laser beam", Micromech. Microeng. **17** (2007)

[2] J. Kruger, W. Kautek, "Ultrashort Pulse Laser Interaction with Dielectrics and Polymers", Adv. Polym. Sci. **168**, 247 (2004)

P-117

Effect of applied electric field in Pulsed Laser Deposition

S. Ohmuro[1], S. Kurumi[1], K. –ich. Matsuda[1], K. Suzuki[1]
[1]Electrical Engineering, Colleg of Science and Technology, Nihon University, Japan
E-mail:cssa14009@g.nihon-u.ac.jp

Mass spectrometry is one of indispensable tools in the field of material sciences and technologies for analyzing characteristics of molecules and ions. The so-called rotating electric field ion mass spectrograph (REFIMS) is of such a mass spectroscopic technique which, in principle, allows one to measure with very high dynamic range as well as high resolution [1]. Recently, the two rotating electric fields mass analyzer employing the REFIMS technology is invented [2]. In a cylindrical coordinate system, when the charged particles are entered along the z-axis in the rotating electric field which rotates around z-axis temporally, they leave the z-axis. In this mass spectrometer, after traveling the charged particles through the first rotating electric field, the particles is entered in the second rotating electric field which rotates in the opposite direction to the first. Thereby, it is possible to return to the z-axis only the particles having specific charge and mass corresponding to the angular velocity of the rotating electric fields. If this technique is applied to Pulsed Laser Deposition (PLD), there is a possibility to realize an element selective PLD with high ion selectivity. In order to realize this combined use of PLD with ion selective mechanism, it is necessary to have the directivity of the ablation plume generated in a vacuum by PLD.

In this study, we investigated the plume induction in the DC Electric field Assisted Pulsed Laser Deposition (DEA-PLD) which induces the ablation plume by applied DC electric field. The DEA-PLD is a method that enable us to separate the charged particles from ablation plume by applied DC electric field and the charge of the particles.

In this paper, we report on the applied voltage dependence of the number of charged particles in DEA-PLD. We focused on the BaO of ionic bonding crystal. Ablation plume generated in a vacuum (pressure: 0.01 Pa) by Nd:YAG laser (wavelength: 355 nm, pulse width: 20 ns, laser fluence: 2.8 J/cm^2) was induced and separated by DC electric field between cathode and anode. The cathode voltage was set to 500 V, and the anode voltage was varied by 100 V from -200 V to -500 V. The cathode current was measured during the PLD process. The number of charged particles was determined as Ba^+ from this current. As a result, the number of charged particles estimated from the measured current was 0.9×10^{12} at -200 V, and the number increased to 2.98×10^{12} at -500 V.

[1] J. H. Clemmons, and F. A. Herrero, *"Mass spectroscopy using a rotating electric field"*, Rev. Sci. Instrum. **69**, 6, 2285 (1998).
[2] M. Hotta and T. Adachi, WO/2014/126227, A1, (2014).

P-118

Numerical Simulation of Laser Processing of Carbon Fiber Reinforced Plastics Including Combustion Effect

Tomomasa Ohkubo[1], Yuji Sato[2], Masahiro Tsukamoto[2]

[1]*School of Media Science, Tokyo University of Technology, 1404-1, Katakura-chou, Hachiouji-shi, Tokyo, 192-0914, Japan*

[2]*Joining and Welding Research Institute, Osaka University, 11-1Mihogaoka Ibaraki-shi Osaka,567-0047, Japan*

E-mail: ookubotmms@stf.teu.ac.jp

1. Introduction

A carbon fiber reinforced plastic (CFRP) consists of carbon fiber and binding polymer and it has higher specific strength compared with metal materials and chemical resistance and dimensional stability. Although laser cutting method is applied to many materials to process these materials, CFRP generates heat affected zone (HAZ) because of differences in thermal properties of carbon fiber and binding polymer. Although many experiments were performed to apply laser cutting technique to CFRP, not enough theoretical or numerical studies are performed about HAZ generation and there is no research considering heat generation of oxidization of materials in the air condition. In this study, heat of combustion was included into calculation model to simulate laser processing of CFRP and validate this model qualitatively.

2. TG-DTA analysis and conditions of our simulation

To develop the new calculation model to consider the effect of combustion and decomposition of each element of CFRP, thermo gravidity analysis (TGA) and differential thermal analysis (DTA) was performed about CFRP in the air condition. The result of TG-DTA experiment is shown in Fig. 1. A two-dimensional model was adopted in this study to calculate the temperature inside the CFRP. A schematic figure of the geometry is shown in **Error! Reference source not found.**. Only the rectangular area surrounding the white dashed line was calculated, and its boundaries were symmetric because the purpose of this study was to clarify what occurs inside the CFRP, not at the surface.

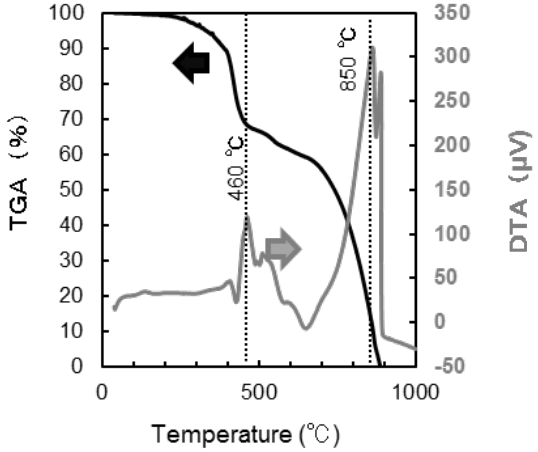

Fig. 1 TG-DTA analysis on CFRP in air

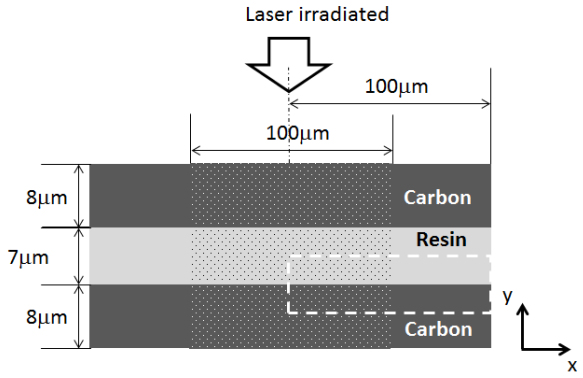

Fig. 2 Schematic figure of the geometry used in our simulation.

3. Results of experiment and numerical simulation

A SEM image of experimental result is shown in Fig. 3. Considering heat generation and absorption from the result of TG-DTA, we calculated heat transfer inside CFRP. Results of calculation are shown in Fig. 4. Comparing with experimental result of Fig. 3, this new model succeeded in simulating HAZ formation in air condition.

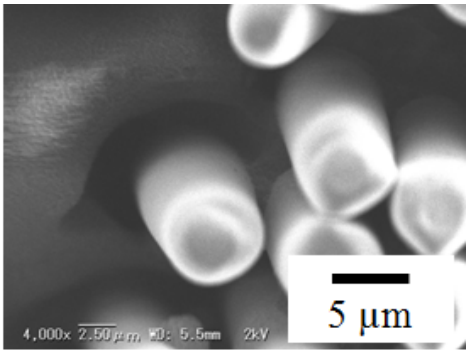

Fig. 3 SEM image of experimental result

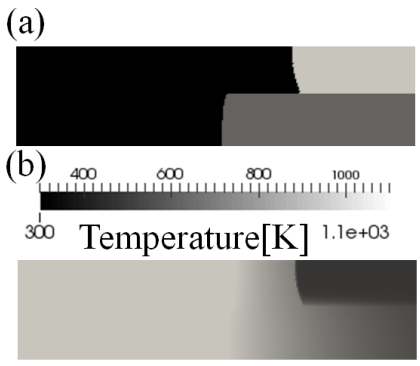

Fig. 4 Results of numerical simulations (a): black area is removed area, dark gray is carbon fiber and light gray is resin. (b): temperature distribution.

P-119

The properties of rare-earth doped zinc oxide/phthalocyanine structures for optoelectronics

M. Novotný[1], P. Fitl[1,2], J. Vlček[1,2], J. Bulíř[1], E. Marešová[1,2], P. Hruška[1,3], L. Fekete[1], M. Vondráček[1], J. Drahokoupil[1], N. Abdellaoui[4], M. Vrňata[2], J. Lančok[1]

1 Institute of Physics, Academy of Sciences of the Czech Republic, Na Slovance 2, 182 21 Prague, Czech Republic
2 Institute of Chemical Technology, Technicka 5, 166 28 Prague 6, Czech Republic
3 Faculty of Mathematics and Physics, Charles University in Prague, 121 16 Prague 2, Czech Republic
4 Institut Lumière Matière, UMR5306 Université Lyon 1-CNRS, Université de Lyon 69622 Villeurbanne cedex, France
E-mail: novotnym@fzu.cz

Zinc oxide (ZnO) is considered as one of the most important material for transparent electronics because of its attractive properties such as a direct wide band gap, nontoxicity, and high stability. It has been envisaged that functionality of the devices can be enhanced substantially by combining two different types of organic and inorganic semiconducting materials. Devices based on p-organic/n-ZnO heterojunction promise a great potential for future applications since p-type organic semiconductors are abundant. The phthalocyanine (Pc) compounds as p-type organics possess good light absorption extending down to the red and near-IR regions, and efficient electron transfer to ZnO. Pcs are known as indispensable components as the donor for the high efficiency bulk-heterojunction organic photovoltaic devices and light emitting diodes. In such devices the electronic properties of the D−A interface play a key role by affecting both the optical absorption induced by solar light and the electron injection to the substrate. ZnO optoelectronics properties can be tuned by appropriate dopants, such as rare earth ions.

Undoped and doped ZnO thin films were grown by Pulsed Laser Deposition (Nd:YAG, λ= 266 nm, τ = 6 ns) from ZnO, Eu_2O_3:ZnO, Pr_2O_3:ZnO, Sm_2O_3:ZnO, and Gd_2O_3:ZnO targets in oxygen ambient at pressure of 10 Pa at substrate temperature of 300°C and room temperature. Fused silica, sapphire and ITO were used as transparent substrates. Metal phthalocyanine thin films were fabricated by organic molecular evaporation (OME).

The structure and morphology of the films were characterized by x-ray diffraction, atomic force microscopy (AFM) and scanning electron microscopy (SEM). Chemical composition and structural properties were examined by NanoESCA. The optical properties were analyzed by spectrophotometry, spectral ellipsometry and photoluminescence. The electrical properties were analyzed by van der Pauw method.

We observed variation of Q band position in Pc absorption spectra as well as its intensity enhancement when doped ZnO is involved. We demonstrated that choice of dopant in ZnO nanostructured films allows to tune optoelectrical properties of ZnO/Pc structures.

P-120

Formation of Diamond-Like Carbon Thin Films by Femtosecond Laser Ablation of a Frozen Cyclohexane Target

T. Nakamura, Y. Wagatsuma, S. Sato

Institute of multidisciplinary research for advanced materials, Tohoku University, Katahira 2-1-1, Aoba-ku, Sendai 980-8577, Japan

E-mail: nakamu@tagen.tohoku.ac.jp

1. Introduction

The formation of diamond-like carbon (DLC) thin films with excellent optical and mechanical properties and high content of tetrahedral (sp^3) bonding is expected by a pulsed laser deposition (PLD) technique using highly intense femtosecond laser pulses. However, the use of a solid target such as graphite in conventional PLD results in the generation of micrometer-sized droplets and fragments derived from the target itself, which are not preferable for the formation of high quality thin films. Instead of solid materials, liquid or frozen targets have a potential to effectively reduce the inclusion of large particulate in the thin film fabrication by PLD [1]. In this study, DLC films were prepared by PLD using a frozen cyclohexane (C_6H_{12}) target. Effect of preparation conditions during film formation on the structure of the DLC films was investigated.

2. Experiment

The film deposition using a frozen cyclohexane target was performed in a specially designed and built in-house vacuum chamber. Several mL of liquid cyclohexane was placed on a target holder, which is connected to a liquid nitrogen reservoir and frozen by thermal conduction in argon gas at atmospheric pressure, then the chamber was evacuated to 10^{-2} Pa subsequently. A femtosecond pulsed laser beam generated from a Ti:Sapphire regenerative amplifier system was introduced into the chamber through a quartz glass window and focused on the surface of a frozen target by a focusing lens with a focal length of 300 mm. The laser fluence on the target surface was set in a range of 5 to 500 J/cm^2. A single crystal silicon plate of 1 inch squares was used as a substrate and placed parallel to the target at a distance of 100 mm. Films were formed at room temperature for different irradiation times from 10 to 180 minutes. The characterization of fabricated DLC films was performed by scanning electron microscopy (SEM), atomic force microscopy (AFM), Raman spectroscopy, X-ray reflectivity (XRR), X-ray photoelectron spectroscopy (XPS) and electron energy loss spectroscopy (EELS).

3. Result

When the femtosecond laser pulses were irradiated on a frozen hexane target, violet-blue soft plume was observed at the surface of the target. All the prepared films with different irradiation conditions had a flat and smooth surface without any fragments (Fig. 1). Bimodal curves corresponding to D band (1350 cm^{-1}) and G band (1580 cm^{-1}), which are characteristic of disordered-carbon structure, were observed in the Raman spectra for all the films fabricated with different laser fluences (Fig. 2). The density of the prepared films was within 1.6-2.1 g/cm^3 indicating that the structure of the prepared films were a:C-H. From the results of the root mean square (RMS) of surface roughness, the low G band peak position and the low I(D)/I(G) value in the Raman spectra of the films, the optimum laser fluence was found to be 50 J/cm^2 for the fabrication of high quality DLC thin film with a flat and smooth surface and high content of sp^3 bonding (Fig. 3). Dominant difference was not observed for the films fabricated for the deposition time over 60 minutes even in the optimal condition for DLC. This result is attributed to the sputtering of the formed DLC film by successively produced high-energetic ablated species from the frozen hexane target.

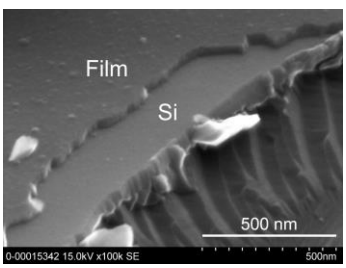

Fig 1. SEM image of fabricated film using a frozen cyclohexane target with the laser fluence of 500 J/cm^2.

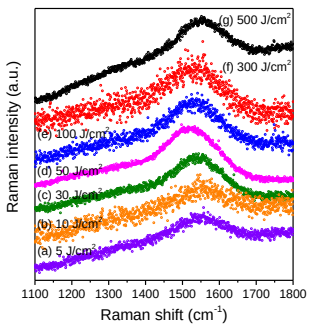

Fig 2. Raman spectra of the fabricated DLC films.

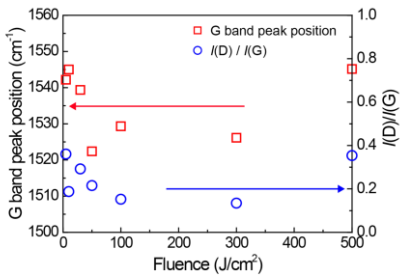

Fig 3. G band position and I(D)/I(G) from Raman spectra of fabricated DLC films.

References

[1] W. Inoue, M. Okoshi and N. Inoue, "Fabrication of diamond-like carbon thin films by femtosecond laser ablation of frozen acetone" Appl. Phys. A **79** 1457 (2004).

P-121

Light Induced Toxicity of Silver Nanoparticles Produced by Laser Ablation

J.J. Naddeo[1,2], Matthew Ratti[1,2], Dr. Julianne Griepenburg[1], Dr. Daniel Bubb[1,3], Dr. Sean O'Malley[1,3], Dr. Eric Klein[2,3]

[1]Department of Physics, Camden, New Jersey 08102, USA
[2]Department of Biology, Camden, New Jersey 08102, USA
Center for Computational and Integrative Biology[3], Camden, New Jersey 08102, USA
Corresponding Author: jnaddeo@gmail.com

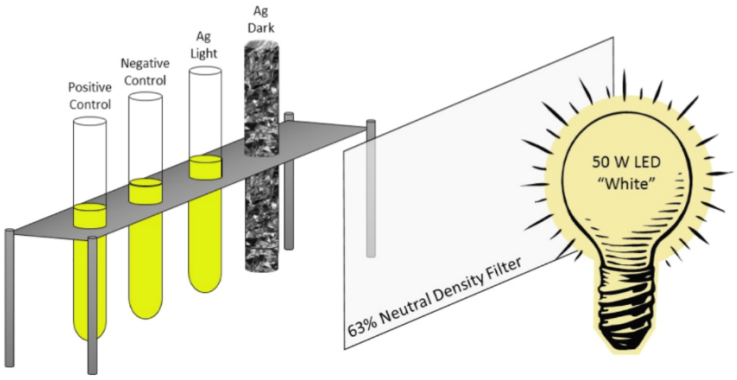

Fig. 1. E.coli cultures supplemented with silver nanoparticles, exposed to light

Abstract

Silver is one of the most studied metals in the biomedical field and has been used for centuries in various forms as an antimicrobial agent dating back to Chaldean dynasty c.a. 4,000 B.C.E. [1]. Silver nanoparticles (AgNP) are of particular interest due to their physical properties, which have been shown to strongly influence antimicrobial activity. Our lab used laser ablation in liquid to synthesize AgNPs, giving us the ability to make "bare" particles, free from precursors that are typically associated with chemical synthetic methods. [2] A Nd:YAG laser at the fundamental wavelength (λ=1064 nm) was used to ablate a pure silver target immersed in a 60 mM sodium dodecyl sulfate solution. As some pathogenic bacteria form resistances to antibiotics, understanding the mechanisms behind AgNPs antimicrobial activity is paramount. A major problem that is preventing the universal application of AgNPs is their possible toxicity to higher organisms. Our current work supports the hypothesis that colloidal suspensions of silver nanoparticles produced by laser ablation, when irradiated with visible light, release a higher concentration of silver ions. Currently the consensus is that AgNPs are toxic due to their ability to release Ag^+ ions. Therefore, an increase in ion release will cause an increase in antimicrobial activity that may allow for lower levels of AgNPs required when treating bacterial infections, thus, limiting off-target toxicity. Our group showed that ablating a pure silver target immersed in a SDS solution produced very concentrated colloidal silver nanoparticle solutions, with hydrodynamic radii of approximately 40 nm. We also showed that this antimicrobial activity was greatly enhanced when the solutions were exposed to visible light at power of approximately 0.7 W. Using the optical properties of the DZ-Ag^+ complex, it was shown that particles exposed to light release ions at a much higher rate relative to particles kept in the dark. The reduced antimicrobial activity of the AgNP in the presence of L-cysteine showed that ions play a major role in the antibacterial effectiveness of AgNPs. As stated above we hope that paired with light, these silver nanoparticles can be employed at a low enough concentration that no adverse effects to mammalian cells will occur, or at the very least the mammalian cell death will remain localized.

References

1. Alexander, J. W. History of the medical use of silver. Surg. Infect. (Larchmt). 2009, 10, 289–292 DOI: 10.1089/sur.2008.9941.
2. Amendola, V.; Meneghetti, M. Laser ablation synthesis in solution and size manipulation of noble metal nanoparticles. Phys. Chem. Chem. Phys. 2009, 11, 3805–3821 DOI: 10.1039/b900654k.

P-123

Confined atmospheric pulsed laser deposition of nanostructured ultrathin films

R McCann [1,2,3] K Bagga[1,2], A Stalcup[2,4], M Vázquez[1,2,4] and D Brabazon[1,2,3]

[1] *Advanced Processing Technology Research Centre, School of Mechanical & Manufacturing Engineering, Dublin City University, Ireland*
[2] *1rish Separation Science Cluster, National Centre for Sensor Research, Dublin City University, Ireland*
[3] *National Centre for Plasma Science and Technology, Dublin City University, Ireland*
[4] *School of Chemical Sciences, Dublin City University, Ireland*
Email: ronan.mccann5@mail.dcu.ie

Control of parameters such as plasma density and electron temperature during pulsed laser deposition (PLD) has a large influence over the characteristics of resultant deposited material [1]. This control can be achieved through laser parameters such as fluence, wavelength, pulse repetition frequency or number of laser shots [2]. Alternatively, process parameters such as target-to-substrate distance or ambient pressure conditions can be altered. For example, when conducted in vacuum or with a low-pressure background gas, stoichiometric thin films can be formed upon deposition. When the plume is confined spatially, the increased plasma density and period can allow for nanoparticle formation via nucleation to occur within the plume. This confinement can be achieved through the use of a sufficiently high pressure of background gas [3] or spatially confining the plasma by placing the substrate in close proximity to the target [4]. Alternatively, the application of ultrashort pulse laser irradiation can also generate nanoparticles within the plume, though the mechanism of nanoparticle formation is fragmentation and decomposition of the target material due to rapid heating [5].

Here we demonstrate confined atmospheric pulsed laser deposition of nanostructured ultrathin films utilising a picosecond pulsed Nd:YAG laser to deposit aluminium nanoparticles onto a cyclic olefin polymer (COP) substrate. These metallic nanostructured coatings are of interest for chemical sensing [6], which is the focus of the current study, but also have applications in areas such as solar power and display technology. This paper presents the potential for provision of such functionalised surface platforms via pulsed laser deposition.

[1] L. Escobar-Alarcón, A. Arrieta, E. Camps, S. Romero, M. Fernandez, E. Haro-Poniatowski, "Influence of the plasma parameters on the properties of aluminum oxide thin films deposited by laser ablation", Appl. Phys. A. 93 (2008) 605–609.
[2] G. Abdellatif, H. Imam, "A study of the laser plasma parameters at different laser wavelengths", Spectrochim. Acta Part B At. Spectrosc. 57 (2002) 1155–1165.
[3] D.B. Geohegan, A.A. Puretzky, G. Duscher, S.J. Pennycook, "Time-resolved imaging of gas phase nanoparticle synthesis by laser ablation", Appl. Phys. Lett. 72 (1998) 2987.
[4] T. Donnelly, J.G. Lunney, "Confined laser ablation for single-shot nanoparticle deposition of silver", Appl. Surf. Sci. 282 (2013) 133–137.
[5] S. Amoruso, R. Bruzzese, X. Wang, N.N. Nedialkov, P.A. Atanasov, "Femtosecond laser ablation of nickel in vacuum", J. Phys. D. Appl. Phys. 40 (2007) 331–340.
[6] S.R. Jim, A. Foroughi-Abari, K.M. Krause, P. Li, M. Kupsta, M.T. Taschuk, et al., "Ultrathin-layer chromatography nanostructures modified by atomic layer deposition", J. Chromatogr. A. 1299 (2013) 118–25.

P-124

PLD of layered double hydroxides for hydrophobic coatings

A. **Matei[1], R. Birjega[1], A.Vlad[1], B.Mitu[1], R.Zavoianu[2], O.D.Pavel[2], M.C. Corobea[3], M. Dinescu[1]**

[1]National Institute for Lasers, Plasma and Radiation Physics, 409 Atomistilor Str., 077125 Bucharest, Magurele, Romania

[2]University of Bucharest, Faculty of Chemistry, Department of Chemical Technology and Catalysis, 4-12 Regina Elisabeta Bd., Bucharest, Romania

[3]National R.&S. Institute for Chemistry and Petrochemistry, ICECHIM, 202 Splaiul Independentei Str., CP-35-274, 060021, Bucharest, Romania

andreea.purice@inflpr.ro

Wettability is a very important property of solid surfaces and is governed by both the chemical composition and the surface topography. Superhydrophobic surfaces/coatings have gained great interest because of their significant potential applications in various fields such self-cleaning, anti-icing, friction reduction, antifouling technologies, microfluidic devices, chemical reactors, biosensors. We report here on the production of hydrophobic composite films of fatty acids/ layered double hydroxides by PLD (pulsed laser deposition) by laser light using three different wavelengths 266, 532 and 1064 nm respectively. Targets were pressed pellets from Mg-Al or Zn-Al LDH (layered double hydroxides) and intercalated fatty acids obtained by precipitation. Analysis of the films demonstrates that crystalline and hydrophobic films with contact angle up to 150^{o} can be obtained, as a function of the deposition parameters and the fatty agent used (lauric acid or stearic acid). Chemical and thermal analysis, X-ray diffraction, IR spectroscopy, scanning electron microscopy, atomic force microscopy and contact angle measurements were the techniques used for the characterization of the deposited thin films.

P-125

Thin films of ferrocene derivatives for non-linear optical applications: laser processed thin films and printed pixels

***Andreea Matei[1], Catalin Constantinescu[1], Bogdana Mitu[1], Iulian Ionita[1,2], Ana Emandi[3,4], Maria Dinescu[1]**

[1]INFLPR – National Institute for Laser, Plasma and Radiation Physics, 409 Atomistilor St, RO-077125, Magurele, Romania
[2]UB – University of Bucharest, Faculty of Physics, 405 Atomistilor St, RO-077125, Magurele, Romania
[3]UB – University of Bucharest, Faculty of Chemistry, 90-92 Panduri St., RO-050663, Bucharest, Romania
[4]INOE2000 - National Institute for Research and Development in Optoelectronics, 409 Atomistilor St, RO-077125, Magurele, Romania
**Corresponding Author e-mail address: andreea.purice@inflpr.ro*

Thin films of ferrocene-based compounds have been deposited by matrix-assisted pulsed laser evaporation (MAPLE), to be further used in nonlinear applications and sensors. The fourth harmonic of a Nd:YAG pulsed laser (4ω / 266 nm, 7 ns pulsed duration) was used in processing the thin films, using typically low fluences (200-400 mJ/cm²) at a repetition rate of 10 Hz. The structure and the morphology of the films were investigated by Fourier-transform infrared spectroscopy (FTIR), scanning electron microscopy (SEM), and atomic force microscopy (AFM) techniques. The optical properties were analyzed by spectroscopic-ellipsometry (SE), while the second harmonic generation (SHG) capabilities were investigated by irradiating the films using a tunable Ti:sapphire laser with maximum emission centred in the near infra-red (~800 nm, 60-100 fs). The 'as-deposited' films were further used as donors in laser-induced forward transfer (LIFT) experiments and their morphological, structural and optical properties of the pixels are reported. The influence of the film thickness and the presence of a metallic dynamic release layer (DRL) are discussed.

P-126

Fabrication of Polyimide Spheres by Pulsed Laser at 355 nm

Yong-Won Ma[1], Bo Sung Shin[1,2], Sang-Mae Lee[2], Moon-Suk Kang[1], Chan Park[1], Sung-Moo Hong[2], Myung-Ju Kim[2]

[1]Department of Cogno-Mechatronics Engineering, Pusan National University, Jangjeon 2-dong, Geumjeong-gu, Busan, Korea
[2]Engineering Research Center for Net-Shape and Die Manufacturing (ERC/NSDM), Pusan National University, Jangjeon 2-dong, Geumjeong-gu, Busan, Korea
E-mail: bosung@pusan.ac.kr

1. Abstract

In this paper, a new fabrication method of micro polyimide(PI) spheres which were processed by Pulsed laser at 355 nm was suggested. A chamber with quartz allowing laser was filled with carbon dioxide (CO_2). Liquid polyimide in the chamber was irradiated by pulsed laser, and then shockwaves were generated over the liquid polyimide. The shockwaves made CO_2 forcibly penetrate into the liquid polyimide. Liquid polyimide baked in the oven at atmospheric pressure, micro-sized polyimide spheres were formed in a regular size. Micro polyimide spheres were studied using transmission electron microscopy (TEM) and scanning electron microscope (SEM). The effects of process parameters such as laser fluence, CO_2 pressure and baking conditions were investigated. This proposed method will be applied in the same way with other types of polymer and gas to make a variety of micro and nano polymer sphere.

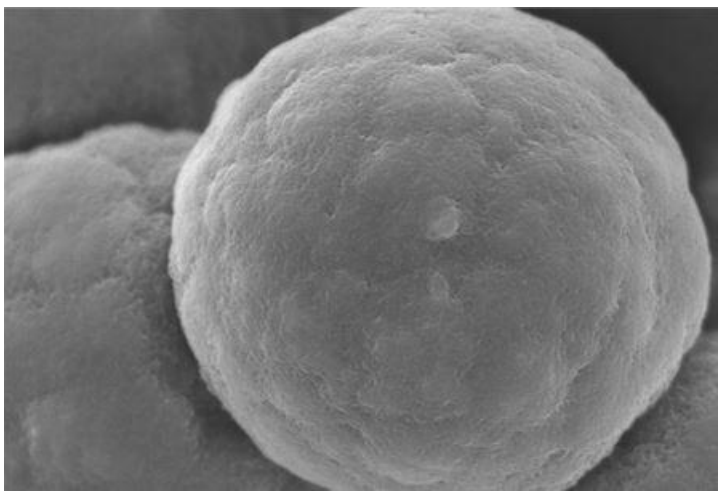

Fig. 1. Polyimide microsphere

P-127

Structural and morphological properties of metallic thin films grown by pulsed laser deposition for photocathode application

A. Lorusso[1]*, F. Gontad[2], G. Maruccio[1,3], E. Chiadroni[4], and A. Perrone[1,2]

[1]Università del Salento, Dipartimento di Matematica e Fisica "E. De Giorgi", 73100 Lecce, Italy
[2]Istituto Nazionale di Fisica Nucleare e Università del Salento, 73100 Lecce, Italy
[3]National Nanotechnology Laboratory, Istituto Nanoscienze-CNR, Arnesano I-73100, Italy
[4]Laboratori Nazionali di Frascati, Istituto Nazionale di Fisica Nucleare, 00044 Frascati, Italy
Corresponding author e-mail: antonella.lorusso@le.infn.it

In this work magnesium, yttrium and lead thin films have been deposited by pulsed laser ablation technique and characterized by different diagnostic methods. All the films revealed a polycrystalline structure; Mg and Y films were uniform while grain morphology characterized Pb films. Such metallic materials are studied because they are proposed as good alternative to copper and niobium photocathodes which are generally used in radiofrequency and superconducting radiofrequency guns, respectively [1, 2]. The relatively low work function and high quantum efficiency of Mg, Y and Pb make possible the employ of these devices as photocathodes improving the performances of the cathode installed in the gun [3]. In this way high brightness electron beam sources can be obtained which are demanded, for example, for the new generation of X-ray free electron lasers. The photoemission performances of the photocathodes based on Mg, Y, and Pb thin films have been also studied. Finally the role of the surface contaminations on the electron photoemission has been discussed for the different materials.

[1] A. Cianchi, et al., "High brightness electron beam emittance evolution measurements in an rf photoinjector", Phys. Rev. Spec. Top., **11**, 032801 (2008)

[2] C. Xu, C. Reece, and M. Kelley, "Characterization of Nb SRF cavity materials by white light interferometry and replica techniques", Appl. Surf. Sci. **274,** 15 (2013)

[2] A. Lorusso, F. Gontad, A. Perrone, and N. Stankova, "Highlights on photocathodes based on thin films prepared by pulsed laser deposition", Phys. Rev. ST Accel. Beams **14** 090401 (2011).

P-128

Systematic investigation of plasma shock evolution from Al target induced by nanosecond Nd:YAG laser ablation

Tianhang Liu, Xun Gao, Zuoqiang Hao, Haiyan Tao and Jingquan Lin*

School of Science, Changchun University of Science and Technology, 130022Changchun, Jilin, China
Corresponding Author: linjingquan@cust.edu.cn

In recent years, with the widely used of the plasma shock wave in laser deposition film coating, laser cleaning, laser propulsion and other related fields, researchers have paid more and more attentions to the dynamic characteristics of plasma shock wave. The laser plasma shock plays a unique role in those applications, and it is strongly dependent on the experimental conditions such as focusing conditions, laser incidence angle, laser wavelength and so on. Up to now, temporal evolution of an Al plasma shock under various experimental conditions has not been fully studied yet.

In this report, evolution of laser plasma shock wave from the Al target that is ablated with a nanosecond IR(1064 nm) and UV(355 nm) laser, under varied incidence angle (normal and with 30 degree to the target normal), and with different focusing conditions (focal point on, ahead of and after the target surface) in air is systematically studied using time-resolved shadowgraph imaging technique. Shadowgraphs of plasma shock evolution under various experimental conditions have been recorded, and correspondingly velocities and pressure of the plasma shock front have been obtained [1]. In the experiment, we have observed a series interesting phenomena (1) With both the normal and oblique laser incidence configurations, evolution of laser plasma shock is strongly influenced by air breakdown which occurs prior to the laser beam reaching the target with the IR and UV laser ablation. (2) An ionization channel is observed for both the laser incidence configurations under the 355 nm laser ablation if focal point is set in front of the target surface. (3) A clear straight boundary between the Al plasma shock and air plasma is observed with the both laser incident configurations. (4) A protrusion appears at the front tip of the shock wave in the shadowgraph with the plasma evolution time around 100 ns if the focal point is at the target surface. (5) Under the oblique incidence, the shock expansion with an ellipsoid-shaped front travelling mainly against the incoming laser beam at the initial stage of laser ablation, and then the shape of shock front turns into a sphere with both UV and IR ablation laser wavelengths. Also an additional spherical plasma shock front travelling normal to the target surface was observed, this parts unify with the one that is against the incoming laser beam, and finally the two form a spherical wave as time delay increases to around 100 ns. The underline physics of those observations are given.

The findings in this work can be utilized in the optimization of laser plasma shock and have the potential in many laser shock application cases such as in the laser film coating, cleaning and other related fields.

This project was supported by National Natural Science Foundation of China under Grant Nos. 61178022.

References

[1] T. Liu, X. Gao, Z. Hao, and J.Lin, " Shadowgraph investigation of plasma shock waves evolution from Al target under 355 nm laser ablation" Chin.Phys. B. 23, 085203 (2014).

P-129

Experimental and Numerical Studies of Nanosecond Laser Processing for Industrial Micromachining Applications

Z. Lin, H. Matsumoto, J. Kleinert, S. Concina,
Electro Scientific Industries Inc., 13900 NW Science Park Drive, OR Portland 97124, USA
A. Otto, R. G. Vázquez, R. Bielak, S. Tatra,
Institute for Production and High Power Laser Technology, Vienna University of Technology, Gusshausstrasse 30, Vienna 1040, Austria
A. N. Volkov, G. Silverstein, O. Ranjbar
Department of Mechanical Engineering, University of Alabama, H. M. Comer Hall, 7th Avenue, Tuscaloosa, AL 35487, USA

Corresponding Author e-mail address: linz@esi.com

In semiconductor device manufacturing, consumer electronics production, and many other industries that widely employ laser-processing technologies, there has been an ever-growing trend towards better processing quality and increasing process throughput. Specifically, this means cutting, drilling, scribing and marking of parts with smaller feature sizes, improved accuracy and at faster processing speed. On the other hand, experimental optimization of laser parameters (wavelength, pulse width, power, repetition rate, etc.) for achieving desired process quality and throughput could involve time-consuming trial-and-error procedures. By integrating different levels of computational approaches, we aim to increase effectiveness in developing process solutions through computer simulations, and help minimizing the time and cost for process development in industrial laser micromachining applications. To this end, a multiphysical nanosecond laser-material simulation package, based on a modified volume-of-fluid (VOF) approach, was developed through a collaborative project between TU-Wien and ESI [1]. The simulation model accounts for the propagation and the interaction of laser beam with work target, phase transformations (melting, evaporation, resolidification and condensation) involving different types of materials, as well as mass and energy transfer in both liquid and vapor phases. During high-power laser ablation, the coupling of laser beam with laser-induced plasma plume can occur and lead to shielding of laser pulse and reduction in the effective energy deposition within the work targets. We develop a hydrodynamic model capable of modeling the effects of plasma shielding and plume dynamics in nanosecond laser ablation of metals under different background gas environments. By leveraging our modeling capabilities of laser and materials interactions, we carry out numerical simulations to address various laser processing needs in industrial micromachining applications. In particular, we simulate nanosecond laser processing of metal targets and multi-layer light-emitting-diodes (LEDs) and show good agreements of the simulation results with experimental observation.

[1] A. Otto, H. Koch, R. Gomez Vazquez, Z. Lin, B. Hainsey, Multiphysical Simulation of ns-Laser Ablation of Multi-Material LED-Structures, Physics Procedia, 56, 1315, 2014

P-131

Laser ablation of CFRP by using picosecond laser and femtosecond laser

O.Kim[1], S.Kim[1], J.Oh[1], Y.Kim[1], H.Kim[2]
[1]*Laser Application Center, Kyungpook Nation University, 80 Daehak-ro, Buk-gu, Daegu, South Korea*
[2]*School of Electronics Engineering, Kyungpook Nation University, 80 Daehak-ro, Buk-gu, Daegu, South Korea*
E-mail: oskim@knu.ac.kr

Carbon fiber-reinforced plastic (CFRP) has been used in various industries to fabricate automobile parts, sports equipment, medical parts, aerospace components, and building materials. CFRP has a high strength-to-weight ratio, does not corrode, and provides outstanding fatigue resistance compared with engineering metals. Therefore, it will likely be used for many more applications in the future.

However, cutting CFRP is known to be difficult because of the different matrix properties and fiber orientation as well as the high level of hardness of the carbon fiber along with the relative volume of the fiber [1]. Conventional mechanical cutting processes such as micro-cutters, milling/machining, or abrasive water-jet machining, can provide high-quality cutting, but when these processes are used to cut CFRP, they have many disadvantages such as considerable tool wear and costs, and limited processing time when [1]. Lasers have been proposed as an alternative technique for cutting CFRP. Laser cutting is a non-contact removal process that avoids the disadvantages of conventional machining methods, but it introduces thermal defects such as a wide heat-affected zone (HAZ). Thermally damaged regions are often reported as the main challenge to overcome in laser-cutting processes [2–4]. As reported in [5, 6], it is therefore challenging to obtain high-quality cuts in CFRP using a laser. Recently, researchers have used various types of lasers to cut CFRP, including a disk laser, single-mode fiber laser, and a picosecond laser. However, these techniques all produce heat effects and poor edge quality. A HAZ is caused when the material is changed from the solid phase to the vapor phase and then to plasma almost instantaneously.

However, unlike conventional laser machining, femtosecond laser and picosecond laser machining reduce collateral damage to the surroundings[7]. Therefore, the ablation properties of the CFRP were experimented by using a picosecond laser and femtosecond laser.

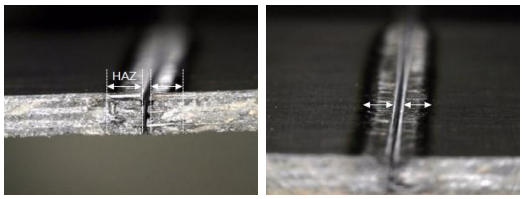

(a) (b)

Fig. 1 1.0-mm-thick CFRP plate after laser cutting with a picosecond laser:
(a) optical surface image and, (b) optical top-view image

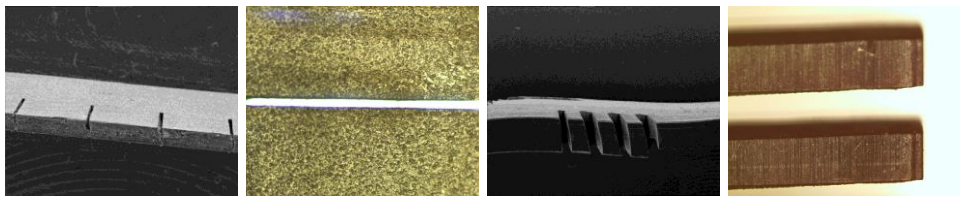

(a) (b) (c) (d)

Fig. 2 0.3-mm-thick CFRP plate after laser cutting with a femtosecond laser
(a) scanning electron microscopy(SEM) surface image, (b) SEM top-view image
1.0-mm-thick CFRP plate after laser cutting with a femtosecond laser
(c) SEM top-view image, (d) optical top-view image

The Experiments results show that heat affected zone was 0 to 8um and cross section was 0 to 60um. Heat affected zone and cross section area was extremely smaller than other lasers. The results of CFRP cutting with femtosecond laser exhibits a clean top and excellent sidewall quality along with a negligible heat affected zone.

In this paper, the characteristics of ultra-short pulsed laser micro-machining have been reviewed and experimentally demonstrated in laser cutting of CFRP.

[1] K. W. Jung, Y. Kawahito, S. Katayama: Int. Welding/Joining conf., (2012) pp. 75-75. (Conference Proceedings)
[2] A. Wolynski, H. Haloui, P. Mucha, A. Gleite, P. French, R. Weber, T. Graf: Proc. ICALEO 2010, (2010). (Conference Proceedings)
[3] P. Mucha: Studienarbeit IFSW 10-37, (2010). (Conference Proceedings)
[4] R. Weber, M. Hafner, A. Michalowski, P. Mucha, T. Graf: Proc. ICALEO 2011, (2011). (Conference Proceedings)
[5] M. Hafner, R. Weber, T. Graf: Neue Messe Stuttgart, (2012). (Conference Proceedings)
[6] C. Freitag, M. Hafner, A. Michalowski, V. Onuseit, R. Weber, P. Berger, T. Graf: LPCC 2012, (2012). (Conference Proceedings)
[7] Eichenholz, Jason M., et al.: Int. Soc. for Op-tics and Photonics, (2006). (Conference Proceedings)

P-132

Printing and surface patterning in liquids by laser and ultrasound ablation

A.A. Asratyan[1], N.A. Bulychev[2], I.N. Feofanov[2], M.A. Kazaryan[2], V.I. Krasovskii[3], K.B. Konovalov[4], V.I. Sachkov[4]

[1] *Gamalei Institute of Epidemiology and Microbiology, 123098, Gamalei Str., 18, Moscow, Russia,*
[2] *P.N. Lebedev Physical Institute, Russian Academy of Sciences, 119991, Leninsky pr., 53, Moscow, Russia,*
[3] *A.M. Prokhorov General Physics Institute, Russian Academy of Sciences, 117942, Vavilova st., 38, Moscow, Russia*
[4] *Joint Stock Company "Istok", 141190, Vokzalnaya Str., 2A, Fryazino, Moscow Region, Russia*
[5] *Siberian Physical-Technical Institute of the Tomsk State University, 634050, pl. Novo-Sobornaya, 1, Tomsk, Russia*
E-mail: kazar@sci.lebedev.ru, kazarmishik@yahoo.com

In this work, the effect of laser and ultrasonic irradiation induced particles motion in liquid phase was studied. If a certain volume with suspension is used as an object in the setup, it could be expected that particles of the suspension affect the formation of the light field and radiation that in turn will cause the motion of the particles. In our experiments it has been shown that erythrocytes chaotically distributed in the central zone of the suspension volume, migrated into the region of the central light spot. Cells at the center broke down and form conglomerates with the size five to ten times exceeding the size of individual cells. The motion of all particles in the illuminated area proved to be light-induced within 20 sec after the formation of conglomerates. The motion was strictly ordered and had a cyclic character. Under certain conditions, conglomerates accumulated near the surface of the object and colliding particles could not leave the central region. Conglomerates grew up to the size of the illuminated surface. The speed of erythrocytes movement has been estimated as 1 cm/sec. When a suspension with transparent particles was used, the following process was observed: particles distributed around the center of the suspension volume migrated into the region of the central light spot and were trapped there due to light pressure. The character of this specific light-dynamic effect apparently differs from a simple capture of particles into a light-induced trap. The special setup applied is based on the so-called shock-wave acceleration in the field of laser radiation. Particles with the size from 1 to 10 μm were used as strongly absorbing particles. At the power of 1-10 W and ultrasonic treatment with 20 kHz repeating pulses, intensive motion of particles along the beam was observed on the screen. The particles colliding with the quartz plate destroyed its surface layer and some of them penetrated at the depth of several μm. The configuration of the treated area corresponded to the shape of computer driving mask. If the penetration depth is known, we can calculate the initial speed. Thus, the speed was estimated as about 10 km/sec. In this case, the possibility of printing and surface patterning in liquids by laser and ultrasound ablations in form of alfabet letters or any like patterns with the special resolution of a few μm is achieved.

This work has been partially supported by RFBR, projects No. 15-02-03559, 14-02-00602, 14-02-31515, 14-02-92019.

P-133

Laser removal of a coating from glass slides of consolidant materials relevant to museum conservation practice

S Haefner[1], B F Johnston and D M Kane

MQ~Photonics Research Centre and Dept. of Physics & Astronomy, Macquarie University ~ Sydney, NSW 2109, Australia
[1]now at Physikalisches Institut, Heidelberg, Germany
deb.kane@mq.edu.au

1. Consolidants used on Australian Aboriginal bark paintings and in museum conservation

Arguably, the most serious conservation issue for Australian Aboriginal traditional bark paintings is de-adhesion of the bound pigments. Consolidation of the pigment (in combination with its original binder) to the bark has been and still is a significant conservation practice on the paintings [1,2]. Past practice has included consolidating the painting as a whole. This alters the texture and colour of the pigments from their as-painted state. There is interest to know if it might be possible to remove some of this consolidant from the surface of the paintings, if it is at least in part in the form of a coating. Paraloid B72, polyvinyl butyral (PVB) and gelatine are the consolidants included in the study. Paraloid B72 is a well regarded consolidant which is used broadly in conservation practice. PVB and gelatine have been used in the past but are not favoured currently. Some research on laser removal of these consloidants from technical samples of Aboriginal bark paintings have been reported [3].

2. Experiment

We report research trialing laser removal of paraloid B72, polyvinyl butyral (PVB) and gelatine from glass microscope slides in order to measure systematic laser ablation and removal rates as dependent on laser wavelength and pulse energy fluence. Both a frequency-doubled Nd:YAG (532 nm), and a frequency-quadrupled Nd:YAG (266 nm) nanosecond pulse duration laser have been used in the study. The material removal is measured using optical surface profiling of the processed sample. An example of single spot processing using 1 to 15 pulses, 532 nm laser, at 6 different pulse fluences are shown in fig.1. The "x" and "y" profiles are quantified to measure the ablation depth and profile.

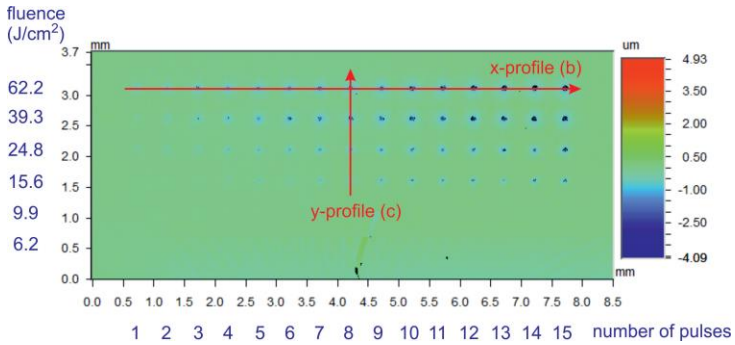

Fig. 1. Array of single and multiple shot experiments with varying fluences for PVB on glass. The number of pulses increases from left to right from one pulse up to 15 pulses. The fluence decreases from top to bottom from 62.2 J/cm^2 to 6.2 J/cm^2.

3. Results and discussion

The study shows that PVB and gelatine can be laser ablated in a controlled manner using the 266 nm wavelength and with pulse fluences between ~2-4 J/cm^2. Paraloid B72 can not be systematically ablated. It bubbles and froths at low and modest pulse fluences and is completed removed with associated damage to the substrate at fluences above 8 J/cm^2. Further outcomes which inform consolidant choice will be reported.

4. Acknowledgements

We are indebted to Mr Colin Macgregor, Manager, Conservation of Materials, Australian Museum, for his advcie on the consolidants and for providing samples of them. Andreas Bilicki completed the optical surface profiling.

5. References

[1] B. Tworek-Matuszkiewicz, "Bark paintings: techniques and conservation', in Caruana, W. (ed.) *Windows on the dreaming: Aboriginal painting in the Australian National Gallery*, (Australian National Gallery and Ellsyd Press, Canberra and Sydney, 1989).

[2] B. Tworek-Matuszkiewicz, B., 'Australian aboriginal bark paintings - their history, structure and conservation', *Reviews in Conservation*, (8) (2007) 15-28.

[3] D M Kane, G Palmer, B F Johnston, S Haefner, A T Bilicki, A Fuerbach and A J J Fernandes, "Studies on Laser Removal of Consolidants & Protective Coatings from Samples of Australian Aboriginal Bark Paintings**, ",** pg 4-11, *Lasers in the Conservation of Artworks IX*, Eds D Saunders, M Strlic, C Korenberg, N Luxford and K Birkholzer, Archetype Publications Ltd, London 2013, ISBN:978-1-904982-87-6.

P-134

Preparation of visible-light-responsive titanium oxides by laser ablation in liquid

R. Kajimoto, Y. Sun, T. Maemoto, Y. Harada and S. Sasa
Nanomaterials Microdevices Research Center, Osaka Institute of Technology
5-16-1 Omiya, Asahi-ku, Osaka 535-8585, Japan
E-mail: ryo02kajimoto@tenor.ocn.ne.jp

Visible-light-responsive type titanium oxides (eg, Ti_2O_3 and Ti_4O_7) compared with titanium dioxide (TiO_2) have many advantages to indicate the absorption in the visible region. It is considered an effective material using a photochemical reaction or photoelectron chemical reactions. Also, as compared with TiO_2 by utilizing the visible-light-responsive type titanium oxides, the electron conductivity is remarkably improved, and the application of the electrode material and a conductive material is expected. In fact, the visible-light-responsive type titanium oxides as high-efficiency electrode material of a solar cell has been reported so far [1]. In this paper, we report fabrication and characterization of visible-light-responsive microsphere titanium oxides by using a liquid-phase laser ablation method.

Fabrication procedure of microsphere titanium oxides is shown in Fig. 1. Titanium oxides with nanoparticles is contained to ethanol solution, which was irradiated with the forth harmonic of a pulsed Nd:YAG laser placed outside the glass cell. The wavelength of the laser radiation was 266 nm, the pulse duration was about 5 ns, and the repetition rate was 10 Hz. After the laser ablation of titanium oxides in liquid, the solution was dropped onto a glass substrate. SEM images of titanium oxides before and after the liquid phase laser ablation were shown in Fig. 2. We successfully fabricated microspheres of titanium oxides by liquid-phase laser ablation, the submicron-sized titanium oxides spheres had high sphericity and crystalline quality as well as good stability under ambient condition. The inset in Fig. 2 shows photograph comparing unmodified white and artificial black titanium oxides by laser ablation in liquid. These results indicate that successful in producing the visible-light-responsive titanium oxides. We also examined heat treatment effects in air of the visible-light-responsive titanium oxides. Figure 3 shows Raman spectra after the annealing of titanium oxides. From these results, we found that anatase-type titanium oxides is formed and visible-light-responsive titanium oxides are maintained at the annealing below 600 ℃.

[1] Xiaobo Chen, Lei Liu,Peter Y. Yu, Samuel S. Mao, "Increasing Solar Absorption for Photocatalysis with Black Hydrogenated Titanium Dioxide Nanocrystals", SCIENCE, Vol. 331, 746.

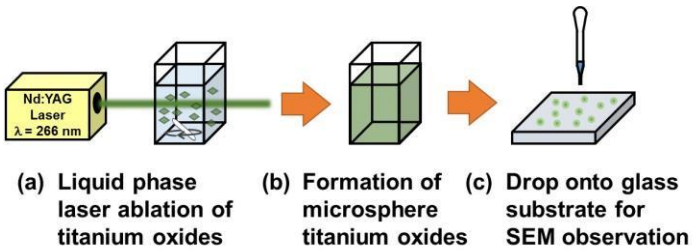

Fig. 1. Schematic diagram of the fabrication procedure of visible-light-responsive type microsphere titanium oxides.

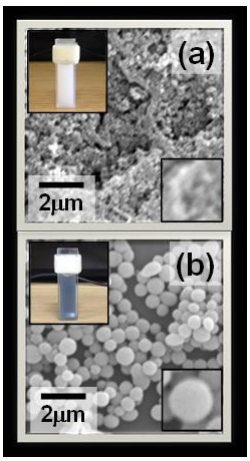

Fig. 2. SEM images of titanium oxides before (a) and after (b) the liquid phase laser ablation.

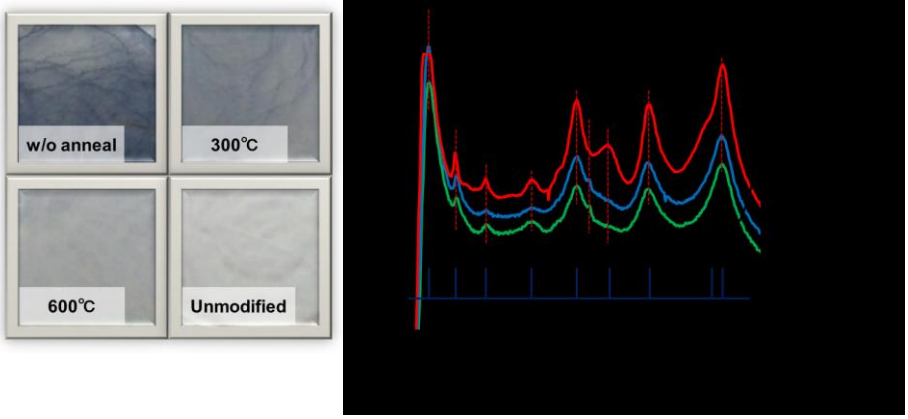

Fig. 3. Photographs of the surface and Raman spectra of titanium oxides without and after the annealing. The peak positions of TiO_2 (White) shown in Fig. 3 is obtained from different structure of a standard TiO_2.

P-135

Bonds and bio- properties of hybrid laser Cr- doped DLC for implants

Miroslav Jelínek[1,2], Marta Vandrovcová [3], Lucie Bačáková [3], Josef Zemek[1], Tomáš Kocourek[1,2], Jan Remsa[1,2],

[1]Institute of Physics, Academy of Sciences of the Czech Republic, v.v.i., Na Slovance 2, 18221 Prague, Czech Republic
[2]Czech Technical University in Prague, Faculty of Biomedical Engineering, nam. Sitna 3105, 27201 Kladno, Czech Republic
[3] Institute of Physiology, Academy of Sciences of the Czech Republic, v.v.i., Videnska 1083, 14220 Prague 4, Czech Republic

jelinek@fzu.cz

Diamond – like carbon (DLC) thin films are frequently used for coating of implants. The problem of DLC layers lies in bad layer adhesion to metal implants. Chromium is used as a dopant for improvement of adhesion of DLC films. Cr-DLC layers were prepared by a hybrid technology using combination of pulsed laser deposition (PLD) from graphite target and magnetron sputtering (continuous stream of material from Cr target). Atomic concentrations of carbon, oxygen, and chromium were determined from C 1s, O 1s, and Cr 2p photoelectron peak areas. Carbon (sp^2 and sp^3 bonds) and concentration of trivalent and toxic hexavalent chromium bonds were also determined by XPS. The sp^3/sp^2 ratio is generally decreasing for higher chromium content and carbide content increasing. The Cr^{6+} spectral signal was identified from the sample surface with the highest Cr contents. Depending on the deposition conditions (laser rep. rate and magnetron power), the concentration of Cr in DLC layers moved from zero to 8.4 at%. XRD revealed no chromium peaks.

In all evaluated time intervals, the population density of Saos-2 cells was the highest on samples containing higher concentrations of chromium (7.1 and 8.4 at%). On day three after seeding, the most apparent focal adhesion plaques revealed by confocal microscopy were also found on samples with the higher concentrations of chromium. The intensity of fluorescence of vinculin, i.e. a protein participating in cell adhesion, was significantly higher on all DLC and Cr-DLC samples than on control microscopic glass slides. However, the expression of collagen type I and alkaline phosphatase was the highest on Cr-DLC samples with lower concentration of Cr (0-1.5 at%). This finding was further confirmed by measurement of the intensity of fluorescence of collagen type I.

We can conclude that higher concentrations of chromium supported cell adhesion and proliferation; however DLC and DLC doped with lower concentration of chromium supported cell differentiation.

Closer experimental details, comparison with contact angles and antibacterial properties [1] and differences in creation and properties of Cr-DLC layers by PLD+ magnetron or by double PLD [2] will be also discussed.

[1] M. Jelinek, T. Kocourek, J. Zemek, J. Mikšovský, Š. Kubinová, J. Remsa, J. Kopeček, K. Jurek. "Chromium-doped DLC for implants prepared by laser-magnetron deposition." *Materials Science and Engineering: C.*, vol. **46**, PP. 381-386 (2015).

[2] P. Písařík, M. Jelinek, T. Kocourek, M. Zezulová, J. Remsa, K. Jurek. "Chromium-doped diamond-like carbon films deposited by dual-pulsed laser deposition". *Applied Physics A.*, vol. **117**, issue 1, PP. 83-88 (2014).

P-136

Thermoelectric YbCoSb Laser Prepared Layers

Miroslav Jelínek[1,2], Radek Zeipl[1], Tomáš Kocourek[1,2], Jan Remsa[1,2], Jiří Navrátil [3]

[1]Institute of Physics of the Academy of Sciences of the Czech Republic, v.v.i., Na Slovance 2, 18221 Prague, Czech Republic
[2]Czech Technical University in Prague, Faculty of Biomedical Engineering, nam. Sitna 3105, 27201Kladno, Czech republic
[3]Institute of Macromolecular Chemistry of the Academy of Sciences of the Czech Republic, v.v.i., Heyrovského nám. 2, 16206 Prague, Czech Republic

jelinek@fzu.c

$CoSb_3$ – based skutterudites has been attracting research interest mainly because of their low thermal conductivity, high Seebeck coefficient and electrical conductivity. The dopation with Yb could help to reduce lattice thermal conductivity without altering the power factor [1]. We studied $Yb_XCo_4Sb_{12}$ layers prepared by pulsed laser deposition method (PLD). A high power pulsed excimer KrF laser (COMPexProTM 205 F, laser λ = 248 nm, τ = 20 ns) radiation was used as an external energy source to vaporize materials of the target and to deposit a thin film. Using PLD we prepared thin films on fused silica substrates and Si(100) substrates, dimension of 1 cm × 1 cm. The stoichiometric $Yb_{0.19}Co_4Sb_{12}$ target was prepared by hot pressing method. Target – substrate distance D_{T-S} was 4 cm or 6 cm.
For D_{T-S} = 4 cm distance we varied ambient argon deposition pressure from 0.5 Pa to 13 Pa, laser repetition rate from 3 Hz to 10 Hz. Substrate temperature was changed from 250 °C to 400 °C. We tested various laser fluencies from 0.8 $J \cdot cm^{-2}$ to 5 $J \cdot cm^{-2}$. Depends on deposition conditions the thickness of layers was from 90 nm to 600 nm. Growth rate moved from 0.06 A/pulse to 0.30 A/pulse. For lower fluencies the growth rate was lower. Films roughness was determined by Alpha-step IQ mechanical profilometer (KLA TENCOR Co.) and by Atomic force microscope (AFM). The lowest roughness (from of about 5 nm to 10 nm) was reached for low laser fluencies and low D_{T-S}, but mechanical quality of films was poor and growth rate low (about 0.1 A/pulse). The layer roughness and homogeneity were characterized also by the Atomic Force Microscope (AFM) Solver NEXT (NT-MDT) operating in dynamic regime with HA_NC tips. The layers surface parameters were calculated from a 50×50 μm area with software NOVA PX. AFM roughness measurements exhibited Ra about three times higher compared to mechanical profilometer. We observed lack of Yb and overlap of Co. Sb was transferred from target to film roughly stochimetrically. Films created at 0.8 Jcm-2 exhibited generally bad stoichiometry.
For D_{T-S} = 6 cm distance the film deposited at Ts = 270 °C, 4 Jcm^{-2}, were studied using AFM, WDX and XRD. Films were crystallografically homogeneous with structure $CoSb_3$.
The quality of thermoelectric layers is expressed by dimensionless figure of merit (thermoelectric efficiency) formula:

$$ZT = (S^2 \sigma T) / \lambda ,$$

where S, σ, T and λ are the Seebeck coefficient, the electrical conductivity, the ambient temperature, and the thermal conductivity, respectively. The electrical conductivity and Seebeck was measured in region from 20 oC to 200 °C. ZT was measured using Harman method. The room temperature ZT was found to be 0.04 resp. 0.05. We calculated thermal conductivity 1.6 - 3.0 $WK^{-1}m^{-1}$. The layers exhibited N- type properties. Obtained results will be discussed in details.

[1] S.R.S. Kumar, D. Cha, N.H. Alshareel, :Lattice dynamics and substrate- dependent transport properties of (In, Yb)- doped skutterudite thin films. Journal of Applied Physics 114, 083710 (2011)

P-137

Scanning thermal microscopy: Characterization of PLD films

Radek Zeipl[1], Miroslav Jelínek[1], Tomáš Kocourek[1], Jan Remsa[1], Jan Vaniš[1,2], Jiří Navrátil[3]

[1] Institute of Physics of the Academy of Sciences of the Czech Republic, v.v.i., Na Slovance 2, 18221 Prague, Czech Republic
[2] Institute of Photonics and Electronics of the Academy of Sciences of the Czech Republic, v.v.i., Chaberská 57, 18251 Prague, Czech Republic
[3]Institute of Macromolecular Chemistry of the Academy of Sciences of the Czech Republic, v.v.i., Heyrovského nám. 2, 16206 Prague, Czech Republic
zeipl@fzu.cz

Thermal conductivity of thermoelectric nano-layers was studied by a scanning thermal microscope working in AC and DC current mode. The microscope's cantilever is being heated by an electrical current and when there is a physical contact or at a very short distance between the measured sample and the cantilever, the probe temperature decreases due to power dissipation into the sample. The temperature change leads to resistance change in the probe which is evaluated using a Wheatstone bridge. The probe's resistivity versus temperature dependency is well known, so the temperature change can be evaluated. For this purpose a simple and reliable method has been developed. The sensitivity of the method is demonstrated on the steep Si substrate-layer boundaries made by a Ga+ Focused Ion Beam technique.

The thermal conductivity experiments were conducted on the single thin layers of different thickness in the range from about 110 nm to 860 nm, prepared by pulsed laser deposition from different hot pressed targets of thermoelectric materials like Bi_2Te_3 and $Yb_{0.19}Co_4Sb_{12}$ on Si (100) substrates 10x10 mm in dimension. We choose Bi_2Te_3 because it has been well established thermoelectric material for more than decade and the bulk $Yb_{0.19}Co_4Sb_{12}$ skutterudite turned out to be material with a possibly high thermoelectric figure of merit. The low thermal conductivity of skutterudite in general is obtained by filling the voids in the structure with small diameter, large-mass interstitials such as for example Yb, Ce etc. The both chosen materials were in a form of thin layer successfully prepared by several deposition methods including Pulsed Laser Deposition in the past.

Deposition took place in Ar atmosphere of 13 Pa, the target to substrate distance was set 40 mm or 60 mm and the base vacuum of the coating system was 5×10^{-3} Pa. The layers were prepared using a high power pulsed excimer KrF laser (COMPexProTM 205 F, laser $\lambda = 248$ nm, $\tau = 20$ ns) with repetition rate of 10 Hz and laser spot 2 x 1 mm^2. For the smoothest Bi_2Te_3 layers were prepared at temperature of 200 °C with the laser fluency of 3 Jcm^{-2}. The $Yb_{0.19}Co_4Sb_{12}$ layers were prepared at 270 °C with 4 Jcm^{-2}. The deposition conditions were chosen based on results of study of influence of the conditions on the layer surface quality which had been done with the objective to prepare smooth i.e. low roughness and homogeneous layers. The increased surface roughness could cause inaccuracy and create difficulties such as artefacts, when using any scanning probe microscope measurement technique, including thermal microscope.

The layers transport and thermoelectric properties such as the in-plain electrical resistivity and the Seebeck coefficient were studied in temperature range from room temperature up to 200 °C. A conventional DC van der Pauw's method was used for the electrical resistivity measurement and the Seebeck coefficient was determined from the variation of the electromotive force for different temperature gradients across the layer. The room temperature thermometric figure of merit was measured by the Harman technique, in which parameters related to electrical conductivity, the Seebeck coefficient and thermal conductivity (that make up thermoelectric figure of merit ZT) are measured at the same place and at the same time with electrical current flowing through the layer. From the ZT value the room temperature thermal conductivity of the layers was estimated. For $Yb_{0.19}Co_4Sb_{12}$ and Bi_2Te_3 layers we got room temperature electrical resistivity of about 7 mΩcm and 1 mΩcm, the Seebeck coefficient of -112 μVK^{-1} and -61 μVK^{-1}, thermoelectric figure of merit about 0.04 and 0.13 and we estimated thermal conductivity of 1.3 $WK^{-1}m^{-1}$ and 0.9 $WK^{-1}m^{-1}$, respectively.

We also present the X-ray Diffraction patterns, the Wavelength Dispersive analysis composition and the Atomic Force Microscope surface morphology of prepared films.

P-138

Synthesis of Rod-Shaped Iron Nanocrystals Using Blue Laser-Assisted Pulsed-Laser Ablation in Liquid Ethanol

R. Ishihara, T. Sagara, S. Kurumi, K. -i. Matsuda, and K. Suzuki
College of Science and Technology, Nihon-University, 1-8-14, Kanda-Surugadai, Chiyoda-ku, Tokyo, Japan
E-mail: csry14004@g.nihon-u.ac.jp

Recently, pulsed-laser ablation in liquid (PLAL) is attracted attention for nanoscale crystal growth. In particular, external field assistant during crystal growth is the key to growth control from the perspective of nanostructure forming. In this study, we investigated the nanosize crystal growth of an iron by the combination of blue continuous-wave (CW) laser irradiation and PLAL. The PLAL was using Nd: YAG laser, growth of nanocrystals were using an Fe bulk target immersed in ethanol solution at room temperature. The laser pulse duration at PLAL was millisecond order. The blue CW laser was irradiated during PLAL for assistance of crystal growth. The obtained nanocrystals showed rod-shaped structure observed by transmission electron microscope images. Additionally, those crystals were maghemite or magnetite with an fcc structure surmised by electron diffraction. This direction in crystal growth has an axial direction of <110>. On this conference, we report the synthesis and structure with shape changing of nanocrystals in CW laser assisted PLAL.

P-139

Planar Square-spiral Inductor Generated from the ITO Film Removal by Using UV Laser Ablation

Ching-Ching Yang, Hsin-Yi Tsai, Yi-Han Chang, Wen-Tse Hsiao, Kuo-Cheng Huang*

Instrument Technology Research Center, National Applied Research Laboratories
20, R&D Rd. VI, Hsinchu Science Park, Hsinchu 300, Taiwan
*E-mail: huangkc@narlabs.org.tw**

Inductive efficiency is the major parameter to induce current for wireless charging module and it would be affected by the electric properties and shape of inductances. In general, the inductances can be made of the Cu coils or the copper (Cu) ring coated on the glass substrate. The quality of the copper (Cu) ring such as the oxidation degree [1] could affect the inductive efficiency. Therein, the planar square-spiral inductances (PSSIs) were designed on a copper-coated glass substrate and employed in the wireless charging module [2-4], and the results in one of studies showed the PSSIs with the Cu thickness of 200 nm and the ratio of 0.75 between line width and pitch has higher efficiency than other PSSIs and the highest induction capacity was 11.34 % [4].

In the study, the indium-tin oxide (ITO) with a thickness of 30 nm was coated on glass for the fabrication of PSSIs, and the patterns were ablated using the UV laser system with the laser of 355 nm. The processing parameters including the pulsed frequencies (80, 100 and 120 kHz) and the scanning speed (500, 1000 and 1500 mm/s) were adjusted to develop the oxidation degree at the edge of patterns, and the patterns with different dimensions and shapes were designed to investigate the variation of the inductive efficiency. The dimension of PSSIs on ITO glass was reduced from 3 × 3 cm^2 to 0.5 × 0.5 cm^2 in the experiments, and the oxidation and contour at the ablated edge were discussed. The efficiency of the inductance from Cu-coated substrate and ITO glass were compared and the ratio between the line width and pitch of patterns was varied to enhance the inductive efficiency up to 5 - 10 %. In addition, the inductances of matrix pattern were designed to discuss the enhanced efficiency compared to the single pattern. The results can provide the information of the relationship between the inductive efficiency and ratio of the patterns, and the designed inductances can be applied in micro wireless charging module in future.

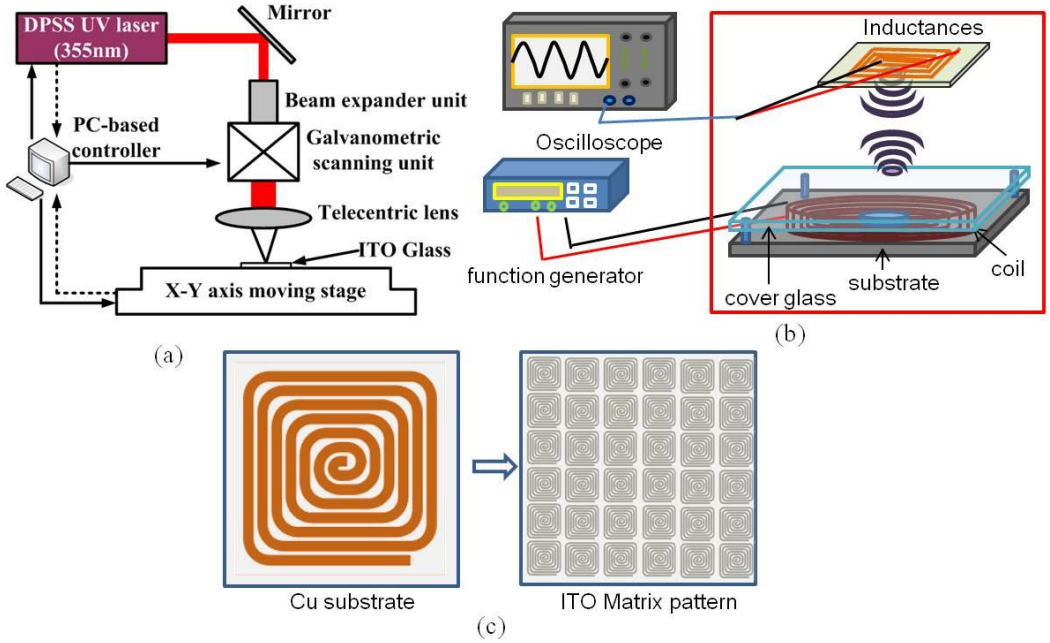

Figure 1: Schematic of the (a) UV laser system (b) inductive efficiency measuring module, and (c) the designed patterns of inductance.

[1] L. Tougiannidis, S. Iezekiel, R. D. Pollard and G. D. Halilis, "An efficient two-layer spiral inductor configuration" IEEE International Conference Mixed Design of Integrated Circuits and Systems (2005).

[2]M. Hershenson, S. Mohan, S. Boyd and T. Lee, "Optimization of inductor circuits via geometric programming" IEEE Design Automation Conference, pp. 994-998 (1999).

[3] N. Klejwa, R. Misra, J. Provine, R. T. Howe, and S. J. Klejwa, "Laser print patterning of planar spiral inductors and interdigitated capacitors", Journal of Vacuum Science & Technology B. 27, 2745-2749 (2009).

[4] C. C. Yang, H. Y. Tsai, C. C. Yang, W. T. Hsiao, K. C. Huang, "Fabricating planar spiral inductances for a wireless charging module by using 355 nm ultraviolet laser ablation, Applied Physics A: Materials Science & Processing, 117, 69-75 (2014).

Wednesday
2 September 2015

Oral presentations

I-09

Soft pulsed laser technologies for transfer of organic materials

I. N. Mihailescu, C. Ristoscu, F. Sima
National Institute for Lasers, Plasma and Radiation Physics, POB MG-36, Magurele, Ilfov, Romania
e-mail: ion.mihailescu@inflpr.ro

Recent results in organic/inorganic composite nanostructured layers synthesized by PLD, MAPLE and LDW are reviewed. The optimum deposition regime was reached based upon the results of investigations by SEM, TEM, SAED, XTEM, AFM, XRD, XPS or FTIR methods. Biocompatibility, bioactivity and biodegradation were assessed by dedicated *in-vitro* tests [1-3].

The coating of metallic implants with composite alendronate-HA or Sr-HA layers by MAPLE and PLD, respectively, was demonstrated to enhance human osteoblasts proliferation and differentiation, while inhibiting osteoclasts growth, with benefic effects for the treatment of bone diseases. Magnesium or strontium substituted OCP deposited by MAPLE on Ti substrates efficiently boost osteoblast activity and differentiation [4].

Urease immobilized by MAPLE in form of thin films was shown to preserve its activity in breaking down and diagnose of urea content in blood.

The application of MAPLE was extended to the transfer and immobilization of IgG molecules. We studied the effect of the lipid addition in the initial solution upon the protein thin films adhesion to substrate.

We showed that the composite PMMA-bioglass films deposited by MAPLE efficiently protects metal implants against the action of human fluids.

The antifungal efficiency of the nano-sized HA and Ag:HA layers obtained by PLD was tested against the Candida albicans and Aspergillus niger strains. The Ti substrates modified with TiO_2 nanotubes covered with Ag:HA thin films demonstrated the highest antifungal activity [5].

The MAPLE obtained nanocomposites Ag:HA-organosolv lignin proved noncytotoxic, supporting the normal development and promoting the proliferation of the adhered human mesenchymal cells. The lignin addition potentiated the anti-microbial activity of HA doped with silver ions against either bacterial or fungal biofilms [6].

Mesotetraphenylporphyrin clean and liquid-free micropatterns on Si substrates were fabricated by LDW. The propulsor metal film thickness was found to be a key parameter, which determines the laser fluence range allowing the clean transfer, predominant mechanism of the blister formation and laser-induced heating of the transferred material.

We conclude that the thin films prepared by PLD, MAPLE and LDW techniques were identical in chemical composition, structure, morphology, and most likely functionality resembling the base material, as proved by physical-chemical characterization and *in-vitro* assays.

[1] V. Nelea, M. Jelinek, I.N. Mihailescu, Biomaterials: new issues and breakthroughs for biomedical applications, in: Pulsed Laser Deposition of Thin Films: Applications-Lead Growth Of Functional Materials, Wiley, Hoboken, New Jersey, 2007, pp. 421–456 (Chapter 18)

[2] Carmen Ristoscu and Ion N. Mihailescu "Laser Technology in Biomimetics", Volker Schmidt, Maria Regina Belegratis (Eds.), Basics and Applications, Series: Biological and Medical Physics, Biomedical Engineering, Springer-Verlag Heidelberg, New York, Dordrecht, London, chapter "Biomimetic Coatings by Pulsed Laser Deposition", Pages 163-191, 2013

[3] Felix Sima and Ion N. Mihailescu, "Laser Technology in Biomimetics", Volker Schmidt, Maria Regina Belegratis (Eds.), Basics and Applications, Series: Biological and Medical Physics, Biomedical Engineering, Springer-Verlag Heidelberg, New York, Dordrecht, London chapter "Biomimetic Assemblies by Matrix-Assisted Pulsed Laser Evaporation", Pages 111-141, 2013

[4] E. Boanini, P. Torricelli, M. Fini, F. Sima, N. Serban, I. N. Mihailescu, A. Bigi, "Magnesium and strontium doped octacalcium phosphate thin films by matrix assisted pulsed laser evaporation", Journal of Inorganic Biochemistry **107**, 65–72 (2012)

[5] S. Eraković, A. Janković, C. Ristoscu, L. Duta, N. Serban, A. Visan, I.N. Mihailescu, G.E. Stan, M. Socol, O. Iordache, I. Dumitrescu, C.R. Luculescu, Dj. Janaćković, V. Miškovic-Stanković, "Antifungal activity of Ag:hydroxyapatite thin films synthesized by pulsed laser deposition on Ti and Ti modified by TiO_2 nanotubes substrates", Applied Surface Science **293**, 37-45 (2014)

[6] A. Janković, S. Eraković, C. Ristoscu, N. Mihailescu (Serban), L. Duta, A. Visan, G.E. Stan, A.C. Popa, M.A. Husanu, C.R. Luculescu, V.V. Srdić, Dj. Janaćković, V. Mišković-Stanković, C. Bleotu, M.C. Chifiriuc, I.N. Mihailescu, "Structural and biological evaluation of lignin addition to simple and silver doped hydroxyapatite thin films synthesized by matrix-assisted pulsed laser evaporation", ournal of Materials Science: Materials in Medicine **26**, 17 (2015)

O-41

Combinatorial Matrix - Assisted Pulsed Laser Evaporation for fabrication of maps of biomaterials

C. Ristoscu[1], F. Sima[1], E. Axente[1], L. E. Sima[2], N. Mihailescu[1], E. Toksoy Oner[3], A. Bigi[4], I. N. Mihailescu[1]

[1] *National Institute for Lasers, Plasma and Radiation Physics, POBox MG-36, Magurele, Ilfov, Romania*
[2] *Department of Molecular Cell Biology, Institute of Biochemistry, Romanian Academy, Bucharest, Romania*
[3] *Marmara University, Turkey*
[4] *Department of Chemistry "G. Ciamician", University of Bologna, Bologna, Italy*
E-mail: carmen.ristoscu@inflpr.ro

We introduce a new method, Combinatorial Matrix-Assisted Pulsed Laser Evaporation (C-MAPLE) for the fabrication of organic biopolymer thin films (Fig. 1) [1]. Structures with compositional gradient are obtained by the simultaneous laser vaporization of two distinct targets. Synchronized matrix-assisted pulsed laser evaporation of levan and oxidized levan cryogenic targets was applied in order to transfer under protection and assemble a two-compound biopolymer film structure. FTIR micro-spectroscopy confirmed the existence of a composition gradient along the length of the sample. Modification of chemical composition from L to OL and the physical texture stayed at the origin of the improved accumulation of cells on discrete film regions (different from the two ends) as compared with all other film areas, which in turn was most probably connected to the appropriate degree of oxidation. I*n-vitro* cell culture assays illustrated characteristic responses of cells to specific surface regions [2]. The cell response induced by the compositional gradient using imaging of early osteoblast attachment and analysis of signaling phosphoprotein expression was investigated. Cells attached along the gradient in direct proportion with oxidized levan concentration. Cell signalling response to the surface composition gradient and roughness has shown that combinations of OL and L (OL-L and L-OL) increase ERK activation as compared to OL or L alone. The analyses revealed a structure-function relationship and beneficial design guidelines. This basically refers to the existence of an optimum mixture between OL and L constituents, and more or less hydrophilic areas. Once identified, the optimum region could be recognized by rapid fluorescence microscopy scanning. The generation of smart discrete materials with desired properties such as the rate of coating dissolution is a prospective, challenging task.

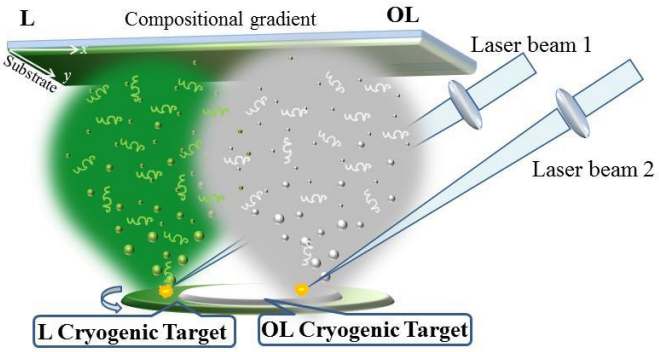

Fig. 1. Design of C-MAPLE experimental set-up.

We demonstrated the use of C-MAPLE to the *in-situ* synthesis of Poly-dl-lactide (PDLLA) and fibronectin (FN) [3]. Confocal and FTIR microscopy evidenced FN packages embedded in the polymeric matrix. The composition of PDLLA and FN was preserved after C-MAPLE as supported by protein staining and FTIR.

C-MAPLE was applied to synthesize crystalline gradient thin films with variable composition of Sr-substituted hydroxyapatite (SrHA) and Zolendronate modified hydroxyapatite (ZOLHA) on Titanium substrates [4]. The inhibitory action of ZOL on osteoclast viability and activity is more efficient than that of Sr, which plays a greater beneficial role on osteoblast proliferation and viability. The deposition method allows to modulate the composition of the thin films and hence the promotion of bone growth and the inhibition of bone resorption.

C-MAPLE opens the possibility to both combine and immobilize two or more organic materials on a solid substrate in a well defined manner by laser evaporation under protection.

[1] F. Sima, E. Axente, L. E. Sima, U. Tuyel, M. S. Eroglu, N. Serban, C. Ristoscu, S. M. Petrescu, E. Toksoy Oner, I. N. Mihailescu, "Combinatorial Matrix-Assisted Pulsed Laser Evaporation: Single-step synthesis of biopolymer compositional gradient thin film assemblies", Applied Physics Letters **101**, 233705 (2012)

[2] E. Axente, F. Sima, L. E. Sima, M. Erginer, M. S. Eroglu, N. Serban, C. Ristoscu, S. M. Petrescu, E. Toksoy Oner, I. N. Mihailescu, "Combinatorial MAPLE gradient thin film assemblies signalling to human osteoblasts", Biofabrication **6**, 035010 (2014)

[3] F. Sima, E. Axente, I. Iordache, C. Luculescu, O. Gallet, K. Anselme, I.N. Mihailescu, „Combinatorial Matrix Assisted Pulsed Laser Evaporation of a biodegradable polymer and fibronectin for protein immobilization and controlled release" Applied Surface Science **306**, 75–79 (2014)

[4] P. Torricelli; F. Sima; E. Axente; M. Fini; I. N Mihailescu; A. Bigi; "Strontium and Zoledronate Hydroxyapatites Graded Composite Coatings for Bone Prostheses; cu mentiunea: accepted for Publication in the Journal of Colloid & Interface Science, February 2015.

O-42

Studies in Laser Cleaning from London Museums Including Some Recent Work on Laser Cleaning of PMMA

D.S. McPhail[1], A.L. Fricker[1], T. Cosnahan[1], B. Keneghan[2], M. Sokhan[3]

1. Imperial College, Department of Materials, London,SW7 2AZ, UK
2. Victoria & Albert Museum, Cromwell Road, London SW7 2RL, UK
3. City & Guilds of London Art School, 124 Kennington Park Road, London SE11 4DJ, UK
E-mail: d.mcphail@imperial.ac.uk

Laser cleaning is being used extensively at the V&A museum, the Natural History Museum, and the City and Guilds College with each institution now owning its own laser(s), and in this talk I will describe some recent success stories. In a series of collaborative programs various analytical techniques operating at different length and energy scales have been used to assess the effectiveness of the laser cleaning and the rate of recontamination of the surface after cleaning. These include optical intereferometry, white light interferometry, atomic force microscopy (AFM), Scanning Electron Microscopy (SEM), Focused Ion beam Secondary Ion Mass Spectrometry (FIB-SIMS) and Secondary Ion Mass Spectrometry (SIMS).

The main case study will involve plastics from the V&A museum. There are a large number of plastic artefacts in museum, and many of the objects are suffering from serious degradation that has arisen from year of storage and display (Fig. 1). Mechanical and solvent based cleaning methods induce some damage or chemical alteration to the plastic's surface and so it seems appropriate to study the potential of laser cleaning. The use of lasers in other areas of conservation has proved highly successful, particularly as it is non-contact and can be performed in-situ. So this preliminary investigation considers the effect of Nd:YAG 1064nm laser light on polymethyl methacrylate (PMMA) surfaces from a materials science perspective. Because polymers have much lower transition temperatures than stone and ceramic and so a higher sensitivity to the laser's energy, the intricacies of the hand held near-infrared laser source are also inspected as control. Theoretical models are developed from previous conservation and non-conservation research to explain results from the experimental irradiation of clean and soiled PMMA samples. It is shown that there is a damage threshold for PMMA at achievable fluences. Above this threshold self-limiting cleaning is assessed. It is also shown that some ring time cracks appear under excessive irradiation.

This work is presented as initial research to aid conservation science in its future challenges of cleaning and maintaining plastic artefacts.

Fig. 1.V&A collection. Degradation of a plastic handbag

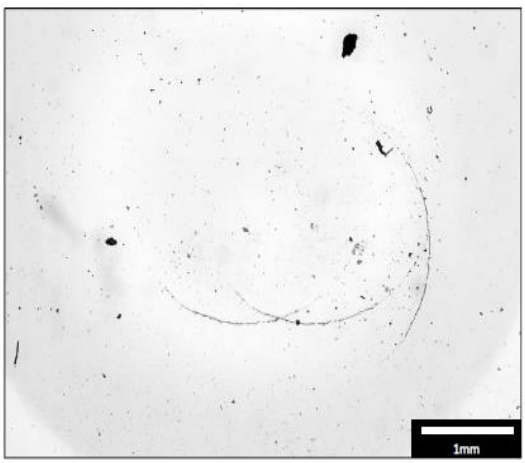

Fig. 2 Typical ring cracks seen on the PMMA surface with a single laser pulse incurring a fluence of 7 Jcm−2.

O-43

Biomimetic multifunctional metallic surfaces produced by femtosecond laser

A. Y. Vorobyev and Chunlei Guo

The Institute of Optics, University of Rochester, Rochester, New York 14627

We created multifunctional metal surfaces by producing a hieratical nano- and micro-structures with femtosecond laser pulses on titanium, platinum and brass. The multifunctional surfaces exhibit excellent broadband light absorption, superhydrophobicity, and self-cleaning effects. The creation of these multifunctional surfaces is inspired by biological surfaces of Lotus leaves and blue Morpho butterfly wings. The enhanced absorption is useful whenever light collection is needed, such as in sensors and solar energy absorbers. The self-cleaning effect will improve the performance of the devices and minimize the maintenance. This surface should also possess other highly desirable functionalities such as anti-corrosion, anti-icing, anti-biofouling, and self-sanitation, since these properties are directly related to superhydrophobicity.

O-44

MAPLE deposition of polymer multilayer structures: overcoming the limitation of solvent-based techniques

A.P. Caricato[1*], M. Mazzeo[1,2], G. Accorsi[2], M. Cesaria[1], C. Leo[1], F. Mariano[2], D. Simeone[2], T. Tunno[1], G. Gigli[1,2,3], M. Martino[1]

[1]*Department of Mathematics and Physics "E. De Giorgi", University of Salento, Via Arnesano, I-73100 Lecce, Italy*
[2]*National NanotechnologyLaboratory (NNL), Istituto Nanoscienze-CNR, Via Arnesano n. 16, I-73100 Lecce, Italy*
[3]*Center for Bio-MolecularNanotechnologies (CBN) of IIT@NNL-UniLe-Lecce, Via Barsanti c/o STAMMS, I-73010 Arnesano (Lecce), Italy*

[*]*E-mail: annapaola.caricato@unisalento.it*

Polymer multilayer deposition represents a serious challenge for solvent-based techniques like spin coating and drop casting since the deposition of even the second layer profoundly affects the first one. To overcome this problems, orthogonal solvents are generally used. However, this strategy, when applicable,limits the deposition to only two layers. The potentialities of the matrix-assisted pulsed laser evaporation (MAPLE) technique have been already demonstrated in the case of bilayer deposition for solar cell application and nanocomposite films.
However, in many cases, the high surface roughness of the films deposited by MAPLE could inhibit the possibility to use it for particular applications, like for example in optoelectronics.
In this paper we report the deposition of a trilayer structure consisting of three light emitting conjugated polymers in a well-defined sequence:
a first spin-coating deposited layer of the blue emitting polymer Poly[9,9-dioctylfluorenyl-2,7-diyl] (PFO), a second MAPLE-deposited layer of the red emitting polymer Poly[2-methoxy-5-(2-ethylhexyloxy)-1,4-phenylene-vinylene](ADS100RE) and athird MAPLE-deposited layer of the green emitting polymer Poly[(9,9-dioctylfluorenyl-2,7-diyl)-co-(1,4-diphenylene-vinyl- ene-2-methoxy-5-{2-ethylhexyloxy}-benzene)] (ADS125GE). The bottom most layer has been deposited by spin coating because of geometrical constraints of the target holder.
The properties of each single layer are reported in terms of surface roughness values and optical/emission properties,investigated by atomic force microscopy (AFM), UV-VIS absorption and photoluminesce (PL) spectroscopy,respectively, together with the behavior of the bi and tri-layer realization. The absorption and photo-emission properties, together with the efficiencies and decay times, of the MAPLE deposited single layers have been compared with that of the films deposited by spin coating obtaining comparable results.
By carefully controlling the laser deposition parameters, layers with roughness values compatible with optoelectronic devices have been obtained. In particular, roughness values less than 7 nm have been obtained for the MAPLE-deposited red (ADS100RE) and green (ADS125GE) single layers and for the bilayer PFO/ADS100RE. In the case of thetri-layer structure a mean roughness value of about 10 nm has been recorded over a scan are of 5×5 μm^2 and photoluminescence spectrum exhibiting emission by all the layers (Fig. 1).
Ourresults are very promising for the realization of a white light polymer-based emitting device.

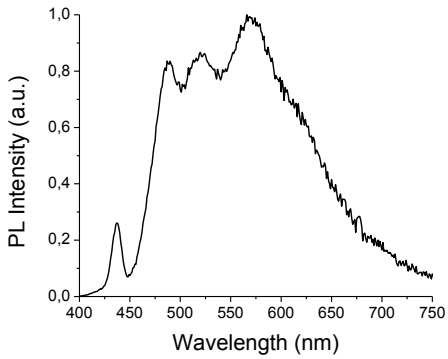

Fig. 1. Photoluminescence spectrum of the MAPLE deposited multilayer.

O-45

In situ monitoring of Laser Induced Periodic Surface Structures formation on polymer films by Grazing Incidence Small Angle X-ray Scattering

Esther Rebollar[1], Daniel R. Rueda[2], Ignacio Martín-Fabiani[2,+], Álvaro Rodríguez-Rodríguez[2], Mari-Cruz García-Gutiérrez[2], Giuseppe Portale[3], Marta Castillejo[1], Tiberio A. Ezquerra[2]

[1] *Instituto de Química Física Rocasolano (IQFR-CSIC), Serrano119, 28006 Madrid, Spain.*

[2] *Instituto de Estructura de la Materia (IEM-CSIC), Serrano 121, 28006 Madrid, Spain.*

[3] *DUBBLE@ESRF, Netherlands Organisation for Scientific Research (N.W.O.), CS40220, 38043, Grenoble, Cedex 9, France*

[+] *Present address: Department of Physics, University of Surrey, Guildford GU2 7XH, United Kingdom*

E-mail: e.rebollar@csic.es

Formation of laser induced periodic surface structures (LIPSS) has been observed on polymers upon irradiation with a linearly polarized laser beam, at wavelengths efficiently absorbed and within a narrow fluence range well below the ablation threshold. LIPSS are the result of the interference between the incoming and the surface-scattered waves, so that an inhomogeneous intensity distribution, together with a feedback mechanism, results in the enhancement of the modulation depth [1]. The use of X-ray scattering techniques with synchrotron radiation can be very useful for LIPSS analysis as they can provide kinetic information in the millisecond range and structural information statistically averaged over a large area of several hundreds of microns.

Poly(trimethylene terephthalate) (PTT) films with a thickness ca. 150 nm and roughness below 1 nm were prepared by spin-coating on silicon wafers. For LIPSS formation we used a Nd:YAG laser (266 nm, 8 ns pulses, 1-10 Hz) at a fluence of 7 mJ/cm^2. The in situ monitoring of LIPSS formation was performed at the DUBBLE beamline of the European Synchrotron Radiation Facility (ESRF, Grenoble, France).

An example of the in situ monitoring of LIPSS formation is shown in Fig. 1 for a laser repetition rate of 5 Hz. The first pattern taken after 25 pulses (5s) is the characteristic one for a spin-coated film in absence of relevant structure. After 200 pulses (40 s), the GISAXS pattern starts exhibiting clear vertical diffraction maxima and for higher number of pulses the diffraction maxima increase both in number and in intensity.

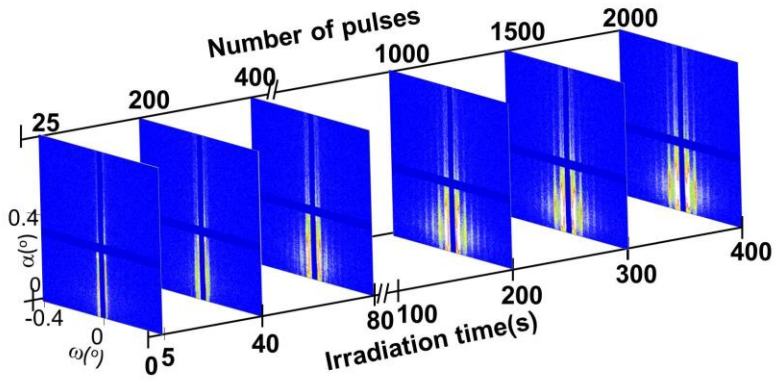

Fig.1. Real time GISAXS patterns as a function of time and number of pulses for a PTT film irradiated with a laser repetition rate of 5 Hz.

The dynamics of LIPSS formation depends on the laser repetition rate. For 10 Hz the period increases with the number of pulses and reaches a plateau at a value close to the laser wavelength while for lower repetition rates the period remains constant, and significantly smaller, independently of the number of pulses. Both the half time and the induction time for LIPSS formation decrease logarithmically with the repetition rate.

When a laser pulse reaches the polymer it heats its surface above the glass transition temperature. Subsequently, the material cools down so that surface inhomogeneities are expected to be enhanced. Then, the next pulse will find a rougher surface thus facilitating the feedback mechanism. For a pulse separation longer than 0.1 s (10 Hz) the feedback effect is reduced although is still present at times as long as 1 s (1 Hz).

The number of maxima appearing in the GISAXS patterns increases with irradiation time and depends on the laser repetition rate. GISAXS patterns obtained for LIPSS can be considered as a one dimensional paracrystalline lattice, where the long range order disappears gradually in a probabilistic way. Modelling provides information about the lattice order. A progressive order improvement of LIPSS is observed as the number of pulses increases, being 10 Hz the repetition rate at which the more ordered structure is found.

References

[1] E. Rebollar, S. Pérez, J.J. Hernández, I. Martín-Fabiani, D.R. Rueda, T.A. Ezquerra, and M. Castillejo, "Assessment and Formation Mechanism of Laser Induced Periodic Surface Structures on Polymer Spin-coated Films in Real and Reciprocal Space," Langmuir **27**, 5596 (2011).

I-10

Diffraction before destruction: Imaging molecules and materials with high-intensity X-ray FEL pulses

Henry N. Chapman[1,2,3]

[1]*Center for Free-Electron Laser Science, DESY, Hamburg, Germany*
[2]*Department of Physics, University of Hamburg, Hamburg, Germany*
[3]*Centre for Ultrafast Imaging, University of Hamburg, Hamburg, Germany*
E-mail: Henry.Chapman@desy.de

The pulses from X-ray free-electron lasers are a billion times brighter than the brightest synchrotron beams available today. When focused to micron dimensions, such a pulse destroys any material, but the pulse terminates before significant atomic motion can take place [1,2]. This mode of "diffraction before destruction" yields structural information at resolutions better than 2 Å, from proteins that cannot be grown into large enough crystals or are too radiation sensitive for high-resolution crystallography [3-5]. Using femtosecond X-ray FEL pulses, doses to the sample can exceed many GGy (1 Gy = 1J/kg), which is thousands of times higher than biological materials can usually tolerate for conventional analysis using synchrotron radiation [6]. The quality of the recovered electron density of protein structures is usually superior to that which is recovered by conventional methods at much lower doses, and samples can be measured at room temperature and physiological conditions rather than at cryogenic temperatures [7]. The ability to obtain high-resolution diffraction data from micron or sub-micron crystals may help to overcome the crystallization bottleneck of structural biology.

A consequence of vaporizing the sample in a single shot is that diffraction data must be collected from many samples (of reproducible structure) in order to build up three-dimensional information [8]. This is the essence of the methodology of serial femtosecond diffraction, and in particular serial femtosecond nanocrystallography (see Fig. 1). The method relies upon key technological advances: the X-ray FEL providing intense pulses that give rise to measurable diffraction patterns from weakly scattering samples; particle injectors that can replenish the sample at the rate of the FEL pulses and which only contribute weakly to background; pixelated X-ray diffraction detectors that can also operate at that frame rate; and software that can process the many millions of data frames that are collected in a typical experiment. At the Linac Coherent Light Source (LCLS), where the repetition rate is 120 Hz, crystalline samples are typically flowed across the path of the focused X-ray beam using a gas-focused liquid jet [9], or a slower extrusion of viscous material [10]. In both cases crystals are hit by chance, usually at a random orientation. Data is processed first by finding the diffraction "hits" [11], followed by indexing and merging of Bragg intensities into a set of three-dimensional structure factors [12]. Phasing of the diffraction to determine the structure then proceeds using conventional protein crystallographic methods, including the possibility of experimental phasing [13].

The approach has opened up new possibilities for structure determination. The short pulses obviously open up the possibility of time-resolved measurements. This includes the measurement of optically induced reactions [14], such as involved in photosynthesis [15], and photoreceptors [16]. Irreversible reactions can be studied, since the sample is constantly replenished. The fact that samples are at room temperature and consist of micron or sub-micron sized crystals also means that microsecond time resolution can be reached in mixing experiments (where the resolution depends on the diffusion time of a chemical into the crystal) [17]. Other benefits of the approach are that it opens new opportunities for phasing diffraction data, which are sorely needed

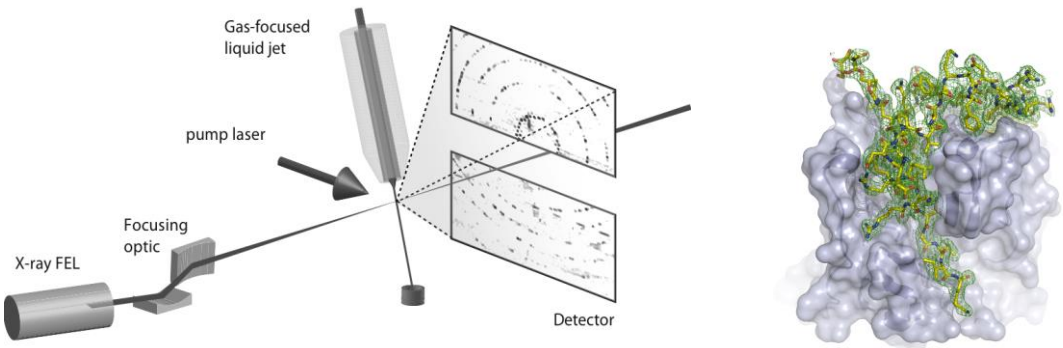

Fig. 1. A serial femtosecond diffraction experiment is carried out by flowing a sample of reproducible particles or crystals across the focused X-ray pulses from a free-electron laser (see left). Here the sample is delivered in a liquid jet [8]. Diffraction data is collected at the repetition rate of the FEL on a pixelated detector. A typical experiment may record more than 50,000 diffraction patterns which are then aggregated to be used to solve the molecular structure. At right is shown the structure of pro-cathepsin B from the Trypanosoma brucei parasite, determined from over 190,000 measured patterns of crystals (from [5]).

in protein crystallography when experimental phasing approaches are not applicable or there are no closely related structures on which to base a starting model. The intensity of the X-ray pulse can be high enough to saturate photoabsorption, particularly of heavier elements. This effect could be used for phasing by observing the specific bleaching of atoms [18]. A difference between data collected at high intensity and low intensity can reveal the substructure of those atoms, akin to isomorphic replacement. Since experiments are carried out in vacuum, data can be collected at relatively low photon energy, allowing such a procedure to be applied to sulfur atoms, which are prevalent in proteins. Another idea is to take advantage of the small crystal size, which gives broad Bragg peaks and often relatively strong scattering along directions normal to crystal facets. Indeed, the Bragg peaks of the infinite reciprocal lattice are convolved with the Fourier transform of the shape of the crystal, as nicely illustrated in Fig. 2. This scattering amplitude between the Bragg spots (or even near to them) yields additional information than the Bragg peaks alone, which by themselves under-sample the underlying molecular transform. Spence *et al* proposed way to recover this underlying molecular transform by dividing out the average shape transform [19], which can then be phased by iterative methods.

The field of protein structure determination using X-ray FELs is still very young, and there are many other developments taking place. We have yet to reach the limit of the smallest samples that can be studied this way, and many innovations indicate the feasibility of reducing the size of crystals all the way to single molecules.

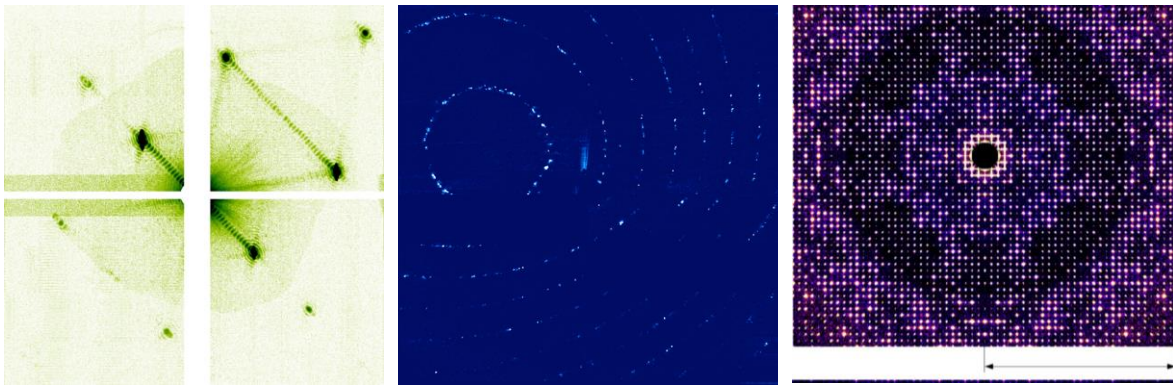

Fig. 2. (left and center) Diffraction patterns from single nanocrystals of photosystem I, measured at LCLS [3]. At left is a pattern collected at low resolution, showing intense Bragg spots and fringes between them. The streaks are perpendicular to facets of the crystal and the fringes are due to truncation of an infinite lattice. A crystal of width of *N* unit cells results in *N*-2 maxima between Bragg peaks. The streaks allow measurement of intensity in between Bragg peaks when patterns are assembled into a 3D reciprocal-space volume, as shown at right [20].

References

[1] R. Neutze, R. Wouts, D. van der Spoel, E. Weckert, and J. Hajdu. Potential for biomolecular imaging with femtosecond X-ray pulses. Nature, **406**, 753–757 (2000).

[2] H. N. Chapman *et al.* "Femtosecond diffractive imaging with a soft-x-ray free-electron laser," Nature Phys, **2**, 839–843 (2006).

[3] H. N. Chapman *et al.* "Femtosecond x-ray protein nanocrystallography," Nature **470**, 73–77 (2011).

[4] S. Boutet *et al.* "High-resolution protein structure determination by serial femtosecond crystallography," Science **337**, 362–364 (2012).

[5] L. Redecke *et al.* "Natively inhibited Trypanosoma brucei cathepsin B structure determined by using an X-ray laser," Science **339**, 227–230 (2013).

[6] A. Barty *et al.* "Self-terminating diffraction gates femtosecond x-ray nanocrystallography measurements," Nature Phot. **6**, 35–40 (2012).

[7] W. Liu *et al.* "Serial femtosecond crystallography of G protein–coupled receptors," Science **342**, 1521–1524 (2013).

[8] M. M. Siebert *et al.* "Single mimivirus particles intercepted and imaged with an x-ray laser," Nature **470**, 78–81 (2011).

[9] D. P. DePonte, *et al*, "Gas dynamic virtual nozzle for generation of microscopic droplet streams," J. Phys. D **41**, 195505 (2008).

[10] U. Weierstall *et al.* "Lipidic cubic phase injector facilitates membrane protein serial femtosecond crystallography. Nat Comm. **5**, 3309 (2014).

[11] A. Barty *et al.* "Cheetah: software for high-throughput reduction and analysis of serial femtosecond X-ray diffraction data," J. Appl. Cryst. **47**, 1118–1131 (2014).

[12] T. A. White *et al.* "CrystFEL: a software suite for snapshot serial crystallography. J. Appl. Cryst. **45**, 335–341 (2012).

[13] T. R. M. Barends *et al.* "De novo protein crystal structure determination from x-ray free-electron laser data," Nature **505**, 244-7 (2014).

[14] A. Aquila *et al.* "Time-resolved protein nanocrystallography using an x-ray free-electron laser," Opt. Express **20**, 2706–2716 (2012).

[15] C. Kupitz *et al.* "Serial time-resolved crystallography of photosystem ii using a femtosecond X-ray laser," Nature **513**, 261–265 (2014).

[16] J. Tenboer *et al.* "Time-resolved serial crystallography captures high-resolution intermediates of photoactive yellow protein," Science **346**, 1242–1246 (2014).

[17] M. Schmidt, "Mix and inject: Reaction initiation by diffusion for time-resolved macromolecular crystallography," Adv. Cond. Matt. Phys. **2013**, 167276 (2013).

[18] S.-K. Son, H. N. Chapman, and R. Santra, "Multiwavelength anomalous diffraction at high X-ray intensity," Phys. Rev. Lett., **107**, 218102 (2011).

[19] J. C. H. Spence *et al*, "Phasing of coherent femtosecond X-ray diffraction from size-varying nanocrystals," Opt. Express **19**, 2866–2873 (2011).

[20] O. Yefanov, et al. "Mapping the continuous reciprocal space intensity distribution of x-ray serial crystallography," Phil. Trans. Roy. Soc. B **369,** 20130333 **(**2014).

O-46

Time-resolved study on periodic microstructure formation in polymers

C. Vass[1], R. Flender[1], B. Kiss[1,2], K. Osvay[1,2]

[1]Department of Optics and Quantum Electronics, University of Szeged, H-6720 Szeged, Dóm tér 9, Hungary

[2]ELI-HU Non-Profit Ltd.., Dugonics tér 13, H-6720 Szeged, Hungary

Corresponding Author e-mail address: vasscsaba@physx.u-szeged.hu

Laser ablation is well suited for material structuring due to the achievable high resolution, good controllability which allow realizing well-defined micropatterns on solid targets. Among many solutions, the interferometric (holographic) etching method is one of the most flexible way to produce surface relief sinusoidal gratings by laser ablation. Here we study the time evolution of grating structures created into polycarbonate (PC) and polymethyl methacrylate (PMMA) by (direct) laser ablation to understand the relevant phenomena during the laser ablation.

The periodic structures were fabricated by a frequency quadrupled nanosecond, Q-switched Nd:YAG pump laser (λ=266 nm, τ=8 ns). The spatially filtered, linearly *s*-polarized UV pulses were steered to the target in two-beam interferometric arrangement, having negligible optical path difference at incident angle of 7.6° and 3°, which corresponds to spatial modulation of ≈1 μm and ≈2,5 μm in the target plane, respectively. The polymer samples were irradiated in the fluence range of 10-800 mJ/cm^2.

The etching setup was completed by an offset-free pumpe-probe system, which consists of a continuous wave HeNe probe laser (λ=632 nm) and amplified photodiode-oscilloscope system. Special care was taken to get distortion- and background-free monitoring of surface evolution. The CW probe beam illuminated the etching area from the backside of the targets. To separate the effect of phase and amplitude grating, the arising reflected +1st (belongs to the both amplitude and phase grating) and +2nd (corresponds only to the phase grating) diffraction order was monitored by individual photodiodes. Colour filters, prisms and irises were used to realize the undisturbed detection of HeNe intensity: the etching UV photons and the flashing scattered 2nd harmonic of Nd:YAG green pulses were completely filtered. Similar system was used for structuring of metals by picosecond pulses [1].

The rise time of the recorded first and second order signals is ≈3 μs, and this section followed by a relatively constant part (see diagrams on Fig.1). This means that the grooves reach their final depth in the first microseconds: the material removal mostly finishes by 3μs. Moreover, in many cases in first diffraction order a transient peak was observed in the first order diffracted beam 1-2 us after the ablating pulse (Fig.1b). The presence and the parameters of this peak depend on the UV laser fluence and also on the type of the material: this peak is detectable in the low (<170 mJ/cm^2) and high fluence range (>500 mJ/cm^2) at PMMA, while it can be observed in the whole studied fluence region at PC target.

The morphology of the gratings was studied by atomic force microscope (AFM). Melted and resolidified structures were observed on those gratings, where the additional peak was detectable (Fig.1b). In case of PC the additional peak was not detected in the medium fluence range, while in these cases the grating quality is high, the grooves are perfectly regular.

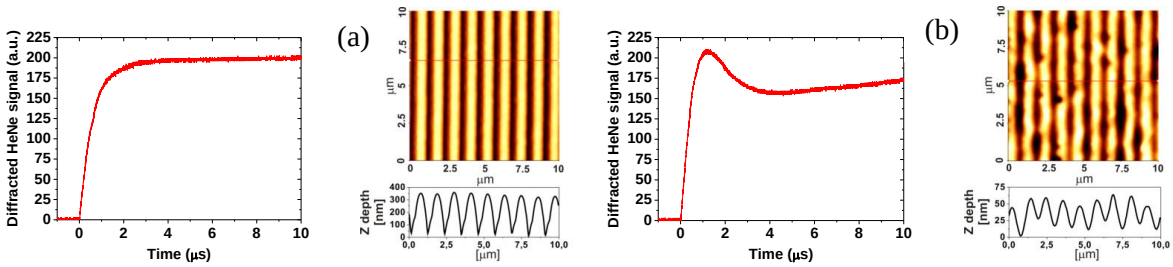

Fig. 1. Detected 1st order signals and AFM images in case of PMMA. Fluence: 385 mJ/cm^2 (a); 615 mJ/cm^2 (b).

However, the transient peak was never observed in the 2nd diffraction order, independently from the UV fluence and type of material. Generally, an amplitude grating does not give rise to diffracted signal in 2nd order. Consequently, the detected 1st order peak can be attributed to a transient amplitude grating, which is due to the different absorption of periodically melted and solid polymer.

On the basis of our experiments the time resolved monitoring of the diffracted signals in the cases of polycarbonate could be a suited method to determine the quality of the ablated gratings, without time consuming ex-situ surface characterization.

[1] J.-H. Klein-Wiele, M.A. Bader, I. Bauer, S. Soria, P. Simon, G. Marowsky, "Ablation dynamics of periodic nanostructures for polymer-based all-optical devices", Synthetic Metals **127** 53-57 (2002)

O-47

Ultrafast laser surgery of dendrites

MA Go[1], C Stricker[1], S Redman[1], H Bachor[2] and VR Daria[1,*]

[1]*Eccles Institute of Neuroscience, Australian National University, Canberra, ACT 0200, Australia*

[2]*Research School of Physics and Engineering, Australian National University, Canberra, ACT 0200, Australia*

**Corresponding Author e-mail address: vincent.daria@anu.edu.au*

Abstract

We use an ultrafast laser to cut dendritic trees of mammalian neurons in the cortex. We show that the cut seals and normal transmembrane ion exchange is restored after ~5 minutes. Subsequently the neurons are functional and able to fire action potentials.

1. Introduction

Focused laser light has found use in cellular surgery as an ultra-sharp scalpel [1-2]. It has been demonstrated in femtosecond (fs) laser surgery that focusing low-energy NIR light on a small volume for a very short duration (fs scale) allows for cutting of neuronal structures such as axons, which have submicron diameters [3]. The working mechanism of fs-laser surgery was initially studied by Vogel et al [4] who observed that ultra-short laser pulses initiate 2P ionization, which induces plasma formation and results in a dramatic, transient, and local increase of the absorption coefficient to a level significantly higher than the linear absorption coefficient. The nonlinear nature of two-photon ionization localizes the cutting energy within the focus thereby minimising damage to surrounding regions. This provides a non-invasive method for precise surgery at the nanoscale.

Here, we use such technique to study how mammalian neurons process its synaptic inputs to arrive at an output. The neurons in the somatosensory cortex processes sensory inputs and generates motor commands among other functions. Such processing and generation of outputs are theorised to be dependent on the neuron's dendritic morphology. Hence, dynamic pruning of dendritic trees could be used to verify theories on neuronal function [5].

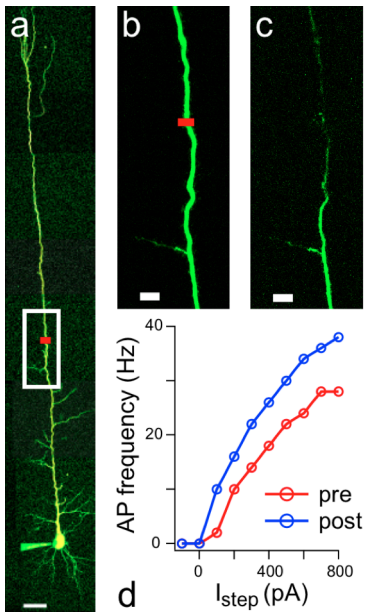

Figure 1. Ultrafast-laser surgery. (a) Fluorescence image of a neuron. Red line indicates location of the cut. Scale 50µm. (b) Magnified view of highlighted area in a before the cut. Scale 10µm. (c) Same area as in b but after the cut.(d) Firing frequency of the neuron versus injected current amplitude before (pre) and after (post) the cut.

2. Results

We used a custom-built two-photon scanning microscope to image neurons in 300 µm thick brain slices from 19 day-old Wistar rats. The slices were cut in ice-cold oxygenated artificial cerebro-spinal fluid and then incubated at 34 ^{o}C for 30 min prior to performing the experiments. Whole-cell voltage-clamp recordings of the cells were done with a Multiclamp 700B. We filled the neuron through the recording electrode which contained 20 µM Alexa fluor 488. Current injections of variable amplitudes served to analyse the neuron's firing properties. Fig. 1a shows the 2P fluorescence image of a cortical pyramidal neuron (magnified in 1b and 1c made before and after the cut respectively). The red line indicates the section at which a cut was targeted. As a consequence of cutting, the cell becomes depolarised and recovers. If the applied energy for cutting exceeds a certain range, the cell fails to recover. Within the cutting parameters, we plot the firing frequency versus the applied injection current (Fig. 1d) and observe differences in the response before and after the cut.

3. Conclusion

We have demonstrated the use of fs Ti:S laser surgery to dynamically prune the neuron's dendritic arbor. The neuron is functional after dendrotomy and the neuron is able to fire action potentials but with an increased firing rate. Such increase is consistent with existing theories that dendritic morphology determines the output response.

4. References

[1] Ando, J et al, Optical trapping and surgery of living yeast cells using a single laser, Rev of Sci Instr 79, 103705 (2008).

[2] Yanik, MF, et al, Functional regeneration after laser axotomy, Nature 432, 422 (2004).

[3] Vuksic, M, et al, Unilateral entorhinal denervation leads to long-lasting dendritic alterations of mouse hippocampal granule cells, Exp Neurology 230, 176 (2011).

[4] Vogel, A, Mechanisms of femtosecond laser nanosurgery of cells and tissues, Applied Physics B-lasers and optics 81, 1015 (2005).

[5] Bekkers, JM and Häusser, M, Targeted dendrotomy reveals active and passive contributions of the dendritic tree to synaptic integration and neuronal output, Proc. Natl. Acad. Sci. U.S.A. 104(27), 11447-11452 (2007)

O-48

Substrate mediated laser ablation and droplet capture for biomolecules analysis by mass spectrometry

B. Fatou [1,2], M. Wisztorski[1], C. Focsa[2], M. Ziskind[2], I. Fournier[1]

[1]*Laboratoire Protéomique, Réponse Inflammatoire et Spectrométrie de Masse, Université Lille 1, F-59655 Villeneuve d'Ascq, France*

[2]*Laboratoire de Physique des Lasers, Atomes et Molécules, Université Lille 1, F-59655 Villeneuve d'Ascq Cedex, France*

E-mail: michael.ziskind@univ-lille1.fr

Since the early 2000s, ambient mass spectrometry (MS) is becoming a powerful tool for direct analysis of samples with minimal preparation. Numerous applications have been demonstrated including the spatially resolved analysis of different regions of biological material. This has promoted the developments of various microsampling techniques like Laser Ablation/ Droplet Capture (LADC)[1,2]. LADC is characterized by the collection into solvent droplets of molecules removed from the sample by laser ablation. The ionization and the mass separation of the captured molecules can then be achieved using conventional MS techniques like Matrix-Assisted Laser Desoption/Ionization (MALDI) or electrospray ionization (ESI).

Laser wavelengths in the UV[1] and IR[2] ranges have already been successfully tested on various biological materials. In this work, LADC approach was investigated on standards from different families of biomolecules (lipid, peptide, protein) and biological tissue sections using nanosecond pulses of a frequency-doubled Nd:YAG laser (532 nm) in conventional reflection geometry. The droplets containing captured materials were collected and analyzed by MALDI MS. At first sight, visible light is not a good candidate to initiate efficient ablation because of the low absorption coefficient of biomolecules in this wavelength range. The addition of dye molecules could overcome this limitation but it complicates the sample preparation. However studies on various parameters of the set-up (including the sample-droplet distance, the laser energy, the sample preparation, the nature of the substrate on which the sample is placed) have demonstrated under certain conditions the efficiency of this approach even in the absence of dye molecules in the samples. This has been attributed to indirect ablation mechanism promoted by the substrate which can advantageously be used for LADC of intact biomolecules from thin tissue sections. First practical application, a spatially resolved proteomic study on rat brain tissue section, is also presented.

[1] O.S. Ovchinnikova, V. Kertesz, G.J. Van Berkel, "Combining transmission geometry laser ablation and a non-contact continuous flow surface sampling probe/electrospray emitter for mass spectrometry based chemical imaging", Rapid Commun. Mass Spectrom. **25**, 3735 (2011)

[2] S.-G. Park, K. K. Murray, "Infrared laser ablation sample transfer for MALDI and electrospray", J. Am. Soc. Mass Spectrom. **22,** 1352 (2011)

O-49

Skin ablation for efficient drug delivery via the laser-induced microjet injector

H. Jang[1], S. Yeo[1] and J. J. Yoh[1*]
[1]*Department of Mechanical and Aerospace Engineering, Seoul National University, 1 Gwanakro, Gwanakgu, Seoul, Korea, 151-742*
E-mail: jjyoh@snu.ac.kr

A handheld-type Er:YAG laser with 2940 nm wavelength and 150 μs pulse duration was built for the purpose of transdermal drug delivery via the laser-induced microjet that is ejected at ~100 m/s in air. A single source of laser beam is split into two: one beam ablates a targeted spot on a skin and another beam drives the injector for fast microjet ejection into a pre-ablated spot (Fig. 1). This combined ablation and microjet injection scheme using a beam splitter utilizes 1:4 laser energy sharing between generation of the micro hole via ablation and the microjet which is generated using the Er:YAG laser. Analysis of the injection mechanism is carried out by studying the response of the elastic membrane that separates a driving water unit for bubble expansion from a drug unit for a microjet ejection. The efficiency of the present delivery scheme is evaluated by the abdominal porcine skin test using the FITC (fluorescein isothiocyanate) staining and the confocal microscopy for quantitative delivery confirmation.

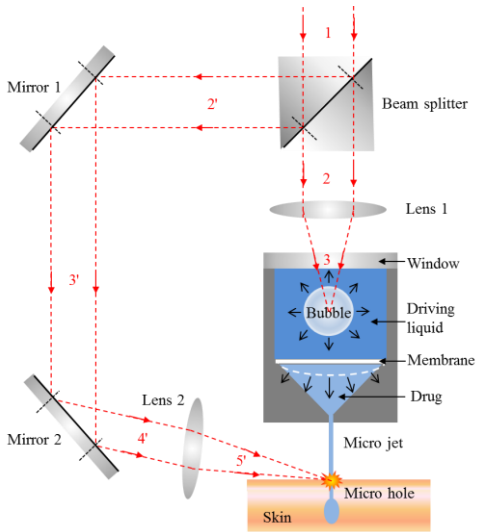

Fig. 1. Schematic of penetration process with combination of skin ablation and microjet ejection via beam splitter

Thursday
3 September 2015

Oral presentations

I-11

Numerical modelling of laser interaction with transparent materials: From description to prediction

N. M. Bulgakova[1,2], V. P. Zhukov[3,4], Y. P. Meshcheryakov[5], T. Mocek[1]

[1]*HiLASE Centre, Institute of Physics ASCR, Za Radnicí 828, 25241 Dolní Břežany, Czech Republic*

[2]*Institute of Thermophysics SB RAS, 1 Lavrentyev Ave., 630090 Novosibirsk, Russia*

[3]*Institute of Computational Technologies SB RAS, 6 Lavrentyev Ave., 630090 Novosibirsk, Russia*

[4]*Novosibirsk State Technical University, 20 Karl Marx ave., 630073, Novosibirsk, Russia*

[5]*Design and Technology Branch of Lavrentyev Institute of Hydrodynamics SB RAS, Tereshkovoi str. 29, 630090 Novosibirsk, Russia*

E-mail: bulgakova@fzu.cz

The interaction of ultrashort laser pulses with transparent optical materials has proven to be a powerful technique of modification of material properties for technological applications based on 3D photonic structures. The physics behind laser-induced modification phenomenon is extremely rich and still far from complete understanding. Even at single pulse irradiation, it involves the multiplicity of physical processes initiated by light absorption and extending to microsecond timescales when a final structure becomes "frozen" in the glass matrix. When ultrashort laser pulses interact with matter, material properties can swiftly start to change already at fs time scale, exhibiting variations of optical response. Modification features can be localized at nanometer scales (e.g., nanogratings and nanovoids, see [1] and references therein). There are no experimental methods with enough resolution to follow the complexity of the processes at such temporal and spatial scales. Consequently, computer modeling plays an increasingly important role in describing dynamics of material evolution and predicting modification structures.

Generally, sophisticated models describing complex phenomena such as laser-induced material modification must be able to demonstrate links between involved processes and predict how the excited matter evolves. Ideally, such models would give scientists new ideas how to control matter evolution in a desired way. In this work, the models will be reported which have been developed to describe the processes excited in the bulk glass during the laser beam propagation with following material evolution up to microsecond time scale. The most sophisticated model to the date consists of two parts. The first part solves Maxwell's equations [2,3] supplemented by the rate and hydrodynamics equations for generated free electrons. The model resolves spatiotemporal dynamics of free-electron population. Its output in the form of the absorbed energy map serves as the initial condition for the second part, the thermoelastoplastic model which models material redistribution. The simulations performed for a wide range of irradiation conditions have allowed to clarify the timescales at which modification occurs after single laser pulses. We demonstrate the ability of the model to quantitatively predict the levels of laser-induced material heating and deformations. The results of simulations of pump-probe experiments have revealed appearance and development of defect-assisted screening of laser light (Fig. 1, left), which must also emerge in multi-pulse irradiation regimes. For the linearly polarized laser beam, the effect of light absorption asymmetry is demonstrated (Fig. 1, middle and right). Finally, a new model will be reported for multi-pulse irradiation regimes that takes into account laser beam scanning. Being simplified, this model, however, enables gaining insight into the roles of defects and heat accumulation.

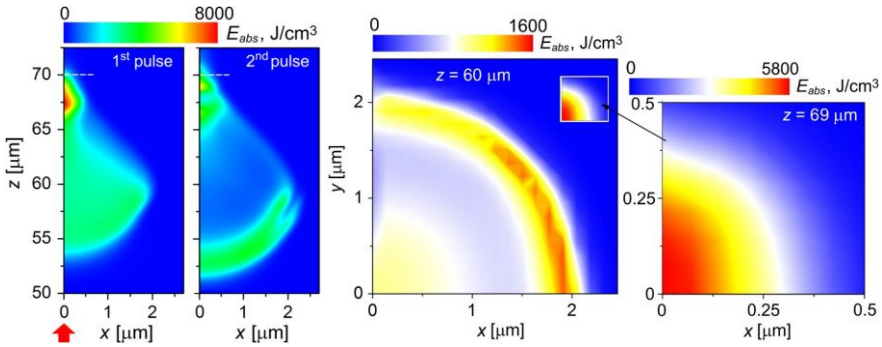

Fig. 1. Absorbed energy maps for pump-probe irradiation regime with several ps separation time between pulses (left). The beam parameters are the following: pulse energy 0.5 μJ, duration 150 fs, NA = 0.4, geometrical focus at 70 μJ from the sample surface. In the middle and right pictures, cross sections of the absorbed energy distribution are given for the 2st pulse demonstrating absorption asymmetry. Laser light is polarized along *x* direction. Note that color scales and dimensions are different for the maps to better highlight the features.

[1] R. Buschlinger, S. Nolte, and U. Peschel, "Self-organized pattern formation in laser-induced multiphoton ionization," Phys. Rev. B. **89**, 184306 (2014).

[2] N. M. Bulgakova, V. P. Zhukov, and Y. P. Meshcheryakov, "Theoretical treatments of ultrashort pulse laser processing of transparent materials: Towards understanding the volume nanograting formation and "quill" writing effect, " Appl. Phys. B **113**, 437-449 (2013).

[3] N. M. Bulgakova, V. P. Zhukov, Y. P. Meshcheryakov, L. Gemini, J. Brajer, D. Rostohar, and T. Mocek, "Pulsed laser modification of transparent dielectrics: what can be foreseen and predicted by numerical simulations?" J. Opt. Soc. Am. B **31**, C8 (2014).

O-50

Laser Induced Periodic Surface Structures of Thin, Complex Multi-Component Films

Juergen Reif [1], Olga Varlamova[1], Markus Ratzke[1], Sebastian Uhlig[1,2], Hans-Michael Krause[3]
[1]*Brandenburgische Technische Universitaet – BTU Cottbus-Senftenberg, Platz der Deutschen Einheit 1, 03046 Cottbus, Germany*
[2]*present address: Fraunhofer IPMS, Maria-Reiche Str., Dresden, Germany*
[3]*IHP, Im Technologiepark, Frankfurt (Oder), Germany*
E-mail: reif@tu-cottbus.de

1. Introduction

Surface modification by the formation of (ultrafast) laser induced periodic surface structures (LIPSS, ripples) has been widely studied during the last few years, and is promising, meanwhile, an increasing number of functional applications, such as controlled wettability, new tribologic properties, or colouring [1]. Nevertheless, the physical mechanisms are still strongly disputed between mainly two models: a static, lithography-like process of structured ablation by interference-modulated irradiation [2], and, on the other hand, self-organized structure formation from a laser induced thermodynamic instability of the material's surface region [3]. It is the intention of the present work to shed more light on this discrepancy by choosing a complex, multilayer thin film target and comparing broadband irradiation by an ultrafast white light continuum [4] and by monochromatic laser light.

2. Experimental outline

The complex target was a piece of a used magnetic 40-Gb hard disk: on a glass substrate covered with a thin titanium buffer layer, the magnetic Co-Pt-Cr magnetic layer is about 100 nm thick, followed by polymer protecting film of about 5 nm thickness.

The irradiation was delivered either by an amplified ti:sapphire laser (800 nm, 100 fs, bandwidth ≈10 nm) or by a white light continuum produced by that laser in an Al_2O_3 crystal (500 ... 700 nm, ≈ 100 fs) at a high number of pulses (mostly 1,000).

3. Results

For white-light irradiation, the first action was, obviously, the complete removal of the polymeric protective layer. Then, several types of regular nanostructures can be observed. At the spot edge, i.e. relatively modest irradiation dose, arrays of isolated long, parallel ripples-like lines have developed, parallel to the laser polarization, They are about 400 nm wide with a separation of about 500 nm. They are between 1.5 and 7 µm long. They extend above the surrounding surface by about 20 nm. Closer inspection reveals an even finer internal ripples-structure of these lines, longitudinally divided into about 200-nm long and 1-nm high segments. In contrast, most of the central part of the spot is densely covered by close-packed round nanoparticles, ranging in diameter from 200 nm in the centre to almost 1µm closer to the edge and extending between 50 and 150 nm above the unaffected target surface outside the spot. On the other hand, however, other regions of the spot, adjacent to the nanoparticles, appear to be completely stripped of the film, down to the bare glass substrate. For irradiation with monochromatic laser light, similar results are obtained.

From the substantial extension of the nanostructures above the original target surface as well as from the complete film removal in the vicinity of – in particular the larger – nanoparticles we conclude that the new film morphology is not the result of mere selective local ablation, as would be inherent in the lithographic model. More likely, we suggest a material reorganization and rearrangement to be responsible for the nano-structure formation. In good agreement with the self-organization model, the irradiation transforms the film into a soft, nearly liquid state which rapidly re-organizes into a new morphology, including de-wetting of the substrate and aggregation in almost spherical nanoparticles, much thicker than the original film. These different "film" morphologies could be compared to different types of thin film formation, e.g. Volmer-Weber (columnar) vs. Frank-van-der-Merwe (layer-by-layer) growth, depending on the competition between material adhesion and cohesion in dependence on the material kinematic energy.

4. References

[1] A.Y. Vorobyev, C. Guo; Laser Photonics Rev. **7**, 385 (2013)

[2] J. Bonse, A. Rosenfeld, J. Krüger; J. Appl. Phys. **106**, 10491015 (2009)

[3] O. Varlamova, J. Reif, S. Varlamov, M. Bestehorn; ch. 1 in *Progress in Nonlinear Nano-Optics*, S. Sakabe, C. Lienau, R. Grunwald, eds. (Springer Int. Publ. 2015)

[4] J. Reif, O. Varlamova, S. Uhlig, S. Varlamov, M. Bestehorn; Appl. Phys. A **117**, 179 (2014)

Modelling field propagation with spatially varying light intensity in Photorefractive media

D. Namarathne, E. Jaatinen
Queensland University of Technology, Brisbane, QLD
E-mail: dinithi.namarathne@qut.edu.au

Intense laser beams can produce higher harmonic generation and other useful nonlinear optical effects when incident upon a suitable medium [1]. However, these same strong optical fields have the potential to damage the sample material. For example, figure 1 shows the observed sample ablation when an intense TEM_{00} laser beam is incident on a ZnO-Au composite structure. To overcome this limitation there is an increasing interest to develop methods which allow nonlinear effects to be observed and measured but without damaging the sample. This requires creating an optical field where the beam's peak intensity remains below the sample damage threshold whilst not limiting other beam attributes that dictate the medium's nonlinear response. For example, in the popular Z scan nonlinear measurement technique [2], the Rayleigh range is an important parameter.

In this paper we propose using higher order TEM transverse modes as fields for undertaking nonlinear optical measurements of samples using the Z scan technique. For the same beam power, these higher order modes have the same Rayleigh range but a much lower peak intensity than the fundamental mode. For example, the TEM_{01}* doughnut mode peak intensity is nearly 5 times lower than an equivalent fundamental TEM_{00} mode with the same power. However, it is not known what impact to the nonlinear response that the higher order mode will have. To date there are few theoretical models presented to investigate a medium's nonlinear response to different beam intensity profiles. The work presented here targets to address this gap by providing a comprehensive theoretical model which enables a deeper understanding of the propagation of light with spatially varying intensity profiles in nonlinear media.

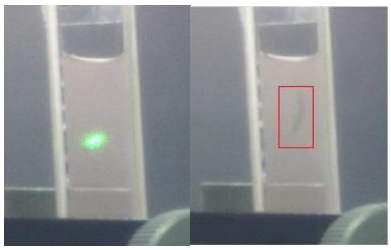

(a) (b)

Fig. 1. a) Shows the area illuminated by high intensity TEM_{00} laser beam
b) Visible line is due to ablation of Au particles

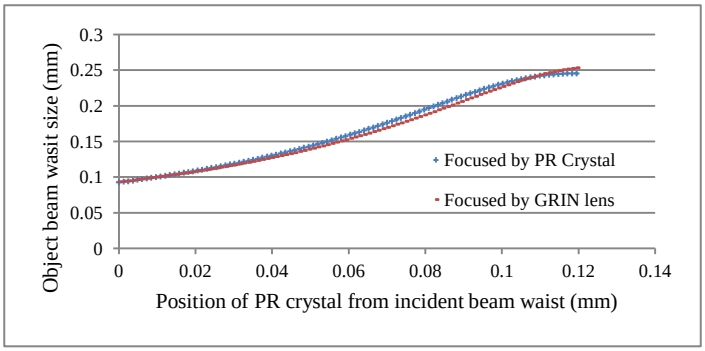

Fig. 2. Comparison between the model produced results and GRIN lens output for TEM_{01}* doughnut beam object waist size

The proposed model investigates the effect of a TEM_{01}* doughnut beam incident on a photorefractive (PR) medium and compares the response to that predicted for a TEM_{00} mode. The PR media is assumed to possess both real and imaginary components of the intensity-dependent refractive index. Considerable amount of beam energy dissipates as beam travels through the medium due to absorption and scattering resulting in a drop in intensity which in turn impacts on the intensity dependent refractive index. To simulate this complex behaviour, the beam propagation method (BPM) is used [3]. In our approach we modify the intensity dependent refractive index term through a Taylor series approximation, which was proven to agree well with previous experimental observations [4]. This has simplified the calculation significantly and allows for the model to be verified by comparison with the known focusing behaviour of a GRIN lens, which also process quadratically varying transverse refractive index profile. To demonstrate this, a GRIN lens with a gradient index constant of 0.339 was placed at various distances from a TEM_{00} mode with a beam waist of 0.1mm, and the final beam waist size determined with the exact analytical solution and with the model. As illustrated in Figure 2, there is good agreement between the exact solution and the model.

The model was then used to analyse various experimental scenarios using media with differing levels of intensity dependent real and imaginary refractive index components (ie. n_2 and β) which are then compared with experimental observations.

References

[1] R.W. Boyd, *Nonlinear optics*, 2nd. ed., (Academic Press, San Diego, CA, 2003)
[2] M. Sheik-Bahae, A.A. Said, T.-H. Wei, D.J. Hagan, and E. W. Van Stryland, "Sensitive measurement of optical nonlinearities using a single beam.", IEEE J Quantum Elect., **26,** 760(1990)
[3] Y. Chung, and N. Dagli, "An assessment of finite difference beam propagation method", IEEE J Quantum Elect., **26,** 1335(1990)
[4] Jones, M.W., E. Jaatinen, and G.W. Michael, "Propagation of low-intensity Gaussian fields in photorefractive media with real and imaginary intensity-dependent refractive index components," Appl. Phys. B **103**, 405(2011)

O-52

Wavelength dependence of nanosecond IR laser-induced breakdown in water: evidence for multiphoton initiation via an intermediate state

N. Linz[1], S. Freidank[1], X.-X. Liang[1], H. Vogelmann[2], T. Trickl[2], A. Vogel[1]
[1]*Institut für Biomedizinische Optik, Universität zu Lübeck, Peter-Monnik Weg 4, 23562 Lübeck, Germany*
[2]*Institut für Meteorologie und Klimaforschung, Forschungszentrum Karlsruhe, Kreuzeckbahn 19, 82467 Garmisch-Partenkirchen, Germany*
E-mail: linz@bmo.uni-luebeck.de

IR laser-induced breakdown in water and aqueous media is utilized for microsurgery in transparent tissues and cells as well as for producing spherical bubbles in basic investigations of cavitation bubble dynamics. Theoretical modeling of the breakdown process requires a clear picture on the fundamental mechanisms providing seed electrons for avalanche ionization, as well as a profound knowledge of the band structure of liquid water and the possible excitation pathways. We present a novel technique of optical breakdown threshold spectroscopy that addresses both issues by investigating the wavelength dependence of the breakdown threshold in water for nanosecond (ns) IR laser pulses.

Avalanche ionization is the most powerful mechanism driving IR ns laser-induced dielectric breakdown. It depends on the availability of seed electrons in the conduction band that can gain energy through inverse Bremsstrahlung absorption and multiply by impact ionization. For ns breakdown, it is still a matter of debate whether such seed electrons are available as background electrons, formed at impurities, or whether they are generated by multiphoton ionization (MPI) of the water itself. If breakdown initiation depends on MPI, the wavelength dependence of the breakdown threshold, $I_{th}(\lambda)$, should exhibit a sharp rise whenever one photon more is needed to overcome the initiation energy E_{ini}. By contrast, if it relies on background electrons or thermal ionization of impurities, the $I_{th}(\lambda)$ curve should vary monotonously.

To date, optical breakdown models treat water as amorphous semiconductor and identify E_{ini} with the band gap energy. However, spectroscopic evidence collected in the past two decades suggests that this approach oversimplifies the band structure and that direct ionization occurs only at considerably higher excitation energies of ≥ 9.5 eV. The previously assumed "ionization energy" of 6.5 eV turned out to be the minimum energy needed for excitation of a valence band electron into a solvated state.

We investigated the optical breakdown threshold in water at 21 wavelengths between 725 nm and 1025 nm using bubble formation as threshold criterion. Measurements were performed using 2-ns IR single-longitudinal mode laser pulses providing a smooth, reproducible temporal pulse shape that is essential for a precise threshold determination. Figure 1 shows the existence of steps in the $I_{th}(\lambda)$ spectrum verifying multiphoton-initiation of nanosecond IR breakdown. The steps in the $I_{th}(\lambda)$ spectrum are consistent with an initiation energy of ≈ 6.6 eV which is considerably smaller than the band gap energy of ≈ 9.5 eV.

We conclude that breakdown initiation likely occurs via excitation of a valence band electron into a solvated state, followed by rapid excitation into the conduction band. Therefore, an additional "initiation channel" involving an intermediate energy level must be introduced into breakdown models for water. Theoretical analysis of the measurement results corroborated our hypothesis on breakdown initiation.

Fitting of model predictions to $I_{th}(\lambda)$ as shown in figure 1 revealed that the seed electron density required to initiate avalanche ionization drops from above 10^{15} cm^{-3} at 725 nm to below 10^{12} cm^{-3} at 1025 nm. Similar seed electron densities as in water will probably be needed also for plasma formation in transparent cells and tissues. However, in those media bio-molecules can provide additional sources for free-electron generation, and the breakdown threshold may be lowered.

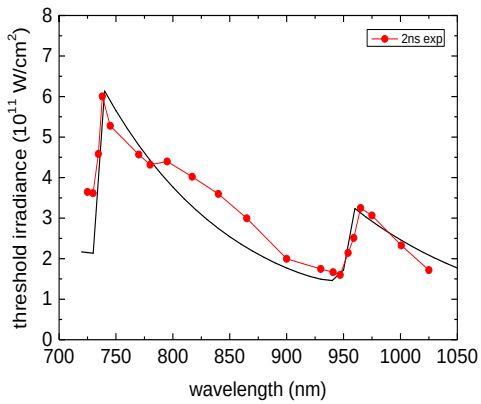

Figure 1 *Wavelength dependence of the irradiance threshold for optical breakdown in water produced by 2-ns laser pulses, compared with model predictions (black line). The steps in the $I_{th}(\lambda)$ spectrum indicate multiphoton initiation of breakdown.*

O-53

Multiphase equations of state for metals under intense laser influences

K. V. Khishchenko
Joint Institute for High Temperatures RAS, Izhorskaya 13 Bldg 2, Moscow 125412, Russia
E-mail: konst@ihed.ras.ru

1. Introduction

Description of the thermodynamic properties of materials under intense laser influences is of both fundamental and practical interests. Equation-of-state models over a wide range from normal conditions to extremely high pressures and temperatures are required for hydrodynamic simulations of a laser–material interaction [1]. Accuracy of simulated results is determined mainly by adequacy of the equation-of-state model for materials in question.

In the work, a new thermodynamic approach to modelling of equation of state for metals with taking into account the polymorphic transformations, melting and evaporation effects is proposed.

2. Multiphase EOS model

The specific Helmholtz free energy F of metals is considered as a sum of three components [2], $F(V, T) = F_c(V) + F_a(V, T) + F_e(V, T)$, describing interparticle interaction at $T = 0$ K (F_c) and thermal contributions by heavy particles (atoms, ions, nuclei) and electrons (F_a and F_e, respectively). Here T is the temperature, V is the specific volume, $V = \rho^{-1}$, ρ is the substance density. The first and second components have different forms for the solid and liquid phases, but the third is defined identically. As distinct from previously obtained multiphase equations of state for metals [3], new functional expressions for the thermodynamic potential are formulated. Those provide for a more correct thermal contribution of heavy particles in the solid and liquid phases.

Multiphase equations of state for iron, gold, tungsten and some other metals are obtained. Calculated results for these substances are given in comparison with experimental data at high temperatures and pressures.

3. Conclusion

The proposed multiphase equations of state provide for a reliable description of the metals properties in a wide range of thermodynamic parameters. That gives an opportunity for effective use of the equations of state in numerical simulations of hydrodynamic processes at intense laser–material interactions.

[1] M. E. Povarnitsyn, T. E. Itina, P. R. Levashov, and K. V. Khishchenko, "Simulation of ultrashort double-pulse laser ablation," Appl. Surf. Science 257, 5168 (2011).
[2] Ya. B. Zel'dovich and Yu. P. Raizer, Physics of Shock Waves and High-Temperature Hydrodynamic Phenomena (Academic Press, New York, 1967).
[3] V. E. Fortov, K. V. Khishchenko, P. R. Levashov, and I. V. Lomonosov, "Wide-range multi-phase equations of state for metals," Nucl. Instr. Meth. Phys. Res. A 415, 604 (1998).

O-54

Non-equilibrium effects in laser-induced plasma plumes

A. N. Volkov, G. Silverstein, O. Ranjbar
Department of Mechanical Engineering, University of Alabama, H. M. Comer Hall, 7th Avenue, Tuscaloosa, AL 35487, USA
Z. Lin
Electro Scientific Industries Inc., 13900 NW Science Park Drive, OR Portland 97124, USA

Corresponding Author e-mail address: avolkov1@ua.edu

Plasma effects in the laser-induced plume flows are known to be important for the laser processing of various material targets by high-power nanosecond pulsed lasers. In particular, the plasma plumes can efficiently absorb the incident laser radiation, thus substantially decreasing the amount of energy absorbed directly by the target, reducing the target temperature, and, finally, decreasing the amount of ablated material. Along with this major "shielding effect", the plasma plume also induces a number of secondary effects like heating and etching of the target by adjacent high-temperature plasma. These plasma-related effects substantially limit the overall efficiency of industrial laser systems and reduce the accuracy of laser machining.

The present work is aimed at the numerical modeling of laser-induced plasma plume expansion. Although a number of diverse models of plasma flow in laser plumes were proposed in the literature, these models were not compared in a unified framework. The major goal of the present work is to accurately quantify the contribution of multiple non-equilibrium effects in laser plasma plume flows.

For this purpose, gas-dynamic and kinetic models of plasma plume expansion into a background gas were developed. The gas-dynamic model solves the one-dimensional continuum equations of the multi-components plume flow and incorporates both equilibrium, based on Saha-Langmuir equations, and non-equilibrium, based on kinetic rates of ionization and recombination, models of plasma. This model accounts for the absorption of the laser radiation in the inverse Bremsstrahlung, the diffusion and heat conduction of individual species, and the difference between temperatures of electrons and heavy particles. The kinetic model is designed for both one- and two-dimensional axisymmetric plume flows and is based on the Direct Simulation Monte Carlo (DSMC) method. This kinetic model is capable of taking into account the same plasma models as the gas-dynamic model. In order to account for the two-temperature effects, the kinetic model is coupled with the continuum equation for the electron temperature. Both gas-dynamic and kinetic models are coupled with the same thermal model of the target. Boundary conditions at the target surface account for the evaporation and condensation, thermionic emission, and back heating of the target by the high-temperature plume. The computational codes implementing these models are designed in order to allow for switching off non-equilibrium models of individual processes and analyzing the contributions of different sources of non-equilibrium. The comparison of results obtained with the gas-dynamic model allows one, in turn, to reveal the effects of translational non-equilibrium in the plume flows, which can be important in the near-surface Knudsen layer and in rarefied regions of the plume. The developed models are used in order to systematically investigate relative contributions of various sources of non-equilibrium in the plume flow for single-pulse nanosecond laser ablation of copper targets in broad ranges of laser fluence and background gas pressure. The background gas pressure varies in simulations from vacuum to atmospheric pressure. The obtained results are compared with simulation and experimental results known from literature. Based on the presented analysis, a series of "minimum" rational models of laser plasma plumes is suggested for different ranges of laser fluence and background gas pressure. These models are further utilized to study the interaction between plumes of two sequential laser pulses in the two-dimensional, axisymmetric framework.

I-12

Ultrashort pulse laser processing of transparent materials – potential and applications

S. Nolte[1,2], K. Bergner[1], F. Dreisow[1], R.G. Krämer[1], D. Richter[1], S. Richter[1], C. Voigtländer[1], and F. Zimmermann[1]

[1]*Institute of Applied Physics, Abbe Center of Photonics, Friedrich Schiller University, Albert-Einstein-Strasse 15, 07751 Jena, Germany*
[2]*Fraunhofer Institute for Applied Optics and Precision Engineering, Albert-Einstein-Strasse 7, 07745 Jena, Germany*
E-mail: stefan.nolte@uni-jena.de

1. Abstract

Ultrashort laser pulses have shown a huge potential for precise microstructuring. Especially the nonlinear interaction processes involved when processing transparent materials offer additional possibilities as e.g. internal structuring without affecting the surface. Applications include precise cutting, welding but also the realization of various photonic components like waveguides, artificial birefringent devices or Bragg gratings.

2. Introduction

Ultrashort laser pulses have a tremendous potential for precise microstructuring. Especially, the possibility to realize three-dimensionally localized modifications within the bulk of transparent materials has generated significant interest. When the pulses are tightly focused into the transparent material, the intensity in the focal volume can become high enough for nonlinear absorption processes. This localized energy deposition results in permanent structural changes inside the sample without affecting the surface. Depending on the processing parameters, either isotropic refractive index changes, self-organized sub-wavelength structures leading to form birefringence or microvoids can be generated in the focus [1]. In addition, for high repetition rates local heat accumulation can occur.

In this presentation a short overview on the fundamentals of femtosecond volume structuring will be given. Different applications including the fabrication of artificial birefringent devices, fiber (FBG) and volume Bragg gratings (VBG) as well as the welding of glasses will be highlighted.

3. Bragg gratings

The possibility to locally modify the refractive index is interesting for a variety of applications. Straightforward is the inscription of waveguiding structures in glasses [2] and crystals [3]. This can be extended to complex 3D waveguide arrangements allowing to mimic physics in other systems [4] or to provide an opportunity for reliable quantum computing [5]. From an application point of view the generation of periodic modifications inside fibers (fiber Bragg gratings - FBG) [6,7] is very attractive. Due to the underlying nonlinear absorption processes, there is no need for any photosensitivity of the material to be structured. Hence, FBG can be inscribed into passive as well as active doped fibers.

For obtaining a reliable periodic pattern, we apply the so-called phase-mask approach. By scanning the focus across the core even large-mode-area fibers can be structured with high homogeneity in order to avoid detrimental effects such as mode coupling. Apart from sensing, promising applications include narrow-bandwidth [8] as well as high-power laser applications.

Nevertheless, the modifications are not restricted to the fiber core or the fiber geometry. By applying the same technique to bulk material volume Bragg gratings (VBG) can be inscribed in different glasses (see Fig. 1) [9]. This provides attractive opportunities, e.g. for laser-diode stabilization (see Fig. 1, right) or beam combining.

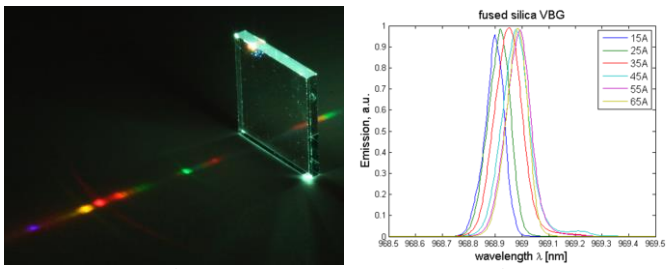

Fig. 1. Left: Two-dimensional VBG inscribed in fused silica. Right: Emission spectra of a diode laser stabilized by fs-written VBG in fused silica for different diode currents.

4. Nanogratings

At slightly higher pulse energies than necessary for inducing homogeneous refractive index changes self-organized periodic nanostructures, so-called nanogratings, can be generated [10-13]. Emerging after several

O-55

Short-pulse laser excitation of quartz: Experiments and modelling of transient optical properties and ablation

L. Haahr-Lillevang[1], K. Wædegaard[1], D. B. Sandkamm[1], A. Mouskeftaras[2], S. Guizard[2], P. Balling[1]
[1]*Department of Physics and Astronomy, Aarhus University, DK-8000 Aarhus C, Denmark*
[2]*Laboratoire des Solides Irradiés/CEA IRAMIS, Ecole Polytechnique, Palaiseau, France*
E-mail: lassehl@phys.au.dk

The ultrafast absorption of laser pulses in dielectrics is an intricate problem to analyse and it currently receives much attention. From a theoretical point of view, many fundamental physical processes must simultaneously be included in a description, e.g. strong field excitation, collisional excitation and the ultrafast changing of optical properties; for a recent review, see [1]. In the current presentation, the changes in the optical properties during the excitation are investigated experimentally in a pump-probe setup, combining time-resolved spectral interferometry and reflectance measurements. Atomic-force-microscopy images of the laser-formed holes are subsequently obtained [2].

The model applied for simulating and understanding the transient changes as well as the final hole depths is a multiple-rate equation model as originally proposed by Rethfeld [3], extended by us to include the propagation of light into the material [4] and in the present material, quartz, to also describe self-trapping of excitons (see also [5]).

Quartz is an interesting material in this context, since the time-resolved optical measurements reveal optical changes in the first picosecond after the pump pulse, consistent with a fast self-trapping of excitons with optical properties described by the Drude-Lorentz model. In materials where self-trapped excitons are known to be absent, e.g. sapphire, the optical properties reaches steady values in the first hundred femtoseconds after the pulse [6].

Figure 1 shows measured atomic-force-microscopy profiles of the holes produced by the laser pulses together with iso-density lines of the conduction-band electrons found in the simulations. The applied model, based on the underlying physical mechanism and containing one set of parameters, enables the explanation of both transient optical measurements and final ablation depths over a large range of intensities, from well below to well above the ablation threshold.

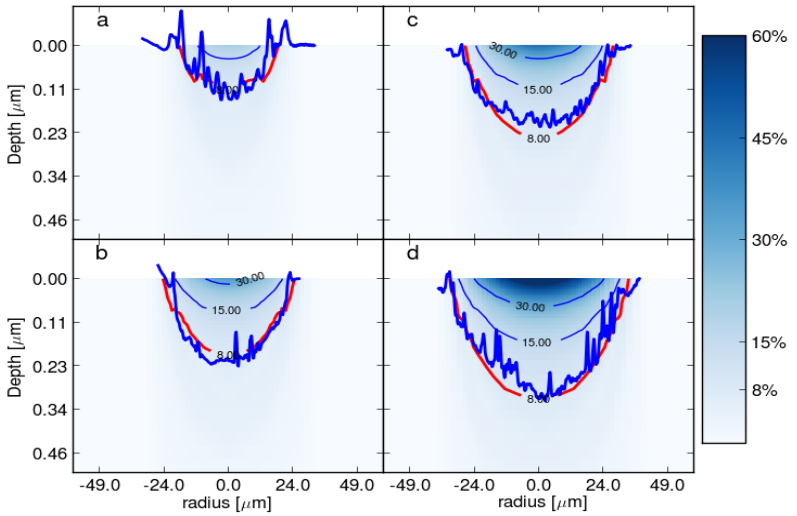

Figure 1: AFM-profiles (blue rugged lines) and simulated results of the spatial distribution of conduction-band-electron densities produced by pulse fluences: a) 7.8 J/cm^2, b) 9.2 J/cm^2, c) 10.7 J/cm^2 and d) 14.3 J/cm^2. The blue gradient colours in the figures represent the ratio between the density of conduction-band electrons and the initial valence-band electron density. Iso-density lines are plotted for 30%, 15% (thin blue) and 8% (thick red), the latter corresponding to the ablation criterion used in the simulations.

1) P. Balling and J. Schou, *Femtosecond laser ablation dynamics of dielectrics: Basics and applications for thin films*, Reports on Progress in Physics, **76**, 036502 (2013).
2) L. Haahr-Lillevang, K. Wædegaard, D. B. Sandkamm, A. Mouskeftaras, S. Guizard and P. Balling, *Short-pulse laser excitation of quartz: Experiments and modeling of transient optical properties and ablation*, Applied Physics A (submitted 2015)
3) B. Rethfeld, Phys. Rev. Lett., **92,** 187401 (2004); B. Rethfeld, Phys. Rev. B, **73,** 035101 (2006).
4) B. H. Christensen and P. Balling, *Modeling short-pulse laser ablation of dielectric materials*, Phys. Rev. B **79**, 155424 (2009).
5) B. Rethfeld, O. Brenk, N. Medvedev, H. Krutsch, and D. H. H. Hoffmann, *Interaction of dielectrics with femtosecond laser pulses: application of kinetic approach and multiple rate equation*, Appl. Phys. A **101**, 19 (2010)
6) K. Wædegaard, D. B. Sandkamm, A. Mouskeftaras, S. Guizard, and P. Balling, *Probing ultrashort-pulse laser excitation of sapphire: From the initial carrier creation to material ablation*, Europhysics Letters **105**, 47001 (2014).

pulses, they are always oriented perpendicular to the laser polarization. By careful analysis we were able to show that the nanogratings consist of small sheet-like cavities arranged periodically [14]. Due to their anisotropy, nanogratings show strong form birefringence. This can be harvested for the fabrication of tailored waveplates with locally varying birefringence. Application examples include polarization converters [15] or structures for advanced microscopy.

4. Welding

A completely different process occurs, when high repetition rates in the order of 1 MHz or above are used. The localized absorption is still based on the nonlinear absorption processes. However, in this case heat from successive pulses accumulates since the pulse-to-pulse separation is shorter than the deposited laser energy needs to diffuse out of the focal volume. The train of ultrashort laser pulses acts here as a point heat source, which can be freely positioned inside the bulk volume.

In order to weld glasses together, the samples just have to be brought into contact and the focus is scanned along the interface. This allows to join the samples without any adhesives or additional layers for increasing the absorption [16]. Bonding strengths of up to the bulk material value can be obtained even for dissimilar glasses with significantly different thermal expansion coefficients, since only a small volume is heated [17,18].

4. Conclusions

Nonlinear processing of transparent materials with intense ultrashort laser pulses opens up various application fields. However, a requirement for a successful utilization is a fundamental understanding of the underlying processes. In this paper an overview of the fundamental processes is given and different applications are highlighted.

5. Acknowledgements

We acknowledge support from the Deutsche Forschungsgemeinschaft (DFG), the German Federal Ministry of Education and Research (BMBF), and the Thuringian Ministry for Education, Science and Culture.

6. References

[1] K. Itoh, W. Watanabe, S. Nolte, and C. B. Schaffer, „Ultrafast processes for bulk modification of transparent materials," MRS Bulletin **31**, 620 – 625 (2006).
[2] K.M. Davis, K. Miura, N. Sugimoto, K. Hirao, "Writing Waveguides in Glass with a Femtosecond Laser," Opt. Lett. **21**, 1729-1731 (1996).
[3] J. Burghoff, S. Nolte, and A. Tünnermann, "Origins of Waveguiding in Femtosecond Laser-Structured LiNbO3", Appl. Phys. A **89**, 127-132 (2007).
[4] Y. Plotnik, M. C. Rechtsman, D. Song, M. Heinrich, J. M. Zeuner, S. Nolte, Y. Lumer, N. Malkova, J. Xu, A. Szameit, Z. Chen, and M. Segev, "Observation of unconventional edge states in 'photonic graphene'," Nature Mater. **13(1)**, 57-62 (2014).
[5] R. Heilmann, M. Gräfe, S. Nolte, and A. Szameit, "Arbitrary photonic wave plate operations on chip: Realizing Hadamard, Pauli-X, and rotation gates for polarisation qubits," Sci. Rep. **4**, 4118 (2014).
[6] J. Thomas, C. Voigtländer, R.G. Becker, D. Richter, A. Tünnermann, and S. Nolte, "Femtosecond pulse written fiber gratings: a new avenue to integrated fiber technology," Laser & Photon. Rev. **6**, 709–723 (2012).
[7] R.J. Williams, R.G. Krämer, S. Nolte, M.J. Withford, "Femtosecond direct-writing of low-loss fiber Bragg gratings using a continuous core-scanning technique," Opt. Lett. **38**, 1918-1920 (2013).
[8] P. Hofmann, C. Voigtländer, S. Nolte, N. Peyghambarian, A. Schulzgen, „550-mW Output Power From a Narrow Linewidth All-Phosphate Fiber Laser," J. Lightwave Tech. **31(5)**, 756-760 (2013).
[9] C. Voigtländer, D. Richter, J. Thomas, A. Tünnermann, and S. Nolte, "Inscription of High Contrast Volume Bragg Gratings in Fused Silica with Femtosecond Laser Pulses", Appl. Phys. A **102**, 35-38 (2011).
[10] Y. Shimotsuma, P.G. Kazansky, J. Qiu and K. Hirao, "Nanostructuring of transparent materials by ultrashort light pulses," Phys. Rev. Lett. **91**, 247405 (2003).
[11] R. Taylor, C. Hnatovsky, and E. Simova, "Applications of femtosecond laser induced self-organized planar nanocracks inside fused silica glass," Laser & Photon. Rev. **2**, 26–46 (2008).
[12] S. Richter, M. Heinrich, S. Döring, A. Tünnermann, S. Nolte, U. Peschel, "Nanogratings in fused silica: Formation, control, and applications," J. Laser Appl. **24(4)**, 4020081-4020088 (2012).
[13] F. Zimmermann, A. Plech, S. Richter, A. Tünnermann, S. Nolte, „On the rewriting of ultrashort pulse-induced nanogratings", Opt. Lett. **40(9)**, 2049-2052 (2015)
[14] F. Zimmermann, A. Plech, S. Richter, S. Döring, A. Tünnermann, and S.Nolte, "Structural evolution of nanopores and cracks as fundamental constituents of ultrashort pulse-induced nanogratings," Appl. Phys. A **114**, 75–79 (2014).
[15] M. Beresna, M. Gecevičius, P.G. Kazansky, and T. Gertus, "Radially polarized optical vortex converter created by femtosecond laser nanostructuring of glass", Appl. Phys. Lett. **98**, 201101 (2011).
[16] S. Richter, S. Döring, A. Tünnermann, and S. Nolte, "Bonding of Glass with Femtosecond Laser Pulses at High Repetition Rates", Appl. Phys. A **103**, 257-261 (2011).
[17] F. Zimmermann, S. Richter, S. Döring, A. Tünnermann, S. Nolte, „Ultrastable bonding of glass with femtosecond laser bursts," Appl. Opt. **52(6)**, 1149-1154 (2013).
[18] S. Richter, F. Zimmermann, S. Döring, A. Tünnermann, S. Nolte, "Ultrashort high repetition rate exposure of dielectric materials: laser bonding of glasses analyzed by micro-Raman spectroscopy," Appl. Phys. A **110(1)**, 9-15 (2013).

O-56

Absorption spectroscopy of atoms in the bubble produced by laser ablation in aqueous solutions

A. Matsumoto, A. Kawasaki, A. Tamura, T. Honda, N. Nishi, K. Amano, T. Sakka
Department of Energy and Hydrocarbon Chemistry, Kyoto University, Kyoto, Kyoto 615-8510, Japan
E-mail: matsumoto.ayumu.78w@st.kyoto-u.ac.jp

1. Introduction

Liquid-phase laser ablation can be used to prepare pure nanoparticle dispersions without additives. Although it has been reported that nanoparticles are observed in the bubble produced by the laser ablation in water [1,2], the mechanism of the formation is not fully clarified. Emission spectroscopy of the laser ablation plasma gives information of the ablated species in the bubble. The lifetimes of the plasma emission and the bubble are several hundred nanoseconds and several hundred microseconds, respectively. To study the formation of the nanoparticles, it is essential to investigate the behavior of the ablated species in the bubble after the plasma quenching. It is expected that absorption spectroscopy gives information of non-emissive species in the bubble. However, it is difficult to transmit the probe light into the bubble since it is very small and the refractive index in the bubble is smaller than outside. In the present study, we perform the absorption spectroscopy of atoms in the ground state in the bubble by employing another laser ablation plasma in water as the probe light source. The plasma in water can be a small and intense continuous emission light source.

2. Experimental

A Q-switch Nd:YAG laser with the wavelength of 1064 nm, the pulse duration of 20 ns, the pulse energy of 12 mJ (laser 1) was focused onto an Al target in water or in a 100 mM NaCl aqueous solution. Another Q-switch Nd:YAG laser with the wavelength of 1064 nm, the pulse duration of 70 ns, the pulse energy of 12 mJ (laser 2) was focused onto a Cu target in water to produce the probe light. The probe light was focused into the bubble produced by the laser 1 in the direction parallel to the Al target surface. The transmitted light was magnified by a 10× objective lens and introduced to an optical fiber bundle connected to a spectrograph equipped with an ICCD camera. The image was measured simultaneously with the spectrum by putting a beam splitter in the light path and using another ICCD camera. By monitoring the image, we adjusted the position of the probe light to put it into the center of the bubble. The time-resolved measurement was performed by controlling the timing of the laser 1 and laser 2 using a delay generator.

3. Results and discussion

Absorption lines of Al atoms ablated from the target were observed at 394.4 and 396.2 nm from 3 to 5 μs after the laser irradiation. On the other hand, absorption lines of Na atoms originating in the solution were observed at 589.0 and 589.6 nm from 4 to 11 μs. By using the absorption coefficients obtained from the literature and the extinction coefficients obtained from the present experiments, we estimated the absolute population densities of the Al and Na atoms in the ground state, $N_{0,\mathrm{Al}}$ and $N_{0,\mathrm{Na}}$. Here, the diameter of the bubble was used as the length of the light path. Also, we assumed that the species in the bubble are homogeneous. The $N_{0,\mathrm{Al}}$ relatively steeply decreased from 7.4×10^{20} m^{-3} at the delay time of 3 μs to 1.1×10^{20} m^{-3} at the delay time of 5 μs while the $N_{0,\mathrm{Na}}$ relatively gradually decreased from 0.81×10^{20} m^{-3} at 4 μs to 0.22×10^{20} m^{-3} at 11 μs. The decrease in both of the densities is attributed to the formation of molecules, oxides, and clusters. The reason for the gradual decrease in the $N_{0,\mathrm{Na}}$ may be that the boiling point of Na (1156 K) is significantly lower than that of Al (2792 K) and consequently the Na atoms remain in the atomic state for longer time in the bubble at low temperature.

[1] W. Soliman, N. Takada, and K. Sasaki, "Growth Processes of Nanoparticles in Liquid-Phase Laser Ablation Studied by Laser-Light Scattering," Appl. Phys. Express **3**, 035201 (2010).
[2] S. Ibrahimkutty, P. Wagener, A. Menzel, A. Plech, and S. Barcikowski, "Nanoparticle formation in a cavitation bubble after pulsed laser ablation in liquid studied with high time resolution small angle x-ray scattering," Appl. Phys. Lett. **101**, 103104 (2012).

O-57

Sub-10fsec to 30 fsec laser ablation: Experimental studies of key features during the first steps of laser ablation around the threshold.

Ali Ajami[1], Chandra S.R.Nathala[1,2] and Wolfgang Husinsky[1]*

1) Institute for Applied Physics, Vienna Technical University, Vienna, Austria

2) Femtolasers Produktions GmbH, Vienna, Austria

** husinsky@iap.tuwien.ac.at*

In this work we report experimental studies of the laser ablation process in the low fsec regime (10-30fsec). The questions addressed are: Can we establish a scenario, how particles are emitted (mass distribution, energy)

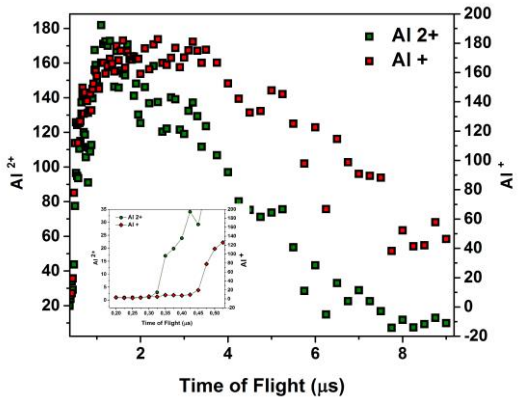

Fig. 1. TOF (Velocity) spectrum of ablated postionized originally neutral species at 7μJ 10 fsec pulses.

for laser fluences at the threshold for ablation. How do they depend on the number of laser pulses? And finally, how do surface structures, in particular, how do High-Spatial-Frequency-Laser-Induced-Periodic-Surface Structures (HSFL), typical for this fluence regime, develop.

For this purpose, a TOF mass spectrometer with laser post-ionization was used to study the mass and velocity distribution of ions and neutrals. A velocity spectrum (actually the measured TOF spectrum) for singly and doubly charged, originally neutral Al atoms from an Al target is shown in Fig. 1. Contrary to the assumption that both should originate from neutral Al atoms, the differences in their velocities indicate a different origin.
The relation between emitted neutrals and ions shows a very pronounced dependency on small fluence changes around the threshold. Also the pulse history is of considerable influence.

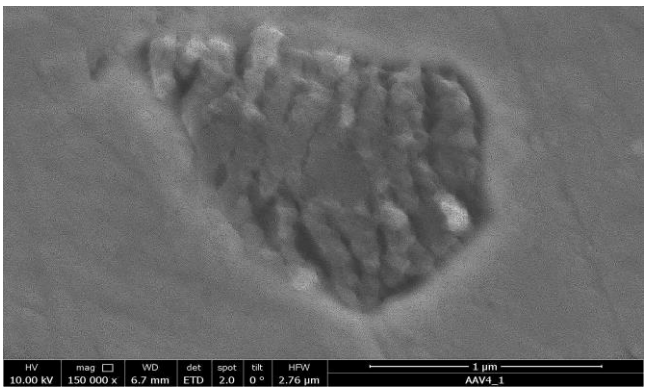

Fig. 2 HFLS for Cu observed in small areas of the laser beam in a fluence regime characterized by mostly neutral particle emission.

Simultaneously we have observed the development of periodic surface structures, which should help to obtain a better understanding of these complex processes. An example is shown in Fig.2.

This work was supported by the Österreichische Forschungsförderungsgesellschaft (FFG) (Project 834325).

O-58

Orientation of periodic grating structures controlled by double pulse irradiations

M. Hashida[1,2], T. Nishii[1,2], Y. Miyasaka[1], H. Sakagami[3], S. Inoue[1,2], and S. Sakabe[1,2]

[1]*Advanced Research Center for Beam Science, Institute for Chemical Research, Kyoto University Uji, Kyoto 611-0011, Japan*

[2]*Department of Physics, Graduate School of Science, Kyoto University, 606-8502 Kyoto, Japan*

[3] *National Institute for Fusion Science, Toki-City, Gifu, 509-5292, Japan*

Corresponding Author e-mail address:hashida@laser.kuicr.kyoto-u.ac.jp

1. Introduction

On metals and semiconductors under irradiation of linear polarized femtosecond laser pulses, laser induced periodic surface structures (LIPSS) were self-organized [1][2] and they were oriented perpendicular to the laser polarization direction. Laser produced LIPSS had an interspace of $0.5\lambda_L$ - $0.85\lambda_L$, which was shorter than the laser wavelength λ_L and its interspaces depended on laser fluence. This dependence was well explained by the parametric decay model [3][4]. An assumption in the model is that, as a consequence of the ultrafast interaction with the laser beam, the solid surface is initially covered by a pre-formed surface plasma with a density much lower than that of the solid. Surface plasma waves are then induced at the interface between free space and the laser-produced surface plasma by parametric decay process. Then, the LIPSS are self-organized. To study the time scale of preformed plasma formation, the double pulse irradiation experiment has been demonstrated. The experimental result suggested that the preformed plasma might be produced in the rising edge of the temporal profile of the laser pulse[5]. However, the detail of LIPSS orientation has not investigated yet and under debated. In this study, cross-polarized double pulses have been used for LIPSS formation to investigate the relation between the laser polarization direction and the LIPSS orientation self-organized on the metal surface.

2. Experiments and results

In the experiments, the T^6-laser system (λ_L=805 nm, τ =40 fs, 10 Hz) was used. The double pulse beam was varied in the time delay from $\Delta\tau$ = 0 to 40ps for the LIPSS formation on titanium. The first pulse fluence F_1 and the delayed pulse fluence F_2 were set to be 50mJ/cm^2 which was below the LIPSS formation threshold of F_{TH} =65mJ/cm^2 for Ti. However, the sum fluence F_1 and F_2 was higher than the F_{TH}. The double pulse beam was collimated and focused to a spot size of 45 μm with flat-topped shape on the Ti target surface with a lens f = 10 cm, at normal incidence in air. The polarization direction of the first pulse was set to be horizontal direction while the delayed pulse was perpendicular direction. The target of titanium was mechanically polished and its roughness was less than 2nm. The number of irradiated double pulse beam was N=50. Laser-produced LIPSS were examined by scanning electron microscopy (SEM; JSM-5560, JEOL). Figure 1 shows SEM images and the FFT power spectra of the surface structures produced by varying the delay time between the first pulse and the delayed pulse. The LIPSS oriented 45degree to both laser polarization directions was self-organized (see Fig1(a)) in the delay time of 0 - 120fs and its interspace was ~ 600nm. The dotted LIPSS structures were produced in the delay time of 1 – 10ps (Fig.1 (b)) while the horizontal direction of LIPSS was obtained for the delay time of 40ps (Fig. 1(c)). The experiment for LIPSS orientation control was demonstrated separately with the double pulse beam with a time delay of 0 fs in which beam composed of a first pulse kept constant fluence of F_1 = 70 mJ/cm^2 and a delayed pulse varied from F_2 = 0 - 70mJ/cm^2. The results show that the direction of LIPSS can control by changing the second laser fluence. Similar results of LIPSS orientation for semiconductor and transparency materials[6][7] have been reported.

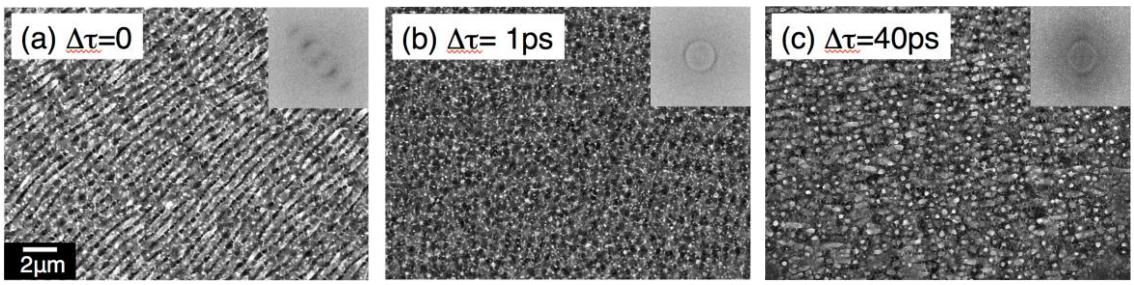

Fig. 1. SEM images and the FFT power spectra (insets) of the surface structures produced by varying the delay time between two pulses. The polarization of first pulse and delayed pulse were horizontal direction <–> and vertical direction ↕, respectively.

Acknowledgments

This study was financially supported by a Grant-in-Aid for Scientific Research (C)(25420728) from the Ministry of Education, Culture, Sports, Science and Technology (MEXT), Japan, and NIFS Collaborative Research Program (NIFS14KNTS031).

References

[1] L. Gemini, M. Hashida, *et al,* J. Appl. Phys. **114**, 194903(2013).
[2] M. Hashida, Y. Ikuta, *et al,* Appl. Phys. Lett.**102**, 174106(2013).
[3] S. Sakabe, M. Hashida, *et al,* Phys. Rev. B **79**, 033409(2009).
[4] K. Okamuro, M. Hashida, *et al,* Phys. Rev. B **82**, 165417(2010).
[5] L. Gemini, M. Hashida, *et al*, Appl. Sur. Sci. (2015) in print.
[6] T. Jia, H. Chen, M.Huang, *et. al*., Phys. Rev. B **72**, 125429 (2005).
[7] Y. Shimotsuma, M. Sakakura, *et. al*, Adv. Mater. **22**, 4039 (2010).

O-59

Laser processing with specially designed laser beam

A.A. Asratyan[1], N.A. Bulychev[2], I.N. Feofanov[2], M.A. Kazaryan[2], V.I. Krasovskii[3], N.A. Lyabin[4], V.I. Sachkov[5], R.A. Zakharyan[3]

[1] Gamalei Institute of Epidemiology and Microbiology, 123098, Gamalei Str., 18, Moscow, Russia,
[2] P.N. Lebedev Physical Institute, Russian Academy of Sciences, 119991, Leninsky pr., 53, Moscow, Russia,
[3] A.M. Prokhorov General Physics Institute, Russian Academy of Sciences, 117942, Vavilova st., 38, Moscow, Russia
[4] Joint Stock Company "Istok", 141190, Vokzalnaya Str., 2A, Fryazino, Moscow Region, Russia
[5] Siberian Physical-Technical Institute of the Tomsk State University, 634050, pl. Novo-Sobornaya, 1, Tomsk, Russia
E-mail: kazar@sci.lebedev.ru, kazarmishik@yahoo.com

The possibility of using laser systems to form beams with special spatial configurations has been studied. The laser systems applied had a self-conjugate cavity based on the elements of copper vapor lasers (LT-5Cu, LT-10Cu, LT-30Cu) with an average power of 5, 10, or 30 W. The active elements were pumped by current pulses of duration 80-100 ns. The duration of laser generation pulses was up to 25 ns. The generator unit included an unstable cavity, where one reflector was a special mirror with a reflecting coating. Various original optical schemes used were capable to explore spatial configurations and energy characteristics of output laser beams in their interaction with micro- and nanoparticles fabricated from various materials. In these experiments, the beam dimensions of the obtained zones varied from 0.3 to 5 mkm, which is comparable with the minimum permissible dimensions determined by the optical elements applied. This method is useful in transforming a large amount of information at the laser pulse repetition rate of 10 – 30 kHz. It was possible to realize the high-precision micromachining and microfabrication of microscale details by direct writing, cutting and drilling (with the cutting width and through-hole diameters ranging from 3 μm to 100 μm) and produce microscale, deep, intricate and narrow grooves on substrate surfaces of metals and non-metal materials. This system is used for producing high-quality micro-scale details without moving the object under treatment. It can also be used for micro-cutting and micro-drilling in a variety of metals such as molybdenum, copper, and stainless steel, with a thickness of up to 300 μm, and in non-metals such as silicon, sapphire and diamond with a thickness ranging from 10 μm to 1 mm with different thermal parameters and specially designed laser beam.

This work has been partially supported by RFBR, projects No. 15-02-03559, 14-02-00602, 14-02-31515, 14-02-92019.

Nanoscale ablation and 3D structuring in porous glass: mechanism and applications

Yang Liao,[1] Jielei Ni,[1] Lingling Qiao,[1] Koji Sugioka,[2] and Ya Cheng[1,*]

[1]*State Key Laboratory of High Field Laser Physics, Shanghai Institute of Optics and Fine Mechanics, Chinese Academy of Sciences, Shanghai 201800, China*

[2]*RIKEN - SIOM Joint Research Unit, RIKEN, Center for Advanced Photonics, Hirosawa 2 - 1, Wako, Saitama 351 - 0198, Japan*

[*]*E-mail: ya.cheng@siom.ac.cn*

The creation of complex three-dimensional (3D) fluidic systems composed of hollow micro- and nanostructures embedded in transparent substrates has attracted significant attention from both scientific and applied research communities. However, it is still a formidable challenge to build 3D micro- and nanofluidic structures with arbitrary configurations using conventional planar lithographic fabrication methods. As a direct and maskless fabrication technique, femtosecond laser micromachining provides a straightforward approach for high-precision, space-selective modification inside transparent materials through nonlinear optical absorption. Recently, we have developed a technique which has enabled rapid fabrication of high-aspect-ratio micro- and/or nanofluidic structures in porous glass with various 3D configurations [1-3].

Figure 1(a) shows a passive microfluidic mixer composed of geometrically complex 3D microchannels. The superior mixing efficiency of the 3D mixer has been confirmed by our numerical as well as experimental results, as evidenced by Figs. 1(b) and 1(c), respectively. Figure 1(d) schematically illustrates an integrated micro-nanofluidic structure which contains an array of nanochannels connected to two microfluidic channels. The transverse width of the nanochannels is only ~40 nm, as shown in Fig. 1(e). Creation of such nanochannels extraordinarily narrower than the laser wavelength is associated with in-volume nanograting formed by irradiating linearly polarized femtosecond laser pulses in dielectric materials. Figure 1(f) shows that the fluorescently stained λ-DNA molecules can be effectively stretched in the nanochannels.

To understand the mechanism of formation of nanochannel as well as in-volume nanograting which is also yet an ununderstood phenomenon [4], the porous glass is a superior material, since it can record the evolution of the nanograting in a 3D volume. Based on the high-fidelity snapshots obtained during the nanograting formation, we suggest that excitation of plasma waves at the interface between the areas modified and unmodified by femtosecond laser irradiation is responsible for the formation of initial periodic nanovoids, which further develop into nanogratings by local field enhancement [5].

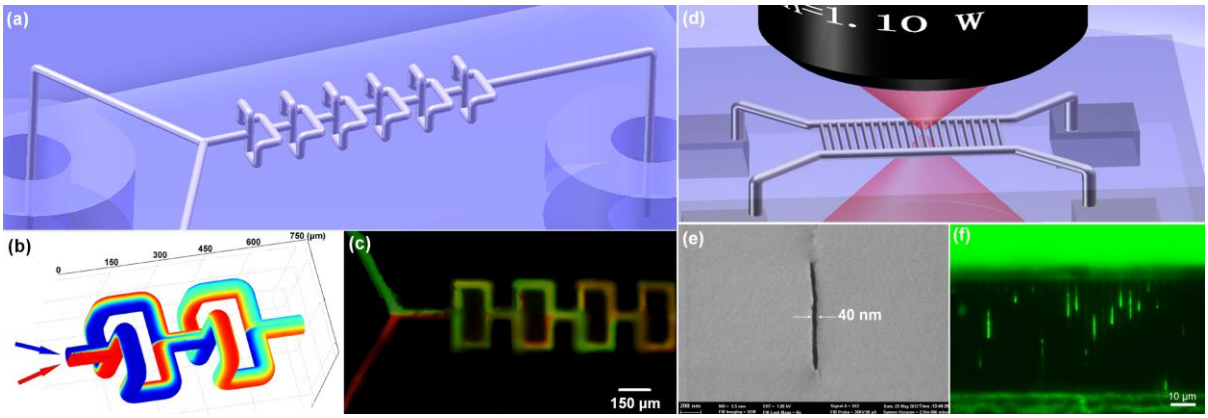

Fig. 1 (a) Schematic of the passive microfluidic mixer; (b) Numerical simulation of mixing result; (c) Fluorescence microscopy image of mixing experiment; (d) Schematic diagram of an array of nanochannels to bridge two microchannels; (e) Cross-sectional SEM micrograph of the nanochannel embedded in consolidated glass; (f) Fluorescent image showing the stretching of λ-DNA in an array of nanochannels.

References

[1] Y. Liao, Y. Ju, L. Zhang, F. He, Q. Zhang, Y. Shen, D. Chen, Y. Cheng, Z. Xu, K. Sugioka, and K. Midorikawa, "Three-dimensional microfluidic channel with arbitrary length and configuration fabricated inside glass by femtosecond laser direct writing," Opt. Lett. **35**, 3225 (2010).

[2] Y. Liao, J. Song, E. Li, Y. Luo, Y. Shen, D. Chen, Y. Cheng, Z. Xu, K. Sugioka, and K. Midorikawa, "Rapid prototyping of three - dimensional microfluidic mixers in glass by femtosecond laser direct writing," Lab Chip **12**, 746 (2012).

[3] Y. Liao, Y. Cheng, C. Liu, J. Song, F. He, Y. Shen, D. Chen, Z. Xu, Z. Fan, X. Wei, K. Sugioka, and K. Midorikawa, "Direct laser writing of sub-50 nm nanofluidic channels buried in glass for three - dimensional micronanofluidic integration," Lab Chip, **13**, 1626 (2013).

[4] Y. Liao, Y. Shen, L. Qiao, D. Chen, Y. Cheng, K. Sugioka, and K. Midorikawa, "Femtosecond laser nanostructuring in porous glass with sub-50 nm feature sizes," Opt. Lett. **38**, 187 (2013).

[5] Y. Liao, J. Ni, L. Qiao, M, Huang, Y. Bellouard, K. Sugioka, and Y. Cheng, "Plasma waves excited at interface by femtosecond laser irradiation enabling formation of volume nanograting in glass," arXiv:1411.2470 (2014)

O-60

Thin film compositional variations in three distinct pressure regimes during pulsed laser deposition

A. Ojeda-G-P[1], J. Chen[1], C. W. Schneider[1], M. Döbeli[2], A. Wokaun[1], T. Lippert[1]

[1] *General Energy Research Department, Paul Scherrer Institut, 5232 Villigen-PSI, Switzerland*

[2] *Ion Beam Physics, ETH Zurich, CH-8093 Zurich, Switzerland*

Corresponding Author e-mail address: thomas.lippert@psi.ch

Abstract

In pulsed laser deposition (PLD) the creation of thin films with complex stoichiometry from a bulk target with similar stoichiometry is presumably the main reason for its widespread application. However, the also widespread use of a background gas, either inert or oxidizing, has important effects in the final film composition as well as on its thickness [1]. Three distinct pressure regimes have been reported [2, 3]: a vacuum like regime, a transition regime in which plume splitting can be detected and a diffusion like regime at the highest deposition pressures. The exact pressure values at which such regimes take place have also been reported, but are not fixed as they depend on many process parameters, e.g. on the masses of the different elements (including the background gas), the laser fluence or the deposition temperature. Nevertheless it is fairly straightforward to identify in which regime the deposition is taking place by using e.g. an ion probe.

We investigate the influence of such regimes on the deposition of different multi-element targets ($BaTiO_3$, $CaTiO_3$, $LiMn_2O_4$ and $La_{0.4}Ca_{0.6}MnO_3$). These targets have been specifically selected based on their element mass ratios, as the masses of the participating elements are central in the transition from one regime to another [4]. A quantitative analysis of the composition at different angular locations and for different pressure regimes is performed. Furthermore, a semi-quantitative plasma analysis is also performed to gather insight into the chemical interactions with the background gas. In some targets ^{18}O isotope is used as a tracer to elucidate the origin of the metal oxygen species.

The first results show a consistent picture on how each pressure regime influences the film thickness, composition and angular distribution (Fig.1), and how these variations depend on the specific mass ratios of the target material. For example, getting a homogeneous thickness is challenging at low pressures, while at $1x10^{-1}$mbar a uniform thickness is achievable although the overall thickness is strongly decreased (Fig. 1a). In terms of composition, depositing films in the transition regime may not work ($1x10^{-2}$mbar Ar in this particular case) and can result in compositional variations of up to 15% for $BaTiO_3$ (Fig.1b). Additionally, the plasma analyses using ^{18}O as tracer show that the metal-oxygen ions (MO^+ and MO^-) are preferentially formed in the plasma through chemical interactions when using a background pressure of $1x10^{-3}$mbar or higher (Fig.1c), and that the oxygen background pressure is the most important source of oxygen for the as-grown thin films at $1x10^{-2}$mbar and above.

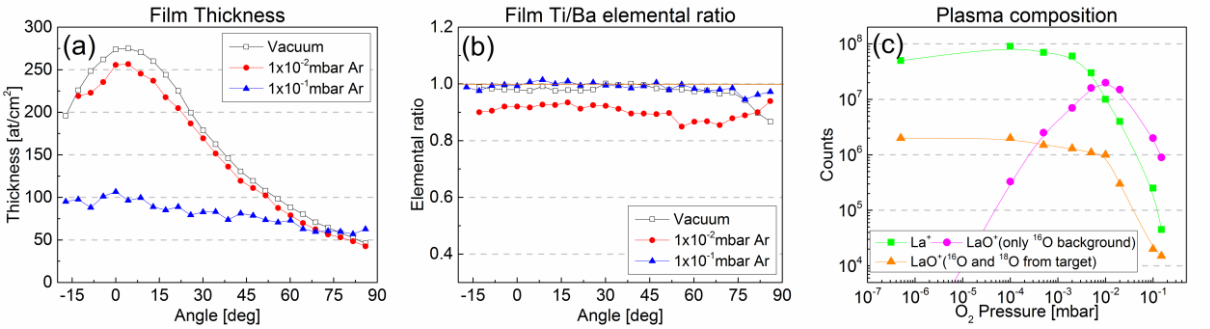

Fig. 1. Angle-resolved film thickness (a) and composition (b) for three argon background-gas pressures using a $BaTiO_3$ target (the compositions and thicknesses were obtained by RBS). The horizontal lines represent the target composition which was also verified by RBS. Compositional variations of the films of up to 15% are seen. (c) Detected amount of positive atomic La^+ and La oxygen species from the target and O_2 background vs. O_2 pressure

Despite the multitude of competing processes that may occur during the deposition and their specific element preference (i.e.: vaporization, diffusion, sputtering…) the goal of this research is to compile a list of simple rules to help the PLD user to optimize the experimental parameters during deposition of multi-element films.

References

[1] J. Schou," Physical aspects of the pulsed laser deposition technique: The stoichiometric transfer of material from target to film," Applied Surface Science, **255**, 5191-5198 (2009).

[2] S. Amoruso, B. Toftmann, J. Schou, "Thermalization of a UV laser ablation plume in a background gas: From a directed to a diffusion like flow," Physical Review E, **69**, 056403 (2004).

[3] Y. Pauleau, "Materials surface processing by directed energy techniques," Elsevier, 2006.

[4] T.E. Itina, W. Marine, M. Autric, "Monte Carlo simulation of pulsed laser ablation from two-component target into diluted ambient gas," Journal of Applied Physics, **82**, 3536-3542 (1997).

O-61

Laser-induced spalling of thin metal film from silica substrate followed by inflation of microbump

N.A. Inogamov[1,2], V.V. Zhakhovsky[2], and K.P. Migdal[2]

[1]*L. D. Landau Institute for Theoretical Physics, Russian Academy of Sciences, 1-A Semenova, 142432, Chernogolovka, Moscow region, Russian Federation*
[2]*All-Russia Research Institute of Automatics, ROSATOM, 22 Sushchevskaya, 127055, Moscow, Russian Federation*
E-mail address: nailinogamov@gmail.com

Dynamics of a gold film of 40-100 nm thick on a silica substrate triggered by fast heating with the use of a subpicosecond laser pulse is studied. After several picoseconds of electron-ion relaxation the pressure waves generated by such heating may result in spalling of the film and its flying away from the substrate after an acoustic time defined by the film thickness and speed of sound in metal, see Fig. 1. Intensity of the heating laser beam has the spatial Gaussian distribution in a cross-section. Therefore,the heating of film surface is nonuniform along cylindrical radius measured from the beam axis. As a result of such heating the velocity distribution in material flying away from the substrate has a maximum at the beam axis [1,2]. Thus, the separated film has dome-like shape which inflates with time. Volume of an empty cavity between the separated film and the substrate increases during inflation. Typical flight velocities are in the range of 30-200 m/s. The inflation stage can last from few to several tens of nanoseconds[1,2] if the diffraction-limited micron-sized laser beams are used [3,4].Capillary forces along the warped flying film decelerate the inflation of dome. There are three possible cases: (i) a low velocity film returns back to a substrate, (ii) a medium velocity film stops and freezes forming microbump [1-5], (iii) a high velocity film tears off from a substrate.Capillary deceleration of a bulging dome focuses mass flow along the dome shell in direction to its axis [1,2]. This results in formation of an axial jet and droplet like structures, see Fig. 1. Our new simulation results and comparisons with experiments are presented. They are important for laser induced forward transfer applications [3] and for nanoplasmonics devices [4]. Authors acknowledge Russian Science Foundation (Grant 14-19-01599).

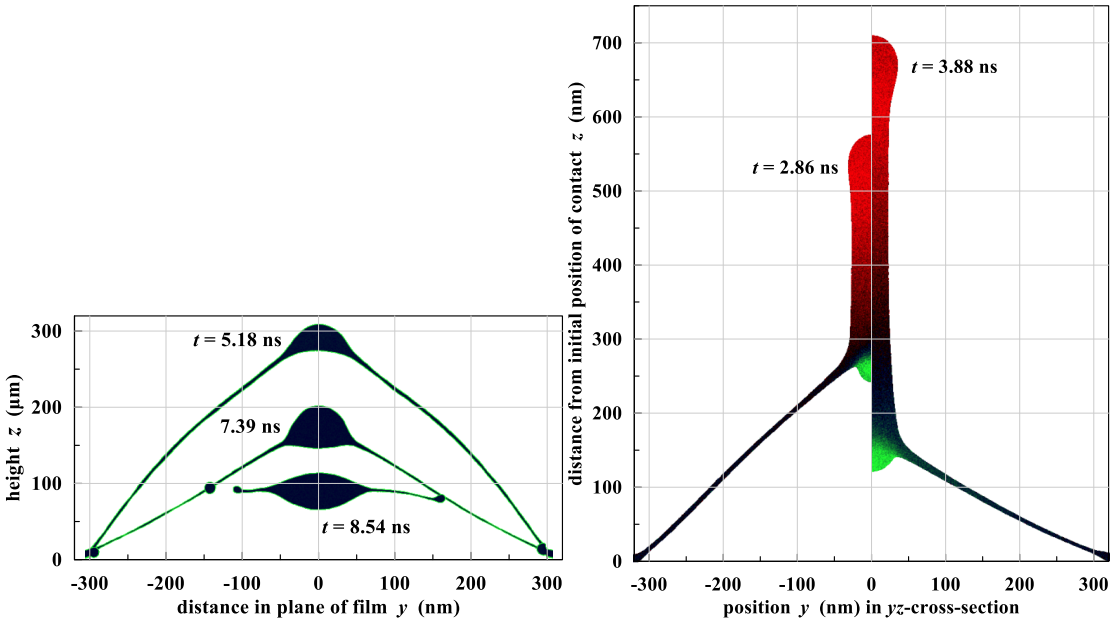

Fig. 1 (Left)MD simulated evolution of a dome after finishing of inflation. Expansion of the dome stops at t~5 ns and it begins to move back to substrate. Between t=7.39 and 8.54 ns the shell breaks and a central droplet flies toward the substrate [1]. Film remains attached to substrate outside of R=300 nm which is a radius of the dome floor. (Right) An instant of maximum inflation and an instant when the dome moves back are shown. While the green-colored shell moves down, the red-colored axial jet moves up.

[1] N.A. Inogamov and V.V. Zhakhovskii, "Formation of Nanojets and Nanodroplets by an Ultrashort Laser Pulse at Focusing in the Diffraction Limit," JETP Lett. **100**(1), 4-10 (2014).
[2] N.A. Inogamov, V.V. Zhakhovskii, and V.A. Khokhlov, "Jet Formation in Spallation of Metal Film from Substrate under Action of Femtosecond Laser Pulse," Journal of Experimental and Theoretical Physics (JETP) **120**(1), 15-48 (2015).
[3] A. Kuznetsov, J. Koch, B. Chichkov, "Nanostructuring of thin gold films by femtosecond lasers," Appl. Phys. A **94**, 221-230 (2009).
[4] M.A. Gubko, W. Husinsky, A.A. Ionin, S.I. Kudryashov, S.V. Makarov, C.R. Nathala, A.A. Rudenko, L.V. Seleznev, D.V. Sinitsyn, and I.V. Treshin, "Enhancement of ultrafast electron photoemission from metallic nanoantennas excited by a femtosecond laser pulse," Laser Phys. Lett. **11,** 065301 (2014).
[5] D.S. Ivanov, Zh. Lin, B. Rethfeld, G.M. O'Connor, T.J. Glynn, L.V. Zhigilei, "Nanocrystalline structure of nanobump generated by localized photoexcitation of metal film," J. Appl. Phys. **107**, 013519 (2010).

O-62

Tin oxide nanostructures prepared by laser ablation in water

T. Owashi[1], M. Honda[2], S. A. Kulinich[2], S. Iwamori[1]

[1]Department of mechanical engineering, Tokai University, Hiratsuka, Kanagawa, Japan
[2]Institute of innovative science and technology, Tokai University, Hiratsuka, Kanagawa, Japan
E-mail address: 4bmkm012@mail.tokai-u.jp

Tin oxide nanostructures have are widely used for a variety of applications, such as gas sensor materials, photocatalysts, transparent conductors, etc. [1-2]. Here, we fabricated tin oxide nanomaterials using laser ablation in liquid (LAL). Nanostructures with various sizes and shapes were prepared. Two types of Nd:YAG lasers (with ms and ns pulses and a wavelength of 1064 nm) were used. The pulse width and laser power were changed to control the product morphology. The products were characterized by transmission electron microscopy (TEM), X-ray photoelectron spectroscopy (XPS), X-ray diffraction (XRD), Raman spectroscopy, and UV-vis spectroscopy. Figures 1 (a,b) are TEM images of nanostructures prepared with ns- and ms- pulsed lasers. The particle shapes are seen in Figs.1 (a,b) to be cubic-like and spherical, respectively. In both cases, the particle size was not strongly affected by the pulse energy.

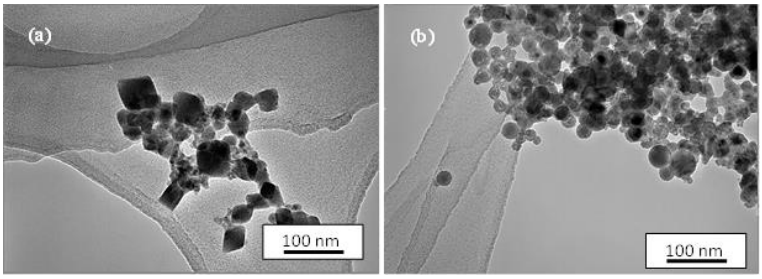

Fig. 1. TEM images of tin oxide nanostructures prepared by LAL with pulse width of (a) 7-9 ns and (b) 1.0 ms.

Figure 2 compares XPS spectra of samples prepared using ns- and ms-pulsed lasers, panels (a) and (b) presenting O1s and Sn3d5 peaks, respectively. The chemical composition of the nanoparticles prepared by means of ns-long pulses is close to SnO_2. Their surface was found to be slightly hydroxylated. Meanwhile, metallic Sn, along with tin oxide and hydroxide, was detected in the particles prepared by means of ms-pulsed laser. With increasing laser power, the fraction of tin oxide in products was found to increase.

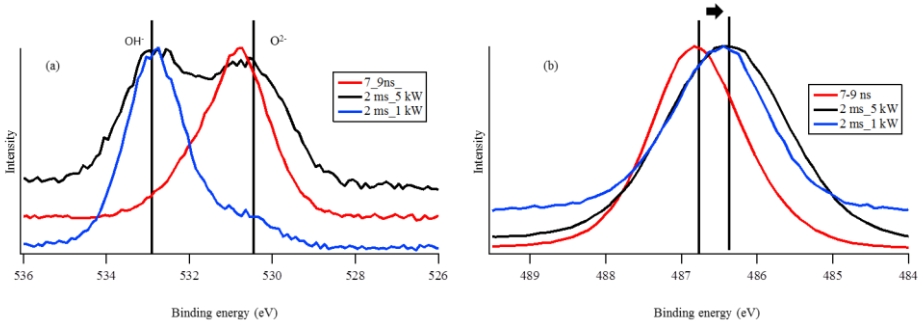

Fig. 2. XPS spectra of tin oxide nanostructures: (a) O1s (b) Sn3d5 peaks.

The Raman spectra (not shown here) of the products prepared by ns-pulsed laser confirmed different oxidation states, assuming coexistence of (SnO and SnO_2). The Raman spectra of the samples prepared by ms-pulsed laser were shown to be power dependent, suggesting the core-shell structure of the particles (with metallic core and oxide shell). We concluded that tinoxide nanocubes and metallic tin nanospheres with oxide coating were generated by ns- and ms-pulsed laser ablation, respectively. Raman spectroscopy revealed different oxidation states in tin oxide nanocubes. Using ms-pulsed laser, the thickness of oxidized layer increased with increasing the laser power in ablation.

References

[1] M. Batzill, U. Diebold, "**T**he surface and materials science of tin oxide," *Progress in Surface Science* 79, 47–154, (2005).
[2] Y.F. Sun, et al., Metal oxide nanostructures and their gas sensing properties: A review, *Sensors*, 12, 2610-2631, (2012).

O-63

Ultrashort pulsed laser ablation threshold dependence on incident wavelength in monocrystalline silicon

Reece N. Oosterbeek[1,2], Owen Bodley[1,2], Simon Ashforth[1,2,3], M. Cather Simpson[1,2,3,4*]

[1] *The Photon Factory, The University of Auckland, Auckland, New Zealand*

[2] *The MacDiarmid Institute for Advanced Materials and Nanotechnology and The Dodd Walls Centre for Quantum and Photonic Technologies, New Zealand*

[3] *Department of Physics, The University of Auckland, Auckland, New Zealand*

[4] *School of Chemical Sciences, The University of Auckland, Auckland, New Zealand*

** Corresponding author email: c.simpson@auckland.ac.nz*

Ultrashort pulsed laser micromachining is an advanced materials processing technique that allows "cold cutting" of almost any material [1]. This is especially of interest in the semiconductor industry, where mechanical cutting of wafers generates large amounts of waste – both in terms of the expensive blades and high purity silicon. Consequently, applying laser micromachining in this area has significant potential for increasing the efficiency and flexibility of semiconductor manufacturing. These industries have already adopted nanosecond pulsed micromachining for certain applications, however this technology is unsuited to silicon dicing due to the large heat affected zone [1]. Ultrashort pulsed laser micromachining avoids this problem, but faces limitations due to slow processing speeds – it is currently too slow to be realistically used in most industrial processes. By tailoring incident femtosecond pulse parameters like wavelength, we hypothesise that femtosecond laser micromachining speed can be increased.

The commonly used metric for evaluation of laser micromachining is the ablation threshold - the energy density required to cause material ablation. In this study, the effect of incident laser wavelength on the ablation threshold of silicon was investigated. Laser ablation was carried out using a Ti:Sapphire pumped optical parametric amplifier (TOPAS-C) producing femtosecond pulses (τ = 110fs, repetition rate = 1 kHz) with wavelengths ranging from 400 nm – 1200 nm. Ablation thresholds were measured using the diagonal scan technique [2, 3], that allows fast and accurate measurement of ablation thresholds and incubation effects. The samples used for ablation testing were monocrystalline silicon, both undoped and with a range of known doping levels.

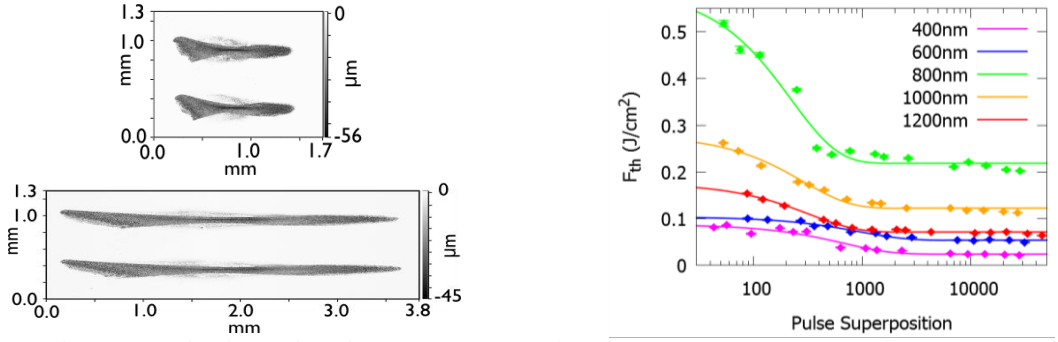

Fig.1. (Left) Examples of surface profiles of diagonal scan ablation features. (Right) Ablation thresholds of undoped silicon at 400 – 1200nm.

Ablation thresholds and incubation effects were measured at a range of wavelengths, with some examples shown in Fig. 1. Significant incubation effects are seen, which fit well to the defect accumulation model seen in Eqn. 1. [4]. Ablation threshold variation with incident wavelength was examined using the incubation curve parameters ($F_{th,1}$ and $F_{th,\infty}$) from Eqn. 1.

$$F_{th,N} = F_{th,\infty} + \left(F_{th,1} - F_{th,\infty}\right).e^{-k(N-1)}$$

The variation in ablation threshold with incident wavelength was compared to calculated values from the Keldysh photoionisation model to explain the trends observed.

References

1. Krüger, J. and W. Kautek, "Ultrashort Pulse Laser Interaction with Dielectrics and Polymers, in Polymers and Light", T.K. Lippert, Editor, Springer Berlin Heidelberg. 247-290.(2004)
2. Samad, R.E. and N.D. Vieira, Jr., "Geometrical method for determining the surface damage threshold for femtosecond laser pulses." Laser Physics, **16** 336-339. (2006)
3. Samad, R.E., et al. "D-Scan Measurement of the Ablation Threshold and Incubation Parameter of Optical Materials in the Ultrafast Regime." in Latin America Optics and Photonics Conference. 2012. Sao Sebastiao: Optical Society of America.(2012)
4. Ashkenasi, D., et al., "Surface damage threshold and structuring of dielectrics using femtosecond laser pulses: the role of incubation." Applied Surface Science, **150** 101-106. (1999)

O-64

Influence of Plume Parameters on Properties of Nanocrystalline ZnO Films Obtained by Pulsed Laser Deposition

E. Zamburg, O. Ageev, I. Shipulin, A. Shumov, M. Ivonin
Southern Federal University, Institute of Nanotechnology, Electronics and Electronic Equipment Engineering,
2 Shevchenko st., Taganrog, 347900, Russia
E-mail: zamburg.evgeniy@gmail.com

Nowadays nanocrystalline ZnO thin films, manufactured by pulsed laser deposition (PLD) method, are used extensively [1]. The fact that properties of ZnO thin films significantly depend on deposition conditions allows using them in various nanoelectronic devices. For instance, ZnO thin films with fractal structure and high resistance are necessary for manufacturing of sorption gas sensors. ZnO thin films with different type of conductivity and with high concentration and mobility of charge carriers are applied as transparent conductive coatings, functional layers of nanoelectronic diode and transistor structures, spintronic and piezoelectric devices [1–4].

Theory of laser ablation implies the impact of a laser beam on the surface of monatomic materials. However, laser ablation is a high temperature process, and it's natural to expect that during the impact of laser beam on complex composition target, dissociation of the molecules of the target material is possible. So, the structure, composition and properties of thin films manufactured by PLD may differ from the structure, composition and properties of the target material. Nevertheless, conservation stoichiometry hasn't received enough attention in the literature, as there is a widespread opinion that in case of laser beam impact on complex composition target, incongruence effect of evaporation does not have enough time to show itself.

The purpose of the paper is to conduct theoretical and experimental studies of the influence of the parameters of the laser plume during laser ablation on the properties of nanocrystalline ZnO thin films.

Based on thermal ablation theory it was shown that the temperature of ablation surface is very high, about 7000 ºC. Therefore, it's possible to assume that ZnO molecules will dissociate affect the composition and properties of the films. Using the gas-dynamic theory of laser ablation made it possible to obtain the ratio for assessing key parameters of plume: temperature of plume, pressure, and concentration of particles.

It was established, that the parameters of plume at different target-substrate distances influence the composition and properties of ZnO thin films. With the target-substrate distance less than 54 mm, the temperature in plume is higher than the dissociation temperature of ZnO (Fig. 1), resulting in the ZnO dissociation. With the target-substrate distance higher than 57 mm the temperature in plume is lower than the dissociation temperature of ZnO, resulting in the formation of thermal conditions conducive to condensation processes and reverse chemical reactions.

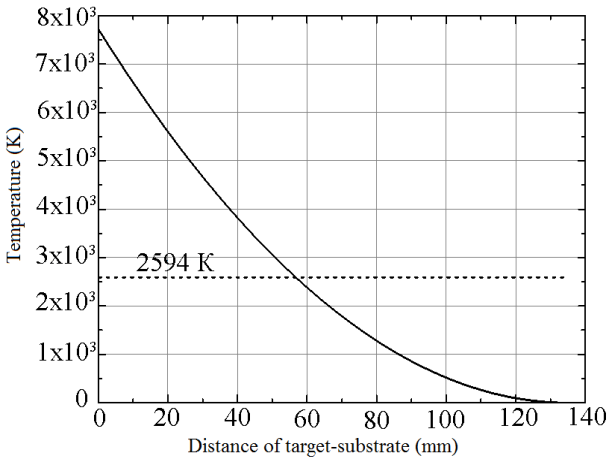

Fig. 1. Influence of target-substrate distance on plume temperature

The dependencies of plume temperature, concentration and pressure of particle on target-substrate distance were established. The results show influence of the parameters of plume on properties of nanocrystalline ZnO thin films. Analytical relations determining the thermodynamic state of the laser plume applied to the laser ablation as a method of technology nanocrystalline materials for nanoelectronic device structures were also established.

[1] H.Morkoc, U. Ozgur. *Zinc Oxide Fundamentals, Materials and Device Technology*, (Wiley-VCH Verlag GmbH & Co., Weinheim, 2009).
[2] E.G. Zamburg, O.A. Ageev, D.A. Golosov, A.M. Alexeev, D.E. Vakulov, Z.E. Vakulov, A.V. Shumov, and M.N. Ivonin, "Researching Influence of IBAD PLD Parameters on Properties of Nanocrystalline ZnO Thin Films", Appl. Mech. Mater. **481**, 55 (2014).
[3] E.G. Zamburg, O.A. Ageev, E.Y. Gusev, D.E. Vakulov, Z.E. Vakulov, A.V. Shumov, and M.N. Ivonin, "Nanocrystalline ZnO Films Grown by PLD for NO_2 and NH_3 Sensor", Appl. Mech. Mater. **475-476**, 446 (2014).
[4] A. P. Dostanko, O. A. Ageev, D. A. Golosov, S. M. Zavadski, E. G. Zamburg, D. E. Vakulov, and Z. E. Vakulov, "Electrical and Optical Properties of Zinc Oxide Films Deposited by the IonBeam Sputtering of an Oxide Target", Semiconductors. **48**, No. 9, 1242 (2014).

I-14

Dynamics of nanostructure formation on metal surfaces induced by ultrashort laser irradiation

J.-P. Colombier[1], E. Bévillon[1], H. Zhang[1], C. Li[1,2], X. Sedao[1], C. Maurice[3], S. Reynaud[1], F. Garrelie[1], R. Stoian[1], F. Pigeon[1]

1) Université de Lyon, F-42023, France, CNRS, UMR5516, Laboratoire Hubert Curien, Université Jean Monnet, 42000 St-Etienne, France
2) State Key Laboratory of Transient Optics and Photonics, Xian Institute of Optics and Precision Mechanics, CAS, 710119 Xian, Shaanxi, China
3) Ecole Nationale Supérieure des Mines de Saint-Etienne, Laboratoire Georges Friedel, CNRS, UMR5307, 42023 St-Etienne, France
E-mail: jean.philippe.colombier@univ-st-etienne.fr

Often under ultrafast laser excitation, structuring of materials on submicron scales occurs via characteristic nanoscale periodic self-arrangement of matter on irradiated surfaces. Nanostructured features are strongly influenced by inhomogeneous light coupling on the local crystal orientation, the nascent topology and the complex material response as the surface material undergoes conditions of extreme nonequilibrium for several picoseconds. In that context, understanding the nature of spatial localization of the absorbed energy requires the knowledge of the transient variation of optical response during irradiation. To provide insights into the dynamics of optical response of a metallic surface, pump-probe ellipsometric measurements and *ab initio* calculations of transport properties have been coupled, shining a new light on the recurring problem of yet unknown optical coupling during Laser-Induced Periodic Surface Structure (LIPSS) formation under ultrashort excitation. Calculations are carried out in the framework of the density functional theory associated to quantum molecular dynamics. The approach allows elucidating the influence of carrier nonequilibrium on optical properties. Simulation of the 3D energy deposition profiles on excited materials based on Finite Difference Time Domain method is then performed to depict the laser pulse interaction with an initially random distributed rough surface, revealing a competition between several periodic energy deposition patterns where light flux can be channeled depending on the nonequilibrium optical properties. Following such localized photoexcitation arrangements, the sub-surface region undergoes phase transformation and thermo-mechanical change at the nanoscale, depending on the surface crystal orientation. Dedicated electron backscatter diffraction experiments reveal that lattice defects are distributed inhomogeneously in the LIPSS profiles and the subsurface region, indicating that LIPSS formation is one of the different relaxation ways. A specific focus involving complex laser excitation mechanisms will be made to the interpretation of this inhomogeneous surface response.

O-65

Interfacial mechanisms and potential applications of novel laser ablated $L1_0$-based nanocomposite magnets

O. Crisan, A.D. Crisan, F. Vasiliu, I. Mercioniu
National Institute for Materials Physics, PO Box MG-7, 077125, Magurele, Romania
Corresponding Author e-mail address: ocrisan@infim.ro

1. Abstract

The present work deals with the characterization and evidences novel phenomena in laser ablated rare-earth (RE) free nanocomposite magnets derived from the FePt and MnAl binary alloy system. Compared with either Nd-Fe-B or Sm-Co permanent magnets (PM), these PM exhibit superior corrosion resistance and can operate at significant higher temperatures due to their higher Curie point. The promising FePt and MnAl systems can provide nanocomposite magnets with good magnetic properties, especially in the high temperature and corrosion-resistant applications. The hard magnetic $L1_0$ FePt phase has high coercivity, high magnetocrystalline anisotropy and its Curie temperature is around 500ºC. Equiatomic FePt is usually first obtained in its soft magnetic A1 fcc structure and until recently, high temperature annealing (600ºC) was thought that is needed in order to promote formation of the hard magnetic ordered $L1_0$ phase. Our group has proven that it is even possible to achieve the hard magnetic phase without post-synthesis annealing. A major step forward is related to the addition of Mn. It has been shown that FeMnPt promotes easier than FePt the $L1_0$ hard magnetic phase. On the other hand MnAl system also exhibit formation of hard magnetic $L1_0$ phase via a two-step reaction process during annealing of as-cast samples. In this work, FeMnPt, and also binary MnAl and ternary FeMnAl are to be studied. These alloys are obtained in form of melt spun ribbons by rapid solidification (RS). Magnetic investigations hint to a possible AFM/FM magnetic transition in FeMnPt, induced by the laser ablation treatment, a transition that has not been reported before in granular alloys. The interplay of structure and magnetic properties is most finely characterized using transmission electron microscopy (TEM), synchrotron XRD, magnetic measurements and neutron diffraction studies.

Acknowledgements

This work was supported by the Swiss Enlargement Contribution in the framework of the Romanian-Swiss Research Programme through contract 142256 / 6 / 2012, financing agencies SNSF – Switzerland and UEFISCDI - Romania.

O-66

The influence of cavitation bubble dynamics and laser fluence on mean particle diameter in laser ablation of metal targets in liquids

Daniel M. Bubb, Sean M. O'Malley, John Tomko, J. J. Naddeo, and Richard Jimenez

Rutgers University – Camden, Camden, NJ 08102, USA
Corresponding Author e-mail address: danny.bubb@rutgers.edu

Recent work in the field of laser ablation of metal targets in liquids has focused on the role of the cavitation bubble dynamics in the formation of nanoparticles [1-3]. Generally, it has been found that bubble generation and collapse plays a strong role in the ejection mechanism for this process [3]. The primary tool for studying the bubble dynamics is the Rayleigh-Plesset Equation [2]:

$$\frac{P_B(t) - P(t)}{\rho_L} = R(t)\frac{d^2R(t)}{dt^2} + \frac{3}{2}[\frac{dR(t)}{dt}]^2 + \frac{4\nu}{R(t)}\frac{dR(t)}{dt} + \frac{2S}{\rho_L R(t)} \qquad (1)$$

Through plume shadowgraphy measurements as shown in **Fig. 1**, we have determined the cavitation bubble radius as a function of time and correlated it with the ablation yield. Our results are typically consistent with what others have seen [2], except for the fact that we obtain a better fit to the unmodified Rayleigh-Plesset equation. These differences may arise from our use of a *ps* laser as opposed to the *ns* lasers used in other studies, and this is an area of active interest for us.

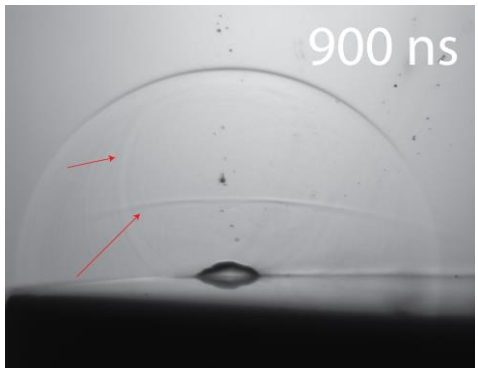

Figure 1 – Image of shockwave showing nascent formation of cavitation bubble

In order to elucidate the influence of cavitation bubbles on the resulting nanoparticle dispersions, we have measured the average particle diameter and used the fitting routine given by Amendola [] which assumes a log-normal distribution for the particles. We find that the particles that are produced by this process do not have a strong size dependence on bubble diameter. These results are interpreted within the latest computational work given by Itina et al [5], and the implications for the mechanism are discussed.

References

[1] Tsuji et al, Preparation of silver nanoparticles by laser ablation in polyvinylpyrrolidone solutions, Applied Surface Science **254**, 5224-5230 (2008).

[2] Soliman et al, Modification of Rayleigh--Plesset Theory for Reproducing Dynamics of Cavitation Bubbles in Liquid-Phase Laser Ablation, J. Journal Applied Physics **49**, 116202 (2010).

[3] Wagener et al., Dynamics of silver nanoparticle formation and agglomeration inside the cavitation bubble after pulsed laser ablation in liquid, Phys. Chem, Chem. Phys. **15**, 3068-3074 (2013).

[4] Povarnitsyn et al., Hydrodynamic modeling of femtosecond laser ablation of metals in vacuum and in liquid, Applied Physics A **117** 175-178 (2014).

[5] V. Amendola et al, Size Evaluation of Gold Nanoparticles by UV-Vis Spectroscopy, J. Phys. Chem. C **113**, 4277-4285 (2009).

O-67

Synthesis of Mg-doped ZnO microspheres by laser ablation in air and their crystal and photoluminescence properties

T. Tanaka[1], F. Nagasaki[1], T. Shimogaki[1] M. Higashihata[1], D. Nakamura[1], H. Ikenoue[1], and T. Okada[1]

[1]Graduate school of information science and electrical engineering, Kyushu University, 744 Motooka, Nishi-ku, Fukuoka 819-0395, Japan

ttanaka@laserlab.ees.kyushu-u.ac.jp

1. Introduction

Zinc oxide (ZnO) has a direct wide band-gap of 3.37 eV and a large exciton binding energy of 60 meV, which is much larger than that of gallium nitride (28 meV) and the thermal energy at room temperature (26 meV). Therefore, ZnO is an excellent candidate material for ultraviolet (UV) emitting devices such as UV light emitting diodes and UV lasers. In addition, ZnO nano/microstructures have attracted considerable attention because of their high crystalline quality and unique structures such as ZnO nanowire[1] and ZnO nanowall[2]. We have succeeded in synthesizing micro-spherical ZnO crystals by a simple laser ablation method in air[3]. In this method, ZnO microspheres are produced by rapid cool down of ZnO droplets generated by laser ablation and crystallization into spherical shape by the surface tension. Thus, it is expected that this synthesizing method may accelerate the doping of impurities in ZnO microspheres. In this study, we succeeded in synthesizing Mg-doped ZnO microsphere using a ZnO sintered target containing of MgO, which is one of the prospective materials due to the large band-gap (7.30 eV) and an ability to increase the band-gap of the ZnO[4]. Interestingly, synthesized Mg-doped ZnO microspheres showed lasing properties with a whispering-gallery-mode (WGM) lasing by optical pumping, and the lasing peaks were blue-shifted compered with a non-doped ZnO microsphere. In this contribution, we report crystalline and emission characteristics of optically-pumped single Mg-doped ZnO microsphere.

2. Fabrication of Mg-doped ZnO microspheres

Mg-doped ZnO microspheres were synthesized by ablating a ZnO sintered target which contains MgO (5 Wt%) using Nd:YAG laser (λ = 1064 nm) in the air. Figure 1(a) shows the SEM image of the Mg-doped ZnO microsphere. Figure 1(b) shows the micro-Raman spectrum of the Mg-doped ZnO microsphere, which indicates that the synthesized Mg-doped ZnO microsphere has a wurtzite-structure.

3. Lasing characteristics Mg-doped ZnO microspheres

The microspheres on a Si substrate was excited by the third harmonics of a Q-switched Nd:YAG laser (355 nm, 5 ns), and the emission from single microsphere was measured by the microscopic-spectroscopy system. Figure 1(c) shows the emission spectra from the Mg-doped and non-doped ZnO microspheres. The non-doped microsphere shows the WGM lasing in 394 nm UV region, which corresponds to the near band edge emission in ZnO, and modal peaks were observed. The mode spacing corresponds to the WGM theory. On the other hand, the spectrum of the Mg-doped microsphere was observed at shorter wavelength region compared with that of non-doped one, indicating an enlargement of the band-gap. Thus, we achieved 374 nm UV emission form the Mg-doped microsphere synthesized by simple laser ablation in air, and demonstrated a novel and simple doping technique in ZnO microsphere fabrication.

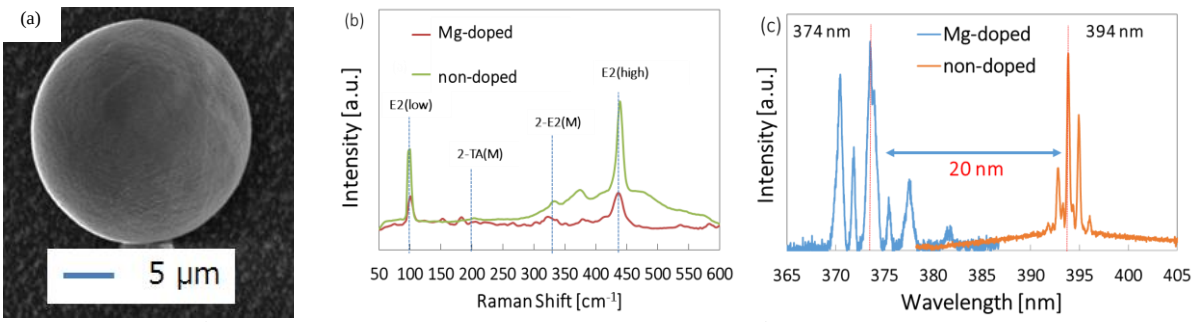

Fig. 1 (a) SEM image of the Mg-doped ZnO microsphere, (b) the micro-Raman spectra of the Mg-doped ZnO microsphere and non-doped ZnO microsphere, and (c) lasing spectra of Mg-doped ZnO microsphere and non-doped ZnO microsphere photoexcited by Nd:YAG laser (λ = 355 nm).

References

[1] Y. Li, G. W. Meng, L. D. Zhang, and F. Phillipp, "Ordered semiconductor ZnO nanowire arrays and their photoluminescence properties," Appl. Phys. Lett., vol. 76, no. 15, p. 2011, 2000.

[2] S.-W. Kim, H.-K. Park, M.-S. Yi, N.-M. Park, J.-H. Park, S.-H. Kim, S.-L. Maeng, C.-J. Choi, and S.-E. Moon, "Epitaxial growth of ZnO nanowall networks on GaN/sapphire substrates," Appl. Phys. Lett., vol. 90, no. 3, p. 033107, 2007.

[3] K. Okazaki, T. Shimogaki, K. Fusazaki, M. Higashihata, D. Nakamura, N. Koshizaki, and T. Okada, "Ultraviolet whispering-gallery-mode lasing in ZnO micro/nano sphere crystal," Appl. Phys. Lett., vol. 101, no. 21, p. 211105, 2012.

[4] W. Q. Peng, S. C. Qu, G. W. Cong, and Z. G. Wang, "Synthesis and temperature-dependent near-band-edge emission of chain-like Mg-doped ZnO nanoparticles," Appl. Phys. Lett., vol. 88, no. 10, p. 101902, 2006.

O-68

Molecular Dynamics Simulations of Laser Ablation of Al-Ni alloys and Al-Ni layer systems

D. Rapp, A. Kiselev, H.-R. Trebin, J. Roth
Institut für Funktionelle Materie und Quantentechnologien, University of Stuttgart, Pfaffenwaldring 57, 70550 Stuttgart, Germany
Email: johannes.roth@fmq.uni-stuttgart.de

1. Introduction: Simulation method, interaction, and parameters

We have studied laser ablation of Al-Ni alloys using molecular dynamics simulations (MD) [1] combined with the two-temperature model (TTM) [2] for the modeling of the electronic contribution to the ablation process.

Several obstacles had to be overcome: the combined MD+TTM program had to be extended to cope with alloys, embedded atom (EAM) interactions had to be tested for the Al-Ni alloys and compared with the experiment with respect to the reproduction of the correct crystal phases and melting temperatures.

The main challenge, however, was the generalization of the two-temperature model to alloys and the determination of the parameters electronic heat capacity, electronic heat conductivity and the electron-phonon-coupling. Several parameters were neither available from experiment nor from ab-initio-calculations and so reasonable averaging procedures had to be found and applied to calculate the parameter values from the data known for neighboring phases.

2. Validation

To test our model we have first simulated the pure metals Al and Ni and reproduced the known simulation results of melting and ablation depth and compared them to hydrodynamical simulations and experiment.

3. Results: Alloys

Next we have studied the alloys bcc-AlNi, fcc-$AlNi_3$, and oP-Al_3Ni. For AlNi we obtained melting depths and an ablation threshold of about 500 J/m^2, no data from experiment have been available. For $AlNi_3$ the ablation threshold is in the range of 400 to 700 J/m^2. In experiments the ablation threshold is considerably higher. But the experiments [3] were not carried out in vacuum and the absorption depth was not given. For Al_3Ni we find ablation thresholds of about 400 J/m^2. Here we observe a phase transition at high fluences to a $L1_2$ phase which is known from the determination of the EAM potential [4]. The melting threshold was 50 to 100 J/m^2 lower than the ablation threshold except for Al_3Ni, where it is considerably lower (about 30 J/m^2). The reason is again the concurrent phase transition.

4. Results: Layers

Finally we have simulated Al layers on Ni substrates. If the Al layer is thin (8 nm), it melts at 40 J/m^2 already while the threshold for the Ni substrate is 250 J/m^2. The Al layer is ablated as a whole at about 480 J/m^2. A thicker Al layer (24 nm) absorbs a lot of laser energy and the Ni substrate melts through heat conduction. Thus the threshold for melting of Ni is 100 J/m^2 higher than in the previous case. At fluences low above the ablation threshold the Al layer is ablated as a whole as before, but at higher fluence (above 900 J/m^2) the ablation depth is reduced and a part of the Al layer is left behind. The explanation is that the largest part of the Al layer vaporizes immediately and thus cools the rest of the sample.

In the case of the thick Al layer AlNi mixtures form at the interface between the two metals. It can be seen that they are molten on the front side and crystalline on the back side with a disordered fcc-AlNi structure.

[1] The simulation program IMD is available from: http://itapmd.github.io/imd/
[2] S.I. Anisimov, B.L. Kapeliovich and T.L. Perel'man, “Electron emission from metal surfaces exposed to ultrashort laser pulses ”, Sov. Phys. JETP **39**, 375(1974).
[3] S. Ma, J.P. McDonald, B. Tryon, S.M. Yalisove, T.M. Pollock, “Femtosecond laser ablation regimes in a single-crystal superalloy”, Metall. Mater. Trans. A **38,** 2349 (2007).
[4] G.P. Purja Pun, Y. Mishin, “Development of an interatomic potential for the Ni-Al system“, Phil. Mag. **89,** 34 (2009).

O-69

Enhanced dielectric properties of Bismuth Zinc Niobate-Silver composite thin films prepared by pulsed laser deposition

P S Krishnaprasad, M K Jayaraj*
Department of Physics, Cochin University of Science and Technology, Kochi, Kerala 682 022
Email: mkj@cusat.ac.in

Abstract:

High k dielectrics has been extensively studied in the past few years for the applications such as gate oxide in thin film transistors, capacitor dielectrics, electrostrictive materials and tunable microwave devices. Dielectric materials like BST, PZT etc in their ferroelectric phase are commonly used for these applications because of their large inherent dielectric constant. But dielectric materials in its ferroelectric phase with its intrinsic hysteresis generally shows a high dielectric loss and they suffer from high leakage current. Rapid development in these area demands dielectric materials with large dielectric constant and tunability together with low dielectric loss. Paraelectric materials with a high dielectric constant and comparatively low dielectric loss are preferred for these type of applications. In the last few years various Bi based pyrochlore structures with general formula $A_2B_2O_7$ has attracted much scientific interest because of their reasonably high dielectric constant (80 to 200) low dielectric loss and large dielectric tunability. Dielectric - metal composite thin films have been found to improve the dielectric properties of the thin films. In the present study we have prepared Ag-$Bi_{1.5}Zn_1Nb_{1.5}O_7$ (Ag-BZN) composite thin film by pulsed laser deposition. As the volume fraction of metals in these composites increase, the dielectric constant and conductivity increase gradually and when the volume fraction of the conductive powder reaches a critical value, the conductivity as well as dielectric constant of the composite increase by several orders of magnitude. The dependence of temperature and oxygen partial pressure on the structural, optical, and electrical properties of the Ag-BZN thin films were studied. The surface morphology and composition were analyzed by AFM and EDX measurements. The dielectric measurements on the thin films were carried out using impedance analyser in the Metal-Insulator-Metal (MIM) structure with Pt as the bottom electrode and Ti/Au as the top electrode. It is found that with low silver content in the film, the dielectric constant of the films has been increased more than 60 times, the leakage current has been reduced by 4 orders, the tunability has been increased up to 80% and FOM factor has been increased by more than 10 times. It makes Ag-BZN composite thin films, a promising material for tunable device applications as well as high k dielectric capacitor applications.

Thursday
3 September 2015

Poster presentations

P-140

Microfabrication of UV transparent fluoric polymer CYTOP using a conventional pulsed green laser

O. Tatsuya[1] and Y. Hanada[1,2]

Hirosaki Univ., Graduate school of Science and Technology 3 Bunkyo-cho, Hirosaki, Aomori 0368561, Japan
RIKEN, 2-1 Hirosawa, Wako, Saitama 3510198, Japan
Corresponding Author e-mail address: y-hanada@hirosaki-u.ac.jp

We demonstrate microfabrication of UV transparent fluoric polymer CYTOP (Asahi glass Corp.) using a conventional pulsed green laser. A CYTOP has unique characteristics such as high transparency, chemical stability and low refractive index and is expected to overcome many problems which conventional transparent material has. For instance, CYTOP has more than 90% high transparency from ca. 200 nm in UV wavelength regions which is useful for thin film coating applications. Low refractive index helps clear microscopic observation in biochip applications. However, due to such unique characteristics, most fluoric polymers are, in general very difficult to microfabricate unless particle beams with high energy such as F_2 laser [1] or synchrotron radiation [2] is provided. For that reason, the fluoric polymer is not yet used for micro-industrial applications. Therefore, we developed crack-free surface microfabrication of CYTOP using a conventional ns pulsed green laser. At first, Nd:YAG laser (532 nm, 500 ps, 1 kHz) was irradiated on a CYTOP surface for ablation and then, fluoride solution was used to selectively etch the ablated regions. Figure 1 shows laser scanning microscopic (LSM) images of the CYTOP edge of the (a) ablated region and (b) wet etched region after ablation.

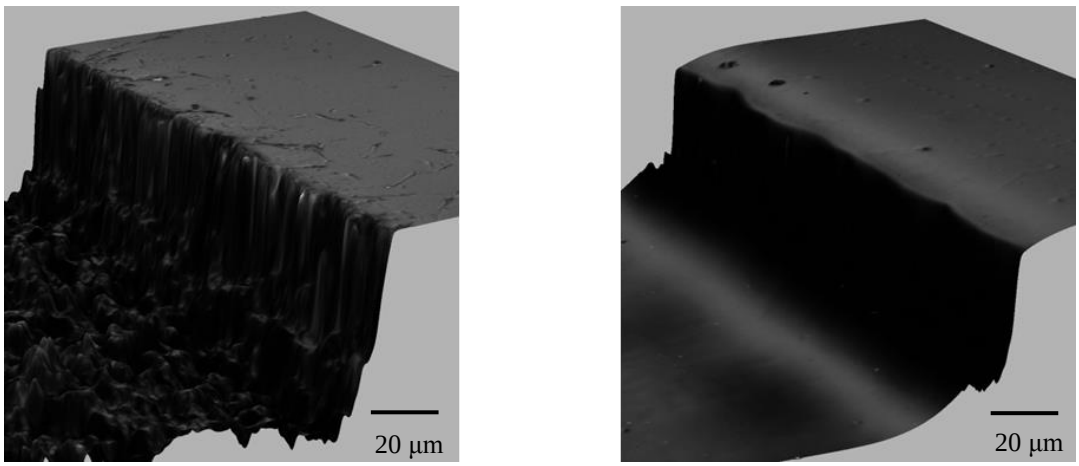

Fig. 1. LSM images of fabricated CYTOP using ns pulsed green laser. (a) after ablation and (b) after wet etching.

From Fig. 1(a), After the green laser ablation, molten regions were produced in the buttom and the edge of the ablated regions and some cracks were also shown at the edge. However, these rough areas were selectively etched after the wet etching as shown in Fig.1(b). In addition, rough surface induced by the ablation and wet etching can be improved by successive annealing ramping up to the glass transition temperature. In this paper, further investigation of the fundamental characteristics of CYTOP microfabrication using a conventional green laser was carried out.

References

1) K. Obata, K. Sugioka, N. Shimazawa, K. Midorikawa, "Fabrication of microchip based on UV transparent polymer for DNA electrophoresis by F_2 laser ablation," Appl. Phys. A, **84**, 251-255 (2006).

2) D. Yamaguchi, T. Katoh, Y. Sato, S. Ikeda, M. Hirose, Y. Aoki, M. Iida, A. Oshima, Y. Tabata, M. Washio, "Micromachining of Crosslinked PTFE by Direct Photo-Etching Using Synchrotron Radiation," Macromol. Symp., **181**, 201-211 (2002).

P-141

Low temperature micro-photoluminescence spectroscopy on laser doped silicon with different surface condition

Young-Joon Han, Evan Franklin, Andreas Fell, Marco Ernst, Hieu T. Nguyen, and Daniel Macdonald

Research School of Engineering, College of Engineering and Computer Science, The Australian National University, Canberra, ACT 0200, Australia
E-mail: young.han@anu.edu.au

Although there have been many studies on laser doping techniques and their applications, the fundamental impacts of the laser process and the resultant characteristics of the processed region are still not completely characterised and understood. In this paper we utilise low temperature micro-photoluminescence spectroscopy (μ-PLS) to investigate shallow layers of laser doped silicon, exploring the impacts of laser doping processes on electronic quality, and thus providing insights into the impacts on the underlying silicon crystal structure.

Micro-scale measurements (with resolution down to 3 μm) enable us to investigate effects of laser processing at specific positions such as boundary/edge of processed and unprocessed regions. In addition, low temperature PLS enables us to identify signals corresponding to laser induced defects or laser induced doping of silicon, which otherwise cannot be observed at room temperature. Samples were prepared with two different surface conditions, chemical mechanical polishing (CMP) and Tetramethyl Ammonium Hydroxide (TMAH) etching, to observe any effect of surface condition on laser doping process. Commercially available, boron-rich spin-on dopant was deposited on high-resistivity n-type float-zone crystalline silicon substrate as a dopant precursor. We employ a 248 nm nanosecond excimer laser, whose beam is homogeneous and rectangular, to melt a shallow layer, thus introducing dopants into the melt subsequent to recrystallisation. A variety of single or multiple repeat pulses is employed, using a range of fluences suitable for light to heavy doping. Neighbouring pulses are arranged such that clear 'overlap' boundaries are present as well as edges between doped and undoped regions. Figure 1 shows the resultant PLS signals, excited with 532nm laser at 79K, for three repeat pulses with fluence of about 4J/cm^2, measured at different positions on different wafer surface types.

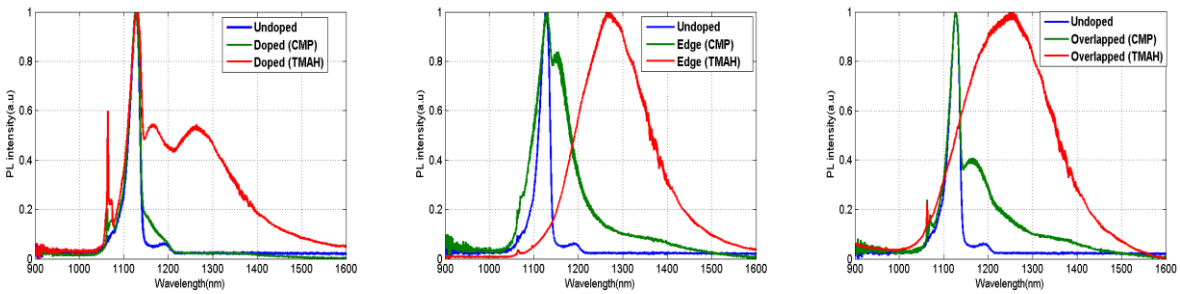

(a) (b) (c)

Fig. 1. Normalized PL spectra, excited with 532nm laser at 79K – (a) at the centre of the doped region, (b) at the edge, (c) at the overlapped on CMP substrate and TMAH etched substrate.

It was observed that for the undoped surfaces, indistinguishable PL signals are observed from CMP and TMAH samples. However, as shown in fig. 1, significantly different PL signals are observed after laser irradiation. Evidence of heavy doping on both samples is indicated by the local PLS peak at around 1160nm due to band gap narrowing effect of heavy doping, though with different peak heights observed due to different depth of doping. Longer wavelength PLS peaks correspond to the signature emissions from dislocation defects, with the well-known D3 dislocation peak observed around 1280 nm. The defect PLS signal on the CMP sample is barely observed at the middle of the doped region, but appears as a 'tail' for the measurements at the boundary regions. On the other hand, the TMAH sample gives dominantly high defects signal in the range of 1200~1500nm, albeit more pronounced again for boundary measurements. Moreover, silicon band-band peak (~1130nm) is buried under the defect signal at the edge due to significantly deep defects. These observations suggest that dislocation defects can be strongly associated with the recrystallization interface at the boundaries of laser-induced melt zones.

By utilizing μPLS, we observed fundamental characteristic of laser doped regions, in particular the presence of both doping and dislocation defects. Notably, different PLS signals at the middle and boundaries of laser doped regions highlights the significant role that the edges of laser doped pulses play in terms of electronic quality and recombination properties. Moreover, different surface conditions or substrate properties appear to affect significantly the impact of laser doping processes on crystal quality and presence of dislocation defects, with a considerably greater level of induced defects observed on initially rougher surfaces than on polished surfaces.

P-142

Prototype of Mini-size Er:YAG Laser Skin Perforator

T.H. Ha[1], S.M. Kim[1], C.W. Lee[1], J.H. Lee[1], Y.J. Kim[1], J.Y. Song[1], D.Y. Kim[2], Y.G. Kim[3]

[1]Korea Institute of Machinery & Materials, Daejeon 305-343, Republic of Korea

[2] GL, Changwon 641-824, Republic of Korea

[3] Jinyoung HNS, Changwon 641-921, Republic of Korea

E-mail: taehoha@kimm.re.kr

1. Introduction

Due to the high absorption of the 2.94 μm wavelength in water-containing tissues like skin [1], Er:YAG laser has the smaller depth of penetration into the skin tissue. Therefore, the laser skin perforators, which work like lancets for collecting capillary blood samples, reduce the patients' pain significantly. Although a large number of studies have been made on the development of Er:YAG laser perforators and the ablation of tissue [1-6], few can satisfy both portability and perforation stability. We have developed the mini-size laser skin perforator which runs by a battery. To our knowledgement, this is the world's smallest laser lancet. We examined the power stability and the performance of the developed device. Also, blood sampling tests from human fingers were carried out to ensure feasibility.

2. Materials and Methods

The major problem for the miniaturization of laser perforators is maintaining proper emitting energy and stability while downsizing the elements. We could reduce the volume down to the dimension of 45×125×25 mm^3 and still sustain output stability by improving both optical and electrical designs. The device mainly consists of a laser resonator, a focusing lens, a battery unit, and a controller unit. The single-pulse laser emission is used for skin poration. The output energy can be adjusted to five levels in order to provide proper ablation energy for each individual patient. Evaluation of the output stability was carried out by measuring Er:YAG laser energy. A band-pass filter was set in front of an energy meter sensor excluding unwanted light from a xenon lamp used for pumping. In order to eliminate the effect of temperature, measurements were conducted under constant temperature condition. The developed perforator showed good pulse-to-pulse stability. For example, the device emitted the average energy of 22.6 mJ per pulse with the standard deviation of 0.8 mJ.

3. Results

The burn paper tests for the different energy levels were performed for the instant and indirect device performance evaluation since heat is the main ablation source [2]. The holes on the thermal paper had oval shapes and the physical size of holes increased with rise in emitting energy. The size varies approximately 160 to 280 μm according to the energy increase. Relatively clean edges were observed for the higher energy output. Actual blood sampling from human fingers was successfully carried out satisfying the minimum blood amount of 0.5 μL for blood glucose tests. Although many conventional laser perforators have maximum output energy of 500 mJ, several tens of mJ appeared to be enough to draw blood using the developed laser perforator. However, the experiments were conducted with a limited number of time and people. The relationship to skin thickness has to be revealed in the future.

4. Discussion

To the best of our knowledge, the developed Er:YAG laser skin perforator is the world's smallest one. The output energy stability and burn paper test results ensured the feasibility of the developed device. Future studies will be required to ascertain the relationship between operating temperature of the perforator and output energy for a reliable blood sampling. Also, the pulse width optimization is needed to further confirm the effect of variable pulse width on skin perforation [3-5]. Furthermore, OCT (optical coherence tomography) observation of skin to measure the size of ablation craters should be performed to find correlation between burn paper test results and actual skin ablation performance.

[1] U. Hohenleutner, S. Hohenleutner, W. Baumler, and M. Landthaler, "Fast and Effective Skin Ablation With an Er:YAG Laser: Determination of Ablation Rates and Thermal Damage Zones," Laser in Surgery and Medicine **20**, 242-247 (1997)

[2] G. Muller, K. Dorschel, and H. Kar, "Biophysics of the Photoablation Process," Laser in Surgery and Medicine **6**, 241-254 (1991)

[3] R. Kaufmann, and R. Hibst, "Pulsed Erbium:YAG Laser Ablation in Cuataneous Surgery," Laser in Surgery and Medicine **19**, 324-330 (1996)

[4] J. T. Walsh, Jr., and T. F. Deutsch, "Er:YAG Laser Ablation of Tissue: Measurement of Ablation Rates," Laser in Surgery and Medicine **9**, 327-337 (1989)

[5] K. A. Khatri, "The effects of variable pulse width of Er:YAG laser on facial skin," Dermatologic surgery **27**, 332-334 (2001)

[6] J. Daici and B. Gaspirc, "Review: Comparison of Er:YAG and Er,Cr:YSGG lasers used in dentistry," Journal of the laser and heath academy **1**, 1-13 (2012)

P-143

Photodisruption of the elastic membrane with the laser-induced cavitation bubble dynamics: an optodynamic study

G. Hawlina[1], B. Drnovšek-Olup[1], J. Možina[2], P. Gregorčič*[2]

[1]*Eye Hospital, University Medical Centre Ljubljana, Grablovičeva 46, 1525 Ljubljana, Slovenia*

[2]*Faculty of Mechanical Engineering, University of Ljubljana, Aškerčeva 6, 1000 Ljubljana, Slovenia*

E-mail: peter.gregorcic@fs.uni-lj.si

Nd:YAG laser photodisruption with nanosecond laser pulses and energies of few millijoules is a well-established tool for intraocular surgery, such as treatment of posterior capsule opacification (PCO) or late-postoperative capsular bag distension syndrome (CBDS) [1]. The PCO and CBDS are post-operative complications of cataract surgery that affects the visual function. The PCO develops due to the lens epithelial cells remaining in the capsular bag after the cataract surgery [2]. Clinically, there are two basic morphological types of PCO, the fibrosis type and the pearl type, which have different cellular origins [3]. On the other hand, the visual function is affected by CBDS due to the accumulation of liquefied material in a closed space between the posterior capsule and the intraocular lens optic [4].

The most effective treatment for PCO and CBDS is a Nd:YAG laser capsulotomy, where the excitation pulse is focused just behind the posterior capsule (typically 100-200 μm). Here, a high-intensity laser pulse induces an optical breakdown resulting in a microexplosion initiated by plasma formation [5]. The plasma expansion is followed by different optodynamic phenomena, such as a shock wave and the cavitation bubble. When a cavitation bubble expands to its maximum volume, it starts to collapse due to the liquid pressure. Under suitable conditions [6, 7] the collapsing bubble develops a liquid jet responsible for the posterior capsule disruption. The procedure is repeated several times, e.g., in a cruciate pattern. In such a way, a central opening in the opacified posterior capsule clears the visual axis. On the other hand, the optodynamic phenomena are responsible also for unwanted collateral effects on many delicate structures which are located very close to the breakdown region.

The bubbles dynamics is determined by *(i)* the distance between the bubble's center and the boundary; and the *(ii)* boundary conditions. In the case of the laser capsulotomy, the boundary conditions depend on the PCO types - fibrosis, pearl or mixed type – which differ by the mechanical properties as well by the distance between the posterior capsule (a thin membrane) and the intraocular lens (a solid boundary). In our previous *in-vivo* study [1], we have shown that both, the PCO type and the distance between the intraocular lens and the posterior capsule significantly affect the total-pulse energy needed to perform the capsulotomy. Understanding of the physical mechanisms that are responsible for these effects is important, since lower total-pulse energy means fewer side effects. However, in our previous *in-vivo* study [1] we have found that an *ex-vitro* experiment under more reproducible and controllable conditions should be performed to clarify the main mechanisms that are responsible for the posterior capsule opening.

In this contribution we will use a high-speed shadowgraphy and a laser-beam-transmission probe [8] to study the laser-induced cavitation bubble dynamics near a solid boundary with a thin elastic membrane. As an excitation source we use a Nd:YAG laser with pulse duration of 6 ns and energy up to 12 mJ, designed for intraocular photodisruption. Our study includes the investigation of membrane and solid boundary photodisruption at different distances between the boundary and the membrane. In such a way we designed an *ex-vitro* model of an intraocular laser surgery, where the distance between the posterior capsule (a thin membrane) and an intraocular lens (a solid boundary) varies form few micrometers (as in the case of the fibrosis PCO type) to several hundreds of micrometers as in the case of CBDS [1]. On the other hand, the perforation of the membrane simulates the wanted effect of the posterior capsule opening, while the damages of the solid boundary represent the side effects that should be avoided during the laser capsulotomy.

[1] G. Hawlina, D. Perovšek, B. Drnovšek-Olup, J. Možina and P. Gregorčič, "Intraocular Photodisruption with Picosecond and Nanosecond Laser-Pulses - Tissue Effects in Cornea, Lens, and Retina" BMC Ophthalmology **14**, 131 (2014).

[2] E. J. Hollick, D. J. Spalton, P. G. Ursell, and M. V. Pande, "Lens epithelial cell regression on the posterior capsule with different intraocular lens materials" Brit. J. of Ophthalmol. **82**, 1182 (1998).

[3] D. J. Apple, K. D. Solomon, M. R. Tetz, E. I. Assia, E. Y. Holland, U. F. C. Legler, J. C. Tsai, V. E. Castaneda, J. P. Hoggatt, J. P., and A. M. P. Kostick, "Posterior Capsule Opacification" Surv Ophthalmol **37**, 73 (1992).

[4] K. Miyake, I. Ota, S. Ichihashi, S. Miyake, Y. Tanaka, and H. Terasaki, "New classification of capsular block syndrome" J. Cataract. Refr. Surg. **24**, 1230 (1998).

[5] A. Vogel, M. R. C. Capon, M. N. Asiyovogel, and R. Birngruber, "Intraocular Photodisruption with Picosecond and Nanosecond Laser-Pulses - Tissue Effects in Cornea, Lens, and Retina" Invest. Ophth. Vis. Sci. **35**, 3032 (1994).

[6] Y. Tomita, A. Shima, "Mechanisms of impulsive pressure generation and damage pit formation by bubble collapse" J. Fluid. Mech. **169**, 535 (1986).

[7] A. Vogel, W. Lauterborn, R. Timm, "Optical and acoustic investigations of the dynamics of laser-produced cavitation bubbles near a solid boundary" J. Fluid. Mech. **206**, 299 (1989).

[8] P. Gregorčič, M. Jamšek, M. Lukač, M. Jezeršek, "Synchronized delivery of Er:YAG-laser-pulse energy during oscillations of vapor bubbles, J. LA&HA **2014**, 14 (2014).

P-144

Blister-based nanosecond-laser-induced forward transfer of large molecules and nanoparticles for gas-phase analysis

A. V. Bulgakov[1], N. Goodfriend[2], N. M. Bulgakova[1], S. V. Starinskiy[1], Yu. G. Shukhov[1], O. Nerushev[2], E. E. B. Campbell[2]

[1]Kutateladze Institute of Thermophysics SB RAS, Lavrentyev ave. 1, Novosibirsk 630090, Russia
[5]EaStCHEM, School of Chemistry, University of Edinburgh, Edinburgh EH9 3FJ
E-mail: ngoodfriend@gmail.com

The detection and characterization of large organic molecules and isolated nanoparticles in the gas phase is an extremely challenging problem but of considerable importance for situations ranging from environmental monitoring to experiments that probe the foundations of physics. A number of analytical techniques, such as mass spectrometry and electron spectroscopy, require intact particles to be introduced into a region of high vacuum. Conventional laser-based methods of nanoparticle transfer like MAPLE, MALDI, and Laser-Induced Forward Transfer (LIFT) use a matrix as a solvent for the particles which is also transferred toward a detector that is often unacceptable for analytical purposes.

Recently, a new matrix-free modification of the LIFT technique for nanoparticle transfer without destruction of the supporting film was proposed [1,2]. In this method, the nanoparticles are spread over a metal film deposited on a transparent substrate and the interaction of a laser pulse with the metal-substrate interface causes, under certain conditions, transient blistering of the film, resulting in gentle transfer of the particles. The efficiency of the method to deliver nanoparticles for mass spectrometry analysis has been demonstrated [3]. In this work, we have performed a detailed study of the blister-based LIFT process to get insight into the mechanisms of particle transfer. As test species, we studied 150-nm-diam gold-coated silica nanoparticles and fullerene C_{60} molecules spread over thin metal films (titanium or nickel) deposited on glass. The films were back-irradiated by ns-laser pulses in high vacuum and transfer process was investigated using a combination of mass spectrometry, time-of-flight measurements, film deposition technique, atomic force microscopy of the irradiated substrates, and theoretical considerations of temperatures and stress in the irradiated film.

The most efficient blister-induced particle ejection is found to occur near, but below, the damage threshold of the film when its deformation is still elastic. The irradiated spot produced under such near-threshold conditions consists of two regions: a central zone completely clean of particles and an external zone where up to 85% of the particles are removed from the surface (Fig. 1). Such a spot structure is assumed to be due to transient melting of the central zone where Marangoni convection is developed. The average velocities of blister-ejected species are found to be ~ 50 m/s for silica nanoparticles and ~ 100 m/s for C_{60} molecules. The nanoparticle velocity distribution is fairly narrow while that of C_{60} is bimodal with a fast population (typical velocity ~ 300 m/s) originated due to thermal evaporation of the molecules. The mechanisms involved into the particle transfer process are discussed. The developed blister-based LIFT method can be widely used in a variety of instruments for gas-phase analysis of different species such as carbon nanostructures, aerosol particles, and biological objects.

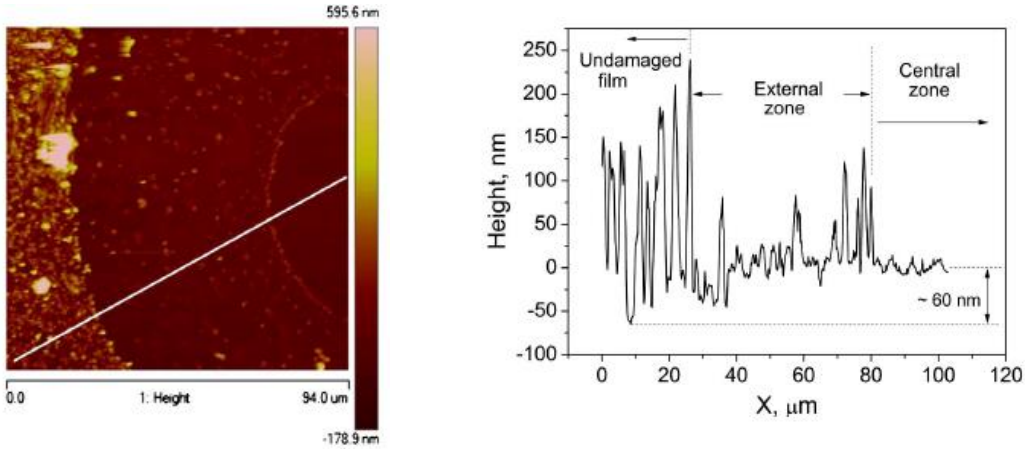

Fig. 1. (Left) AFM image and (right) surface height profile of the LIFT-produced spot on a 250-nm Ti film with gold-silica nanoparticles.

[1] T. V. Kononenko, P. Alloncle, V. L. Konov, and M. Sentis, "Laser transfer of diamond nanopowder by metal film blistering," Appl. Phys. A **94**, 531 (2009).

[2] M. S. Brown, N. T. Kattamis, and C. B. Arnold, "Time-resolved study of polyimide absorption layers for blister-actuated laser-induced forward transfer," J. Appl. Phys. **107**, 083103 (2010).

[3] A. V. Bulgakov, N. Goodfriend, O. Nerushev, N. M. Bulgakova, S. V. Starinskiy, Yu. G. Shukhov, E. E. B. Campbell, "Laser-induced transfer of nanoparticles for gas-phase analysis," J. Opt. Soc. Am. B **31**, C15 (2014).

P-145

Crystalline hydroxyapatite thin coatings produced by Nd:YAG 532nm Pulsed Laser Deposition at room temperature

G. C. Gomes[1], F. F. Borghi[2], R. O. Ospina[1], F. O. Borges[3], E. O. L. Meza[1] and A. Mello[1]

[1]*Centro Brasileiro de Pesquisas Físicas, Rua Doutor Xavier Sigaud, 150 - Urca, Rio de Janeiro-RJ, Brasil – 22290-180*

[2] *University of Sydney, Camperdown /Darlington Campus, NSW 2006, Sydney, Australia*

[3]*Instituto de Física, Universidade Federal Fluminense, Avenida General Milton Tavares de Souza, s/nº - Niterói-RJ, Brasil – 24210-346*

E-mail: gabriela@cbpf.br

Due to a rising demand for dental and orthopedic implants, new technologies are being developed to increase their chemical stability and body acceptance. Among others, some thin films deposition techniques was been applied for coating metals with bioactive ceramics, mainly calcium phosphates (CaP) [1,2] - natural component of human bone, in order to increase the implant's bioactivity as bone substitutes [2,3]. The most widely used commercial method of bioceramic coatings is Plasma Spray (PS) [4]. Nevertheless, some PS disadvantages leads to the research of other techniques like radio frequency magnetron sputtering (RFMS) and pulsed laser deposition (PLD). PLD has shown to be a promising bioceramic coating technique due to its good results as high adhesion to the substrates, stoichiometry, crystallinity and surface roughness.

In this work, the 2nd harmonic of a Nd:YAG laser (532 nm) operating in the range of 50 to 350mJ and repetition rate of 10Hz was used to produce crystalline hydroxyapatite (HAp) coatings over silicon and titanium substrates at room temperature and vacuum environment. No further heat treatment was necessary to produce the crystalline coatings, but to verify the material stability and the possible presence of other hidden phases; in-situ heating was performed during PLD for some coatings.

The structure, composition and morphology of those coatings were analyzed by synchrotron radiation grazing angle x-ray diffraction (GAXRD), Fourier transformed infrared spectroscopy (FTIR), scanning electron microscope (SEM) and atomic force microscopy (AFM).

The produced coatings were all hydroxyapatite free of other CaP phases, mainly crystalline and copying the HAp target stoichiometry (Ca/P=1.67). The morphology of all coatings showed a high roughness of some micrometric particles splashed over a dense nanometer layer.

In addition, optical emission spectroscopy (OES) [5] was applied to investigate the plasma composition.

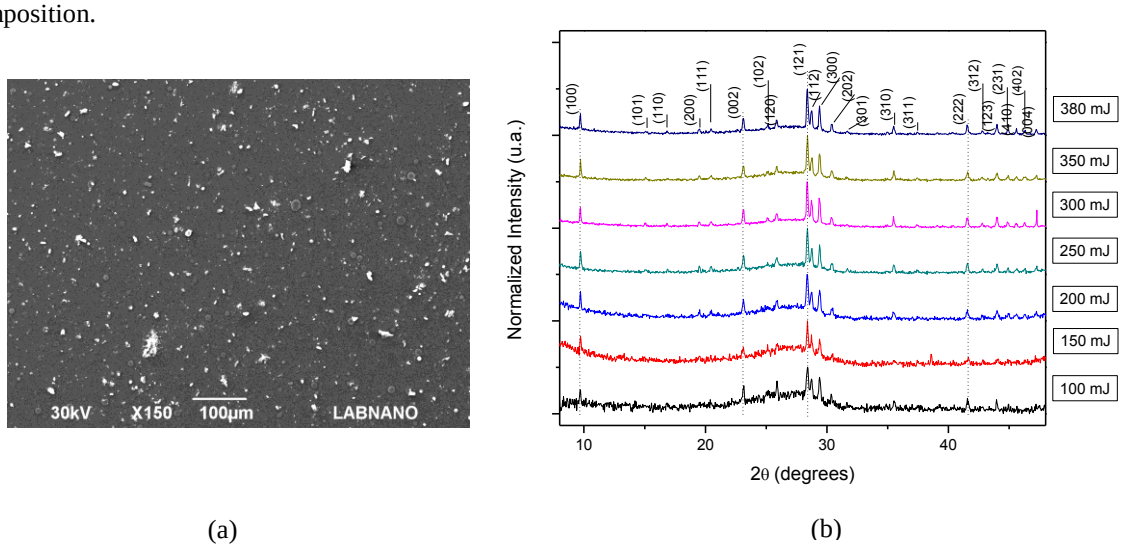

(a) (b)

Fig1. (a) SEM image (b) and GAXRD patterns for the HAp coatings produced by Nd:YAG 532nm.

References

[1] Y. Suda, H. Kawasaki, T. Ohshima, S. Nakashima, S. Kawazoe and T. Toma, "Hydroxyapatite Coatings on Titanium Dioxide Thin Films Prepared by Pulsed Laser Deposition Method". Thin Solid Films. **506-507**, 115-119 (2006).

[2] R. A. Surmenev, M. A. Surmeneva, A. A. Ivanova, "Significance of Calcium Phosphate Coatings for the Enhancement of new Bone Osteogenesis – a review". Acta Biom. **10**, 557-579 (2014).

[3] R. Pa, N. Mohan, Y. Yokogawa, H. Varma, "Pulsed Laser Deposition of Hydroxyapatite on Nanostructured Titanium Towards Drug Eluting Implants". Mat. Sc. and Eng. **33**, 2899-2904 (2013).

[4] F. J. Garcia-Sanz, M. B. Mayor, J. L. Arias, J Pou, B. Leon, M. Perez-Amor, "Hydroxyapatite Coatings: A Comparative Study Between Plasma-Spray and Pulsed Laser Deposition Techniques" Journal of Mat. Sc.: Mat. in Med. **8**, 861-865 (1997).

[5] C. Aragón, J.A. Aguilera, " Characterization of laser induced plasmas by optical emission spectroscopy: A review of experiments and methods". Spec. Acta Part B: Atomic Spect. **63**, 893-916 (2008).

P-146

Textured graphene synthesis by pulsed laser ablation for surface-enhanced Raman scattering

T. Tite[1], C. Donnet[1], A. –S. Loir[1], C. Maddi[1], F. Bourquard[1], S. Reynaud[1], J. –Y. Michalon[1], F. Vocanson[1], V. Barnier[2], and F. Garrelie[1*]

[1] *Université de Lyon, F-69000, Lyon, France, Université de Saint-Étienne, Laboratoire Hubert Curien (UMR 5516 CNRS), 42000 Saint-Étienne, France*

[2]*Laboratoire Georges Friedel, Ecole Nationale Supérieure des Mines, 42023 Saint-Etienne, France*

Corresponding Author : garrelie@univ-st-etienne.fr

Abstract

We report a processing route to produce large scale textured few-layer (fl) graphene at low temperature based on the catalytic conversion of thin Diamond-Like Carbon films grown by Pulsed Laser Deposition, and highlight its potential applications as a surface-enhanced Raman scattering (SERS) platform. The formation of fl-graphene film was confirmed by Raman spectroscopy, and surface morphology was inspected by scanning electron microscopy. We have shown that the diffusion of Ni atoms through a Si substrate and the concomitant formation of nickel silicides compounds offer a good template to design simply the surface properties of graphene with nanoscale roughness. The textured fl-graphene films decorated with gold nanoparticles are introduced as new hybrids materials that can be used as highly efficient SERS devices to detect various molecules. The detection at very low concentration aminothiophenol and methyl parathion, which are active molecules of commercial insecticides, was further demonstrated. This robust device, without any need of graphene transfer, presents a stable detection for up to one year under ambient conditions.

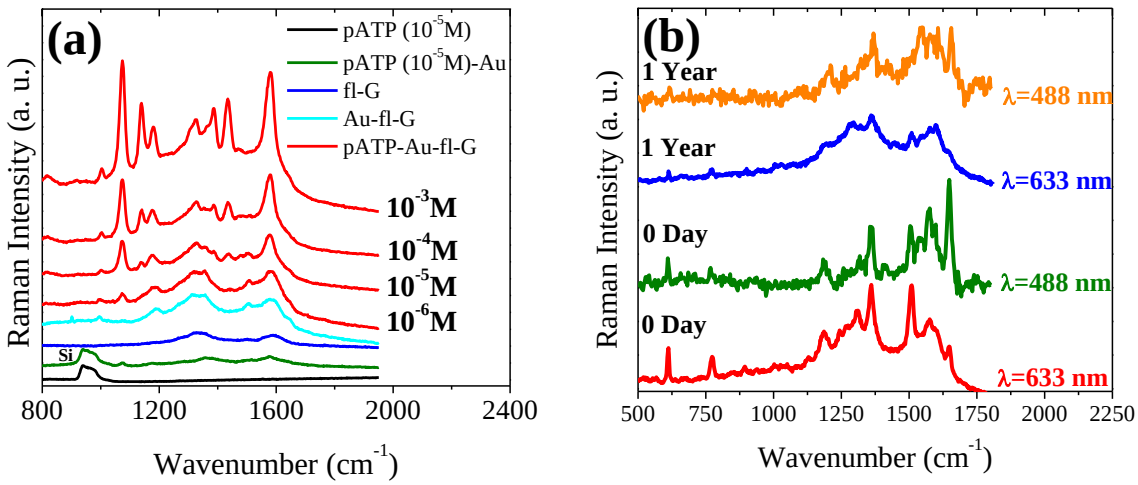

Figure 1: (a) Raman spectra at 633 nm of pATP(10^{-5}M) on Si, pATP(10^{-5}M) on AuNPs deposited on Si, fl-graphene, AuNPs/fl-G, and pATP on AuNPs/fl-G at different pATP concentration (10^{-6}M, 10^{-5}M, 10^{-4}M, 10^{-3}M). The arrows indicate the peak signature of pATP used for Raman mapping. (b) SERS Raman at 488 and 633 nm of R6G (10^{-6}M) on AuNPs/fl-G freshly obtained and after 1-year.

P-147

Laser ablation of ZnS nanoparticles in liquids

YuLin Gan[1], Li Wang[1], ChengHan Li[1], RongPing Wang[2]

[1]*College of Applied Sciences, Beijing University of technology, 100 PingLeYuan ChaoYang District, Beijing, China, 100124*

[2]*Laser Physics Centre, Research School of Physics and Engineering, Australian National University, Canberra ACT 0200, Australia*

Abstract

We have prepared ZnS nanoparticles using pulsed laser ablation in liquid media with an aim to produce ZnS nanoparticles with controllable ideal structural and physical properties. The particle size, structure and physical properties have been systematically investigated by X-ray diffraction (XRD), Raman spectra, high-resolution transmission electron microscopy (HRTEM), selected area electron diffraction (SAED) and energy dispersive spectroscopy (EDS). The ZnS nanoparticles were confirmed to possess the sphalerite structure from XRD and SAED patterns. Chemical composition of the nanoparticles was found to be stoichiometric ZnS as shown in the EDS results. HRTEM images exhibited well-arranged lattices with two space of 0.274nm for [200] and 0.317nm for [111]. Furthermore, we observed clear shift of Raman peaks in Raman spectra of the nanoparticles with different size which can be due to the size confinement effect in phonon modes. The present results demonstrated that, pulsed laser ablation in liquids is effective and promising to nanoparticles with controllable size in large scales.

P-148

Effect of substrate temperature on structure and luminescence properties of YVO_4:Eu thin films grown by PLD

K.E Foka[1], B.F Dejene[1], H.C Swart[2]

[1]*Department of physics, University of the Free State (Qwaqwa), private Bag x13, Phuthaditjhaba, 9866, South Africa*

[2]*Department of physics, University of the Free State, P. O. Box 339, Bloemfontein, 9300, South Africa*

E-mail: fokake@gmail.com

1. Abstract

YVO_4:Eu thin film is a special material phosphor with many potential applications. YVO_4:Eu thin films phosphor has high resolution devices such as cathode ray tubes and flat panel display device [1]. YVO_4:Eu has the strong red emission line ($^5D_0$-$^7F_2$ emission transition at 614 and 619 nm), by the energy transfer to Eu^{3+} ion following absorption of UV light into VO_4^{3-} group [2]. YVO_4 thin films can be prepared by different methods, like sol-gel, pulse laser deposition, vacuum deposition, etc. YVO_4:Eu phosphor thin films were grown using a pulse laser deposition (PLD) technique on silicon substrate. One of the most important things in the deposition of a phosphor thin film is the stoichiometric transfer of the target material to the substrate. In this report the films were grown at the various substrate temperatures and oxygen pressure. The substrate temperatures were varying from 200 to 400 ℃ and the oxygen pressure from 20 to 80 mTorr. YVO_4:Eu phosphor thin films were characterized using various techniques like X-ray diffraction (XRD), photoluminescence (PL), scanning electron microscopy (SEM) and atomic force microscopy (AFM). The structure of YVO_4:Eu thin films matched well with tetragonal phase (JCPDS Card 17-341) and no second phase was detected. The results of PL showed that the emission spectra is consisted of peaks at 594 nm, 618 nm, 651 nm and 699 nm which correspond to the magnetic transition of $^5D_0$-$^7F_1$ and electric dipole transition of $^5D_0$-$^7F_{2,3,4}$ respectively. The major peaks at around 594 nm ($^5D_0$-$^7F_1$) and 618 nm ($^5D_0$-$^7F_2$) correspond to the orange and red colours, respectively. The crystal field splitting of the of $^5D_0$-$^7F_{2,3,4}$ transition indicate that the film is well crystalline. AFM showed that the average grain size and the roughness of the YVO_4:Eu thin films were found to increase with an increasing substrate temperature.

2. References

[1] S. Yi, J. S. Bae, B. C. Choi, K. S. Shim, H. K. Yang, B. K. Moon, J. H. Jeong, and J. H. Kim, ″Surface morphology and photoluminescence characteristics of Eu-doped YVO_4 thin films, ″ Optical Materials 28, 703 (2006).

[2] W. Kang, J. Park, D. Kim, and K. Suh, ″Pulse Laser Deposition of YVO_4:Eu Phosphor Thin Films for Low temperature Fabrication, ″ Bull. Korean Chem. Soc. 22, 921 (2001).

P-149

Rare earth doped cobalt ferrite thin films grown by PLD: influence of the deposition conditions

Georgiana Bulai[1], Ioan Dumitru[1], Silviu Gurlui[1], Bertrand Chazallon[2], Cristian Focsa[2]

[1]*Faculty of Physics, Alexandru Ioan Cuza University, 700506 Iasi, Romania*

[2]*Laboratoire de Physique des Lasers, Atomes et Molécules (UMR 8523), Université Lille 1 Sciences et Technologies, 59655 Villeneuve d'Ascq, France*

E-mail: cristian.focsa@univ-lille1.fr

The interest in rare earth elements and their influence on the microstructure and magnetic properties of substituted ferrite is related to the occupancy of the 4f electron shell (from 0 (La) to 14 (Lu)) and magnetic moments (from 0 (La) to 10.6 μB (Dy)). Due to their moderate elastic constants and the large orbital component in their moments, the lanthanide metals display the largest known magnetostrictions [1]. The RE elements present large ionic radii which, when substituting cations with smaller ionic radii in other types of structures, can determine a change in cell symmetry and thus generate internal stress. As a consequence, not only the structural properties of the material are changed (e.g. increased cell parameter, decreased average crystallite and grain dimensions) but also the magnetic and dielectric properties of substituted materials [2,3].

Motivated by the mentioned characteristics of rare earth (RE) elements and by the magnetic and magnetostrictive response of cobalt ferrite, our work was focused on the investigation of RE induced changes in structural and magnetic properties of $CoFe_{1.8}RE_{0.2}O_4$ films deposited by laser ablation in different conditions. The varied experimental parameters were target-substrate distance, laser fluence, pressure, deposition time and substrate temperature. The structural properties were analysed using profilometry, SEM/EDX, XRD and Raman spectroscopy. The magnetic and magneto-optic characteristics were studied by means of VSM and MOKE techniques.

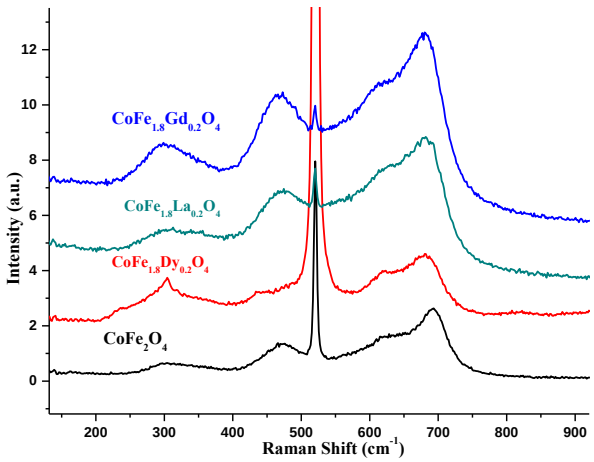

Fig. 1. Raman spectroscopy results of the rare earth doped cobalt ferrite samples deposited at a 400°C substrate temperature

The presence of the RE with large ionic radii determined a distortion of the spinel structure. The Raman vibrational mode of the octahedral sublattice (Figure 1) presented a shift to lower frequencies indicating an increase in cation-oxygen length. This result was further confirmed by XRD measurements were an increase in cell parameter was observed. The VSM results revealed that the magnetic response of the samples depends on the magnetic moment of the rare earth element.

References

[1] *J. Jensen, A. R. Mackintosh, Rare Earth Magnetism (Clarendon press • Oxford, 1991);*

[2] *E. Pervaiz, I. H. Gul, Influence of Rare Earth (Gd3+) on Structural, Gigahertz Dielectric and Magnetic Studies of Cobalt ferrite, J. Phys. Conf. Ser.* ***43****, 012015 (2013);*

[3] *L. Zhao, H. Yang, X. Zhao, L. Yu, Y. Cui, S. Feng, Magnetic properties of CoFe2O4 ferrite doped with rare earth ion, Mater. Lett.* ***6****, 1–6 (2006).*

P-150

Tailoring the physical properties of plasma mirrors antireflection coatings

M. Filipescu*, V. Ion, A. Vlad, T. Nedelea, D. Colceag, M. Dinescu
National Institute for Lasers, Plasma and Radiation Physics, Magurele, RO-077125 Bucharest, Romania
** e-mail: mihaela.filipescu@gmail.com*

Due to the increasing number of facilities based on ultra-short high power lasers systems, the interest for producing highly-resistant optical components, particularly mirrors, to be used in the beam transfer become very current. Solutions for these mirrors are based on heterostructures consisting in combinations of dielectric materials with different refractive indices. Starting from targets of Ta_2O_5, Al_2O_3, SiO_2, and HfO_2 in a controllable oxygen atmosphere, thin layers were grown by pulsed laser deposition and radio-frequency assisted pulsed laser deposition. The experimental parameters for obtaining single layer and layers combination were established after their careful characterization by specific techniques as AFM, XRD, spectroellipsometry, SIMS, SEM, HR-TEM and electrical measurements for the dielectric properties characterization. Then, optical components – demonstrators with controlled antireflection characteristics were obtained, based on dielectric layers with optimized properties and deposition architecture, compatible with plasma mirror generation, capable to withstand high energies ultra-short laser pulses. Simultaneously, computer simulation studies regarding the phenomena that rise when a high energy ultra-short laser beam hits a material were performed using Particle in Cell-Finite Difference Time Domain method.

This work was supported by a grant from MEN-UEFISCDI, project PN-PCCA 38/2014.

P-151

Preparation of vanadium oxide thin films modified with Ag using an hybrid deposition configuration

F. Gonzalez-Zavala[1], L. Escobar-Alarcón[1]*, D. A. Solís-Casados[2], S. Romero[1], C. Rivera-Rodríguez[3], E. Haro-Poniatowski[4]

[1] *Departamento de Física, Instituto Nacional de Investigaciones Nucleares, Apdo. Postal 18-1027, México DF 11801, México.*
[2] *Centro Conjunto de Investigación en Química Sustentable UAEM-UNAM, Toluca, Estado de México, 50200, México.*
[3] *Departamento de Estudios del Ambiente, Instituto Nacional de Investigaciones Nucleares, Apdo. Postal 18-1027, México DF 11801, México.*
[4] *Departamento de Física, Universidad Autónoma Metropolitana Iztapalapa, Apdo. Postal 55-534, México, D.F., México.*

**corresponding author: luis.escobar@inin.gob.mx.*

Abstract

The versatility of the laser ablation technique allows the possibility of implementing different variants in order to improve some characteristics of the deposits, as well as to obtain new materials. In this work, the application of an hybrid deposition configuration to deposit vanadium oxide thin films modified with different amounts of silver is reported. The samples were synthesized combining a vanadium plasma, produced by laser ablation, with a flux of vapor of silver, produced by thermal evaporation. In order to control the amount of Ag incorporated in the film, the Ag deposition rate was varied. In this way, films with different properties were prepared ablating a high purity vanadium target. A Nd:YAG laser with emission at the third harmonic (355 nm) and 10 ns pulse duration was used as energy source. The structural, morphological, compositional and optical properties were studied in detail by Raman spectroscopy, Scanning Electron Microscopy, Atomic Force Microscopy, X-ray Photoelectron spectroscopy, Elastic Forward Analysis and UV-Vis spectroscopy. The obtained results reveal that films with variable Ag content from 3.0 to 26 at.% were obtained. The as-deposited films, consist of a mixture of vanadium oxide and metallic vanadium according with the X-ray Photoelectron spectroscopy results. Raman spectra reveal amorphous films with very smooth surfaces. In order to promote crystallization and oxidation of the remaining vanadium, the films were subjected to thermal treatments at different temperatures: 250, 350 and 450°C. At 450°C the samples show V_2O_5 thin films with good crystalline quality and depending on the silver content the samples show very different surface morphologies (Figure 1). Optical characterization indicate that as the Ag content increases the optical bang gap increases from 3.2 to 3.4 eV.

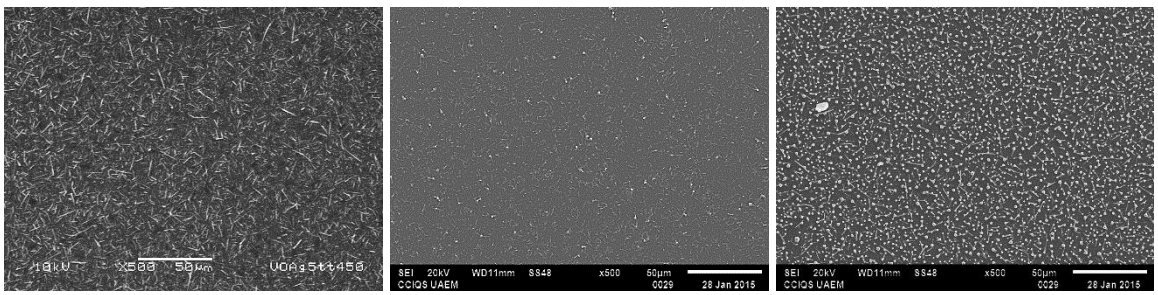

Fig. 1. SEM micrographs of vanadium oxide thin films modified with different silver content: a) 3 at. %, b) 6 at. %, c) 26 at. %.

P-152

Characterization of structural and luminescence properties of blue-green $SrAl_xO_y:Eu^{2+}$, Dy^{3+} thin films deposited by PLD system.

Francis B. Dejene[1*]

[1]*Department of Physics, University of the Free State (Qwaqwa Campus), Private Bag X13, Phuthaditjhaba, 9866, South Africa*
** Corresponding author: Tel: +27 58 718 5263; Fax: +27 58 718 5444; E-mail: dejenebf@ufs.ac.za*

Abstract

Aluminates are in general are large band gap oxides. They are being investigated with increasing interest for application as phosphors in cathode ray tubes, fluorescent lamps and Hg-free discharges with VUV output. Because of their large optical gap, they are suitable hosts for investigating transitions from higher excited states of rare earth ions, and other non-linear luminescent processes. In this work, Europium ion doped strontium aluminates ($SrAl_xO_y:Eu^{2+};Dy^{3+}$) blue-green phosphors have been prepared by pulse laser deposition method on quartz and/or silicon substrate. The synthesized thin films were characterized by X-ray diffraction (XRD), scanning electron microscopy (SEM), electron diffraction spectroscopy (EDX), excitation, emission and lifetime measurements. The dependence of various structural, optical and morphological properties of the prepared thin films on growth conditions has been discussed and the results are compared with those reported in earlier literature. In addition, the effects of annealing temperature, time and Eu^{2+}/Eu^{3+} ion doping concentration on PL were investigated in detail. The $SrAl_xO_y:Eu^{2+};Dy^{3+}$ films exhibited blue-green emission at 500 nm and strong red emission at 614 nm, which were, respectively ascribed to the ($^5D_0 \rightarrow {}^7F_1$) and ($^5D_0 \rightarrow {}^7F_2$) transitions of Eu^{3+}.

Keywords: $SrAl_x0_y:Eu^{2+};Dy^{3+}$, Pulsed laser Deposition, Growth parameter, Molar ratios, Structure, Luminescence

P-153

Structural and luminescence properties of yellow $Y_3Al_50_{12}:Ce^{3+}$, thin film phosphors prepared by Pulsed Laser Deposition.

F.B. Dejene *
Department of Physics, University of the Free State (Qwaqwa Campus), Private Bag X13, Phuthaditjhaba, 9866, South Africa
* Corresponding author: Tel: +27 58 718 5307; Fax: +27 58 718 5444;
E-mail: dejenebf@ufs.ac.za

Recently oxide phosphors have gained much attention because of the variety of materials available and chemical stability as compared to sulfide phosphors. $Y_3Al_5O_{12}$ Eu^{2+} (YAG) crystal is an excellent host material which is able to compatibly accept divalent and/or trivalent activators from both rare earth and transition metal groups. It is well known that YAG is a highly efficient yellow phosphor. However, these phosphors in the form of thin films have not yet been fully realized due to technical difficulties. We prepared thin film type YAG phosphors on silicon (110) substrate using a pulsed laser deposition technique. The luminescent and structural properties of thin film phosphors were monitored as a function of key processing parameters such as oxygen partial pressure inside the deposition chamber, deposition time, laser energy density and the type of post deposition treatments used. The surface morphology of the as grown thin films was strongly affected by the growth process. EDS (electron diffraction spectroscopy) confirm the presence of the Y, Al, O, Ce and and Si. Even though we could not obtain homogenous phases, by optimizing these processing parameters, thin films with large homogenous areas and a high photoluminescence could be produced. XRD measurements revealed $Y_3Al_5O_{12}$ structure when grown at low temperature from 500°C to 1000°C, however, other phases such as $YAlO_3$ and $Y_4Al_2O_9$ are observed as impurities. The PL results, which are in good agreement with the XRD data, showed that $Y_3Al_5O_{12}$ phase was relatively dominant in the film deposited in a vacuum, so emission spectra is strong at around 580 nm .

P-157

Pulsed Laser Deposition and Characterization of Single Crystal Cobalt Ferrite Films with Biphase Composition

Juan de la Figuera,[1] Adrian Quesada,[2] Laura Martín-García,[1] Mikel Sanz,[1] Mohamed Oujja,[1] Esther Rebollar,[1] Pilar Prieto,[3] Angel Muñoz-Martín,[3] Michael Foerster,[4] Lucía Aballe,[4] José F. Marco,[1] Marta Castillejo[1*]

[1]*Instituto de Química Física "Rocasolano", CSIC, 28006 Madrid, Spain*
[2]*Instituto de Cerámica y Vidrio, CSIC, 28049 Madrid, Spain*
[3] *Centre for Micro Analysis of Materials, Universidad Autónoma de Madrid, 28049 Madrid, Spain*
[4]*Alba Synchrotron Light Facility, CELLS, 08290 Barcelona, Spain*
**marta.castillejo@iqfr.csic.es*

Cobalt ferrite, $(Fe^{3+})_A[Co^{2+}Fe^{3+}]_BO_4$, where A and B refer to tetrahedral and octahedral lattice sites, is the ferrite with the highest magnetocrystalline anisotropy. It presents antiferromagnetic order, a reduced magnetic moment, when compared with magnetite, and a high Curie temperature. These singular properties have attracted the interest for magnetic applications of this material. In particular, thin single crystal films of cobalt ferrite are being explored to engineer the magnetic easy axis through the manipulation of the strain state of the film by the choice of the substrate and other deposition parameters.

In this work we have grown single crystalline films of cobalt ferrite by pulsed laser deposition using an IR laser under conditions similar to those used to fabricate magnetite films [1,2]. Pulses of 15 ns at 1064 nm, delivered by a Q-switched Nd:YAG laser (repetition rate of 10 Hz), served for ablating cobalt ferrite sintered targets in a deposition chamber at 10^{-5} Torr. We used fluences of 4 J/cm^2 and typically 1.5 10^5 pulses to grow deposits on $SrTiO_3$(100) (STO) substrates, both undoped and doped with 0.1% Nb, heated to 780 K. Under these conditions the thickness of deposits was measured by atomic force microscopy (AFM) to be around 250 nm. A multi-analytical approach was used to characterize the films and included, in addition to AFM, the use of X-ray diffraction, Rutherford Backscattering spectroscopy, micro-Raman spectroscopy, Integral Conversion Electron Mössbauer Spectroscopy, X-ray photoelectron spectroscopy and low energy electron diffraction. X-ray absorption and circular dichroism measurements were also performed at the CIRCE beamline of the Alba Synchrotron Light Facility.

The grown films have three main distinctive characteristics. First, diffraction experiments indicate a single crystal growth with relaxed lattice spacing. Second, their morphology consists of small rectangular and larger square islands with well-defined sizes (Fig. 1). The rectangles are oriented along either the [100] or the [010] substrate directions, while the squares, with around two orders of magnitude lower density, are oriented along the [110] and [1-10] directions. Third, Mössbauer spectra of the films differ from those of the target and indicate that they are composed of a mixture of magnetite (or Co-poor) and Co-enriched cobalt ferrite. Collected data support a segregated two-phase composition for the films, consisting in rectangular islands of cobalt ferrite and square islands of magnetite. The origin of these two components is discussed to arise in the poor oxidizing conditions of the growth process, that are insufficient to maintain all the Fe in a 3+ valence state. Given that the film is single crystal and both phases are well lattice-matched, we expect that the present films represent a novel avenue for the formation of magnetite-cobalt ferrite composites of tunable properties.

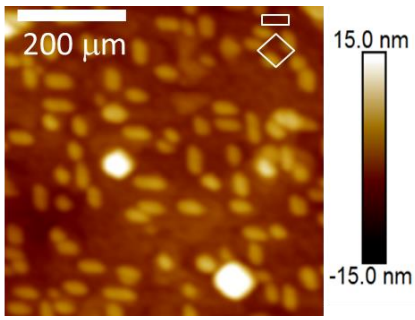

Fig. 1. AFM height image of a cobalt ferrite film grown by IR-PLD on STO:Nb at 780 K. The rectangle and squares in the upper right corner have the typical dimension of the two types of nanostructures observed on the deposits.

References

[1] M. Monti, M. Sanz, M. Oujja, E. Rebollar, M. Castillejo, F. J. Pedrosa, A. Bollero, J. Camarero, J. L. F. Cuado, N. M. Nemes, F. J. Mompean, M. Garcia-Hernndez, S. Nie, K. F. McCarty, A. T. N'Diaye, G. Chen, A. K. Schmid, J. F. Marco, J. de la Figuera, J. App. Phys. 114, 223902 (2013).

[2] M. Sanz, M. Oujja, E. Rebollar, J. F. Marco, J. de la Figuera, M. Monti, A. Bollero, J. Camarero, F. J. Pedrosa, M. García-Hernández, M. Castillejo, Appl. Surf. Sci. 282, 642 (2013).

P-158

Decoration of silica nanowires forests with Au nanoparticles by PLD

A.P. Caricato[1*], C. Leo[1], M. Cesaria[1], F.Gontad[1], V. Resta[1], A. Taurino[2], M.G. Manera[2], A. Convertino[3], R. Rella[2], M. Martino[1]

[1]*Department of Mathematics and Physics "E. De Giorgi", University of Salento, Via Arnesano, I-73100 Lecce, Italy*
[2]*Institute for Microelectronics and Microsystems (IMM-CNR)Strada Provinciale per Monteroni, -73100 Lecce, Italy*
[3]*Institute for Microelectronics and Microsystems (IMM-CNR) Unit of Roma, Via del Fosso del Cavaliere 100, 00133 Roma, Italy*

[*]*E-mail: annapaola.caricato@unisalento.it*

The production of metallic nanoparticles (NPs), specially Au NPs, is a subject that attracts a great interest for the fabrication of sensors for biological and chemical applications, and also in the field of Surface Enhanced Raman Spectroscopy. These NPs, once deposited on 1-dimensional structures, such as silica nanowires (NWs), can be chemically functionalized with biological receptors and tested by exploiting DNA/DNA or antigen/antibody reactions, monitoring in real time the variation of the Au NPs surface Plasmon resonance (SPR). However, the deposition of Au NPs on complex substrates like silica NWs forests is a very challenging goal. In order to overcome such a difficulty, the Pulsed Laser Deposition (PLD) technique is an excellent alternative to chemical based approaches, due to the nature of the process, which involves very energetic particles and high fluxes of ablated materials and offers a good adhesion on different substrates even at room temperature.Thus, the PLD allows obtaining uniform coverage of bi-dimensional and tri-dimensional substrates with high density NPs layers and as an additional advantage of the process there is no need of NPs functionalization.

In this work we report the deposition of Au NPsdirectly grown on silica NWs forests through PLD analyzing the influence of the number of laser shots used for the deposition on theirmorphology and optical properties. The Au NPs were deposited in an high vacuum chamber with a pulsed Ar Fexcimer laser (20 ns, 193 nm), at an energy density of 2.5 J/cm^2 and a repetition rate of 10 Hz, on two different sets of substrates: the silica NWs forests and also on quartz substrates for comparison.

The morphological analysis of the samples deposited on quartz substrates shows a uniform coverage of the substrate surface with the NPs, increasing its size with the number of laser pulses used for the deposition. Similar behavior can be found in the silica NWs that appearuniformly covered bythe NPs, as shown in figure 1 where the Au NPs are effectively distributed along the whole NWs surface.The optical characterization of the Au NPs on both substrates shows the typical localized plasmonic resonance peak.

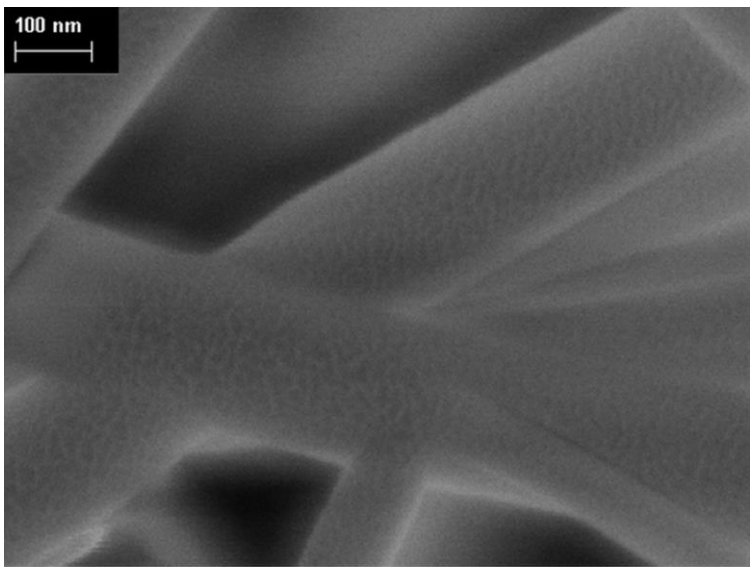

Fig. 1. SEM image of Au NPs decorating the silica NWs.

P-160

Nitrogen plasma assisted Femtosecond Pulsed Laser Deposition of a-C:N films for environmental analytical microsystems and *in situ* plume analysis

C. Maddi[(a)], F. Bourquard[(a)], T. Tite[(a)], N. Zehani[(c)], P. Fortgang[(c)], A.-S. Loir[(a)], V. Barnier[(b)], T.C. Rojas[(d)], J. C. Sánchez-López[(d)], C. Chaix[(c)], N. Jaffrezic-Renault[(c)], K. Wolski[(b)], C. Donnet[(a)], F. Garrelie[(a)]

(a) *Université de Lyon, F-69003, Lyon, France, Université de Saint-Étienne, Laboratoire Hubert Curien (UMR 5516 CNRS), 42000 Saint-Étienne, France*

(b) *Laboratoire Georges Friedel, Ecole Nationale Supérieure des Mines de Saint-Étienne, France*

(c) *Université de Lyon, F-69003, Lyon, France, Université Claude Bernard Lyon 1, Institute des Sciences Analytiques (UMR 5280 CNRS), 69100 Villeurbanne, France*

(d) *Instituto de Ciencia de Materiales de Sevilla (CSIC-US), Avda. Américo Vespucio 49, 41092 Sevilla, Spain*

florent.bourquard@univ-st-etienne.fr

Within the field of carbon based materials generation and characterization, nitrogen doped amorphous carbon (a-C:N) thin films have demonstrated a wide potential range of applications, in particular as active elements of electrodes and sensors in the chemical and biomedical fields. Nitrogen containing amorphous carbon (a-C:N) thin films have been elaborated by femtosecond Pulsed Laser Deposition (fs-PLD), coupled with a DC plasma assistance. Various nitrogen pressures (0-10 Pa) and Direct Current (DC:0-400V) bias were used to introduce nitrogen on a wide range of concentration, extending up to N content of 28 %at.

The ablation plume expansion has been studied with intensified CCD (ICCD) gating through both optical emission spectroscopy (OES) and direct 2D spectral-resolved imaging. The ICCD time resolution (5ns) allows for a precise determination of the arising time of the different species observed via OES, such as C^+, C, C_2 and CN. The use of 10 nm wide interferential filters for 2D imaging of the plasma allows us to gain spectral resolution when imaging the plume dynamics. This has been exploited to address the kinetic and spatial behavior of C-N and C-C bonding during plume expansion in nitrogen pressure or nitrogen plasma. Comparative studies were carried in argon atmosphere and argon plasma, as well as in vacuum, to determine the precise influence of the DC plasma on the dynamics of the ablation plume and on the bonding nature of the various species. The results of those studies are correlated with the properties of the deposited films.

The structure and chemical composition of the thin films have been studied through Multi-wavelength (MW) Raman spectroscopy, X-ray photoelectron spectroscopy (XPS), Electron energy-loss spectroscopy (EELS) and Reflection electron energy loss spectroscopy (REELS). Cyclic Voltammetry (CV) has been performed in order to characterize electrochemical properties. During deposition, the intensity of the reactive activated species in the plasma plume is increased owing to the DC biased assistance when compared to the inert N_2 atmosphere. These deposition conditions induce an overall increase of nitrogen contents in the films and the formation of sp^2 rich graphitic-like structures.

The a-C:N films are shown to exhibit better electrochemical properties than pure a-C films, representing thus promising electrode material for electrochemical detection of biopathogen molecules and pollutant traces.

P-162

ZnSb-based thermoelectric thin films by PLD and combined PLD-sputtering system

A. Bellucci[1,2], S. Orlando[3], E. Cappelli[1], F. Di Fonzo[4], F. Fumagalli[4], L. Medici[5], A. Mezzi[6], S.Kaciulis[6], and D.M. Trucchi[1]

[1]*CNR-ISM, Montelibretti Section, Via Salaria km 29.300, 00015 Monterotondo (RM), Italy*
[2]*Dipartimento di Fisica, Sapienza Università di Roma, Piazzale A. Moro 5, 00151 Roma, Italy*
[3]*CNR-ISM, Tito Scalo Section, Zona Industriale, 85050 Tito Scalo (Pz), Italy*
[4]*Center Nano Science Technology at Polimi, I.I.T., Via Pascoli 70/3, 20133 Milano, Italy*
[5]*CNR-IMAA, Zona Industriale, 85050 Tito Scalo (Pz), Italy*
[6]*CNR-ISMN, Via Salaria km 29.300, 00015 Monterotondo (RM), Italy*
E-mail: alessandro.bellucci@ism.cnr.it

The request of thermoelectric thin films is involving increasingly several research groups for their attractive low-power applications and the possibility to fabricate flexible and efficient devices. Among the thermoelectric materials, ZnSb represents a promising candidate in the temperature range 400-600 K since it is a cheap, non-toxic and potentially high-performing material.
The feasibility of Pulsed Laser Deposition (PLD) as a powerful deposition technique for nanostructuring thermoelectric films has been demonstrated in [1, 2]. The deposition of p-type and n-type doped ZnSb thin films has been performed by fs-PLD and by a fs-PLD/DC sputtering co-deposition system in order to compare the dopant inclusion within the ZnSb matrix, aimed at finding the recipe able to maximize the films thermoelectric performance.
Structural, compositional and thermal characterizations have been carried out to study and to demonstrate thermal and chemical stability of the samples. Electronic performance has been analysed by carrier concentration, mobility, electrical resistivity and the Seebeck coefficient, thus obtaining the evaluation of the power factor as a function of the doping. Finally, preliminary measurements of thermal conductivity by TDTR (Time-Domain ThermoReflectance), obtained by a fs-laser pump-and-probe setup, are discussed.

References

[1] A. Bellucci, E. Cappelli, S. Orlando, L. Medici, A. Mezzi, S. Kaciulis, R. Polini, and D. M. Trucchi, "fs-pulsed laser deposition of PbTe and PbTe/Ag thermoelectric thin films", Appl. Phys. A 117(1), 401-407 (2014)
[2] E. Cappelli, A. Bellucci, L. Medici, A. Mezzi, S. Kaciulis, F. Fumagalli, F. Di Fonzo, and D. M. Trucchi, "Nano-crystalline Ag-PbTe thermoelectric thin films by a multi-target PLD system", Appl. Surf. Sci. (2015), http://dx.doi.org/10.1016/j.apsusc.2014.12.031

P-163

The effect of different species of gases on material properties of Eu^{3+} doped Y_2O_2S thin films phosphor deposited by Pulsed Laser Deposition method.

AG Ali[1]*, BF Dejene[1] and HC Swart[2].

[1]Department of Physics, University of the Free State (Qwaqwa Campus), Private Bag X13, Phuthaditjhaba, 9866, South Africa.

[2]Department of Physics, University of the Free State, P.O. Box 339, Bloemfontein, 9300, South Africa.

* Corresponding author: E-mail: aliag@qwa.ufs.ac.za

1. Introduction

Y_2O_2S nanocrystals doped with trivalent RE ions have particularly attracted considerable interest in terms of high chemical durability and thermal stability [1]. It has been widely investigated as the host for RE ions for optical application. It has a broad transparency range(0.2- 8μm) with a band gap of between 5.6-5.8 eV, a high refractive index, better thermal conductivity, and low photon energy that makes it an attractive choice as host materials[2]. Synthesis of rare earth doped Y_2O_2S based nanophosphor has been accomplished through a variety of techniques such as sol gel method, co-precipitation etc. Among various methods, combustion method has been studied extensively due to its simplicity and easiness to control the particle size of the products. In this study Y_2O_2S: Eu^{3+} thin films have been deposited with the pulsed laser deposition technique under different species of gases and the material properties dependence of Y_2O_2S:Eu^{3+} were reported. The deposition was carried out under vacuum, argon and oxygen atmosphere.

2. Results

The synthesis and characterization of Eu^{3+} doped yttrium oxysulfide (Y_2O_2S) nanophosphors were undertaken in the current work. Trivalent europium doped Y_2O_2S nanophosphors were prepared by combustion synthesis method using thiourea as an oxidizing fuel. As-prepared powders were deposited on a Si (100) substrate by pulsed laser deposition method. The structural and morphological properties of Y_2O_2S: Eu^{3+} nanophosphors were characterized with X- ray diffraction (XRD), Atomic force microscopy (AFM), Scanning electron microscopy (SEM), UV-vis and Photoluminescence (PL) measurements. X-ray diffraction patterns show mixed phases of cubic and hexagonal. Photoluminescence measurement indicates intense red emission around 619 nm due to $^5D_0 \rightarrow {}^7F_2$ transition of Eu^{3+}. Scanning Electron Microscopy (SEM) show agglomerates of crystalline particles with spherical shapes. Atomic Force Microscopy (AFM) further confirmed the crystallinity of the films. UV measurement gave a band gap of about 4.7 eV. This phosphor may be good promising material for applications in the flat panel displays.

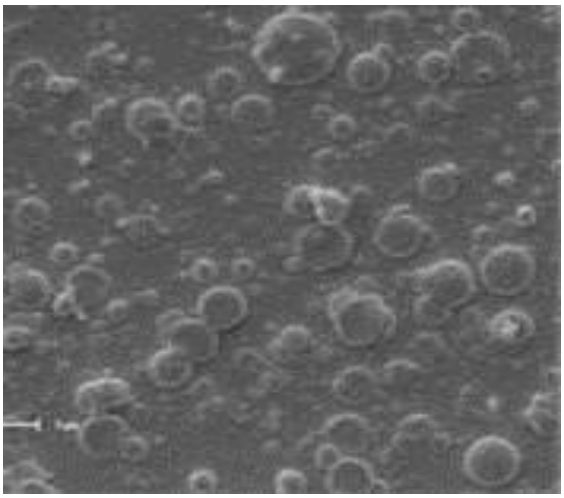

Fig. 1: SEM micrograph of Y_2O_2S:Eu^{3+} thin film deposited in vacuum ambient

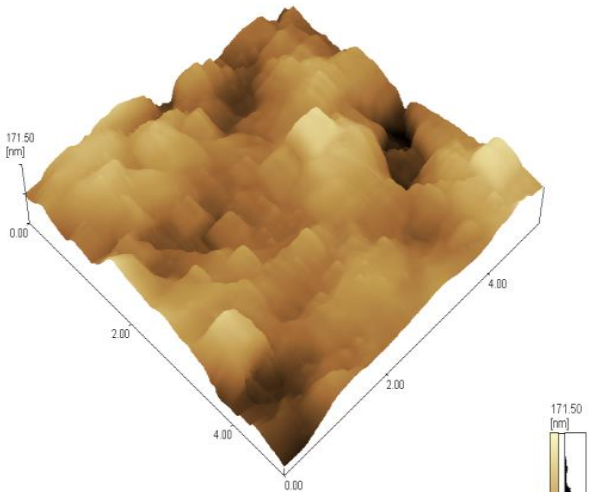

Fig. 2: AFM image of Y_2O_2S: Eu^{3+} thin film deposited in vacuum ambient

3. Reference

[1] G. kumar Das, T. Thatt, Y. Tan, J. Phy. Chem C. 112, 11211-11217 (2008).
[2] H. Wang, M. Uehar, H. Nakamura et al, Adv. Mat. 17, 2506 (2005).

P-164

Effect of annealing temperature on structural and luminescence properties of Eu^{3+} -doped Y_2O_3 red phosphor thin films by PLD method.

AG Ali[1*], BF Dejene[1] and HC Swart[2].

[1*]*Department of Physics, University of the Free State (Qwaqwa Campus), Private Bag X13, Phuthaditjhaba, 9866, South Africa.*
[2]*Department of Physics, University of the Free State, P.O. Box 339, Bloemfontein, 9300, South Africa.*
** Corresponding author: E-mail: aliag@qwa.ufs.ac.za*

1. Introduction

Trivalent europium-doped yttrium oxide (Y_2O_3:Eu^{3+}) is an important phosphor system extensively applied in colour-television pictures tubes owing to higher luminescent efficiency and the saturation degree in color and of late, in field-emission display devices[1]. Among the metal oxides, Y_2O_3:Eu^{3+} have found various useful technological applications due to their thermal, optical and chemical stability and excellent mechanical properties such as high strength and fracture toughness [2]. Physical and chemical techniques including chemical precipitation [8–10], alkalide reduction, sol-gel, combustion, pyrolysis, solvothermal and hydrothermal synthesis have been employed for the synthesis of nanoparticles, nanotubes, nanorods, nanowires, nest-like structures of Y_2O_3:Eu^{3+} and the related compounds. In this study Y_2O_3: Eu^{3+} powder was synthesized by sol-combustion technique. As- prepared powder was deposited on Si (100) substrate using pulsed laser deposition technique. The thin films were annealed at temperatures between 600 and 900^{0}C. Temperature dependence characteristics of Y_2O_3:Eu^{3+} were reported.

2. Results

X-ray diffraction patterns shows pure cubic phase. It was observed that high temperature annealing improved the crystallinity of the films. Photoluminescence measurement indicates intense red emission around 626 nm due to $^5D_0 \rightarrow {}^7F_2$ transition of Eu^{3+}. Scanning Electron Microscopy (SEM) show agglomerates of crystalline particles with spherical shapes for as-prepared films. After annealing at high temperature, SEM also confirms that the crystallinity of the films improved. Atomic Force Microscopy (AFM) further confirmed the crystallinity of the films at higher annealing temperatures. UV measurement gave a band gap in the range of 4.6-4.8ev. It was concluded that the annealing temperature plays an important role in the luminescence intensity and crystallinity of these films. This phosphor may be good promising material for applications in the flat panel displays.

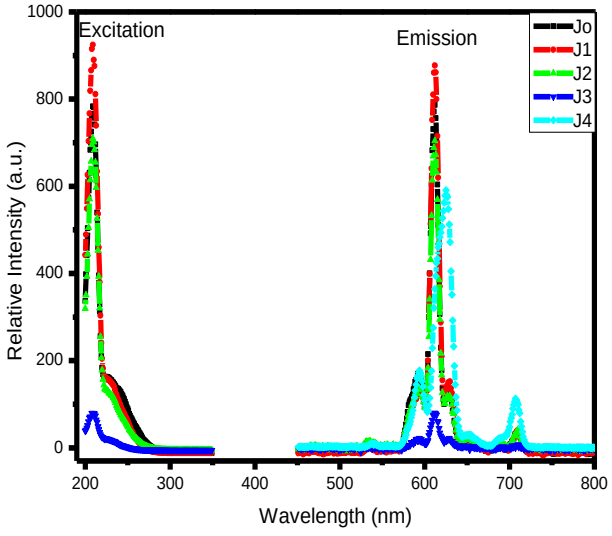

Fig. 1. The excitation and emission spectra of Y_2O_3: Eu^{3+} thin films annealed at (a) J1=600 (b) J2=700 (c) J3=800 (d) J4=900^{0}C

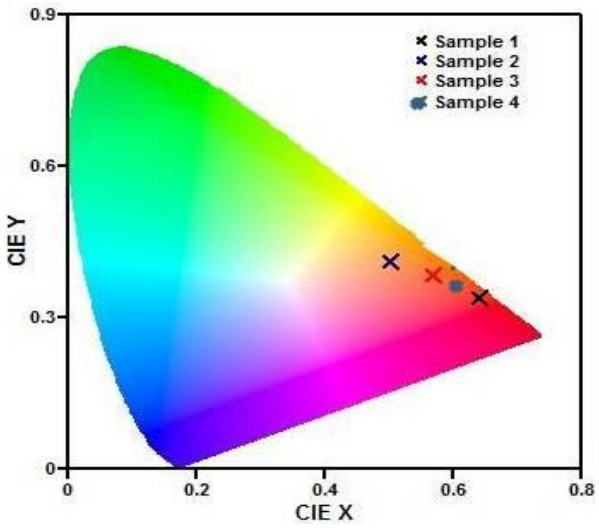

Fig. 2. Chromacity co-ordinates of the PL spectra for the sam ples annealed at (1) 600, (2) 700, (3) 800 and (4) 900^{0}C

3. Reference

[1] Katsumata T, Nabae T, Sasajima K. Growth and characteristics of long persistent SrA1204 and CaA1204 based phosphor crystals by a floating zone technique. *J. Cryst. Growth***,** 1998, 83: 361.
[2] Kinoshita T, Yamazaki M, Kawazoe H, et al. Long phosphorescence and photo stimulated luminescence in Tb ion activated reduced calcium aluminate glasses. J. *Appl . Phys***.,** 1999, 86: 3729.

P-168

Control and optimization of an energetic sub-picosecond laser-driven hard x-ray K_α source with a high pulse repetition rate

Y. Azamoum, V. Tcheremiskine, P. Blandin, R. Clady, L. Charmasson, N. Sanner, O. Uteza and M. Sentis

Laboratoire Lasers, Plasmas et Procédés Photoniques
Aix-Marseille Université - UMR 7341 CNRS, Luminy, Marseille, France.
Email: azamoum@lp3.univ-mrs.fr

We report our latest results on development of a K_α x-ray source produced by high intensity femtosecond laser solid interaction. The control and optimization of such a source is subject of high current interest in regard with a very dynamic growth and diagnostic demand of novel diagnostics at ultrafast science domain [1]. Such laser plasma source is characterized by a micrometric size (comparable to the size of a laser focal spot) and sub-picosecond duration. It exhibits an isotropic emission with a characteristic line spectrum (dominantly K_α line at photon energy determined by target material) superimposed on a weak bremsstrahlung continuum.

Several techniques are being developed to produce intense femtosecond x-ray sources. In accelerator community, large scale free electron laser facilities (LCLS, FLASH ...) [2] can now deliver brightest and shortest x-ray beams ever. In parallel, alternative and complementary methods based on laser produced plasma have been developed to produce compact radiation sources such as secondary x-ray sources of K_α radiation or Betatron radiation based on the emission of electrons accelerated in laser wake field. Indeed, the intense activity on the production of such radiation is motivated by countless applications in fundamental science, industry, biology and medicine. While the micrometric source size allows high spatial resolution coupled with phase contrast technique, favorable for bio-medical imaging [3], the combination of sub-Angstrom structural resolution of x-rays with ~100fs temporal resolution allows for studying ultrafast changes of crystal lattice structure under optical excitation [2].

Being focused on the target surface, an intense fs laser pulse creates plasma, where electrons are accelerated by the laser field via different absorption mechanisms. We consider the regime of intense non-relativistic interaction (10^{16} - 10^{18} W/cm^2) and high-contrast p-polarized fs pulses. It results in the vacuum heating (Brunel effect) as dominant mechanism of plasma absorption, leading to characteristic energies of accelerated "hot" (suprathermal) electrons of tens keV and higher. Coming in collisions with atoms of the target material, the hot electrons are scattered producing spectrally-continuous bremsstrahlung radiation and create vacancies in the atom inner shells, resulting in the characteristic line emission. The K_α emission is dominant due to the highest rate of the K-shell population. At hot electron energies of several times the K-shell ionization threshold, the K-shell ionization cross-section reaches its maximum resulting in higher efficiencies [4]. Owing to a fast energetic relaxation of hot electrons in the target material, the produced x-ray pulse has sub-picosecond duration.

Photon fluxes of K_α emission of up to 10^{10} photons/s have been attained using laser system delivering few mJ per pulse with 1-kHz repetition rate [5]. In the present work our goal is to deliver higher K_α photon fluxes (up to 10^{12}photons/s) using a new and unique high-contrast (10^9@ns and 10^8@10ps) Ti:Sa (800nm) laser system delivering 10TW/250mJ/25fs at 100 Hz repetition rate. With such high contrast and energetic pulses, we expect to obtain a source size of $\leq 10\mu m$ thanks to a deformable optical mirror and attain energy conversion efficiency into K_α photons higher than 10^{-5}.

An optimization of the X-ray source size, brightness and efficiency as a function of laser intensity, temporal contrast ratio and incidence angle will be presented with a particular emphasis on the temporal contrast ratio since the role of this parameter in producing K_α X-rays with high efficiency is still controversial. Beside this unique laser source, the experimental setup includes a vacuum interaction chamber with a silver-coated off-axis parabolic mirror (metal-substrate,90°, f=150mm, f/3.5) which focuses the intense fs laser into a ~ limited diffraction spot size (owing to the aberration correction with the help of a large ellipsoidal deformable mirror working at 45 ° angle of incidence) at the surface of a motorized rotating disk Mo target (17keV) or Cu target (8keV). This setup allows to work at a repetition rate of 100 Hz and to deliver more than 10^6 pulses with the same target disk. X-ray diagnostics for the parametric study include Xray-PMTs, X ray-spectrometers, direct and indirect X ray-CCDs.

References

[1] Jannick Weisshaupt , Vincent Juvé , Marcel Holtz *et al*., "High-brightness table-top hard X-ray source driven by sub-100-femtosecond mid-infrared pulses", Nature Photonics ,vol **8**, (2014).

[2] T. Elsaesser and M. Woerner, "Perspective: Structural dynamics in condensed matter mapped by femtosecond x-ray diffraction", J, Chem. Phys.**140**, 020901 (2014).

[3] R. Toth, J. C. Kieffer, S. Fourmaux, T. Ozaki and A. Krol, "In-line phase-contrast imaging with a laser-based hard x-ray source", Rev. Sci. Instrum. **76**, 083701 (2005).

[4] F. Ewald H. Schwoerer and R. Sauerbrey, "Kα radiation from relativistic laser-produced plasmas", Europhys. Lett., **60** (5), pp. 710–716 (2002).

[5] F. Zamponi, Z. Ansari, C.v. Korff Schmising *et al*., "Femtosecond hard X-ray plasma sources with a kilohertz repetition rate", Applied Physics A, vol. **96**, pp. 51-58, 2009.

P-169

New High-Pressure Silicon Phases Formed in Fs-Laser Induced Confined Microexplosion

L. Rapp[1,2], B. Haberl[3], C. J. Pickard[4], J. E. Bradby[3], J. S. Williams[3], E. G. Gamaly[1], A. V. Rode[1]

[1]*Laser Physics Centre, Research School of Physics and Engineering, The Australian National University, Canberra ACT 0200 Australia*
[2]*Laboratoire LP3, Aix-Marseille Universite, FR-13288, France*
[3]*Electronic Materials Engineering, Research School of Physics and Engineering, The Australian National University, Canberra ACT 0200 Australia*
[4]*Department of Physics and Astronomy, University College London, London WC1E 6BT, UK*

avr111@physics.anu.edu.au

Intense ultrafast laser pulses tightly focused in the bulk well below the surface of transparent material interact with matter in the condition where the conservation of mass is fulfilled. Plasma produced by the laser pulses in confined geometry generates strong shock waves with the pressure at the shock wave front exceeding several times the Young modulus of solid material. Irreversible structural changes, often considered as damage, occur at an intensity level above the optical breakdown threshold. The essential distinctive feature of laser-driven microexplosion is that the modified material remains compressed and confined in a strongly localized region inside a bulk, and can be investigated later by Raman spectroscopy, electron beam, x-ray, and other structural diagnostics techniques. The extreme conditions produced in the ultrafast laser driven micro-explosion can serve as a novel microscopic laboratory for high-pressure studies above 10^{12} Pa (10 Mbar), well beyond the pressure levels achieved in diamond anvil cell.

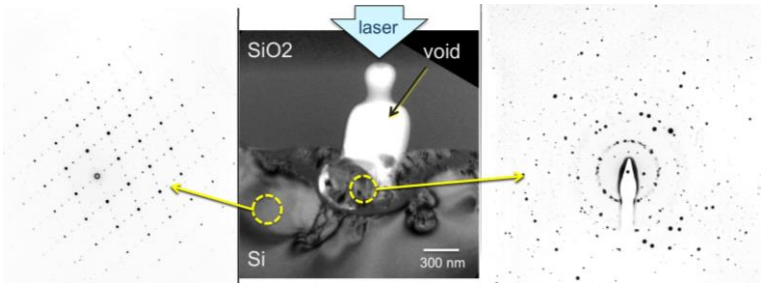

Figure 1. Transmission electron microscope image of a void formed by a single fs-laser pulse focused on Si-surface buried under a layer of SiO_2 (centre) and electron diffraction pattern from a pristine diamond-cubic silicon (left) and from a shock-wave affected area showing the presence of new tetragonal high-pressure phases of Si-BT8 and Si-S12 [3].

Here we expand the confined microexplosion method into the domain of non-transparent materials such as Silicon [1,2]. In this presentation we report the observation of two new pressure-induced tetragonal metastable polymorphs of Si formed via these highly non-equilibrium conditions of a confined microexplosion. Electron diffraction analysis of laser-modified Si clearly reveals the presence of crystal structures currently not assigned to any known phases of silicon. Silicon polymorphs, which are metastable in ambient conditions, under pressure demonstrate a wide range of characteristics, from semiconducting to metal, and even predicted to form superconducting phases, signifying their scientific and technological importance. In addition to some diffraction spots that we can not identify, three tetragonal phases are observed, two of which BT8 and ST12 have been predicted theoretically [4,5] but have previously never been observed experimentally, and one (Si-VIII) has only been observed in a single experimental study under very rapid unloading [6]. The formation of these tetragonal polymorphs, reliably repeatable in several microexplosion experiments, is evidence that Si has undergone pressure-induced transitions into the realm of the metallic high-pressure phases that are formed above 11 GPa [7]. The ability of ultrafast lasers to locally modify the electronic properties of silicon with sub-micron precision via non-equilibrium pressure/temperature processes with repetition rates up to and above 10^5 shots per second opens up novel opportunities for nanoelectronics through the incorporation of such nanostructures into semiconductor devices.

[1] E. G. Gamaly, L. Rapp, V. Roppo, S. Juodkazis and A. V. Rode, New J. Phys. **15**, 025018 (2013).
[2] L. Rapp, B. Haberl, J. E. Bradby, E. G. Gamaly, J. S. Williams, A. V. Rode, Appl. Phys. A **114**, 33-43 (2014).
[3] L. Rapp, B. Haberl, C. J. Pickard, J. E. Bradby, J. S. Williams, E. G. Gamaly, A. V. Rode, under preparation for publication.
[4] J.-T. Wang, C. Chen, H. Mizuseki, Y. Kawazoe, Phys. Rev. Lett. **110**, 165503 (2013).
[5]. B. D. Malone, J. D. Sau, M. L. Cohen, Phys. Rev. B **78**, 035210 (2008).
[6]. Y.-X. Zhao, F. Buehler, J. R. Sites, I. L. Spain, Sol. State Comm. **59**, 679-682 (1986).
[7]. J. C. Jamieson, Science **139**, 762-764 (1963).

P-171

Thermal effects on the rapid bubble growth in the laser-induced microjet injector for transdermal drug delivery

S. Yeo[1], H. Jang[1], and J. J. Yoh[1*]

[1]*Department of Mechanical and Aerospace Engineering, Seoul National University, Seoul 151-742, Republic of Korea*

E-mail: jjyoh@snu.ac.kr

A handheld-type Er:YAG laser with 2940 nm wavelength and 150 μs pulse duration was built for the purpose of generating the laser-induced microjet that is ejected at ~100 m/s in air. The strength of the microjet depends on the bubble dynamics from beam-water interaction within the driving chamber as well as the discharging of the drug solution underneath the elastic membrane that separates the drug from the driving liquid. The confinement pressure within the chamber depends on the volumetric growth of the bubble, which determines the extent of membrane deflection, thereby accelerating the microjet through a nozzle. Figures 1 and 2 show rough bubble surface and maximum bubble volume at 87 ℃, suggesting that the thermal effects play instrumental role in the performance of a microjet injector.

The enhancements in jet volume (dosage) and repeated jet generation are achieved which are aimed at making the injector suitable for general clinical use as well as for tattooing.

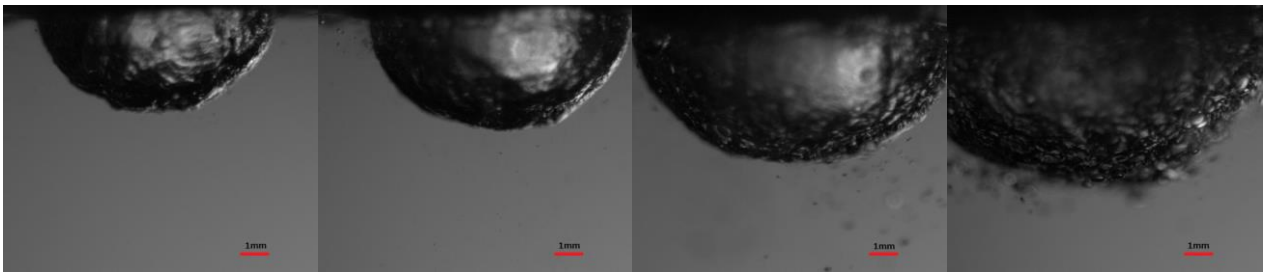

Fig. 1 Laser-induced vapor bubbles in the water of different temperatures (36 ℃, 50 ℃, 75 ℃, 87 ℃)

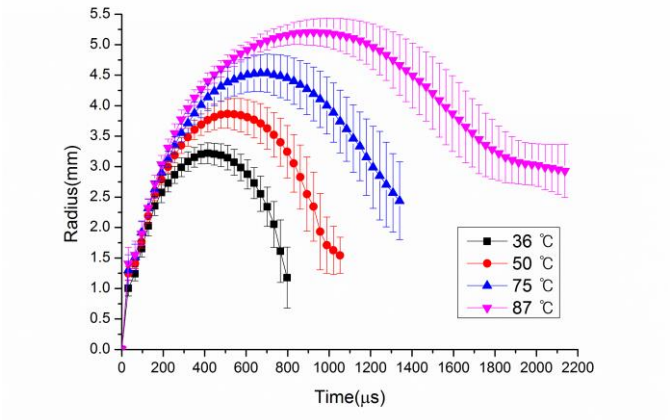

Fig. 2 Bubble growth in different water temperatures

Fig. 3 SNU logo tattooed on the porcine skin

P-172

Biodegradability of poly(lactic-co-glycolic acid) after irradiation of femtosecond laser pulses

A. Shibata[1], S. Yada[1], M. Terakawa[1,2]

[1]*School of Integrated Design Engineering, Keio University, 3-14-1 Hiyoshi, Kohoku-ku, Yokohama 2223-8522, Japan*

[2]*Department of Electronics and Electrical Engineering, Keio University, 3-14-1 Hiyoshi, Kohoku-ku, Yokohama 2223-8522, Japan*

E-mail: terakawa@elec.keio.ac.jp

Biodegradable polymers have attracted considerable interest as a high biocompatible biomaterial, since they degrade into non-toxic materials in the body. In applications to drug delivery system, biodegradable polymers could achieve a precisely controlled rate of drug release by degrading carriers, if the biodegradation profiles could be controlled. In applications for tissue scaffolds, the scaffold should have demanded degradability to exist until tissue regenerates sufficiently, and to degrade after tissue regeneration completes. Several methods to modify the biodegradability of polymers including copolymerization and microporous structure formation have been reported. Laser processing is a high-throughput method which enables us to process desired spot even after molding. Remarkably, femtosecond laser realizes precise processing of polymers via multiphoton absorption. In this paper, we investigate the effect of femtosecond laser irradiation on biodegradability of poly(lactic-co-glycolic acid) (PLGA), a widely used biodegradable polymer. Femtosecond laser pulses (τ = 100 fs) at 800 nm or 400 nm central wavelengths were focused onto a surface of PLGA with spot size of 100 μm at normal incidence using plano-convex lens. The repetition rate was 1 kHz. Each sample was placed in a vial after laser irradiation and fully immersed in a 5 mL phosphate-buffered saline (PBS). Vials were placed in a water bath at 37^0C. The ablated area of sample was observed with digital microscope after immersion for 0-24 hours. With 800 nm in wavelength, the ablated area formed under irradiation conditions of 1.0 J/cm^2 with 15000 pulses did not expand dramatically after 24 hours immersion [Fig. 1]. It is notable that the ablated area formed with 400 nm in wavelength under irradiation conditions of 0.15 J/cm^2 with 15000 pulses shows expansion with elapse of time [Fig. 2]. To discuss the difference, the modification of chemical structure of the surface of PLGA before and after laser irradiation was analyzed by using X-ray photoelectron spectroscopy (XPS). The result shows that more dissociation of C-O bond and C=O bond occurred after laser irradiation with 400 nm wavelength than the irradiation with 800 nm. For comparison, the ablated area formed mechanically using a milling machine, was also evaluated and we found no significant change even after 24 hours immersion. These results show the potential of femtosecond laser processing to fabricate degradability controlled scaffolds.

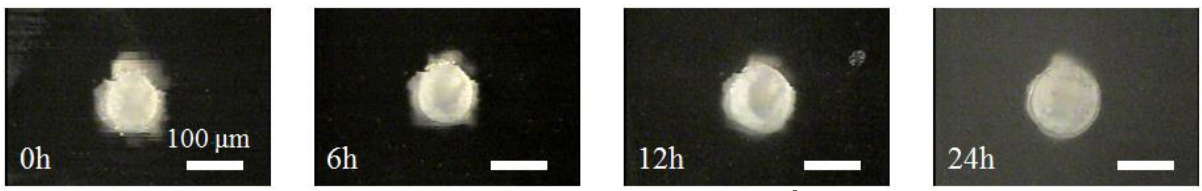

Fig. 1. Microscope images of ablated area formed under the irradiation condition of 1.0 J/cm^2 with 15000 pulses at 800 nm after immersion in PBS for 0, 6, 12, 24 hours. Scale bars indicate 100 μm.

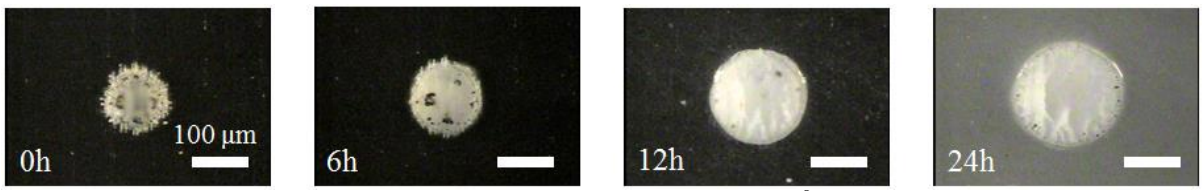

Fig. 2. Microscope images of ablated area formed under the irradiation condition of 0.15 J/cm^2 with 15000 pulses at 400 nm after immersion in PBS for 0, 6, 12, 24 hours. Scale bars indicate 100 μm.

P-173

Thin film production from a compressible organic target by laser irradiation: from material destruction at high target pressure to material drop-out at low pressure

Catalin Constantinescu[1,2], Andreea Matei[1,2], Maria Dinescu[2] and Jørgen Schou[1,*]

[1] *DTU Fotonik, TechnicalUniversity of Denmark, DK-4000 Roskilde, Denmark*
[2] *INFLPR – National Institute for Laser, Plasma and Radiation Physics, 409 Atomistilor St, RO-077125, Magurele, Romania*

[*] *Corresponding Author e-mail address: josc@fotonik.dtu.dk*

The protein lysozyme is used as a model system for film deposition of complex organic molecules [1]. Its properties are well-known, it has a significant signal for the mass analysis by MALDI (Matrix-Assisted Laser Desorption/Ionization) and an activity test which is not too complicated. We have recently demonstrated that such films can be produced by laser irradiation without an external matrix, but by utilizing the residual water in lysozyme powder as a matrix [2]. Thin film production of an organic material without an external matrix, e.g. toluene or water ice, reduces the background pressure considerably and facilitates the deposition of organic molecules without compounds between the film molecules and the matrix molecules. Uniform thin films of proteins in a dry environment are difficult to produce in the thickness range of 10-100 nm, and typically these films can be used for sensors and for patterning of organic systems, as well as for other biotechnical and pharmaceutical applications.

In contrast to most inorganic powders, lysozyme powder can be prepared to a target with a pressure that varies by more than one order of magnitude, i.e. from 10 to 130 bar. A standard deposition at 2 J/cm^2 with laser light at 355 nm and a target preparation pressure of 60 bar leads to a deposition of about 6 ng/cm^2 per pulse. The pressed target density at 60 bar is about 0.6 of the crystalline lysozyme density. The target preparation was carried out by pressing the lysozyme powder with a calibrated piston.

The increase of target preparation pressure leads to a considerable enhancement of the deposition rate, which varies by a factor of 3 from the lowest pressure at 10 bar up to the highest at 130 bar. However, the number of intact molecules transferred to the film on a substrate falls off by almost two orders of magnitude in the same pressure interval, as determined by quantitative MALDI and described in ref. [2]. The lysozyme molecules are presumably destroyed by the high preparation pressure already in the target or early in the ablation process. It means that the high deposition rate at high target pressure just reflects the high number of lysozyme fragments rather than intact molecules in the film. Films deposited at high target pressure are thus of limited quality, even though they are faster to produce.

A surprising observation, which could not be quantified, was that a target prepared with low pressure (< 30 bar) mounted with a perpendicular surface fell out of the holder after few laser shots. The thermal impact of the laser pulses was apparently sufficient to eject material at low internal adhesion. At low pressure a target holder mounted with an inclination of 45^o to the horizontal plane had to be used, such that the expanding lysozyme did not fall out. At such low pressure a substantial part (up to 0.5) of the ablated lysozyme was ejected in chunks, which could be collected on a horizontally placed plate below the target.

Most of the films as well as those studied in ref. [1,2] were thus prepared at the optimum target pressure at 60 bar. The influence of the target pressure on these ablation phenomena will be discussed in great detail.

[1] A. Purice, J. Schou, P. Kingshott and M. Dinescu, "Production of active lysozyme films by matrix assisted pulsed laser evaporation at 355 nm", Chem. Phys. Lett. **435**, 350 (2007)

[2] M. Tabetah, A. Matei, C. Constantinescu, N. P. Mortensen, M. Dinescu, J. Schou and L. V. Zhigilei, "The minimum amount of "matrix" needed for matrix-assisted pulsed laser deposition of biomolecules", J. Phys. Chem. B **118**, 13290 (2014)

P-174

Femtosecond laser induced periodic nanostructure on PET surface for controlling of cell elongation

Yuji Sato, Masahiro Tsukamoto, Togo Shinonaga, Takuya Kawa
Joining and welding reserach institute, Osaka university (11-1 Mihogaoka, Ibaraki-shi Osaka, 567-0047, JAPAN)
Graduate school of engineering, Osaka university (1-1 Yamadaoka, Suita-shi, Osaka, 565-0871 JAPAN)
sato@jwri.osaka-u.ac.jp

1. Introduction

Periodic nanostructures were formed on a polyethylene terephthalate (PET) film surface with a femtosecond laser. The PET is clinically applied for biomaterials such as an artificial blood vessel, an artificial ligament, and soft tissue material because of having weather resistance, chemical resistance and bio inert property. When the PET was implanted in human body, proteins and cells were adhered randomly to grow from living body tissues. If the cell adherence is controlled by the material itself, it is possible to enhance the proliferation of living body tissue.

In our previous study, the periodic nanostructures were formed on a TiO2 film by femtosecond laser irradiation. In cell cultivated test on the treated TiO2 film, cells elongations along the grooves of the periodic nanostructures were observed. From the results, it was indicated that the periodic structure could control the direction of cell elongations (1). It was important for control of cells elongation to form tissue orientation and 3D cell cultivation. However, only limited research has been reported to form the periodic structure on plastic surface with an excimer laser or ion beam.

In this study, a new method of periodic nanostructure formation on PET surface was developed with femtosecond laser at wavelength of 1045 nm. In order to evaluate the surface morphology, atomic force microscopy (AFM) analysis was conducted on treated and un-treated PET surface. A cell (MG-63) cultivated test were carried out on the treated and un-treated PET surface.

2. Experimental procedure and results

A commercial femtosecond laser system was used for this experiment. The wavelength, pulse duration, repetition rate and beam diameter of the femtosecond laser were 1035 nm, 400 fs, 100 kHz, and 5 mm, respectively. The PET film was put on between a fused silica glass and a silicon wafer, and then the femtosecond laser was scanned on the silicon wafer passing the PET film at the scanning speed of 27 mm/s. The periodic nanostructure were created the backside of PET film and Si wafer surface. AFM images of the Si wafer surface and backside surface of PET are shown in Fig.1 (a) and (b) for laser fluence of 45 mJ/cm2, (c) and (d) for laser fluence of 50 mJ/cm2, respectively. From the results, the period and height of periodic nanostructures formed on PET 50 mJ/cm^2 were about 650 nm and 80 nm, respectively.

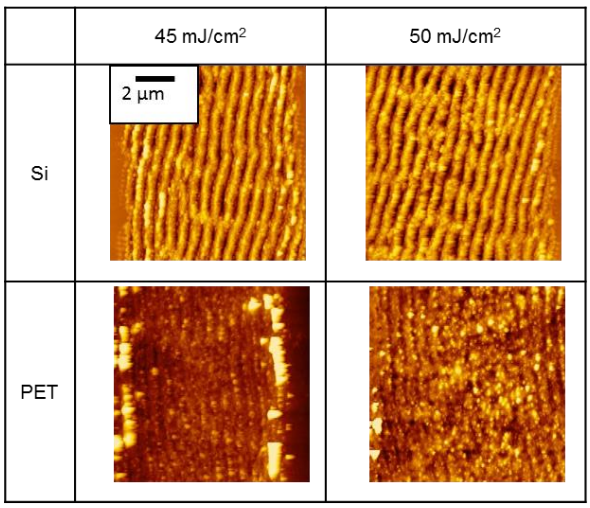

Fig.1 Periodic nanostructure on Si and PET surface with femtosecond laser

(1) T. Shinonaga, M. Tsukamoto, A. Nagai, K. Yamashita, T. Hanawa, M. Takahashi, N. Matsushita, X. Guoqiang and N. Abe, “Cell spreading on titanium dioxide film formed and modified with aerosol beam and femtosecond laser”, Appl. Surf. Sci., Vol. 288, 649-653, (2014).

P-176

Simultaneous laser induced periodic nanostructuring and diffraction-assisted micropatterning of thin polymer films

Esther Rebollar[1], Jaime J. Hernández[2,+], Daniel E. Martínez-Tong[2,#], Mari-Cruz García-Gutiérrez[2], Tiberio A. Ezquerra[2], Marta Castillejo[1]

[1] *Instituto de Química Física Rocasolano (IQFR-CSIC), Serrano119, 28006 Madrid, Spain.*
[2] *Instituto de Estructura de la Materia (IEM-CSIC), Serrano 121, 28006 Madrid, Spain.*
[+] *Present address: Instituto Madrileño de Estudios Avanzados en Nanociencia (IMDEANanociencia), Faraday 9, Ciudad Universitaria de Cantoblanco, 28049 Madrid, Spain.*
[#] *Present address: Département de Physique, Faculté des Sciences, Université libre de Bruxelles (ULB), Boulevard du Triomphe, 1050 Brussels, Belgium*
E-mail: e.rebollar@csic.es

Formation of laser induced periodic surface structures (LIPSS) has been observed on polymers upon irradiation with a linearly polarized laser beam as the result of the interference between the incoming and the surface-scattered waves [1]. Alternatively, irradiation through a mask induces the formation of a diffraction pattern so that the patterning effects depend on the mask size and its distance to the sample [2].

Poly(bisphenol A carbonate) (PBAC) films with a thickness ca. 150 nm and roughness below 1 nm were prepared by spin-coating on silicon wafers. Samples were irradiated through TEM grids with squared holes of 90 and 420 μm size using a Nd:YAG laser (266 nm, 8 ns pulses, 10 Hz). The morphology of the polymer films was characterized by atomic force microscopy (AFM) and surface properties were studied by water contact angle, colloidal probe technique and peak force quantitative nanomechanical mapping (PF-QNM).

Fig. 1 shows an example of the structures obtained on the surface of a PBAC film irradiated through a TEM grid using laser parameters for optimal LIPSS formation. The square diffraction pattern produced by the grid hole is easily noticeable. Circular areas containing LIPSS with several periodicities are formed at the corners of the square, while at the centre we observe LIPSS with periods close to the laser wavelength and parallel to the laser polarization.

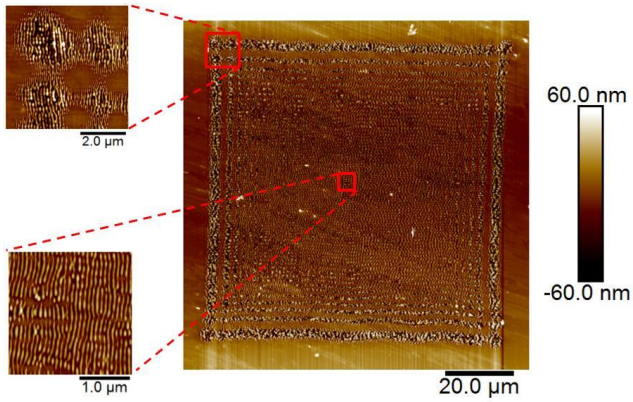

Fig.1. AFM height image of a PBAC film irradiated with 1200 pulses of 266 nm at 7 mJ/cm^2 through a TEM grid (hole size: 90 μm).

When irradiation takes place either at fluences or with number of pulses lower than those required for optimal LIPSS formation, only the diffraction pattern of the mask is imprinted on the film. The water contact angle of samples endowed with only LIPSS (no diffraction mask applied) decreases in comparison to the pristine PBAC sample. However, for diffraction patterned films or with combination of diffraction pattern and LIPSS, the water contact angle increases. The adhesion force measured by the colloidal probe technique is very similar for pristine samples and for samples with only LIPSS. In the case of films with both kinds of structures, a significant increase of the adhesion force is observed close to the edge of the irradiated square for a distance to the edge of ca. 15 μm, where micro- and nanostructures are present. At the nanoscale, no significant differences are observed in the adhesion force.

In conclusion, we have shown that it is possible to simultaneously induce both micro- and nanopatterning of polymer surfaces using a diffraction mask and irradiation conditions optimal for LIPSS formation. Additionally, significant changes of surface properties are observed for areas with micro- and nanostructures.

References

[1] E. Rebollar, S. Pérez, J.J. Hernández, I. Martín-Fabiani, D.R. Rueda, T.A. Ezquerra, and M. Castillejo, "Assessment and Formation Mechanism of Laser Induced Periodic Surface Structures on Polymer Spin-coated Films in Real and Reciprocal Space," Langmuir **27**, 5596 (2011).

[2] E. Haro-Poniatowski, E. Fort, J. P. Lacharme, and C. Ricolleau, "Patterning of nanostructured thin films by structured light illumination", Appl. Phys. Lett. **87**, 143103 (2005).

P-177

Ultrashort laser ablation of load bearing and skull cortical bone tissue: A comparative study

Simon Ashforth[1,2,3], Reece N. Oosterbeek[1,3], Owen Bodley[1,3], M. Cather Simpson[1,2,3,4*]

[1]*The Photon Factory, The University of Auckland, Auckland, New Zealand*

[2]*Department of Physics, The University of Auckland, Auckland, New Zealand*

[3]*The MacDiarmid Institute for Advanced Materials and Nanotechnology and The Dodd Walls Centre for Quantum and Photonic Technologies, New Zealand*

[4]*School of Chemical Sciences, The University of Auckland, Auckland, New Zealand*

** Corresponding author email: c.simpson@auckland.ac.nz*

Ultrashort laser pulses have proved to be a successful tool in many medical applications, however they have yet to experience widespread use for hard tissue ablation. Several studies have been performed to study ultrashort pulsed laser ablation properties of bone tissue and have yielded promising results especially for applications in microsurgical procedures such as in the ear, spine, sinus and skull. Lasers can overcome several problems associated with mechanical tools such as such as drill bit wander [1] and excessive temperature rise (and tissue death) as a result of friction at the tool-tissue interface [2].

Laser pulses in the micro- and nanosecond regime have been found to produce thermally generated defects in bone tissue [3] that result in carbonization around the ablation site and lead to increased healing times paired with a higher risk of infection and bone necrosis [4, 5]. Femtosecond lasers are an excellent candidate for bone cutting and machining due to their 'cold cutting' mechanism; ablation of hard dielectric materials can occur with minimal thermal or mechanical side effects. One of the most important parameters for characterizing laser ablation is the ablation threshold, the minimum amount of energy per unit area required to remove material. Investigations have been conducted in order to determine this parameter in cortical bone and report range of values from ~3.3 Jcm^{-2} to 0.6 Jcm^{-2} [7-9]. However, few studies have been performed comparing the ablation parameters between cortical bone in load bearing and skull structures.

Our previous studies in ex vivo bovine and ovine cortical bone samples in load bearing structures identified the ablation threshold, incubation parameters and optimal factors that affect the laser cutting rate. These results have shown promise with increased accuracy, prevision and no heat damaged to the surrounding structures whilst achieving comparable material removal to conventional microsurgical tools. These results on cortical bone are not necessarily representative for femtosecond laser surgery of all types of bone; the structural characteristics of bones depend upon their location and function within the animal.

This study identifies and ocmpares the ultrashort pulsed laser ablation properties of load bearing bone and skull bone using a Ti:Sapphire (Coherent Legend Elite) femtosecond laser (τ = 110 fs, Repetition Rate = 1 kHz, λ = 800 nm). Using the diameter regression technique, the ablation threshold of cortical load bearing and skull bone is determined and incubation effects characterized. 1 mm ablation cut lines have been utilized to characterize the ablation rates and achievable depths as a function of incident laser power. Ablation features dimensions, volumes and quality of cut and collateral tissue damage were measured using several methods, optical profilometry, scanning electron microscopy and optical microscopy.

References

[1] K. L. Wiggins and S. Malkin, "Drilling of Bone." J. Biomech. **9**, 553 (1976)

[2] K. M. Sasaki, A. Aoki, S. Ichinose and I. Ishikawa, "Ultrastructural analysis of bone tissue irradiated by Er:YAG laser." Lasers Surg. Med. **31** 322 (2002)K. M. Sasaki, A. Aoki, S. Ichinose and I. Ishikawa, "Ultrastructural analysis of bone tissue irradiated by Er:YAG laser." Lasers Surg. Med. **31** 322 (2002)

[3] M. D. McKee, "Effects of CO2-laser irradiation in-vivo on rat alveolar bone and incisor enamel, dentin and pulp." J. Dent. Res. **72**, 1406 (1993)

[4] G. W. Allen and J. C. Adrian, "Effects of carbon dioxide laser radiation on bone: An initial report." Mil. Med. **146**, 120 (1981)

[5] B. Girard, D. Yu, M. R. Armstrong, B. C. Wilson, C. M. L. Clokie and R. J. D. Miller, "Effects of femtosecond laser irradiation on osseous tissues." Lasers Surg. Med. **39**, 273 (2007)

[6] J. Neev, L. B. Da Silva, M. D. Feit, M. D. Perry, A. M. Rubenchik, and B. C. Stuart, "Ultrashort pulse lasers for hard tissue ablation," IEEE J. Sel. Top. Quantum Electron. **2(4)**, 790 (1996).

[7] L. T. Cangueiro, R. Vilar, A. M. Botelho do Rego, and V. S. F. Muralha, "Femtosecond laser ablation of bovine cortical bone," J. Biomed. Opt. **17(12)**, 125005 (2012).

[8] V. Wieger, S. Zoppel, and E. Wintner, "Ultrashort pulse laser osteotomy," Laser Phys. **17(4)**, 438 (2007)

[9] B. Emigh, R. An, E. M. Hsu, T. H. R. Crawford, H. K. Haugen, G. R. Wohl, J. E. Hayward, and Q. Fang, "Porcine cortical bone ablation by ultrashort pulsed laser irradiation," J. Biomed. Opt. **17(2)**, 028001 (2012).

P-179

Laser ablation of UV curing polymer and compositions

E. Loktionov[1], A. Pavlov[1], Yu. Protasov[1], V. Telekh[1]
[1]Bauman Moscow State Technical University, 2nd Baumanskaya str. 5-1, 105005 Moscow, Russia
E-mail address: stcpe@bmstu.ru

1. Introduction

Solid rather than liquid active media are used in pulsed laser plasmatrons despite sophisticated transportation and dosing system need for a long-term operation. Liquid media could be more preferable due to transportation and dosing (down to 10^{-14} l) being well developed, but plasma generation of those results in intensive droplet formation and kinetic energy losses. Combination of liquids transportation advantages and solids plasma generation efficiency might resolve this trade-off. Liquid-to-solid transition can be induced by cooling down to sublimation temperature, thermo-, photo- or electron induced polymerization (curing). Light cured polymers seem to be very useful as active media for plasma generators, since they can be solidified very fast (ca. 30 ms) just before impact.

2. Experimental conditions and results

For the first time we have investigated mass flow rates, momentum coupling coefficient, specific impulse and energy efficiency (at 30 J/cm^2) of both liquid and solid phase of acrylic UV-ink ca. 0.5 μl droplets cured by 405 nm laser diode under 213, 266, 355, 532 and 1064 nm nanosecond (12-17 ns) laser irradiation at ambient conditions. Except mechanical performance, curing could be identified from photoluminescence and Raman spectra.

At 1064 nm irradiation either glass substrate or even underlying PVDF force sensor, not polymer were damaged due to low spectral absorption. At second harmonic efficiency performance the lowest of obtained. At 266 nm irradiation solid and liquid phases of investigated UV-inks have demonstrated about similar characteristics relation known for water and ice: liquid phase had greater ablation threshold (4.67 vs. 1.02 J/cm^2 – the lowest of obtained), mass flow rate (6.77 vs. 0.35 mg/J) and momentum coupling coefficient (0.933 vs. 0.167 mN/W), solid phase had greater specific impulse (476 vs. 138 s), and energy efficiency was about equal, data obtained for cured ink match well those known for PMMA. At 213 nm an unexpected ablation threshold increase was observed, that could be explained by intensive luminescence energy losses – it's 5 times more intensive for liquid ink and results in about same ratio of ablation thresholds of liquid to cured states the highest of obtained.

The most interesting results were obtained at 355 nm irradiation that matches curing optimum specified for this ink (365±15 nm). Data on specific ablated mass and recoil momentum show that high-power pulsed radiation induces curing (its rate is proportional to square root of radiation intensity) at nanosecond scale, so irradiation performance became about equal for initially solid and cured medium for fluence over 40 J/cm^2 (Fig. 1).

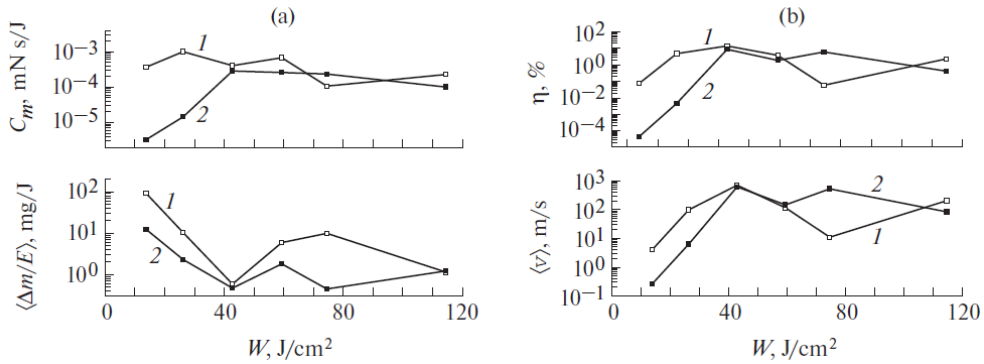

Fig. 1. The dependence of characteristics of the laser ablation efficiency of a PPC on the energy density of radiation at λ3 ~ 355 nm

3. Conclusions

The obtained results demonstrate that light cured polymers can be used as a working media for laser plasmatrons. In case of high-power irradiation with a wavelength close to an optimal one for photopolymerization, no preliminary curing illumination is needed, and laser-to-plasma kinetic energy efficiency can be even greater than for initially cured medium. Use of light curing polymers makes special active media (incl. heterogeneous and homogenous mixes) preparation, transportation and dosing much easier.

The results have been obtained at "Beam-M" (RFMEFI59014X0001) facility at BMSTU.

P-180

Periodic Nanostructures Produced on Ti Substrate with Femtosecond Laser for Controlling of Cell Spreading in Multi Direction

T. Kawa[1], M. Tsukamoto[2], T. Shinonaga[2], P. Chen[3], A. Nagai[3], T. Hanawa[3],

[1]Graduate School of Engineering, Osaka University, 1-1 Yamadaoka, Suita, Osaka 565-0871, Japan
[2]Joining and Welding Research Institute, Osaka University, 11-1, Mihogaoka, Ibaraki, Osaka, 567-0047, Japan
[3]Institute of Biomaterials and Bioengineering, Tokyo Medical and Dental University, 2-3-10 Kanda-Surugadai Chiyoda-ku, Tokyo 101-0062, Japan

kawa@jwri.osaka-u.ac.jp

Titanium (Ti) is one of the most used biomaterials in metals, because of its high corrosion resistance and strength. However, Ti has problems for bioinert, so it is necessary to add new function to Ti substrates. Recently, it is known that microstructures formation on material was one of the useful method for controlling the cell spreading[1]. Previously, we reported that the periodic nanostructures lying perpendicular to the laser electric field polarization can be formed on TiO_2 film with a femtosecond laser using the fundamental wavelength of 775 nm[2]. Cell tests indicated that cell spreading occurs along the grooves of the periodic nanostructures[2]. However, control of cell spreading on periodic nanostructure of Ti substrates has not yet been investigated. We also focused on the direction of grooves of periodic nanostructures. The grooves of periodic nanostructures might be changed by controlling the laser electric field polarization vector *E*. If periodic nanostructures with multi directional grooves were formed on Ti substrates, the direction of cell spreading might be controlled in multi direction. The control of cell spreading in multi direction on Ti substrates would contribute to the creation of new functional biomaterials.

In this study, we try to create periodic nanostructures with multi directional grooves on Ti surface by scanning of the femtosecond laser spot while the laser electric field polarization *E* was controled. We also examined cell spreading on the Ti substrates by using the periodic nanostructures with multi directional grooves. Commercial femtosecond Ti: sapphire laser system was used in the experiment. The wavelength, repetition rate and pulse duration of the femtosecond laser were 775 nm, 1 kHz and 150 fs, respectively. SEM images of the Ti substrates after scanning of the femtosecond laser spot were shown in Fig. 1. As Fig. 1 shows, periodic nanostructures, lying perpendicular to the laser electric field polarization vector *E*, were clearly formed on the irradiated Ti substrates. The groove directions of the periodic nanostructures were changed by controlling the laser electric field polarization vector. Periodic nanostructures with multi directional grooves on the Ti substrates were formed. Cell testing revealed that cells spread along the grooves of the periodic nanostructure. Then, cell spreading in multi direction was also observed. These results suggested that the direction of cell spreading on Ti was controlled by formation of periodic nanostructure with the multi directional grooves.

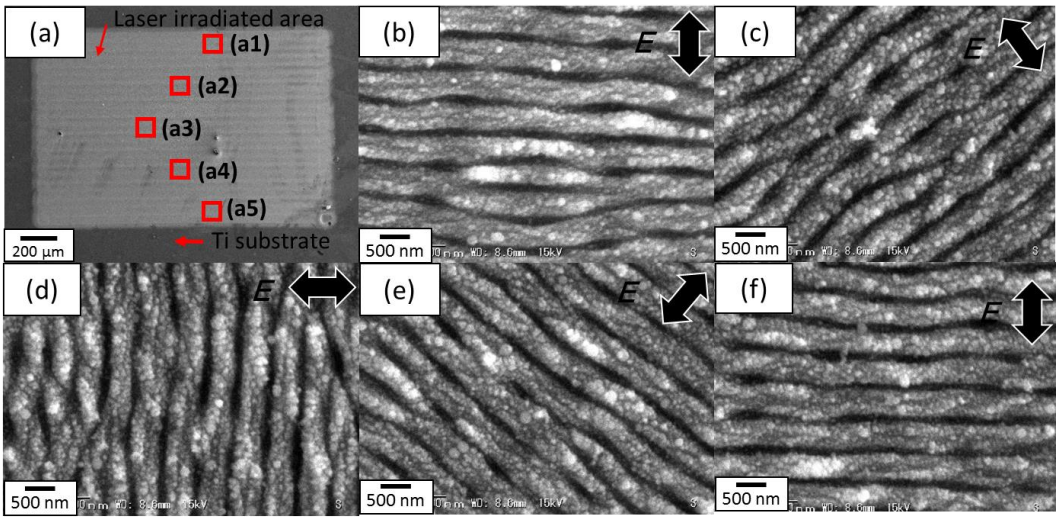

Fig. 1. (a)SEM image of Ti substrate after scanning of the femtosecond laser spot. High magnification SEM images of (a1),(a2),(a3),(a4) and (a5) in (a) are shown in (b),(c),(d) ,(e) and (f), respectively. *E* is laser electric field polarization vector.

[1] Yoshinari: Inplant Materials, Implant Surfaces and Interface Processes Part 3. Implant surfaces and interface processes, The Journal of the Tokyo Dental College Society, **103**, No.7, 565-572 (2003)
[2] Shinonaga, T et al.: Cell spreading on titanium dioxide film formed and modified with aerosol beam and femtosecond laser, Applied Surface Science, **288**, 649-653 (2014)

P-181

The influence of pulse duration, wavelength and fluence on laser induced structure formation from the viewpoint of dental applications

Anett Gárdián[1], Roland Masa[1], Judit Budai[2], Miklós Füle[3], Kinga Turzó[1], Zsolt Tóth[1]

[1]Department of Oral Biology and Experimental Dental Research, Faculty of Dentistry, University of Szeged, H-6720, Tisza Lajos krt. 83.
[2]Department of Optics and Quantum Electronics, University of Szeged, H-6725 Szeged, Dóm tér 9.
[3]High Intensity Laser Laboratory, Department of Experimental Physics, University of Szeged, H-6725 Szeged, Dóm tér 9.
Corresponding Author e-mail address: miklos.fule@gmail.com

1. Introduction

Titanium and its alloys are the most preferred materials in dental implantology due to their biocompatible feature. Dental implants are more and more used in dentistry to replace lost teeth. Mechanical roughness of the implant surface plays a significant role in osseointegration. Increased contact area can strengthen the connection between the implant and the bone. To determine the nano- and microscale roughness for achieving a better attachment of bone forming cells is an up-to-date demand.

Surface structuring by lasers is widely investigated from the viewpoint of dental applications e.g. [1]. The underlying mechanisms of structure formation are extensively studied, especially in the case of subpicosecond laser – matter interaction. In our previous works [2-4] surface morphologies induced on silicon by different lasers were investigated. It is still under discussion how structure evolution is influenced by interference phenomena and capillary wave effects.

The aim of this work is to find those parameters, which have remarkable influence on the nano- and micro-scale roughness of titanium surfaces and finally control the surface structures by tuning the appropriate process parameters.

2. Materials and Methods

Structure formation by titanium-sapphire and KrF excimer laser irradiation on silicon and titanium samples are studied under the same conditions. For the investigation of structure forming effects the pulse duration and the fluence are varied. Titanium-sapphire laser provides pulses in the near infrared region (central wavelength: 780 nm) with a tuneable pulse duration from 30 fs to 30 ps. The other applied laser source is a frequency doubled distributed-feedback dye-laser, which pulses are amplified by a KrF excimer laser delivering pulses at 248 nm from 200 fs to 20 ps. Structured surfaces have been investigated by scanning electron microscopy (SEM). SEM images were analysed with fast Fourier transformation (FFT) and based on this the periodicities (the characteristic sizes) are evaluated.

3. Results

Interference effects have been clearly observed when using 2-5 laser pulses. Below ablation threshold linear patterns appear while slightly above ablation threshold circular waves surround the forming splashes. In both cases the scale length is approximately the same as the wavelength of the applied laser. Therefore the characteristic size of the resulting morphology strongly depends on the wavelength. The scale length slightly decreases and its amplitude increases with increasing pulse number below ablation threshold. Illuminating by five laser pulses and exceeding the ablation threshold the surface becomes irregularly rough. Pulse durations influence the contrast and the amplitude of the forming periodic surface structures. In the future cell-culture experiments will be done to test the biocompatibility of these samples.

References

[1] M. Bereznai, I. Pelsőczi, Z. Tóth, K. Turzó, M. Radnai, Z. Bor, and A. Fazekas, "Surface modifications induced by ns and sub-ps excimer laser pulses on titanium implant material", Biomat. **24,** 4197 (2003).

[2] M. Füle, A. Gárdián, J. Budai, and Z. Tóth, "Comparative Study of the Surface Nanostructure Formation on Different Surfaces Generated by Low Number of fs Laser Pulses", J. Laser Micro Nanoen. **10,** 74 (2015).

[3] Z. Tóth, I. Hanyecz, A. Gárdián, J. Budai, J. Csontos, Z. Pápa, and M. Füle, "Ellipsometric analysis of silicon surfaces textured by ns and sub-ps KrF laser pulses", Thin Solid Films, **571**, 631 (2014).

[4] M. Füle, A. Gárdián, J. Csontos, J. Budai, and Z. Tóth, "Ti: Sapphire laser ablation of silicon in different ambients", J. Laser Micro Nanoen. **9**, 119 (2014).

P-182

Patterning of organic semiconductors for photovoltaic applications by LIFT technology

Přemysl Fitl[1,2], Martin Vrňata[1], Jan Vlček[1,2], David Tomeček[1], Dušan Kopecký[1], Michal Novotný[2] and Ján Lančok[2]

[1] Dept. of Physics and Measurement, Institute of Chemical Technology Prague, Technická 3, 166 27, Prague 6, Czech Republic,
[2] Dept. of Analysis of Functional Materials, Institute of Physics AS CR v.v.i Na Slovance 1999/2, 182 21 Prague, Czech Republic
E-mail:fitlp@vscht.cz

Laser Induced Forward Transfer (LIFT) is a widely used technique for elegant deposition and patterning of various materials (eg. Metals, oxides, organic substances and even biological material). The most typical attribute of LIFT technique (as presented by many authors) is utilization of short laser pulses with duration from ps to tens of ns with very high energy per pulse. Such approach requires of usage of expensive laser sources. Our work is focused to alternative instrumentation of LIFT - possibilities of usage of continuous wave (CW) lasers for local deposition and patterning of organic semiconductors.

The source substrates were prepared as follows: Thin glass slides with sputtered metal layer (gold, platinum, copper, silver - thickness ~ 100 nm) were cleaned and dried. Side with sputtered metal was then covered with a thin layer of purified organic semiconductors - Perylene, Perylene anhydride, Zn and Sm Phthalocyanines, AlQ3 and Fullerene C60, deposited by organic molecular evaporation in high vacuum chamber (10-5 Pa, dep. Rate ~ 0.1-3nm/min, substrate temp. 20 – 300 °C). The temperature of deposition source and substrate was selected for each substance so as to achieve optimal growth rate and to avoid thermal decomposition of materials. In the next step CW laser depositions were carried out from these substrates. The deposition apparatus include micro CNC machine (minimal step adjustable to 300 nm) equipped with the semiconductor laser (405 nm, 10 - 50 mW, spot 6 microns) in continual mode and focusing optics. The distance between source substrate and target (i.e. glass, silicon or alumina sensor substrates) was varied between 1-100 micrometers. Deposition process was held in an inert gas (Argon, Nitrogen) at atmospheric pressure. Morphology and microstructure were studied by optical, electron microscopy and AFM. Chemical composition of deposited structures was studied by FTIR and compared with that of source substances. It was proved that chemical structure of all chosen substances is not affected by this deposition technique. The best lateral resolution of prepared structures was obtained for source layer thickness of 100-150 nm. Employing our CW-LIFT technique we are able to achieve precise and reproducible laser transfer of organic semiconductors to the target substrate with lateral structural resolution of 14 microns.

Selected substances are widely used in the form of thin film for novel organic photovoltaic devices. CW-LIFT deposition and patterning could improve conversion efficiency and other properties of these devices. We can make an assumption that CW-LIFT technique could be used also for other organic semiconductors used in organic photovoltaics which can be deposited by organic molecular evaporation.

Acknowledgements
This work was supported by project GA CR no. 14-10279S

P-183

Human mesenchymal stem cells interaction with nano and microtextured surfaces

Valentina Dinca[1], Livia Elena Sima[2], Laurentiu Rusen[1], Iulia Anghel[1] and Maria Dinescu[3]
1National Institute for Lasers, Plasma and Radiation Physics, Bucharest, Romania
2 Department of Molecular Cell Biology, Institute of Biochemistry, Romanian Academy, *Bucharest, Romania*
E-mail: valentina.dinca@inflpr.ro

Abstract

Cell anatomy and function can be regulated by various physical stimuli, such as the architecture/topography of the substrates used for cell cultures. In this work, various nano- and micro-scale peaks and troughs topographies were obtained by femtosecond laser direct texturing. The obtained structures were analyzed by scanning electron microscopy, atomic force microscopy, X-ray diffraction. The contact angle measurements revealed a change in the hydrophilic character of the unstructured area towards hydrophobic character when texturing was applied.
The contact guidance and morphological parameters of human mesenchymal stem cells (hMSCs) adhering to with either steep or curved edges was quantified. Analysis by fluorescence and scanning electron microscopy showed that on peaks and troughs microtopographies, cells were aligned and contacted intimately the underlying granulated structures. The minimum depth to induce cell alignment response was 0.5 μm. The efficacy of cell nuclei alignment along the troughs was significantly higher on curved than on steep topographies. Between the more restrictive straight edges a decrease in nuclei width was evidenced. Our results indicate that substrate micropattern features play a key role in hMSCs spreading response and more importantly that even smoother patterns than grooves and ridges are able to provide contact guidance. Our results demonstrate potential use of laser micropatterned Zirconia to modulate cell fate during bone implantation.

Funding and acknowledgments: This work was supported by a grant of the Romanian National Authority for Scientific Research, CNCS – UEFISCDI, under the project PN-II-PT-PCCA 239/2014.

P-184

Sericin-tethered graphene artificial composite matrix obtained by MAPLE for MC3T3-E1 pre-osteoblasts studies

Valentina Dinca[1], Valentina Mitran[2], Nicu-Doinel Scarisoreanu[1], Raluca Nicoleta Ion[2], Patricia Neacsu[2], Laurentiu Rusen[1], Simona Brajnicov[1], Anca Bonciu[1,3], Valentin Ion[1], Anisoara Cimpean[2], Maria Dinescu[1]

1National Institute for Lasers, Plasma and Radiation Physics, Bucharest, Romania
2 University of Bucharest - Department of Biochemistry and Molecular Biology, Bucharest, Romania
Physics Faculty, Bucharest University, Bucharest,Romania
E-mail: valentina.dinca@inflpr.ro

Abstract

An artificial matrix consisting of graphene and sericin was obtained on titanium based alloy substrates via Matrix Assisted Pulsed Laser Evaporation technique. The morphology and topography of the artificial matrix from atomic force microscopy (AFM) and scanning electron microscopy (SEM) analysis was characterized by porous micro and nano cavities, having an average roughness of 388 nm. FTIR spectra showed no significant distorsions of the functional bands of the deposited matrices when compared with control surfaces. The degradability of the samples was quantified by AFM and ellipsometry measurements.

The biocompatibility, and cellular behaviour of the osteoblasts on the graphene-sericin matrix were compared to those of cells cultured on Ti based alloys and sericin alone. Focal adhesion molecule (vinculin) expression was analyzed from the fluorescence images showing highly activated areas at when cultured on the artificial matrix. The release of lactate dehydrogenase (LDH) and LIVE/DEAD assay showed no cytotoxic effect and a sustained cell survival on the analyzed surfaces. To this end, in this work, a biocompatible artificial composite matrix with potential in bone tissue engineering applications was engineered.

Funding and acknowledgments: This work was supported by a grant of the Romanian National Authority for Scientific Research, CNCS – UEFISCDI, under the project PN-II-PT-PCCA 213/2014.

P-185

Indirect laser surgery

V. A. Kamensky[1], V. V. Elagin[2], M. A. Shakhova[2], V. V. Kazakov[1], V. Bredikhin[1], N. Bityurin[1]
[1]Institute of Applied Physics, RAS, Nizhniy Novgorod, Russia
[2]Nizhniy Novgorod State Medical Academy, Nizhniy Novgorod, Russia
E-mail: bit@appl.sci-nnov.ru

In direct laser surgery, one employs the laser radiation for direct processing of a tissue. In indirect laser surgery, the laser radiation is employed to modify the tissue not directly, for instant, by heating the strongly absorbing tip at the end of the optical fiber using this heated tip for the tissue resection.
In the present communication, we show that the absorbing tip allows the decrease in the power of effective cutting of the laser scalpel at the wavelength of 0.97 μm. It changes the resection speed as well as the characteristics of the damage of the tissues adjacent to the incision in experiments on model media and experimental animals.
The performed research demonstrates that a laser scalpel with a fiber tip having a strongly absorbing coating operating with the output power of 3 W proves to be most efficient for making contact incisions. It provides maximum tissue cutting speed and small coagulation area and, consequently, less thermal damage of the surrounding tissues. The morphological study of the laser incision area shows that the depth of thermally damaged region in the center of the exposure area decreases from 901 μm with the use of a clear fiber tip to 417 μm in the case of a resin and carbon coating.
We investigate the acoustic phenomena accompanying the heating of the tip immersed into a water medium. We analyze the spectrum of acoustical noise in the frequency band of several MHz. This noise can relay on the generation of the small bubbles that can be useful for some surgery processes.
This work was supported by the RSF grant No. 14-15-00840.

P-186

Hybrid subtractive and additive 3D microprocessing using femtosecond laser for functional biochip fabrication

Koji Sugioka, Jian Xu, Felix Sima, Jian Xu, Dong Wu, Katsumi Midorikawa
RIKEN Center for Advanced Photonics, Wako, Saitama 351-0198, Japan
E-mail: ksugioka@riken.jp

Extremely high peak intensity achieved by femtosecond laser allows nonlinear multiphoton absorption to be induced in transparent materials, which provides versatility in terms of the materials that can be processed. More interestingly, irradiation with tightly focused femtosecond laser pulses inside transparent materials makes three-dimensional (3D) micro- and nanofabrication possible due to efficient confinement of the nonlinear interactions within the focal volume. Using this feature, both types of subtractive and additive 3D manufacturing are available. Specifically, the former process involves femtosecond laser internal modification followed by wet chemical etching (Femtosecond Laser Assisted Wet Etching: FLAE) which directly fabricate 3D microfluidic structures inside glass, while the latter one is two-photon polymerization (TPP) of photocurable resin to create 3D polymer micro and nanostructures even with complicated geometries. In this paper, we propose to conjugate these two processes to further enhance performance of femtosecond laser processing for fabrication of highly functional biochips [1-3].

The hybrid process consists of two main steps. The first step is to fabricate 3D microfluidic structure by FLAE of photosensitive Foturan glass. The second step is to integrate functional microcomponents into the resulting glass 3D microfluidic structure for device functionalization by the TPP procedure.

This technique was applied to fabricate functional biochips to demonstrate efficient mixing of different kinds of fluids, on-chip synthesis of nanomaterials, and parallel cell detection and counting. Figure 1 (a) shows a center-pass optofluidic microlens array consisting of seven microlenses and an M-shaped confining wall with 9 μm-diameter apertures fabricated by TPP for the cell counting. The center-pass optofluidic microlens array is integrated in the closed Y-shaped glass microfluidic channel fabricated by FLAE as shown in Fig. 1 (b). Each microlens produces approximately the same intensity at the focal positions (within ±5%) under white-light illumination, while the confining wall restricts 6~8 μm-width cells to passing through the edges of two adjacent microlenses resulting in great enhancement of the probability in cell detection. The device demonstrates coupling-free parallel cell counting with a 100% success rate by monitoring the optical intensity variations at each spot. As a result, this method features both easy operation and high performance. Furthermore, the confining wall can filter deformed cells having larger width.

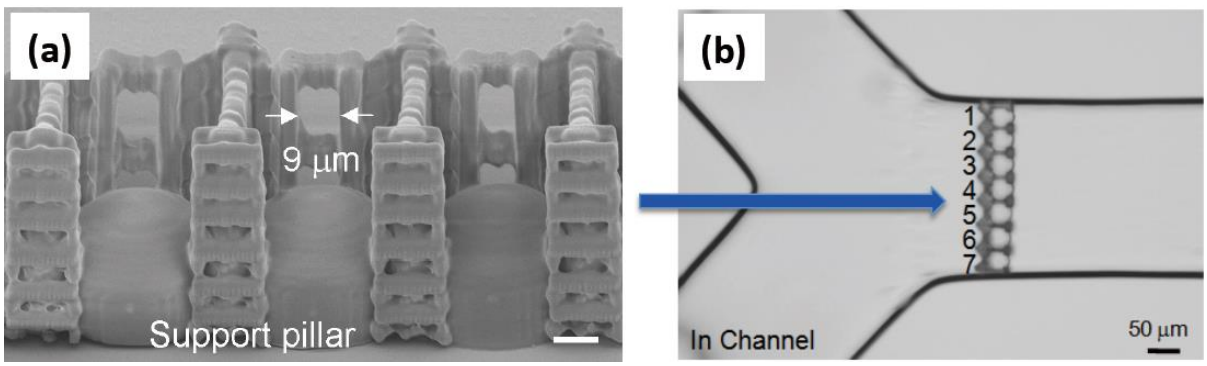

Fig. 1. (a) SEM image of a center-pass optofluidic microlens array consisting of seven microlenses and an M-shaped confining wall with 9 μm-diameter apertures fabricated on glass surface by TPP. (b) Optical microscope image of 3D glass microfluidics integrated with the center-pass optofluidic microlens array for coupling-free parallel cell counting.

References

[1] D. Wu, S. Wu, J. Xu, L. Niu, K. Midorikawa, and K. Sugioka, "Hybrid femtosecond laser microfabrication to achieve true 3D glass/polymer composite biochips with multiscale features and high performance: the concept of ship-in-a-bottle biochip", Laser Photon. Rev. **8**, 458-467 (2014).

[2] D. Wu, J. Xu, L. Niu, S. Wu, K. Midorikawa, and K. Sugioka, "In-channel integration of designable microoptical devices using flat scaffold-supported femtosecond-laser microfabrication for coupling-free optofluidic cell counting", Light Sci. Appl. **4**, e228 (2015).

[3] D. Wu, L. G. Niu, S. Z. Wu, J. Xu, K. Midorikawa, and K. Sugioka, "Ship-in-a-bottle femtosecond laser integration of optofluidic microlens arrays with center-pass units enabling coupling-free parallel cell counting with 100% success rate," Lab Chip (2015). DOI: 10.1039/c4lc01439a

P-187

Development of a real time mass spectrometry instrument for non-invasive ex-vivo and in-vivo analysis based on IR laser ablation

B. Fatou[1,2], M. Wisztorski[1], C.Focsa[2], M. Salzet[1], M. Ziskind[2], I. Fournier[1]

[1]*Laboratoire Protéomique, Réponse Inflammatoire et Spectrométrie de Masse, Université Lille 1, F-59655 Villeneuve d'Ascq, France*

[2]*Laboratoire de Physique des Lasers, Atomes et Molécules, Université Lille 1, F-59655 Villeneuve d'Ascq Cedex, France*

E-mail: michael.ziskind@univ-lille1.fr

Since the past decade there has been an increasing interest for the development of various ambient mass spectrometry (MS) techniques allowing for ex-vivo tissue analysis by microsampling[1-4]. However, most of these techniques are incompatible with in-vivo conditions. Currently, only Rapid Evaporative Ionization MS (REIMS) using standard electrosurgical tools for ionization was demonstrated as solution for in-vivo medical conditions[5].

Here, we want to explore the potential of another solution based on the laser ablation of tissues, using a ns-pulsed IR Optical Parametric Oscillator (OPO) tuned at 2.94 µm. The ablated material is collected by suction and transferred to the MS instrument through a PTFE tubing connected to the inlet of a 3D ion trap MS instrument just directly in front of the transfer capillary.

The effect of various parameters including laser energy, irradiation time, aspiration flow rate or MS tuning was studied using model bovine liver tissue samples. The instrument was then tested for real-time in-vivo analysis by studying skin molecular profiles from fingers of different people.

The obtained results show the feasibility of the technology as well as its low invasiveness (damages and pain) character which clearly demonstrates its interest for clinical applications.

[1] Z. Takats, J. M. Wiseman, B. Gologan, R.G. Cooks, "Mass Spectrometry Sampling Under Ambient Conditions with Desorption Electrospray Ionization" Science **306**, 471 (2004)

[2] P.J. Roach, J. Laskin, A. Laskin, " Nanospray desorption electrospray ionization: an ambient method for liquid-extraction surface sampling in mass spectrometry", Analyst **135**, 2233 (2010)

[3] J. A. Stolee, A. Vertes, "Toward Single-Cell Analysis by Plume Collimation in Laser Ablation Electrospray Ionization Mass Spectrometry", Anal. Chem. **85**, 3592 (2013)

[4] O.S. Ovchinnikova, M. Lorenz, V. Kertesz, G.J. Van Berkel, "Combining Laser Ablation/Liquid Phase Collection Surface Sampling and High-Performance Liquid Chromatography−Electrospray Ionization-Mass Spectrometry" Anal. Chem. **85**, 10211 (2013)

[5] K.-C. Schäfer, T. Szaniszlo, S. Gûnther, J. Balog, J. Dénes, M. Keseru, B. Dezso, M. Toth, B. Spengler, Z. Takats, " In situ, real-time identification of biological tissues by ultraviolet and infrared laser desorption ionization mass spectrometry" Anal. Chem. **83**, 1632 (2011)

P-188

Interfacial Indentation Test of Laser Surface Modified AISI H13 tool steel thermal barrier coatings

M. S. Reza[1], S. N. Aqida[1,2]

[1]Faculty of Mechanical Engineering, Universiti Malaysia Pahang, 26600 Pekan, Pahang, Malaysia
[2]Automotive Engineering Centre, Universiti Malaysia Pahang, 26600 Pekan, Pahang, Malaysia
E-mail: mdreza@ump.edu.my

Adhesion is one of the most important parameters which influence the development of thermal spray coatings and interfacial indentation test (IIT) was used to evaluate adhesion of coatings. The effect of spraying parameters on the coatings adhesion of laser surface modification of H13 tool steel as well as its toughness was investigated. The investigation deals with the application of a continuous CO2 laser to laser surface modified H13 tool steel surface and consequently deposited by Atmospheric Plasma Spray (APS). Different laser power and scanning speed were investigated in order to improve the overall mechanical property of H13 tool steel surface. The changes in mechanical properties were investigated in terms of its' micro hardness and micro-structure using Micro Hardness Tester Machine and optical microscope. Improvements in micro hardness is performed at higher laser power and moderate scanning speed. Too much increase in power density can be detrimental to the final property of H13 surface and too slow scanning speed increase overlap percentage causes decrease in mechanical properties i.e. micro hardness. Further, the experiment continues with the deposition of thermal barrier coatings (TBC) of bond coat and top coat using Atmospheric Plasma Spray (APS) technique. Three controlled factors of input current, powder feed rate and stand-off-distance were investigated to coat the TBC layer. The coating thickness and percentage of porosity were measured using IM7000 inverted optical microscope while fracture toughness of between coatings were measured using MMT-X7 Matsuzawa Hardness Tester Machine with Vickers Indenter. The microscopy findings indicated variations of Fracture Toughness, K with coating porosity and coating thickness at different parameters settings. The obtained results revealed that the adhesion increase with the decrease in porosity and increase in coating thickness of bond coat and top coat. These findings are significant to enhance surface properties of semi-solid forming H13 tool steel die and prolong its' lifecycle.

Index Terms— Atmospheric plasma spray, Fracture Toughness, K, yttria stabilized zirconia, laser surface modification, surface roughness

P-189

Laser induced breakdown spectroscopy for in situ elemental analysis of deep sea minerals

Sung Hyun Pyun[1], Dae Hoon Lee[1], Kwan Tae Kim[1] and Young Hoon Song[1]
[1]*Korea Institute of Machinery and Materials, Daejeon 305-303, South Korea*
E-mail: shpyun@kimm.re.kr

1. Introduction

A few countries that possess manned deep sea submarines thrives to explore and develop marine resources including manganese pavements, nodules and hydrothermal crust deposits. Those precious mineral resources are developed on a small scale and sparsely distributed on the ocean floor. Thus, the detailed mineral survey is needed, obtaining mineral specimens by using a robotic arm for further elemental analysis before determining the mining localities. Considering that the allowed time for underwater navigation is extremely limited and the mineral sampling process using a robotic arm is time-consuming, a technology for real-time, in situ elemental analysis of deep sea mineral is becoming a necessity. Laser induced breakdown spectroscopy (LIBS) has been widely used for real-time elemental analysis of various kinds of materials in solid, liquid and gaseous state [1]. In this study, we developed a LIBS system for preliminary study on the in situ analysis of deep sea minerals.

2. Experiment

A 1064 nm Nd:YAG Q-switched laser with the pulse energy of up to 400 mJ and the pulse duration of 8 ns was used to generate up to 50 MW for effective plasma formation and evolution on the sample surfaces. The pulsed laser beam is focused (100 mm focal length) to the surface of deep sea mineral samples including manganese pavements and hydrothermal deposits. The light emitted from the plasma generated right above the surface is collected and delivered through the two plano-convex lenses to the optical fiber which is then connected to the spectrometer of a spectral resolution of 0.1 nm. A double pulse Nd:YAG laser at 532 nm was also used to enhance the emission signal. The plasma temperature, volume and ion density is increased as well as the decay time of line intensities when double pulse LIBS is applied [2]. The first pulse is mainly used for ablating the material, while the second pulse is irradiated to the plume of the first pulse producing finer aerosol [3]. A delay generator of a 10 ns resolution is coupled to the double pulse laser to control the delay time between the two pulses.

3. Results

The temporal evolution of laser induced plasma and its decay on the target surface is examined using a high speed camera. When using the double pulse laser of 532 nm wavelength, the time interval between the initial and the latter pulse was optimized for maximum SNR of the plasma emission signal. We successfully detected several key elements, including Mn, Fe, Co, Ni and Cu from the several deep sea mineral samples including manganese pavements and hydrothermal deposits. One of the measured emission spectra of manganese pavements using a 200 mJ pulse with 8 ns pulse duration is described in Fig. 1.

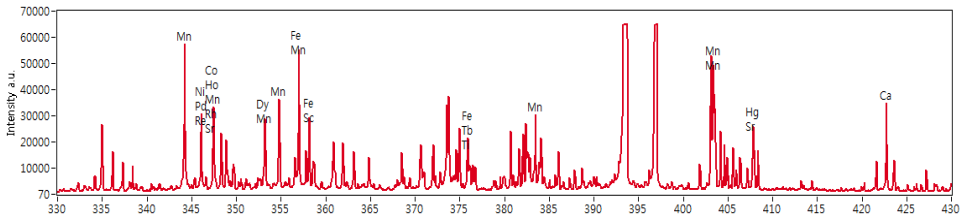

Fig. 1. Measured emission spectrum of a deep sea manganese pavement

4. Summary

We utilized the LIBS technique to unveil the possibility of real-time, in situ elemental analysis of deep sea minerals including manganese pavements and hydrothermal deposits using a single pulse and double pulse Nd:YAG laser at 1064 nm and 532 nm respectively. Our preliminary results strongly support the potential of LIBS application for in situ analysis of deep sea minerals.

5. References

[1] D.W. Hahn, N. Omenetto, "Laser-induced breakdown spectroscopy (LIBS), Part I: Review of basic diagnostics and plasma-particle interactions: Still-challenging issues within the analytical plasma community, Applied Spectroscopy **64**, No 12 (2010).
[2] V.I. Babushok, F.C. DeLucia Jr., J.L. Gottfried, C.A. Munson, A.W. Miziolek, "Double pulse laser ablation and plasma: Laser induced breakdown spectroscopy signal enhancement," Spectrochim. Acta PartB **61**, 999-1014 (2006).
[3] J. Gonzalez, C. Liu, J. Yoo, X. Mao, R. E. Russo, " Double-pulse laser ablation inductively coupled plasma mass spectroscopy," Spectrochim. Acta Part B **60**, 27-31 (2005).

P-190

Laser spectroscopy for noninvasive gas monitoring in patients with dysfunctions

C. Popa[1,2], M. Petrus[1], A. M. Bratu[1], M. Patachia[1], S. Banita[1], C. Matei[1], D. C. Dumitras[1]

[1]*National Institute for Laser, Plasma and Radiation Physics, Laser Department, 409 Atomistilor St., PO Box MG-36, 077125 Magurele, Romania*

[2]*University Politehnica of Bucharest, Faculty of Applied Sciences, Physics Department, 313 Splaiul Independentei, Bucharest- 060042, Romania*

E-mail: cristina.achim@inflpr.ro

The quest for non-invasive and real-time monitoring tools is a characteristic of the modern medicine. The technique that is developed in this research complies with this requirement, ensuring the advantages of health state assessment by monitoring the evolution of gaseous biomarkers in human body. We chose to characterize by breath air the assessment of ammonia and ethylene in mental disorders, but the techniques can be easily extended to other pathological issues [1-3].

The first objective of the present study was to analyze the oxidative stress marker in breath samples of patients with mental disorder before and after the treatment.

The second objective was to analyze the deficiency of amino acids marker in breath samples of patients with mental disorder before and after the treatment; subsequently, laser spectroscopy was used to assess the exhaled breath compounds of the study peoples.

The breath gases in the exhalation of patients exhibited significant differences from the breath gases in the exhalation of healthy controls.

In conclusion, the data from this study support the hypothesis of the oxidant/antioxidant balance as a key component that may contribute to mental disorder pathology.

Based on a non-invasive sampling method, stable in biological materials, and easy to measure, we conclude that laser spectroscopy analyses of breath ethylene/ammonia in alveolar air appeared to distinguish patients with mental disorder from healthy controls [4-6].

Although laser spectroscopy is a sensitive, non-invasive and real time method to accurately analyze breathing gas concentrations, finding a sensitive, specific and non invasive biomarker of mental disorder, which could be measured in alveolar air, still remains an important task.

Acknowledgments

We gratefully acknowledge the financial support of the Sectoral Operational Programme Human Resources Development 2007-2013 of the Ministry of European Funds through the Financial Agreement POSDRU/159/1.5/S/132395, CNCS-UEFISCDI, project number LAPLAS 3/PN 09 39 and project number PN-II-PT-PCCA-2013-4-0608 (72/2014) .

References

1 D.C. Dumitras, S. Banita, A.M. Bratu, R. Cernat, D.C.A. Dutu, C. Matei, M. Patachia, M. Petrus and C. Popa, "Ultrasensitive CO_2 laser photoacoustic system" ,Infrared Physics & Technology Journal **53**, 308-314,(2010).

2 D. C. Dumitras, D. C. Dutu, C. Matei, A. M. Magureanu, M. Petrus and C. Popa, "Laser photoacoustic spectroscopy:principles,instrumentation,and characterization" Journal of Optoelectronics and Advanced Materials**, 9**, 3655-3701 (2007).

3 C. Popa, Ş. Băniţă, A. M. Bratu, M. Paţachia, C. Matei, and D. C. Dumitraş, "The level of ethylene biormarker in renal failure of elderly patients analyzed by photoacoustic spectroscopy", Laser Physics **23**, No. 12, doi:10.1088/1054-660X/23/12/125701, Article ID 125701 (2013)

4. C. Popa, D. C. Dumitraş, M. Paţachia, and S. Băniţă, "Testing fruits quality by photoacoustic spectroscopy assay", Laser Physics **24**, No. 10, doi:10.1088/1054-660X/24/10/105702 , (2014)

5 C. Popa, "IR spectroscopy study of the influence of inhaled vapors/smoke produced by cigarettes at active smokers", Journal of Biomedical Optics 20(5), 051003, [DOI: 10.1117/1.JBO.20.5.051003]

6. Cristina Popa, " "Human respiration in wavelenghts", ISBN: 978-3-659-61401-9, LAP Lambert Academic Publishing (2014)

P-191

Analysis of copper sulfide contaminant in solid transformer insulation using vacuum ultraviolet laser induced breakdown spectroscopy

Aparna N[1]*, Nilesh J. Vasa[1], R. Sarathi[1], P.B. Bisht[1], J. Sundara Rajan[2], P. Hayden[3], M. B. Alli[3], J. T. Costello[3]

1) Indian Institute of Technology Madras, Chennai-600036, Tamil Nadu, India, 2) Central Power Research Institute, Bangalore-560080, Karnataka, India, 3) Dublin City University, Glasnevin, Dublin 9, Ireland

*E-mail: *aparna.neettiyath@gmail.com*

Time integrated spatially resolved Vacuum-Ultraviolet Laser Induced Breakdown Spectroscopy (VUV-LIBS) is proposed and demonstrated for the detection of trace copper and sulfur contaminants in the transformer insulation. It has been reported that copper sulphide (Cu_2S) diffusion in transformer insulation media is a major threat to the effective functional life of transformers [1,2]. In the present work, a methodology using VUV-LIBS was identified to study the diffusion of Cu_2S into the solid insulation, the oil impregnated pressboard (OIP).

A Q switched Nd^{3+}: YAG laser (wavelength 1064 nm and pulse duration 20 ns FWHM) was used for the VUV-LIBS experiment. The emission spectra were spatially resolved using a foreslit of width 50 µm located between the plasma and the entrance slit of the spectrometer. The wavelength range of the spectrometer was optimized for 50 to 90 nm where there is minimum interference from the emission lines of virgin pressboard. Emission lines of SIII (68.3 nm), SIV (66.6 nm) in the OIP were indicative of the presence of the diffused sulfur contaminant. The results were correlated with the LIBS studies based on the emission line of sulfur (S III 279.73 nm) in the visible region. For enhancing further the emission signal intensity of sulfur lines, a Helium gas ambience was used and was optimized for maximum signal detection. A calibration of sulfur emission intensity was attempted using samples of known sulfur concentration. The emission lines of copper were also analyzed in the vacuum ultraviolet region of the spectrum.

Keywords: vacuum ultraviolet laser induced breakdown spectroscopy (VUV-LIBS), copper sulfide, oil impregnated pressboard (OIP)

[1] R. Maina, V. Tumiatti, M. Pompili, R. Bartnika., "Corrosive sulfur effects in transformer oils and remedial procedures" IEEE transactions on Dielectrics and Electrical Insulation, vol.**16**, no.6, pp.1655-1663, (2009).

[2] Aparna N, Nilesh J. Vasa, R. Sarathi, J. Sundara Rajan, "Feasibility study for detecting copper contaminants in transformer insulation using laser induced breakdown spectroscopy", Appl. Phys A.,Volume 117, Issue 1 , pp 281-288 (2014).

P-193

Laser-induced breakdown spectroscopy and shadowgraphic analysis of selective thin-layers removal by laser ablation

M. S. Rabasović[1], D. Šević[1], N. Lukač[2], M. Jezeršek[2], J. Možina[2], P. Gregorčič*[2]
[1]*Institute of Physics, University of Belgrade, Pregrevica 118, 11080 Zemun, Serbia*
[2]*Faculty of Mechanical Engineering, University of Ljubljana, Aškerčeva 6, 1000 Ljubljana, Slovenia*
E-mail: peter.gregorcic@fs.uni-lj.si

Selective laser ablation of thin layers means subliming or vaporising a thin (i.e., under 100 μm) layer without damaging the substrate or the intermediate underlying layer. This is especially important in several applications, such as rapid prototyping of printed circuit boards. In this case it is essential that the copper is removed from an engraved track without damaging the composite substrate under the copper, while the damaged substrate may carbonize and therefore cause the unwanted altering of its electrical properties [1]. Since the laser-engraved track depth significantly varies with different parameters, such as copper layer thickness, surface conditions, and processing-laser parameters, an adaptation of the laser-processing parameters is needed to achieve optimal results. However, the current laser engraving systems lack of an on-line monitoring method that would enable selective layer removal of changing surface properties during the laser processing.

Several methods of detecting the acoustic waves and plasma spectrum during the thin layer removal have been investigated [1, 2, 3]. Here, the acoustic waves have been measured by a microphone and a laser-beam-deflection probe [4, 5]. The main idea behind these methods is to detect the time-of-flight of the shock wave, which is generated during the laser ablation. Since the shock wave's velocity varies with the optodynamic energy-conversion efficiency [6], this results in different time-of-flights at a constant distance between the probe or microphone and the laser-material interaction site. Here, the main idea is that the optodynamic energy-conversion efficiency changes when the ablated material changes, e.g., since a thin layer is already removed and the ablation of the substrate takes place. The second type of the method for monitoring the removal of thin layers is laser-induced breakdown spectroscopy (LIBS) that enables the spectrum analysis of the plasma emission generated during the laser-material interaction. In such a way, the identification of the elemental composition of the material being ablated is possible [7].

In the presented study we simultaneously use two monitoring methods, the shadowgraphy [6] and LIBS [8] for the analysis of laser ablation of copper from a printed circuits board. Here, a laser pulse of 5 ns having the energy of 16 mJ at 1064 nm was used to ablate an 18-μm-thin copper layer from the substrate. On the basis of shadowgraphs of the shock wave induced by a laser ablation, we measured the optodynamic energy-conversion efficiency. Our results show that this efficiency, defined as the ratio between the mechanical energy of the shock wave and the excitation-pulse energy, is significantly higher for the laser-pulse-copper interaction than for the interaction between the excitation pulse and the substrate. The presented shadowgraphic results enable a better insight into the shock wave dynamics that is important to understand and optimize measurements with other optodynamic methods, such as a laser-beam-deflection probe and microphone measurements. LIBS was simultaneously employed in our experimental setup. Thus, the optical emission from plasma plume was collected by using a spectrograph and recorded with a streak camera. Here, the time-resolved streak images enable monitoring of temporal evolution of the ionic and atomic emission lines. We will show that advancing of laser ablation through the copper layer and reaching of the substrate can be estimated by tracking the intensity ratio of doublet Copper lines (515.3 nm and 521.8 nm) and doublet Aluminium lines (394 nm and 396 nm). Therefore, our results confirm that LIBS method enables an on-line monitoring needed for selective thin-layers laser removal.

[1] A. Gorkič, D. Kovačič, and J. Diaci, "Analysis of sonic waves generated during laser engraving of printed circuits" Int. J. Adv. Manuf. Tech. **42**, 138 (2009).
[2] J. Diaci and J. Možina, "A Study of Blast Wave-Forms Detected Simultaneously by a Microphone and a Laser Probe during Laser Ablation" Appl. Phys. A **55**, 352 (1992).
[3] T. Tong, J. G. Li, and J. P. Longtin, J. P., "Real-time control of ultrafast laser micromachining by laser-induced breakdown spectroscopy" Appl. Optics **43**, 1971 (2004).
[4] J. Diaci, "Response Functions of the Laser-Beam Deflection Probe for Detection of Spherical Acoustic-Waves" Rev. Sci. Instrum. **63**, 5306 (1992).
[5] R. Petkovšek, P. Gregorčič, and J. Možina, "A beam-deflection probe as a method for optodynamic measurements of cavitation bubble oscillations" Meas. Sci. Technol. **18** (2007).
[6] P. Gregorčič, J. Zadravec, J. Možina, and M. Jezeršek, "Optodynamic energy-conversion efficiency during laser ablation on metal surfaces measured by shadow photography" Appl. phys. A, **117**, 353 (2014).
[7] T. J. Li, Q. H. Lou, Y. R. Wei, F. Huang, J. X. Dong, and J. R. Liu, "Laser-induced breakdown spectroscopy for on-line control of selective removal of cobalt binder from tungsten carbide hardmetal by pulsed UV laser surface ablation" Appl. Surf. Sci. **181**, 225 (2001).
[8] M. S. Rabasović, B. P. Marinković, and D. Šević, "Time-Resolved Optical Spectra of the Laser Induced Indium Plasma detected using a Streak Camera", IEEE Trans. Plasma Sci. **42**, 2588 (2014).

P-194

Role of Material Properties on Signal Enhancement in Nd:YAG-CO_2 DPLIBS

P. J. Skrodzki, J. R. Becker, P. K. Diwakar, and A. Hassanein

Center for Materials Under eXtreme Environment (CMUXE), School of Nuclear Engineering, Purdue University, West Lafayette, IN 47906, USA

Email address: pskrodzk@purdue.edu

Abstract

Laser-induced breakdown spectroscopy (LIBS) is a well-known analytical technique for elemental detection entailing spectral analysis of plasma formed through laser ablation. Among numerous advantages, LIBS is practical for robust, *in-situ* and remote analysis of various single- or multi-element materials, namely metals and dielectrics. Although the standard technique suffers from low sensitivity, alternative methods exist which bode signal enhancement over the standard. Double-pulse LIBS (DPLIBS) involves optimization of spatial and temporal coupling for two laser pulses in order to improve spectral emissions from plasma formed via laser ablation. However, signal improvement varies often significantly between targets of different properties. The objective of this study is to compare signal sensitivity between conventional single-pulse LIBS (SPLIBS) and DPLIBS techniques for pure element samples of varying properties. The study investigates laser-material interaction for Nd:YAG SPLIBS and near-collinear Nd:YAG-CO_2 DPLIBS schemes. Analysis involves correlation of such material properties as atomic weight, melting and boiling point, thermal parameters, optical reflectivity and ionization potential to observed signals and plasma characteristics. Target samples chosen for varying properties include metals of varying Z: Al, Mg, Co, Fe, Sn, Cu, Cr, Ta, and W. Signal intensity, signal-to-noise and signal-to-background as well as plasma persistence, excitation temperature and electron density constitute parameters of merit for signal as well as plasma analyses, respectively. Results suggest thermal properties parallel intensity variation while signal (including background of spectra) varies largely with the atomic mass of the target element between proposed SPLIBS and DPLIBS techniques. Ultimately, mechanisms involved for signal enhancement in DPLIBS are discussed in context of laser-material interaction and material physical properties.

P-195

Laser Ablation Sampling at Ultrashort Wavelength

R. Delmdahl, B. Fechner
Coherent LaserSystems GmbH & Co. KG, Hans-Boeckler-Str. 12, D-37079 Goettingen, Germany
E-mail: ralph.delmdahl@coherent.com

Abstract

Pulsed excimer lasers are the most powerful 193 nm laser processing tools on the market and have a history of success in demanding industrial laser markets such as refractive surgery, microelectronics manufacturing or laser engraving. High pulse energies of some 10 to several 100 mJ are available already from compact, stand-alone excimer lasers which are easily integrated into laser ablation systems for LA-ICP-MS solid sample analysis. This is because their 6,4 eV photons are generated directly without the need for frequency conversion. The high pulse energy is usually transformed into high fluence levels favourable in the case of optically transparent specimens or when analysing a variety of geological samples. Today, homogenized 193 nm laser optical systems for LA-ICP-MS analysis such as the GeoLasPro provide nanosecond pulsed output for ablation with better than 1% rms shot-to-shot stability and on-sample fluence levels as high as 45 J/cm2. LA-ICP-MS has come a long way since its introduction over 25 years ago. Whereas the first generation of laser systems started out with infrared lasers, today's most advanced solid sampling systems are predominantly using UV excimer lasers driving accuracy and precision achieved in analysing soils and sediments, gemstones, quartz samples, calcite, fluorite and other materials. Ultra-precise excimer lasers at 193 nm ensure optimum ablation quality and get the most out of the resolution and signal processing capabilities of the attached ICP-MS instrumentation.

P-196

Nanoparticles Enhanced Laser Induced Breakdown Spectroscopy: applying nanoparticle to LIBS

A. De Giacomo[1,2], M. Dell'Aglio[2], O. De Pascale[2], R. Gaudiuso[1], C. Koral[1], G. Valenza[2]
[1]*Chemistry Department, University of Bari, Via Orabona 4, 70125 Bari-Italy*
[2]*CNR-IMIP, Via Amendola 122/D, 70126 Bari-Italy*
e-mail: alessandro.degiacomo@uniba.it

Many approaches have been proposed in the last decade to improve LIBS performances, like Multi-pulse LIBS, Resonance LIBS and various hyphenated techniques. Although these techniques have been successful applied, they require complex experimental set-up and additional costs that decrease the LIBS' appeal for users, who generally use compact commercial systems and are not interested in developing deep expertise in laser techniques.
On the other hand development of knowledge on nanotechnology is having a great impact in analytical chemistry like in mass spectrometric techniques, high resolution microscopy and gas sensors.
Starting from these considerations we have recently proposed Nanoparticle Enhanced LIBS (NELIBS) [1,2] in order to strongly improve the efficiency of the laser-matter interaction by exploiting the physical features of noble metal nanoparticles (NP) for what concerns their electrical, optical and thermal properties. NELIBS is based on the deposition of a colloidal solution of noble metal NP on the sample surface and does not require any change in the LIBS set-up and so can be directly applied to traditional LIBS commercial system achieving an emission intensity 1-2 orders of magnitude higher than LIBS. In this work the fundamental aspects of NELIBS is be discussed in correlation with quantitative analysis of conductor samples (metals and alloys), high refractive index samples (glasses) and biological samples. In the case of conductor the NELIBS enhancement is ascribed to the coupling effect of the laser field with the surface plasmonic field inducing instantaneous electron field emission and a more efficient breakdown ignition. On the other hand NPs on transparent medium can be applied in order to tune the surface refraction index of the sample and optimize the breakdown and plasma induction. Finally the lower ablation threshold of sample covered with NPs allows to apply LIBS to fresh leaves, where conventional LIBS does not work efficiently. Although huge difference in laser breakdown process and in the emission signal observed during NELIBS and LIBS, it has been observed that the plasma features are very similar in both the techniques, confirming the possibility of applying the same analytical methodologies.

[1] A. De Giacomo, R. Gaudiuso, C. Koral, M. Dell'Aglio, O. De Pascale "Nanoparticle Enhanced Laser Induced Breakdown Spectroscopy (NELIBS): effect of nanoparticles deposited on sample surface on laser ablation and plasma emission" Spectrochim. Acta Part B. **98**, 19 (2014)
[2] A. De Giacomo, R. Gaudiuso, C. Koral, M. Dell'Aglio, O. De Pascale "Nanoparticle-Enhanced Laser Induced Breakdown Spectroscopy of metallic samples" Anal. Chem. **85**, 10180 (2013)

P-197

Spectroscopic analysis of the breath from subjects with type 2 diabetes

M. Petrus[1], C. Achim[1,2], A-M Bratu[1], S. Banita[1], M. Patachia[1],
C. Matei[1,2] and D. C. Dumitras[1]
[1]*Department of Lasers, National Institute for Laser, Plasma and Radiation Physics, 409 Atomistilor St., PO BOX MG-36, 077125, Bucharest, Romania*
[2]*University POLITEHNICA of Bucharest, 313 Splaiul Independentei St., Bucharest, Romania*
E-mail address: mioara.petrus@inflpr.ro

Concerning the complications associated with type 2 diabetes, the emission of ethylene from the human breath as a consequence of oxidative stress determination by lipid peroxidation was monitored using laser photoacoustic spectroscopy (LPAS) [1,2]. Lipid peroxidation (LP) is the oxidative degradation of polyunsaturated fatty acids (PUFA) induced by free radicals (reactive molecules that posses an unpaired electron. The cell damage started by free radicals action on biomolecules plays a very important role in the pathogenesis of some diseases, such as cancer, cardiopulmonary bypass, Alzheimer, atherosclerosis and inflammation. Under stress conditions (e.g. ionising radiation, toxic chemical substances, chronic or acute diseases, etc), the free radical production is significantly increased.

Breath analysis has long been recognized as a potentially powerful tool for the diagnosis and study of medical diseases [3,4]. The molecular profile of breath will be the product of the composition of the inspiratory air and the volatile molecules that are present in the blood. The bulk matrix of breath is a mixture of nitrogen, oxygen, carbon dioxide, water vapors and the inert gases. Over 1,000 compounds have been identified to be present in exhaled human breath with concentrations range from ppb to ppt levels. Approximately, 35 of the identified compounds in the exhaled breath have been established as biomarkers for particular diseases and metabolic disorders [3-7]. Diabetes mellitus is a group of metabolic diseases characterized by hyperglycemia resulting from effects of insulin action, insulin secretion or both [5,6]. Diabetes has taken place as one of the most important diseases worldwide, reaching epidemic proportions. Diabetes is a major source of morbidity, mortality, and economic cost to the society. In addition to this, diabetics are also at risk of experiencing chronic complications such as coronary heart diseases, retinopathy, nephropathy and neuropathy, and foot ulceration. Oxidative stress plays an important role in the pathogenesis and the complications of diabetes. Hyperglycemia results in overproduction of oxygen free radicals, which contributes to the progression of diabetes.

Ethylene as biomarkers for lipid peroxidation in humans can be detected in the exhaled breath by means of very sensitive gas sensors based on high resolution molecular spectroscopy. To this purpose, a CO_2 laser photoacoustic spectroscopy system (CO_2LPAS) for online ethylene monitoring in subjects with type 2 diabetes. The high resolution laser spectroscopy is able to detect trace gases in human breath with high sensitivity and can help medicine and science in understanding the life processes and designing sensors useful for non-invasive clinical diagnostic procedures. The method was applied in a study of the correlation between the exhaled ethylene and the complication related with type 2 diabetes. The results seems to indicate an increase in ethylene concentrations at subjects with different complications due to diabetes. Additional work is needed to confirm the reported results and to take same advantage from them, and in general from the possibility offered by the LPAS facility.

[1] C. Popa, D.C.A. Dutu, R. Cernat, C. Matei, A.M. Bratu, S. Banita, and D.C. Dumitras, "Ethylene and ammonia traces measurements from the patients' breath with renal failure via LPAS method," Appl Phys B 105, 669–674 (2011).
[2] D.C. Dumitras, D.C. Dutu, C. Matei, A.M. Magureanu, M. Petrus, C. Popa," Laser photoacoustic spectroscopy: principles, instrumentation, and characterization," J. Optoelectron. Adv. Mater. 9(12), 3655-3701 (2007).
[3] T.H. Risby, Volatile organic compounds as markers in normal and diseased states, Disease markers in exhaled brath: basic mechanisms and clinical applications, Series I: A life and Behavioural Sciences vol. 346, N. Marczin, M. Yacoub (Eds.), IOP Press, pp. 113-122 (2002).
[4] G. Giubileo, A. Puiu, G. Argiro, P. Rocchini, E. Borra, Analysis of the breath from patients treated by anti-tumour radio-therapy, Laser Physics, 41 (2): 243-249 (2004).
[5] A. Mezzetti, F. Cipollone, and F. Cuccurullo, "Oxidative stress and cardiovascular complications in diabetes: isoprostanes as new markers on an old paradigm," Cardiovascular Research, vol. 47(3): 475–488 (2000).
[6] F. Giacco and M. Brownlee, Oxidative stress and diabetic complications, Circ Res. 107(9): 1058–1070 (2010).
[7] C. Wang, and P. Sahay,"Breath analysis using laser spectroscopic techniques: breath biomarkers, spectral fingerprints, and detection limits," *Sensors (Basel)*, 9(10), 8230-8260 (2009).

P-199

Suitability of laser-induced breakdown spectroscopy in screening potential additives to mitigate fouling deposits

S. Balakrishnan[1], V. Midhun Reddy[1], N.J. Vasa[2*], R. Nagarajan[1]

[1]Deparment of Chemical Engineering, [2]Department of Engineering Design, Indian Institute of Technology Madras, Chennai 600036, India.

[*]email address: njvasa@iitm.ac.in

Abstract: Condensable alkali vapors present in the flue gas play a vital role in promoting the formation of fouling deposits and their growth. A decrease in alkali vapors in flue gas suppresses the growth rate of fouling deposits, and increases the thermal efficiency of a coal-fired thermal power plant. An increase in alkali content in ash - generated by burning a coal with an additive -compared to ash generated by combusting the coal without an additive indicates a decrease in alkali vapors in flue gas. Elemental composition of coals is one of the key parameters to measure in order to assess coal quality and its behavior during combustion. In this study, the suitability of laser-induced breakdown spectroscopy (LIBS) in detecting and quantifying alkali elements in coals was investigated [1,2]. In the experiment, a pulsed Nd^{3+}:YAG laser at a wavelength of 1064 nm with a pulse interval of 10 ns and pulse repetition rate of 10 Hz was used. Five additives – kaolinite, alumina, silica, magnesia, and pumice – were tested on four Indian coals for their capability to confine alkali elements to ash during coal combustion. Two additive concentrations and two combustion temperatures were employed to study the effect of concentration and combustion temperature, respectively, on retention of alkali elements to ashes. The technique was used to identify additives to trap both sodium and potassium to ash.

Keywords: Fouling; Mitigating ash deposition; Laser-induced breakdown spectroscopy; Additive technique; Alkalis retainment.

References

[1] T. Ctvrtnickova, M. P. Mateo, A. Yanez, G. Nicolas, "Laser induced breakdown spectroscopy applicationfor ash characterization for a coal fired power plant," Spectrochim Acta Part B **65**, 734-737 (2010).

[2] L. Zhang, L. dong, H. Dou, W. Yin, S. Jia, "Laser-induced breakdwon spectroscopy for determination of the organic oxygen content in anthracite coal iunder atmospheric conditions," Appl. Sperctosc. **62**, 458-463 (2008).

P-200

Fast atomic diffusion in solid state amorphous thin films irradiated with low fluence laser pulse in UV

V.S. Teodorescu[1], C. Ghica[1], A.V. Maraloiu[1], A. Kuncser[1], A.M. Lepadatu[1], I. Stavarache[1], M.L. Ciurea[1], N.D. Scarisoreanu[2], A. Andrei[2], M. Dinescu[2]

[1]National Institute of Material Physics, 105 bis Atomistilor Street, 077125 Bucharest-Măgurele, Romania
[2]National Institute of Plasma Lasers and Radiation, 409 Atomistilor Street, 077125 Bucharest-Măgurele, Romania
E-mail: teoval@infim.ro

Thin amorphous films were irradiated with 266 nm radiation of the Nd-YAG laser. Experiments were performed on SiGe amorphous films [1] and TiGeO amorphous films obtained by RF magnetron sputtering deposition [2]. Low value laser fluence well below the ablation or melting threshold was used.

Before and after laser irradiation, the films structure was studied by SEM, AFM and TEM methods. The TEM specimens were prepared by cross section technique. This method allows the study of structural modifications, induced by the laser pulse action in the thin surface layer corresponding to the radiation absorption depth in the film. The modifications of the surface layer atomic composition, effect which is directly related with the atomic diffusion induced by the laser pulse action, were studied using the HAADF-STEM imaging and the EDX line scan analyze technique.

The SiGe amorphous films with 170 nm thickness were obtained by RF magnetron sputtering using Si:Ge ratio of 45:55. After laser pulse irradiation with 30 mJ/cm^2 fluence, which is well below the experimental 50 mJ/cm^2 value, which is the experimental threshold value for melting , the surface layer show a gradual crystallization which develop in depth to about 50 nm after 10 laser pulse irradiation. In the same time with the crystallization process, the Ge atoms concentration grows in the 10 nm film surface layer and the region under this layer is depleted in Ge, as revealed by the EDX line scan analyze. This diffusion effect takes place in solid state phase in the time of laser pulse action. Considering that the normal values of Ge diffusivities is solid state at 1000 K are of the order of magnitude of 10^{-16} cm^2/s, the diffusion length is of the order of several pm. However, the redistribution of Ge in the surface layer shows a real diffusion coefficient of the order of 10^{-4} cm^2/s, which is characteristic for liquid state.

A similar fast diffusion effect takes place in the case of laser pulse irradiation of TiGeO amorphous films. These films with 350 nm thickness were deposited with the Ge:TiO_2 ratio of 50:50, and their annealing at 900 K leads to formation of a nanostructurated crystalline film containing Ge(Ti)O_2 rutile, Ti(Ge)O_2 anatase and Ge cubic phases [2]. The laser irradiation of the as deposited TiGeO amorphous film was performed perpendicular to the film surface using 100 laser pulses and a fluence of 15 mJ/cm^2 . After the laser irradiation the film structure remains amorphous. A wave like relief with a quasi-period of 200 nm was produced a on the film surface and the surface layer nanostructure was modified in a depth of 50 nm. An interesting effect of Ge atoms segregation in nanometric amorphous spheres takes place under the film surface. These Ge spheres have size from 5 to 20 nm and are embedded in the TiGeO amorphous matrix depleted in Ge. The surface temperature estimations lead to a maximum temperature of about 700 K, which is well below the Ge or Ge and Ti oxides melting temperature. However, the laser pulse action probably can trigger the glass transition effect, which produces a softening of the amorphous matrix and give the possibility to the surface relief appearance. Even so, the fast diffusion of Ge atoms forming the Ge amorphous nanospheres, cannot be explained only with this softening.

In conclusion, the experimental facts reveal that in the case of UV pulse laser irradiation of Ge content amorphous films, using fluence values less than the melting threashold, a fast atomic diffusion effect takes place. This efect takes place in solid state phase and show diffusivity values like in the liquid state phase.

References

[1] V.S. Teodorescu, C. Ghica, A.V. Maraloiu, A.M. Lepadatu, I. Stavarache, M.L. Ciurea, N.D. Scarisoreanu, A. Andrei, M. Dinescu, "Nanoscale fast Diffusion in Laser Irradiated SiGe Thin Films", 2013 Proceesing Nanotech, Washington, USA, vol.1, pp 109-112, 2013

[2] Stavarache.I, Lepadatu. A-M, Teodorescu. V.S., Galca. A.C., Ciurea M.L "Annealing induced changes in the structure, optical and electrical properties of GeTiO2 nanostructured films",.Applied Surface Science, **309**, 168-174 , 2014

P-203

Thermodynamics and Kinetics of d-Metals in Two-Temperature States

K. P. Migdal[1], Yu. V. Petrov[2], D. K. Il`nitsky[1], V. V. Zhakhovsky[1,3], K. V. Khishchenko[3], N. A. Inogamov[1,2]
[1]*Centre of Fundamental and Applied Research, All-Russia Research Institute of Automatics, 22 Sushchevskaya, Moscow 127055, Russia*
[2]*Landau Institute for Theoretical Physics, Russian Academy of Science, 1a Academika Semyonova, Chernogolovka 142432, Russia*
[3]*Joint Institute of High Temperature, Russian Academy of Science, 13/19 Izhorskaya, Moscow 125412, Russia*
E-mail: migdal@vniia.ru

The relaxation between initially cold lattice and femtosecond laser heated electrons is in a focus of the experimental and computational studies during last decade [1]. A detailed knowledge of 3d electron band structure in copper is crucial to determine electron temperature in a two-temperature (2T) state from X-ray absorption spectroscopy (XAS) measurements.

An advanced model of 2T state based on the simple model [2] was developed for d-metals including copper and gold. The model includes an equation of state (EoS), electron heat conductivity and electron-ion coupling as functions of density and both ion and electron temperatures. Contribution of hot electrons to the 2T EoS is derived from DFT calculations with the use of VASP code. Cold energy and ion contribution to the 2T EoS are taken from a semi-empirical EoS for copper in electron-ion equilibrium [www.ihed.ras.ru/rusbank].

Electron heat conductivity was calculated using either QMD simulation performed with ABINIT code or an analytical method [2] based on the Boltzmann kinetic equation, which was extended in this work. The change of 3d electron density of state (DoS), shown in Fig. 1 (left panel), caused by compression or electron heating was taken into account in calculation of electron transport coefficients using the analytical method [2]. Electron-ion coupling, which guides the electron-ion relaxation in metals, was obtained with an approach [2] utilizing Kaganov-Lifshitz-Tanatarov theory. The coupling was calculated to be significantly dependent on both electron temperature and density (Fig. 1, right panel), and yet it is in good agreement with the experimental data obtained at the temperature 2200 K and zero-pressure equilibrium density [3].

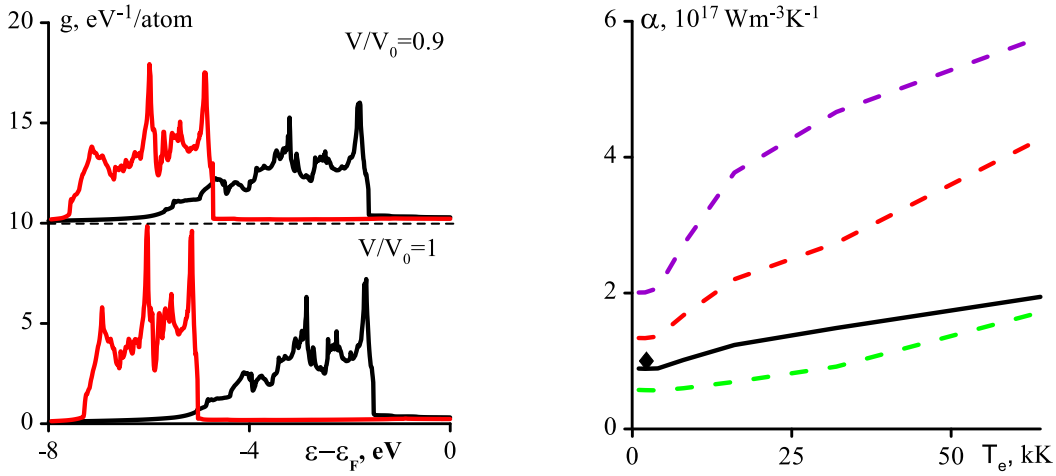

Fig. 1. Left: Densities of states (DoS) for copper with cold (black lines) and hot (red lines; T_e=55,000 K) electrons. DoS for hydrostatically compressed copper at V/V_0=0.9 are shifted up on 5 eV^{-1}/atom with respect to DoS at equilibrium density ρ=8930 kg/m^3. Fermi energy for compressed copper is different by 10.5 eV from Fermi energy of 8.7 eV in equilibrium state of copper. Right: Electron-ion coupling α for copper at different electron temperatures and densities. Black solid line shows α at the equilibrium density, purple dashed line – α at V/V_0=0.8, red dashed line – α at V/V_0=0.9, green dashed line – α in stretched copper with V/V_0=1.1. Diamond shows the experimental α for equilibrium condition with T=2200 K and zero-pressure equilibrium density [3].

The model developed for two-temperature hydrodynamic (2T-HD) simulation of electron-ion relaxation allowed us to obtain distributions of electron and ion temperatures across a submicron foil during the electron-ion relaxation timescale in the range of 1-10 ps. We demonstrate that the electron temperature distribution is not spatially uniform in such thin foils within picoseconds after laser irradiation. The calculated rates of thermal transfer from electron to ion subsystem were used in combined 2T-HD and MD simulations to study effect of 2T electron-ion relaxation on foil expansion. This work was partially supported by RFBR (grant No. 13-02-1078).

1 B. I. Cho, K. Engelhorn, A. A. Correa, T. Ogitsu, C. P. Weber, H. J. Lee, J. Feng, P. A. Ni, Y. Ping, A. J. Nelson, D. Prendergast, R. W. Lee, R. W. Falcone, and P. A. Heimann, "Electronic Structure of Warm Dense Copper Studied by Ultrafast X-Ray Absorption Spectroscopy", Phys. Rev. Lett. 106, 167601 (2011).

2 Yu. V. Petrov, N. A. Inogamov, and K. P. Migdal, "Thermal Conductivity and the Electron-Ion Heat Transfer Coefficient in Condensed Media with a Strongly Excited Electron Subsystem", JETP Letters. 97(1), 20 (2013).

3 H. E. Elsayed-Ali, T. B. Norris, M. A. Pessot, and G. A. Mourou, "Time-Resolved Observation of Electron-Phonon Relaxation in Copper", Phys. Rev. Lett. 58, 1212 (1987).

P-204

Cross-sectional image of femtosecond laser-induced periodic surface structures on yttria-stabilized zirconia

M. Kakehata[1], H. Yashiro[1], A. Oyane[2], A. Ito[3], and K. Torizuka[1]

[1] *Electronics and Photonics Research Institute, National Institute of Advanced Industrial Science and Technology (AIST), Central 2, 1-1-1 Umezono, Tsukuba, Ibaraki 305-8568 Japan.*

[2] *Nanosystem Research Institute, National Institute of Advanced Industrial Science and Technology (AIST), Central 4, 1-1-1 Higashi, Tsukuba, Ibaraki 305-8562. Japan.*

[3] *Human Technology Research Institute, National Institute of Advanced Industrial Science and Technology (AIST), Central 6, 1-1-1 Higashi, Tsukuba, Ibaraki 305-8566, Japan.*

E-mail: kakehata-masayuki@aist.go.jp

Formation of laser-induced periodic surface structures (LIPSS) by ultrashort pulse lasers has been investigated for variety of materials. The low spatial frequency LIPSS（LSFL） is explained by the interaction of the incident light and the scattered light on the surface [1]**.** For metals and semiconductors, the direction of the periodic line structure of LSFL is generally perpendicular to the polarization direction. For some dielectrics, LSFL parallel to the polarization have been reported [2]. The Y_2O_3-stabilized tetragonal ZrO_2 polycrystal (3-mol % Y_2O_3-doped ZrO_2, 3Y-TZP), which is one of fine engineering ceraimcs, offers advantages in application for mechanical components and medical implants due to its high resistance to fracture and flexural strength. Femtosecond laser ablation can be a suitable method to modify the surface roughness of 3Y-TZP [3], however, there has been no report on LIPSS for 3Y-TZP. In this paper, we report the formation of LIPSS and cross sectional image of LIPSS on 3Y-TZT for the first time, which can be utilized to modify the surface characteristics of fine ceramics.

A laboratory made Ti:Sapphire laser system was employed for experiment. It generates 800nm-centered 80-fs FWHM pulses at 560Hz repetition rate. The beam was focused by lenses to the sample with controlling polarization by using waveplates. The shot number was controlled by a mechanical shutter. The 3Y-TZP samples are made from a fine powder (TZ-3YB-E, Tosoh) with sintering temperature at 1350 ºC. The surface was wet-polished to mirror quality (Ra<0.05μm) by a manufacturer. The ablated surfaces were observed by a laser scanning microscope and scanning electron microscopes (SEM). In order to take cross-sectional images of LIPSS, a focused ion beam (FIB) etching was employed (FIB-SEM, XVision 200DB, Hitachi High-tech). Before FIB etching, the surface was coated by 100nm-thick Pt as a conduction layer and by 500-nm thick W as a guard layer for FIB.

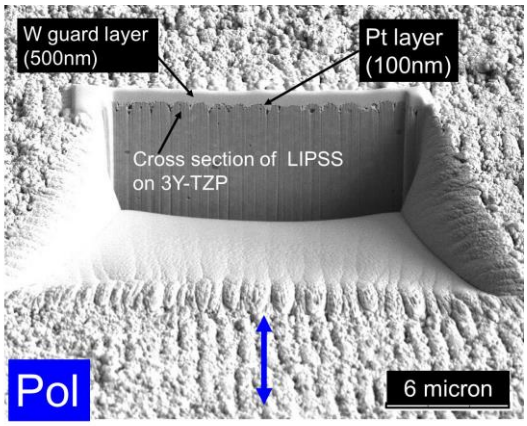

Fig. 1. Cross-sectional SEM picture of LIPSS generated on 3Y-TZP. B**l**ue **a**rrow indicates direction of the laser polarization. The observation angle relative to the 3Y-TZP surface normal is 54 deg. The top surface of the sample is covered with guard layer of W.

Figure 1 shows SEM picture of the W-coated surface and the cross-section of LIPSS on 3Y-TZP. The LIPSS was generated with 40-shots irradiation of the laser pulses at a fluence of 4 J/cm^2. The LIPSS is grating like structure with a period of 700-900nm/cycle for linearly polarized light with the lines parallel to the polarization direction. From the cross-sectional image obtained with different electron detectors for SEM and scanning ion microscope (SIM), we could clearly observe grains of polycrystal and some modified layers with < 100-nm thickness on the LIPSS on 3Y-TZP.

[1] J. E. Sipe, J. F. Young, J. S. Preston, and H. M. van Driel, "Laser-induced periodic surface structure. I. Theory," Phys. Rev. **B27,** 1141 (1983).

[2] S. Höhm, A.Rosenfeld, J Krüger, and J. Bonse, "Femtosecond laser-induced periodic surface structures on silica, " J. Appl. Phys. **112**, 014901 (2012).

[3] R. A. Delgado-Ruíz1, J. L. Calvo-Guirado1, P. Moreno, J. Guardia, G. Gomez-Moreno, J. E. Mate-Sánchez, P. Ramirez-Fernández, and F. Chiva, "Femtosecond laser microstructuring of zirconia dental implants," J. Biomed. Mater. Res., **96B**, 91 (2011).

P-205

Dynamics of gold and silver films initiated by femtosecond laser pulse

N.A. Inogamov[1], V.V. Zhakhovsky[2], V.A. Khokhlov[1], Yu.V. Petrov[1], K.P. Migdal[2]
[1]*L. D. Landau Institute for Theoretical Physics, Russian Academy of Sciences, Akademika Semenova, 1-A, 142432, Chernogolovka, Moscow region, Russian Federation*
[2]*All-Russia Research Institute of Automatics, ROSATOM, Sushchevskaya, 22, 127055, Moscow, Russian Federation*
E-mail address: nailinogamov@gmail.com

Metal films on dielectric substrates are widely used in laser experimentsand technologies (LIFT, LIBT, nanoparticles production, microelectronics, etc.) [1-3]. Dynamics of films on substrate differs from dynamics of free-standing foils due to mechanical response of substrate, see Fig. 1. Also motion of the films is significantly different from dynamics of bulk targets if the film thickness is of the order of or less than thermal depth heated by a laser pulse [3-6], which is typically ~40-150 nm in metals. The same absorbed laser energy makes a thin film hotter than a bulk target since the thermal conductance of dielectric is low. From the other hand, an ultrashort laser pulse generates tensile stress in a film. An amplitude of stress increases as an absorbed fluence increases. Above the separation threshold, the stretching action of tensile stress separates the film from substrate because usually the metal – substrate contact is the weakest (for stretching) plane in the metal – substrate system, see Fig. 1. Combination of higher heating and the weak plane together with interaction of two rarefaction waves decreases the threshold for separation of film from substrate relative to the ablation threshold for a bulk target.

We present the new theoretical and simulation results concerning two-temperature thermophysics and hydrodynamics of irradiated silver and gold films for various conditions, in which the influence of absorbed fluence, thickness, and cohesion strength are discussed. Behavior of film below and above the separation threshold is analyzed. Evolution of optical properties is investigated. Dynamics of separation is studied. Hydrodynamic interaction between a film and substrate plays a significant role in the separation of a film and its fly out from substrate. The separation threshold is defined. Simulation results are compared with experimental studies. Support from Russian Science Foundation 14-19-01599 is acknowledged.

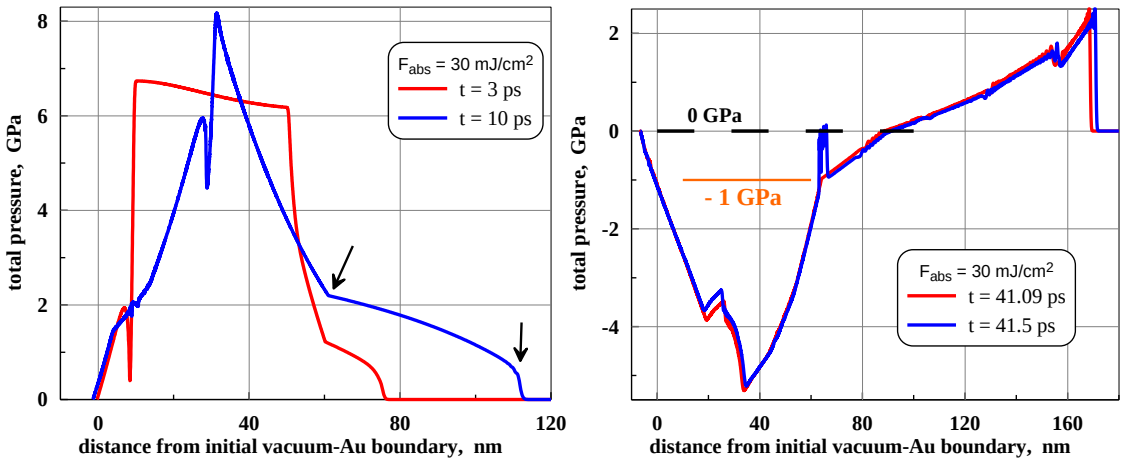

Fig. 1 (Left)The rise of total pressure (electron+ion contributuions) is due to laser heating (at early stage a main contribution is from electrons) in the begining and next because of energy transfer from electrons to ions. Ion Gruneisen parameter is higher than electron one, therefore the same energy results in higher pressure. Two rarefaction waves propagate one from the vacuum boundary at the left side and another from the gold-glass contact initially located at 60 nm. The arrows mark current positions of contact and shock in glass. (Right) Separation of film from glass. Two instants, one just before separation, and another just after, are shown. The pressure increase toward zero indicates beginning of separation. Laser pulse duration is 100 fs. Pulse comes from the left side. Rarefaction from vacuum boundary creates tensile stress, that comes to the contact and stretches it. Film separates from glas when tensile stress overcomes the cohesive strength, which is assumed to be equal 1 GPa in this simulation.

[1] C. Unger, J. Koch, L. Overmeyer, and B.N. Chichkov, "Time-resolved studies of femtosecond-laser induced melt dynamics," Optics Express **20**(22), 24864 (2012).
[2] T. Tomita, M. Nishikino, N. Hasegawa, Y. Minami, R. Takei, M. Baba, T. Eyama, S. Takayoshi, T. Kaihori, T. Morita, Y. Hirano, T. Kawachi, M. Yamagiwa, and T. Suemoto, "Time-Resolved Soft X-Ray Imaging of Femtosecond Laser Ablation Processes on Metals," JLMN-Journal of Laser Micro/Nanoengineering **9**(2), 137-142 (2014).
[3] D.S. Ivanov, A.I. Kuznetsov, V.P. Lipp, B. Rethfeld, B.N. Chichkov, M.E. Garcia, and W. Schulz, "Short laser pulse nanostructuring of metals: direct comparison of molecular dynamics modeling and experiment," Appl. Phys. A **111**, 675-687 (2013).
[4] B.J. Demaske, V.V. Zhakhovsky, N.A. Inogamov, I.I. Oleynik, "Ablation and spallation of gold films irradiated by ultrashort laser pulses," Phys. Rev. B **82**, 064113 (2010).
[5] N.A. Inogamov and V.V. Zhakhovskii, "Formation of Nanojets and Nanodroplets by an Ultrashort Laser Pulse at Focusing in the Diffraction Limit," JETP Lett. **100**(1), 4-10 (2014).
[6] N.A. Inogamov, V.V. Zhakhovskii, and V.A. Khokhlov, "Jet Formation in Spallation of Metal Film from Substrate under Action of Femtosecond Laser Pulse," Journal of Experimental and Theoretical Physics (JETP) **120**(1), 15-48 (2015).

P-206

Case study on the ultrafast laser ablation of thin aluminium films: dependence on laser parameters and film thickness

A. Horn[1], M. Olbrich[1], E. Punzel[1], J. Kubistova[1], R. Roesch[2], R. Oettking[2], B. Muhsin[2], H. Hoppe[2], and J. Schille[1]

[1]*Laserinstitut Hochschule Mittweida, University of Applied Sciences Mittweida, Technikumplatz 17, 09648 Mittweida, Germany*
[2]*Institut für Physik, Ilmenau University of Technology, Langewiesener Str. 22, 98693 Ilmenau, Germany*
Email: horn4@hs-mittweida.de

High-quality micro-structuring of thin metallic films, e.g. no debris, no burr and no damage of the substrate is of increasing interest for thin film electronics, like organic electronics [1]. Laser ablation using ultra-short pulsed laser radiation allows removing thin film with very high spatial resolution and working with high repetition rate as well with high through-put. In this work the ultrafast ablation of thin films of aluminium on BK7 glass is investigated as function of wavelength (1026 nm and 257 nm), pulse duration (200 fs to 10 ps), number of pulses per point (1 to 10), temporal separation of pulses (10 ps to 1 ms), and film thickness (10 nm to 300 nm). The ablation $F_{Thr,abl}$ and melting threshold peak fluences $F_{Thr,melt}$ are determined. The experimental data are compared with numerical simulations. The model combines the simulation of the beam propagation by using Finite Differences Time Domain (FDTD) method with Yee-algorithm and the calculation of the temperature distribution by solving the coupled heat transfer equation of the Two Temperature Model (TTM). All simulations were performed two-dimensionally with axial symmetry and by using Graphic Processor Units (GPU). The optical properties of the thin Al-films were determined experimentally by ellipsometry and the thermo-physical properties were taken from literature [2] including the dependence of the electron temperature. The change of the optical properties due to the rising electron temperature caused by the the laser pulse is taking into account by the Lorentz-Drude model [3]. The removal of the molten material is considered by a simplified approach applying the recoil pressure [4].

The peak threshold fluence determined by focused IR femtosecond laser radiation (λ = 1026 nm, t_p = 280 fs, d_f = 26.8 µm) feature an incubation dependence on the number of pulses (Fig. 1 left). After irradiating the surface with single laser pulses below $F_{Thr,abl}$, the thin Al-film is not removed completely, but its density is changed and a porous layer of re-solidified aluminium with a well confined external border is detectable by SEM, light microscopy and laser scanning microscopy (Fig. 1 right). Due to the Gaussian intensity distribution of the laser radiation at fluences above $F_{Thr,abl}$ the layer is removed in the central region completely and a bumpy border is detectable around the removed area.

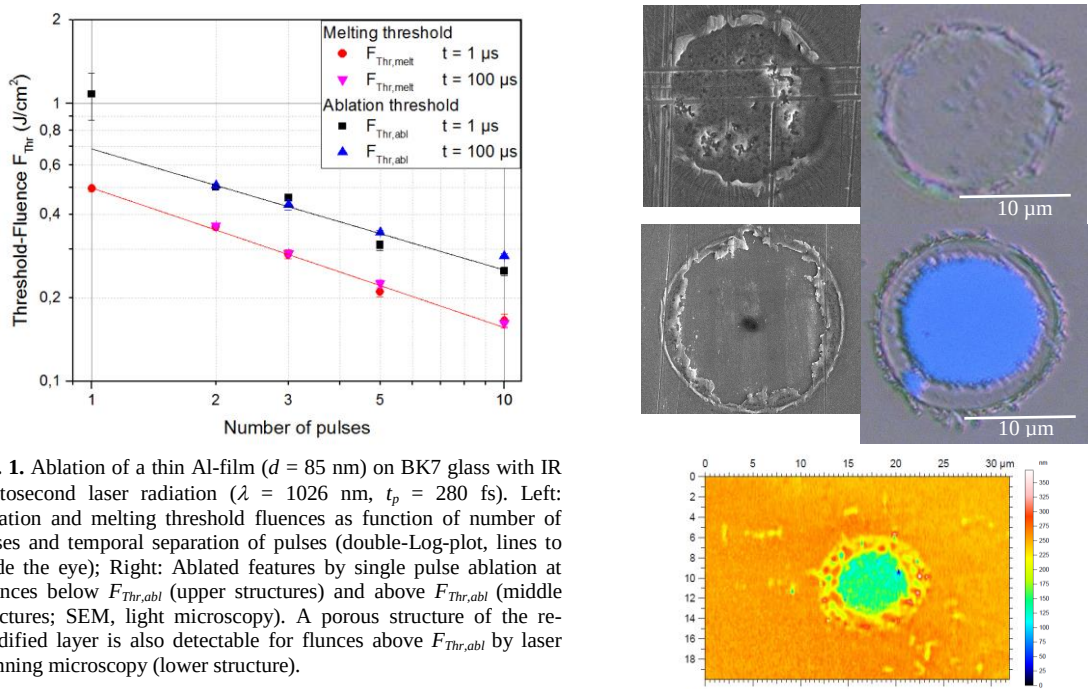

Fig. 1. Ablation of a thin Al-film (d = 85 nm) on BK7 glass with IR femtosecond laser radiation (λ = 1026 nm, t_p = 280 fs). Left: Ablation and melting threshold fluences as function of number of pulses and temporal separation of pulses (double-Log-plot, lines to guide the eye); Right: Ablated features by single pulse ablation at fluences below $F_{Thr,abl}$ (upper structures) and above $F_{Thr,abl}$ (middle structures; SEM, light microscopy). A porous structure of the re-solidified layer is also detectable for flunces above $F_{Thr,abl}$ by laser scanning microscopy (lower structure).

[1] A. Horn, C.-C. Kalmbach, J. González, V. Schuetz, U. Stute, L. Overmeyer "Laser-Surface-Treatment for Photovoltaic Applications," Phys. Proc. **39**, 709 – 716 (2012)
[2] Lin, Z., Zhigilei, L., and Celli, V. "Electron-phonon coupling and electron heat capacity of metals under conditions of strong electron-phonon nonequilibrium,", Phys. Rev. B **77**, 075133 (2008)
[3] Rakic, A. D., Djurišic, A. B., Elazar, J. M., and Majewski, M. L. "Optical Properties of Metallic Films for Vertical-Cavity Optoelectronic Devices," Appl. Opt. **37**, 5271 – 5283 (1998)
[4] Courtois, M., Carin, M., Le Masson, P., Gaied, S., and Balabane, M. "A new approach to compute multi-reflections of laser beam in a keyhole for heat transfer and fluid flow modelling in laser welding," J. Phys. D: Appl. Phys. **46** 505305 (2013)

P-207

Investigations about oligothiophene donor-acceptors systems

A. Guarnaccio [1], M. D'Auria [2], R. Racioppi [2], R. Teghil [1,2], P. A. Loukakos [3], D. Anglos [3], D. Catone[4], *P.* O'Keeffe[5], G. Lendvay [6], A. Santagata[1*]

[1] CNR-ISM U.O.S. Tito Scalo, Zona Ind. – 85050 Tito Scalo (PZ) – Italy

[2] Department of Science, University of Basilicata, Via dell'Ateneo Lucano 10 – 85100 Potenza – Italy

[3] Institute of Electronic Structure and Laser-IESL, Foundation for Research and Technology Hellas – FORTH, 71110 Heraklion, Greece

[4] CNR-ISM, Via del Fosso del Cavaliere, 100 - 00133 Roma - Italy

[5] CNR-ISM, Area della Ricerca di Roma 1, Monterotondo Scalo - Italy

[6] Research Centre for Natural Sciences, Institute of Materials and Environmental Chemistry, Hungarian Academy of Sciences, 1025 Budapest, Magyar Tudósok krt. 2 - Hungary

Presenting Author E-mail: antonio.santagata@cnr.it

Recently, in our group a new synthetic pathway has been developed for getting a donor-acceptor π-conjugated fullerene-oligothiophene-fullerene triad compound in which the three constituents are linked covalently by two ethynyl bridges [1].

Starting from this potentially interesting compound we performed photophysical steady-state and transient pump-probe measurements in solution in order to study the electron dynamics processes involved after the photoexcitation. In parallel, electronic structure calculations have been performed on some related donor-acceptor systems with different electron acceptor groups (*e.g.*, -Br; –CHO and -ethynyl). The results of exploratory quantum chemical methods were used to evaluate the energetics of excited electronic states and the absorption spectra as well as the nature of the excitations. In this work the agreement between experimental and TD-DFT data will be reported and discussion about the role of solvents during the charge transfer process will be presented.

[1] M. D'Auria, A. Guarnaccio, R. Racioppi, A. Santagata, R. Teghil, "Synthetic Approach to and Characterization of a Fullerene–DTBT–Fullerene Triad" Synlett, **24**(8), 943, (2013).

P-208

Hydrodynamic simulation of aluminum target surface irradiated by a femtosecond laser pulse

B. Chimier, F. Deneuville, F. Dorchies, G. Duchateau, and C. Fourment
Université de Bordeaux-CNRS-CEA, Centre Laser Intenses et Applications (CELIA), Talence F-33405, France
E-mail: chimier@celia.u-bordeaux1.fr

Studying the surface motion of a metal sample during and after a sub-picosecond laser heating presents a great interest to understand the structural evolution along with the phase transition dynamics. An accurate description of the surface dynamics is essential to understand the interplay between energy absorption and relaxation processes.

The surface dynamics of aluminum sample irradiated by a femtosecond laser pulse was measured at CELIA using the Aurore Ti:sapphire laser facility (800 nm, 30 fs, up to 6 mJ at 1 kHz repetition rate) [1]. The laser beam was split into two beams. The pump beam was focused on a 300 nm thick aluminum layer deposited on optical quality glass. The probe beam was used to set up a Frequency Domain Interferometry diagnostic. The position evolution of the aluminum surface was measured with a sub-picosecond time resolution and a 1 nm accuracy. The results show that the surface sample remains sharp during the time of observation. This over dense expansion of the surface is due to a nanometer oxide layer present on the aluminum target surface. This layer plays the role of a plug which inhibits the plasma ejection and keeps the surface in a condensed phase.

To investigate the influence of the oxide layer on the surface relaxation, simulations were performed with 1D Lagrangian hydrodynamic code ESTHER [2]. In the calculations, the sample was composed of an aluminum target surrounded by a Al_2O_3 layer. The oxide layer is assumed to be transparent to the laser with a constant optical index of 1.76. The pump laser energy is absorbed by the aluminum electrons behind the oxide layer. The deposited laser energy is transferred to the aluminum lattice after the end of pump irradiation. A two-temperature equation of state based on the multiphase equilibrium equation of state Bushman, Lomonosov and Fortov [3] is used for aluminum, and aluminum oxide is described by the SESAME table 7411. To include the oxide mechanical resistance in our 1D simulation, the oxide layer is assumed to behave as a membrane – i.e., a thin plate subject to large external stretching forces applied at its circumference.

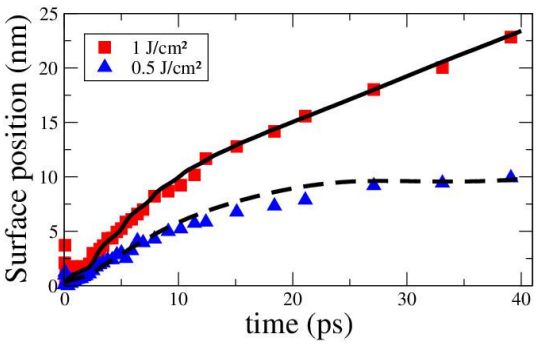

Fig. 1. Calculated and measured evolution of Al target surface irradiated by 0,5 J/cm² (blue triangles for experiment, and dashed line for simulation) and 1 J/cm² (red square for experiment, and line for simulation).

The calculated and measured Al-Al2O3 interface motions are presented in Fig. 1 for a 300 nm aluminum target surrounded by a 10 nm thick oxide film, and irradiated with fluences of 0.5 and 1J/cm². A good agreement is observed between the calculated and experimental results. The simulation exhibits a sharp aluminum boundary as in the experiment. During the first five picoseconds, the oxide layer retains the aluminum expansion without mechanical resistance. After, the oxide layer induces a mechanical resistance which slows down the surface expansion. Finally, the oxide layer breaks, and the expansion velocity of the aluminum surface becomes roughly constant.

[1] F. Deneuville, B. Chimier, D. Descamps, F. Dorchies, S. Hulin, S. Petit, O. Peyrusse, J.J. Santos, and C. Fourment, "Sub-picosecond and nanometer scale dynamics of aluminum target surface heated by ultrashort laser pulse," Appl. Phys. Lett. **102**, 194104 (2013).
[2] J. P. Colombier, P. Combis, F. Bonneau, R. Le Harzic, and E. Audouard, "Hydrodynamic simulations of metal ablation by femtosecond laser irradiation," Phys. Rev. B **71**, 165406 (2005).
[3] A. V. Bushman, I. V. Lomonosov, and V. E. Fortov, "Models of wide-range equations of state for matter under conditions of high energy density," Sov. Technol. Rev. B **5**, 1 (1993).

P-209

Dissociative double ionization of acetylene in strong laser field

Atia-tul-noor[1,*], Han Xu[1], X. Wang[1] , D. Kielpinski[1,2], R. T. Sang[1,2], I. V. Litvinyuk[1]

[1] *Centre for Quantum Dynamics and Australian Attosecond Science Facility, Griffith University, Nathan, QLD 4111, Australia*
[2] *ARC Centre of Excellence for Coherent X-Ray Science, Griffith University, Nathan, QLD 4111, Australia*
**atia-tul-noor@griffithuni.edu.au*

We studied the molecular dynamics in a strong laser field by investigating the dissociative double ionization of acetylene which is one of the symmetric organic and important polyatomic molecules for understanding the photo-initiated process. Using the COLTRIMS technique [1] in combination with pump probe technique we mapped different dissociation pathways. Two body fragment channels are dominated. Pump and probe pulses were produced with Mach-zehnder interferometer. The pump and probe pulses were overlapped in space and time at zero delay and directed into the COLTRIMS main chamber. Inside the chamber the laser beams were tightly focused by a silver coated spherical mirror of focal length 75mm onto the supersonic jet. The laser pulse had duration of 6 fs with a central wavelength of 800 nm. The Pump power was 15mW and probe power was 6mW.The Probe power was set in such a way that no $C_2H_2^{++}$ ions could be created by probe pulse. The ions were extracted onto a time-and position-sensitive channel plate detector by a uniform electric field 15 V/cm. The ionic products such as H^+,CH^+,C^+, CH_2^+, C_2H^+, $C_2H_2^{++}$, $C_2H_2^+$ were detected. To analyse the correlated ion pairs, we only selected the pairs of fragments with total momentum close to zero and they are separated by the PIPICO (Photo ion photo ion coincidence) method.
Following two body breakup channels were selected for the double ionization of acetylene

$$C_2H_2^{++} \rightarrow H^+ + C_2H^+ \quad \text{P channel}$$
$$C_2H_2^{++} \rightarrow CH^+ + CH^+ \quad \text{A Channel}$$
$$C_2H_2^{++} \rightarrow C^+ + CH_2^+ \quad \text{V Channel}$$

KER spectra for three breakup channels are presented in the figure 1.

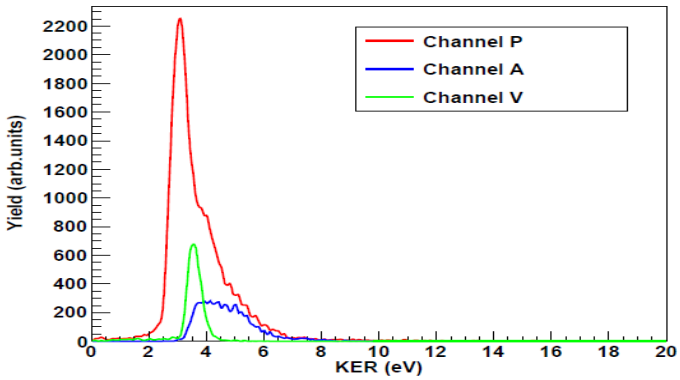

Fig1. A comparison of KER vs Yield for three channel.

The deprotonation channel shows the largest yield as compared to the other channels. These spectra reveal time dependent features that reflect the behaviour of dissociation of molecule which we will discuss in our paper.

Reference.

[1] Han Xu, Tian-Yu Xu, Feng He, D. Kielpinski, R.T.Sang and I.V. Litvinyuk, "Effect of nuclear mass on carrier-envelope-phase controlled electron lacalization in dissociating molecules," *Phys. Rev.A*, vol. 89, p. 041403(R), (2014).

Friday
4 September 2015

Oral presentations

I-15

High-resolution ultrafast laser ablation-based chemical imaging of energy materials

Vassilia Zorba
Lawrence Berkeley National Laboratory, Berkeley CA 94720
Corresponding Author e-mail address: vzormpa@lbl.gov

One of the main objectives in laser ablation-based chemical analysis is increasing spatial and depth resolution. In this work we use ultrafast laser ablation in the optical far- and near- fields to identify the spatial resolution limitations in laser-ablation based chemical analysis, and to reduce limits of detection down to the attogram scale. These all-optical femtosecond laser technologies are implemented in a number of energy applications, and in particular in the analysis of interfacial layers in Li-ion battery systems, as well as for 3D chemical imaging of different components of the battery cell. The chemical distributions of these systems are correlated to their electrochemical performance, and serve to develop strategies for enabling next-generation high-energy density Li-ion technologies. These results demonstrate the flexibility of laser ablation-based chemical analysis for high-resolution and high-sensitivity elemental imaging of complex energy systems, in real-time and at atmospheric pressure conditions.

O-70

LIBS spectroscopy meets the ocean. Chemical analysis of archeological materials in Mediterranean waters

Javier Laserna
Departamento de Química Analítica, Universidad de Málaga, Spain

After decades of development in laboratories and land operations, chemical analysis of submerged objects is starting to become a reality. While the analysis of water at variable depth has been demonstrated in the past using florescence spectroscopy and Raman spectroscopy, determination of the atomic composition of submerged objects is much a more complex task. Technology based on laser-induced breakdown spectroscopy (LIBS) has been recently developed for such sub-sea operations. This paper will discuss the operating parameters of a marine LIBS analyzer. Metals, alloys, rocks, marble, concrete, can be analyzed at a depth of up to 50 m. The system has been tested in several coastal surveys in Mediterranean waters.

O-71

Two-Step Laser Mass Spectrometry (L2MS) analysis of soot particles surface composition: new developments on the VUV single photon ionization

C. Irimiea[1], Y. Carpentier[1], I. K. Ortega[1], M. Ziskind[1], A. Faccinetto[2], E. Therssen[2], C. Focsa[1]

[1]Laboratoire de Physique des Lasers, Atomes et Molécules (UMR CNRS 8523), Université de Lille 1, 59655 Villeneuve d'Ascq cedex, France

[2]Laboratoire de Physicochimie des Processus de Combustion et de l'Atmosphère (UMR CNRS 8522), Université de Lille 1, 59655 Villeneuve d'Ascq cedex, France

cristian.focsa@univ-lille1.fr

Accurate analyses of soot particle surface composition are aimed at a better understanding of various topics such as their growth processes in flames, their hazardous effect on health and their hydroscopic properties or their potential role as ice condensation nuclei in the atmosphere. In our laboratory, we characterize the species adsorbed on soot particles at low-trace level by Laser Desorption – Laser Ionization – Time-of-Flight Mass Spectrometry (L2MS). Besides the dominating polycyclic aromatic hydrocarbon (PAH) component, we search for other classes of molecules which could modify the physical and chemical properties of soot particles. We developed original laser-based approaches on the one hand to control the ionic / neutral content of the desorbed species and on the other hand to selectively identify the aliphatic component from the aromatic one during the ionization step of the neutrals. Various samples have been analyzed including pure aromatic and aliphatic samples, mixtures, synthetic soot, and model laboratory flame soot.

The soot surface is probed either with the second (532 nm) or fourth (266 nm) harmonic of a nanosecond Nd:YAG laser. While mostly neutral species are produced at 532 nm, the production of ion or neutral can be controlled by the laser fluence of the 266 nm beam. The ionization of the desorbed neutral species is performed by the collimated 266 nm beam from a second Nd:YAG laser or by the focused 118 nm beam generated in a home-made Xe-cell by tripling the third harmonic (355 nm) of the Nd:YAG laser [1]. In the former configuration, only species exhibiting absorption band around 266 nm and ionization energies lower than 9.3 eV, including especially π stabilized polyaromatic species, can be selectively detected by resonant two-photon ionization (R2PI). In the latter case, most of the condensed-phase species can be single-photon ionized (SPI) since their ionization energies are lower than 10.5 eV. The successive use of both ionization wavelengths allows us to distinguish thus the aromatic component from the aliphatic one. The species in the desorption plume are finally mass-analyzed using a Time-of-Flight Mass Spectrometer.

As a preliminary work, we tested the effects of the available wavelengths in both desorption and ionization steps on PAH pellets and various aliphatic compounds and mixtures. We report the effect of the fluence on the desorption pattern. In a second step, we produced and analyzed synthetic soot samples with a controlled-concentration coverage in standard PAH and aliphatic mixtures. In this manner, we can an estimate a limit of detection of our apparatus and compare it in the various configurations. Finally, the method has been applied to soot collected from a laboratory turbulent flame.

[1] D. J. Butcher, "Vacuum Ultraviolet Radiation for Single-Photoionization Mass Spectrometry: A Review", Microchemical Journal **62,** 354–362 (1999).

O-72

Decoration of silicon nanowires with laser ablated silver nanoparticles for surface-enhanced Raman spectroscopy

C. D'Andrea[1], M. J. Lo Faro[2,3], A. Irrera[2], P.M. Ossi[4], F. Neri[5], F. Priolo[1,3,6], B. Fazio[2], S. Trusso[2]

[1]MATIS IMM - CNR, Via Santa Sofia 64, I-95123 Catania, Italy
[2]IPCF - CNR, V.le F. Stagno d'Alcontres 37, I-98156 Messina, Italy
[3]Dipartimento di Fisica ed Astronomia, Università di Catania, Via Santa Sofia 64, I-95123 Catania, Italy
[4]Dipartimento di Energia, Center for Nanoengineered Materials and Surfaces-NEMAS, Politecnico di Milano, via Ponzio 34-3, I-20133 Milano, Italy
[5]Dipartimento di Fisica e Scienze della Terra, Università di Messina, V.le F. Stagno d'Alcontres, 31, 98166, Messina, Italy.
[6]Scuola Superiore di Catania, Via Valdisavoia 9, I-95123 Catania, Italy
E-mail: trusso@me.cnr.it

To detect specific molecules at very low concentration is of particular interest in many areas including biology, analytical chemistry, cultural heritage. Raman spectroscopy provides a clear fingerprint to identify a chemical species, but it is a second order, inefficient process with scattering cross-sections of the order of 10^{-30} cm^2 per molecule, preventing detection and recognition of molecular species at very low concentrations. Nanostructured metallic surfaces, mainly gold and silver, lead to giant amplifications of the Raman scattering cross sections. The enhancements strongly depend on the morphologies of the metallic substrates: nanoparticle (NP) size, shape and mutual arrangement on the surface *i.e.* NP spatial density and interparticle spacing. Many efforts have been made to improve Raman enhancement by controlling the optical and morphological properties of the substrates. In this respect, a three-dimensional SERS active structure can be more effective with respect to a planar substrate since the number density of metallic NPs and the volume probed by the laser spot are both increased. In this work, we present a method to decorate silicon nanowires (Si NWs) with silver NPs deposited by pulsed laser ablation. Si NWs were prepared as follows: an n-doped (10^{15} at/cm^2) crystalline silicon substrate was soaked at room temperature in an aqueous solution containing silver nitrate ($AgNO_3$) 0.02 M, as metal precursor and fluoridric acid (HF) 5 M as etching agent. The silver salts dissociate in the solution, thus realizing a precipitation of silver NPs that randomly distribute on the silicon surface. Locally, just underneath the region covered by metal NPs silicon oxide forms that is subsequently removed by the HF. So silver NPs sink into the silicon bulk, leading to the formation of Si NWs during the etching. Depending on the adopted etching time Si NWs with different lengths (L=1.8 μm and 3.5 μm) were grown. Decoration of the Si NWs with silver NPs was achieved by pulsed laser ablation (PLA). In previous works [1-3] we have shown that effective SERS substrates can be grown by PLA of silver target in presence of an inert (Ar) controlled atmosphere. Different morphologies, ranging from isolated spherical NPs to nearly percolated structures, result by changing two parameters: laser shot number and Ar pressure, keeping fixed all the other relevant deposition parameters. Here silver NPs were grown on the surface of Si NWs using laser pulse numbers ranging between 30000 and 60000. Laser fluence was kept fixed at about 2.0 J/cm^2 and Ar pressure at 70 Pa. The evolution of NP morphology on the surface of Si NWs was investigated by SEM microscopy. SEM cross-section images of the Si NWs show that NPs and their distribution not only depend on the laser pulse number but also on NP position along the Si NW surface. We observe that NPs on top of the Si NWs are larger and less spaced than NPs lying at NW bottom, near the substrate.

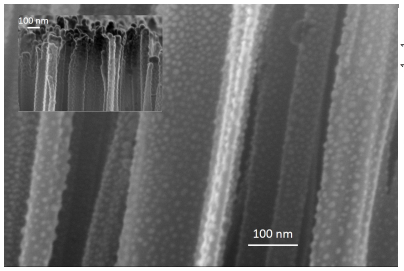

Fig. 1

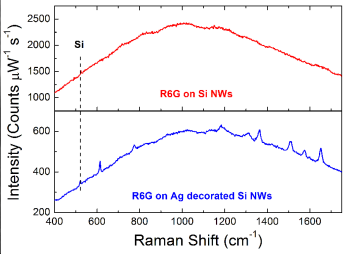

Fig. 2

In Fig.1 SEM cross-section of shows Si NWs decorated by silver NPs acquired at half height of the Si NWs (L=1.8 μm): typical NP size, 7.5 nm. In the inset is shown the cross-section image acquired at the top where NP size was estimated to be about 8.4 nm. Even if a deep optimization of the SERS activity was not performed, rhodamine 6G was detected at concentration level of 10^{-6}M (see Fig.2).

[1] C. D'Andrea, F. Neri, P.M. Ossi, N. Santo, S. Trusso, "The controlled pulsed laser deposition of Ag nanoparticle arrays for surface enhanced Raman scattering", Nanotechnology, **20**, 245606 (2009).

[2] E. Fazio, F. Neri, P.M. Ossi, N. Santo, S. Trusso, "Growth process of nanostructured silver films pulsed laser ablated in high-pressure inert gas", Appl. Surf. Sci., **255**, 9676 (2009).

[3] P.M. Ossi, F. Neri, N. Santo, S. Trusso, "Noble metal nanoparticles produced by nanosecond laser ablation", Appl. Phys. A, **104**,829 (2011)

O-73

Comparison of fs and ns lasers for Blister-Based Laser-Induced Forward-Transfer

N. Goodfriend[1], A. V. Bulgakov[2], N. M. Bulgakova[2], S. V. Starinskiy[2], Yu. G. Shukhov[2], O. Nerushev[1], E. E. B. Campbell[1]

[1]EaStCHEM, School of Chemistry, University of Edinburgh, Edinburgh EH9 3FJ
[2]Kutateladze Institute of Thermophysics SB RAS, Lavrentyev ave. 1, Novosibirsk 630090, Russia
ngoodfriend@gmail.com

1. Introduction

Blister-Based Laser-Induced Forward-Transfer (BB-LIFT) is a recent technique [1,2] which has shown the potential to project neutral nanoparticles into the gas phase without inducing damage. The technique potentially has considerable advantages over alternative methods of producing gas phase targets of nanoparticles or large molecules such as Laser-Induced Acoustic Desorption (LIAD) or MALDI. When using nanosecond lasers for BB-LIFT the underlying substrate can undergo significant heating [3] which may then also lead to thermally-induced fragmentation of thermally-desorbed molecules. In order to avoid this, we are investigating the use of fs laser pulses to induce blister formation and impulsive molecular transfer to the gas phase to provide relatively dense gas phase targets for advanced spectroscopy studies.

2. Methodology and Results

Direct comparisons of ns and fs BB-LIFT of gold-coated silicon nanoparticles (150 nm diameter) and fullerene molecules (1nm diameter) were carried out to determine the blister formation mechanism, the collimation of the desorbed particle beams and the velocity distributions for the two different laser conditions. Angular distributions were determined by depositing the desorbed particles on a substrate and analysing the particle distribution using a combination of optical and atomic force microscopy. Velocity distributions were determined by using laser ionisation time-of-flight mass spectrometry. Blister formation was investigated by SEM and AFM studies as a function of laser fluence and by in situ optical imaging.
We will present a detailed comparison of the ns and fs results, discuss the potential of the technique as a practical source for spectroscopy experiments and describe the mechanisms leading to particle emission in both cases.

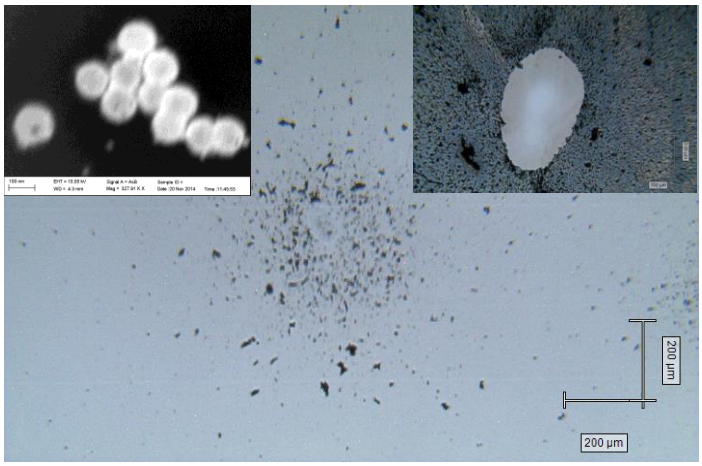

Fig. 1. Shows an optical microscope image of deposited gold coated silicon nanoparticles (main picture) with an optical image of the blister which caused the deposit (top right) alongside an SEM image of the deposited nanoparticles (top left).

[1] T. V. Kononenko, P. Alloncle, V. L. Konov, and M. Sentis, "Laser transfer of diamond nanopowder by metal film blistering," Appl. Phys. A **94**, 531 (2009).

[2] M. S. Brown, N. T. Kattamis, and C. B. Arnold, "Time-resolved study of polyimide absorption layers for blister-actuated laser-induced forward transfer," J. Appl. Phys. **107**, 083103 (2010).

[3] A. V. Bulgakov, N. Goodfriend, O. Nerushev, N. M. Bulgakova, S. V. Starinskiy, Yu. G. Shukhov, E. E. B. Campbell, "Laser-induced transfer of nanoparticles for gas-phase analysis," J. Opt. Soc. Am. B **31**, C15 (2014).

Oxygen vacancies, a crucial role playing on structural, magnetic, and electrical properties of epitaxial manganite thin films

Haizhong Guo[1,*], Xu He[1], Zhenzhong Yang[1], Jia-ou Wang[2], Kui-juan Jin[1, 3], Riqiang Zhao[1], Lin Gu[1,3], Yaqing Feng[1], Wenjia Zhou[1], Xiaolong Li[4], Chen Ge[1], Qian Wan[1], Meng He[1], , Caihao Hong[2], Zhiying Guo[2], Can Wang[1], Huibin Lu[1], Ibrahim Kurash[2], and Guozhen Yang[1,3]

[1]Beijing National Laboratory for Condensed Matter Physics, Institute of Physics, Chinese Academy of Sciences, Beijing 100190, People's Republic of China

[2]Beijing Synchrotron Radiation Facility, Institute of High Energy Physics, Chinese Academy of Sciences, Beijing 100049, People's Republic of China

[3]Collaborative Innovation Center of Quantum Matter, Beijing, China

[4]Synchrotron Radiation Facility (SSRF), Shanghai Institute of Applied Physics, Chinese Academy of Sciences, Shanghai 201204, People's Republic of China

E-mail address: hguo@iphy.ac.cn

Mixed-valence manganites gain increasing significance due to their attractive properties of half-metallic character and colossal magnetoresistive response rendering them as the ideal materials for applications in oxide spintronics devices and for the study of fundamental physical properties. On the other hand, the rich array of phenomena found in oxides is largely due to oxygen, since oxygen tends to pull electrons away from other atoms resulting in strong electronical fields at the interatomic scale. To gain a deep insight in the effects of oxygen vacancies on the electronic structure of mixed-valence manganites, two epitaxial manganite $La_{2/3}Sr_{1/3}MnO_3$ (LSMO) thin films were epitaxially grown at high and low oxygen pressures, which are referred as HP and LP, respectively. The degraded transport properties of LP can be attributed to the effects of the oxygen vacancies. We are known that the oxygen vacancies will be formatted when the LSMO thin films grown below 26 Pa, inducing a charge transition disproportionation of the $Mn^{4+} \rightarrow Mn^{3+}$. The enhanced Mn^{3+} concentration may segregate into imhomogeneous patches, resulting in patches where the magnetic ordering varies from antiferromangetic (Mn^{3+}-O-Mn^{3+}) and ferromagnetic (Mn^{3+}-O-Mn^{4+}) interactions. On the other hand, depletion of oxygen from the Mn-O-Mn chain reduces the coordination of Mn cations, destroying the Mn^{3+}-O-Mn^{4+} interactions. These would cause the degraded the magnetic and transport properties in LP.

To characterize the crystalline structures of the LSMO thin films, state-of-the-art sophisticated aberration-corrected scanning transmission electron microscopy (STEM) techniques of the high-angle annular dark-field (HAADF) and annular-bright-field (ABF) micrographs were utilized. From the line profiles in of ABF images it is worth noting that the profile in HP is almost identical, and exhibits ordering, indicating HP is high structural quality with proper oxygen stoichiometry. However, the height of the profile in LP is randomly distributed, indicating that the LP sample is oxygen-deficient. The evolution of electron correlation in LSMO thin films with oxygen vacancies has been studied employing a combination of Mn 2p resonant photoemission spectroscopy, x-ray photoemission, and band structure calculations. Our findings highlight the key role of the oxygen vacancies on the structural and electrical properties and demonstrate an approach to tune the properties by controlling the oxygen vacancies in oxide thin films.

I-16

Ultrafast lasers on a chip: Progress towards making the femtosecond world mainstream

Steve Madden
Laser Physics Centre, Research School of Physics and Engineering,
Australian antional University, canberra, ACT, Australia
stephen.madden@anu.edu.au

1. Introduction

Ultrafast mode locked lasers have revolutionised many areas of science and industry since their inception, and continue to drive scientific research and select new industrial applications. They have to date however failed to penetrate into more mainstream applications despite a plethora of potential uses. The main reasons for this are the relatively high costs of suitable devices and the lack of small form factor platforms integrated with other functionality. This is of course exactly the domain of planar integrated devices, which in electronic form have wrought massive changes in society over the last 30 years. The question is then raised of whether suitable fully chip based ultrafast lasers are possible with the necessary performance levels for a broad range of applications?

2. Requirements

Performance requirements vary by application, for the low end of the scale (integrated sensors, metrology devices, instrumentation, etc) peak powers of a few KW in 1-200fs pulses at GHz to ~50MHz repetition rates are adequate. For material processing, sub 100fs pulses with >10MW peak power and tens of MHz rates (ie 10-100W average power) are desirable. These requirements dictate several parameters for planar technology. Firstly a high gain amplifier is required for GHz rates where the cavity could be as short as 1cm. Secondly, a low loss dispersion tailored passive waveguide is needed in lengths to ~1m for lower repetition rate applications. Thirdly high saturated power outputs are required. In addition all the other components for a laser must be integratable (pump coupling, frequency selective mirrors, mode locking mechanism). To date, existing chip scale mode locked results, [1-4] representing the best to date in several technologies, have not met these.

3. Current status and prospects

We propose the use of rare earth doped glass waveguides to attain the necessary parameters. It is clear a MOPA architecture will be required and for long cavity lengths a relatively high index waveguide system is needed to enable the cavity to be coiled. The recent demonstration of TeO_2 based ultra-low loss waveguides, high gain amplifiers, and waveguide lasers [5-7] provides a strong foundation, the main barrier to fully integrated devices now being the mode locker. To this end we are currently researching waveguide based graphene saturable absorbers, Figure 1 showing the first integration of a graphene monolayer on a TeO_2 waveguide. More results and further discussion on planar laser technology illustrating a path to obtaining the performance requirements outlined above will be presented at the conference.

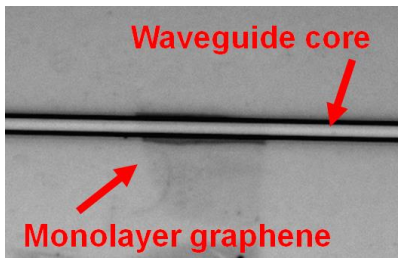

Fig. 1. Micrograph showing Tellurium dioxide waveguide with graphene sheet transferred for saturable absorber tests.

[1] D. I. Nikitichev, et al., “High peak power and sub-picosecond Fourier-limited pulse generation from passively mode-locked monolithic two-section gain-guided tapered InGaAs quantum-dot lasers” Laser Physics, **22**, 715 (2011)
[2] H. Suche, "Mode-locked and Q-switched Ti:Er:LiNbO3 waveguide lasers", Proc. SPIE **3622**, Rare-Earth-Doped Materials and Devices III, 92 (April 1, 1999)
[3] H.Byun et al., "Integrated Low-Jitter 400-MHz Femtosecond Waveguide Laser", IEEE Phot. Tech. Lett. **21** 763 (2009)
[4] S.Beecher et al., "320fs pulse generation from an ultrafast laser inscribed waveguide laser mode-locked by a nanotube saturable absorber", App. Phys. Lett. **97** 111114 (2010)
[5] S.Madden & K.Vu, "Very low loss reactively ion etched Tellurium Dioxide planar rib waveguides for linear & non-linear optics," Opt. Exp. **17** 17645 (2009)
[6] K.Vu & S.Madden, "Tellurium dioxide Erbium doped planar rib waveguide amplifiers with net gain & 2.8dB/cm internal gain," Opt. Express **18** 19192 (2010)
[7] K. Vu, S. Farahani, and S. Madden, "980nm pumped erbium doped tellurium oxide planar rib waveguide laser and amplifier with gain in S, C and L band," Opt. Express **23**, 747-755 (2015)

O-75

Plasma-Enhanced Pulsed Laser Deposition of metal-oxide films: studying the plasma physics for enhanced process control

S. Rajendiran[1], J. Colgan[2], A.K. Rossall[1], A. Gibson[1], E. Wagenaars[1]
[1] *York Plasma Institute, Department of Physics, University of York, York, YO10 5DD, UK*
[2] *Theoretical Division, Los Alamos National Laboratory, Los Alamos, NM 87545, USA*
Email: erik.wagenaars@york.ac.uk

1. Introduction

Metal-oxide thin films such as ZnO, Al_2O_3, MgO, and TiO_2 are widely used in industry and academia, e.g. in microelectronics, photonics, catalysts and as possible indium-free transparent conductors. Pulsed Laser Deposition (PLD) is a plasma-based deposition technique for metal-oxide films that is highly versatile, but suffers, like most alternative thin-film deposition techniques, from limitations in control and predictability of film quality because of a lack of fundamental understanding of the underlying physical processes. The aim of the presented research is twofold. First, to combine experiments and modelling to provide a fundamental understanding of the underlying physics of the different phases of the PLD process. Second to enhance the control options for the PLD process by introducing Plasma-Enhanced PLD (PE-PLD): a combination of traditional PLD with an electrically-produced plasma as a source for reactive oxygen species. The ultimate goal is to develop a predictive computer model that enables us to design thin-film deposition processes for specific applications rather than finding them empirically.

2. Understanding the physics of different phases of the PLD process

The PLD process can be described as three phases with interconnected, but distinctly different physics involved: laser ablation, plasma plume expansion and interactions, and thin-film formation. In this paper we present experimental and modelling studies of the laser ablation and plume expansion phases.

The 2D hydrodynamic code POLLUX [1] is used to model the laser-solid interaction and plasma formation of a Zn ablation with a Nd:YAG nanosecond-pulsed laser. The POLLUX simulations show the interaction of the leading edge of the laser pulse with the solid target, creating a high-density plasma in front of the surface. Subsequently, the laser does no longer reach the solid surface, it is primarily absorbed in the plasma via inverse Bremsstrahlung. In this early phase of PLD, the plasma plume has temperatures of about 10 eV, is highly ionised, and travels with a velocity of roughly 10-100 km/sec away from the target.

After the 10 ns laser pulse has finished there is no more energy input into the plasma. However, the plume has only travelled a few mm from the target surface and has not yet reached the substrate, which is typically a few tens of mm away. The plasma therefore enters the plume expansion phase. Inside the plasma plume, the plasma cools down and expands and collision chemistry changes the composition of the plume via e.g. electron impact ionisation and 3-body electron-ion recombination. Time-integrated optical emission spectroscopy shows that Zn I and Zn II emission lines dominate light emission in the visible range. Since the measurements are time-integrated they are dominated by the plume expansion phase (μs time scales) instead of the ablation phase (10 ns). Comparison with the Los Alamos plasma kinetics code ATOMIC [2] reveals an average temperature around 1 eV, confirming a significant drop in plasma temperature during the expansion phase.

3. Plasma-Enhanced PLD

Finally, a new form of PLD is introduced, plasma-enhanced PLD. In PE-PLD we combine the laser-produced metal ablation plasma with an electrically-produced oxygen plasma to provide separately controlable sources of species for the deposition of metal-oxide films. With this method a Zn target is ablated which subsequently expands into an oxygen plasma rather than neutral oxygen gas. This oxygen plasma contains well-characterised and controllable, reactive oxygen species such as atomic oxygen, ozone and singlet delta oxygen. This method offers additional control of the Zn and O interactions and concentrations in the depositing ZnO plasma.

[1] G.J. Pert, "Two-dimensional hydrodynamic models of laser-produced plasmas," J. Plasma Phys. **41**, 263 (1989).
[2] N.H. Magee, J. Abdallah, J. Colgan, P. Hakel, D.P. Kilcrease, S. Mazevet, M. Sherrill, C.J. Fontes, H.L. Zhang, in *"14th Topical Conference on Atomic Processes in Plasmas"*, J.S. Cohen, S. Mazevet, D.P. Kilcrease ed. (AIP Conference Proceedings, New York, pp. 168–179, 2004).

O-76

Resonance effect of the secondary vapor-bubble's oscillations induced by a synchronized delivery of Er:YAG-laser pulses

P. Gregorčič*, N. Lukač, J. Možina, M. Jezeršek
Faculty of Mechanical Engineering, University of Ljubljana, Aškerčeva 6, 1000 Ljubljana, Slovenia
E-mail: peter.gregorcic@fs.uni-lj.si

Effective irrigation, including debriding, cleaning and the decontamination of anatomical cavities, is one of the most important challenges in different areas of dentistry, such as endodontics, implantology, periodontics and bone surgery [1]. For example, one of the main goals in nonsurgical endodontic treatment is the efficient cleaning and decontamination of the smear layer, bacteria and dentine debris within the root canal system [2]. Recent studies [2, 3] have proven that the usage of a free-running erbium:yttrium aluminium garnet (Er:YAG) laser that radiates low-energy pulses (20-60 mJ) with durations of 50 µs is a very promising technique for endodontic treatment of the root canal. In these treatments, the Er:YAG-laser pulse with a wavelength of 2.94 µm is delivered through a fiber tip into the coronal portion of the pulpa chamber, filled with a liquid, such as water or sodium hypochlorite. Due to the very high absorption coefficient ($\mu_a = 1.247\times10^6$ m^{-1}) of Er:YAG light in water more than 70% of all the pulse's light is absorbed within an only 1-µm-thick water layer. Thus, the water is locally and instantly heated over its boiling point and a vapor bubble starts to expand at the fiber tip's end [4, 5].

After the explosive boiling, the vapor bubble starts to expand. When it reaches its maximum volume, it is nearly empty and starts to collapse due to the pressure of the surrounding liquid. This collapse, in turn, initiates the secondary bubble's growth and collapse. The process repeats itself, resulting in the so-called secondary vapor-bubble's oscillations. Here, each oscillation has less energy and therefore reaches smaller volume due to the energy dissipation during each oscillation [5, 6]. The ratio between the mechanical energy of two successive oscillations can be defined as the oscillation energy-conversion efficiency.

In this contribution we will present our recent results of a synchronized delivery of multiple Er:YAG-laser pulses [7]. Here, the first pulse induces a vapor bubble, while the role of the subsequent pulses is to increase the oscillation energy-conversion efficiency. To investigate this, we have developed a method called a laser-beam-transmission probe (LBTP) that enables online monitoring of the bubble's oscillations. This LBTP method was calibrated by the simultaneously employed laser shadowgraphy. As an excitation laser for water ablation we employed a free-running Er:YAG laser, designed for laser dentistry. The laser was running in the sub-microsecond pulse regime at ultra-low-energy (less than 2 mJ) with frequencies up to 100 kHz.

In the experiments we measured the oscillation energy-conversion efficiency as a function of the delay between the primary and secondary laser pulse. We show that the variation of this delay results in a resonance effect of the oscillation energy-conversion efficiency. Here, the resonance effect is obtained when the second pulse is delivered at the end or slightly after the bubble's first collapse. On the other hand, if the second pulse is delivered before the end of the bubble's first oscillation, it decreases the energy-conversion efficiency of the laser treatment. The presented method, called Photo Acoustic Synchronized Transients (PHAST), has great potential to open new opportunities for further development of modern laser-based dental treatments and to further improve upon their safety and efficiency.

[1] M. Lukač, and G. Pustovrh, "Modeling Photoacoustic Efficiency during Erbium Laser Endodontics" J. LA&HA **2013**. 1 (2013).
[2] E. DiVito, O. A. Peters, and G. Olivi, "Effectiveness of the erbium:YAG laser and new design radial and stripped tips in removing the smear layer after root canal instrumentation" Laser. Med. Sci. **27**, 273 (2012).
[3] E. Deleu, M. Meire, and R. G. Moor, "Efficacy of laser-based irrigant activation methods in removing debris from simulated root canal irregularities" Laser. Med. Sci. **30**, 831 (2015).
[4] A. Vogel, and V. Venugopalan, "Mechanisms of pulsed laser ablation of biological tissues" Chem. Rev. **103**, 577 (2003).
[5] P. Gregorčič, M. Jezeršek, and J. Možina, "Optodynamic energy-conversion efficiency during an Er:YAG-laser-pulse delivery into a liquid through different fiber-tip geometries" J. Biomed. Opt. **17**, 075006 (2012).
[6] R. Petkovšek, and P. Gregorčič, "A laser probe measurement of cavitation bubble dynamics improved by shock wave detection and compared to shadow photography" J. Appl. Phys. **102**, 044909 (2007).
[7] P. Gregorčič, M. Jamšek, M. Lukač, M. Jezeršek, "Synchronized delivery of Er:YAG-laser-pulse energy during oscillations of vapor bubbles, J. LA&HA **2014**, 14 (2014).

O-77

Dynamics of laser-induced cavitation bubble in liquid studied by high-speed stroboscopic videography: Effects of liquid viscosity

Rie Tanabe, Shugo Kurata, Kazuki Nakayama, and Yoshiro Ito
Nagaoka University of Technology, 1603-1, Kamitomioka, Nagaoka, Niigata, Japan
itoy@vos.nagaokaut.ac.jp

Cavitation bubbles are generated when laser pulses are focused in liquid. Dynamics of cavitation bubbles attract much interest in fluid dynamics, materials processing in liquids, medical and biological applications and there are considerable numbers of researches on the subject [1-4]. In this paper, dynamics of the cavitation bubble induced by a focused laser pulse in liquid was investigated through the high-speed laser stroboscopic videography technique developed by authors group. In this imaging method [5, 6], a high-repetition rate, short pulse laser is combined to a high-speed video camera and successive 100 images can be obtained as fast as 1 μs interval. Using the system, videos of cavitation bubbles triggered by single laser pulse can be recorded with an effective shutter speed of as short as 35 ps, which is determined by pulse duration of the high-repetition rate laser, and thus very sharp images are recorded even at 1 MHz frame rate.

Pure water and silicon oil were used as liquid media. The silicon oils used have kinematic viscosities of 10, 100, 1000, 10000, and 100000 cSt, and consist of the same chemical composition, with only slightly different properties. Therefore, our observation can reveal effects of the viscosity on bubble dynamics.

A pulse from a nano-second Nd:YAG laser at 1064 nm with pulse energy of 50 mJ was focused at 10 mm below the liquid surface in a glass cell. Focusing lens was an objective lens of 50x. Laser-induced cavitation bubble was generated in all liquids. When the bubble was generated, the initial shape was elliptical, elongated along laser-incident axis, vertical direction in our case. The bubble expands and then collapses several times with the decrease in size and its shape and position are changed along its cycle as shown in lower row of Figure 1, where initial center position of the sphere was indicated by a dotted line. The center of the first bubble was at the focus position and did not move during its expanding and shrinking period. The center of the second bubble formed after the first bubble collapse was, however, moved downward continuously during its expansion and shrinkage. The shape of the second and the followed bubbles were asymmetric spheres with irregular shape boundaries. Maximum size of the bubble measured in horizontal direction varies little for pure water and silicon oils of viscosities less than 1000 cSt and was about 5 mm. For silicon oils with 10000 and 100000 cSt, the size becomes smaller and was about 3 mm. Details of differences in dynamics of the laser-induced bubbles due to the viscosity will be presented.

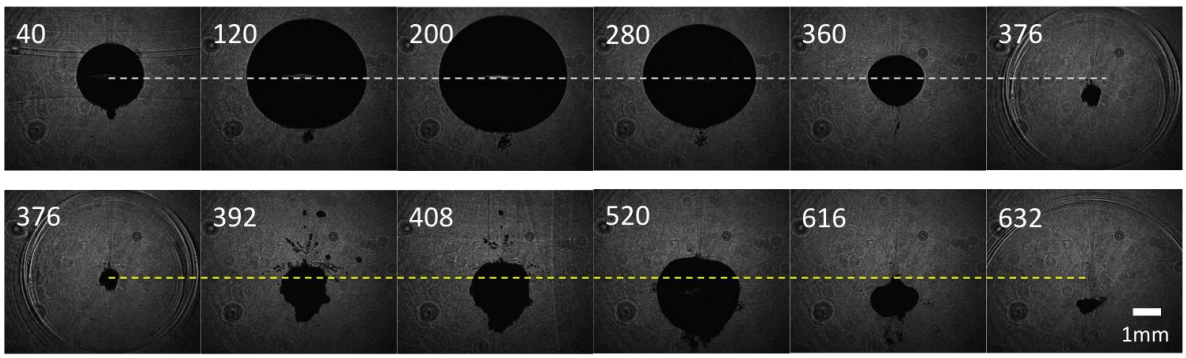

Figure 1. Selected images from the video showing the dynamics of the cavitation bubble generated by single nano-second laser pulse in pure water. Numbers in the pictures indicates the time from the laser irradiation. Gray dotted line shows the center position of the first bubble and yellow dotted line shows that of the second bubble formed after the first bubble collapse.

[1] A. Vogel, S. Busch and U. Parlitz, Shock wave emission and cavitation bubble generation by picosecond and nanosecond optical breakdown in water, J. Acoust. Soc. Am., **100**, 148 (1996)

[2] I. Akhatov, O. Lindau, A. Topolnikov, R. Mettin, N. Vakhitova and W. Lauterborn, Collapse and rebound of a laser-induced cavitation bubble, Phys. Fluids **13**, 2805 (2001)

[3] R. Petkovšek and P. Gregorčič, A laser probe measurement of cavitation bubble dynamics improved by shock wave detection and compared to shadow photography, J. Appl. Phys., **102**, 044909 (2007)

[4] As a recent review, W. Lauterborn and A. Vogel, Shock wave Emission by Laser Generated Bubbles, Technology Reference Library, **8**, 67 (2013)

[5] Y. Ito, R. Tanabe and N. Mohri, Self-Sharpening of Tungsten Electrode in Single, High-Current Discharge: Its Dynamics and Mechanism, Annals of the CIRP **56**, 1 (2007)

[6] T. T. P. Nguyen, R. Tanabe and Y. Ito, Effects of an absorptive coating on the dynamics of underwater laser-induced shock process, Appl. Phys. A **116**, 3 (2014)

O-78

Dynamics of cavitation bubbles induced by laser ablation in liquid nitrogen at various temperatures

Koichi Sasaki and Shingo Harada
Division of Quantum Science and Engineering, Hokkaido University, Kita 13, Nishi 8, Kita-ku, Sapporo 060-8628, Japan
sasaki@qe.eng.hokudai.ac.jp

1. Introduction

This work is motivated by two previous works. One is the synthesis of TiN nanoparticles by laser ablation of a titanium target in liquid nitrogen [1]. The liquid nitrogen used in the previous work was at the boiling point (77 K). The other previous work is that we observed the growth of nanoparticles in a cavitation bubble induced by laser ablation in water [2]. Nanoparticles were stored inside the cavitation bubble until its collapse. Since the cavitation bubble had a high temperature and a high pressure at the collapse [3], the structure of nanoparticles was affected by the dynamics of the cavitation bubble [4,5]. In this work, we try to control the dynamics of ablation-induced bubbles in liquid nitrogen by controlling its temperature. We expect the control of the structure of nitride nanoparticles synthesized by laser ablation in liquid nitrogen.

2. Experiment

We developed a special chamber, which was composed of four shells, to realize laser ablation in liquid nitrogen at various temperatures. The outermost shell was a vacuum chamber which worked for the thermal isolation. The second shell was filled with liquid nitrogen. Although the liquid nitrogen in the second shell was always at the boiling point, the temperature was lower than 77 K by reducing its pressure using an oil rotary pump. The third shell was also filled with liquid nitrogen at pressures between 0.1 and 0.2 MPa. The liquid nitrogen in the third shell was cooled down by the liquid nitrogen in the second shell, so that we obtained liquid nitrogen at a lower temperature than the boiling point in the third shell. The inner most shell was used for collecting synthesized nanoparticles. The liquid nitrogen in the innermost shell was connected to the third shell. A titanium target was installed in the innermost shell, and it was irradiated by Nd:YAG laser pulses at 532 nm from the normal direction. A shadowgraph imaging system employing a high-speed camera and a white lamp was used to record the bubble dynamics.

3. Results and discussion

When the temperature of liquid nitrogen in the innermost shells was 77 K, which was the boiling temperature of liquid nitrogen at 0.1 MPa, the expansion of the bubble was not followed by the shrinkage. We observed the change in the bubble shape from a hemisphere to distorted one after the maximum size. After that, we observed that the bubble was shredded into small bubbles at a delay time longer than 1 ms. In contrast, we observed the shrinkage of the bubble at a temperature of 66 K. The shrinkage was followed by the collapse and the reformation of the secondary bubble. This behaviour is similar to the behaviour of a cavitation bubble induced by laser ablation in water at room temperature. When we pressurized the liquid nitrogen in the innermost shells up to 0.2 MPa with keeping the temperature at 66 K, the maximum bubble size became smaller and the collapse of the bubble became earlier. In addition, we observed the formation of the third cavitation bubble at 0.2 MPa and 66 K, which may be due to the fact that the boiling point at 0.2 MPa is higher than that at 0.1 MPa.

The aforementioned behaviours of laser-induced bubbles are understood by considering the cavitation parameter [6]. It is known that the bubble dynamics is dominated by the inertia when the cavitation parameter is greater than 10, and in this case we can obtain a cavitation bubble with the hard collapse. On the other hand, the energy dissipation via the heat transfer becomes serious when the cavitation parameter is smaller than 10^{-2}, and in this case we cannot expect the collapse of the bubble. The cavitation parameter in the present experimental condition was approximately 0.2 at the maximum. This cavitation parameter is smaller than that in laser ablation in water (roughly 10); however, we obtained a bubble with the dynamics of the collapse and the reformation. Because of the relatively small cavitation parameter, there is a possibility that the temperature and the pressure at the collapse are lower than those in a cavitation bubble induced by laser ablation in water. We are now trying to evaluate the pressure and the temperature of the bubble at the collapse by solving the Rayleigh-Plesset equation.

[1] N. Takada, T. Sasaki, and K. Sasaki, Appl. Phys. A **93**, 833 (2008).
[2] W. Soliman, N. Takada, and K. Sasaki, Appl. Phys. Express **3**, 035201 (2010).
[3] W. Soliman, T. Nakano, N. Takada, and K. Sasaki, Jpn. J. Appl. Phys. **49**, 116202 (2010).
[4] N. Takada, A. Fujikawa, N. Koshizaki, and K. Sasaki, Appl. Phys. A, **110**, 835 (2013).
[5] W. Soliman, N. Takada, N. Koshizaki, and K. Sasaki, Appl. Phys. A, **110**, 779 (2013).
[6] I.W. Florschuetz and B.T. Chao, Trans. ASME, Ser. C, J. Heat Transf. **87**, 209 (1965).

AUTHOR INDEX DIVIDER GOES HERE

Author index